Ecological stability of Indo-Pacific coral reefs during Quaternary climatic fluctuations: Case studies from Vanuatu and Egypt.

DISSERTATION

zur Erlangung des akademischen Grades

d o c t o r r e r u m n a t u r a l i u m

(Dr. rer. nat.)

im Fach Biologie

eingereicht an der

Lebenswissenschaftlichen Fakultät

der Humboldt-Universität zu Berlin

von

Dipl.-Geol. Heike Mewis

Präsident der Humboldt-Universität zu Berlin

Prof. Dr. Jan-Hendrik Olbertz

Dekan der Lebenswissenschaftlichen Fakultät

Prof. Dr. Richard Lucius

Gutachter/innen:

1. Prof. Dr. Wolfgang Kießling
2. Prof. Dr. Liliane Rueß
3. Prof. Dr. Thomas Brachert

Tag der mündlichen Prüfung: 25. Februar 2016

Zusammenfassung

Korallenriffe, ob fossil oder rezent, stellen durch ihre Größe und Lebensdauer einmalige biologische und geologische Strukturen dar, an denen sich über Beobachtungen zu Veränderungen ihrer organismischen und sedimentologischen Zusammensetzung über einen langen Zeitraum hinweg Rückschlüsse auf u.a. Klimaveränderungen und Meeresspiegelschwankungen durchführen lassen. Rezente Riffe gelten als bedroht durch Klimaerwärmung und Versauerung der Meere durch den steigenden Gehalt von CO_2 in der Atmosphäre, und anthropogen induzierte Habitatzerstörung und Verschmutzung der Meere. Verschiedene Zukunftsszenarien, die auch schon in der erdgeschichtlichen Vergangenheit der Korallenriffe beobachtet wurden, werden in diesem Zusammenhang diskutiert, u.a. Adaption/Akklimatisierung, Migration in höhere Breiten und Dezimierung. Besonders pleistozäne Riffe spielen eine große Rolle bei der Analyse von Riffen auf Klimaveränderungen, da sie 1) von den gleichen Taxa errichtet wurden, die auch die heutigen Riffe bauen, 2) aufgrund ihrer guten Erhaltung eine ausreichend analytische Auflösung erlauben und 3) Riffe auch im Pleistozän dramatischen Klimaschwankungen ausgesetzt waren. In tektonisch aktiven Gebieten sind oft eine ganze Serie von fossilen Riffterrassen aus verschiedenen Interglazialen erhalten, an denen man hervorragend faunistische Veränderungen untersuchen kann. Am besten sind pleistozäne Riffe in der Karibik untersucht, während aus dem viel größeren Indo-Pazifik, der auch über eine deutlich höhere Biodiversität verfügt, bisher nur wenige quantitative Studien vorliegen. Bisherige Studien zeigen eine erstaunliche Stabilität und Langlebigkeit der Korallengemeinschaften hinsichtlich Diversität und taxonomischer Zusammensetzung trotz extremer Meeresspiegelschwankungen und starker klimatischer Veränderungen im Pleistozän und Holozän.

Die vorliegende Arbeit behandelt zwei Regionen, aus der quantitative Daten auf Artniveau über die Zusammensetzung der fossilen Korallengemeinschaften bisher fehlten: das tropische Vanuatu (Südpazifik) und der subtropische Sinai, Ägypten (nördliches Rotes Meer). Die konkrete Fragestellung war, ob sich Veränderungen der Riff-Gemeinschaften eher in höheren Breiten als in niederen beobachten lassen, und inwiefern diese Regionen die These der Stabilität bestätigen. Außerdem erlauben Riffe in Ägypten aufgrund der deutlich geringeren tektonischen Hebungs-Raten auch Rückschlüsse faunistischer Veränderungen in kleinem Maßstab innerhalb einer Sequenz. Die Daten wurden mit Hilfe von Linientransekten und, wenn notwendig, in Sammelproben erfasst, bevor sie statistisch in R ausgewertet wurden.

In Vanuatu sind mindestens 7 fossile Riffterrassen mit einem Alter von etwa 5000 - 400.000 Jahren überliefert, von denen 4 detailliert untersucht werden konnten. Veränderungen in der Diversität wurden sowohl lateral als auch vertikal beobachtet, die allerdings hauptsächlich in Abhängigkeit von beprobten Riffzonen sind. Die Riffe waren insgesamt über die Interglaziale bin ins mittlere Holozän hinweg weitestgehend stabil. Nur die Gattung *Acropora* scheint erst in den letzten 96.000 Jahren häufiger zu werden, wobei taphonomische Veränderungen dabei eine untergeordnete Rolle zu spielen scheinen.

In Ägypten wurden quantitative und binäre Daten aus der jüngsten interglazialen Terrasse (MIS 5e) mit rezenten Daten aus dem Roten Meer verglichen und eine Migration von Arten nach Norden während des letzten Interglazials hin belegt: Die pleistozänen Terrassen aus dem Golf von Aqaba zeigen eine höhere Diversität als rezente Riffe im gleichen Gebiet. Beim Vergleich mit Daten aus anderen Regionen des arabischen Raums zeigt sich, dass die Korallengemeinschaft des Pleistozäns aus dem nördlichen Roten Meer die größte Ähnlichkeit mit den Korallengemeinschaften aus dem rezenten zentralen Roten Meer besitzt, welches als Diversitätshotspot des westlichen Indo-Pazifiks bekannt ist. Diese Beobachtung unterstützt frühere Arbeiten, die eine Verschiebung der Riffdiversität in höhere Breiten verbunden mit einer Abnahme der Diversität in niederen Breiten aufzeigten, sowie Studien, die das nördliche Rote Meer und besonders auch den Golf von Aqaba als mögliches Refugium für Korallen im Zuge der weiteren Klimaerwärmung sehen. Inwieweit diese in der Vergangenheit genutzte Möglichkeit durch anthropogen verursachte Habitatzerstörung besonders auch entlang der Touristenzentren im Roten Meer, sowie der ebenfalls dazu kommenden

Ozeanversauerung tatsächlich auch zukünftig für Korallen machbar ist, bleibt fraglich. Jedoch zeigen meine Ergebnisse, dass Riffe unter Abwesenheit von menschlichen Einflüssen durchaus in der Lage waren auch mit starken Umweltveränderungen zurecht zu kommen

Abstract

Fossil and recent coral reefs provide the opportunity to study detailed time-series of ecological data in the form of variations in reef coral community structure during past episodes of environmental change. This is because they accumulate at vast thicknesses of biogenic sediments during their long lifetime. Recent reefs face major threats from global warming, ocean acidification, habitat destruction, and pollution. Three different future scenarios of biological response, which have also been observed in the geological record of reefs, are currently being discussed: Adaption/acclimatization, migration, and destruction. Especially Pleistocene reefs play an important role when assessing the response of coral reefs to climate change, because they 1) are built largely by the same taxa as modern reefs, 2) their good preservation due to their young geological age allows for a good analytical resolution, and 3) they regularly experienced dramatic climatic and sea level changes throughout the Pleistocene. In tectonically active regions, a whole series of uplifted Pleistocene terraces from different interglacials allow for the comparison of coral assemblages from different reef building episodes during frequently shifting climate and sea level regimes. Pleistocene reefs from the Caribbean are well studied and understood, while the much larger Indo-Pacific region with a greater coral diversity is represented by only a few quantitative studies on community ecology. Previous studies observed an astonishing persistence and stability in community composition and diversity throughout several interglacial episodes until today, which is contradictory with the claim that coral reefs are especially sensitive to climate change.

The present study deals with two Indo-Pacific regions that so far lacked any quantitative data of fossil reef communities at the species level: tropical Vanuatu (Coral Sea) and subtropical Sinai, Egypt (northern Red Sea). The major goal of the study was to test if changes in faunal composition are more pronounced at higher than at lower latitudes, and if coral communities from both regions confirm previous observations of long-term stability and persistence throughout the Pleistocene. Also, reefs from Sinai allow for inferences on faunal change at smaller scales within a reef sequence, due to the much lower uplift rate. Data was collected using line transects and additional bulk samplings if necessary, and analyzed statistically using R.

In Vanuatu at least seven fossil reef terraces with ages between 5,000 and 400,000 years are preserved, of which four could be studied in more detail. A great variability was observed among terraces and especially among sub-environments within terraces. Reefs remained stable in terms of diversity throughout the Pleistocene and Holocene but it seems that the dominance of the coral genus *Acropora* is a fairly recent phenomenon in Vanuatu, because this genus does not play a large role in terraces older than 96,000 years (MIS 5c), and its absence cannot be solely explained by taphonomic or sampling biases.

In Egypt quantitative and binary data from the last interglacial episode (MIS 5e) were compared with data from the recent Red Sea and adjacent regions. The Pleistocene reefs from the Gulf of Aqaba display a higher diversity than comparable recent reefs from the same region. Also, when comparing Pleistocene coral data to those of recent Arabic regions, the Pleistocene coral assemblage shows the highest similarity with the recent coral communities from the central Red Sea, which is known as a diversity hotspot in the western Indian Ocean. This observation confirms earlier studies that demonstrated a range expansion of tropical reef communities towards higher latitudes, and is supports studies that suggest the northern Red Sea and especially the Gulf of Aqaba as future refuge for corals during climate warming. More detailed predictions remain difficult, however, as we currently do not know enough about the influence of ocean acidification and anthropogenically induced habitat destruction, especially along the tourist centers of the northern Red Sea. Nevertheless, results of the present study indicate that coral reefs were able to cope with dramatic environmental changes in the absence of anthropogenic impact.

Acknowledgements

First of all I wish to thank my supervisor Prof. Dr. Wolfgang Kießling for his guidance, support, and patience. Julien Millet, who started together with me, and accompanied me in both field seasons - thank you for your support in the field and providing pictures. Special thanks to Prof. Dr. Ulrich Radtke and his laboratory for ESR dating, Prof. Dr. Thomas Kenkmann and the mineralogical laboratory at the MfN for allowing and supporting X-ray diffractometry on some of my samples. Special thanks also the Red Sea Environmental Center in Dahab for logistical support, and especially to Christian von Mach (Alter) and Nina Milton for their temporary and pleasant company in the field, including insight into their work about the ecology of recent reefs and environmental issues. I also want to thank Guy Cabioch† for logistical support in the South Pacific and the Department of Environment and Conservation/Ministry of Land's and Natural Resources, Port Vila, Vanuatu for permissions and support, students from the University of the South Pacific for temporary company in the field and the medical staff from the Vila Bay Health center and Private Hospital in Port Vila for taking care of me in an emergency situation. I also want to thank Georg Heiß, Moshira Hassan and her students for their temporal company during the field work in Ras Mohammed. Special thanks to Prof. Dr. Moshira Hassan also for putting so much afford into helping us with export permits for our Egyptian samples.

Many thanks also to Johannes Müller for patiently English proof-reading and useful comments. Thanks also to my two beloved, sweetest daughters, who were so patient with me during the last months and had to do without me over so many weekends. We will catch up on everything from now on. Thanks also to my mother, Marlies Mewis, for spending so much time on entertaining our daughters, cooking delicious meals and taking care of us throughout the time. I owe you a lot. And finally thanks to my whole family and all friends who stood by me and accompanied me over the last years. I am done now.

TABLE OF CONTENTS

*Parts of these sections have been published before in *Coral Reefs*, 2013 (as cited in the heading if appropriate), but are now extended and modified.

LIST OF FIGURES

LIST OF PLATES

1. INTRODUCTION

Reefs have existed for about two billion years and experienced dramatic climatic and environmental change in their history. Over the entire Neogene period and also today scleractinian corals and calcareous algae were the main reef builders of these complex biogenic structures, that even managed to expand in abundance and latitude despite increasing global cooling in the Neogene, indicating that reef growth is not generally dependent on geological factors, but also biologically controlled (Kiessling 2009). Coral reefs are home to over a million species (Knowlton *et al.* 2010) and sustain over 500 million people worldwide (Moberg & Folke 1999). Tragically, coral reefs are endangered hotspots of biodiversity and among the most vulnerable habitats to future climate change (Pandolfi *et al.* 2011); in fact, one third of all zooxanthellate reef-building coral species are considered to be threatened by global extinction (Carpenter *et al.* 2008). The proportion of threatened coral species exceeds that of most terrestrial animal groups, apart from amphibians (Carpenter *et al.* 2008). The major threats are associated with bleaching and diseases driven by elevated sea surface temperatures (SST), sea level fluctuations and ocean acidification, enhanced by anthropogenic disturbances (Pandolfi 1999; Hoegh-Guldberg *et al.* 2007; Veron *et al.* 2009; Pandolfi *et al.* 2011). The symbiosis of corals and photosynthetic dinoflagellates is negatively affected by positive anomalies in SST (Wooldridge 2013), whereas an increase in SST of only 1 - 2 °C for more than four months causes coral bleaching (Eakin *et al.* 2010). The last big El Niño in 1997/98 caused the worst coral bleaching in history, and another dramatic mass mortality event due to coral bleaching is expected to occur within the next months (Witze 2015). In total, 16% of the world's coral has been lost already due the last bleaching event (Carpenter *et al.* 2008) and some countries like the Maldives lost up to 90% of their reef coverage (Bianchi *et al.* 2006). Most coral reefs already exist in environments near their upper thermal limits (Glynn 1993; Coles & Riegl 2013), and the big question is how they will respond to future temperature rise. Different scenarios are discussed among scientists, among those adaptation and acclimatization (Hoegh-Guldberg 2014; Palumbi *et al.* 2014) as well as biogeographic shifts of corals to higher latitudes along with a decline at lower latitudes (Hoegh-Guldberg 1999; Carpenter *et al.* 2008; Descombes *et al.* 2015). However other authors expressed a pessimistic view. Descombes *et al.* (2015) doubt that the shift to higher latitudes will be a realistic option in the near future, because ocean acidification due to higher atmospheric CO_2 will decrease the capability to produce aragonitic skeletons. Muir *et al.* (2015) shows that the lower dose of photosynthetically available radiation during winter in higher latitudes would severely constrain reef development. These authors therefore predicted a decline of coral reefs (Descombes *et al.* 2015; Muir *et al.* 2015). Climate change has occurred repeatedly in the geological past, and adaptation, migration, and extinction are major evolutionary consequences that can be derived from the fossil history of coral reefs (Pandolfi & Kiessling 2014). The Pleistocene, with its fluctuations between warmer (interglacial) and colder (glacial) periods at relatively short time scales and with species compositions largely identical to those of modern reefs, allow for a direct comparison with the present and could help predicting the response of reefs to current climate change. Especially the last interglacial episode (Eemian, MIS 5e, see below), when temperatures (McKay *et al.* 2011) and sea level (Siddall *et al.* 2007) were well above today's averages, is supposed to provide information on the behavior of coral reefs facing higher temperatures. Kiessling *et al.* (2012) have shown that reef corals moved towards higher latitudes in the Eemian, relative to today. Because this affected both the leading (the poleward range edges) and trailing edges (the equatorward range edges) of coral ranges, equatorial reefs declined in diversity.

1.1 Paleoenvironmental background of this study – The Pleistocene

The beginning of the Quaternary 2.58 Million years ago (Gibbard *et al.* 2010) marked the onset of dramatic global cooling and a strong cyclic fluctuation of relatively cold glacial and relatively warm interglacial episodes (Wefer & Berger 2000). With glaciations and deglaciations also the eustatic sea level fluctuated dramatically (Waelbroeck *et al.* 2002; Siddall *et al.* 2007), which led to a severe reduction in shelf areas during glacial episodes over the past 800,000 years at an approximately 100,000 year cycle with an amplitude of sea level of about 130 m. Before, the dominant period was of shorter duration and of smaller amplitude (Shackleton & Opdyke 1973; Lambeck *et al.* 2002). During the successive interglacials the global sea levels did not exceed their present positions by more than a few meters (Murray-Wallace 2002; Waelbroeck *et al.* 2002; Siddall *et al.* 2007). The Pleistocene and Holocene epochs are divided into marine oxygen-isotope stages (MIS) deduced from oxygen isotope data, reflecting changes in temperature derived from data from deep sea core samples. Working backwards from the present, which is MIS 1 in the scale, stages with even numbers have high levels of oxygen isotope ^{18}O (versus ^{16}O) and represent cold glacial periods, while the odd-numbered stages have low levels of ^{18}O and represent warm interglacial intervals (Cohen & Gibbard 2011, and see Figure 1.3.1). The stages are sometimes subdivided into substages when interglacials comprise several peaks of ^{18}O levels. MIS 5, which is the last interglacial before the LGM is subdivided into horizons, ordered alphabetically from *a* to *e*, with *a* being the youngest horizon. MIS 5e (128 - 116 ka BP) is the best known interglacial episode, often referred to as Eemian. MIS 5b and d represent sea level lowstands within that episode, while 5a and c represent highstands, but not reaching the maximum of 5e. Sea level was well below today's level in all 6 to 4 episodes, except for 5e, when global seal level was higher by 2 to 4 m as derived from fossil corals from a tectonically stable part of Western Australia (Stirling *et al.* 1998).

Glacial episodes are not well documented in coral reefs, because reefs from these times are usually submerged und far below today's sea level (Tager *et al.* 2010). Only a few studies directly studied submerged reef terraces from Hawaii, Australia, and the Caribbean (Macintyre 1972; Harris & Davies 1989; Lidz *et al.* 2003; Faichney *et al.* 2009, 2011), but none of them did it in a quantitative manner. However, via seismic and echo-sound techniques these studies provided evidence that reefs existed during glacial episodes and thus the reefs followed the glacioeustatic sea level fluctuations. Even in the Red Sea, Nir (1969) could document glacial reefs via echo-sound in up to 100 m depth. He identified two submerged terraces, one between 15 and 25 m, and one between 60 and 65 m. Both are interpreted as fringing reefs during a sea level lowstand. In 100-130 m depth a distinctive steepening of the slope can be observed at several locations along the coasts of Sinai, Sudan, Saudi Arabia, and the Gulf of Aqaba (Gvirtzman & Friedman 1977; Gvirtzman 1994). This breakpoint is interpreted as the lowest erosional base level during the last glacial maximum (LGM), (Gvirtzman & Friedman 1977), and is in accordance with other studies that estimate the glacioeustatic sea level during the LGM at 120-130 m below the recent sea level (Fairbanks 1989). The drowning of glacial reefs is the reason why Pleistocene reef corals are largely known from interglacial episodes, when ice melting associated with polar warming caused global sea levels to rise at around the level of today or even some meters higher (Lisiecki 2005; Jouzel *et al.* 2007; McKay *et al.* 2011). Paleoclimatic proxy data and modeling suggest that warming during the last interglacial (LIG) was more modest than suggested by temperature reconstructions from Arctic and Antarctic ice cores. The latter prove that the LIG temperatures exceeded modern temperatures by 4-5°C in these polar regions (Andersen *et al.* 2004; Jouzel *et al.* 2007), while compilations of faunal and geochemical proxy data suggest that global average temperatures were only 1.5°C warmer than today (Turney & Jones 2010). The average SST was only 0.7°C higher (McKay *et al.* 2011). Proxy data and climate models agree in suggesting very small temperature change in the tropics and stronger and more uniform warming at higher latitudes (Andersen *et al.* 2004; Turney & Jones 2010; McKay *et al.* 2011).

1.2 Ecology of coral reefs

Coral reefs are among the ecosystems with the highest biodiversity on this planet, probably even more than tropical rainforests (Spalding *et al.* 2001). Occupying less than one percent of the ocean floor, coral reefs are home to more than twenty-five percent of marine life (Spalding *et al.* 2001). Figure 1.1 (Veron *et al.* 2011) shows the global distribution of zooxanthellate reef coral diversity. The so-called 'Coral Triangle' that comprises the marine waters of East-Indonesia, Papua New Guinea, Philippines, Solomon Islands and Timor-Leste, contains at least 500 species of reef-building corals in each ecoregion (Veron *et al.* 2011) and is the well-defined Indo-Pacific centre of coral diversity.

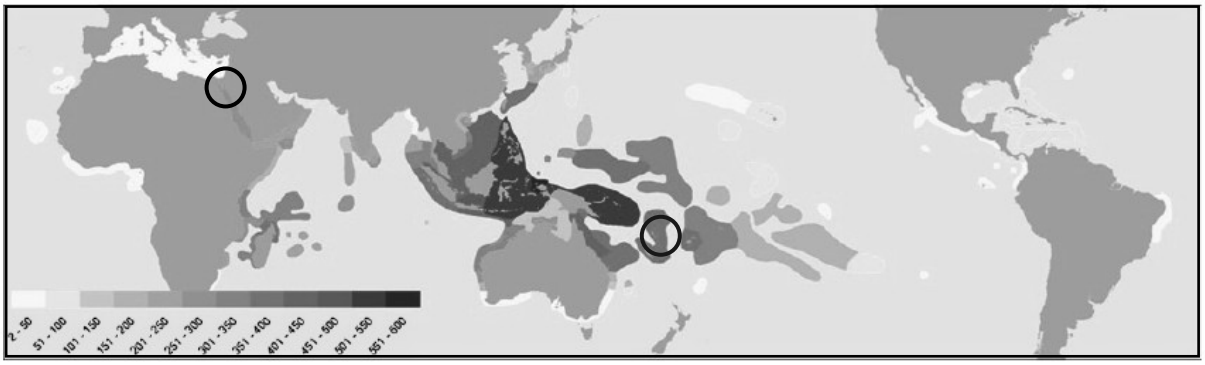

Figure 1.2.1: Global biodiversity of zooxanthellate corals. The colors indicate the total species richness in the different biogeographic regions (from Veron *et al.* 2011). The coral triangle comprises the darkest red zone. The black circles mark the field work areas Sinai (Egypt) and Vanuatu (see section 1.5).

In conjunction with changing SST diversity decreases latitudinally from there (Veron *et al.* 2011) northward to Japan, and southward along the west and east Australian coasts, respectively. Longitudinally, diversity decreases eastward across the Pacific. In the Indian Ocean, diversity is more uniformly distributed longitudinally. Diversity in the Atlantic is relatively depauperate and there is a deep evolutionary divergence between Atlantic and Indo-Pacific species (Fukami *et al.* 2004); there are no hermatypic species in common between the Atlantic and Indo-Pacific (Veron *et al.* 2011). High diversity is either a result of a high level of endemism or the overlap in the range of species with wide ranges (Veron 1995). Diversity in the coral triangle is created by the latter reason: with 605 species it amounts to 83% of all reef coral species living in the Indo-Pacific or 76% globally. The Red Sea/Arabian Sea with a total of 333 coral species has the highest endemism worldwide with 7.4% of the species being endemic (Veron *et al.* 2011). Patterns of endemism are created by isolation either because of geographic distance or geographic enclosure (Veron *et al.* 2011). The coral diversity in the central Red Sea is the highest for the western Indian Ocean (Spalding *et al.* 2001).

A highly biodiverse ecosystem is supposed to be more resilient to changing conditions and can better withstand disturbances (Naeem & Li 1997; DiMichele *et al.* 2004; Kiessling 2005). Resilience describes the ability of a system to absorb disturbances without fundamentally shifting to a different community state. *Hotspot* is a term frequently used to denote a relatively restricted geographic area containing exceptionally high levels of biodiversity and/or endemism (Mittermeier *et al.* 1998). Current hotspots of coral diversity occur in regions with the warmest SST, such as the coral triangle, the Maldives and the central Red Sea, because these regions served as refugia during cold periods of the Quaternary (Pellissier *et al.* 2014). The central Red Sea has the highest diversity in the western Indian Ocean (Spalding *et al.* 2001). Descombes *et al*. (2015) predict that these hotspots will also be the first to show a reduction in habitat suitability under warmer climate. These observations correspond with the conclusion that the Caribbean, with its not very diverse reefs, has the largest proportion of corals in high extinction risk categories, and the coral triangle with the warmest SST has the highest proportion of species in all categories of elevated extinction risk (Carpenter *et al.* 2008). Corals in oceanic islands of the Pacific generally have the lowest proportion of threatened species (Carpenter *et al.* 2008).

1.2.1 Types of coral reefs and reef zones

Three major types of coral reefs are usually recognized based on their large-scale reef morphology: fringing reefs, barrier reefs, and atolls (Darwin 1842). Barrier reefs are extensive linear reef complexes, separated from the shore by a lagoon. Atolls are roughly circular structures, surrounding a central lagoon with a presumed volcanic basement. This study examined fossil Pleistocene fringing reefs that are often preserved as distinct terraces along recent shorelines. Fringing reefs are simple in terms of their morphology (Kennedy & Woodroffe 2002). They consist of reefs that are close to the shore and often even shore-attached, usually forming a relatively thin veneer of seaward thickening carbonate sediments over the basement (Steers & Stoddart 1977) with three different reef zones: forereef (or slope), reef crest and backreef. However, the distinction between different reef types is not always unambiguous (Davis 1928; Kennedy & Woodroffe 2002), and so is also the terminology used in the literature.

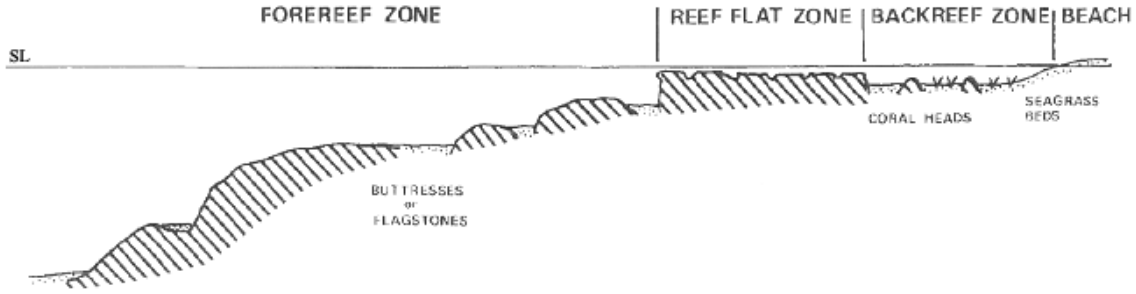

Figure 1.2.2 Typical reef zonation of a Red Sea fringing reef with a shallow backreef zone (not always present), an often wide reef flat zone, exposed at low tide, and a steep drop-off to the forereef zone (= slope). SL = Sea level (Dullo & Montaggioni 1998).

Various transitional forms of fringing reefs are distinguished on the basis of the existence of a deeper backreef channel (or backreef zone = 'boat channel') between the reef crest and the shoreline (Guilcher 1988). The simplest fringing reefs do not have a backreef channel. Here, the reef crest is attached to the shoreline. Sometimes, a small backreef channel occurs, which is only 1.5 deeper than the reef-flat surface, with minor sediment accumulation and scattered corals. These two types are widely distributed in the Red Sea region. Several grades of deeper and wider backreef channels occur in fringing reefs; the widest and deepest having lagoonal characters (Kennedy & Woodroffe 2002).

A greater distinction can be made between backreef areas composed of reef flats and those composed of backreef channels. Both are usually submerged at high tide, but often much of the reef flat landward of the crest is exposed at low water (Kennedy & Woodroffe 2002). Near-horizontal reef flats that dry at lowest tides are widespread in the Red Sea region. A real crest does not exist, instead the reef front forms a nearly vertical drop-off of 2-4 m height (Dullo & Montaggioni 1998). In Vanuatu the recent crest is directly attached to the shore and the slope begins immediately, but gently. Therefore extensive reef flats as in Egypt do not exist. In this study the terms reef crest and flat consequently used synonymously for very shallow and exposed flat/crest environments that are constructed differently in both regions. Fringing reefs will preferentially accrete vertically as long as there is accommodation space available (Kennedy & Woodroffe 2002). If either the reef has reached the sea surface, or due to a relative sea-level fall, or due to tectonic uplift it will prograde seaward.

The term "patch reef" is commonly used in this study to refer to comparatively small, isolated outcrops of coral reef. Patch reefs can occur in association with any of the main reef types, but a distinct zonation is missing.

1.3 Geology of coral reefs

Coral reefs are both biological and geological structures. The coral reef community lives only on the surface veneer of the reef, on top of dead skeletal material left behind by previous reef-builders. As such coral reefs provide the opportunity to study detailed time-series of ecological data in the form of variations in reef coral community structure during past episodes of environmental change, because they accumulate a vast thicknesses of biogenic sediments during their long lifetime. Carbonate production by reefs is supposed to play a major role in the global carbon cycle (Kleypas *et al.* 1999a; Gattuso & Buddemeier 2000; Suzuki & Kawahata 2003; Vecsei 2004) with one sixth of the carbonate produced annually in the oceans of the world (Langer *et al.* 1997). Most of the produced carbonate accumulates in situ, while the rest is washed into the oceans (Milliman 1993; Milliman & Droxler 1996). Sedimentologically, coral reefs represent the end products of processes such as construction, destruction and sediment deposition (Montaggioni & Braithwaite 2009). Construction occurs by reef builders, such as corals and coralline algae, green algae (*Halimeda*), molluscs and benthic foraminifera, destruction is caused by bioerosion and wave energy leading to sedimentation processes, and sediment deposition occurs through destruction within the reef or through transported material from adjacent areas.

Coral skeletons consist of aragonite, which is metastable and recrystallizes to calcite over time in the presence of water. The recrystallization of aragonite into calcite reconfigures the crystal lattice from a high energy state to a lower energy state so that the calcium carbonate mineral is no longer metastable (Vernon & Clarke 2008). Fossil corals may contain all grades of aragonite to calcite conversions, from being 100% aragonitic to being 100% recrystallized into calcite. Recrystallization is an indicator for diagenetic or alteration processes. The presence of water in especially humid tropical climates favors the alteration of aragonite.

The other important factor when studying fossil reefs is the role of tectonic activity and relative sea level. As mentioned above, sea level during interglacial periods has varied around today's sea level. A higher sea level during the LIG relative to the present one has left fossil coral reefs as distinct terraces between 0 and 10 m altitude accessible on land along tectonically stable shorelines. Nevertheless, there is debate as to the height reached by sea level during the LIG (e.g., Lambeck *et al.* 2011; Murray-Wallace & Woodroffe 2014). Recent studies emphasize that the elevation and age of the last interglacial shoreline varies geographically in response to isostatic adjustments to the distribution of former icesheets and water loads (Dutton & Lambeck 2012; Woodroffe & Webster 2014). There is, however, no doubt that tectonic uplift is responsible for terraces from outside the peak interglacials, such as MIS 5a and MIS 5c when sea level was below today's level, and also for older terraces at higher altitudes, such as MIS 7 and upwards. Nonetheless, tectonic uplift is nowhere fast enough to uplift glacial terraces. Coral reefs tend to respond to changing sea level in three ways: They either *keep-up*, growing at a rate approximating that of sea-level rise, or lag behind the sea surface but later, when sea level decelerates or is stable, *catch-up*. In some cases reef growth cannot be maintained and the reef is drowned (*give-up*) (Neumann & Macintyre 1985) as it occurred along many of the shelf margins of the Caribbean (Macintyre 1988). Tectonically, uplifted coral reefs are especially valuable for studies on Pleistocene reefs as they are usually dominated by keep-up reefs that follow the rising phase of sea level and therefore preserve long sequences of upward-growth. However, Cabioch *et al.* (2003) have shown that during very rapid eustatic rise as caused by meltwater pulses during the Holocene deglaciation reefs of Vanuatu switch from keep-up to catch-up responses. The combination of tectonic uplift and oscillating sea levels, results in younger reefs progressively onlapping over older reefs, generally at lower elevations, producing an inverted horizontal sequence of terraces. Along many active plate margins, there are sequences of successive highstands from a series of interglacials preserved as sequences of terraces (Woodroffe & Webster 2014). The locality in Vanuatu chosen for this study is situated in an highly active zone with an uplift rate of up to 1 mm/year and a series of terraces from Holocene to MIS 11 is preserved there (Lecolle *et al.* 1990). Although the interglacial record of reef corals extends through the entire Pleistocene, available coral data is dominated by those of the LIG (Kiessling *et al.* 2012), and especially to MIS 5e when the sea level was higher than the present sea level (Figure 1.3.1).

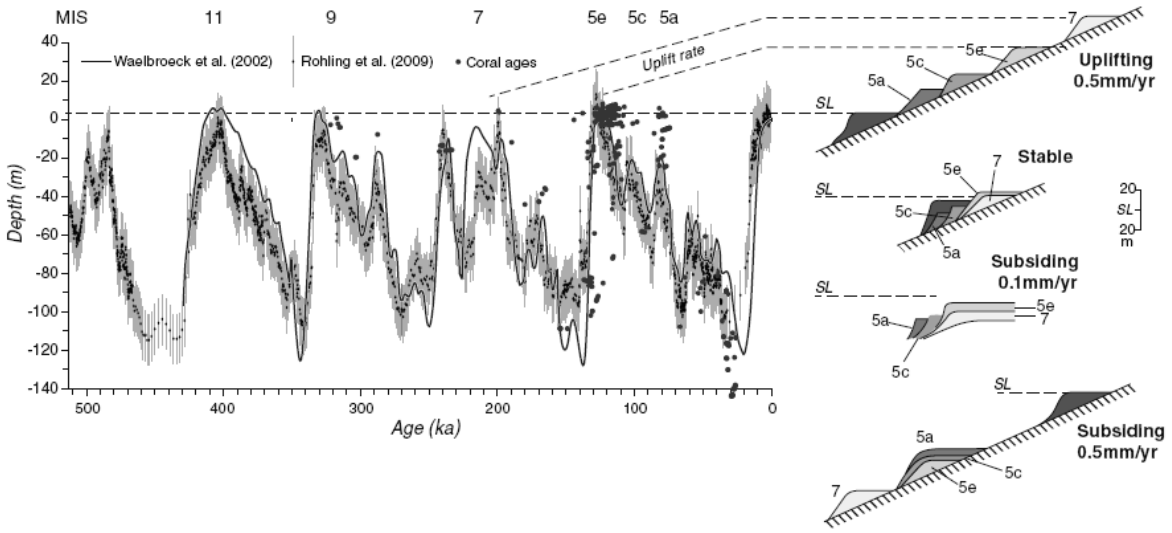

Figure 1.3.1: Reconstructions of sea level over the past 500 ka based on continuous records, compiled from the Red Sea by Rohling et al. (2009, 2012), modified by Waelbroeck et al. (2002). Points show the distribution of the most reliably dated corals for samples >25 ka (data from Medina-Elizalde 2013). Schematic representation of reef terraces on shorelines that have different histories of vertical movement are shown to the right with highstands identified representing marine oxygen isotope stage (MIS) 7 and substages 5e, 5c and 5a (from Woodroffe & Webster 2014).

Even within the Holocene there has been substantial geographical variation in sea level over the past 10 ka because the rate of glacio-eustatic change slowed with disappearance of most northern hemisphere ice sheets (Woodroffe & Webster 2014). In the Indo-Pacific, Holocene sea level rose at a rate of around 6 mm/year up to 6500 years BP, when it reached a level close to present (Chappell & Polach 1991; Chappell *et al.* 1998). There are hints that in the Indo-Pacific the sea level was even up to 1 m higher than during the mid-Holocene (Grossman *et al.* 1998) before levels fell again to its current position in the late Holocene. A Holocene terrace can sometimes be recognized at 0 - 1 m altitude across the Indo-Pacific (Pirazzoli *et al.* 1988; Lambeck *et al.* 2011). This may result in emergent Holocene reef flats, being responsible for relative extensive flats in some regions, such as along the Red Sea (Figure 1.3.2). Consequently, reef growth in the Indo-Pacific is concentrated on the slope, while the crests/flats are barren and well cemented (Dullo 2005). In the tropical Atlantic relative sea level is still rising in contrast to global ocean levels, which is caused by the siphoning effect (Mitrovica & Peltier 1991) that leads to flourishing reef flats and crests (Dullo 2005). At our study site

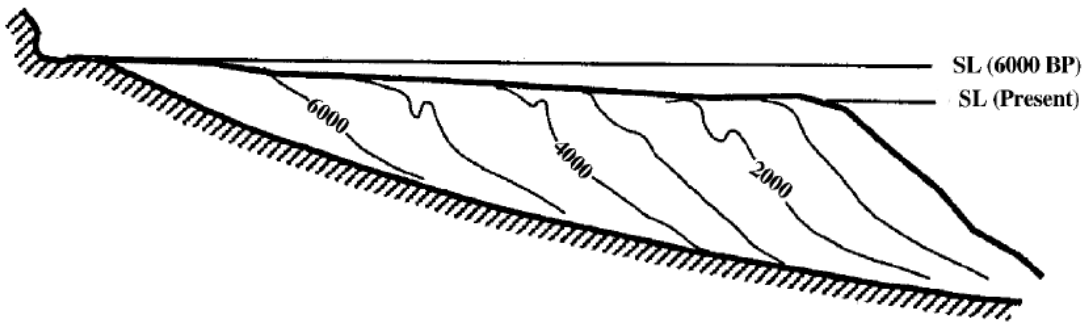

Figure 1.3.2: Fringing reef growth model of Chappell (1983), demonstrating the possible origination of emergent and extensive reef flats as preserved in the Red Sea.

Uplifted Holocene terraces in Vanuatu and other tectonically active plate margins are elevated well above sea level and occur between the MIS 5a reef and the recent reef as illustrated in the sketch of Figure 1.3, where an uplift of only half the rate is presumed. Also in Egypt a series of fossil reef terraces is preserved, but the role of tectonic uplift for the LIG and Holocene highstands are still debated (Lambeck *et al.* 2011). I will refer to this issue in chapter 5. Whereas the debate about the magnitude of Holocene sea level fluctuations has been constrained to within the order of a meter, it is perhaps not surprising that sea level during MIS 5e remains a subject of debate, with uncertainties of up to 3 m depending on author and locality (see Siddall *et al.* 2007 and Lambeck *et al.* 2011 for detailed discussions).

In conclusion, the exact morphology of reef terraces at any particular coast is dependent on the actual height that was attained by the sea at each of the highstand periods, the continuity of tectonic displacement, and the growth response of the reef during each highstand (Woodroffe & Webster 2014).

1.3.1 Ecological succession in fossil reefs (Mewis & Kiessling 2013)

One of the fossil reefs in Southern Sinai, Egypt, preserves a whole successional sequence and was therefore studied in more detail. The theory of ecological succession is a major theme in ecology and describes a process by which an ecological community changes orderly and predictably after disturbance or initial colonization of a new habitat, leading to a self-perpetuating condition (Ricklefs 1990). Ecological succession can be either allogenic, which means that extrinsic factors control community evolution, or autogenic, meaning that any shift in community composition is the result of species interactions. A large number of studies tested and verified ecological succession in fossil coral reefs: Most of these studies focused on Paleozoic reefs and came to the conclusion that fossil reef succession is largely autogenic (Alberstadt *et al.* 1974; Walker & Alberstadt 1975; Copper & Grawbarger 1978; Méndez-Bedia & Soto 1984; Martin *et al.* 1989). They also identified four successional stages to be generally present in fossil reefs: a stabilization stage, a colonization stage, a diversification stage and a domination stage. The first three stages record a gradual increase in biomass, diversity, and niche specialization through time, producing a stabilized highly integrated community. The change from diversification to domination stage is often abrupt (Walker & Alberstadt 1975). The first three stages are commonly interpreted as an autogenic succession whereas the domination zone, characterized by a few dominating species, may also be allogenic and driven by shallowing of the reef and the resulting physical and ecological consequences. Stable environmental conditions are a precondition for a fully developed autogenic succession (Copper 1988). This primary—climax zonation can be observed in short-term as well as in long-term successions, but long-term successions are driven primarily by orbital or geological rather than ecological processes (Karlson 1999). Three hypothetical models of successions have been proposed by Connell and Slatyer (1977), who emphasized the character of biological interactions in influencing the successional changes. The facilitation model is equivalent to the community-controlled succession defined by Walker and Alberstadt (1975). It posits that only a few species can colonize a particular site, and then modify the environment so that other species can start colonizing. The tolerance model suggests that later species are simply late arrivals or slowly growing species that are able to cope with the limitation of available resources left by the first arriving species. The inhibition model assumes that there are no faunal replacements until disturbance leads to an opening of the community. Most successional models are based on ancient fossil reef complexes, which differ in several aspects from modern coral reefs (Kiessling *et al.* 1999). Studies on Neogene and Quaternary reefs are therefore of special importance.

1.4 Previous studies of Pleistocene reefs

Pleistocene reef terraces have been subject to a number of studies with respect to sea level changes, microfacies, diagenesis, age, and faunal composition. The two best-studied uplifted sites with a series of reef terraces from different interglacials and representing the most detailed records

of the late Pleistocene are the Huon Peninsula, Papua New Guinea (Chappell 1974, 1986; Chappell *et al.* 1996; Ota & Chappell 1999; Yokoyama *et al.* 2001) and Barbados (Kenneth J. Mesolella 1970; Schellmann & Radtke 2004; Thompson & Goldstein 2005), largely referred to as 'Huon Peninsula Model' and 'Barbados Model'. These two models provide a level of stratigraphic discrimination in relation to Pleistocene sea level events that no other sequence worldwide has reached so far (Montaggioni & Braithwaite 2009). The few available studies on community ecology of Indo-Pacific Pleistocene reefs primarily concentrate on the Huon Peninsula (Pandolfi 1996, 1999; Pandolfi *et al.* 2006; Tager *et al.* 2010). Nine successive highstands investigated there display a clear constancy in species composition and diversity (Pandolfi 1996, 1999), and show a high similarity to equivalent modern reef zones (Nakamori *et al.* 1995) A larger number of studies analyzed the Pleistocene reefs preserved along the Caribbean coasts with regard to their community structure (e.g., Jackson 1992; Aronson & Precht 1997; Greenstein *et al.* 1998; Pandolfi 2001a, b; Pandolfi & Jackson 2001, 2006; Aronson *et al.* 2002; Pandolfi *et al.* 2002; Klaus & Budd 2003; Meyer *et al.* 2003). Caribbean coral reefs are well understood and recent paleoecological reconstructions in this region have highlighted the collapse of coral communities at the regional level, which is unprecedented within the Holocene (Greenstein *et al.* 1998; Aronson *et al.* 2002; Aronson & Precht 2008) and Pleistocene (Jackson 1992; Greenstein *et al.* 1998; Pandolfi 2001a; Pandolfi & Jackson 2006). Nevertheless, also during the Pliocene and early Pleistocene, Caribbean reefs reveal changes in numerical dominance and relative abundance of coral genera, also known as the *Plio-Pleistocene turnover*, and demonstrate that neither dominance nor taxon can be associated with persistence (Edmunds *et al.* 2014). Van Woesik *et al.* (2012) defined biological traits of coral species and processes, and could show a strong relationship between Plio-Pleistocene trajectories and modern vulnerability. The Plio-Pleistocene episodes of regional extinction are strongly related to the vulnerability of modern corals (van Woesik *et al.* 2012). That the Pleistocene reef corals from the Huon Peninsula show evidence of persistence and stability over broad time scales (Pandolfi 1996, 1999; Tager *et al.* 2010), which is confirmed by drill cores from the Great Barrier Reef (Webster & Davies 2003) is a striking discrepancy to the instability and vulnerability of living corals (e.g., Hoegh-Guldberg *et al.* 2007; Carpenter *et al.* 2008; Hoegh-Guldberg 2011) that also affects Indo-Pacific recent reefs, and challenge conventional ecological views of coral reefs as mainly disturbance-driven ecosystems with ephemeral species compositions (Karlson 1999) that are derived mainly from studies on restricted spatial and temporal scales (Pandolfi 2010). Pandolfi (2010) and other studies by the same author (Pandolfi 1999, 2002) emphasize that the spatial and temporal scale is important to assess variance and persistence.

The Pleistocene reef terraces of the Red Sea have been studied intensively with respect to sea level changes, microfacies, diagenesis, age, and faunal composition (Veeh & Giegengack 1970; Gvirtzman & Friedman 1977; Gvirtzman & Buchbinder 1978; Andres *et al.* 1988; Dullo 1990; Hoang & Taviani 1991; Brachert & Dullo 1991; Strasser *et al.* 1992; El Moursi *et al.* 1994; Gvirtzman 1994; Plaziat *et al.* 1995, 2008; Bosworth & Taviani 1996; Strasser & Strohmenger 1997; El-Asmar 1997; El-Sorogy 2002, 2008; Lambeck *et al.* 2011; Parker *et al.* 2012a; Mewis & Kiessling 2013; Kora *et al.* 2014). However, none of these studies ever quantitatively analyzed and compared the species compositions of the fossil reef communities preserved within the Pleistocene terraces with recent reef communities of the Red Sea, even though studies on living corals (Riegl & Piller 2003; Fine *et al.* 2013) highlight the role of the Red Sea as a refuge for corals for the future warming. Studies on fossil reefs of Vanuatu focused on postglacial reef growth, sea level reconstructions and tectonic implications only (Lecolle *et al.* 1990; Cabioch & Ayliffe 2001; Dickinson 2001; Neef & McCulloch 2001; Cabioch 2003; Cabioch *et al.* 2003, 2006; Wirrmann *et al.* 2011). Information on the species composition of Pleistocene reefs from Vanuatu do not exist at all.

1.5 Scope and structure of this study

As emphasized above, coral reef communities appear to be unstable over historical time scales. They appear as vulnerable and threatened structures that are in urgent need for management policies of conservation. However, on geological time scales, reefs reveal an astonishing stability (Jackson 1992; Pandolfi 1996; Tager *et al.* 2010), especially in the Indo-Pacific. Studies that analyze the relative abundance of species from fossil communities provide a rich resource from which the response of living assemblages to contemporary environmental change can be derived (Pandolfi & Kiessling 2014). The present study, therefore, aims to fill gaps of quantitative data for Indo-Pacific Pleistocene coral reefs. Two different localities were chosen for this project:
1) Vanuatu as a volcanic archipelago in the tropical southern Pacific at the eastern margin of the highly diverse Coral Sea, located directly south of the Coral Triangle with a high species diversity of about 300 recent reef coral species (Spalding *et al.* 2001), but a low endemism, far away from the continental ice shields, and
2) the subtropical Egyptian northern Red Sea with a lower total diversity of about 128 species, but a high endemism.

Specifically I want to test the following hypotheses:

1. If Indo-Pacific reefs display stability and persistence throughout the Pleistocene then the Pleistocene reef communities from Vanuatu should not reveal any significant differences between comparable reef zone communities from different interglacial periods.

2. The Pleistocene Red Sea reefs are expected to be more disturbed than the reefs from Vanuatu, because the water exchange between the Red Sea and the Indo-Pacific was largely restricted during glacial episodes, due to sea level lowstands.

3. Nevertheless, the northern Red Sea should show a higher diversity during the Eemian compared to today in case it was a suitable refuge during climate warming as suggested by several authors (Riegl & Piller 2003; Montaggioni 2005; Fine *et al.* 2013).

4. The Red Sea shore exhibits a minor uplift rate and reef sequences should reflect successional patterns. If an autogenic succession occurred, a successional replacement of species under stable environmental conditions should be observed. An allogenic succession should comprise temporary assemblages that interact with their physical environment, which eventually regulates coral species diversity.

In order to test these hypotheses, my study aims to

1. Provide new quantitative data from regions where no quantitative studies on Pleistocene reef communities have so far been performed. Vanuatu and Egypt are well known for their sequences of Pleistocene terraces, but abundance data of their species compositions are lacking.

2. Reconstruct the ecology of fossil communities based on the collected quantitative data. In both studies area fringing reefs are the predominant reef types.

3. Compare the fossil communities between Pleistocene and Holocene interglacial episodes (Vanuatu) and between Eemian and recent communities (Egypt).

4. Test for autogenic succession in a well-exposed Pleistocene reef complex near Dahab on the Sinai Peninsula (Egypt) that exhibits a distinct vertical zonation.

5. Compare tropical (Vanuatu) and subtropical (Egypt) Pleistocene reefs to each other and evaluate the results within a global context, especially regarding their presumed stability.

After presenting the material (data) and methods used in this study (chapter 2), I will provide a detailed taxonomy of the identified corals (chapter 3). Chapter 4 deals with Vanuatu, giving a more detailed introduction into the geology and geography of the island chain, present results of the analyses of the collected data from there, and discuss the results in the local context. Chapter 5 is similarly structured as chapter 4 and deals with the Egyptian study sites. Additionally, data from recent reefs taken from the literature are used to compare them against the last interglacial records. Finally, Chapter 6 puts the results from Egypt and Vanuatu into a global context, and into the current climate change debate about the future of coral reefs.

2. MATERIAL AND METHODS

2.1 Material

The quantitative coral data used in this study were collected in Vanuatu and Egypt mainly by myself. For the purpose of comparison literature data was used as denoted below. The data describes species or genus abundances, measured as number of specimens per sample. All data used in this study are provided in the Appendices and on the CD attached to this thesis. All GPS data used in this study that are marked in the maps in the respective studies are also listed in the Appendices. They were transferred into the Google Earth system that uses the Geographic Coordinate System (GCS) with WGS84 datum. Coordinates in maps and tables are given in degrees, minutes, and seconds (DMS). The altitudes provided by the GPS devices were unreliable the closer we were to sea level. The altitudes measured by the devices at the beach in Egypt range from -8 to 20 m, so that all altitudes provided in this thesis were own assessments in the field or corrected with the help of profiles, especially at the higher altitudes of Vanuatu. However, for the latter the information given by the GPS devices were largely consistent with constructed profiles.

2.1.1 Datasets from Vanuatu

Two datasets were generated from the field work in Vanuatu between 09/26/2008 and 10/03/2008. One consists of 1224 data points and contains all line transect data, whereas the second contains 610 data points from bulk samplings. The latter is limited to corals. Details on sampling protocols are detailed in chapter 2.3. The datasets from Vanuatu are listed in Appendix I.

2.1.2 Dataset from Egypt

One dataset was created from the field work in Egypt from 03/28/2009 to 04/19/2009, consisting of 2937 datapoints from line transects. The complete data is provided in Appendix II.

2.1.3 Literature data

Data of recent coral distributions in the Red Sea and adjacent regions was taken from the appendix of Sheppard & Sheppard (1991). Presence-absence data of coral species were summarized in the northern Red Sea, the central Red Sea, the southern Red Sea, the Arabian Sea, the Gulf of Oman, and the Persian Gulf. Additional data from other authors were also taken into account (Vaughan 1907; Burchard 1979, 1983; Scheer & Pillai 1983; Hoeksema 1989). All records marked with a question mark by Sheppard & Sheppard (1991) were excluded from the dataset, as well as most azooxanthellate corals, apart from those that occurred in Pleistocene data. Taxa with unclear taxonomic status that could not be synonymized were also eliminated from the dataset. The complete list can be seen in Appendix 2, with 0 = absence, 1 = presence. The Pleistocene data in this table consists of my observations (transformed to presence/absence data), with additional data provided by El-Sorogy (2002, 2008) and Kora *et al.* (2014). Other literature data of Pleistocene corals could not be used here because they could not be assigned to one of the regions of Sheppard & Sheppard (1991). El-Sorogy (2002, 2008) provides data exclusively from the northern Red Sea, namely the areas around Safaga and Hurghada. Data from Kora *et al.* (2014) provide data from Marsa Alam, which is located already relative close to the central Red Sea region as defined by Sheppard & Sheppard (1991). However, excluding the data provided by Kora *et al.* (2014) does not change the pattern resulting from the analyses. Data from the northern Red Sea provided by Sheppard & Sheppard (1991) were compared to data collected in the Gulf of Aqaba by Alter (2004) and completed if records were missing for the northern Red Sea in the Sheppard & Sheppard (1991) dataset. Single occurrences of one taxon within one geographic region (singletons) are excluded from this binary dataset because this only applies to Pleistocene occurrences from this dataset and most of these taxa still occur in the region today (Veron 2000), but have not been recorded by Sheppard & Sheppard (1991). They therefore cannot be used for a comparison at the regional level. In the context of diversity studies, singletons are usually ignored, because their presence might disturb the structure of the dataset (Legendre & Legendre 1998) and/or contain misleading artifactual

patterns (M. Pease 1985; Alroy 1998; Foote 2000). See chapter 5 for discussion of details on this topic.

The resulting dataset thus contains 78 coral taxa from the Pleistocene of the northern Red Sea. The dataset was analyzed with reduced sampling bias, excluding all species that have no occurrence in the Pleistocene. This leaves 66 (139) species from the recent Northern Red Sea, 71 (148) from the central Red Sea, 62 (112) from the southern Red Sea, 29 (45) from the Persian Gulf, 38 (69) from the Gulf of Oman, and 44 (82) from the Arabian Sea. The brackets show the original unbiased numbers. The number of collected specimens for the respective region is unfortunately not available, so that in the binary data set the number of species is also representing the number of the data points from each region. For reducing taxonomic biases, *Echinopora forskaliana* from this study were also counted as *Echinopora gemmacea*, because Sheppard & Sheppard (1991) most likely used them as synonym (see chapter 3).

For small-scale comparisons of the local Pleistocene data from Dahab and Ras Mohammed Alter (2004) provided recent data from a dive site at Dahab with 2845 specimens and 178 identified species. A table (Appendix II-III) was therefore created that combines the recent and fossil localities . Genera that contain many unidentified species in the Pleistocene data were combined to genus sp. in the recent dataset, in order to make the datasets more comparable. After omitting species with no Pleistocene record 2579 specimens distributed among 40 taxa (species and/or genera) remain in the Alter (2004) dataset.

2.1.4 Material sampled

The reference specimens collected from Vanuatu are housed in the Museum für Naturkunde in Berlin, Germany. The reference specimens collected in Egypt are currently housed in the Red Sea Environmental Centre in Dahab, Egypt. Due to bureaucratic difficulties and later political revolutions it was impossible to export the samples to Germany, despite valid permission and a lot of effort and time invested in that issue. Nevertheless, the collected specimens were examined and documented using photographs during a second trip to Dahab in November 2011.

2.1.5 Pictures and Figures

All photos were taken by myself, unless noted otherwise with the name of the photographer. The scale bar in all plates of Chapter 3 is 10 mm, unless noted otherwise. Maps were generated using Google Maps and Google Earth, unless noted otherwise. Figures taken from other sources are noted as such in the respective legend. Most of the figures in the results sections were created with R version 3.1.1. (2014), and sometimes modified with Adobe Illustrator CS2. All other figures and plates were edited or created with the help Adobe Illustrator CS2 and/or Adobe Photoshop CS2.

2.2 Methods

2.2.1 Taxonomic Methods

The quantitative analyses were at species level if possible. However, not all corals could be identified to species level, largely due to poor preservation. In cases of doubt qualifiers such as "cf.", "aff." and "?" were added or the specimens were only identified to genus level. This leads to an underestimation of species diversity, especially in *Acropora* spp. and *Porites* spp. Specimens that could not be identified to genus level were excluded from the quantitative analyses. The respective data points were only included in the total coral coverage analyses.

Species identification was primarily based on Scheer and Pillai (1983), Sheppard and Sheppard (1991), and Veron (2000) applying the species concepts of Veron (2000), with additions from recent studies on the evolutionary relationships among corals (Fukami *et al.* 2008; Kitahara *et al.* 2010; Huang *et al.* 2011, 2014b; Budd *et al.* 2012; Kitano *et al.* 2014). The World Register of Marine Species (WoRMS Editorial Board 2015) was used to confirm valid names and provided the synonymy lists. Gross identification was already performed in the field, but refined in the laboratory via both close-up pictures of samples that could not be brought to Germany (Egyptian samples), as well as samples exported to and studied in Berlin (Vanuatu data).

2.2.2 Terminology

Identification of fossil corals is traditionally based on skeletal characters. Most scleractinian corals in this study are zooxanthellate, colonial and hermatypic, unless noted otherwise. The identification of the growth form is often less clear in fossil than in recent reefs, because fossil preservation of corals is often fragmentary. Nevertheless, it is mostly possible to infer from the preserved remains to the overall form.

The skeleton of an individual polyp is the corallite, a tube that contains vertical plates radiating from the centre. The tube itself is the corallite wall and the plates are the septo-costae, with septa being the same structure inside the corallite wall and costae outside the wall. The tubes are joined together by horizontal plates and other structures, collectively called the coenosteum. In most corals, the septa are of different lengths and have a cyclical symmetry. They are usually in cycles with 6 septa in the 1st cycle, 6 in the 2nd cycle, 12 in the 3rd, 24 in the 4th and so-on. In reality, this cyclical arrangement is often unclear. The genus *Porites* has a unique septal plan, which is used extensively in taxonomy for the identification of species (Veron 2000).

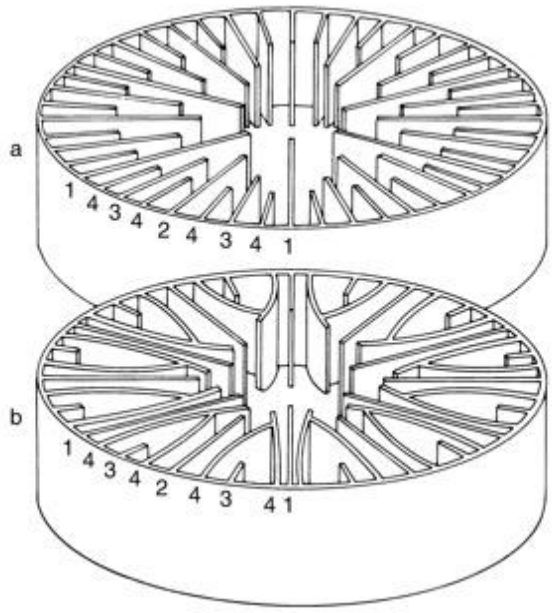

Figure 2.2.1: Septa arrangement of Hexacorallia, illustrating the different orders. (a) Normal cycles of septa, (b) pourtàles plan (septa of the 4th cycle curve in front of those of the 3rd cycle and fuse). Numbers indicate cycles. Figure taken from Veron (2000).

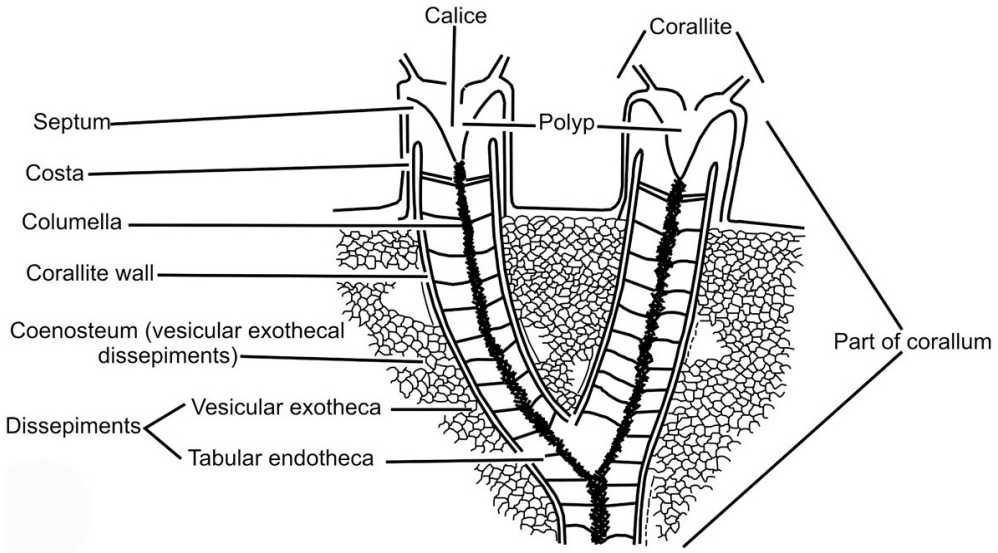

Figure 2.2.2 (from Budd *et al.* 2010): Traditional morphological features used in scleractinian classification. Drawing from Wells (1956, p. F336, *Treatise on Invertebrate Paleontology*), illustrating several primary skeletal architectural features (corallite, septum, costa, columella, wall, coenosteum, dissepiments).

Terms frequently used for coral identification

Skeletal components:

Corallite: Skeleton of the individual polyp.

Calice: The upper surface of a corallite (usually a cavity) bounded by the wall.

Coenosteum: Sponge-like skeletal matrix. In general, the coenosteum is located between the walls of adjacent corallites.

Septo-costae: Divided by the wall into two components:
1. Septa - inside the corallite
2. Costae - outside the wall (in the coenosteum).

Septal teeth: Sharp tooth-like or lobed structures along the margins of septa.

Columella: The inner margins of the septa of most families usually have inward-projecting teeth , which intertwine and form a tangle. This tangle is of different shape in different taxa.

Paliform lobes: Pillar-like projections on the inner margin of some or all of the septa, often forming a neat crown around the columella.

Colony growth forms

Massive: Solid and similar in shape in all dimensions.

Encrusting: Adhering to substrate.

Branching: Forming branches of various kinds.

Plate-like/laminar: The colonies are primarily two-dimensional and solid. They may be partly or wholly attached to the substrate, but are not encrusting and do not closely follow the contours of the substrate.

Columnar: Colony forms dominating columns.

Foliose: Colonies have leaf-like fronds or consist of thin sheets that are not encrusting.

Corallite growth forms

Intratentacular budding: Parent polyp divides itself into two or more daughter polyps.

Extratentacular budding: Daughter corallites grow on the side of the parent colony.

Cerioid: Massive colonies with corallites sharing common walls.

Plocoid: Colonies have corallites with distinct walls separated by the coenosteum.

Phaceloid: Colonies with corallites adjoined only toward their bases.

Meandroid: Colonies with corallites aligned in valleys separated by ridges; adjacent valleys share the same ridge.

Flabello-meandroid: Corallites are meandroid, but have their own walls, which are not connected and only share a common base.

Petaloid: Corals in which finely textured skeletal material envelops a number of septo-costae, so that they appear as a flower-like structure.

A common modification of all descriptive terms is the addition of the prefix sub to the term (e.g. submassive, subcerioid, sub-equal), meaning ‘less than’ or ‘not quite’. Other, more particular terms used for describing coral morphology are explained when used in Chapter 3.

2.2.3 Sampling design

Two regions were chosen for field work: The South Pacific and the northern Red Sea. Both are located in tectonically active zones with exposed emerged reef terraces. Also, both are characterized by a relatively high coral diversity. While Vanuatu is placed within the tropical latitudes, the northern Red Sea is situated in the subtropics. These two areas give us the opportunity to directly study similarities or dissimilarities of coral reef communities with regard to climate change at different latitudes. Field work was performed by Prof. Dr. Wolfgang Kießling (supervisor), Julien Millet (second PhD student) and myself. In Vanuatu we were temporarily accompanied by students from the University of the South Pacific and members of the Department of Environment and

Conservation belonging to the Ministry of Land's and Natural Resources, Vanuatu. In Egypt, we were temporarily accompanied by Christian Alter and Nina Milton from the Red Sea Environmental Centre in Dahab, Dr. Georg Heiß, Prof. Dr. Moshira Hassan and some of her students from the American University in Cairo.

Our sampling was confined to suitable outcrops, which were very limited in the densely vegetated Vanuatu. Sampling sought to characterize coral communities during a single reef-building episode over spatial and environmental scales. As such, data from one site represent data from one reef building episode. The Pleistocene reefs in Vanuatu and Egypt, as elsewhere, consist of in situ reef framework and transported accumulations of reef debris (Hubbard 1997). The framework includes corals in life position, as well as corals toppled by bioerosion and storms that were not transported far from their location of growth and death. In contrast, large accumulations of fragmented coral debris occur as strand lines due to storms (Woodley *et al.* 1981), and are identifiable by independent sedimentological criteria (Blanchon *et al.* 1997). Sampling of obviously transported reef debris was avoided.

Two different sampling techniques were applied in Vanuatu, even though only one was originally planned: Point intercept transects (PIT), which measure objects at specific intervals either below the transect tape, or below and to the side of the transect tape. With sufficient points they can provide comparable information to LIT (Hill & Wilkinson 2004). The PIT method is a linear method similar to the Line intercept transect (LIT) method (Loya 1972; English *et al.* 1997), with the difference that the reef facies is recorded only at fixed intervals along the transect without recording any length measurements (Dodge *et al.* 1982; Hill & Wilkinson 2004). In this study the interval of 10 cm was used. Facon *et al.* (2016) have shown that with this short interval and a high identification level, the PIT 10 method is, next to the LIT method, the most suitable method to gain data that allow for proper statistical analyses, but the LIT method is much more time consuming. Segal & Castro (2001) came to the similar conclusion that PIT is an adequate methodology to detect differences among sites, but that LIT should be preferred when investigations concentrate on coral colonies, such as for bleaching and disease studies. Since the focus of this study is on differences among sites, the PIT method was deemed the most effective method for the study of fossil reefs.

Transects had a length of 15 m if possible. However, depending on the outcrop situation, also shorter transects were taken, in order to gain data at all. Transects were always as long as possible and always within the same facies of one site. The number of transects depends on the size of the site. The distance between transects was at least 50 cm. All faunal and lithological constituents that intercepted the points on the transects were recorded, including sediment, calcareous algae, mollusks, and corals. Our censuses differ from a transect on a living reef, where data would also be obtained on the relative abundance of soft-bodied organisms. Corals were identified to the lowest possible taxonomic level in the field, and samples collected for later in-depth identifications. All other reef dwellers, and especially the molluscs, were the subject of another thesis and therefore left out of my own study. The goal was to provide an extensive and comprehensive view on the ecology of Pleistocene reef communities from Egypt and Vanuatu from different perspectives. As such, in this present study the non-coral transect data was only used to calculate the coral coverage of each transect/site, and otherwise ignored.

The PIT method was always applied in Egypt, but did not deliver sufficient data in Vanuatu. For the latter bulk sampling supplemented the transect data. The bulk sampling method is a common method for geological/mineralogical samples. In a small area of maximally 25-30 m^2 all coral samples, independent of taxonomy or preservation, were collected or counted within a short time. This method allowed us to gain an overview of the community composition even in outcrops that are only partly accessible. However, this method is neither linear nor standardized as the PIT method, such that the resulting dataset was analyzed separately with the same methods and compared to the transect data from same sites.

2.2.4 Data analyses

Data were analyzed using R version 3.1.1 (2014), and the vegan 2.2-0 package (Oksanen *et al.* 2014). Package 'ca' (Nenadic & Greenacre 2007) was used for correspondence analyses. Package 'stats' (R Core Team 2014) was used to calculate correlation coefficients and other standard statistical metrics. Package 'Hmisc' (Harrell *et al.* 2015) was used for one plotting.

2.2.4.1 General statistical methods

All transect data was used to calculate the coral coverage within transects, terraces and/or sites. For this purpose gaps caused by soil, vegetation or gravel in the transect raw data were excluded and the proportion of corals (including *Millepora*) in relation to matrix and non-corals was calculated and are given as percentages. For all sites the mean coral coverage from the transect data and the respective standard deviation (SD) are given.

A correlation of age and calcite content of samples from Vanuatu was performed using the nonparametric Spearman rank correlation coefficient (ρ) using the `cor.test()` function in R with the parameter `method="spearman"`.

2.2.4.2 Subsampling and standardization

The recent species richness differs distinctively from that of Pleistocene reefs. Kiessling *et al.* (2012) compared pantropical data from last interglacial (LIG) and recent reefs. The latter contain information on 730 species, while the LIG data contains only 269 species. Kiessling *et al.* (2012) showed a significant correlation between per-species occurrence counts now and then. The less common a species is today, the less probable is its occurrence in the LIG. As such, it can be concluded that the probability of being preserved further declines with even older interglacials (MIS 7 and 9) in the Vanuatu data. Much of the resulting differences in diversity are likely due to taphonomic biases, because Pleistocene corals are usually sampled from outcrops, where they are exposed to weathering and diagenetic alteration. Kiessling *et al.* (2012) have shown that downgrading recent coral data to Pleistocene levels does not influence the results in comparison to the recent raw data, but makes them more comparable to the LIG data. Consequently this method was applied to the recent datasets of this study, which were downgraded to Pleistocene occurrences before being compared to each other. Some taxa that are hardly distinguishable at species level in fossil material are reduced to their genus levels when being compared. Diversity results of downgraded (sampling and taphonomic bias reduced) datasets were compared to the results of the studies from which the data were taken to ensure that the resulting downgraded dataset still gives a reliable picture. Especially *Acropora* as a highly diverse recent genus is underrepresented in the fossil record, due to its delicate morphological structures. When comparing terraces of older ages to each other, the analyses were repeated with a preservation-standardized dataset that excludes *Acropora* and other fragile taxa to further reduce taphonomic bias. All fragile, branching and solitary taxa were excluded from that preservation-standardized dataset: *Acropora* spp., *Alveopora* spp., *Fungia* spp., *Millepora* spp., *Pavona cactus*, *Pavona varians*, *Pocillopora* spp., *Sandalolitha* spp., *Seriatropora hystrix*, *Stylophora* spp., *Tubipora musica*. Thus, this dataset contains only massive taxa.

All datasets have been compared using specimen-based rarefaction (Raup 1975). Rarefaction allows the calculation of species richness for a given number of individual samples, based on the construction of so-called rarefaction curves. This curve is a plot of the number of species as a function of the number of samples. The problem when sampling species in a community is that the larger the number of specimens sampled, the more species will be found. Rarefaction curves are created by randomly re-sampling the pool of *N* samples multiple times and then plotting the average number of species found in each sample (1,2, ... N). A rarified species number thus generates the expected number of species in a small collection of *n* individuals (or *n* samples) drawn at random from the large pool of *N* samples (Gotelli & Colwell 2001). This number allows the comparison of species richness in a comparable pool of samples. Rarefaction curves generally grow rapidly at first, because this is when the most common species are found, but the curves flatten when only the

rarest species remain to be sampled. As such, the trend of the curve already gives an evaluation of the goodness of sampling a certain assemblage.

Additionally, the datasets were subsampled and compared applying the Shareholder quorum subsampling method (Alroy 2010a), in the following referred to as SQS. It samples the occurrence frequency distribution to a pre-specified level of coverage (= the quorum) rather than imposing uniform sampling. As such it avoids the dampening of genuine fluctuations in diversity that characterize analyses using classical rarefaction (Alroy 2010a, b). The quorum should be higher than 0.4 and lower than 1. I decided to use a quorum of 0.7, but results for all quorum levels will be displayed graphically. I used the SQS R function version 3.3 available on John Alroy's website (Alroy 2011).

Datasets were submitted to Wisconsin double standardization prior to creating distance matrices. In this method, the abundance values are first standardized by species maximum standardizations, and then by sample total standardization. Bray & Curtis (1957) used this method for ordination purposes and achieved a more uniform basis for comparison than with simpler standardization methods. If the range value is too large, vegan automatically square root transforms the data before submitting it to Wisconsin double standardization for ordination purposes. This combination of the two standardizations often improves the quality of an ordination (Oksanen 2015).

2.2.4.3 Diversity metrics

Species richness is always an underestimation, because many species will remain unseen in a collection (Palmer 1990; Colwell & Coddington 1994). To estimate the number of unseen species I used the abundance-based coverage (ACE) diversity estimator (Chao & Lee 1992; Chao & Yang 1993) in the vegan package using `estimateR()`. This method uses an estimator when all species are equally probable, and then adds a correction based on the variance of the distribution (Bunge & Fitzpatrick 1993). O'Hara (2005) compared different species richness estimators and found that ACE seems to be an underestimate, so that it can only provide lower limits of species richness. However, none of the other estimators delivered reliable results (O'Hara 2005), and knowing the lower bounds of the expected species richness is sufficient for the purpose of this study. ACE values are given with their respective standard errors (SE). It considers the value of SD as well as sample size. As such, the SE gets smaller when samples get larger.

Additionally to the subsampling methods described above, which compare the species richness of different sites, diversity can also be described using the Shannon Wiener Index (H):

$$H = -\sum_{i=1}^{S} p_i ln\, p_i$$

with p_i = proportion of individuals belonging to the i_{th} species (S). The evenness (J) of the community was calculated as: J = H/ln S, where S = number of species in the community.

To gain a better understanding of the distribution and complexity of the coral communities we used the logarithms of species abundances to assess rank-abundance distributions (RADs). RAD plots (Whittaker 1965) display logarithmic species abundances against species rank order. These plots are supposed to be effective in analyzing types of abundance distributions in communities. The function `radfit()` in vegan fits some of the most popular models: The null model (or "Broken Stick", MacArthur 1957), the pre-emption model (or geometric series, Motomura 1932), the Zipf model (Zipf 1949), the Zipf-Mandelbrot model (Mandelbrot 1977, 1982), and the log-normal model (Preston 1948; McGill *et al.* 2007). The null model represents the most complex community structure with the highest evenness, whereas the pre-emption model is the simplest community structure with the lowest evenness. In the latter model each species pre-empts a constant fraction of the same space (May 1975), and would thus expected to be found in pioneer or frequently disturbed communities. The Zipf and Zipf-Mandelbrot models are closely related and both presume that the presence of a species can be seen as dependant on previous physical conditions and previous species occurrences. They are assumed to represent a successional process where colonists that arrive later

are more specialized than the pioneer species and are therefore rarer (Gray 1987). Log-Normal and Zipf models are generalized linear models (glm) with a logarithmic link function. Zipf-Mandelbrot adds one nonlinear parameter to the Zipf model, and is fitted using nonlinear models (Oksanen *et al.* 2014). The log-normal model describes the most common distribution in Mesozoic-Cenozoic marine communities (Wagner *et al.* 2006) and is typical for mature communities with moderate complexity (McGill *et al.* 2007). It is a continuous probability distribution of a random variable whose logarithm is normally distributed. We would expect log-normal or Broken Stick models in very even and well established communities. In contrast to the log-normal model, the Broken Stick model represents a group of species of almost equal abilities competing for the same niche space (Tokeshi 1993).

The Akaike information criterion (AIC) was used to obtain the best model fit: AIC = 2k – 2ln(L), with k = number of parameters, and L = maximized value of the likelihood function for the estimated model (Akaike 1974).

2.2.4.4 Ecological metrics

Communities were compared using the Bray-Curtis (BC) dissimilarity index (d^{BCD}, (Bray & Curtis 1957), which has been shown to be one of the most robust coefficients for the analysis of taxonomic composition data (Faith *et al.* 1987):

$$d^{BCD}(i,j) = \frac{\sum_{k=0}^{n-1} \left| y_{i,k} - y_{j,k} \right|}{\sum_{k=0}^{n-1} \left(y_{i,k} + y_{j,k} \right)}$$

with i, j = the objects that are compared, k = index of a variable, and n = total number of variables y.

Ordinations were used to display a visual summary of the pattern of BC dissimilarities among the samples. The technique employed in this study was global non-metric multidimensional scaling (NMDS, Kruskal 1964), which has been shown to be one of the most effective methods available for the ordination of taxonomic composition data (Kenkel & Orloci 1986; Minchin 1987), and because it makes no assumptions about the underlying distribution of the data (Kiessling *et al.* 2011). NMDS, function `metaMDS` in vegan, represents each sample as a point in a coordinate space with a given number of dimensions, such that the distances between each pair of points are, as far as possible, in rank order with the corresponding dissimilarities in taxonomic composition. The degree to which the distances depart from a perfect rank order fit is measured by a quantity known as "stress" and the ordination with minimum stress is found by a successive improvement algorithm. NMDS was applied to the same matrix of BC values, which was used in the ANOSIM tests. NMDS ordinations were computed in two dimensions, which was sufficient based on the stress value. For comparison a detrended correspondence analysis (DCA) was performed, which is a method widely used to identify main factors of gradients in large, but species-poor datasets. DCA is the further development of classical correspondence analysis correcting for biases such as the arch effect (Hill & Gauch 1980). However, DCA can still produce stronger distortions than NMDS and most ecologists have embraced NMDS as the method of choice (e.g., Edinger *et al.* 2001; Pandolfi & Jackson 2001; Pandolfi 2002; Benzoni *et al.* 2003; Greenstein & Pandolfi 2008; Kiessling *et al.* 2011). DCA differs from NMDS in that it is seeking eigenvectors to explain as much of the overall variance as possible instead of projecting quantitative distance metrics between multiple variables on a (in this study) two dimensional plot. DCA results of my data are however relatively similar to NMDS results, and thus DCA was not further used in this study.

Dissimilarities were also investigated using hierarchical clustering with the Ward's method (Ward Jr. 1963). It attempts to form clusters keeping the variances within the clusters as small as possible. Ward's method is based on the linear model criterion of least squares. Although the computation of within-group sums of squares (SS) is based on a Euclidean model, the Ward method produces meaningful results from distances that are Euclidean or not (Borcard *et al.* 2011), and as such is also based on the BC matrix here.

Whittaker (1960) divided diversity into several components. The best known are diversity in one spot (α-diversity) and the diversity along gradients (β-diversity). The basic diversity indices are indices of alpha diversity. Almost everybody understands β-diversity as a measure of general heterogeneity (Tuomisto 2010a, b), i.e. how many more species are in a collection of sites compared to an average site. Beta diversity can, however, also be measured directly using dissimilarity indices. Dissimilarities were computed based on presence-absence data as well as abundance data. For presence-absence data I used the Sørensen similarity (S_S, Sørensen 1948) : $S_S = 2a/(2a + b + c)$, where a = number of species common to both sites, b = number of species unique to the first site, and c = number of species unique to the second site. It can be simply calculated for all sites in vegan with binary data using the command `1-vegdist(data, binary=TRUE)`.

I applied several β-diversity indices using the function `betadiver`() for abundance data (Koleff *et al.* 2003). This study uses the Arrhenius species–area model $S = kX^z$, where X is the area (size, here represented by the number of samples) of the patch or site, and c and z are parameters (Arrhenius 1921). Parameter z gives the steepness of the species area curve and is a measure of β-diversity. It is commonly regarded that $z \approx 0.3$ implies random sampling variability, and only higher values mean real systematic differences (Oksanen 2015). Function `betadisper()` was used to analyze beta diversity with respect to ecological and geographical groups (Anderson 2006; Anderson *et al.* 2006). This study uses `adonis()`, a multivariate ANOVA based on dissimilarities that is directly analogous to MANOVA (multivariate analysis of variance), but nonparametric - a "permutational MANOVA" (Anderson 2001; McArdle & Anderson 2001). Function `adonis()` partitions dissimilarities for the sources of variation, and uses permutation tests to inspect the significances of those partitions. Adonis is used here to study beta diversity between ecological and geographical or spatial groups in the respective data. It uses the β-diversity z of the Arrhenius model. Adonis is supposed to be more robust than other methods like ANOSIM (Clarke 1993), function `anosim()` in vegan, which was also performed in order to test the significance of taxonomic differences with regard to reef environment and site. ANOSIM uses the BC dissimilarity matrix instead of a β-diversity index, but only the rank order of the matrix values and not the BC index directly (Pandolfi & Jackson 2001). Additionally, geographical and environmental groups were submitted to the analysis of multivariate homogeneity of group dispersions (ANOVA, function `betadisper()` in vegan). While the function `adonis()` is analogous to multivariate analysis of variance and calculates the differences in the group means, the function `betadisper()` calculates the differences in group homogeneities and is the multivariate analogue of Levene's test of the equality of variances (Levene 1960; Oksanen 2015).

The significance of group variability in the latter model, a standard parametric ANOVA of the distances to the spatial medians as group centroids was performed. Additionally a permutation test was carried out, which gives a simple way to compute the sampling distribution for any test statistic, under the strong null hypothesis of no dispersion between groups. A third test, the Tukey's honest significant difference test (Tukey's HSD) was conducted to find means that are significantly different from each other. This test compares all possible pairs of means, and is based on a studentized range distribution, which is the difference between the largest and smallest data in a sample measured in units of sample standard deviations. Tukey's HSD test is considered to be the best when sample sizes are not equal, which is the case in this study.

2.3 X-Ray diffractometry

Prior to dating it is important to know about the diagenetic alteration of corals, which is approximated by the proportion of calcite in the aragonitic skeleton. Candidate corals of each locality were analyzed using X-ray powder diffraction. In comparison to other methods of X-ray diffraction analysis, powder diffraction allows for rapid, almost non-destructive analysis of multi-component mixtures without the need for extensive sample preparation (Cullity 1956). In order to get an average picture of the composition of each sample, very small fragments from different part of the samples were scraped off before being reduced to powder (silt size) in a mortar. A small amount covering the tip of a spatula was then glued to a special foil.

The STOE & CIE STADI P diffractometer at the Museum für Naturkunde Berlin was run at 40kV and 40mA for the analysis, which was supervised by Prof. Dr. Thomas Kenkmann (now at Albert-Ludwigs-University Freiburg). The results were interpreted with the WinXPOW software. X-rays are generated in an X-ray tube with copper anode. Diffraction occurs as waves interact with a regular structure whose repeat distance is about the same as the wavelength. X-rays have wavelengths on the order of a few angstroms, the same as typical interatomic distances in crystalline solids (Cullity 1956). The resulting data are presented as a diffractogram in which the X-ray intensity is recorded as a function of the measured angle of diffraction 2θ. All diffraction patterns were prepared as step-scans with the following parameters: a starting 2θ (10-20°) angle, a step size (0.5 or 1 degree), a step time (100-180s), and an ending 2θ angle (70-80°). The X-ray diffraction itself allows for qualitative results only. To get quantitative information, which is important especially for the U-Th dating, it is necessary to compare the obtained diffractograms with reference diffractograms. Therefore one sample of pure aragonite (a) and one of pure calcite (c) where crushed and treated with the same methods as for the samples described above, and then weighted and mixed to obtain six additional samples: 1-100%a, 2-100%c, 3-50%a50%c, 4-80%a 20%c, 5-90%a10%c, 6-98%a2%c. These were then compared to our samples. Preferentially samples of massive *Porites* were used, but if not available, faviid corals were also suitable for the analysis as previously shown by Pirazolli *et al.* (2004).

2.4 Age dating

Electro Spin Resonance (ESR) dating belongs to the group of radiation-induced dating methods (e.g. luminescence) and has been applied in earth sciences and archaeology since Ikeya (1975) presented this method on stalactites. The method has since been further improved and is now comparable to radiocarbon (C^{14}) dating results (Radtke *et al.* 2003), and to the mass spectrometric ^{230}Thorium/^{234}Uranium (Th/U) dating (Schellmann & Radtke 2001, 2004; Schellmann *et al.* 2004). Nevertheless, Schellmann *et al.* (2004) have shown that when comparing corals from MIS 5 many ESR data are systematically 5% to 10% younger than the corresponding U/Th dating results. One of the reasons might be the post-depositional recrystallization of the aragonitic coral structure (Schellmann & Radtke 2004). However, the C^{14} and the U/Th method are strongly limited by age and recrystallization status. In contrast to the U/Th method, the ESR method is less vulnerable to recrystallization and allows a dating as far back as 500–600 ka (Pirazzoli *et al.* 1991; Schellmann & Radtke 2001), and was thus considered as the appropriate method for dating the older reef terraces preserved in Vanuatu. ESR dating is based on the measurement of the number of paramagnetic centers in a mineral. These centers are generated by alpha-, beta-, and gamma-radiation of the natural radioelements such as U, Th, and K. This radiation causes charge to be trapped at defects in the crystal lattice of minerals, such as aragonite and calcite. The amount of trapped charge accumulation increases over time and can be quantified by the ESR dating method, which then gives a date of the burial time of sedimentation. An ESR-age is a function of the radiation rate and the atomic lattice defects which have been produced by radiation over time and in which unpaired 'free' electrons are trapped. The ESR-signal intensity is proportional to the concentration of trapped electrons in the mineral. However this defect concentration does not yet tell anything about the age

unless it is put into relation to the radiation doses. Two parameters have to be determined: the equivalent or accumulated dose ($D_{e,}$ derived from the ESR-signal) and the annual dose rate (D_o) derived from cosmic rays and radionuclides in the vicinity of the sample (Schellmann *et al.* 2008). The annual (cosmic) dose rate is directly related to the depth in which the sample was buried, latitude and elevation, and which is therefore being considered for the interpretation of the results. The surrounding radioactivity can be calculated by the determination of the Uranium content of a sample. In aragontic material such as corals, the internal dose rate is caused almost completely by Uranium, which corals absorb from seawater during their lifetime or shortly after death and of which corals usually have a high content (Schellmann *et al.* 2008). The equivalent dose is calibrated by the construction of so-called growth curves. The sample is artificially irradiated and is thus made artificially older. The calculation can be summed up with the following equation (Schellmann *et al.* 2008):

$$ESR\ age = \frac{accumulated\ paleodose\ (Gy)}{radiation\ rate\ (Gy/year)} = \frac{equivalent\ dose}{average\ annual\ dose\ rate} = \frac{D_e(Gy)}{D_o(Gy/year)}$$

The results are given in *Gray* (Gy), which is the absorption of one joule of energy, in the form of ionizing radiation per kilogram of matter: $1\ Gy = 1\frac{J}{kg} = 1\frac{m^2}{s^2}$.

ESR dating was performed by Prof. Dr. Ulrich Radtke in his laboratory at the University of Cologne with an ESR-spectrometer. The samples used for the dating method were chosen by myself, considering the results of the X-ray diffractometry. Two samples were 100% recrystallized and were therefore not sent for dating.

3. TAXONOMY OF PLEISTOCENE AND HOLOCENE CORALS FROM EGYPT AND VANUATU

3.1 Coral taxonomy – some introductory words

"The corals constitute a chaotic collection of individuals, and the uncertainty as to what may be considered as species is the first problem that must confront anyone who happens to study corals from his own resources on an isolated coral-reef." (Frederic Wood Jones, *On the Growth Forms and Supposed Species in Corals,* 1907)

Coral taxonomy is a challenge in many respects. Not only makes the high degree of morphological variation, even within the same species, taxonomic assessment often difficult, but coral systematics based on morphology have been recently challenged by molecular studies suggesting that classical coral taxonomy is in urgent need of revision (Fukami *et al*. 2004, 2008). In fact, Fukami *et al*. (2008) have shown that 11 out of 16 classical scleractinian families are not monophyletic (Figure 3.1.1), a dramatic difference relative to the classical hypotheses of coral relationships based on morphological traits. Furthermore, the remaining five traditional families both gained new and lost old members. Over the last decade, and while writing this thesis, coral taxonomy has been greatly advanced by integrating genetic data with morphological characters (Budd *et al.* 2010; Huang *et al.* 2014b; Kitano *et al.* 2014), thus shedding some light onto the "chaotic collection of individuals". The traditional macromorphology-based taxonomy identified five to seven suborders (Vaughan & Wells 1943; Wells 1956), while it is now widely accepted that scleractinian corals comprise only three, but highly divergent clades (Figure 3.1.1), i.e. the "basal", the "complex", and the "robust" corals (Fukami *et al.* 2008; Kitahara *et al.* 2010; Stolarski *et al.* 2011; Huang *et al.* 2014a, b; Kitano *et al.* 2014). Recent studies suggest that the picture is even more complex, with the robust coral group being a lineage that is embedded within the complex coral group (Fukami *et al*. 2008; Kitahara *et al*. 2010) and several genera of azooxanthellate corals being basal to both (Kitahara *et al*. 2010). The molecular results also prove the distinctiveness between Atlantic and Pacific scleractinian taxa (Fukami *et al.* 2004) as several families have now been suggested to be largely or exclusively Atlantic, i.e. the newly defined Mussidae, the Meandrinidae, the Oculinidae, as well as some genera such as *Favia*.

In this study, species identification is often based on one or two specimens, all of them fossil, and has therefore relied upon traditional, typological, macrostructural analysis. Even though some recent studies have started to redefine and evaluate morphological characters with respect to the results of the molecular studies for some major clades, a paleontological approach to the taxonomy on species level of modern scleractinian corals is still lacking.

Species identification, if possible, is important for ecological interpretation. A complete list of specimens and species can be found in Appendix I (Vanuatu data) and Appendix II (Egypt data). Table 3.1 at the end of this chapter provides environmental preferences of the fossil species. Next to Bromfield (2013), who published a detailed taxonomy of Miocene to early Pleistocene Indo-Pacific corals, this is the first detailed taxonomy of late Pleistocene Indo-Pacific corals. (Note that Humblet *et al*. (2015) recently published an identification guide for Quaternary corals, which is helpful for generic identifications for the very common genera *Acropora*, *Isopora*, *Montipora*, and *Porites* based on macromorphological characters of internal structures. These genera have in common that they possess very small corallites, which are prone to destruction in various taphonomical processes)

Figure 3.1.1(next page, modified from Fukami *et al*. 2008): Phylogenetic relationships among scleractinian (mostly zooxanthellate) corals and outgroups. Topology was inferred by Bayesian analysis, based on combined mitochondrial *cox1* and *cob* DNA sequences. Numbers on main branches show percentages of Bayesian probability (>70%) and bootstrap values (>50%) in ML analysis. Dashes mean bootstrap values <50% in ML. Numbers in circles show the connection of trees from A to D. Bars in black indicate possible new family level groupings. Numbers (1, 2) following species names indicate that different colonies of the species had different haplotypes. My study contains members of the colored traditional families.

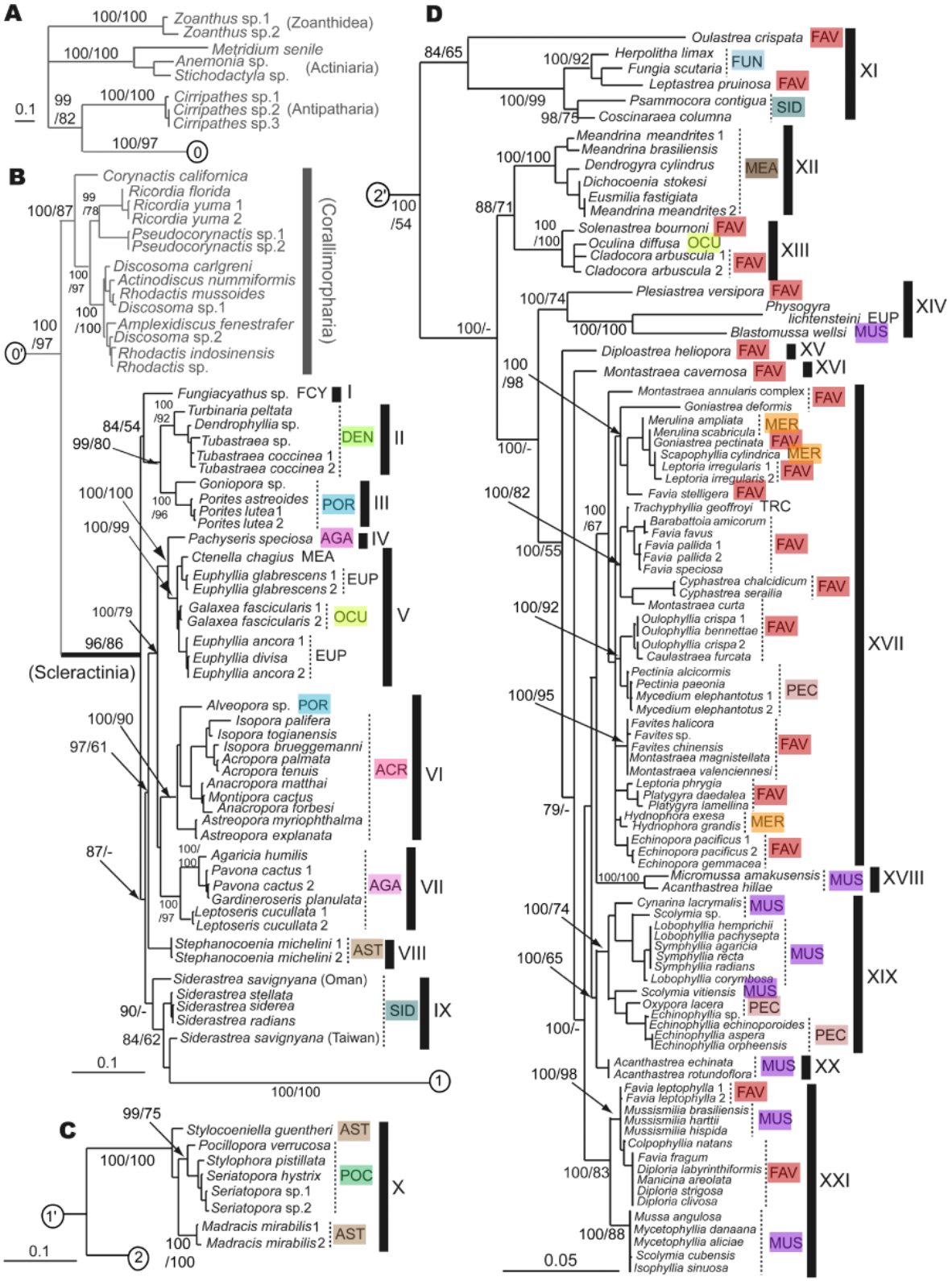

A - outgroups, B - complex corals and corallimorphans, C - Pocilloporidae, D - robust corals.
ACR: Acroporidae, AGA: Agariciidae, AST: Astrocoeniidae, DEN: Dendrophylliidae, EUP: Euphylliidae, FAV: Faviidae, FCY: Fungiacyathide, FUN: Fungiidae, MEA: Meandrinidae, MER: Merulinidae, MUS: Mussidae, PEC: Pectinidae, POC: Pocilloporidae, POR: Poritidae, OCU: Oculinidae, SID: Siderastreidae, TRC: Trachyphyllidae

3.2 Systematic classification

Cnidaria HATSCHEK 1888

Anthozoa EHRENBERG 1834

Hexacorallia HEACKEL 1866

Scleractinia BOURNE 1900

3.2.1 Acroporidae VERRIL 1902

The Acroporidae are a well-defined family, and one of the five monophyletic clades, which are currently accepted. The results of Fukami *et al.* (2008) suggest that *Alveopora* (previously Poritidae) should be included.

3.2.1.1 Genus *Acropora* OKEN1815

(Plate 3.1c-f)

Type species: *Millepora muricata* LINNAEUS 1758 = *Acropora muricata* (LINNAEUS 1758)

General remarks

Acropora is one of the three monophyletic genera next to *Porites* and *Siderastrea* that contains Atlantic and Indo-Pacific species (Fukami *et al.* 2008). Even though *Acropora* can be easily recognized at genus level, it is very difficult to distinguish fossil specimens at species level. They are rarely preserved in-situ, but mostly only in small pieces of branches, affected my mechanical forces through transport and wave action. Even when preserved in-situ, the small corallites usually show traces of erosion, which makes identification at species level difficult. *Acropora* occurs in recent and fossil reefs of Vanuatu and Egypt, but is surprisingly rare in the Pleistocene of Vanuatu. Identification and taxonomy of *Acropora* species is also controversial in recent specimens, due to their high species richness – it is by far the most species rich genus with 182 known species after Veron (2000) – and interspecific similarities, as well as their high intraspecific phenotypic-environmental variability. Veron (2000) therefore defined species groups, based on a combination and growth-form characters, which is helpful for grouping recent species directly underwater, but do not have a well defined taxonomic basis (Veron 2000).

Diagnosis

All *Acropora* species are branching and mostly bushy or plate-like. However, there is a wide range of growth forms that can be helpful for identification in recent reefs. For fossil *Acropora*, when preserved in pieces only, growth form is not diagnostic. The genus is distinct because of the two types of corallites: small radial corallites along the branches and one larger, bisymmetrical axial corallite on top of each branch. Corallites of *Acropora* do not possess columellae, they are 0.7 to 1.3 mm in diameter. The corallite walls and the coenosteum are porous, the corallites are round in cross-section and protrude several mm from the surface. Usually there are 12 fully developed septa.

The preservation of most specimens from Vanuatu and Egypt is too poor for species identification. The assignment to *Acropora* is largely based on its ramose morphology, the porous coenosteum, the lack of a columella, and the axial corallite.

Ecology

Acropora is always zooxanthellate and colonial. It is by far the most abundant coral genus in most recent Indo-Pacific reefs (Veron 2000), where it dominates intertidal and subtidal communities.

Acropora often outcompetes other corals in shallow tropical reefs, especially where the water is clear. The colonies can grow up to 10 cm per year.

Acropora muricata (LINNAEUS 1758)
(Plate 3.1a, Figure 3.2.1)

Original name *Madrepora (Eumadrepora) muricata* LINNAEUS 1758

Synonymized names
Acropora arbuscula (DANA 1846) (synonymy)
Acropora copiosa NEMENZO 1967 (synonymy)
Acropora formosa (DANA 1846) (synonymy)
Acropora gracilis (DANA 1846) (synonymy)
Acropora laevis CROSSLAND 1952 (synonymy)
Acropora varia NEMENZO 1967 (synonymy)
Madrepora (Eumadrepora) muricata LINNAEUS 1758 (previous combination)
Madrepora brachiata DANA 1846 (synonymy)
Madrepora formosa DANA 1846 (synonymy)
Madrepora gracilis DANA 1846 (synonymy)
Madrepora muricata (LINNAEUS 1758) (old combination)
Madrepora stellulata VERRILL 1902 (synonymy)
Madrepora virgata DANA 1846 (synonymy)
Millepora muricata LINNAEUS 1758 (original combination, basionym)

General remarks

This is the one of two *Acropora* species that could be identified with some confidence. In the fossil reef of Dahab it occurs as single species stands at one corner of the slope. As it also occurs as dominant species in recent reefs of the Gulf of Aqaba, forming large single species stands, and because of its in-situ preservation it is quite distinct. The *formosa* - *muricata* debate is not finally solved, because Veron (2000) does not accept the synonymization. However, the two species have been synonymized in this study.

Figure 3.2.1: Single species stand of *Acropora muricata* at one corner of the Dahab reef complex.

Diagnosis

Acropora muricata forms arborescent colonies with cylindrical branches. The branches are relatively short and compact, which is typical for shallow water colonies. In deeper water the colonies would have more open branches. The axial corallites are exert, while the radial corallites are tubular.

Ecology

The ecological variation of this species indicates a shallow water habitat, where colonies are exposed to stronger mechanical forces. *A. muricata* typically occurs in reef slopes and lagoons. Here, it occurs on the edge of the upper slope of a fringing reef as single species patch (Figure 3.2.1).

Acropora monticulosa (BRÜGGEMANN 1879)

(Plate 3.1b)

Original name *Madrepora monticulosa* BRÜGGEMANN 1879

Synonymized names *Madrepora monticulosa* BRÜGGEMANN 1879 (original combination, basionym)

General remarks

The species is conspicuous in the field, because the branches of this *Acropora* species form plates built of compacted branches with digitate smaller branches growing upwards like fingers from the plate. They occurred in several terraces in Vanuatu.

Diagnosis

The isolated subcolonies are digitate, with thick branches tapering to a small axial corallite. The radial corallites are uniform in size an arranged in rows.

Ecology

The pyramid-shaped and short branches indicate that the colonies were exposed to relatively strong wave action. This species usually lives on upper reef slopes.

3.2.1.2 Genus *Astreopora* DE BLAINVILLE 1830

Type species: *Astraea opthalma* LAMARCK 1816 = *Astreopora myriophthalma* (LAMARCK 1816)

General remarks

Even though it is not one of the common genera, this genus could be identified both in Vanuatu and in Egypt. This might be due to its generally massive appearance, which facilitates preservation of characters. *Astreopora* is a conspicuous genus and can generally be easily identified. Nevertheless, identification at species level is again more difficult. Only one species could be identified with confidence. The other specimens either lack sufficient preservation or could not be assigned to a species with certainty.

Diagnosis

The colonies can be massive, laminar or encrusting, with immersed or conical corallites. *Astreopora* can be distinguished from *Montipora* by the size of its corallites. The latter has usually smaller corallites (<1mm). The corallites are distinct and separate, round in cross-section and 1-4 mm in diameter. There are numerous, neatly spaced septa and a compact columella.

Ecology

Astreopora occurs on reef flats and reef slopes. It usually shows endolithic borings by polychaetes and *Lithophaga* species.

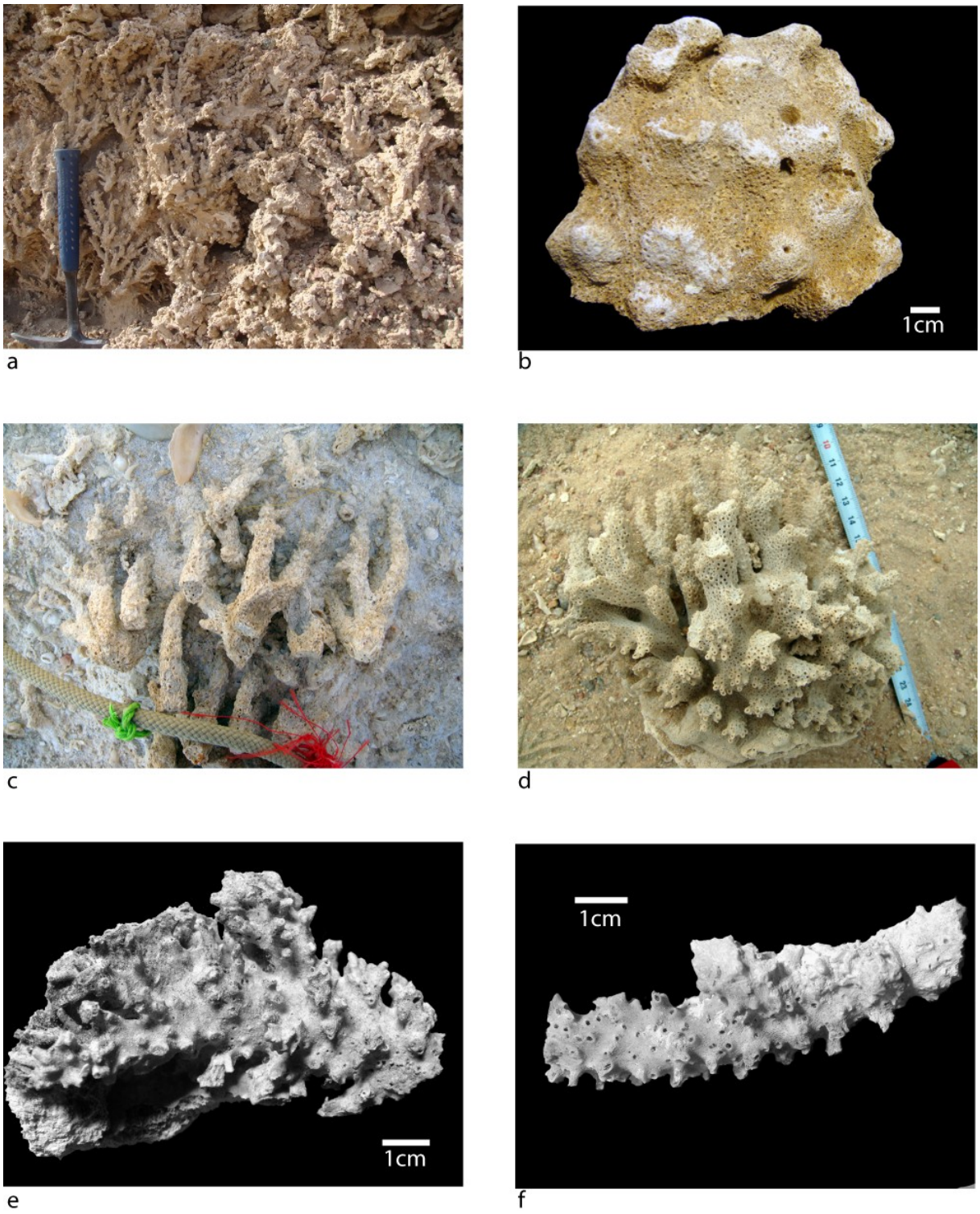

Plate 3.1:
a - *Acropora muricata*, single-species stand, Dahab, Egypt
b - *Acropora monticulosa*, Pleistocene 1, Vanuatu
c - *Acropora sp.*, in-situ preservation, LT50, Ras Mohammed, Egypt
d - *Acropora sp.*, colony preservation, Ras Mohammed, Egypt
e - *Acropora sp.*, Holocene, Vanuatu
f - *Acropora sp.*, typical preservation, Holocene, Vanuatu

Astreopora myriophthalma (LAMARCK 1816)
(Plate 3.2a, b, f)

Original name	*Astrea myriophthalma* LAMARCK 1816
Synonymized names	*Astrea myriophthalma* LAMARCK 1816 (original combination, basionym) *Astrea pulvinaria* LAMARCK 1816 (synonymy) *Astreopora arenaria* BERNARD 1896 (synonymy) *Astreopora ehrenbergi* BERNARD 1896 (synonymy) *Astreopora eliptica* YABE & SUGIYAMA 1941 (synonymy) *Astreopora kenti* BERNARD 1896 (synonymy) *Astreopora ovalis* BERNARD 1896 (synonymy) *Astreopora profunda* VERRILL 1872 (nomen nudum, synonymy) *Astreopora stellae* NEMENZO 1964 (synonymy)

General remarks

This species could be identified in Vanuatu as well as in Egypt. It is the most common of all *Astreopora* species.

Diagnosis

The colonies of *Astreopora myriophthalma* are usually hemispherical and the corallites are evenly spaced and conical with rounded, upright or outwardly directed openings. They are about 1.5 mm in diameter. The coenosteum has outwardly directed papillae.

Ecology

A. myriophthalma occurs in most reef habitats where the water is not too turbid.

3.2.1.3 Genus *Montipora* BLAINVILLE 1830

(Plate 3.2c-e)
Type species: *Montipora verrucosa* (LAMARCK 1816)

General remarks

Montipora resembles *Porites* at first glance, but can be distinguished by its tiny, superficially empty corallites. The genus could be found in several localities in Vanuatu as well as in Egypt. However, identification at species level was not possible either due to preservation (Vanuatu) or lack of material in the laboratory (Egypt). Similar to *Acropora*, *Montipora* is a species-rich genus and the similarity among species in combination with the very small size of the corallites is a further challenge.

Diagnosis

This genus can show all shapes of colonies, but usually forms leafy, encrusting, plate-like, or semi-massive colonies with numerous intermediates. A single colony usually has more than one growth form. Distinctive is the empty appearance of the small corallites, being only 0.25 – 1 mm in diameter, because there is no columella. The septa consist of vertical rows of inward projecting spines and the walls are porous. Species identification is based on differences in the structure of the coenosteum, which hardly preserved in fossils. The coenosteum can be plain, without elaborations, or may develop various elaborations with papillae, tuberculae, ridges or verrucae.

Ecology

This genus is ecologically unspecific as it is present in all reef habitats, from the high-energy upper reef slopes to deeper calm lagoonal habitats.

a

b

c

d

e

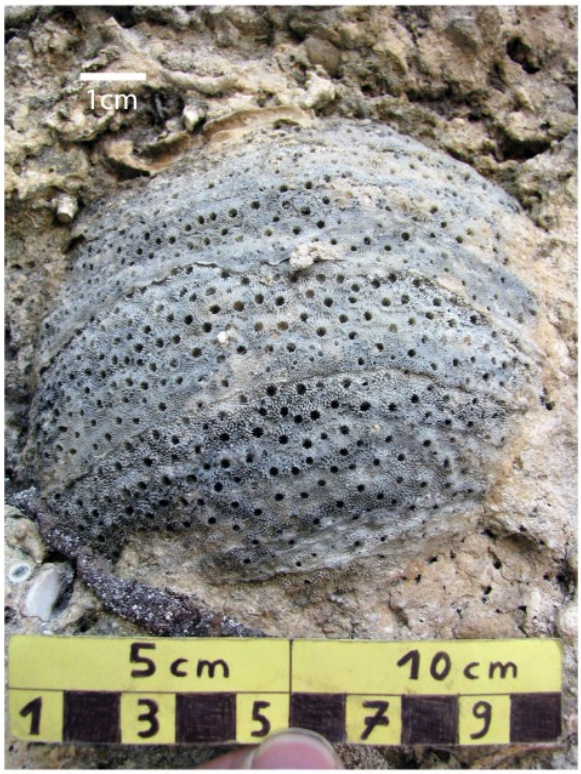

f

Plate 3.2 (previous page):
a - *Astreopora myriophthalma*, large in-situ colony, LT1, Pleistocene, Dahab, Egypt
b - *Astreopora myriophthalma*, close-up picture of the same colony
c - *Montipora sp.*, encrusting in-situ colony, LT 47, Pleistocene, Ras Mohammed, Dahab
d - *Montipora sp.*, sample from the Holocene of Vanuatu
e - *Montipora sp.*, along with *Lobophyllia* sp., Holocene, Vanuatu, picture taken by J. Millet
f - *Astreopora myriophthalma*, hemispherical in-situ colony, Holocene, Vanuatu, by J. Millet

3.2.1.4 Genus *Alveopora* DE BLAINVILLE 1830

Type species: *Madrepora daedalea* FORSKÅL 1775 = *Alveopora daedalea* (FORSKÅL 1775)
(Plate 3.13a)

General remarks

This is a conspicuous genus, whose position within the Poritidae has been doubtful already before recent genetic analyses. It is now accepted to belong to Acroporidae. Due to its porous structure it is probably underrepresented in the fossil record, but I found specimens in the few well preserved outcrops of Vanuatu. Nevertheless, identification at the species level was not possible.

Diagnosis

The most remarkable feature of this genus is its very porous, light structure. The corallites are rounded or polygonal and about 1.4 to 6 mm in diameter. They are crowded or closely united by their brittle walls. There are 12-24 hardly distinguishable septa that seem to originate from the corallite wall. The shared wall is pierced by pores. There is little internal structure in the corallite.

Ecology

Alveopora is an Indo-Pacific genus that can sometimes be common, but is mostly not. It primarily occurs in protected reef environments.

3.2.2 Agariciidae GRAY 1847

General remarks

This relatively well defined zooxanthellate family is largely monophyletic (Fukami *et al.* 2008; Kitahara *et al.* 2010), only the genus *Pachyseris* was recently placed into euphylliids (*Pachyseris* could be identified neither in Vanuatu nor in Egypt in this study). Kitahara (2010) shows that the Agariciidae are formed by *Gardineroseris*, *Pavona*, and *Agaricia*, of which the latter is the only Atlantic genus. *Leptoseris* is in need of further revision to reveal its exact evolutionary position, but the above studies put it into Agariciidae. Atlantic species have been moved to the genus *Helioseris* (Kitahara *et al.* 2012), such that *Leptoseris* is endemic to the Indo-Pacific.

Diagnosis

The Agariciidae are characterized by their septa that are continuous between adjacent corallites. Walls are poorly developed and the small corallites are immersed. All recent members of this family are colonial and hermatypic.

3.2.2.1 Genus *Gardineroseris* SCHEER & PILLAI 1974

Type species: *Gardineroseris planulata* (DANA 1846)

Gardineroseris planulata (DANA 1846)
(Plate 3.3c)

Original name *Agaricia planulata* DANA 1846

Synonymized names
Agaricia planulata DANA 1846 (original combination, basionym)
Agaricia ponderosa GARDINER 1905 (synonym)
Agaricia ponderosa var. minikoiensis GARDINER 1905 (synonym)
Agariciella minikoiensis (GARDINER 1905) (synonym)
Agariciella planulata (GARDINER 1905) (previous combination)
Agariciella ponderosa (GARDINER 1905) (synonym)
Asteroseris planulata (DANA 1846) (previous combination)
Gardineroseris ponderosa (GARDINER 1905) (synonym)
Pavona (Polyastra) planulata (DANA 1846) (previous combination)
Pavona (Polyastra) ponderosa (GARDINER 1905) (synonym)

General remarks

This genus contains only one species that can be easily distinguished from other Agariciidae. It occurs in the Pleistocene of Egypt, but was not observed in the line transects.

Diagnosis

G. planulata has distinctive polygonal, cerioid corallites with acute walls that are 4 to 6 mm in diameter and 2 to 4 mm in depth. The numerous, fine septa merge with the columella in deep cavities.

Ecology

This species typically occurs on reef slopes in clear to moderately turbid water from very shallow to 25 m depth.

3.2.2.2 Genus *Leptoseris* EDWARDS & HAIME 1849

(Plate 3.3d)
Type species: *Leptoseris fragilis* MILNE EDWARDS & HAIME 1849

General remarks

Leptoseris was found in the Pleistocene and Holocene of Vanuatu and Egypt. Due to its delicate construction usually only small pieces are preserved, which makes identification at the species level problematic.

Diagnosis

This genus usually builds foliaceous colonies, consisting of thin and smooth leafs with regular septocostae. Colonies usually possess a central corallite. The corallites are interconnected by very fine septocostae, whereas walls are absent.

3.2.2.3 Genus *Pavona* LAMARCK 1801

Type species: *Madrepora cristata* ELLIS & SOLANDER 1786 = *Pavona cactus* (FORSKÅL 1775)

General remarks

Pavona is a widespread genus with problematic taxonomy at the species level. It could be recorded in the Pleistocene of both Vanuatu and Egypt. Similar to *Leptoseris* its fragile construction often leads to fragmentary preservation. As much of the identification is based on colony construction, identification was usually impossible. However, some well-preserved colonies allow for a glance into its diversity in the Pleistocene study areas.

Diagnosis

The growth forms range from encrusting to foliaceous or branching with bifacial or unifacial leaves. Walls are absent and the corallites are interconnected by septocostae alternating in size, merging in a columella. The corallites are 0.5 to 3 mm in diameter and may also be separated by more or less prominent ridges.

Pavona cactus (FORSKÅL 1775)

(Plate 3.3a)

Original name *Madrepora cactus* FORSKÅL 1775

Synonymized names
Lophoseris knorri MILNE EDWARDS & HAIME 1851 (synonym)
Madrepora cactus FORSKÅL 1775 (original combination, basionym)
Madrepora cristata ELLIS & SOLANDER 1786 (synonym)
Pavona cristata (ELLIS & SOLANDER 1786) (synonym)
Pavona formosa DANA 1846 (synonym)
Pavona praetorta (DANA 1846) (synonym)
Pavona venusta DANA 1846 (synonym)

General remarks

This species could be identified in Vanuatu as well as in Egypt.

Diagnosis

The colonies consist of small, vertical and irregular leaves. The leaves are up to 5 mm thick with septa running in rows parallel to the edges of the leaf. The rows of septa are separated by corallites that by 3 to 4 mm in diameter.

Ecology

The species is mostly found in sheltered and lagoonal areas. It well tolerates sediment, and reaches its greatest abundance and colony size between 3 and 10 m deep in calm areas.

Pavona varians VERRILL 1864

(Plate 3.3b)

Original name *Pavona varians* VERRILL 1864

Synonymized names
Lophoseris repens BRÜGGEMANN 1877 (synonym)
Pavona percarinata RIDLEY 1883 (synonym)
Pavona repens (BRÜGGEMANN 1877) (synonym)
Pavonia intermedia GARDINER 1898 (synonym)

General remarks

This species was identified in several localities of Vanuatu.

Diagnosis

P. varians is an encrusting species that may have leafy edges. Calices are cerioid, though the surface of the colonies are ridged with collines, giving a low, convoluted appearance.

Ecology

The species is found between the surface, in crevices in the reef crest, to at least 45 m deep, and is equally common on clear water reef slopes and turbid back-reef habitats. It appears to be a rapidly colonizing species, which occupies parts of dead corals. Thus it is the species most likely to be found colonizing the dead basal parts of large colonies of *Goniopora* and *Porites* species, which dominate in back-reef areas.

3.2.3 Astrocoeniidae KOBY 1890

This family contains only one Indo-Pacific genus, which could also be identified in the Pleistocene of Vanuatu and Egypt. Fukami *et al*. (2008) have shown that this family is paraphyletic with the Atlantic genus *Stephanocoenia* forming a separate clade, whereas the Atlantic genus *Madracis* and the Indo-Pacific genus *Stylocoeniella* group with Pocilliporidae. The family is therefore most probably no longer valid.

3.2.3.1 Genus *Stylocoeniella* YABE and SUGIYAMA, 1935

Type species: *Stylocoenia hanzawai* YABE & SUGIYAMA 1933 = *Stylocoeniella armata* (EHRENBERG 1834)

General remarks

This genus contains only three valid species and only one could be identified in the Pleistocene with confidence. The genus occurs in the dataset of Vanuatu, but was also identified in the Pleistocene of Egypt outside the transects.

Diagnosis

Stylocoeniella forms encrusting colonies, with immersed corallites of 0.5 to 1.4 mm in size. Characteristic are the two cycles of septa and the styliform columella. The coenosteum surface is spiny.

Stylocoeniella guentheri (BASSETT-SMITH 1890)
(Plate 3.3e-f)

Original name *Stylophora guentheri* BASSETT-SMITH 1890

Synonymized names *Stylophora guentheri* BASSETT-SMITH 1890 (original combination, basionym)

Diagnosis

The corallites are widely spaced and only 0.5 to 1 mm in diameter with only 6 prominent septa. The second cycle is hardly developed. The coenosteum spines are small but distinctive.

Ecology

S. guentheri occurs in shady habitats where it can form encrusting sheets.

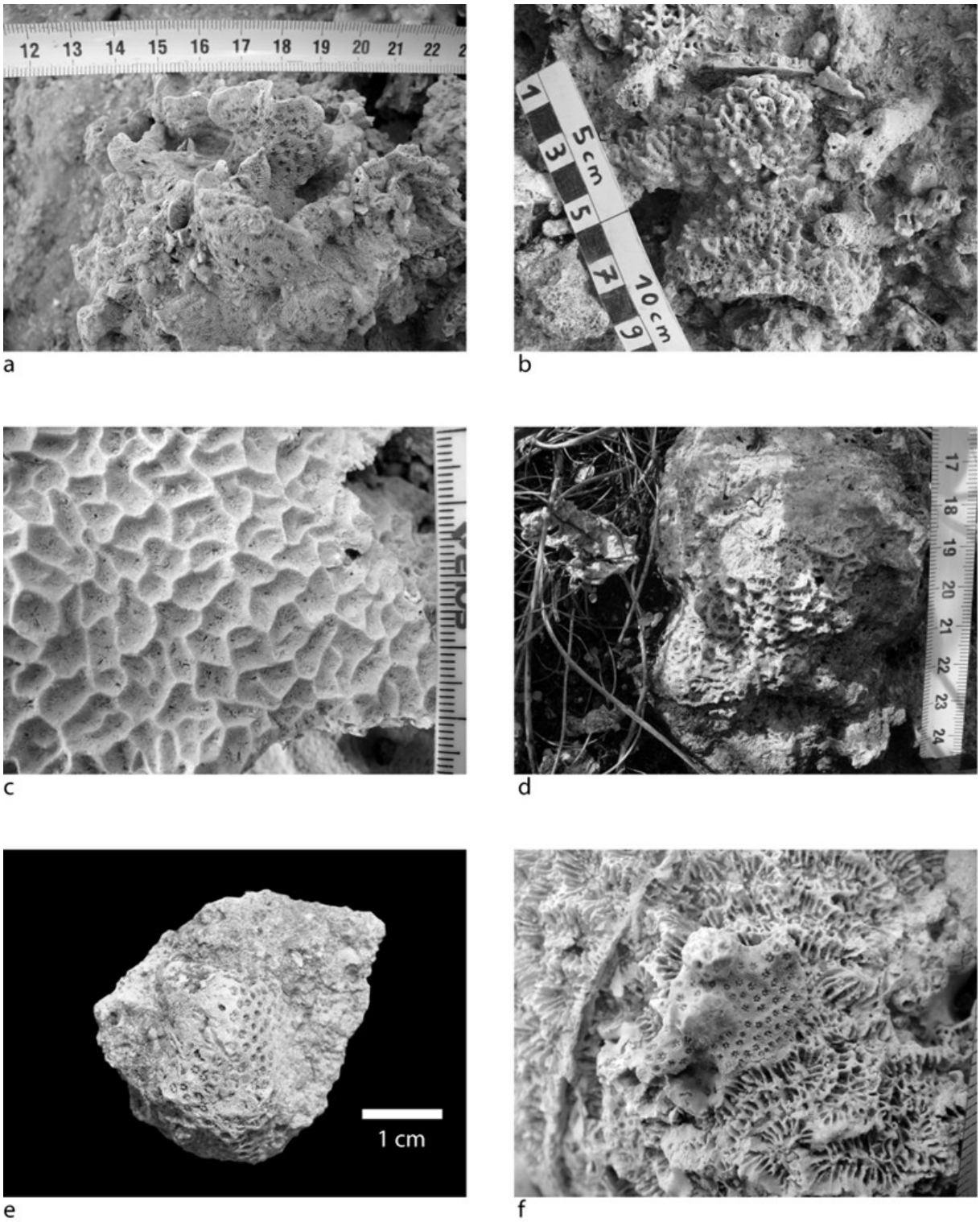

Plate 3.3:
a - *Pavona cactus*, Pleistocene, LT18, Dahab, Egypt
b - *Pavona varians*, Holocene, Vanuatu, picture taken by J. Millet
c - *Gardineroseris planulata,* Pleistocene, Ras Mohammed, Egypt
d - *Leptoseris sp.*, Pleistocene 1, Vanuatu
e - *Stylocoeniella guentheri*, Pleistocene 1, Vanuatu
f - *Stylocoeniella guentheri* growing on *Platygyra daedalea*, Pleistocene, Ras Mohammed, Egypt

3.2.4 Dendrophylliidae GRAY 1847

The Dendrophylliidae are the only family that remains completely unchanged after the molecular study of Fukami *et al*. (2008). This family is mostly azooxanthellate.

3.2.4.1 Genus *Tubastraea* LESSON 1829

Type species*: Tubastraea coccinea* LESSON 1829

Veron (2000) refers to this genus as "*Tubastrea*", but in the original description by Lesson (1829) this genus is written "*Tubastraea*" (see also Cairns (2000, 2001)). Tubastraea is azooxanthellate living in exposed parts of coral reefs all over the world along with zooxanthellate corals.

Tubastraea micranthus (EHRENBERG 1834)
(Plate 3.4a-b, Figure 3.2.2)

Original name *Tubastrea micrantha* EHRENBERG 1834

Synonymized names
Dendrophyllia aequiserialis MILNE EDWARDS & HAIME 1848
Dendrophyllia micrantha (EHRENBERG 1834)
Dendrophyllia micrantha var. grandis CROSSLAND 1952
Dendrophyllia nigrescens DANA 1846
Dendrophyllia viridis Milne EDWARDS & HAIME 1848
Oculina micranthus EHRENBERG 1834
Tubastrea micrantha EHRENBERG 1834 (genus misspelling)

General remarks

The species occurred in one spot at Ras Mohammed, but not inside transects. The specimens from Egypt consist mostly of broken pieces, but accumulate in high densities on a single spot. Above that spot, in-situ colonies in growth position could be seen at one clearly defined area inside the reef body along with a high accumulation of gastropods (Figure 3.2.2).

Diagnosis

Tubastraea micranthus is a dendroid coral with branches that are 10 to 20 mm thick and repeatedly dividing. The corallites grow laterally along the branches and are 5 to 8 mm in diameter and 10 to 15 mm in length. Septa are in three cycles with the tertiaries being incomplete and inconspicuous. Columellae are well developed.

Ecology

This species is known for its patchy distribution. It occurs in greatest abundance in water below 20 m deep and can occur in cavities of even very shallow reef crests.

Figure 3.2.2: *Tubastraea micranthus* high above the accumulation of broken pieces, along with large gastropods. Picture by J. Millet.

3.2.4.2 Genus *Turbinaria* OKEN 1815

Type species: *Madrepora crater* PALLAS 1766 = *Turbinaria crater* (PALLAS 1766)

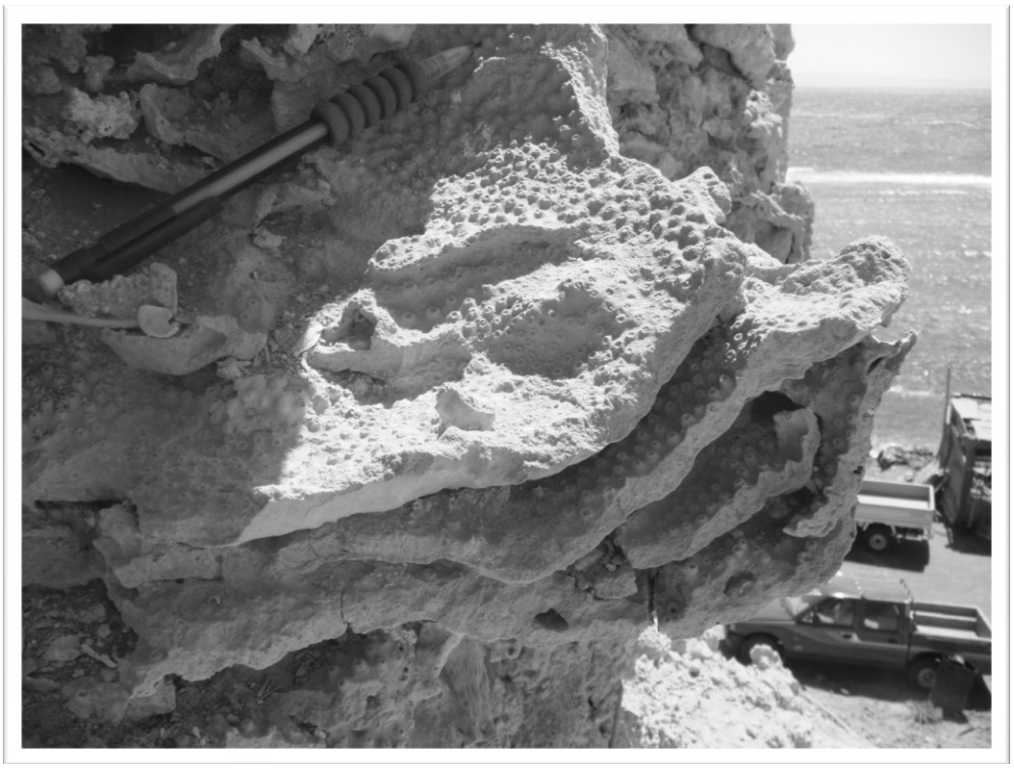

Figure 3.2.3: *Turbinaria reniformis* at the Pleistocene reef of Dahab.

General remarks

This genus is distinctive, but identification at the species level is difficult as the species are mainly distinguished by their different corallite size. One species in the Egyptian Pleistocene could be identified. Small pieces were found in Vanuatu as well, but poor preservation did not allow for further identification.

Diagnosis

The species of this genus may form laminar, encrusting or foliaceaous colonies with round corallites and a porous coenosteum. The septa are short and the columella is broad and compact.

Ecology

Sheppard & Sheppard (1991) showed that in the Red Sea members of this genus are usually found in sedimented and sandy areas, where they form large colonies of vertical, interlocking plates (Figure 3.2.3).

Turbinaria reniformis BERNARD 1896

(Plate 3.4c, Figure 3.2.3)

Original name	*Turbinaria reniformis* BERNARD 1896
Synonymized names	*Turbinaria lichenoides* BERNARD 1896 (synonym?) *Turbinaria reptans* BERNARD 1896 (synonym?) *Turbinaria veluta* BERNARD 1896 (synonym?)

General remarks

One beautifully preserved colony was found in the main reef complex in the Pleistocene of Dahab (Figure 3.2.3).

Diagnosis

The colonies of *T. reniformis* build mostly horizontal, unifacial laminae. The corallites are about 2.5 mm in diameter and widely spaced with thick walls. The coenosteum is smooth.

Ecology

This species is known to form large colonies on fringing reefs where the water is turbid.

3.2.5 Merulinidae VERRILL 1866

As could be recently shown by molecular and also morphological studies (Fukami *et al*. 2004; Budd *et al*. 2012; Fukami *et al*. 2008; Kitahara *et al*. 2010; Huang *et al*. 2011; Budd & Stolarski 2011 Huang *et al*. 2014) Faviidae do not represent a monophyletic group, even though most of the genera exhibit a suite of superficial morphological similarities. In fact, it is the most polyphyletic of all families in Fukami's *et al*. (2008) analyses, with taxa scattered in several clades. Atlantic "faviids" and Pacific "faviids" are clearly distinct. Budd (2009) referred to this mess, including all taxa belonging to clade XVII (Fukami *et al.* 2008), as the 'Bigmessidae', which is a quite telling designation. Recent studies started to clean up the taxa (Huang *et al.* 2011, 2014b; Budd *et al.* 2012), but it is still a long way to go until this issue will be finally solved. Thus, the 'Bigmessidae' comprise the traditional families Faviidae, Merulinidae, Pectinidae and Trachyphyllidae, all of which have not been monophyletic before (Fukami *et al*. 2008). Nevertheless, most genera of 'Bigmessidae' were monophyletic, except *Favia*, *Favites*, *Goniastrea*, and *Montastrea* (Huang *et al.* 2011). Based on the molecular studies by Fukami *et al*. (2008) and Huang *et al*. (2011), as well as detailed examinations of coral morphology at the corallite and subcorallite scales (Budd & Stolarski 2011), Merulinidae VERRILL 1865 was expanded to include all members of 'Bigmessidae'. Faviidae was demoted to the subfamily Faviinae as a group limited to the Atlantic, and the remaining two families were synonymized (Budd *et al*. 2012).

All traditional „faviid“ taxa have a more or less massive phenotype and are of a robust appearance, which was the main reason why they have traditionally been put into a single family. The colonies are therefore often preserved, in contrast to the skeletal details, which makes it sometimes difficult to distinguish between the different genera, let alone the different species. Many specimens, especially from Vanuatu, were therefore declared as „Faviidae" indet. and thus excluded from detailed quantitative analyses. For the Egyptian samples it was mostly possible to identify the different genera.

3.2.5.1 Genus *Cyphastrea* (LAMARCK 1816)

Type species: *Astrea microphthalma* LAMARCK 1816 = *Cyphastrea microphthalma* (LAMARCK 1816)

General remarks

Cyphastrea is considered a close relative of *Dipsastraea*. It occurs in the study areas of Vanuatu and Egypt. The preservation of skeletal characters that are necessary for identification at the species level is often poor, due to the small size of the corallites. In Egypt two species could be distinguished but only one could be clearly identified. Poorly preserved or questionable specimens are referred to as *Cyphastrea* sp., which leads to a realistic diversity within this genus in the analyses.

Diagnosis

This genus is distinctive because of its small plocoid corallites that never exceed 3 mm in diameter. Most species are massive or encrusting. They tend to form large colonies exceeding 50 cm across. The costae are restricted to the corallite wall and the coenosteum is spiny. The septa are arranged in three cycles without conspicuous paliform lobes.

Cyphastrea serailia (FORSKÅL 1775)

(Plate 3.4d-f, Figure 3.2.4)

Original name	*Madrepora serailia* FORSKÅL 1775
Synonymized names	*Cyphastrea brueggemanni* QUELCH 1886 (synonym) *Cyphastrea conferta* NEMENZO 1959 (synonym) *Cyphastrea danai* MILNE EDWARDS 1857 (synonym) *Cyphastrea serialis* (FORSKÅL 1775) (wrong spelling) *Cyphastrea suvadivae* GARDINER 1904 (synonym) *Madrepora serailia* FORSKÅL 1775 (original combination, basionym)

General remarks

This species is widespread and at least some of the specimens from Vanuatu may also belong to this species.

Diagnosis

C. serailia can form very large massive colonies with a smooth surface. It is distinguished from the other common *Cyphastrea* species by having 12 primary septa that unite with the columella. The round corallites are 1.5 to 2.5 mm in size and all relatively equal in appearance.

Ecology

This species can be found in all reef environments, but is especially known to occur on reef flats in conditions of raised salinity and temperature, and on clear water reef slopes down to at least 40 m. Colonies may reach a large size (Figure 3.2.4).

Figure 3.2.4: Cyphastrea cf. serailia - large isolated colonies next to the main Dahab reef

3.2.5.2 Genus *Echinopora* LAMARCK 1816

Type species: *Echinopora rosularia* LAMARCK 1816 = *Echinopora lamellosa* (ESPER 1795)

General remarks

Members of this genus could be identified in Vanuatu as well as in Egypt, but only specimens from Egypt were sufficiently preserved for identification at species level. *Echinopora* may have a wide range of growth forms - from massive to encrusting, from laminar to arborescent. The collected specimens are all laminar or submassive to massive.

Diagnosis

The corallites are 5 to 10 mm in diameter and plocoid. The septa are exert and dentate, the columellae are usually prominent.

a

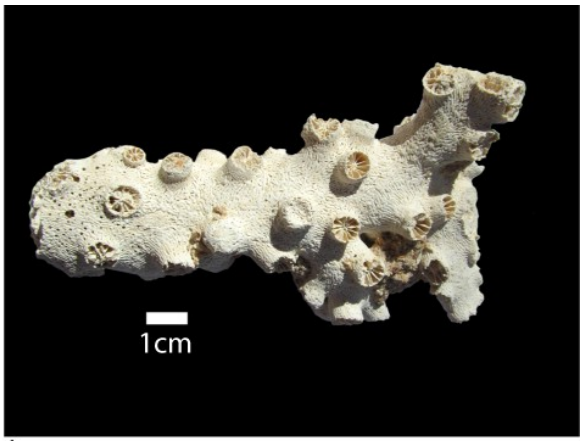

b

c

d

e

f

Plate 3.4:
a - *Tubastraea micranthus*, in-situ accumulation, Ras Mohammed, Egypt, picture taken by J. Millet
b - *Tubastraea micranthus*, sample from above locality
c - *Turbinaria reniformis*, LT7, Dahab, Egypt
d - *Cyphastrea* cf. *serailia*, Dahab, Egypt
e - *Cyphastrea serailia*, well preserved colony, Ras Mohammed, Egypt
f - *Cyphastrea serailia*, close-up of above colony

Echinopora forskaliana (MILNE EDWARDS & HAIME 1849)
(Plate 3.5a-c)
Original name *Astrea forskaliana* MILNE EDWARDS & HAIME 1849

General remarks

This species is common in the Pleistocene of Egypt. All specimens of *Echinopora* that could be identified to species level belong to this species based on corallite details. Nevertheless, there is some confusion about the species name and the descriptions. According to Veron (2000) the mostly massive and sometimes laminar specimens of my samples would belong to *E. forskaliana.* However, Sheer & Pillai (1983) as well as Sheppard & Sheppard (1991) would assign these specimens to *E. gemmacea,* which especially Scheer & Pillai (1983) describe as very variable in skeletal details and growth forms. The latter authors synonymized *E. forskaliana* with *E. gemmacea*. Here, I assigned the specimens to *E. forskaliana* according to Veron's (2000) definition and his description of corallite sizes and skeletal details. He describes *E. gemmacea* as bifacial, but the laminar specimens from this study are only unifacial.

Diagnosis

The collected specimens are mainly massive, some are unifacial laminar. The corallites are mostly tall and conical, between 5 to 10 mm in diameter. Long and short septocostae alternate and run mostly continuously between the septa.

Ecology

The species is especially common in shallow reef environments. *E. gemmacea (=forskaliana)* is described to be especially found on reef flats in severe environmental conditions and on both exposed and turbid reef slopes at all depths to over 30 m (Sheppard & Sheppard 1991).

3.2.5.3 Genus *Dipsastraea* BLAINVILLE 1830

(Plate 3.5d - *Dipsastraea sp.)*
Type species: *Madrepora favus* FORSKÅL 1775 = *Dipsastraea favus* (FORSKÅL 1775)

General remarks

The traditional genus "Favia" OKEN 1815 is paraphyletic and now splits up into the Atlantic *Favia* MILNE EDWARDS 1857 and the Indo-Pacific *Dipsastraea* (Budd *et al.* 2012; Huang *et al.* 2014b). The Atlantic *Favia fragum* belongs to another molecular clade together with some other Atlantic genera (Fukami *et al*. 2008) and is now placed in the newly defined Mussidae that are exclusively Atlantic (Budd *et al.* 2012). The Indo-Pacific *Dipsastraea* is represented in all study areas in Egypt and Vanuatu. Nevertheless, identification at the species level is almost impossible without samples (for Egypt) and with the poor preservation status of many specimens (Vanuatu). Skeletal details as the number of septa and the development of paliform lobes are necessary information for species identification. One species in Egypt could be identified with certainty. *Dipsastraea* is clearly underrepresented in the diversity analyses.

Diagnosis

To identify *Dipsastraea* three taxonomic features are distinctive and have to be present at the same time: 1. plocoid calices that are 2. basically monocentric and 3. show intratentacular budding. Huang *et al*. (2014) also defined some skeletal features that distinguish *Dipsastraea* from other genera of the newly defined Merulinidae, but these are ambiguous, and in fact more distinct in comparison to the Atlantic *Favia* than within *Dipsastraea*.

Dipsastraea pallida (DANA 1846)
(Plate 3.5f)

Synonymized names
Astraea (Fissicella) denticulata DANA 1846 (synonym)
Astraea cellulosa VERRILL 1872 (synonym)
Astraea denticulata DANA 1846 (synonym)
Astraea ordinata VERRILL 1866 (synonym)
Favia amplior (MILNE EDWARDS & HAIME 1849) (synonym)
Favia denticulata (DANA 1846) (synonym)
Favia doreyensis MILNE EDWARDS & HAIME 1849 (synonym)
Favia laccadivica GARDINER 1904 (synonym)
Favia okeni MILNE EDWARDS 1857 (synonym)
Favia pallida (DANA 1846) (original combination, basionym)
Favia tubulifera KLUNZINGER 1879 (synonym)
Goniastrea serrata ORTMANN 1889 (synonym)
Heliastrea borradailei GARDINER 1904 (synonym)
Parastrea amplior MILNE EDWARDS & HAIME 1849 (synonym)
Parastrea verrilleana MILNE EDWARDS & HAIME 1849 (synonym)

General remarks

D. pallida is the most common of all *Dipsastraea* species and quite abundant. It is likely that some of the unidentified *Dipsastraea* specimens from Vanuatu also belong to this species. Nevertheless, identification is based on Egyptian specimens.

Diagnosis

This species forms massive colonies with corallites from 5 to 11 mm in diameter. The number of septa is irregular and somewhere between 18 to 36 with paliform lobes being present.

Ecology

As mentioned above, this coral is widespread and abundant - thus it is unspecific in its environmental preferences. It occurs on reef slopes in depths between 5 and 35 m, in exposed outer reefs, in back-reef environments, and on calmer reef crests. Interestingly it also occurs on reef flats and can tolerate salinities of up to 48 ppt (Sheppard & Sheppard 1991).

3.2.5.4 Genus *Favites* LINK 1807

Type species: *Favites astrinus* LINK 1807 = *Favites abdita* (ELLIS & SOLANDER 1786)

General remarks

Favites is a large and relatively common genus with generally massive or sub-massive colonies. It is always cerioid with intratentacular budding. In contrast to *Goniastrea*, which is also cerioid, *Favites* budding occurs close to the periphery of the mother corallite so that the daughter polyp is much smaller and the colony thus has a much more irregular appearance. Identification at species level is always hard, because they are all very similar - in skeletal details as well as in ecological preferences. Three species could be identified with some confidence, whereas one is only tentatively identified. These four species are still assigned to this otherwise paraphyletic genus, even though the position of *Favites pentagona* within or not *Favites* needs further future research (Huang *et al*. 2014), and *Favites rotundata* has been only recently moved into Favites Huang *et al*. (2014).

Diagnosis

This genus can be recognized by usually being massive and cerioid. The corallites are between 5 to 17 mm in size and are monocentric, and the calices usually polygonal. The major septa are of equal width as the thecal wall, often without paliform lobes.

Ecology

Similar to *Dipsastraea*, *Favites* is common on reefs at mid-depths and most of them cannot tolerate greater environmental stress (Sheppard & Sheppard 1991).

Favites rotundata VERON, PICHON & WIJSMAN-BEST 1977
(Plate 3.5e)

Original name *Favites rotundata* VERON, PICHON & WIJSMAN-BEST 1977

Synonymized names
Dipsastraea rotundata (VERON, PICHON & WIJSMAN BEST 1977) (previous combination)
Favia rotundata (VERON, PICHON & WIJSMAN BEST 1977) (previous combination)

General remarks

This species is relatively distinct, because of the size of its corallites. It occurred in the Pleistocene of Egypt, but is not abundant. After Veron (2000) moved this species into *Favia,* Budd *et al*. (2012) consequently placed it within *Dipsastraea*, but Huang *et al*. (2014) recently move this species into *Favites*, which is the accepted nomenclature and corresponds to the original description by Veron *et al*. (1977). However, while writing this thesis this species belonged to three different genera, and the probability is high that this was not the last change. The era of the 'Bigmessidae' is not yet over and the confusion of which status is accepted or not is more erroneous than marking the traditional status. This species is represented by two specimens from Egypt only, of which only one occurs within the transects.

Diagnosis

As mentioned above, the most distinct feature of the species is the large corallite size of up to 2 cm. The corallites are subplocoid, mostly circular and possess thick walls. There are 50 - 60 septa. The neither real plocoid nor real cerioid growth might have been one reason for moving this species between *Favia* and *Favites.*

Ecology

This species occurs especially on slopes and in lagoons, mostly on exposed, clear water slopes below 7 m depth.

Favites pentagona (ESPER 1794)
(Plate 3.6b)

Original name *Madrepora pentagona* ESPER 1795

Synonymized names
Aphrastrea deformis (LAMARCK 1816) (synonym)
Astraea deformis LAMARCK 1816 (synonym)
Astrea deformis LAMARCK 1816 (synonym)
Favia adduensis GARDINER 1904 (synonym)
Favites gailei CHEVALIER 1971 (synonym)
Favites parvicella NEMENZO 1959 (synonym)
Goniastrea rudis MILNE EDWARDS & HAIME 1849 (synonym)
Madrepora pentagona ESPER 1795 (original combination, basionym)
Plesiastrea haeckeli BRÜGGEMANN 1878 (synonym)
Prionastraea gibbosissima MILNE EDWARDS & HAIME 1849 (synonym)
Stephanocoenia maldivensis GARDINER 1904 (synonym)

General remarks

This species could be identified in all study areas and is probably one of the most common species of *Favites* and relatively easily identified due to its small calices.

Diagnosis

F. pentagona usually forms massive and large colonies. The relatively deep calices are 5 to 8 mm in diameter with a polygonal, usually five-sided outline. There are 24 to 36 septa, of which 12 to 16 reach the columella, and septa possess paliform lobes.

Ecology

This species can be found in shallow reef environments throughout the Indo-Pacific. It cannot tolerate salinities over 45 ppt.

Favites flexuosa (DANA 1846)
(Plate 3.6a)

Original name *Astraea flexuosa* Dana, 1846

Synonymized names *Astraea flexuosa* Dana, 1846 (original combination, basionym)
Favites ellisiana Verrill, 1901 (synonym)

General remarks

This species could be identified in the Pleistocene localities of Egypt, where it is occasionally common.

Diagnosis

F. flexuosa is a relatively conspicuous species due to its size. The massive colonies reach a large size and the angular corallites are between 18 and 22 cm long, about 15 mm wide and 10 mm deep. The walls are thick and there are up to 75 prominent septa with large teeth. Paliform lobes are absent or weakly developed.

Ecology

This species grows mainly in intermediate depths, but it is able to tolerate moderate sediment input, which leads to occurrences on back-reef slopes and in lower depths.

Favites cf. spinosa (KLUNZINGER 1879)
(Plate 3.6c)

General remarks

This taxon could not be identified down to species level with certainty. However, given its similarity with *F. spinosa,* which occurs in the Western Indo-Pacific and the Red Sea, this taxon is tentatively referred to this species. It is distinctive from other unidentified *Favites* species.

Diagnosis

The characters that it shares with *F. spinosa* are the relatively small massive and rounded colonies with small corallites (6 to 10 mm) that are deeply excavated and possess angular walls. The septa that have prominent teeth are widely spaced and in two alternating orders. Paliform lobes are not preserved.

Ecology

F. spinosa occurs in a wide range of reef environments and is therefore unspecific.

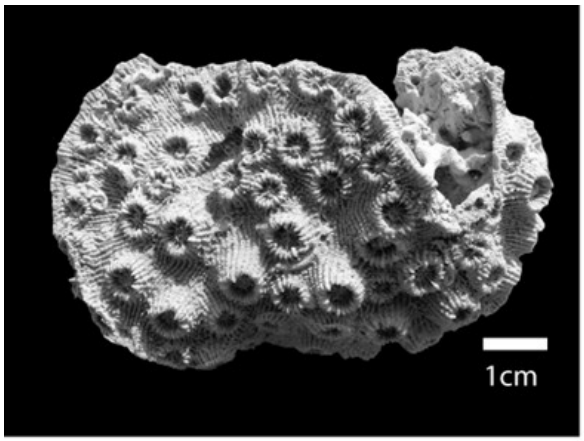

a

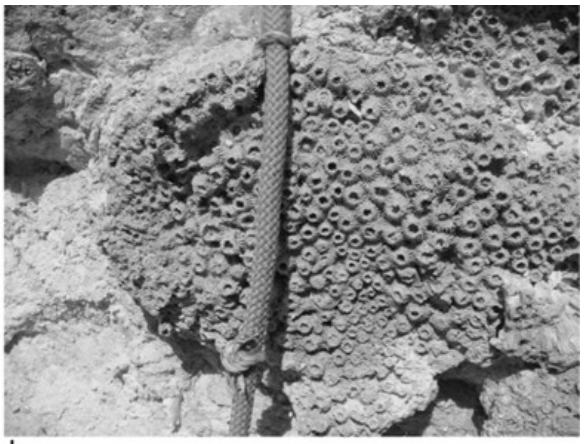

b

c

d

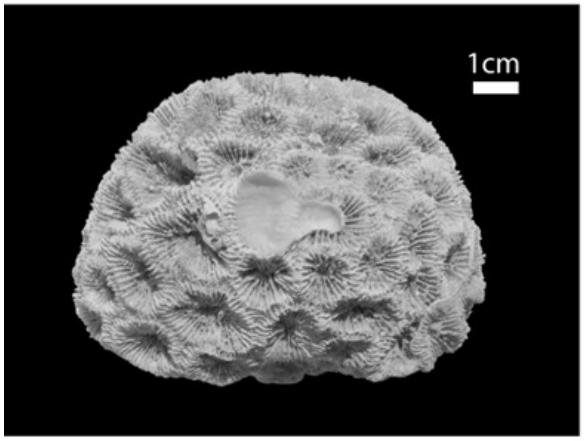

e

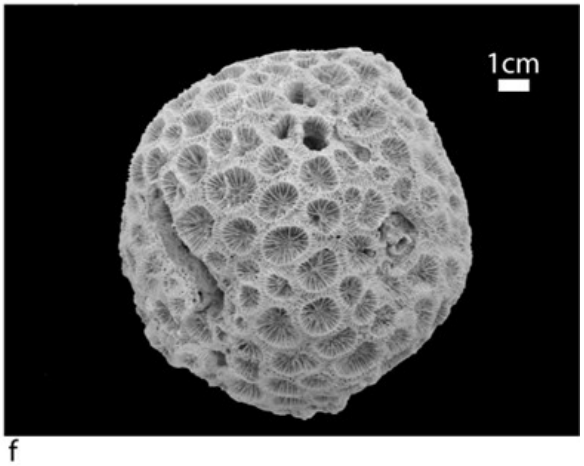

f

Plate 3.5:
a - *Echinopora forskaliana*, laminar specimen, Ras Mohammed, Egypt
b - *Echinopora forskaliana*, submassive specimen, LT48, Ras Mohammed, Egypt
c - *Echinopora forskaliana*, massive specimen, LT47, Ras Mohammed, Egypt
d - *Dipsastraea sp.*, typical preservation, Pleistocene 1, Vanuatu
e - *Favites rotundata*, Ras Mohammed, Egypt
f - *Dipsastraea pallida,* Ras Mohammed, Egypt

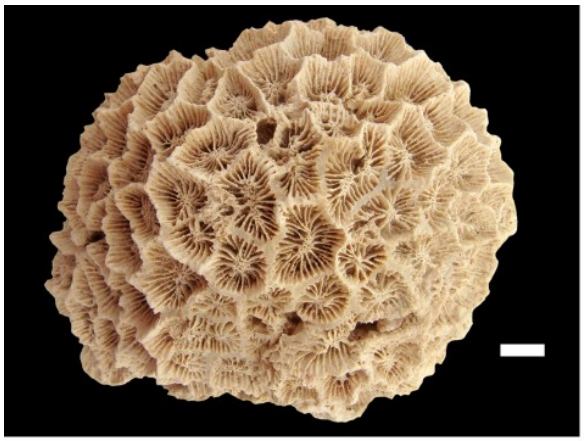
a

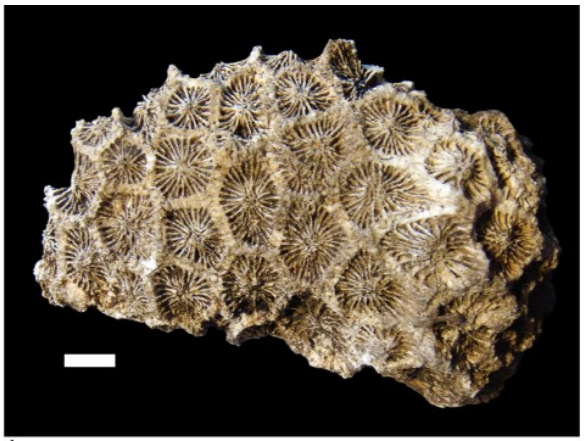
b

c

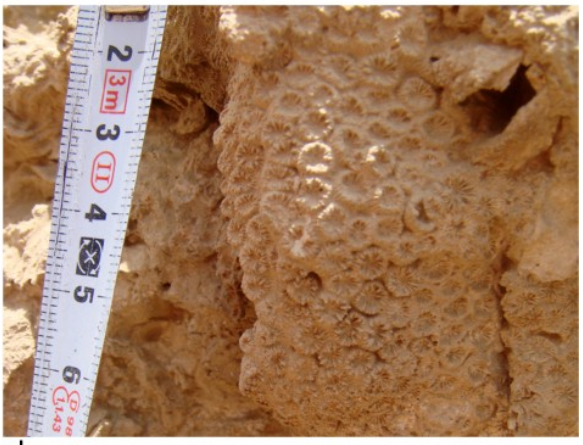

d


e

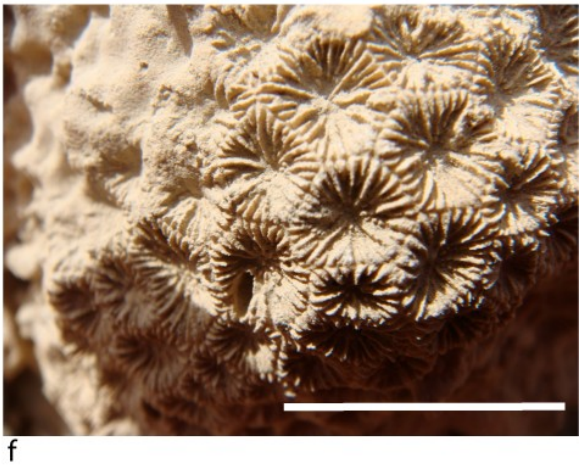
f

Plate 3.6:
a - *Favites flexuosa*, Pleistocene, Ras Mohammed, Egypt
b - *Favites pentagona,* Pleistocene 1, Vanuatu
c - *Favites* cf. *spinosa*, LT34, Ras Mohammed, Egypt
d - *Leptastrea bottae*, LT27, Dahab, Egypt
e - *Leptastrea transversa*, LT15, Dahab, Egypt
f - *Leptastrea transversa*, close-up picture of the same specimen

3.2.5.5 Genus *Leptastrea* MILNE EDWARDS & HAIME 1848

Type species: *Leptastrea roissyana* MILNE EDWARDS & HAIME 1849 = *Leptastrea purpurea* (DANA 1846)

General remarks

This genus could be identified in several Egyptian localities. Its current status is Scleractinia incertae sedis, but it is probably closely related to fungiids and Siderastreidae (Fukami *et al.* 2008; Kitahara *et al.* 2010). According to Veron's traditional taxonomy the genus belongs to "Faviidae".

Diagnosis

The genus is relatively distinctive with its small, cerioid to subplocoid corallites that are only between 2.5 and 6 mm in size. The colonies are massive or encrusting. The skeleton is dense and there is an intercorallite groove where the costae terminate. However, identification at the species level is more difficult, due to strong similarities among species and missing samples.

Leptastrea transversa KLUNZINGER 1879

(Plate 3.6 e-f)

Diagnosis

The species forms massive colonies with rounded to polygonal corallites that are 3 to 5 mm in size. The septa are in four cycles, of which the first two are almost equally developed, and plunge steeply near the columella.

Ecology

The species is relatively common in a wide range of habitats, and prefers exposed reef slopes with clear to moderately turbid water.

Leptastrea bottae MILNE EDWARDS & HAIME 1849

(Plate 3.6 d)

Original name	*Cyphastrea bottae* MILNE EDWARDS & HAIME 1849
Synonymized names	*Cyphastrea bottae* MILNE EDWARDS & HAIME 1849 (original combination, basionym) *Leptastrea agassizi* VAUGHAN 1907 (synonym?) *Leptastrea hawaiiensis* VAUGHAN 1907 (synonym?) *Leptastrea immersa* KLUNZINGER 1879 *Leptastrea solida* MATTHAI 1914 (synonym) *Orbicella (Leptastrea) bottae* (MILNE EDWARDS & HAIME 1849) (previous combination) *Orbicella (Leptastrea) inaequalis* (KLUNZINGER 1879) (synonym)

Diagnosis

The colonies are massive to encrusting with circular and cylindrical corallites. The septa are arranged in three cycles, the longest being distinctively larger and exert.

Ecology

This species occurs in all shallow reef environments.

3.2.5.6 Genus *Goniastrea* MILNE, EDWARDS & HAIME 1848

Type species: *Astrea retiformis* LAMARCK 1816 = *Goniastrea retiformis* (LAMARCK 1816)

General remarks

Goniastrea is a common genus and occurs in almost all studied localities. However, its taxonomic evaluation is similarly complicated as that of *Dipsastraea* and *Favites.* The genus is strongly polyphyletic and cannot be unequivocally solved phylogenetically at this point (Huang *et al*. 2014). *Goniastrea* loses several members, and potentially gains at least one new member from "*Favia*" (*Dipsastraea stelligera*). The nine accepted species of *Goniastrea* (*G. columella, G. edwardsi, G. favulus, G. minuta, G. pectinata, G. ramosa, G. retiformis, G. stelligera,* and *G. thecata)* are

probably more closely related to *Merulina* and *Scapophyllia* than to *Favia* and *Favites* (Huang at al. 2014). The two most common *Goniastrea* species (*G. edwardsi* and *G. retiformis*) within my study remain in this genus, while *Goniastrea aspera* was moved to the resurrected genus *Coelastrea* VERRILL 1866 together with one former *Favia* species, and is apparently not closely related to *Goniastrea*. For the former *Goniastrea peresi* Huang *et al*. (2014) erected the new genus *Paramontastraea* HUANG & BUDD 2014 (see below at species description).

Diagnosis

The colonies are massive and possess cerioid corallites, while some species become sub-meandroid to meandroid. Intratentacular budding gives rise to equal-sized daughter corallites rather than the unequal sizes produced in *Favites*. Paliform lobes are mostly well developed and characteristic.

Ecology

This genus is often dominant on intertidal mudflats, rock platforms and reef flats (Veron 2000). Some species are very well adapted to withstand aerial exposure.

Goniastrea retiformis (LAMARCK 1816)

(Plate 3.7c-d)

Original name	*Astraea retiformis* LAMARCK 1816
Synonymized names	*Astraea eximia* DANA 1846 (synonym) *Astraea retiformis* LAMARCK 1816 (original combination, basionym) *Astraea spongia* EHRENBERG 1834 (synonym) *Astrea retiformis* LAMARCK 1816 (new combination) *Goniastrea bournoni* MILNE EDWARDS & HAIME 1849 (synonym)

General remarks

This is by far the most common species that could be identified in the field, especially in Egypt. It is relatively distinct and may be a dominant species in certain localities (see results). Veron (2000) and other authors distinguish it from *Goniastrea edwardsi*, which is highly similar to *G. retiformis*. Differences are minor and Scheer & Pillai (1981) lump both species together. Nevertheless, here I follow Veron (2000) and distinguish these species.

Diagnosis

This species forms massive colonies that tend to grow large, over 1 m across, while the corallites are small and usually only 3 to 4 mm in diameter. The calices are four to six sided and deep, with thin, sharp walls. The septa are in three cycles and alternate strongly. The first order septa bear thin, well developed paliform lobes.

Ecology

G. retiformis occurs on shallow water reef slopes. It is always a member of reef flat communities and especially abundant in areas where water temperatures and salinity may rise.

Goniastrea edwardsi CHEVALIER 1971

(Plate 3.9a)

Original name	*Goniastrea edwardsi* CHEVALIER 1971
Synonymized names	*Astraea parvistella* DANA 1846 (synonym?) *Goniastrea capitata* STUDER 1880 (synonym?) *Goniastrea parvistella* (DANA 1846) (synonym?) *Goniastrea solida* MILNE EDWARDS & HAIME 1848 (synonym?)

General remarks

This species could be identified in the Egyptian localities.

Diagnosis

As mentioned above *G. edwardsi* is very similar to *G. retiformis*. Both build large colonies with small corallites, but septa are more irregular and the paliform lobes on the first cycle are thick. The walls of the calices are broader and less sharp. The colonies appear less regular than those of *G. retiformis.*

Ecology

This species is widespread on all clear water reef slopes. It is ecologically more generalist than *G. retiformis*.

3.2.5.7 Genus *Coelastrea* VERRILL 1866

Coelastrea aspera (VERRILL 1866)
(Plate 3.9b)

Original name	*Goniastrea aspera* VERRILL 1866
Synonymized names	*Astraea (Fissicella) magnifica* (DANA, 1846) (synonym) *Favites aspera* (VERRILL 1866) (previous combination) *Goniastrea aspera* VERRILL 1866 (original combination, basionym) *Goniastrea equisepta* NEMENZO 1959 (synonym) *Goniastrea incrustans* DUNCAN 1889 (synonym) *Goniastrea mantonae* CROSSLAND 1952 (synonym) *Goniastrea spectabilis* (VERRILL 1872) (synonym) *Prionastraea spectabilis* VERRILL 1872 (synonym)

General remarks

One specimen of *C. aspera* could be identified in the Pleistocene terraces of Vanuatu and Egypt, respectively.

Diagnosis

This species is quite similar to other monocentric species of *Goniastrea*, especially to *G. retiformis*, but the corallites are larger (> 5mm). The colonies are massive to encrusting with thick walled corallites that are angular in shape. Paliform lobes are poorly developed, which is untypical for *Goniastrea*.

Ecology

It is usually found in intertidal habitats where different colonies may adjoin to form large colonies that can reach sizes over 5 m across, so that it may be a dominant species. It also occurs in most shallow, tropical reefs in protected turbid environments until 15 m depth with smaller colonies.

Plate 3.7 (next page):
a - *Goniastrea edwardsi*, Holocene, Vanuatu, picture taken by J. Millet
b - *Coelastrea aspera*, Pleistocene 1, Vanuatu
c - *Goniastrea retiformis*, Ras Mohammed, Egypt
d - *Goniastrea retiformis*, close-up of the corallite details, same colony
e - *Paramontastraea peresi,* with scalloped, leafy margin, Ras Mohammed, Egypt
f - *Paramontastraea peresi,* same colony with view on corallites

a

b

c

d

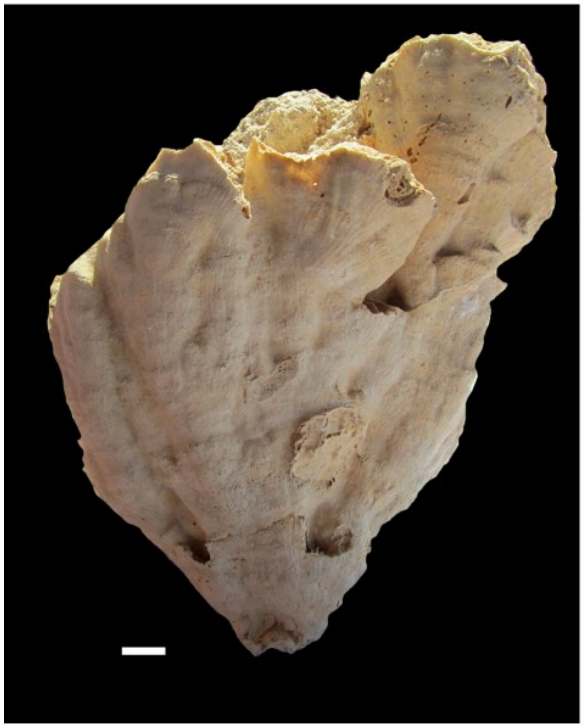

e

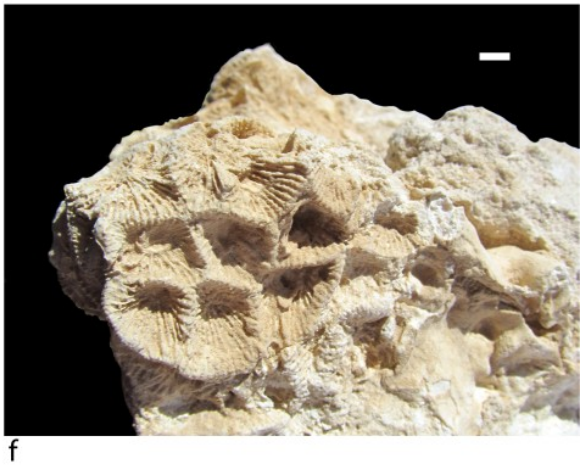

f

3.2.5.8 Genus *Paramontastraea* HUANG & BUDD 2014

Paramontastraea peresi (FAURE & PICHON 1978)
(Plate 3.7e-f)

Original name *Favites peresi* FAURE & PICHON 1978

Synonymized names
Favites peresi FAURE & PICHON 1978 (original combination, basionym)
Goniastrea peresi (FAURE & PICHON 1978) (previous combination)

General remarks

This species was identified in Egyptian localities and is relatively distinct. However, its generic position is again problematic. Before Veron (2000) moved it into *Goniastrea* this species belonged to *Favites*, but it seems that neither of these genera has close affinities to this species (Huang *et al.* 2014). The latter authors erect the genus *Paramontastraea* for *Goniastrea peresi*, *Montastrea serageldini*, and *Plesiastrea salebrosa*.

Diagnosis

The characteristically scalloped colony margin is partially preserved in only one of the collected specimens. Nevertheless, the corals could be identified with confidence. The angular calices are about 10 to 20 mm across, and 6 to 10 mm deep. The walls are thin and sharp and the septa low and thin. The numerous septa are narrow and bear a conspicuous ring of paliform lobes around the columella.

Ecology

In contrast to most other species of this genus *Goniastrea*, *P. peresi* is less common in environmentally stressed areas, and rare on reef crests and flats. It usually occurs in shallow reef environments.

3.2.5.9 Genus *Leptoria* MILNE EDWARDS & HAIME 1848

Type species: *Meandrina phrygia* (ELLIS & SOLANDER, 1786) = *Leptoria phrygia* (ELLIS & SOLANDER, 1786)

General remarks

This genus only contained one species until 1990, when Veron erected a second species.

Diagnosis

This massive genus is characterized by its long and sinuous, neatly arranged valleys, which is a distinctive feature.

Leptoria phrygia (ELLIS & SOLANDER 1786)
(Plate 3.7a-b)

Original name *Madrepora phrygia* ELLIS & SOLANDER 1786

Synonymized names
Leptoria gracilis (DANA 1846) (synonym)
Leptoria tenuis (DANA 1846) (synonym)
Madrepora phrygia ELLIS & SOLANDER 1786 (original combination, basionym)
Maeandrina gracilis DANA 1846 (synonym)
Maeandrina phrygia (ELLIS & SOLANDER 1786) (previous combination)
Maeandrina tenuis DANA 1846 (synonym)
Meandrina phrygia (ELLIS & SOLANDER 1786) (previous combination)
Platygyra gracilis (DANA 1846) (synonym)
Platygyra phrygia (ELLIS & SOLANDER 1786) (previous combination)

General remarks

L. phrygia was relatively common in the localities of Vanuatu, but was not found in the Egyptian study areas.

Diagnosis

This meandroid species is distinct, because its valleys are particularly long with extensive straight sections. The valleys are narrower than those of *Platygyra* species with an average depth of 4 mm. The columella is usually vertically undulated and sometimes interrupted.

Ecology

The species is common and largely restricted to shallow waters.

3.2.5.10 Genus *Astrea* LAMARCK 1801

(Plate 3.8d, *Astrea sp.*)

Type species: *Astrea guettardi* DEFRANCE 1826 † Miocene, Dax (Atlantic).

General remarks

The traditional genus *Montastrea* VAUGHAN & WELLS 1943 has always been problematic and not clearly defined. Molecular studies have shown that it is not monophyletic and should therefore be revised. It contains Atlantic and Pacific members that are clearly not closely related (Fukami *et al.* 2008). Consequently, the genus was split into three different genera (Budd *et al.* 2012), of which two belong to the newly defined Merulinidae. The former *Montastrea annularis* complex was assigned to *Orbicella* DANA 1846, while the other Atlantic species remain are now referred to as *Montastraea* BLAINVILLE 1830. The Indo-Pacific *Montastrea* species were assigned to the resurrected genus *Phymastrea* MILNE EDWARDS & HAIME 1848 (Budd *et al.* 2012) but are now placed in the resurrected genus Astrea LAMARCK 1801 (Huang *et al.* 2014). One species is preserved in the Pleistocene of Egypt, but did not occur inside transects. The specimens from Vanuatu are too poorly preserved for identification at the species level but place with Astrea.

Diagnosis

Astrea sp. builds massive colonies with monocentric and plocoid corallites. In contrast to the plocoid genera *Dipsastraea*, *Leptastrea*, and *Cyphastrea*, daughter corallites are generally formed by extratentacular budding. This usually leads to calices that are relatively more separated from each other and more conical or rounded.

Astrea curta (DANA 1846)

(Plate 3.8c)

Original name

Astrea curta DANA 1846

Synonymized names

Astraea lamarckiana MILNE EDWARDS & HAIME 1849 (synonym)
Astraea laperousiana MILNE EDWARDS & HAIME 1849 (synonym)
Astraea quadrangularis MILNE EDWARDS & HAIME 1849 (synonym)
Astraea solidior MILNE EDWARDS & HAIME 1849 (synonym)
Montastraea curta (DANA 1846) (previous combination)
Montastrea curta (DANA 1846) (previous combination, wrong genus spelling)
Orbicella coronata DANA 1846 (synonym)
Orbicella curta DANA 1846 (original combination, basionym)
Orbicella funafutensis GARDINER 1899 (synonym)
Orbicella rotumana GARDINER 1899 (synonym)
Orbicella vacua CROSSLAND 1952 (synonym)
Orbicella wakayana GARDINER 1899 (synonym)
Phymastrea curta (DANA 1846) (previous combination)

a

b

c

d

e

f

Plate 3.8:
a - *Leptoria phrygia*, Pleistocene 1, Vanuatu
b - *Leptoria phrygia*, Pleistocene 3, large colony, Vanuatu
c - *Astrea curta*, Ras Mohammed, Egypt
d - *Astrea* sp., Pleistocene 3, Vanuatu
e - *Gyrosmilia interrupta*, several colonies growing on each other, Ras Mohammed, Egypt
f - *Gyrosmilia interrupta*, close-up of above colony, Pleistocene, Ras Mohammed, Egypt

General remarks

A. curta plots close to *Cyphastrea* in Fukami's *et al.* (2008) study and has recently been assigned to the genera *Phymacea* (Budd *et al.* 2012) and *Astrea* (Huang *et al.* 2014). *Astrea curta* is the latest synonym. This species is represented by only one specimen from Egypt, and was not encountered in transects.

Diagnosis

The circular corallites of this species are 4 to 7 mm in size and plocoid. The septa are arranged in three cycles, with the first two being almost indistinguishable. The first order septa possess paliform lobes.

Ecology

Sheppard & Sheppard (1991) observed this species mainly in the mid-depths of fore-reef slopes, whereas Veron (2000) mentions that it especially occurs on reef flats.

3.2.5.11 Genus *Platygyra* EHRENBERG 1834

(Plate 3.9a - *Platygyra sp.*)

Type species: *Platygyra labyrinthica* EHRENBERG 1834 = *Platygyra lamellina* (EHRENBERG 1843)

General remarks

Platygyra occurs in all study areas, but is more abundant in Egyptian localities than in Vanuatu. Identification at the species level is challenging, because all species show similar skeletal modifications along environmental gradients, and some species are generally similar. In Vanuatu identification was especially difficult due to strong erosional processes that deleted skeletal details. Nevertheless, one relatively distinct species was identified. In Egypt, identification was sometimes easier, when species occurred next to each other and could be directly compared.

Diagnosis

The colonies of this genus are massive and usually meandroid, only a few are monocentric or sub-meandroid. There are no paliform lobes and the columellae do not have centers, but spongy structures.

Platygyra crosslandi (MATTHAI 1928)

(Plate 3.9f)

Original name *Coeloria crosslandi* MATTHAI 1928

Synonymized names *Coeloria crosslandi* MATTHAI 1928 (original combination, basionym)

General remarks

P. crosslandi is relatively distinct and occurred in Egyptian localities.

Diagnosis

This species forms short valleys with 1.5 to 2 mm thick and rounded walls. The septa are thickened at the wall and bear exert irregular teeth. Columellae may be developed.

Ecology

It occurs in most shallow reef environments.

Platygyra pini CHEVALIER 1975

(Plate 3.9b)

General remarks

This species could be identified in some localities of Vanuatu, but was not abundant.

Diagnosis

P. pini is a monocentric to short valley species and therefore distinct. The walls are thick and have rounded edges. The septa are thin and evenly spaced.

Ecology

This species usually occurs in all shallow reef environments.

Platygyra daedalea (ELLIS & SOLANDER 1786)
(Plate 3.9c, e)

Original name *Madrepora daedalea* ELLIS & SOLANDER 1786

Synonymized names
Astroria astraeiformis MILNE EDWARDS & HAIME 1849 (synonym)
Astroria daedalea (ELLIS & SOLANDER 1786) (previous combination)
Astroria esperi MILNE EDWARDS & HAIME 1849 (synonym)
Caeloria daedalea (ELLIS & SOLANDER 1786) (previous combination)
Coeloria astraeiformis (MILNE EDWARDS & HAIME 1849) (synonym)
Coeloria daedalea (ELLIS & SOLANDER 1786) (previous combination)
Coeloria esperi (MILNE EDWARDS & HAIME 1849) (synonym)
Coeloria rustica (DANA 1846) (synonym)
Madrepora daedalea ELLIS & SOLANDER 1786 (original combination, basionym)
Maeandra astraeiformis (MILNE EDWARDS & HAIME 1849) (synonym)
Maeandra daedalea (ELLIS & SOLANDER 1786) (previous combination)
Maeandrina daedalea (MILNE EDWARDS & HAIME 1849) (previous combination)
Maeandrina rustica DANA 1846 (synonym)
Meandrina daedalea (ELLIS & SOLANDER 1786) (previous combination)
Platygyra astraeiformis (MILNE EDWARDS & HAIME 1849) (synonym)
Platygyra esperi (MILNE EDWARDS & HAIME 1849) (synonym)
Platygyra rustica (DANA 1846) (synonym)

General remarks

This is the most common of all *Platygyra* species and common in Egyptian localities. It probably also occurs in Vanuatu, but could not be identified with sufficient confidence.

Diagnosis

P. daedalea is fully meandroid with valleys that are 5 to 7 mm wide and 5 to 8 mm deep. The walls are angular and the septa exert and in two orders. The columella is ragged, but the centers are distinct.

Ecology

P. daedalea occurs in most reef environments over all depths except on reef flats.

Platygyra lamellina (EHRENBERG 1834)
(Plate 3.9d)

Original name *Maeandra lamellina* EHRENBERG 1834

Synonymized names
Coeloria arabica KLUNZINGER 1879 (synonym)
Coeloria bottai MILNE EDWARDS & HAIME 1849 (synonym)
Coeloria forskaliana MILNE EDWARDS & HAIME 1849 (synonym)
Coeloria lamellina (EHRENBERG 1834) (previous combination)
Coeloria laticollis MILNE EDWARDS & HAIME 1849 (synonym)
Coeloria leptoticha KLUNZINGER 1879 (synonym)
Coeloria subdentata MILNE EDWARDS & HAIME 1849 (synonym)
Maeandra lamellina EHRENBERG 1834 (original combination, basionym)
Meandrina lamellina (EHRENBERG 1834) (previous combination)
Platygyra labyrinthica EHRENBERG 1834 (synonym)

General remarks

This species is similar to *P. daedalea* in terms of valley size and general appearance, but there are skeletal differences.

Diagnosis

P. lamellina is fully meandroid. The walls are thicker than those of *P. daedalea*, and its septa are uniformly exert and rounded. The columella may be well developed, but does not form distinct centers.

Ecology

As *P. daedalea*, it is unspecific, but prefers backreef margins.

Plate 3.9 (next page):
a - *Platygyra sp.*, typical preservation, Pleistocene 1, Vanuatu
b - *Platygyra pini*, Pleistocene 1, Vanuatu
c - *Platygyra daedalea*, Ras Mohammed, Egypt
d - *Platygyra lamellina,* LT22, Dahab, Egypt
e - *Platygyra daedalea*, LT17, Dahab, Egypt
f - *Platygyra crosslandi*, LT20, Dahab, Egypt

a

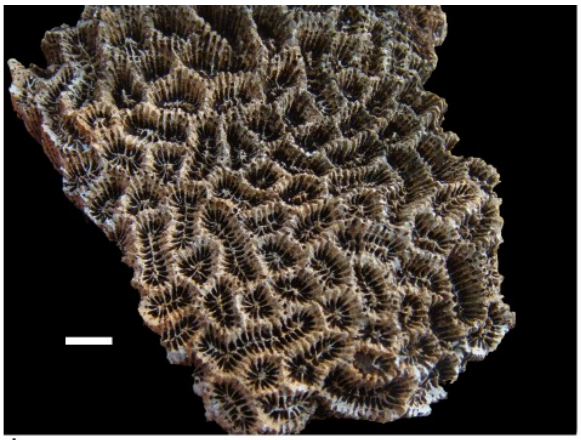

b

c

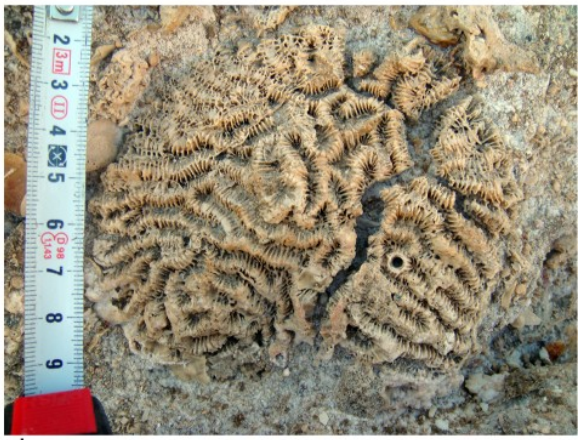

d

e

f

3.2.5.12 Genus *Hydnophora* Fischer & von Waldheim 1807

Type species: *Hydnophora demidovii* Fischer & von Waldheim 1807 = *Hydnophora exesa* (Pallas 1766)

General remarks

Hydnophora is a conspicuous genus and easy to identify even at the species level. I found one species in the Pleistocene terraces of Egypt. The genus belongs to the traditional family Merulinidae, and remains stable within the extended family Merulinidae.

Diagnosis

Hydnophores are common walls, built by septocostae that intersect and form a conical mound. They are characteristic and eponymous for this genus. The corallites sit at the base of the hydnophores and are 3.0 to 4.0 mm in size. In addition the appearance of the hydnophores is useful for identification at the species level.

Ecology

In general this genus is known to be abundant in lagoonal environments.

Hydnophora microconos (Lamarck 1816)

(Plate 3.10e-f)

Original name	*Monticularia microconos* Lamarck 1816
Synonymized names	*Hydnophora klunzingeri* Rehberg 1892 (synonym) *Hydnophorella microconos* (Lamarck 1816) (previous combination) *Madrepora exesa* Ellis & Solander 1786 (homonym, synonym) *Monticularia microconos* Lamarck 1816 (original combination, basionym)

General remarks

H. microcons occurs in both Egyptian localities, Dahab and Ras Mohammed. It is distinguished from other *Hydnophora* species by the size of its hydnophores.

Diagnosis

This species forms massive and rounded colonies with small and uniform hydnophores of 2-5 mm in size. A columella is present. The tops of adjacent hydnophores are 2 - 5 mm apart.

Ecology

This genus is environmentally unspecific and can occur in all reef environments. Nevertheless, Sheppard and Sheppard (1981) mention that this species is rarely found in a depth of more than 5 meters, thus making it an indicator for very shallow reef crests. Veron (2000) observed this species in lagoonal environments of the Pacific, but in the Red Sea especially on reef crests.

3.2.5.13 Genus cf. *Mycedium* Oken 1815

Type species: *Madrepora elephantotus* Pallas 1766 = *Mycedium elephantotus* (Pallas 1766)

General remarks

Mycedium is now assigned to the Merulinidae, along with other members of the former Pectinidae (Fukami *et al.* 2008; Kitahara *et al.* 2010; Huang *et al.* 2014b) and all other 'Bigmessidae'. The Pectinidae are polyphyletic and no longer constitute a valid family.

Diagnosis

The colonies are laminar and composed of thin plates. The corallites do not possess thecal walls. Two specimens could be identified in Egypt, one in Vanuatu. Due to their poor preservation they could not be examined more closely, but were assigned to the genus cf. *Mycedium* sp. *Mycedium* has characteristically nose-shaped corallites with only one side of the wall projecting up to 8 mm. The corallites are 6 to 12 mm in diameter and the coenosteum is costate.

Ecology

This genus occurs in sheltered reef environments.

3.2.6 Fungiidae DANA 1846

The Fungiidae are a distinctive and well defined family traditionally consisting of mostly solitary and free-living zooxanthellate corals. It is one of the four families that remains monophyletic (Fukami *et al.* 2008), but it gains new members that are not solitary and free-living: *Leptastrea* (further analyses necessary; Huang *et al.* 2014), *Psammocora*, *Coscinaraea* and *Oulastrea*. The latter genera are described here in the context to their traditional relatives. Fungiidae (including newly assigned genera) are restricted to the Indo-Pacific, and occur in the Pleistocene of Vanuatu as well as in Egypt.

The solitary genera have septo-costae radiating as septa from the mouth on the upper surface and as costae from the center of the undersurface. This conspicuous appearance also gave them their common name "mushroom corals". The solitary genera usually can be found on coarse sand. Only few species, which usually belong to *Cycloseris,* can be found on fine sands or mud. However, in the Red Sea, most of the species are common on reefs and unconsolidated coral rubble where the slope is less than 45° steep (Sheppard & Sheppard 1991).

3.2.6.1 Genera *Fungia* Lamarck 1801 and *Cycloseris* MILNE EDWARDS & HAIME 1849

(Plate 3.10a-c, *Fungia sp.*)

Type species: *Madrepora fungites* LINNAEUS 1785 = *Fungia fungites* (LINNAEUS 1785)

General remarks

These two genera are treated as a single complex as they are only distinguished by their size and a few skeletal details. In contrast to *Cycloseris*, *Fungia* usually occurs in reef environments, which makes it most likely that the specimens from this study belong primarily to *Fungia*. Nevertheless some small specimens may either be juvenile *Fungia* or *Cycloseris*. Specimens could be found in Vanuatu as well as in Egypt. In the latter case, identification at genus and species levels was impossible due to missing samples, and the preservation of the samples from Vanuatu was too poor for a reliable identification. If a solitary coral was preserved within the transect, it was mostly covered with matrix and only parts of the specimens could be observed.

Diagnosis

The species of these two genera are free-living and solitary. *Cycloseris* is usually smaller than 5 cm, whereas *Fungia* grows larger than 5 cm, i.e. up to 30 cm. Both are circular and expose one central mouth. *Fungia* can also be elongate. The septae of *Fungia* have larger teeth, and the costae elongate spines. The costae and septa of *Cycloseris* have small, grain-like teeth.

Ecology

Cycloseris is most common on sandy substrates, whereas *Fungia* is more common on rubble and hard substrate.

3.2.6.2 Genus *Ctenactis* VERRILL 1864

Type species: *Madrepora echinata* PALLAS 1766 = *Ctenactis echinata* (PALLAS 1766)

Ctenactis echinata (PALLAS 1766)

(Plate 3.10d)

Original name *Madrepora echinata* Pallas 1766

Synonymized names
Ctenactis triangularis MONDAL & RAGHUNATHAN 2013 (synonymy)
Fungia (Ctenactis) echinata (PALLAS 1766) (previous combination)
Fungia asperata DANA 1846 (synonym)
Fungia echinata (PALLAS 1766) (previous combination)
Fungia echinata var. parvispina DÖDERLEIN 1902 (synonym)
Fungia echinata var. undulata DÖDERLEIN 1902 (synonym)
Fungia gigantea DANA 1846 (junior synonym)
Fungia pectinata EHRENBERG 1834 (synonym)
Haliglossa echinata (PALLAS 1766) (previous combination)
Herpetolithas ehrenbergii LEUCKART 1841 (synonym)
Herpetolithas ruepellii LEUCKART 1841 (synonym)
Madrepora echinata PALLAS 1766 (original combination, basionym)

General remarks

One specimen of *Ctenactis* occurred in the Holocene terrace of Vanuatu and one in the Pleistocene of Dahab. However, these specimens did not occur in the line transects or bulk samples, and thus were not used in the analyses.

Diagnosis

This genus is similar to *Fungia,* but distinct by its elongation and prominent axial furrow that may have one or several mouths. The collected specimens probably belong to *Ctenactis echinata* as only one central mouth is recognizable.

Ecology

Ctenactis echinata is a common and widespread fungiid coral. It can be found on fore- and backreef slopes and rubble, but not on soft substrate, between 5 and 25 m depth.


a


b


c

d


e


f

Plate 3.10:
a - ***Fungia sp.***, LT49, Ras Mohammed, Egypt
b - ***Fungia sp.***, Holocene, Vanuatu
c - ***Fungia sp.***, Ras Mohammed, Egypt
d - ***Ctenactis echinata***, Holocene, Vanuatu
e - ***Hydnophora microconos***, LT1, Dahab, Egypt
f - ***Hydnophora microconos***, Ras Mohammed, Egypt

3.2.7 Euphylliidae ALLOITEAU 1952

This family has been poorly defined before molecular studies (Fukami *et al.* 2008), have shown that the family is polyphyletic. It loses and gains several new members. The two relevant genera of this study have only recently been assigned to this family including two genera identified in this study (Fukami *et al.* 2008; Kitahara *et al.* 2010). The morphological characters of this family are in urgent need of a new evaluation, but one of the features that also the new members seem to share are the solid and widely spaced, exert septa, which have little or no ornamentation.

3.2.7.1 Genus *Galaxea* OKEN 1815

Type species: *Madrepora fascicularis* LINNAEUS 1767 = *Galaxea fascicularis* (LINNAEUS 1767)

General remarks

This genus formerly belonged to Oculinidae GRAY 1847, but Fukami *et al.* (2008) and Kitahara *et al.* (2010) assigned it to Euphyllidae. Oculinidae is now an exclusively azooxanthellate and Atlantic genus. *Galaxea*, however, is a zooxanthellate and hermatypic coral that can be found in the Pleistocene of Vanuatu as well as in the Pleistocene of Egypt. In the latter area it is common and sometimes dominant, building large single species stands. Two species could be identified with certainty.

Diagnosis

Galaxea has a very distinctive skeleton. The corallites are strongly plocoid, consisting of tall, thin-walled, cylindrical tubes within a porous smooth coenosteum. The number of cycles of the exert septa can be used for species identification. Columellae are usually absent or poorly developed.

Galaxea fascicularis (LINNAEUS 1767)
(Plate 3.11e, Figure 3.2.5)

Original name	*Madrepora fascicularis* LINNAEUS 1767
Synonymized names	*Galaxea aspera* QUELCH 1886 (synonym) *Galaxea ellisi* (MILNE EDWARDS & HAIME) (synonym) *Galaxea esperi* (SCHWEIGGER 1820) (synonym?) *Galaxea fragilis* QUELCH 1886 (synonym?) *Galaxea heterocyathus* ORTMANN 1889 (synonym) *Galaxea hexagonalis* (MILNE EDWARDS & HAIME 1848) (synonymy) *Galaxea hexagonalis* (MILNE EDWARDS & HAIME) (synonym?) *Galaxea hystrix* DANA 1846 (synonym) *Galaxea irregularis* (MILNE EDWARDS & HAIME) (synonym) *Galaxea lawisiana* NEMENZO 1959 (synonym) *Galaxea quoyi* (MILNE EDWARDS & HAIME) (synonym) *Galaxea tenella* BRÜGGEMANN 1879 (synonym) *Madrepora fascicularis* LINNAEUS 1767 (original combination, basionym) *Sarcinula hexagonalis* MILNE EDWARDS & HAIME 1848 (synonymy)

General remarks

This widespread species can be found in the Pleistocene of Vanuatu and Egypt. It is especially common in the Pleistocene of Egypt, but particularly occurs in single species stand patch reefs (Figure 3.2.5) rather than within larger reef bodies.

Diagnosis

G. fascicularis can build large colonies that are usually massive or columnar. Smaller colonies are encrusting or form cushions. The corallites are 7 to 15 mm in diameter and up to 10 mm exert, with septa usually in 4 cycles, of which most of them reach the columella.

Ecology

The species is ecologically unspecific as it occurs in a wide range of habitats. It may be a dominant species on inshore fringing reefs, which can be clearly observed also in the Pleistocene of

Egypt (Figure 3.2.5). *G. fascicularis* is mostly common in depths of 5 - 20 m, but can be abundant in turbid waters of less than 5 m depth.

Figure 3.2.5: *Galaxea fascicularis*, patch reef in Ras Mohammed, Egypt.

Galaxea astreata (LAMARCK 1816)
(Plate 3.11f)

Original name	*Caryophyllia astreata* LAMARCK 1816
Synonymised names	*Anthophyllum clavus* DANA 1846 (synonym) *Anthophyllum musicale* (LINNAEUS 1767) (synonym) *Caryophyllia astreata* LAMARCK 1816 (original combination, basionym) *Galaxea clavus* DANA 1846 (synonym) *Galaxea musicalis* (LINNAEUS 1767) (synonym) *Madrepora musicale* LINNAEUS 1767 (synonym?)

General remarks

This species could be identified in the Pleistocene of Vanuatu only.

Diagnosis

Colonies of *G. astreata* are submassive columnar or encrusting. The corallites are circular, not more than 3 to 4.5 mm in diameter and 2 to 3 mm exert. The septa are in 2 to 3 cycles, of which only 8 to 12 reach the columella.

Ecology

The species is known from reef environments where it is protected from strong wave action.

3.2.7.2 Genus *Gyrosmilia* MILNE EDWARDS AND HAIME 1851

Type species: *Manicina interrupta* EHRENBERG 1834 = *Gyrosmilia interrupta* (EHRENBERG 1834)

Gyrosmilia interrupta (EHRENBERG 1834)
(Plate 3.8e-f)

Original name *Manicina interrupta* Ehrenberg, 1834

Synonymized names *Manicina interrupta* Ehrenberg, 1834

General remarks

Gyrosmilia interrupta is the only known species of this genus. It was not included in the study of Fukami *et al*. (2008), who found that the newly defined Meandrinidae, to which *Gyrosmilia* traditionally was assigned, only include Atlantic genera. *Gyrosmilia* has recently been transferred to the Euphylliidae, but since two further former meandrinid Pacific genera were not included in Fukami's study, the true relationship of *Gyrosmilia* remains unclear. *G. interrupta* was found in the Pleistocene of Ras Mohammed.

Diagnosis

The colonies are up to 30 cm in size and meandroid with long valleys. The valleys formed by the corallites are about 8 mm in width, and septa of adjacent valleys often join at the top of the thin wall, where their line of contact is marked by a thin ridge. The septa have a radius over the top of the wall of 2-3 mm and plunge steeply. A columella is missing.

Ecology

Veron (2000) observed *G. interrupta* in shallow and calm reef environments, whereas Sheppard &Sheppard (1991) described this species to occur at mid to deep depths on all reef slopes (in the Arabian areas), and found it equally common in moderately turbid as well as clear water reef slopes.

3.2.8 Lobophylliidae DAI & HORNG 2009

Budd *et al.* (2012) resurrected the clade Lobophylliidae, which contains most of the former Indo-Pacific Mussidae and three genera that formerly belonged to the family Pectinidae. All mussid-like corals in this study belong to the Lobophylliidae.

However, the typical morphological characters that defined the traditional family are still valid for the new Indo-Pacific family: They are all zooxanthellate with solid skeletal structures. Also, they have large calices and prominent septal teeth. Only three genera were found in the study areas.

3.2.8.1 Genus *Acanthastrea* MILNE EDWARDS & HAIME 1848

Type species: *Acanthastrea spinosa* MILNE-EDWARDS & HAIME 1850 = *Acanthastrea echinata* (DANA 1846)

General remarks

The new position of *Acanthastrea* cannot be defined with certain, and it is probably paraphyletic within Lobophyllidae Budd *et al.* (2012). A more detailed examination is necessary - not only in molecular studies, but also in regard of morphological differences.

Diagnosis

Acanthastrea builds massive or encrusting colonies with monocentric, cerioid to subplocoid corallites that are 12 to 50 mm in size. The skeletal structures are "faviid"-like, but without paliform lobes and large septal teeth. One species that occurs in the study areas of Vanuatu as well as in those of Egypt could be identified with confidence. The other specimens are poorly preserved, so that necessary skeletal details are not well enough preserved.

Acanthastrea echinata (DANA 1846)

(Plate 3.11a)

Original name *Astraea echinata* DANA 1846

Synonymized names
Acanthastrea grandis MILNE EDWARDS & HAIME 1849 (synonym)
Acanthastrea hirsuta MILNE EDWARDS 1857 (synonym)
Acanthastrea spinosa MILNE EDWARDS & HAIME 1848 (synonymy)
Astraea echinata DANA 1846 (original combination, wrong genus spelling)
Astrea echinata DANA 1846 (original combination, basionym)
Astrea patula DANA 1846 (synonym)
Favia hirsuta (MILNE EDWARDS 1857) (synonym)
Favites hirsuta (MILNE EDWARDS 1857) (synonym)

General remarks

A. echinata occurs in almost all coral reefs throughout the Indo-Pacific. It may be confused with larger *Favites* species, when only regarding the skeleton, but the septal spines are thicker and sharper than in the latter genus.

Diagnosis

The colonies are massive and rarely grow very large. The corallites are between 10 and 25 mm in diameter and are cerioid to subplocoid and circular in shape, with thick walls. The septa have large pointed teeth.

Ecology

This species is the most common of all *Acanthastrea* species and widespread, tolerating a wide range of environments. It favors shallow water environments, including crevices on exposed reef crests.

Genus Lobophyllia DE BLAINVILLE 1830

Type species: *Madrepora corymbosa* FORSKÅL 1775 = *Lobophyllia corymbosa* (FORSKÅL, 1775)

General remarks

This genus is distinct and occurs in both study areas.

Diagnosis

Lobophyllia is distinct with its phaceloid colonies. The corallites and valleys are usually large (15 mm to 7 cm in length and 10 to 20 mm wide) and the exert septa possess very long teeth. The columella centers are distinct.

Lobophyllia corymbosa (FORSKÅL 1775)

(Plate 3.11b)

Original name *Madrepora corymbosa* FORSKÅL 1775

Synonymized names
Lobophyllia eydouxi MILNE EDWARDS & HAIME 1849 (synonym)
Lobophyllia fistulosa MILNE EDWARDS & HAIME 1849 (synonym)
Lobophyllia ringens MILNE EDWARDS & HAIME 1849 (synonym)
Lobophyllia rudis MILNE EDWARDS & HAIME 1849 (synonym)
Madrepora corymbosa FORSKÅL 1775 (original combination, basionym)
Mussa cactus DANA 1846 (synonym)
Mussa corymbosa (FORSKÅL 1775) (previous combination)
Mussa eydouxi (MILNE EDWARDS & HAIME 1849) (synonym)
Mussa fistulosa (MILNE EDWARDS & HAIME 1849) (synonym)
Mussa glomerata (MILNE EDWARDS & HAIME 1849) (synonym)
Mussa ringens (MILNE EDWARDS & HAIME 1849) (synonym)
Mussa rudis (MILNE EDWARDS & HAIME 1849) (synonym)

General remarks

L. corymbosa builds the largest colonies in this genus, sometimes reaching over 1 m in diameter (see Figure 3.2.6) in the Red Sea (Veron 2000). Outside the Red Sea colonies rarely exceed 0.5 m across. The species occurs in both study areas, but in Vanuatu colonies are much smaller than in Egypt.

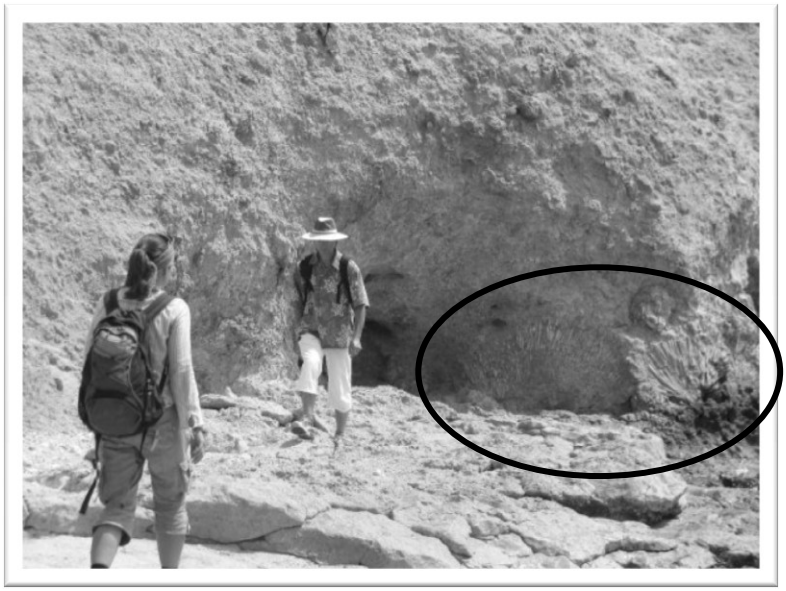

Figure 3.2.6: Some large colonies of *L. corymbosa* growing in the background, close to visitor center, Ras Mohammed, Egypt. Photo by Y. Al Sharḳawi.

Diagnosis

The species is monocentric, with frequent budding resulting in di- and tricentric calices. Nevertheless it is never meandroid. The round, monocentric calices are about 2 cm in diameter. They are deep and possess well defined walls. The septa are thick near the walls and become thinner within the calices. The septal teeth are tall and blunt, decreasing in size towards the columella.

Ecology

This species is particularly abundant in sheltered areas, especially large colonies occur exclusively in sheltered localities. It often occurs adjacent to or on sandy backreef areas and among coral rubble.

Lobophyllia hemprichii (EHRENBERG 1843)
(Plate 3.11c)

Original name

Manicina hemprichii EHRENBERG 1834

Synonymized names

Caryophyllia cristata (ESPER 1789) (synonym)
Lobophyllia aspera MILNE EDWARDS & HAIME 1849 (synonym)
Lobophyllia costata (DANA 1846) (synonym)
Lobophyllia cristata (ESPER 1789) (synonym)
Lobophyllia echinata Milne EDWARDS & HAIME 1849 (synonym)
Lobophyllia flexuosa Milne EDWARDS & HAIME 1849 (synonym)
Lobophyllia sinensis Milne EDWARDS & HAIME 1849 (synonym)
Lobophyllia tenuidentata MILNE EDWARDS & HAIME 1849 (synonym)
Madrepora cristata ESPER 1789 (synonym)
Manicina hemprichii EHRENBERG 1834 (original combination, basionym)
Mussa aspera (MILNE EDWARDS & HAIME 1849) (synonym)
Mussa brueggemanni QUELCH 1886 (synonym)
Mussa costata DANA 1846 (synonym)
Mussa cristata (MILNE EDWARDS & HAIME 1849) (synonym)
Mussa cytherea DANA 1846 (synonym)
Mussa distans KLUNZINGER 1879 (synonym)
Mussa echinata (MILNE EDWARDS & HAIME 1849) (synonym)
Mussa erythraea KLUNZINGER 1879 (synonym)
Mussa flexuosa (MILNE EDWARDS & HAIME 1849) (synonym)
Mussa hemprichii (EHRENBERG 1834) (previous combination)
Mussa multilobata DANA 1846 (synonym)
Mussa sinensis (MILNE EDWARDS & HAIME 1849) (synonym)
Mussa solida TENISON-WOODS 1879 (synonym)

Mussa studeri VON MARENZELLER 1901 (synonym)
Mussa tenuidentata (MILNE EDWARDS & HAIME 1849) (synonym)

General remarks

The species is widespread and was found in both study areas.

Diagnosis

L. hemprichii forms meandroid, phaceloid series with a single row of centers down each valley, the latter dividing irregularly as growing space permits. The septa taper in thickness from the wall to the columella and have tall, sharp teeth. The major septa are highly thickened.

Ecology

L. hemprichii is an upper reef slope species, growing near the surface to at least 20 m depth.

3.2.8.2 Genus *Symphyllia* MILNE EDWARDS & HAIME 1848

Type species: *Meandrina sinuosa* QUOY & GAIMARD 1833 = *Symphyllia sinuosa* (QUOY & GAIMARD 1833)

General remarks

This genus could only be found in the Pleistocene terraces of Vanuatu.

Diagnosis

Symphyllia is a distinct genus, because it contains large, meandroid forms that are either flat-topped or dome-shaped. The observed specimens are mostly flat-topped. The valleys are wide compared to meandroid "faviid" corals. The columellae are broad and compact and the septa are large and possess long teeth. A groove usually runs along the top of the walls.

Symphyllia recta (DANA 1846)
(Plate 3.11d)

Original name *Mussa recta* DANA 1846

Synonymized names
Mussa nobilis DANA 1846 (synonym)
Mussa recta DANA 1846 (original combination, basionym)
Symphyllia hemispherica TENISON-WOODS 1879 (synonym)
Symphyllia nobilis (DANA 1846) (synonym)

Diagnosis

The observed specimen is massive and flat on top. The valleys are 12 to 15 mm wide and highly sinuous.

Ecology

This species is common on upper reef slopes and fringing reefs.

a

b

c

d

e

f

Plate 3.11:
a - ***Acanthastrea echinata***, Holocene, Vanuatu, picture taken by J. Millet
b - ***Lobophyllia corymbosa***, Ras Mohammed, Egypt
c - ***Lobophyllia hemprichii,*** Pleistocene, Ras Mohammed, Egypt
d - ***Symphyllia recta***, Pleistocene 1, Vanuatu
e - ***Galaxea fascicularis***, within ***Acropora*** patch, Dahab, Egypt
f - ***Galaxea astreata***, Holocene, Vanuatu

3.2.9 Pocilloporidae GRAY 1842

The family Pocilloporidae is exclusively Indo-Pacific today. It retains all its conventionally assigned genera and remains monophyletic. Pocilloporidae are among the most common corals on reef flats, in lagoons, and in shallow intertidal habitats. They are considered weedy and opportunistic species and are among the first to colonize new substrates. In frequently disturbed environments, *Pocillopora* and *Stylophora* are the two dominant genera.

3.2.9.1 Genus *Pocillopora* LAMARCK 1816

Type species: *Pocillopora acuta* LAMARCK 1816

General remarks

Pocillopora contains some of the most widely distributed species, but also has many regional endemics. Today only two species live in the Red Sea. The genus can be found in the Pleistocene reefs of both Vanuatu and Egypt. All species expose a wide range of environmentally correlated growth forms, which sometimes lead to identification problems. This and the poor preservation are responsible for many unidentified *Pocillopora* specimens in my samples.

Diagnosis

Pocillopora is a conspicuous genus, due to the presence of verrucae, which cover the colonies. Verrucea are granules or wart-like nodules. The colonies are mostly arborescent, with clumped branches. The corallites are small and immersed, with 0.5-1mm in diameter and crowded so densely that the corallite walls touch each other. There is little internal structure, the septa are usually rudimentary developed in two cycles.

Pocillopora verrucosa (ELLIS & SOLANDER 1786)
(Plate 3.12a-b)

Original name	*Madrepora verrucosa* ELLIS & SOLANDER 1786
Synonymized names	*Madrepora verrucosa* ELLIS & SOLANDER 1786 (original combination, basionym) *Pocillopora danae* VERRILL 1864 (synonym) *Pocillopora hemprichi* EHRENBERG 1834 (synonym)

General remarks

This species occurred in several localities in both study areas.

Diagnosis

P. verrucosa builds usually smaller colonies than *P. damicornis*, being usually less than 50 cm across and composed of uniform upright branches. The verrucae are evenly spaced, but irregular in size.

Ecology

P. verrucosa occurs in almost all reef environments, but is especially common on fore-reef slopes of moderate exposure.

Pocillopora damicornis LINNAEUS 1758
(Plate 3.12c)

General remarks

P. damicornis is probably one of the most abundant coral species (Sheppard &Sheppard 1991). It occurs in the Red Sea as well as in the Coral Sea around Vanuatu.

Diagnosis

The colonies of this species form compact clumps that may reach a size of several meters. Branches and verrucae intergrade with each other so that there is no clear distinction between them.

It has thinner branches and less verrucae than *P. verrucosa.* It also exhibits more branching than the latter.

Ecology

This species is widely distributed, can be found in very shallow water and up to 40 m deep, in turbid and calm waters, and in lagoons and reef slopes. It is ecologically unspecific and can also tolerate sedimented conditions.

3.2.9.2 Genus *Seriatopora* LAMARCK 1816

Type species: *Seriatopora subulata* LAMARCK 1816

General remarks

This conspicuous genus could only be found in Vanuatu. All specimens could be assigned to the same species.

Diagnosis

The colonies of this genus are always branched. These branches are narrow and not more than 5 mm in diameter. They usually form thickets with needle-like tips. The calices are only about 1 mm in diameter and the coenosteum is covered by fine spinules. They possess a styliform columella and only six poorly developed septa. The corallites are more or less arranged in rows.

Seriatopora hystrix DANA 1846

(Plate 3.12 e-f)

General remarks

This is probably the most common species of this genus and the colonies may form extensive species stands. Only small pieces have been preserved, but not a single in-situ specimen. This makes sense when regarding the fragile construction of this genus. Nevertheless, whereas these small pieces never occurred isolated, they were counted only as one specimen for the bulk samples.

Diagnosis

Colonies of this species have very thin (1 to 4 mm) tapering branches. The linear alignment of the corallites is conspicuous.

Ecology

S. hystrix occurs in a wide range of reef environments and can be found on intertidal reef flats and reef slopes, but is especially abundant in backreef or lagoonal areas.

3.2.9.3 Genus *Stylophora* SCHWEIGGER 1820

Type species: *Madrepora pistillaris* ESPER 1797 = *Stylophora pistillata* ESPER 1797

General remarks

Stylophora is probably the only major genus that has a higher diversity in the western Indian Ocean and in the Red Sea than in the central Indo-Pacific. All species exhibit substantial variation in growth form along geographical and ecological gradients, which led to different views about the number of species and synonyms in the literature. Nevertheless, the identification of one species was possible.

Diagnosis

The colonies are usually branching, sometimes becoming submassive. The genus is similar to *Seriatopora*, but less fragile and not needle-like. The branches are slightly laterally flattened, have rounded tips and are usually at least 1 cm in diameter. The corallites are 0.5 to 1.5 mm in diameter

and have six main septa that unite with a styliform columella. In contrast to *Seriatopora*, the corallites of *Stylophora* are irregularly scattered.

Stylophora pistillata ESPER 1797
(Plate 3.12d)

Original name *Stylophora pistillata* ESPER 1797

Synonymized names
Madrepora pistillaris ESPER 1797 (synonym)
Pocillopora andreossyi AUDOUIN 1826 (synonym)
Porites pistillata (ESPER 1797) (previous combination)
Porites subdigitata LAMARCK 1816 (synonym)
Sideropora mordax DANA 1846 (synonym)
Sideropora pistillata (ESPER 1797) (previous combination)
Sideropora subdigitata (LAMARCK 1816) (synonym)
Stylophora cellulosa QUELCH 1886 (synonym)
Stylophora digitata (PALLAS 1766) (synonym)
Stylophora mordax (DANA 1846) (synonym)
Stylophora palmata DE BLAINVILLE 1830
Stylophora pistillaris (ESPER 1797) (synonym)
Stylophora prostrata KLUNZINGER 1879 (synonym)
Stylophora septata GARDINER 1898 (synonym)
Stylophora sinaitica BRÜGGEMANN 1877 (synonym)
Stylophora stellata VERRILL 1864 (synonym)

General remarks

This species occurs in both study areas.

Diagnosis

The colonies are usually branching with blunt-ended branches, becoming thick and submassive depending on the habitat. The corallites may be immersed, conical or hooded. Additionally to the six major septa, a second cycle of six short septa may be present. The coenosteum is covered by fine spinules.

Ecology

S. pistillata is a common species that occupies an enormous range of habitats. It may be a dominant species on exposed reef fronts, but may also occur in extreme conditions of turbidity.

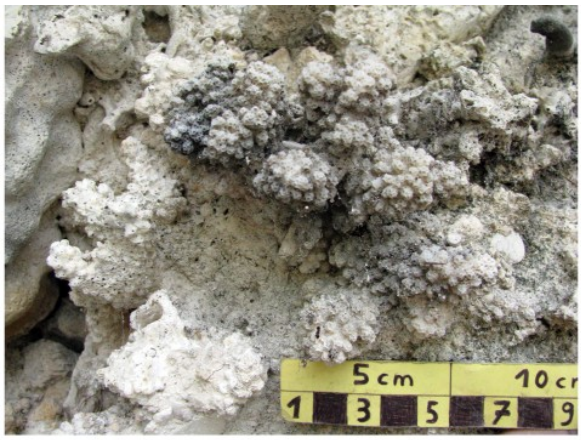

a

b

c

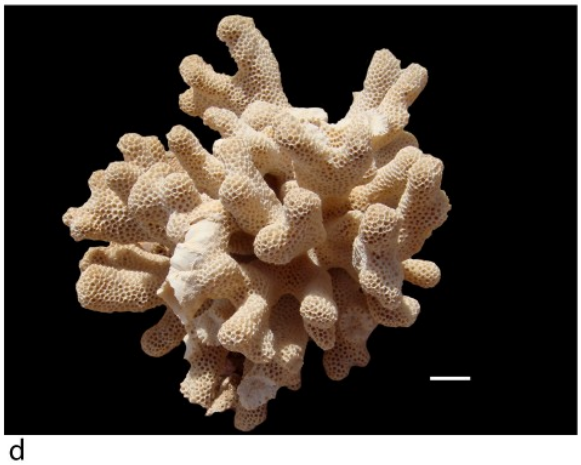

d

e

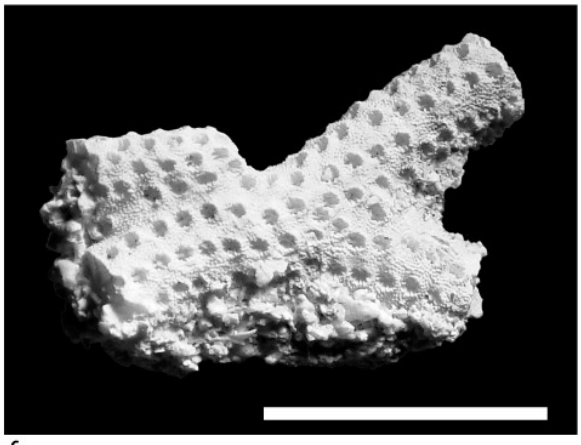

f

Plate 3.12:
a - *Pocillopora verrucosa,* in-situ position, Holocene, Vanuatu
b - *Pocillopora verrucosa*, Ras Mohammed, Egypt
c - *Pocillopora damicornis,* in-situ position, LT50, Ras Mohammed, Egypt
d - *Stylophora pistillata*, Ras Mohammed, Egypt
e - *Seriatopora hystrix*, typical preservation in matrix, Pleistocene 1, Vanuatu
f - *Seriatopora hystrix*, close-up picture of sample, Pleistocene 1, Vanuatu

3.2.10 Poritidae Gray 1842

The Poritidae are one of the non-monophyletic families, but probably can retain their family status as only genus *Alveopora* has been moved to the Acroporidae (Fukami *et al.* 2008; Kitano *et al.* 2014). However, Kitano *et al.* (2014) have shown that within this family some taxonomic changes will likely occur, but this does not affect any poritid species examined in this study. Four extant genera remain in the family, i.e. *Porites*, *Goniopora*, *Stylaraea* and the newly erected genus *Bernardpora* KITANO & FUKAMI 2014. *Porites* occurs in all tropical oceans, whereas the three other genera are exclusively Indo-Pacific.

The family is widely distributed, and tends to dominate in backreef or lagoonal habitats. Three genera have been preserved in the study areas. Especially in *Porites* corallite characters, on which identification is mainly based, are small and sometimes very variable, making some species difficult to tell apart. Also small collected fragments from colonies of unknown shape make identification often impossible. Veron (2000) provided detailed diagnostic criteria for *Porites* using details of the complex corallite structure. Most of the collected samples were not suitable for species identification. If they were, it was possible without microscopic details.

3.2.10.1 Genus *Goniopora* DE BLAINVILLE 1830

Type species: *Goniopora pedunculata* QUOY & GAIMARD 1833

General remarks

Goniopora is less problematic than *Porites* in regard of its identification, because the corallites are a little bit bigger and there are fewer genera, but in recent reefs it is mostly recognized by characters of soft tissues (always 24 tentacles that are extended day and night, specific coloration). It is common in the Pleistocene and Holocene reefs of Vanuatu, while only two specimens could be identified in the Pleistocene reefs of Egypt.

Diagnosis

Goniopora forms massive or columnar colonies. The corallites have thick porous walls, 24 compacted septa in three cycles, and columellae. The larger first 2 cycles are distinct, while the 3rd merges with the former at close proximity of the corallite wall. The corallites are 2.2 to 5.0 mm in diameter, rounded or hexagonal. The septal margins are pitted or spiny and seem to come up from the floor of the corallite.

Ecology

Extant *Goniopora* frequently forms extensive monospecific or multi-specific stands in inshore environments dominated by terrigenous sediments as well as offshore areas that are influenced by river runoff. Thus, *Goniopora* can be found in turbid water and in areas generally protected from wave action. Local dominance in certain habitats may be related to their sediment-rejecting ability. It only occurs in the Indo-Pacific.

Goniopora tenuidens (QUELCH 1886)

(Plate 3.13c)

Original name *Rhodaraea tenuidens* QUELCH 1886

Synonymized names *Rhodaraea tenuidens* QUELCH 1886 (original combination, basionym)

General remarks

This is probably the most common *Goniopora* species that could be identified in several terraces of Vanuatu, but not all specimens could be assigned with confidence due to poor preservation.

Diagnosis

The colonies can be massive, hemispherical or irregular. The corallites are rounded with thin walls and have six paliform lobes. They are closely compacted.

Ecology

Goniopora tenuidens is a common species that occurs in subtidal reef environments, especially in lagoons.

Goniopora minor CROSSLAND 1952 = *Goniopora pedunculata* QUOY & GAIMARD 1833
(Plate 3.13b)

Original name *Goniopora pedunculata* QUOY & GAIMARD 1833

Synonymized names *Goniopora minor* CROSSLAND 1952 (synonymy)

General remarks

Veron (2000) and most other authors still refer to *G. minor*, and so do I to avoid confusion, even though WoRMS (2015) regard *G. pedunculata* as the valid name.

Diagnosis

The colonies are submassive, hemispherical or encrusting, with oval or rounded corallites with thick walls that are 2-3 mm in diameter and 1 mm deep. The third cycle of septa is incomplete. The columella is well developed. There are usually 6 thick pali, which are in contact, forming a crown. All septal structures are heavily granulated.

Ecology

Goniopora minor is a common species that occurs in subtidal reef environments, especially in lagoons.

3.2.10.2 Genus *Porites* LINK 1807

(Plate 3.13e-f, 3.14a,f - *Porites sp.*)
Type species: *Porites polymorphus* LINK 1807 = *Porites porites* (PALLAS 1766)

General remarks

Porites is next to *Acropora* one of the most challenging genera, if not even the most challenging one. According to Veron (2000) there are 52 valid species, of which most are very difficult to distinguish, especially in the field, due to their similarity and small size of the corallites. The corallite characters may vary within colonies and between colonies in different environments as well as between colonies from different latitudes. *Porites* is geographically widely distributed, a true cosmopolitan. It is a common genus in the Indian Ocean and conspicuous at the genus level. Thus, it is also one of the most common genera in this study, in Egypt as well as in Vanuatu.

Diagnosis

The colonies are flat, massive, encrusting, nodular or branching. They are covered by small, immersed corallites filled with septa. The corallites are only 0.6 to 1.3 mm in size, rounded, polygonal or closely united by the walls. The septa may be visible in the calices, exposing three septal cycles. The first 2 cycles are dominant and form 12 septa with a paliform lobe at the inner end, while the 3rd cycle merges with the former at close proximity of the corallite wall. The columellae are usually submerged.

Ecology

Porites is a abundant genus in backreef margins and lagoons.

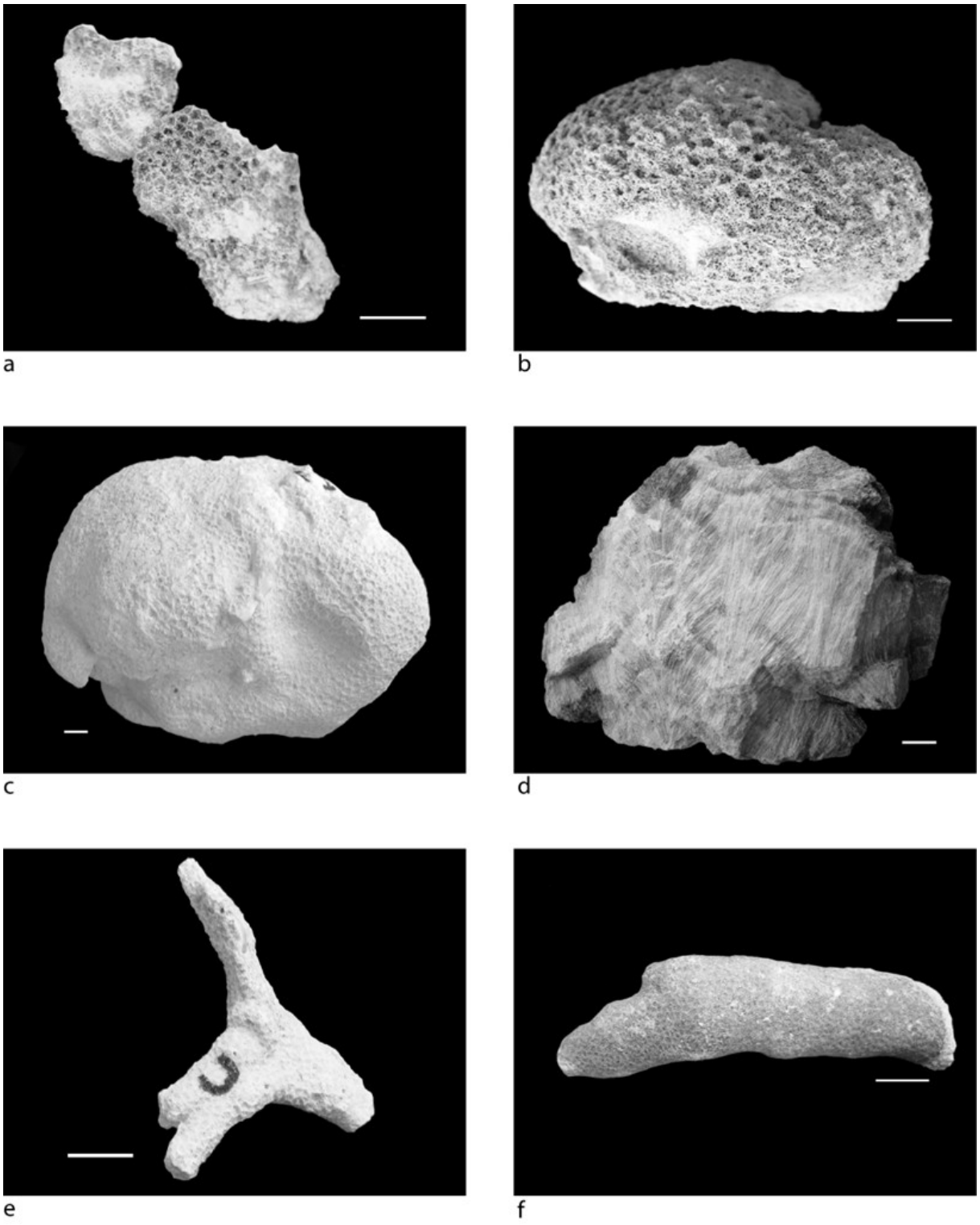

Plate 3.13:
a - *Alveopora sp.*, Holocene, Vanuatu
b - *Goniopora minor*, Holocene, Vanuatu
c - *Goniopora tenuidens*, Holocene, Vanuatu
d - *Porites lobata/lutea*, internal structure, Pleistocene 1, Vanuatu
e - *Porites sp.*, branching species, Holocene, Vanuatu
f - *Porites sp.*, different branching species, Pleistocene 1, Vanuatu

Porites lobata DANA 1846/*Porites lutea* QUOY & GAIMARD 1833

(Plate 3.14c-e)

General remarks

As it is almost impossible to distinguish between fossil *Porites lobata* and *Porites lutea* via pictures and also in the field, I decided to treat them as *Porites lobata/lutea* complex. They are similar in every sense, morphologically as well as ecologically. *Porites lobata/lutea* is common in the Pleistocene of Egypt and in the Pleistocene of Vanuatu. It is also common in the recent reefs of both areas.

Diagnosis

Porites lobata/lutea can be identified by its smooth surface, massive growth forms and sometimes huge colonies.

Ecology

They are commonly found together in backreef margins and intertidal areas, sometimes forming microatolls. Both are very common and may form huge colonies of more than four meters in size (Veron 2000). Also in the Pleistocene those giant colonies can be found.

Porites nodifera KLUNZINGER 1879

(Plate 3.14b)

Original name *Porites nodifera* KLUNZINGER 1879

Synonymized names *Porites clavaria* LAMARCK 1816 (synonym)

General Remarks

This species is restricted to the Red Sea, Persian Gulf and Eastern Africa (Veron 2000).

Diagnosis

The colonies are compact clusters of columns, which have a smooth surface. Individual colonies tend to be isolated subcolonies. Small colonies usually consist of nodular subcolonies. The corallites are polygonal, 1.5 to 1.75 mm in length, and shallow. The paliform lobes are poorly developed.

Ecology

P. nodifera is a shallow water species, generally living in less than 5 m depth and tolerating salinities of up to 48‰ (Sheppard and Sheppard 1991). Its presence is especially notable in highly saline, shallow areas where sea grass dominates. *P. nodifera* is also supposed to be common on reef slopes with normal Red Sea salinities (about 40-42 ‰), but there it does not form extensive single species stands (see Figure 3.2.7 for a fossil stand), which could be observed in the lowermost reef zone at Dahab. Huge single species stands of *P. nodifera* can also be observed today in very shallow areas of the Gulf of Aqaba (personal observation).

Figure 3.2.7: *Porites nodifera*, single species stands in patch reefs along the coast north of Dahab.

a

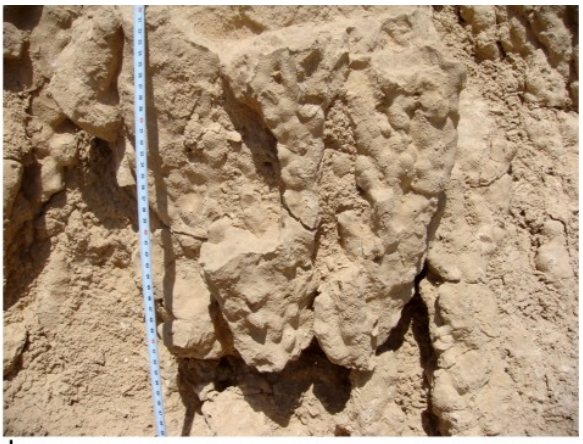

b

c

d

e

f

Plate 3.14:
a - *Porites sp.*, branching species, LT40, Ras Mohammed, Egypt
b - *Porites nodifera*, Dahab, Egypt
c - *Porites lobata/lutea*, large colony, Ras Mohammed, Egypt
d - *Porites lobata/lutea,* Pleistocene 1, Vanuatu
e - *Porites lobata/lutea,* microatoll, LT32, Ras Mohammed, Egypt
f - *Porites sp.*, Ras Mohammed, Egypt

3.2.11 "Siderastreidae" VAUGHAN & WELLS 1943

The Siderastreidae are paraphyletic. Fukami *et al.* (2008) defined two distantly related clades, with one clade formed by the genus *Siderastrea*, which has no other close relatives, and an Indo-Pacific clade consisting of *Psammocora* and *Coscinaraea*. *Psammocora* and *Coscinaraea* are closely related to the Fungiidae (Fukami *et al*. 2008; Kitahara *et al*. 2010). However, both genera are not monophyletic and further studies are necessary to identify their phylogenetic relationships.

3.2.11.1 Genus *Psammocora* DANA 1846

Type species: *Pavonia obtusangula* LAMARCK 1816 = *Psammocora contigua* (ESPER 1794)
(Plate 3.15f)

General remarks

The taxonomy of *Psammocora* is problematic. The species are very variable, and many different names were used for one and the same species in the past. Identification at species level was not possible here. This genus was recorded several times in the Pleistocene terraces of Egypt.

Diagnosis

Psammocora can build almost all types of colony forms from massive to columnar, laminar or encrusting. The corallites of all species of this genus are conspicuously small (< 5mm) and shallow with indistinct walls. For species identification a characteristic (petaloid) pattern of septa and septocostal structures are considered.

Ecology

Psammocora is ecologically unspecific.

3.2.11.2 Genus *Coscinaraea* MILNE EDWARDS & HAIME 1848

Type species: *Coscinaraea bottae* MILNE EDWARDS & HAIME 1848 = *Coscinaraea monile* FORSKÅL 1775

General remarks

Coscinaeraea is similar to *Psammocora*, but can be distinguished by the larger size of its corallites. Two specimens were found in Ras Mohammed. Only three species occur in the Red Sea today.

Coscinaraea monile (FORSKÅL 1775)
(Plate 3.15e)

Original name	*Coscinaraea monile* Forskål 1775
Synonymized names	*Coscinaraea bottae* MILNE EDWARDS & HAIME 1848 (synonym) *Coscinaraea donnani* GARDINER 1905 (synonym)

General remarks

C. monile is distinctive. Nevertheless the species shows a wide range of habitat-related skeletal variations.

Diagnosis

The colonies of this species are usually encrusting or massive. The one collected within this study is dome-shaped and only about 10 cm in size. The species shows intratentacular budding with calices being monocentric or in short meandroid series. The calices are 3 to 7 mm across and 2 to 5 mm deep with thick walls. The septa are thick, even and finely serrated.

Ecology

C. monile is a common species in the Red Sea, especially in deeper slopes or in turbid water of back-reef slopes. It is also commonly found in holes on reef flats, but cannot tolerate salinities above 45 ppt (Sheppard & Sheppard, 1991).

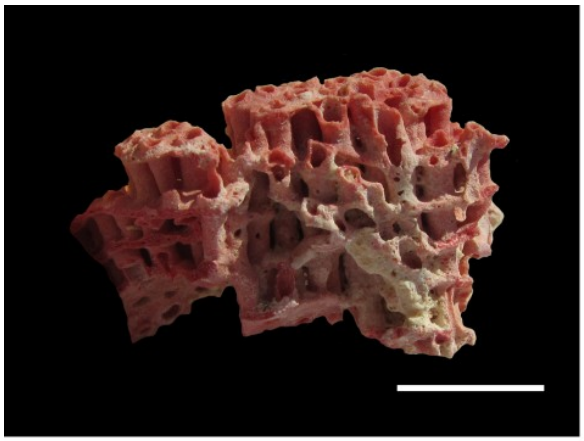

a

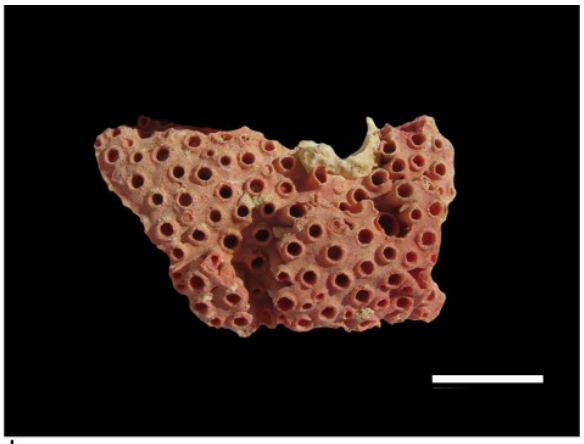

b

c

d

e

f

Plate 3.15 (previous page):
a - *Tubipora musica*, Pleistocene , Ras Mohammed, Egypt
b - *Tubipora musica,* same specimen from above
c - *Millepora sp.*, massive specimen, Pleistocene, Ras Mohammed, Egypt
d - *Millepora sp.*, recent branching specimen, Dahab, Egypt
e - *Coscinaraea monile,* LT44, Ras Mohammed, Egypt
f - *Psammocora sp.,* LT15, Dahab, Egypt

Cnidaria HATSCHEK 1888
Anthozoa EHRENBERG 1834
Octocorallia HAECKEL 1866

3.2.12 Tubiporidae EHRENBERG 1828

3.2.13 Genus *Tubipora* Linnaeus 1758

Tubipora musica LINNAEUS 1758
(Plate 3.15a-b)

Original name *Tubipora musica* LINNAEUS 1758

Synonymized names *Tubipora purpurea* PALLAS 1766 (synonym)

This genus is represented by only one species, *Tubipora musica*, which can be easily identified by its red skeleton. The color is also preserved in fossil specimens. Vertical (organ pipe-like) tubes are interconnected by irregular thin vertical folia, which led to the common name „Organ pipe coral“. This species was found in the Pleistocene of Egypt as well as in the Holocene and LIG terraces of Vanuatu.

Cnidaria HATSCHEK 1888
Hydrozoa OWEN 1843
Anthoathecatae CORNELIUS 1992

3.2.14 Milleporidae FLEMMING 1828

3.2.14.1 Genus *Millepora* LINNAEUS 1758

(Plate 3.15c-d)

Millepora is a sessile hydrozoan genus that possesses an aragonitic skeleton, and can therefore be preserved in the fossil record. However, the fossil record is scarce and the preservation often poor. Today, *Millepora* is one of the main reef builders next to scleractinian corals in tropical coral reefs. This is not mirrored in the fossil record. Especially in the Red Sea it is very common today, and probably was common in the Pleistocene, because more Pleistocene *Millepora* was found in Egypt than in the fossil terraces of Vanuatu. *Millepora* can be branching, plate-like, massive or encrusting, and can be identified by their smooth surface and the larger gastropores (gastrozooids) of about 0.1 mm that are surrounded by 5-7 smaller dactylopores (dactylozooids). Identification at the species level was not attempted. All identified specimens are referred to as *Millepora* sp.

3.3 Environmental preferences of the investigated coral species

Table 3.3.1: Environmental preferences of the taxa identified on species level. 0 = no typical occurrences, 1 = typical occurrences. A "0" in the columns "Vanuatu" or "Egypt" does not mean that the respective taxon does not occur there nowadays or during the Pleistocene, but that it was not found or identified within this study.

Species	Vanuatu	Egypt	Upper slope	Deeper slope	Backreef	Lagoon	Crest/ flat	Intertidal	turbid	calm	preferred	Depth	Salinity tolerance
Acanthastrea echinata	1	1	1	1	1	1	1	1	1	0	unspecific	shallow	unspecific
Acropora muricata	0	1	1	0	0	0	0	0	1	0	slope	shallow	unspecific
Acropora monticulosa	1	0	1	0	0	0	0	0	1	0	slope	shallow	unspecific
Astreopora myriophthalma	1	1	1	0	1	1	0	0	0	1	unspecific	shallow	unspecific
Coscinaraea monile	0	1	0	1	1	0	0	0	1	0	unspecific	deep	low
Cyphastrea serailia	1	1	1	1	1	1	1	0	1	1	unspecific	shallow	high
Echinopora forskaliana	0	1	1	1	1	1	1	0	1	1	unspecific	shallow	unspecific
Echinopora gemmacea	0	1	1	1	1	1	1	0	1	1	unspecific	unspecific	unspecific
Dipsastraea pallida	0	1	1	1	1	1	1	0	1	1	unspecific	unspecific	high
Favites rotundata	0	1	1	0	1	1	0	0	1	0	slope	unspecific	low
Favites cf. spinosa	0	1	1	1	1	1	0	0	1	1	unspecific	unspecific	unspecific
Favites flexuosa	0	1	0	1	1	1	0	0	0	1	backreef	unspecific	unspecific
Favites pentagona	1	1	1	0	1	1	0	0	1	1	unspecific	shallow	Low
Galaxea astreata	1	0	1	0	1	1	0	0	0	1	unspecific	shallow	Unspecific
Galaxea fascicularis	1	1	1	0	1	1	1	1	1	0	unspecific	shallow	Unspecific
Gardineroseris planulata	0	1	1	0	0	0	0	0	1	1	slope	unspecific	Unspecific
Coelastrea aspera	1	1	0	0	1	1	1	1	1	0	intertidal	shallow	unspecific
Goniastrea edwardsi	1	1	1	0	0	0	1	1	1	0	intertidal	shallow	high
Paramontastraea peresi	0	1	1	0	1	1	0	0	1	1	unspecific	shallow	unspecific
Goniastrea retiformis	1	1	1	0	0	0	1	1	1	0	intertidal	shallow	high
Goniopora minor	1	0	0	0	1	1	0	0	0	1	lagoon	shallow	unspecific
Goniopora tenuidens	1	0	0	0	1	1	0	0	0	1	lagoon	shallow	unspecific
Gyrosmilia interrupta	0	1	1	1	1	1	0	0	1	1	unspecific	unspecific	unspecific
Hydnophora microconos	0	1	1	0	1	1	1	1	1	1	unspecific	shallow	unspecific
Leptastrea bottae	0	1	1	0	0	1	0	0	1	1	unspecific	shallow	unspecific
Leptastrea transversa	0	1	1	0	0	0	0	0	1	1	slope	shallow	unspecific
Leptoria phrygia	1	0	1	0	1	1	0	0	0	1	unspecific	shallow	unspecific
Leptoseris mycetoseroides	0	1	1	1	1	1	0	0	0	1	unspecific	unspecific	unspecific
Lobophyllia corymbosa	1	1	1	0	1	0	0	0	0	1	backreef	shallow	unspecific

Species	Vanuatu	Egypt	Upper slope	Deeper slope	Backreef	Lagoon	Crest/ flat	Intertidal	turbid	calm	preferred	Depth	Salinity tolerance
Lobophyllia hemprichii	1	1	1	0	0	0	0	0	0	1	slope	shallow	unspecific
Aspera curta	1	0	1	0	0	0	1	0	1	1	unspecific	unspecific	unspecific
Pavona cactus	1	1	0	0	1	1	0	0	0	1	sheltered	shallow	unspecific
Pavona varians	1	0	1	1	1	1	0	0	1	1	unspecific	unspecific	unspecific
Platygyra crosslandi	0	1	1	0	1	1	0	0	1	1	unspecific	shallow	unspecific
Platygyra daedalea	1	1	1	0	1	1	0	0	1	1	backreef	shallow	unspecific
Platygyra lamellina	0	1	1	0	1	1	0	0	1	1	unspecific	shallow	unspecific
Platygyra pini	1	0	1	0	1	1	0	0	1	1	unspecific	shallow	unspecific
Pocillopora damicornis	0	1	1	1	1	1	1	0	1	1	unspecific	unspecific	unspecific
Pocillopora verrucosa	1	1	1	1	1	1	1	0	1	1	unspecific	unspecific	unspecific
Porites lobata/lutea	1	1	0	0	1	1	1	1	1	1	backreef	intertidal	unspecific
Porites nodifera	0	1	0	0	1	1	1	1	1	1	unspecific	shallow	high
Seriatopora hystrix	1	0	1	0	1	1	1	1	1	1	unspecific	shallow	unspecific
Stylocoeniella guentheri	1	0	1	0	1	1	0	0	0	1	unspecific	unspecific	unspecific
Stylophora pistillata	1	1	1	1	1	1	1	1	1	1	unspecific	unspecific	unspecific
Stylophora subseriata	0	1	1	0	1	1	1	0	1	1	unspecific	unspecific	unspecific
Symphyllia recta	1	0	1	0	0	0	0	0	1	0	slope	shallow	unspecific
Tubastraea micranthus	0	1	0	1	0	0	1	0	0	1	unspecific	crevities	unspecific
Tubipora musica	1	1	1	0	1	1	1	0	0	1	sheltered	shallow	unspecific
Turbinaria reniformis	0	1	1	0	0	0	0	0	1	0	fringing reef	shallow	unspecific

4. PLEISTOCENE AND HOLOCENE REEFS OF VANUATU

Vanuatu is extraordinarily well suited for studying Pleistocene coral reefs because of its special tectonic situation. The islands have a relatively high and constant uplift rate of up to 1 mm/a (Jouannic *et al.* 1982; Lecolle & Bernat 1985; Lecolle *et al.* 1990) in a tropical environment, which allows studying also older Pleistocene reef terraces from several interglacial episodes (Figure 4.1). Also, Vanuatu with its position at the eastern margin of the Coral Sea and south of the Coral Triangle provides high scleractinian diversity.

Figure 3.3: View from the beach close to Port-Havannah over to the island of Moso with its distinct reef terraces. Photo by W. Kießling.

4.1 Geographic Situation and Geological background

Vanuatu is a narrow volcanic archipelago in the tropical South Pacific, between latitudes 13° (Torres Group in the North) and 21°S (Aneityum in the South), and longitudes 166° and 171°E, belonging to the New Hebrides (NH) island arc system (Figure 4.1.1b). The NH island arc is located in the south-western Pacific between New Caledonia, Fiji and the Solomon Islands (Figure 4.1.1a). It also represents the eastern margin of the Coral Sea, which is one of the coral diversity hotspots, with about 300 scleractinian species (Spalding *et al.* 2001). The 83 islands of Vanuatu, of which 65 are inhabited, have a total land area of 12,190 square kilometers. The New Hebrides island arc is being significantly modified by collision with several submarine ridges and plateaus. Three collisions are presently occurring along the 1400 km length of the arc (Meffre & Crawford 2001), which are associated to the circum-Pacific seismic belt or „Ring of Fire". Thus, the tectonic situation is complex, but mainly related to the subduction of the Indo-Australian plate beneath the Pacific plate (Lecolle *et al.* 1990). The subduction zone lies approximately 120 km west of the island arc, whereas east of the arc lies the North Fiji Basin (Figure 4.1.1a). Our study site is located on Efaté Island, which is the main island with the capital Port Vila in the Southwest. Efaté is situated near the centre of the Vanuatu Archipelago and is affected by a series of periodic uplifts correlated with the different subduction zones and the active volcanism on the island. The reef facies discordantly overlies a volcanic lithology (Figure 4.1.1c) on large parts of the island (Lecolle & Bernat 1985; Lecolle *et al.* 1990). Several emerged Quaternary reef terraces can be identified, which result either from the general uplift associated with transgression and regression cycles, or from faulting (Guilcher 1974). Lecolle *et al*. (1990) took 35 U/Th datings of fossil corals from Efaté. They obtained the most complete profile in the western area, which we picked as our study area. One Holocene and four major Pleistocene terraces were identified ranging in age from 103,000 to probably 300,000 yrs. B.P. Faults are radially oriented and almost perpendicular to the terraces. The average uplift rate in this area is 0.9 - 1 mm/a (Lecolle *et al.* 1990).

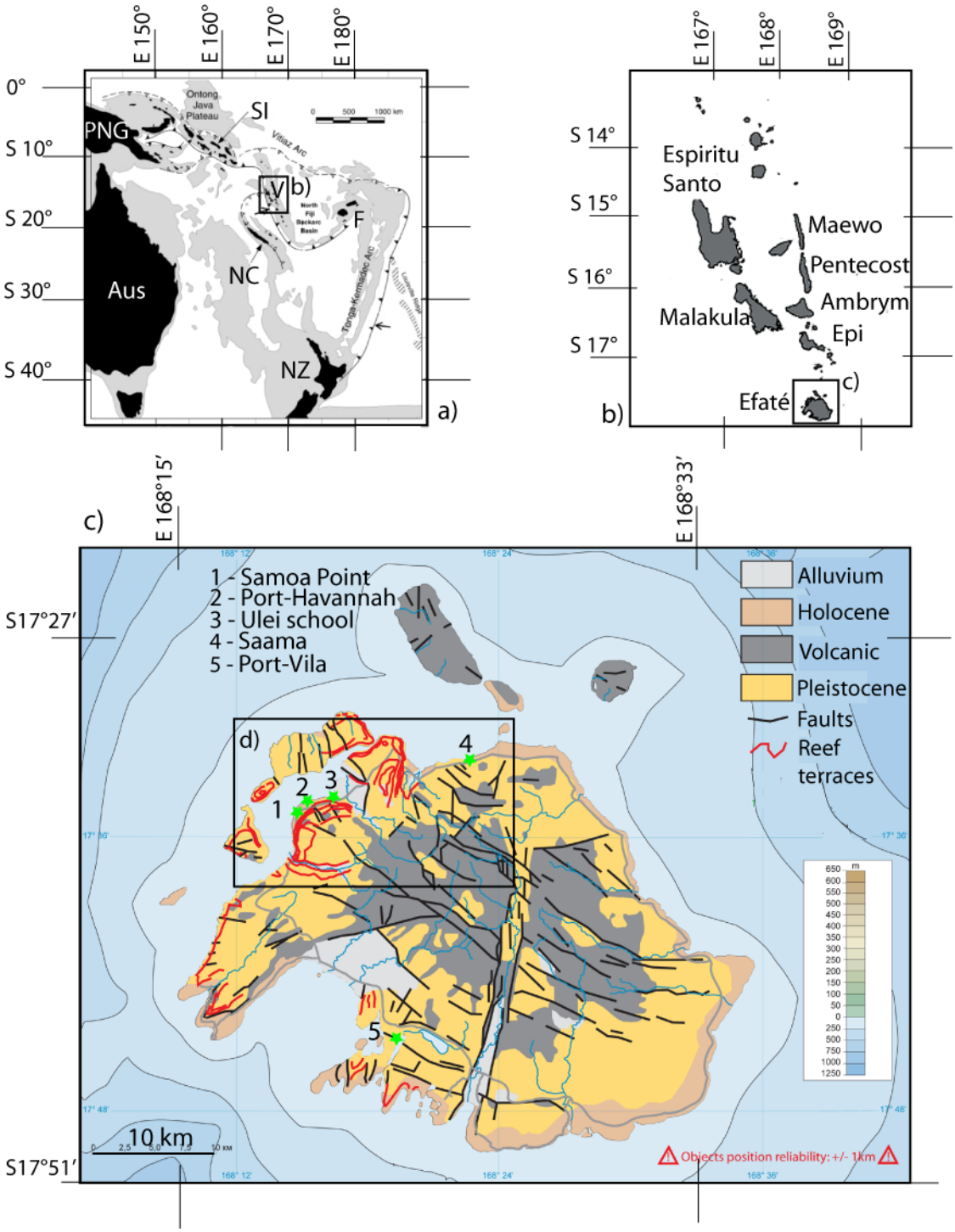

Figure 4.1.1: Geographic situation of Vanuatu and study sites. a) Tectonic map of the south-western Pacific (redrawn after Meffre & Crawford 2001). Solid lines with solid triangles show active subduction zones. The shaded area is the 2500 m contour after Kroenke (1984). Aus - Australia, PNG - Papua New Guinea, V - Vanuatu, SI - Salomon Islands, F - Fiji, NC - New Caledonia, NZ - New Zealand. b) Close-up of central Vanuatu. Efaté in the south is the island with the capital Port Vila and our study sites. c) Close-up of Efaté and its Geology. Relevant cities marked with green stars. Redrawn after Lecolle *et al.* (1990) by Julien Millet and me. Volcanic lithology includes all volcanic formations. Holocene and Pleistocene lithologies are all carbonates. d) (next page) North-western Efaté with all sites and morphological features. Map modified from Google Earth and Lecolle *et al.* (1990).

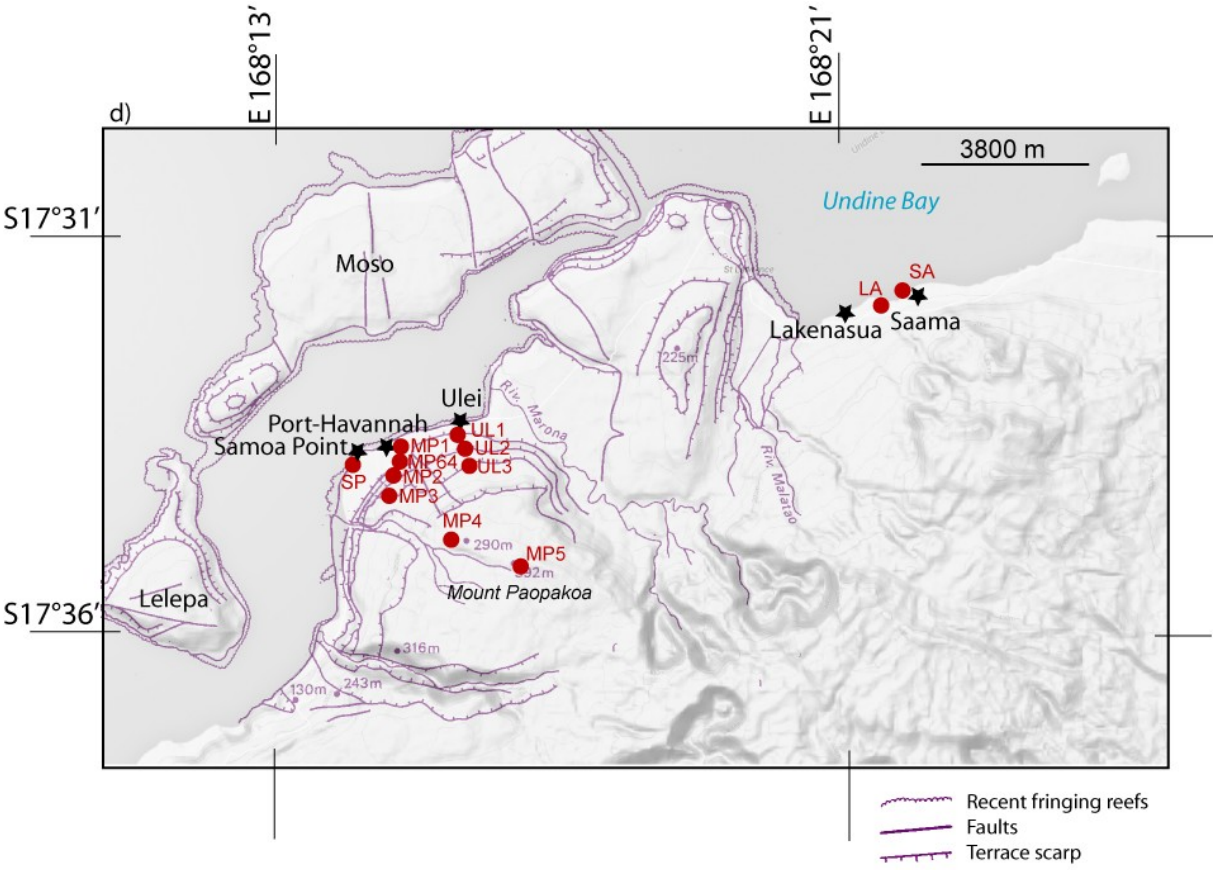

(Figure 4.1.1 continued)

Being a tropical country, Vanuatu has a relatively uniform temperature throughout the year. The warmest month is February and the coolest is August. On Efaté (Port Vila, Figure 4.1.2), the average minimum temperature in February is 22°C and the average maximum temperature 31°, while in August the average is 17°C minimum and 26°C maximum. Relative humidity ranges between 81% and 86%. Average rainfall ranges from 86 mm in August to 323 mm in March (source: Vanuatu Meteorological Services). The predominant wind flows in any season are the trade winds from the southeast.

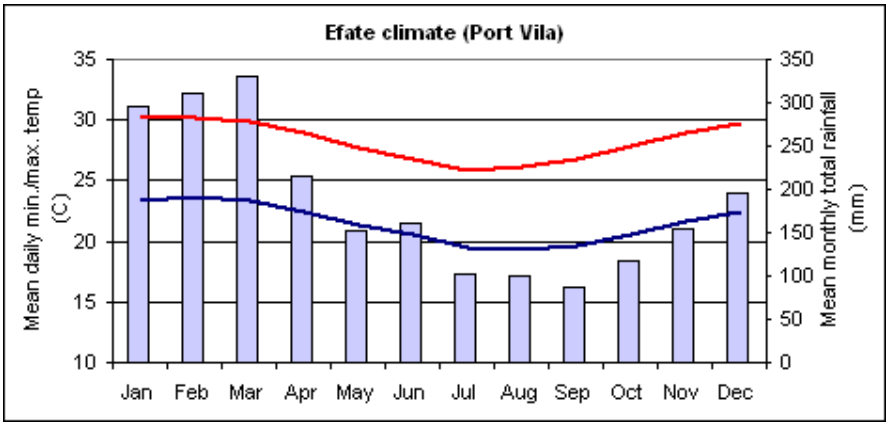

Figure 4.1.2: Climate of Efaté. Average minimum (blue) and maximum (red) temperatures and average rainfall per month. Data source: WMO-Vanuatu Meteorological Service.

The climate in Vanuatu and the geological setting around volcanoes favors the growth of coral reefs, as already observed by Darwin (1842). Efaté is surrounded by an almost continuous narrow fringing reef (Lecolle *et al*. 1990, Figure 4.1.1d) with steeply sloping forereefs close to the shores (Guilcher 1974; Done & Navin 1990). There are no barrier reefs surrounding the islands and the fringing reefs are directly exposed to the open ocean, except some smaller islands occurring close to the main islands (like Moso and Lelepa) in north-west Efaté. All fossil Quaternary coral reefs are fringing reefs as well (Guilcher 1974). They either grow (or grew) around volcanoes or around previously raised fringing reefs. The morphology and biology of Vanuatu's recent coral reefs have been studied by several authors (Guilcher 1974; Done & Navin 1990; Veron 1990). Veron (1990) provided the first list of hermatypic corals of Vanuatu listing 296 species belonging to 62 genera. For the Pleistocene, there have been several studies on the emerged Quaternary reef terraces from Vanuatu in regard of sea level events, carbonate facies and tectonics, showing that the raised reefs provide a long-term record of vertical plate motion in this complex zone, and thus a long-term record of glacial and interglacial sea-level variations as well as uplift events. However, so far there have been no studies on the ecology and diversity of Pleistocene and Holocene emerged reefs from Vanuatu.

4.2 Sites

The study sites in north-west Efaté are shown in Figure 4.1.1d. We concentrated on the few available paths through the jungle along Mount Paopakoa (aka Mount Erskine), situated south of Ulei and Port-Havannah. Mount Paopakoa is a volcano[1], on the slopes of which extensive reef growth occurred throughout the Pleistocene. Due to the uplift of the islands, several terraces are preserved, which can be inferred from isohypes on the close-up map of Figure 4.1.1d, but can be hardly seen in the field due to the dense vegetation. However, a view from the distance over to the Island of Moso (Figure 4.1) reveals the terraces. A radio mast was built on top of Mount Paopakoa, to which a small unpaved road was created. Along this road vegetation was destroyed by slash-and-burn land cleaning, which allowed us to study small exposed areas of the Pleistocene reef terraces. Based on the topography and the preservation status of the specimens, we could identify three different terraces along that road up to the mast. Fresh road sections allowed us to study better preserved samples than along our second profile, which we started directly behind our accommodation at Ulei, where we tried to find a way through the dense jungle. The slope was much steeper there and we could not reach the top of the mountain from there. Preservation was poor. The climate is tropical, and humidity and vegetation lead to strong erosional processes on lime-stones. The two profiles are shown in Figure 4.3.1 along with the dating results.

4.2.1 Ulei Profile

UL1: 17°34'18.61"S/168°16'8.81"E, ~80 m in altitude

This site is a dry creek not far above Ulei school, where strongly eroded Pleistocene limestone was covered by rubble from the creek, as well as by moss and roots. One transect (LT5 with 11.9 m in length and 120 points) was taken perpendicular to the shore.

UL2: 17°34'21.86"S, 168°16'12.63"E, ~90 m in altitude

The second site near Ulei is a burned clearing in the middle of the forest (Figure 4.2.1). The top of a fossil reef is preserved, but strongly eroded and with many gaps due to soil and vegetation. Three transects (LT1 with 15 m in length and 151 data points, LT2 with 15 m in length and 151 data points, and LT3 with 12.8 m in length and 129 points) and one bulk sample (UL2B) were taken here. Many red algae and some traces of bioerosion are conspicuous in the field.

[1] assumed by own observations. We found basalt layers among reef terraces.

Figure 4.2.1: Site UL2. The picture shows the clearing and the overall condition of this site.

UL3: 17°34'31.83"S, 168°16'18.27"E, 125 m in altitude

This poorly exposed site is situated along a fault, because one part of the N-S trending cliff N-S is higher than the other. The limestone is strongly weathered, karstified (Figure 4.2.2), and covered by vegetation. One transect (LT4 with 12.4 m in length and 125 data points) and one bulk sample (UL3B) were taken.

Figure 4.2.2: UL3 - typical outcrop situation along the Ulei profile.

4.2.2 Mount Paopakoa - Profile:

MP1: 17°34'33.81"S, 168°15'18.45"E, 22m in altitude

This is the first outcrop along the road (Figure 4.2.3) up to the radio mast on top of Mount Paopakoa. Extensive bulk sampling was done here. Next to relatively well preserved corals, a large number of molluscs and *Halimeda* chips are preserved. Corals are mainly massive or encrusting.

Figure 4.2.3: Road section at MP1. Bulk sampling was performed on the road and within the vegetated area next to it. Photo by W. Kießling.

MP55: between MP1 und MP64, around 55 m in altitude

This next road section up to Mt. Paopakoa is again rich in sandy layers that contain a large number of molluscs. Corals can be found scattered between the sands. Bulk sampling was again the method of choice.

MP64: 17°34'39.30"S, 168°15'19.78"E, ~ 80 m in altitude

Further up the road another bulk sampling was done, including 5 m of altitude difference. Many bioclasts are contained in the limestone here.

MP2: 17°34'44.85"S, 168°15'17.01"E, 105 m in altitude

Due to a steeper slope, we had the impression in the field that this was a second terrace. Next to the road, a cliff of about 8m height is exposed (Figures 4.2.4). It is a grainstone with molluscs, then algal crust and patchy corals in the top. The preservation is poor and there is dense vegetation on top and around. The limestone is very porous. Two transects (LT7 with 15 m in length and 151 points & LT8 with 11.7 m in length and 117 points) and one bulk sample were taken at the cliff and along the road next to the cliff.

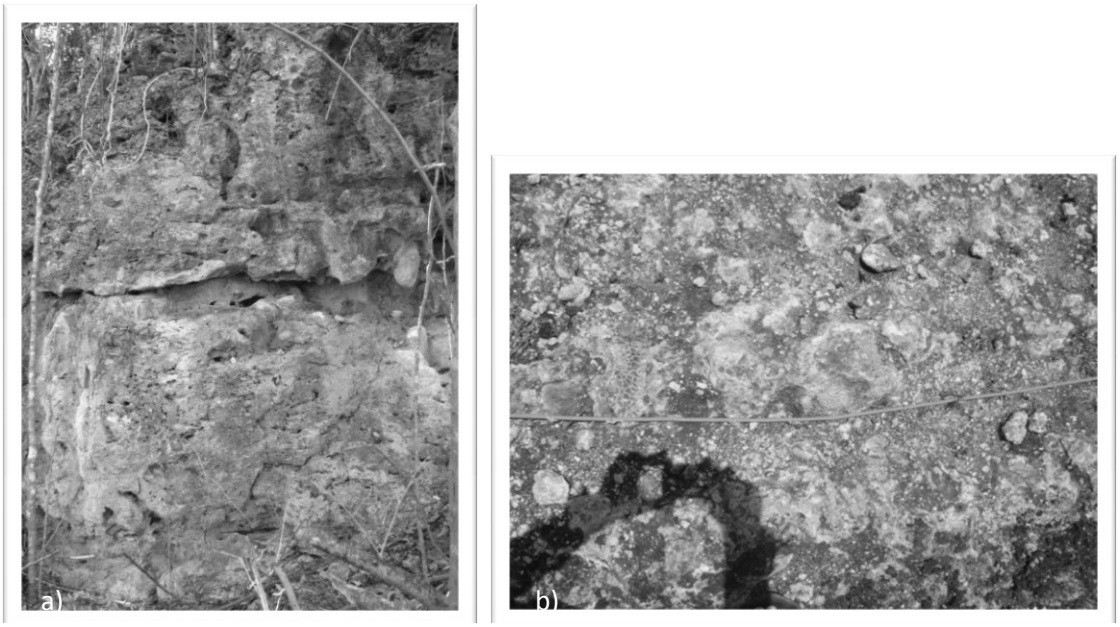

Figures 4.2.4: Cliff (a) and top of the (b) road at MP2. Massive corals dominate.

MP3: 17°34'54.71"S, 168°15'15.76"E, 130 m in altitude

This site is a plateau above MP2. The dense vegetation did again allow for bulk sampling only. Corals were encrusting, hemispherical or plate-like. The limestone matrix is a rudstone with plenty of red algal fragments, borings and gastropods. Ninety percent of the corals were found in growth position.

MP4: 17°35'25.83"S, 168°16'5.99"E, 297 m in altitude

Almost on top of Mount Paopakoa along a relatively fresh road (Figure 4.2.5), a bulk sample and a transect perpendicular to the shore (LT6 with 15.3 m in length and 154 points) were taken. The preservation is better than in some younger outcrops due to the freshness of the road section.

Figure 4.2.5: Street outcrop of MP4. In the background, the mast marks the top of Mt. Paopakoa with MP5 below it. Picture taken by W. Kießling.

MP5: 17°35'40.94"S, 168°16'57.91"E, 392 m in altitude

This outcrop is next to the radio mast on top of Mt. Paopakoa (in the background of Figure 4.2.5). The limestone is strongly recrystallized and only a few rocks with a few fossils, mostly massive corals were accessible. Some molluscs are also preserved.

4.2.3 Holocene terraces

Sa1: 17°32'28.70"S, 168°21'49.07"E, 0 m in altitude
La: 17°32'37.62"S, 168°21'28.89"E, 10 m in altitude

Reconnaissance studies were carried out at Saama (Sa1) and Lakenasua (La1). The latter one was dated by Lecolle *et al*. (1990). The goal was to verify the ages of 12,000 an 20,000 years that the authors had gained from dating samples from Lakenasua, as this would be a time just around the last glacial maximum; however, Lecolle *et al*. (1990) already suggested to handle these results with care due to the strong calcification of the samples, which is always a problem for U/Th dating. Only two samples from poorly preserved small rocks at 10 m altitude were taken for age dating. Data from this site do not appear in any further analysis, because the site was too small for statistically relevant sampling and not well enough preserved for age dating.

Sa1 is a small beach near Saama village (Figure 4.2.6). The outcrop is today in the intertidal area and thus strongly eroded. One transect parallel to the shore (LT9 with 12.5 m in length and 126 points) and one bulk sample were taken here.

Figure 4.2.6: Holocene terrace exposed at the beach of Saama village.

SP: 17°34'38.42"S, 168°14'45.14"E, 0-5 m in altitude
Sp1: 17°34'30.95"S, 168°14'51.06"E, 0-5 m in altitude

These sites at Samoa Point, west of Port Havannah, were found and examined by W. Kießling and J. Millet. Here, Holocene cliffs are well preserved at the beach. Massive and plate-like corals alternate with *Acropora* and *Fungia* facies. I created bulk sampling data from samplings and pictures taken by my colleagues. Of course, this artificial data has to be interpreted with care. Nevertheless, a huge number of *Acropora* in-situ and debris (Figure 4.2.7) can be found here, more than in any other of our sites.

Figure 4.2.7: Outcrop situation at Samoa Point. *Acropora* and other branching corals seem to dominate the community. Picture taken by J. Millet.

4.3 Results

4.3.1 Age dating results, recrystallization and diagenesis

Samples were dated using the ESR-dating method by the laboratory Prof. Dr. Ulrich Radtke in Cologne. As described in Chapter 2.4 this method is based on the natural radiation damage that occurs in minerals as a result of uranium uptake and external effects. This damage is usually repaired in living tissue, but accumulates in dead tissue. Thus, the approximate age can be deduced from the extent of the radiation damage. For the calculation of this damage it is also important to know the depth, in which the sample was buried. As we did not know the original depth of the samples, the ESR age was calculated for different potential depths for most samples (0.2 m, 1 m, and 3 m depth). In general it can be assumed that our samples were not deeply buried, and that the first estimate of 0.2 m depth is the most likely one for most sites

Table 4.3.1 shows the results obtained from the ESR-dating. Four groups of ages could be identified that are defined as follows for the further analyses:

Holocene

This terrace includes the two sites at the beach of Samoa Point with ages between 4,216 - 4,824 years, and the sites La1 und Sa1. This group represents an age of the terrace that correlates with the sea level highstand after the decay of the large ice sheets was completed at around 7000 years. This time is largely referred to as the Holocene Climate Optimum (HCO) in the Northern Hemisphere, but studies along the Great Barrier Reef indicate that the tropical sea surface temperature 5350 years ago was 1° C warmer than today (Gagan *et al.* 1998) also in the tropical Southern Hemisphere.

Pleistocene 1

This group includes sites from the Ulei and mainly from the Mt. Paopakoa profile and represents an age between about 70,000 and 80,000 years, roughly agreeing with MIS 5a.

Pleistocene 2

This group is defined by one result from one site (UL2) only and is about 140,000 years old, marking either the onset of MIS 5e or more likely MIS 7 when paying respect to the limits of the ESR dating method. This issue will be discussed later. For the analyses it is important that this terrace is distinct from the other Pleistocene terraces.

Pleistocene 3

This group is again obtained from one site (MP4) only, and is at least about 220,000 years old.

Pleistocene 4

Site MP5 from the top of Mt. Paopakoa could not be dated, because the samples were 100% recrystallized. However, the topographic situation renders likely an age considerably older than 200,000 years. Based on the results of Lecolle *et al*. (1990), the general topography and the sea level development during the Pleistocene, MP5 likely corresponds to MIS 11 (Table 4.4.1).

The results (Figure 4.3.1: The two profiles with all the sites along Mt. Paopakoa with the results from the ESR-dating.) also show that altitude and age do correspond within the profiles, but not among them. The profiles are located each on the other side of a distinct fault that is oriented perpendicular to the terraces (Figure 4.1.1). The sample from MP3 is more strongly recrystallized than the other samples, which is a potential explanation for the different age estimate suggesting a much younger age of about 34,000 years. Accordingly, MP3 is grouped with the next older samples of Pleistocene 1. Here, we also come to the limits of ESR-datings, which have to be considered for the interpretation of the results: Comparisons of ESR-dating to other dating methods, especially to U/Th - ages, have shown that ESR results are systematically 5 - 10 % younger than corresponding U-series ages (Schellmann & Radtke 2004; Schellmann *et al.* 2004). The latter authors conclude that for an accurate ESR based chronostratigraphy a large number of samples from more than one site in one

terrace would be necessary. Also, they suggest using only the oldest ESR dating result for the interpretation. In our case it was not possible to analyze more than this number of samples, so we have to handle the results with great care. Despite the limitations, however, our results allow to generate distinct groups of sites, which correspond to the topology seen within the profiles in Figure 4.3.1.

Chappell *et al*. (1996) provided an equation to reconstruct the uplift rate for reef terraces: U=(H -S)/t, with U = uplift rate, H = height above sea level of the dated coral sample, t = age of the sample, and S = reference sea level. The reference sea level can be taken from Siddall *et al*. (2007): +2 m to + 4 m above today's sea level during MIS 5e (exposed terraces in tectonically stable parts of Western Australia), -5 m to -15 m below today's sea level during MIS 7 (mixed evidences), -3 m to +4 m for MIS 9, and -10 m to +10 m during MIS 11. Cabioch (2003) has shown that the uplift rate in Vanuatu was relatively constant within the last 23 ka. Emanating from a constant uplift rate of 0.9 to 1 mm/a in this area (Lecolle *et al*. 1990) throughout the last 400 ka, we would accordingly expect to find MIS 5e (115 - 130 ka BP) between 115 an 135 m altitude, MIS 7 (194 - 238 ka BP) between 179 m and 233 m altitude, MIS 9 (300 - 337 ka BP) between 297 m and 341 m, and MIS 11 (374 - 424 BP) between 364 m and 434 m altitude. The ESR dating results gained in this study reveal a different pattern and would indicate different uplift rates between the middle terraces of the profiles, with Pleistocene 2 in the UL profile being found at the same altitude as Pleistocene 1 in the MP profile, whereas MP1 and ULW1 are equal and fit to my estimates. MP5, which has not been dated, can be observed at the same altitude in both profiles. This discrepancy will be discussed later.

In order to obtain an understanding of the quality of our samples from the different sites, their degree of recrystallization was examined as described in Chapter 2.3. The results are shown in Table 4.3.1. The Spearman rank correlation coefficient was calculated in order to test for a correlation between age and preservation, namely the calcite content, of the samples. For that purpose the samples from La1 and MP5 were excluded, because no age dating was possible for them. MP3 was excluded as well since the result is a clear underestimation of the age. The other ages are taken from Table 4.3.1 (ESR-dating results). UL1 and UL3 ages are rough estimates, because they are from the same terrace as UL2 (see Figure 4.3.1).

The results suggest that the recrystallization is not generally dependent of the age of the samples, giving a correlation coefficient of $\rho = 0.43$ with no significance ($p = 0.19$). The recrystallization and thus the diagenetic state of the samples is mainly dependent on other parameters, such as exposition to environmental forces (vegetation, climate, carst) after uplift. However, ρ is high enough to assume that the age also plays a role in so far that it increases the probability to be exposed to physical and/or chemical influences that favor diagenetic processes.

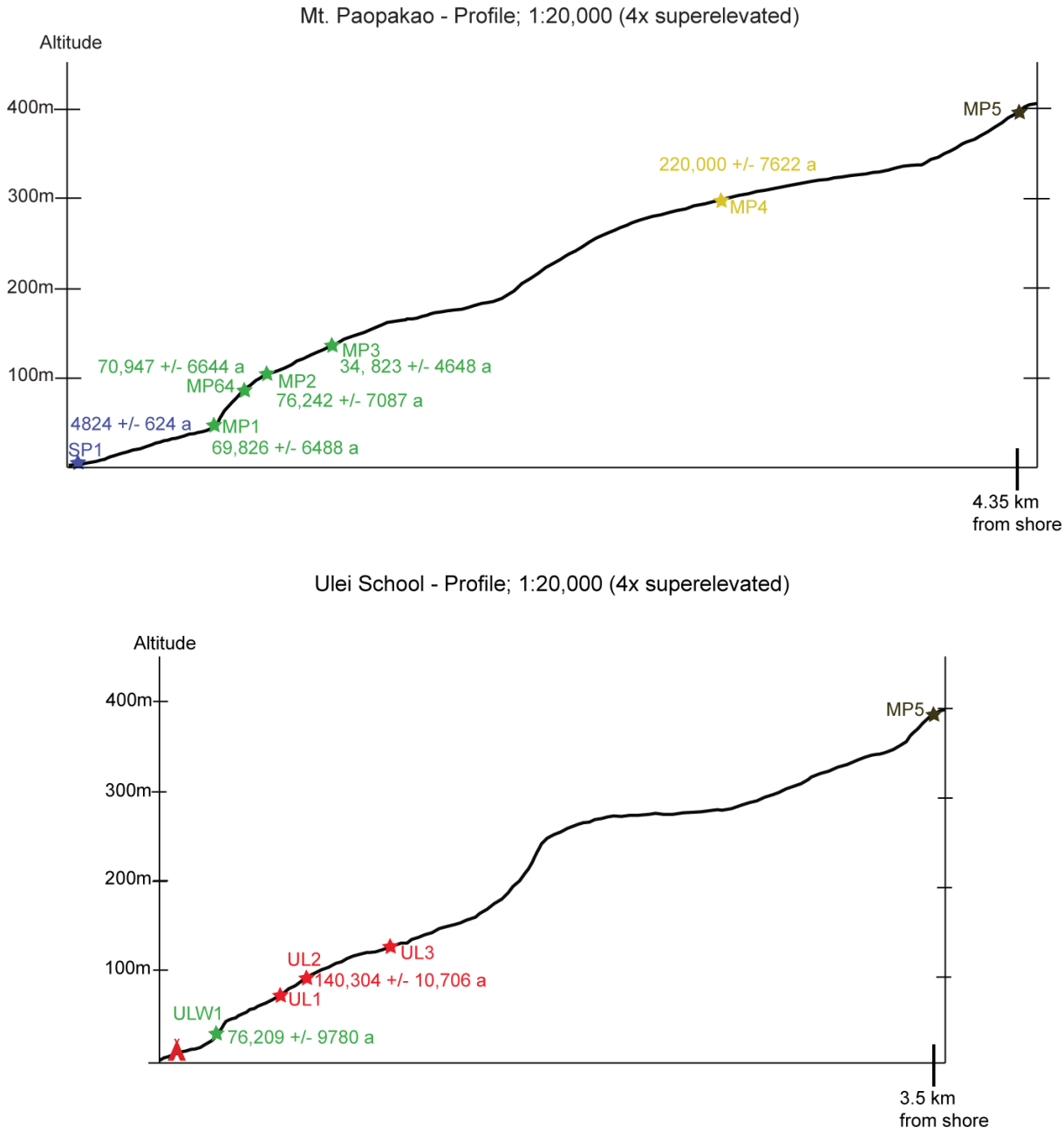

Figure 4.3.1: The two profiles with all the sites along Mt. Paopakoa with the results from the ESR-dating.

Table 4.3.1: ESR-dating results for several assumed depths. D_o (Gy/year) = annual dose rate, D_e (Gy) = equivalent (accumulated) dose. *G.* sp. = *Gonipora* sp., *P.* sp. = *Porites* sp. Aragonite and Calcite content are given as well as the altitude in which the sample was taken. Four groups of ages could be identified and are named as follows in the further thesis: blue = Holocene, green = Pleistocene 1, red = Pleistocene 2, yellow = Pleistocene 3.

Sample	Species	Altitude (in m)	Aragonite (in %)	Calcite (in %)	U	U (dev +/-)	D_o (µGy/a)	D_o (dev +/-)	D_e (Gy)	D_e (dev +/-)	depth (m)	depth (dev +/-)	age (a)	age (dev +/-)
Sa1k	"faviid" indet.	0	100	0	2.33	0.23	455	30	1.93	0.04	0.2	0.1	**4,216.00**	291.00
							412	27			1	0.1	**4,660.00**	320.00
							371	27			3	0.1	**5,167.00**	391.00
SP1a	*G.* sp.	0	100	0	2.86	0.29	510	35	2.46	0.37	0.2	0.1	**4,824.00**	624.00
							467	32			1	0.1	**5,268.00**	681.00
ULW1	*P.* sp.	35	96	4	2.71	0.27	747	51	56.96	2.14	0.2	0.1	**76,209.00**	9,780.00
							712	49			1	0.1	**79,932.00**	10,281.00
MP1Ba	*P.* sp.	40	100	0	2.1	0.21	616	40	43.02	2.86	0.2	0.1	**69,826.00**	6,488.00
							581	37			1	0.1	**74,109.00**	6,822.00
							547	38			3	0.1	**78,544.00**	7,552.00
MP64e	*P.* sp.	80	100	0	3.42	0.34	865	61	61.38	3.78	0.2	0.1	**70,947.00**	6,644.00
							830	60			1	0.1	**73,949.00**	7,022.00
							798	58			3	0.1	**76,877.00**	7,323.00
UL2B3	"faviid" indet.	90	74	26	2.19	0.21	766	53	107.53	3.46	0.2	0.1	**140,304.00**	10,706.00
							731	52			1	0.1	**147,034.00**	11,479.00
							698	52			3	0.1	**153,920.00**	12,490.00
MP2x	*P.* sp.	105	88.6	11.4	3.18	0.32	837	60	63.86	3.78	0.2	0.1	**76,242.00**	7,087.00
							803	57			1	0.1	**79,532.00**	7,350.00
							770	58			3	0.1	**82,852.00**	7,937.00
MP3Sd	*P.* sp.	130	78	22	2.31	0.23	550	34	19.45	2.22	0.2	0.1	**34,823.00**	4,648.00
MP4Sj	*P.* sp	297	100	0	2.63	0.26	992	68	219.1	6.19	0.2	0.1	**220,918.00**	7,622.00
							922	65			3	0.3	**237,510.00**	29,666.00

4.3.2 Comparison of diversity, species richness and similarity within and between different datasets

Two sampling methods were applied during the field work in Vanuatu. As shown in section 4.2, the outcrops were mostly not suitable for line transects, such that bulk sampling was the method of choice to gather a larger amount of data. The transects contain up to 64% gaps, which means that 64% of the data points did not reveal lithological information, but rather soil or vegetation. The bulk sampling method allowed collecting data randomly from everywhere, where access to limestone was possible. Matrix and non-coral reef dwellers were only considered to calculate the coral coverage (see Chapter 2). Otherwise all non-coral data were excluded from further analyses. The raw data of both methods are available in Appendix I. Table 4.3.2 shows the transect data with specimens numbers, species numbers and diversity indices of transects and/or by terrace gained from transect data. It also shows the coral coverage that was calculated from the raw transect data as percentage of corals in the total data amount (excluding gaps). Table 4.3.3 shows the species richness and diversity of sites and terrace gained from bulk sampling data. Species richness varies among the studied fossil reef assemblages in the different sites, but in all of them corals were the main carbonate-forming group, as shown by coral coverage. Other common reef dwellers were mollusks and coralline algae. Also two coralline demosponges, which represent the first record from the Pleistocene, were found (Millet & Kiessling 2009).

Pleistocene 4 was excluded from further analyses because the data set is too small. Transect data do not play a big role in all further analyses, but were used for comparison and to test trends apparent from the bulk sampling data.

For the bulk sampling data some analyses were performed at both species and genus level in order to test if identification at genus level delivers similar signals as analyses at species level. As shown in Chapter 3, the identification at species level can be challenging for many Pleistocene corals. Pandolfi (2001b) has shown that there are some differences between species and genus level patterns in Quaternary coral communities, but that they have little effect on paleoecological interpretations. Table 4.3.4 contains the bulk sampling genus data with richness and diversity indices. A further dataset was created that contains massive taxa only. By excluding fragile corals, I attempted to reduce the taphonomical bias of taxa that are easily eroded and/or washed away. Therefore, delicate taxa as *Acropora*, *Alveopora*, *Millepora*, *Pavona*, *Pocillopora*, *Seriatropora, Stylophora*, *Tubipora* were excluded, as well as the solitary genera *Fungia* and *Sandalolitha* that have a greater chance to be washed away after death or during diagenesis and/or erosion. Analyses based on this preservation-standardized dataset were also performed at both species and genus level. It should be mentioned that species level identification was not possible for all specimens, so that the species dataset is rather a mix of species and genus level identifications. The resulting data is presented in the overview of Tables 4.3.3 and 4.3.4 for species and genus analyses, respectively.

Table 4.3.2: Overview of line transect (LT) data and distribution among terraces after cleaning the data from gaps, matrix, and other reef dwellers. The mean coral coverage per terrace is the mean of the coral coverage in each transect. SD = standard deviation of the mean coverage, Sobs = number of observed species in LT and terrace, N = number of observed specimens in LT and terrace, H = Shannon–Wiener Index of Diversity, J = Evenness, SR21 = number of species after rarefaction (N = 21), ACE = coverage-based richness estimation that gives the estimate for the minimum total number of species we might observe in the respective terrace, SE = standard error of ACE, SQS = shareholder quorum subsampling for a coverage level of 70% after 1000 trials.

Terrace	LT No.	*N* (LT)	S_{obs} (LT)	*N* (terrace)	S_{obs} (terrace)	Coral Coverage (mean ± SD in %)	*H*	*J*	$S_{R\ 21}$	ACE ± SE	SQS q =0.7
Holocene	LT9	50	9	50	9	48.5	1.84	0.84	7.17	9.52 ± 1.34	3.89
Pleistocene 1	LT7	38	4	72	8	41.4 % ± 13	1.16	0.84	4.85	13.51 ± 1.9	1.44
	LT 8	34	6								
Pleistocene 2	LT1	17	5	89	14	42.4 % ± 20.9	2.24	0.56	8.92	16 ± 1.8	6
	LT2	13	5								
	LT3	11	2								
	LT4	2	2								
	LT5	46	8								
Pleistocene 3	LT6	22	8	22	8	43.6	1.76	0.85	7.82	13.58 ± 1.89	4.54

Table 4.3.3: Overview of species richness and diversity in bulk sampling data and distribution among terraces. *Sobs* = number of observed species in raw data (raw) and preservation-standardized (ps) data per terrace, *N* = number of observed specimens in raw and ps data per terrace, *H* = Shannon–Wiener Index of Diversity per terrace, *J* = Evenness per terrace, S_{R40} = number of species after rarefaction (*N* = 40) for comparing to subsampled genus data, S_{R21} = number of species after rarefaction (*N* = 21) for comparison to subsampled transect data, ACE = coverage-based richness estimation that gives the estimate for the minimum total number of species we might observe at the respective sites, SE (ACE) = standard error of ACE. SQS = shareholder quorum subsampling for a coverage level of 70% after 1000 trials. All diversity and species observations and estimations per terrace are given for raw and ps data respectively. Pleistocene 4 has not been considered for any detailed analysis, due to its small sample size. Samples from ULW und La were collected for age dating purposes only.

Terrace	Site	*N* (raw, site)	S_{obs} (raw, site)	*N* (raw, ter-race)	*N* (ps)	S_{obs} (raw, ter-race)	S_{obs} (ps)	*H* (raw)	*H* (ps)	*J* (raw)	*J* (ps)	$S_{R\,40}$ (raw)	$S_{R\,40}$ (ps)	$S_{R\,21}$ (raw)	$S_{R\,21}$ (ps)	ACE ± SE (raw)	ACE ± SE (ps)	SQS (raw) q =0.7	SQS (ps) q=0.7
Holocene	La	2	1	146	98	36	23	2.94	2.52	0.82	0.8	18.43	15.33	12.27	10.52	46.43 ± 3.7	28.26 ± 2.78	15.24	9.17
	Sa1	35	10																
	SP	84	27																
	SP1	27	17																
Pleistocene 1	MP1	67	21	264	228	33	25	2.96	2.69	0.85	0.84	17.99	15.42	12.53	11.18	36.67 ± 2.78	27.13 ± 2.41	13.67	10.06
	MP2	40	9																
	MP3	39	13																
	MP55	26	10																
	MP64	89	20																
Pleistocene 2	UL2	28	8	47	41	11	9	2.15	1.96	0.9	0.89	10.53	8.95	8.69	7.71	12.72 ± 1.4	10.05 ± 1.23	5.72	4.66
	UL3	19	7																
	ULW	1	1																
Pleistocene 3	MP4	72	13	72	72	13	13	1.99	1.99	0.78	0.78	10.83	10.83	8.32	8.32	15.84 ±1.7	15.84± 1.7	5.17	5.21
Pleistocene 4	MP5	12	4	12	12	4	4	1.24		0.89									

Table 4.3.4: Overview of genus richness and diversity in bulk sampling data and distribution among terraces. *Sobs* = number of observed genera in raw data (raw) and preservation-standardized (ps) data per terrace, *N* = number of observed specimens in raw and ps data per terrace, *H* = Shannon–Wiener Index of Diversity per terrace, *J* = Evenness per terrace, S_{R40} = number of genera after rarefaction (*N* = 40), S_{R21} = number of genera after rarefaction (*N* = 21) for comparison to subsampled transect data, ACE = coverage-based richness estimation that gives the estimate for the minimum total number of genera we might observe at the respective sites, SE (ACE) = standard error of ACE. SQS = shareholder quorum subsampling for a coverage level of 70% after 1000 trials. All diversity and genera observations and estimations per terrace are given for raw and ps data respectively. Pleistocene 4 has not been considered for any detailed analysis, due to its small sample size.

Terrace	Site	*N* (raw, site)	S_{obs} (raw, site)	*N* (raw, ter-race)	*N* (ps)	S_{obs} (raw, ter-race)	S_{obs} (ps)	*H* (raw)	*H* (ps)	*J* (raw)	*J* (ps)	$S_{R\,40}$ (raw)	$S_{R\,40}$ (ps)	$S_{R\,21}$ (raw)	$S_{R\,21}$ (ps)	ACE ± SE (raw)	ACE ± SE (ps)	SQS (raw) q =0.7	SQS (ps) q=0.7
Holocene	La	2	1	146	98	25	17	2.67	2.22	0.82	0.79	15.37	11.88	11.01	8.79	29.27 ± 2.54	24.07 ± 2.7	9.54	5.85
	Sa1	35	10																
	SP	84	19																
	SP1	27	14																
Pleistocene 1	MP1	67	20	264	222	25	18	2.63	2.32	0.82	0.80	14.34	11.43	10.73	9.01	29.03 ± 2.63	21.5 ± 2.24	8.9	6.22
	MP2	40	7																
	MP3	39	13																
	MP55	26	10																
	MP64	89	16																
Pleistocene 2	UL2	28	7	47	41	10	8	2.11	1.91	0.92	0.92	9.7	7.98	8.38	7.22	10.78 ± 1.18	8.31 ± 1.03	5.38	4.33
	UL3	19	7																
	ULW	1	1																
Pleistocene 3	MP4	72	10	72	71	10	9	1.59	1.54	0.69	0.70	8.47	7.95	6.65	6.39	12.06 ±1.5	10.04± 1.25	2.91	2.74
Pleistocene 4	MP5	12	4	12	4	4	4	1.24		0.89									

All five resulting datasets were subsampled using rarefaction and shareholder quorum subsampling (SQS). The rarefaction curves are presented in Figure 4.3.2, the SQS curves in Figure 4.3.3. Whereas the trends in species/genus richness and diversity of the bulk sampling data are always similar, no matter if regarding raw data, preservation-standardized data, or genus/species levels, the transect data show a different trend. In the bulk sampling data Holocene and Pleistocene 1 are best sampled and are similarly diverse regarding the estimated abundance (ACE), whereas Pleistocene 2 and 3 are poorly sampled and appear low in diversity. However, sampling especially in the Holocene is not sufficient, as the steep curve suggests. The abundance-based coverage estimator (ACE) supports these results for the bulk sampling data. In the transect data, differences are less distinct. Here, only the Holocene, which is represented by one transect only, appears to be less diverse, while the other three terraces reveal a similar level of species richness. The Shannon-Wiener diversity and evenness indices produce similar results. Diversity would be similarly high in the youngest Pleistocene terrace and the Holocene terrace for the bulk sampling data, whereas it declines with age in the older terraces. This trend can also be observed with genus data only and with preservation-standardized data. The transect data reveals more differences in diversity among terraces, with Pleistocene 1 being the least diverse and Pleistocene 2 the most diverse. Interestingly the evenness is similar between all five datasets (species and genus bulk data, preservation-standardized each and transect data). However, differences in evenness among the terraces within the bulk sampling datasets are greater than they are in the transect dataset. Here, three terraces are almost identically even with an evenness of 0.84 and 0.85, while Pleistocene 1 has an evenness of only 0.56. Differences between transect and bulk data are greatest in the youngest and oldest Pleistocene terrace. All results are shown in Table 4.3.3 (species level) and Table 4.3.4 (genus level). SQS supports these results, but the differences within the two groups (Holocene & Pleistocene 1 versus Pleistocene 2 and Pleistocene 3) are less distinct than suggested by all other methods.

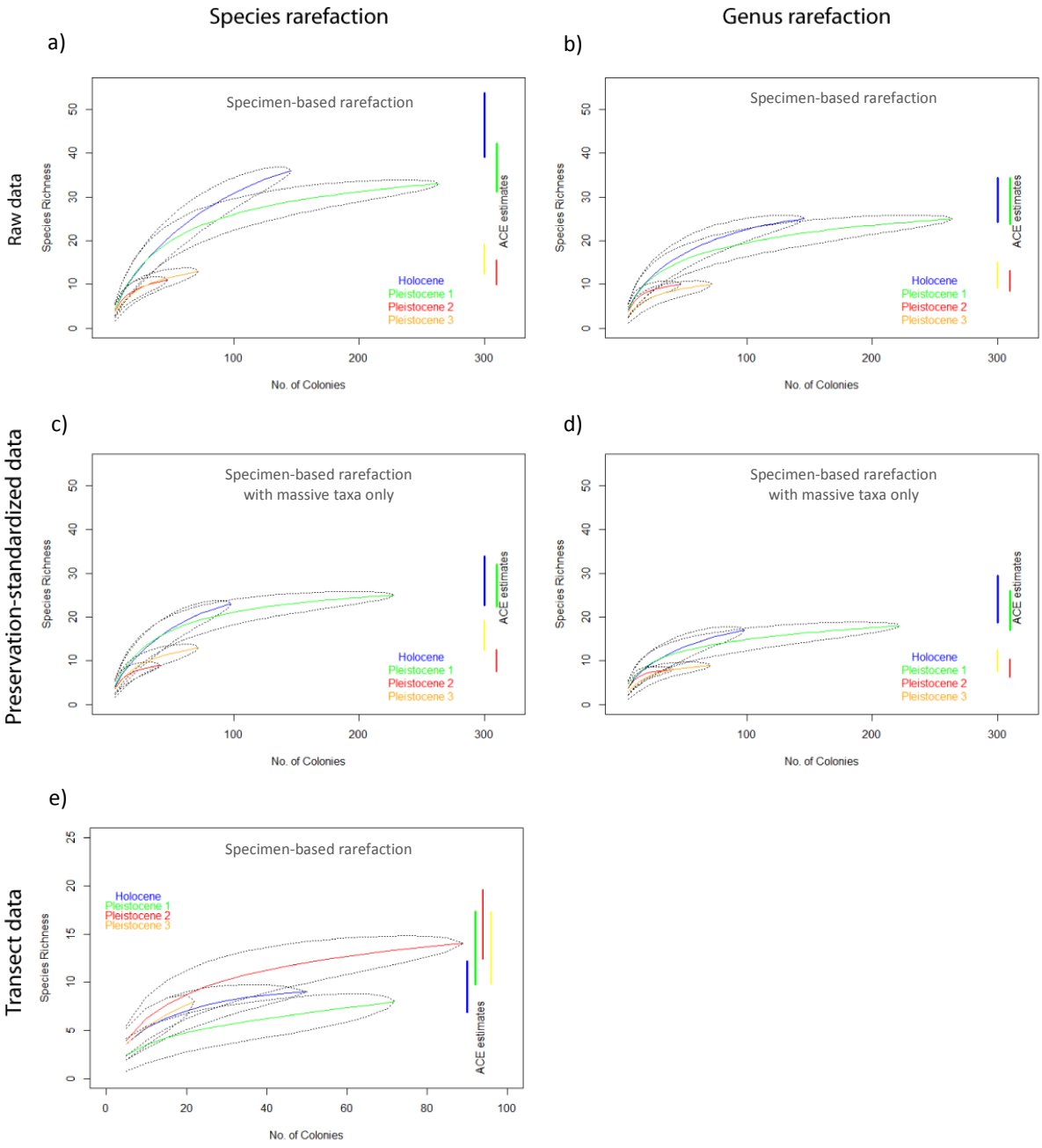

Figure 4.3.2: Rarefaction curves and abundance-based coverage estimator (ACE) of all datasets by terrace using individual-based rarefaction. a), c) and e) show the species rarefaction; b) and d) genus rarefaction. a) and b) show the curves of the raw bulk sampling data, c) and d) show the curves of the preservation-standardized bulk sampling data where all fragile taxa were pruned from the analyses, e) shows the curves of the transect data. The total richness estimator (ACE) was plotted in intervals (expected values +/- 2*SE). SE is the standard error of ACE.

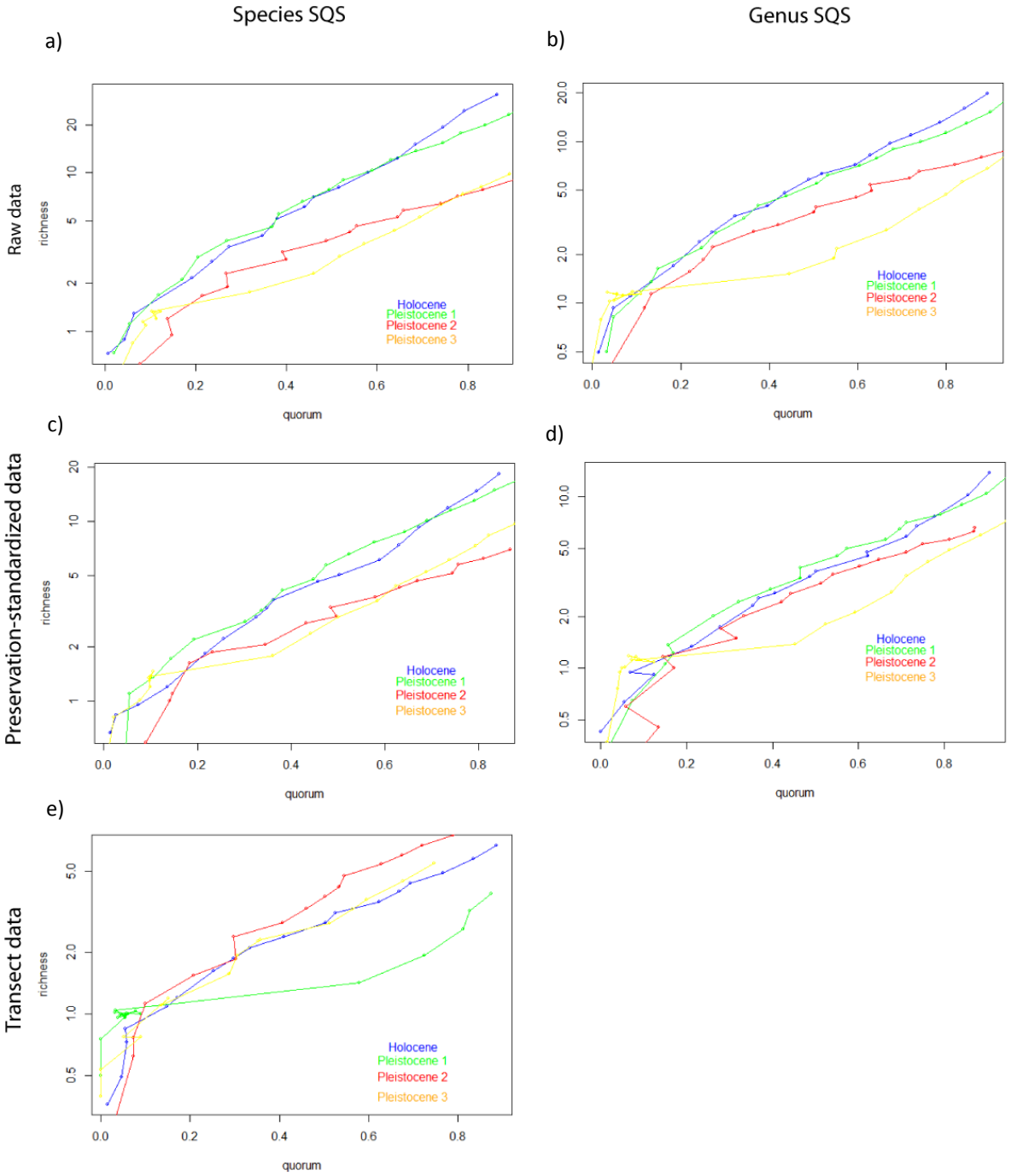

Figure 4.3.3: Shareholder quorum subsampling curves, showing the subsampled richness for different coverages. Table 4.3.3 shows the subsampled richness for q = 0.7 after 1000 trials. a), c) and e) show the SQS curves of species data; b) and d) SQS curves of genus data. a) and b) show the curves of the raw bulk sampling data, c) and d) show the curves of the preservation-standardized bulk sampling data where all fragile taxa were pruned from the analyses, e) shows the curves of the transect data.

The Spearman's correlation coefficient has been calculated between the Shannon-Wiener-Index of diversity and the age of the terraces (Table 4.3.5). Despite the small sample size, the results strongly suggest to be careful with the bulk sampling results depending on identification and standardization level. There is a distinct decrease in diversity correlated with age towards lower diversity level in the bulk sampling data, defined as indicated in Table 4.3.5.

Table 4.3.5: Correlation of diversity indices of different identification and standardization levels with approximate age of the terraces. Spearman's rho (ρ) and respective *p*-values are given. *H* = Shannon-Wiener-Index of diversity. The last column summarizes the identification and standardization levels discussed.

	ρ	*p*	Level
***H* raw genus data**	-1	0.08	1
***H* raw species data**	-0.8	0.33	2
***H* preservation-standardized genus data**	-0.8	0.33	2
***H* preservation-standardized species data**	-0.6	0.42	3
***H* transect data**	0	1	

The lowest level (level 1) is the correlation coefficient showing the highest negative correlation of diversity and age in the raw genus data, while the preservation-standardized species has the highest level (level 3), expressed by the lowest negative correlation coefficient among the bulk sampling datasets. Diversity of raw species data and preservation-standardized genus data are identical (level 2), which is likely due to the fact that the species dataset contains a high number of genus identifications only. Also, the raw data and preservation-standardized data of Pleistocene 3 are identical in the bulk sampling data, because only massive taxa have been preserved there. If the datasets were larger and more species identified to species level, there would probably be distinction between these datasets. However, the transect data shows no correlation at all between diversity and age. This fact shows that the bulk sampling data is strongly biased, and that this bias can only be derogated by a high level of identification and standardization of the bulk sampling data. The four bulk sampling rarefactions show that with a decreasing level sampling also appears to be more sufficient indicated by less steep curves, which is helpful in small datasets. Nevertheless, the overall trend of the bulk sampling data results do not change with higher standardization level and lower identification level. However, the rarefaction curves and the ACE estimates support the strong discrepancy between transect and bulk sampling data.

For a first comparison of the similarities between all five datasets in species/genus presence/absence composition the Sørensen similarity (Table 4.3.6) was calculated for the five datasets: The raw data of species and genus bulk sampling datasets, the preservation-standardized species and genus dataset and the transect dataset. Despite the differences in diversity, the similarities reveal similar trends. The lower the identification level and the higher the standardization level, the more similar are the datasets. The preservation-standardized genus level bulk sampling data reveals the highest degree of similarity between the terraces. Holocene and Pleistocene 1 are more similar to each other than all other terraces are to those and among each other. The transect data, however, deliver a different pattern. Here, Holocene and Pleistocene 3 are more similar to each other than to any other terrace, whereas Holocene and Pleistocene 1 are among the least similar terraces. Differences among the Pleistocene terraces are small, meaning that all appear to be relative similar to each other in terms of species composition. Here, it has to be kept in mind that the Holocene data lacks sufficient transect data.

Table 4.3.6: Sørensen's similarity between terraces (bulk sampling species and genus, transect data, and preservation-standardized bulk sampling species and genus data)

Bulk sampling raw data (genus) - level 1				Bulk sampling raw data (species) - level 2				Transect data			
	H	**P1**	**P2**		**H**	**P1**	**P2**		**H**	**P1**	**P2**
P1	0.76			**P1**	0.64			**P1**	0.42		
P2	0.57	0.57		**P2**	0.47	0.5		**P2**	0.54	0.52	
P3	0.51	0.57	0.6	**P3**	0.37	0.48	0.5	**P3**	0.67	0.53	0.54

Preservation-standardized genus data (BS) - level 2				Preservation-standardized species data (BS) - level 3			
	H	**P1**	**P2**		**H**	**P1**	**P2**
P1	0.80			**P1**	0.67		
P2	0.64	0.62		**P2**	0.56	0.53	
P3	0.61	0.67	0.71	**P3**	0.50	0.50	0.55

The transect dataset was not used for further analyses because it is too small and results, especially those of the Holocene data, would be misleading. Also the genus data was omitted. As shown above, it may give some trends but the small sample size prevents any further in-depth analysis. Despite the discrepancy between transect and bulk data, the latter one was examined in detail. Two datasets remain in the analyses: bulk sampling species data and preservation-standardized bulk sampling species data.

4.3.3 Community structure

Rank-abundance distribution (RAD) curves (Figure 4.3.4) have been created out of the two remaining datasets to gain insights into the community structure of the coral communities from the different terraces. The best sampled terrace (Pleistocene 1) shows a log-normal distribution. The worst sampled, but according to the above indices most even community (Pleistocene 2) shows the null model (aka "Broken Stick"). Holocene and Pleistocene 3 show a Zipf-Mandelbrot distribution. The differences between raw and preservation-standardized data are negligible. A detailed overview of the results, including the AICs, is given below in Table 4.3.7.

In Pleistocene 3, where the Zipf model has the lowest AIC (= 47.14), the AIC for the lognormal distribution (AIC = 48.58) is lower than the one for the Zipf-Mandelbrot (AIC = 49.14) distribution, and all three of them (Zipf, Zipf-Mandelbrot and lognormal) are very similar. In the bulk sampling data the evenness of the Pleistocene 3 data is the lowest of all terraces - as such it has the simplest community distribution in comparison to the other terraces. This is, however, not the case in the transect data, where all Pleistocene terraces are similar even.

Table 4.3.7: RAD results for the four terraces and two datasets. The best modelfit (marked with bold numbers) has the lowest AIC.

	Holocene				**Pleistocene 1**			
	a) Raw Data		b) Preservation-standardized data		c) Raw data		d) Preservation-standardized data	
No. of species	36		23		33		25	
Total abundance	146		98		264		228	
Model	**Deviance**	**AIC**	**Deviance**	**AIC**	**Deviance**	**AIC**	**Deviance**	**AIC**
Null	37.61	137.53	21.63	86.7	18.03	130.76	13.76	102.15
Preemption	34.15	136.07	19.06	86.14	21.83	136.56	15.06	105.46
Lognormal	19.87	123.79	10.12	79.19	**3.22**	**119.95**	**1.8**	**94.19**
Zipf	13.72	117.64	**5.58**	**74.65**	14.18	130.91	10.83	103.23
Zipf-Mandelbrot	**9.18**	**115.11**	4.32	75.4	9.18	127.9	5.78	100.17
	Pleistocene 2				Pleistocene3			
	a) Raw Data		b) Preservation-standardized data		c) Raw data		d) Preservation-standardized data	
No. of species	11		9		13		13	
Total abundance	47		41		72		72	
Model	**Deviance**	**AIC**	**Deviance**	**AIC**	**Deviance**	**AIC**	**Deviance**	**AIC**
Null	**2.02**	**35.72**	**1.32**	**29.54**	12.11	52.12	12.11	52.12
Preemption	1.26	36.96	0.87	31.09	11.59	53.61	11.59	53.61
Lognormal	1.47	39.16	0.89	33.11	4.56	48.58	4.56	48.58
Zipf	3.79	41.49	2.87	35.08	**3.13**	**47.14**	**3.13**	**47.14**
Zipf-Mandelbrot	1.01	40.71	NA	NA	3.13	49.14	3.13	49.14

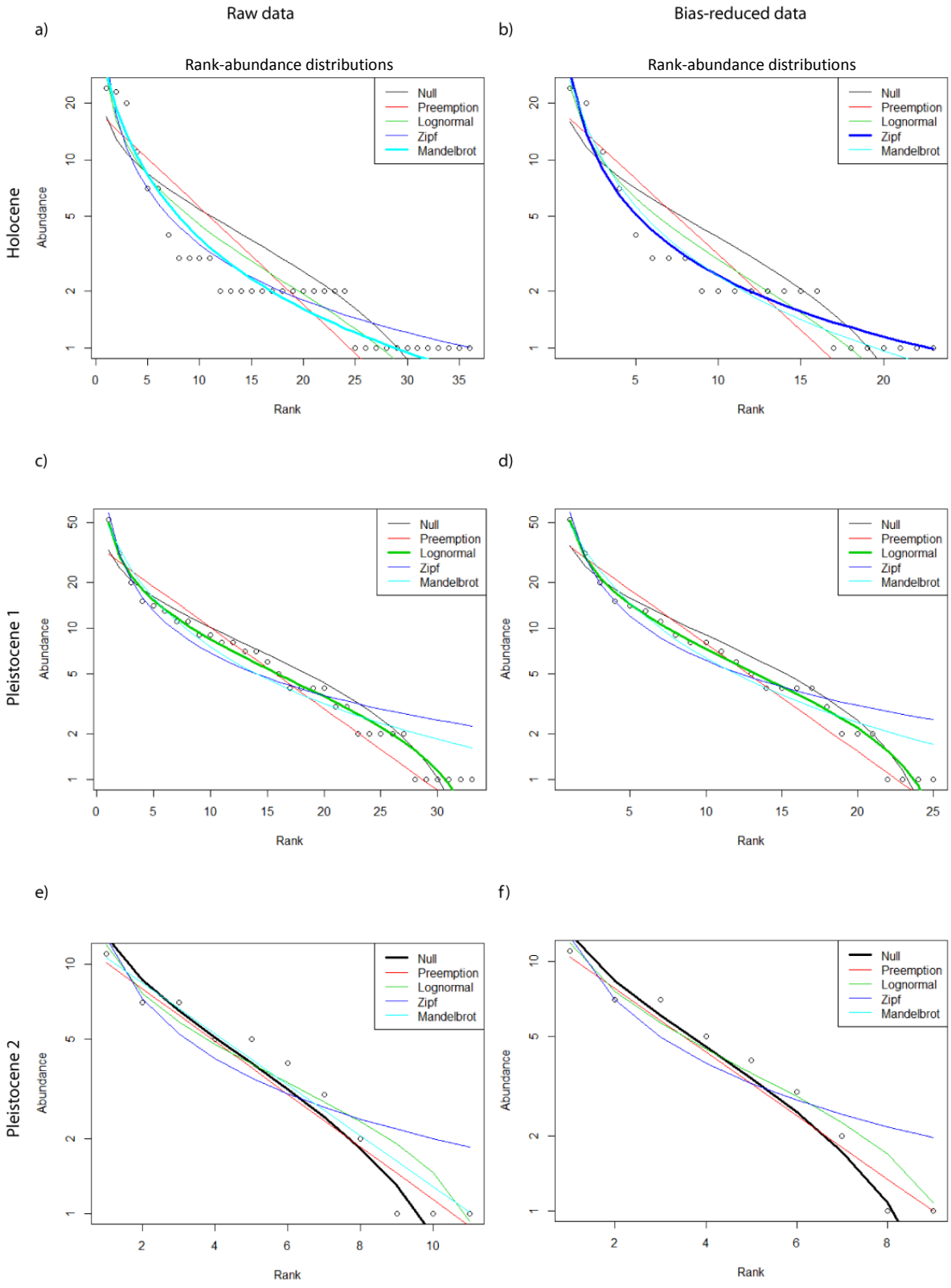

Figure 4.3.4: Rank-abundance distributions of Pleistocene and Holocene terraces generated from bulk sampling data. a), c), e), and g) of raw data. b), d), f) and h) of preservation-standardized data with massive taxa only. The thicker curves represent the best fit model with the lowest AIC.

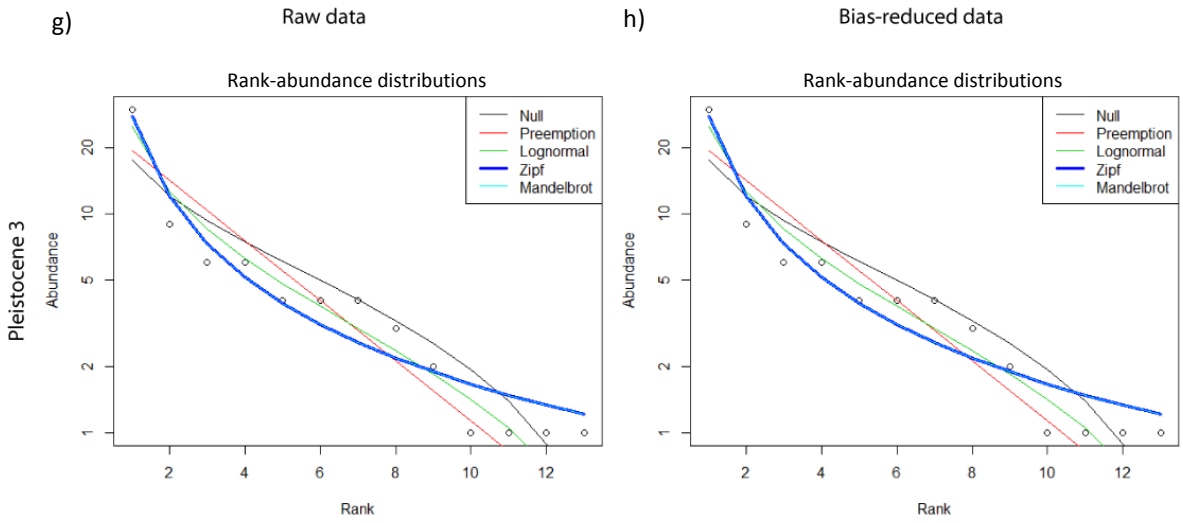

Figure 4.3.4 (continued).

Based on the shown negligible differences between raw bulk sampling data and preservation-standardized bulk sampling data, only the first one will be considered in the following sections. For the ecological analyses the greater number of data is more important than the small reduction of bias trough preservation-standardization, which leads to a loss of information especially in the two younger terraces. For the ecological reconstructions, data will be further delimited to species occurrences with environmental information.

4.3.4 Dissimilarities among and within terraces

The terraces and sites of the bulk sampling data were clustered with the hierarchical Ward's method (Figure 4.3.5) in order to display a visual summary of Bray-Curtis dissimilarities among and within terraces (Table 4.3.8 and Table 4.3.9). As already observed when comparing species richness and diversity as well as Sørensen's similarity, Holocene and Pleistocene 1 are similar to each other, as are Pleistocene 2 and 3. Sites with less than 20 specimens were omitted from further analyses. When comparing sites within the cluster dendrogram, it becomes obvious that there must be ecological gradients within the terraces and that dissimilarities among terraces are less important than dissimilarities among environments: Pleistocene 3 (MP4) is more closely related to one of the Holocene sites (Sa1) than to any of the other Pleistocene terraces, and UL2 (Pleistocene 2) plots among sites from Pleistocene 1.

Table 4.3.8: Bray-Curtis dissimilarities of Wisconsin standardized bulk sampling data among terraces.

Bray-Curtis dissimilarity (terraces)			
	Holocene	**Pleistocene 1**	**Pleistocene 2**
Pleistocene 1	0.61		
Pleistocene 2	0.85	0.65	
Pleistocene 3	0.68	0.71	0.65

Table 4.3.9: Bray-Curtis dissimilarities of Wisconsin standardized matrix of bulk sampling data among sites with more than 20 specimens.

Bray-Curtis dissimilarity (sites)									
	MP1	**MP2**	**MP3**	**MP4**	**MP55**	**MP64**	**Sa1**	**SP**	**SP1**
MP2	0.78								
MP3	0.68	0.68							
MP4	0.71	0.63	0.71						
MP55	0.79	0.85	0.81	0.89					
MP64	0.52	0.66	0.63	0.73	0.72				
Sa1	0.72	0.84	0.89	0.59	0.90	0.85			
SP	0.76	0.94	0.80	0.96	0.83	0.73	0.88		
SP1	0.79	0.83	0.77	0.84	0.81	0.68	0.87	0.61	
UL2	0.78	0.85	0.71	0.77	0.75	0.57	0.87	0.91	0.78

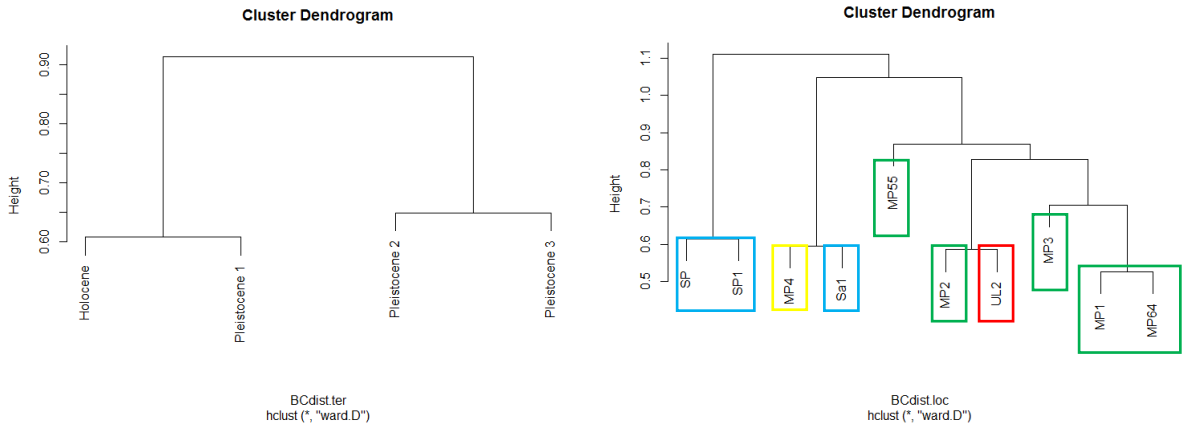

Figure 4.3.5: Cluster Dendrograms based on Bray-Curtis dissimilarity matrices and hierarchical clustering with the Ward's method. a) Dissimilarities among terraces, b) dissimilarities among sites. Blue = Holocene, Green = Pleistocene 1, Red = Pleistocene 2, Yellow = Pleistocene 3.

4.3.5 Ecological reconstruction

As described in Chapter 4.2 there was no possibility to identify fossil reef zonation in the field, because outcrops were too small and preservation poor. Therefore species composition was used to reconstruct the reef environment. For that purpose Table 3.1 (in Chapter 3) was created, which contains the available environmental information for all identified species. Accordingly all taxa that could not be identified to species level were removed for the reconstruction. Many species occur in several environments, and only a few taxa show specific preferences. Thus, different reconstruction methods were tested for suitability. First, the environment was reconstructed using taxa that show a preference for a certain environment (Table 4.3.10). The second approach was more quantitative, i.e. data were tabulated by the number of taxa of all sites occurring in the different environments (Table 4.3.11). Taxa that occur in several environments were counted repeatedly for all environments, in which they can be observed.

Table 4.3.10: Number of species occurrences that show preference for one certain environment in the different sites. Sites with no or only one environmental information were omitted.

Site	Backreef	Fringing reef	Intertidal	Lagoon	Slope	Unspecific
MP1	4	0	0	0	0	3
MP2	1	0	9	0	0	5
MP3	0	0	0	0	1	5
MP4	0	0	9	0	1	5
MP55	0	0	0	0	5	5
MP64	3	0	1	0	5	11
SP	3	0	0	1	2	11
SP1	1	0	1	2	1	3
UL2	1	0	0	0	0	1

Table 4.3.11: Quantitative species occurrences of the different sites in the different environments in which they may occur.

Site	Upper slope	Deeper slope	Backreef	Lagoon	Crest/Flat	Intertidal
MP1	3	0	7	7	5	5
MP2	15	0	6	5	9	9
MP3	6	0	5	5	0	0
MP4	15	0	5	5	9	9
MP55	10	2	5	5	3	1
MP64	19	7	15	12	9	9
SP	15	8	17	16	11	5
SP1	7	2	7	6	3	2
UL2	2	1	2	1	1	1

As can already be seen in the Cluster dendrogram, ordination via non-metric multidimensional scaling (NMDS) shows that the dissimilarity between communities from different times is often less than that for communities from separate sites during the same time. This becomes most obvious in Figure 4.3.6, when all sites with more than two specimens were included in the NMDS. There is no distinctive temporal grouping or linear changes of assemblages; instead they appear scattered throughout the plot, even with regard to the small number of sites in most terraces. Note the greater dissimilarity exhibited by assemblages within a single reef-building episode versus that between reef-building episodes; for example, the two assemblages from Pleistocene 2 are more dissimilar to each other than they are to certain assemblages from Pleistocene 1 and 3 respectively, and they each are separated in time from each other by around 70 ka. Thus, it seems that the sites are sorted more by an environmental gradient than by time. To test this further I used the function `envfit` in vegan to plot environmental information onto the NMDS plot. Figure 4.3.7 provides the NMDS plotted along with the preferred environmental information. It shows a clear trend towards slope and intertidal communities, whereas lagoon and backreef communities are on a relative similar gradient.

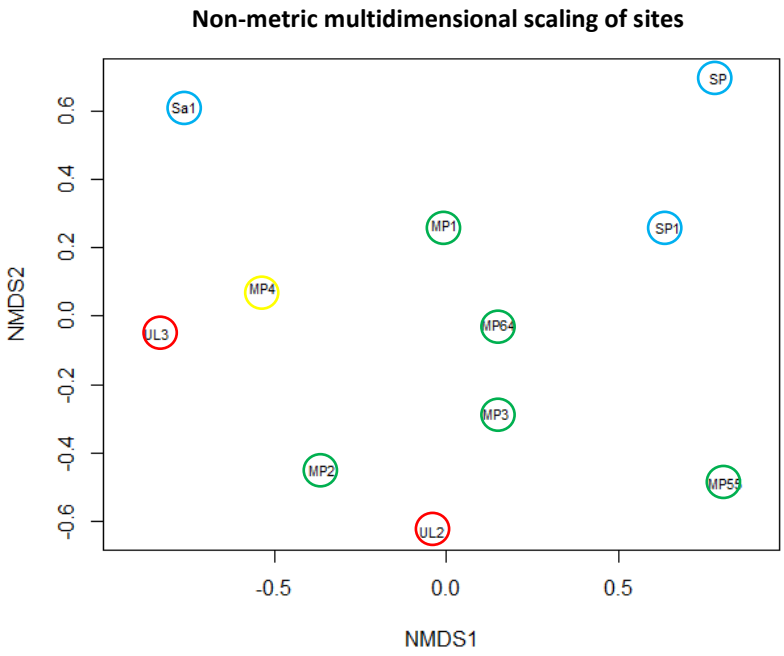

Figure 4.3.6: Non-metric multidimensional scaling (NMDS) ordination of sites with more than two specimens. The NMDS was calculated in two dimensions. Distance is based on a Bray-Curtis matrix. Data is standardized by Wisconsin double standardization. The minimum stress value was 0.12. Blue = Holocene, Green = Pleistocene 1, Red = Pleistocene 2, Yellow = Pleistocene 3.

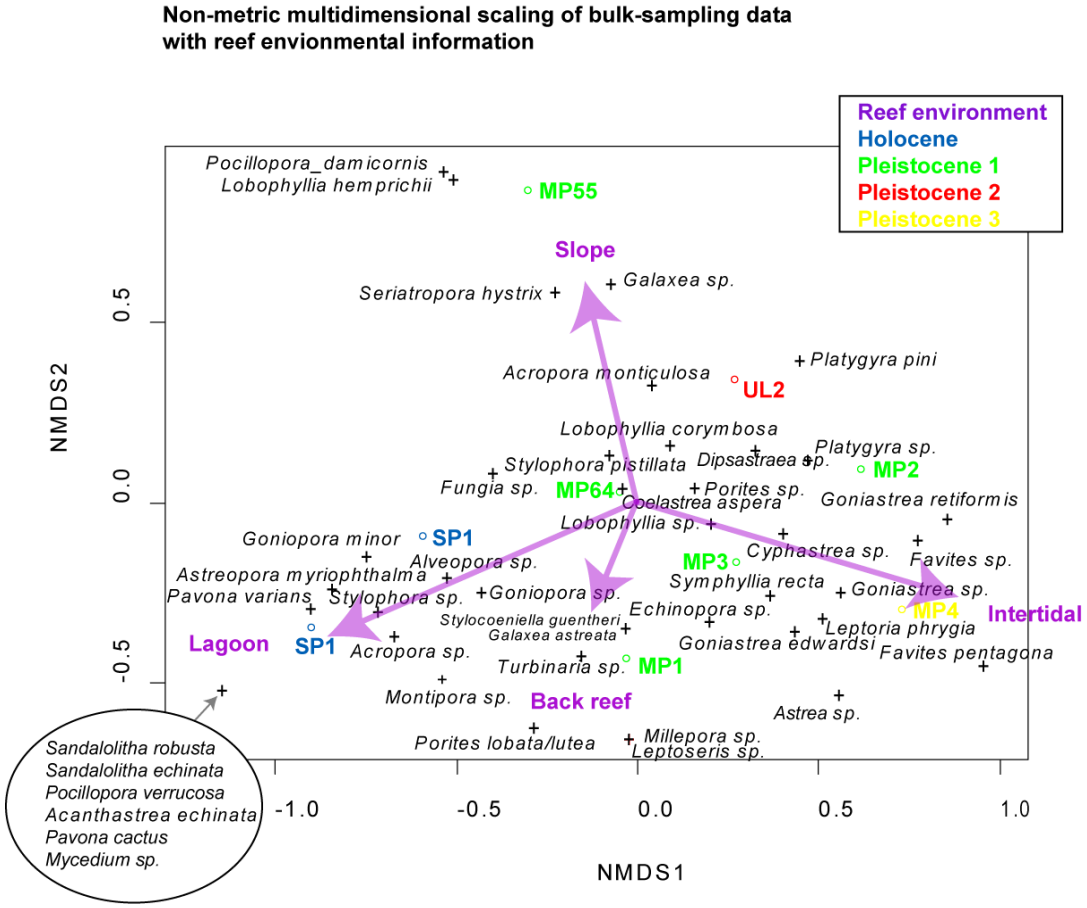

Figure 4.3.7: Non-metric multidimensional scaling (NMDS) ordination of sites, species and there preferred environments within the different terraces of the study sites in Vanuatu. The NMDS was calculated in two dimensions. Distance is based on a Bray-Curtis matrix. Both datasets are standardized by Wisconsin double standardization. The minimum stress value was 0.08. *p*-values: backreef = 0.9, intertidal = 0.14, lagoon = 0.11, slope = 0.5.

When regarding the quantitative (all environmental occurrences of a species = "allenocs") approach, where all environments in which a specific taxon occurs were counted repeatedly (Table 4.3.11) without only regarding the preferred environment, results are similar. Figure 4.3.8 shows this dataset on the same Bray-Curtis dissimilarity NMDS plot as the dataset with the preferred reef environments. Backreef and lagoon are again close together, but change their positions. For intertidal and slope communities, however, the outcome is almost identical to the preferred fitting.

In both ordinations, Pleistocene 1, which is comprised of more assemblages than the other terraces, shows a clear ecological gradient from slope to intertidal communities. The sites SP and SP1 are geographically close together and thus also do not show any strong dissimilarities in community composition. The species inhabiting these sites preferred a lagoonal/backreef environment. MP4 is the site with the strongest intertidal trend in both, the ordination with the preferred environmental fitting, and in the "allenocs" ordination (Figure 4.3.7 & Figure 4.3.8). MP55 is the site with the strongest slope trend in all three ordinations. The *p*-values of environmental fits show no significance in the environmental fit for any ordination. Nevertheless there is a clear trend, which makes sense when regarding the species composition without statistical background. Also other reef dwellers, like the frequent occurrence of *Halimeda* in site MP1 gives a hint that the statistical reconstruction of the environmental information provides a useful tool when important geoecological details essential for identifying reef zones are missing. *Halimeda* particles are usually mixed with other skeletal materials during reef accretion, and are often associated with semi-exposed to sheltered fringing reefs and in lagoonal settings of atolls (Montaggioni 2005).

Table 4.3.12: Number of taxa with their respective salinity preferences.

	high	low	unspecific
MP1	0	0	7
MP2	9	0	6
MP3	0	0	6
MP4	9	1	5
MP55	0	0	10
MP64	1	0	19
SP	0	0	19
SP1	1	0	8
UL2	0	0	2

Some taxa can tolerate a higher salinity than others. Only two variables could be used: The information how many species in a certain site can tolerate high salinities, and how many of them are unspecific. Only one taxon in one site, namely *Favites pentagona* in MP4, shows an explicitly low salinity tolerance (Table 4.3.12), but had to be excluded from the analysis because only one specimen was preserved.

The environmental fit (Figure 4.3.9) is again not significant, but the outcome makes sense when regarding the environmental reconstructions of the above ordinations. Taxa that preferentially occur in intertidal communities show a high salinity tolerance.

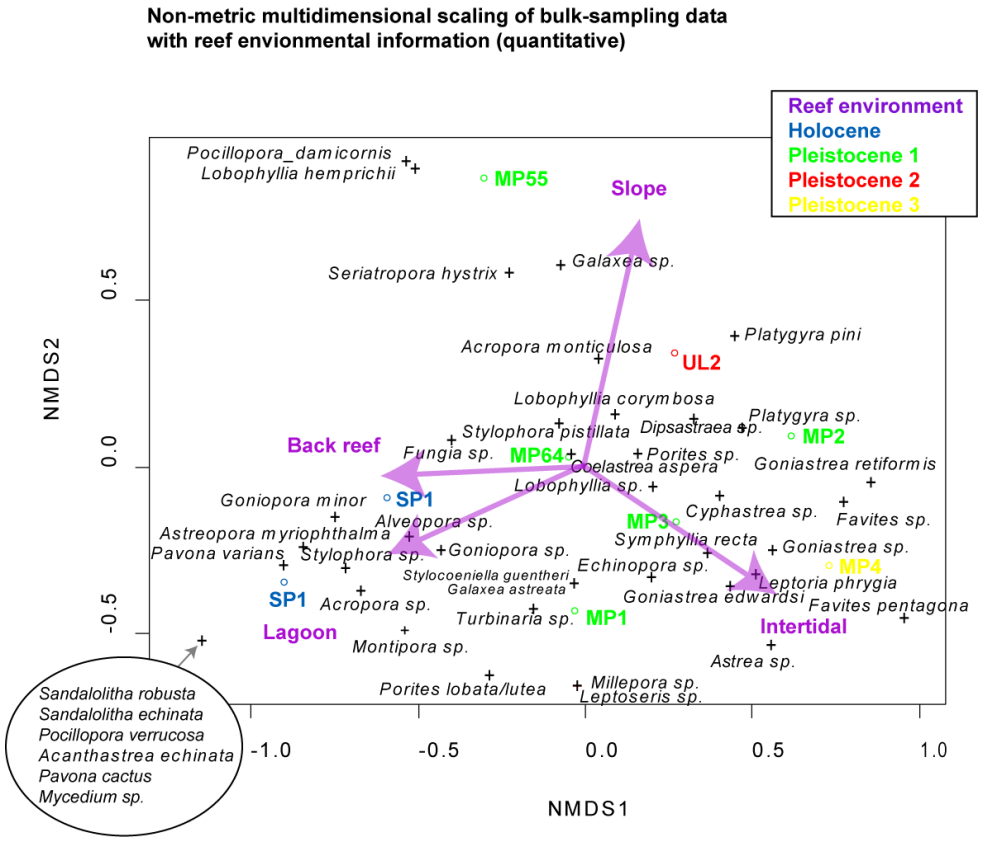

Figure 4.3.8: Ordination is the same as in Figure 4.3.7, but function `envfit` plotted "allenocs" data of Table 4.3.11 on the ordination. *P*-values: backreef = 0.45, intertidal = 0.3, lagoon = 0.39, slope = 0.21, crest = 0.98. The latter one is not displayed, because the information is not distinct enough.

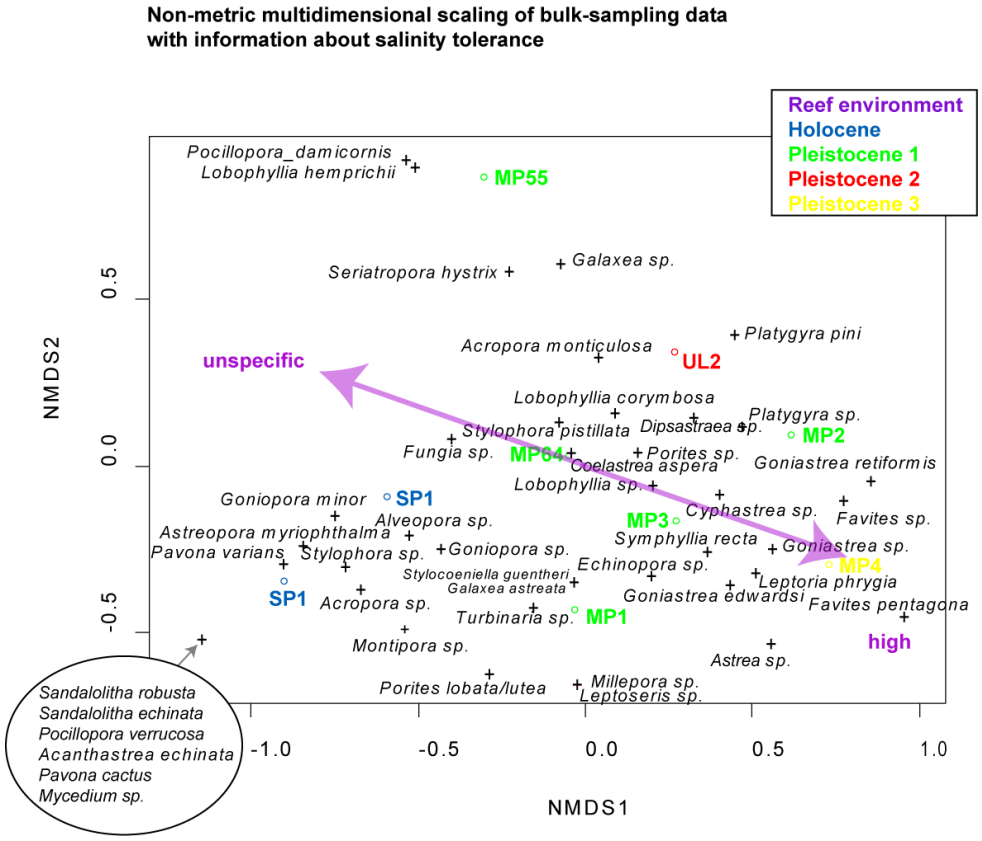

Figure 4.3.9: Ordination is the same as in Figure 4.3.7. *P*-values: high = 0.19, unspecific = 0.19.

4.3.6 Beta diversity with respect to environmental information

The beta diversity based on the Arrhenius species–area model among and within terraces is shown in Table 4.3.13 and Table 4.3.14, the latter one excluding La1, ULW and MP5 for previously mentioned reasons.

Table 4.3.13: Beta diversity based on the Arrhenius species-area model among terraces.

	Holocene	Pleistocene 1	Pleistocene 2
Pleistocene 1	0.45		
Pleistocene 2	0.62	0.58	
Pleistocene 3	0.71	0.61	0.58

Table 4.3.14: Beta diversity based on the Arrhenius species-area within terraces. H = Holocene, P1 = Pleistocene 1, P2 = Pleistocene 2, P3 = Pleistocene 3.

	MP1 (P1)	MP2 (P1)	MP3 (P1)	MP4 (P3)	MP55 (P1)	MP64 (P1)	Sa1 (H)	SP (H)	SP1 (H)	UL2 (P2)
MP2 (P1)	0.68									
MP3 (P1)	0.5	0.63								
MP4 (P3)	0.56	0.54	0.69							
MP55 (P1)	0.75	0.75	0.56	0.72						
MP64 (P1)	0.45	0.67	0.54	0.66	0.62					
Sa1 (H)	0.63	0.75	0.8	0.56	0.77	0.79				
SP (H)	0.66	0.87	0.68	0.89	0.74	0.62	0.79			
SP1 (H)	0.66	0.69	0.62	0.74	0.7	0.55	0.77	0.49		
UL2 (P2)	0.73	0.37	0.61	0.7	0.74	0.51	0.83	0.78	0.53	
UL3 (P2)	0.58	0.46	0.68	0.58	0.82	0.7	0.61	0.87	0.74	0.55

As already observed in the ordinations, the beta diversities are independent of the age of the site but are correlated to environmental conditions. To visualize this, a grouping by age and a grouping by assumed environment were tested against each other. The environmental assessment is based on the Bray Curtis dissimilarity, the cluster dendrogram and the environmental fit in ordinations of section 4.3.5. It therefore represents rather a similarity in species composition. Sites Sa1 and UL3 were included on the basis of the ordination in Figure 4.3.7. Accordingly Sa1 is treated as distinct environment. Its position will be discussed further below. MP1 and MP64 are most closely related in the cluster dendrogram and in the ordination. According to their contained coral taxa and the preservation of *Halimeda* chips in the framestone matrix, these sites are grouped together as sheltered fringing reef slope communities. Sp1 and SP build the second distinct group, declared as lagoonal (comprising lagoonal and backreef affinities from the NMDS) according to the environmental plotting. Both groups (sheltered and slope) build crown groups of two different clades in the cluster dendrogram. The other sites cannot be objectively distinguished from each other, especially when including UL3, and are therefore represented by one general cloud of slope environments.

Both the multivariate ANOVA based on dissimilarities (ADONIS) and the analysis of similarity (ANOSIM) tests showed no significant differences in taxonomic composition among assemblages from different times, regardless of whether MP4 was included (Table 4.3.15). However, ADONIS does show significant differences in taxonomic composition among assemblages from different reef environments, regardless of their age. ADONIS almost shows a significance with a *p*-value of 0.6. The (ANOVA, function `betadisper` in vegan) confirms significance. Pleistocene 3 had to be excluded from the latter analysis because it consists of only one assemblage, but it can be assumed that it

would not change the non-significance of the grouping by age. Pairwise permutation tests and Tukey's honestly significant difference (HSD) test of the outcome of the `betadisper` analyses show no significant difference between any of the terraces, but there are some strongly significant differences between certain environments. As already inferred from the ordination and cluster dendrogram, there is a significant difference in community composition between the lagoonal habitat of the SP communities and those of the sheltered reef slope communities MP1 and MP64. The permutation test did not deliver results for Sa1, but Tukey's HSD confirmed that Sa1 is significantly different from all other communities. The latter test does, however, not confirm significant differences between the other communities. Slope communities are not distinct from any of the other groups in either test.

Table 4.3.15: Summary of metrics used to assess the degree of similarity among Pleistocene reef communities from different reef environments and times from Efaté, Vanuatu. Adonis included the terrace Pleistocene 3, which contains only one site. All other metrics in the age group excluded Pleistocene 3 and MP4. Metrics were repeated with the preservation-standardized dataset.

	Raw Data	
	Grouped by age	**Grouped by reef environment**
ADONIS	R^2 = 0.38; *p* = 0.09	R^2 = 0.36; *p* = 0.03
ADONIS excluding MP4	R^2 = 0.31; *p* = 0.06	
ANOSIM	R = 0.21; *p* = 0.15	R = 0.35; *p* = 0.06
ANOSIM excluding MP4	R = 0.30; *p* = 0.07	
ANOVA (Betadisper)	F = 0.12; *p* = 0.89	F = 14.45; *p* = 0.002
Permutation test for F		
Pairwise comparisons		
Holocene - Pleistocene 1	Observed/permuted *p* = 0.96/0.97	
Holocene - Pleistocene 2	Observed/permuted *p* = 0.72/0.78	
Pleistocene 1 - Pleistocene 2	Observed/permuted *p*= 0.61/0.63	
Sheltered - Lagoon		Observed/permuted *p* = 2.2E-30/0.001
Sheltered - Slope		Observed/permuted *p* = 0.08/0.08
Lagoon - Slope		Observed/permuted *P* = 0.67/0.67
Tukey's HSD test		
95% family-wise confidence level		
Holocene - Pleistocene 1	*P* = 1	
Holocene - Pleistocene 2	*p* = 0.9	
Pleistocene 1 - Pleistocene 2	*P* = 0.9	
Sa1 - Lagoon		*p* = 0.005
Sa1 - Sheltered		*P* = 0.017
Sa1 - Slope		*P* = 0.002
Sheltered - Lagoon		*p* = 0.52
Slope - Lagoon		*p* = 0.96
Slope - Sheltered		*p* = 0.2

4.4 Discussion

4.4.1 Diversity and ecology of fossil reef terraces from Vanuatu

The results of this study suggest that the variability in the taxonomic composition of reef coral assemblages among sites within one terrace is greater than that among terraces from different interglacial episodes. This is consistent with previous studies from the Indo-Pacific region (Pandolfi 1996) and also from the Caribbean (eg., Pandolfi & Jackson 2001; Pandolfi 2001; Pandolfi 2002). Differences among reef terraces from Vanuatu may be explained by sampling bias as shown by the comparison between transect data and bulk sampling data. The differences in diversity between terraces that occur in the bulk sampling dataset cannot be confirmed with the transect data, which give a more objective result than bulk sampling. This is, however, not surprising, because transect data like the PIT 10 (point intercept transects with 10 cm intervals) are among the most robust methods to gain quantitative data (Facon *et al.* 2016). Bulk sampling was here not performed in a manner that it would allow for proper standardization. This sampling bias is the largest problem. Bulk sampling data and transect data give contrary signals concerning the diversity of all terraces. In the bulk sampling data Pleistocene 1 is the most diverse, whereas in the transect data it is the least diverse and Pleistocene 2 the most diverse. Using rarefaction on the transect data, all Pleistocene terraces reveal a similar species richness, whereas SQS suggest stronger differences between Pleistocene 1 and the other three terraces. The Holocene contains only one transect from Saama village, which was poorly preserved, so that the difference to the Pleistocene terraces in all methods, except for SQS, can be explained by sampling bias. SQS seems to be the more robust method for excluding sampling bias. The rarified and SQS bulk sampling data, however, gives another signal. Here, Pleistocene 1 and Holocene appear similarly diverse, while Pleistocene 2 and 3 are also similar and distinct from the younger two terraces. However, since the transect data cannot confirm this distinctiveness, I refrain from over-interpreting the bulk-sampling data in relation to diversity.

The interpretation of the Holocene is problematic insofar that I had to rely on only a few samples and some pictures. The potential of the outcrops at Samoa Point is probably far better than what is presented here. There is no doubt that diversity in the Holocene of Samoa Point is much higher than in any other of our sites, which is supported by the glimpse that we could catch with the bulk sampling data. Here, preservation plays the main role. The Holocene limestone cliffs along the beaches have not undergone many ten thousands of years of humid tropical climates and tectonic forces, but only about 5,000. Nevertheless, also the poorer preserved older terraces are remarkably similar in diversity as the transect data suggest, especially when considering the strong underestimation in diversity due the low species resolution in the older terraces. At least 48 different taxa could be identified out of 541 specimens from five reef-building episodes in the bulk sampling data and 20 out of 233 from four different reef episodes in the transect data. Thus, the species density is similar in both datasets: 11.65 % in the transect versus 11.27 % in the bulk sampling data.

The analysis of community structure did not show distinct differences between preservation-standardized and raw-data. Only in the Holocene the curves differ with a Zip-Mandelbrot distribution in the raw-data curve and a Zipf curve in the preservation-standardized dataset. Nevertheless, the Zipf-Mandelbrot model is derived from Zipf's law as described in Chapter 2, so that this difference might be negligible, especially when considering the unconventional sampling method at Samoa Point that already bears a potential source of error. However, this is just another hint that the potential of the outcrops at Samoa Point has not been tapped. For the other terraces with better technical sampling methods the results are discussed in the respective sections below. In those datasets the taphonomy - reconstructed by the reduced dataset - did not have any influence on the distribution model. Probably the complexity of the community structure makes the differences that occur after taphonomical events insignificant for the big picture.

The reconstruction of the reef ecology was the most interesting part in this chapter. The most comprehensive previous study of reef ecology in Vanuatu was performed by Done and Navin (1990), who studied numerous recent coral reefs in various environmental settings along the main islands of Vanuatu. The main differences they could observe are between "oceanic" exposed (outer) reefs and sheltered reefs. Our sites in the north-west of Efaté belong to the more sheltered reefs

since the islands of Moso and Lelepa are protecting the area from the open ocean. Done and Navin (1990) define four typical assemblages of coral species that characterize several parts of the reefs:

1. Outer reef slopes with abundant coralline algae and robust-branching corals (*Acropora* spp. and Pocilloporidae) in the reef crest zones, and with massive and branching corals including *Goniopora* spp. on the steeper slopes.
2. Sheltered parts of outer reefs with various species belonging to *Acropora* and *Montipora*.
3. Open embayments with massive domal *Porites* and *Acropora* spp.
4. Sheltered embayments with soft corals (that do of course not play a role in fossil communities) accompanied by domal *Porites* spp. and various branching species of *Acropora* and *Porites*.

Cabioch (2003) has shown that this characterization is suitable also for the reconstruction of the postglacial reef development in drilling cores from Espiritu Santo (Vanuatu), where he studied the reef growth and sea level changes of the last 23,000 years at a tectonically active zone. This characterization is hence also used to interpret my results.

4.4.2 Age reconstruction

The second important issue studied in Vanuatu is the dating of the terraces. Table 4.4.1 shows a summary of the results of previous studies and this study, and Figure 4.4.1 graphically displays the relation of the collected altitude and age data. The colors correspond to those of the different terraces used in my results. Obviously there is some discrepancy in the results between mine and those of other authors, especially in the middle terraces. The Holocene is distinct, and also the youngest Pleistocene terrace, which can be confidently correlated with MIS 5a at an altitude between at least 27 and about 60 m. Here, the results of all previous studies and mine are consistent.

Table 4.4.1: Dating results along Mt. Paopakoa (Mt. Erskine) from this study and previous studies. All sites are more or less taken along the same profile. The paleo-sea level is the sea level that was calculated by the respective authors (+/- above today's sea level). Terrace is the obvious or estimated reef building episode/marine isotopic stage. Caution must be exerted with our UL-profile data as they were taken on the other side of a fault in comparison to the rest of the samples. Especially UL2 needs to be put in brackets and is listed here only in the interest of completeness.

Site	Age (ka)	Altitude (m)	Paleo-sea level	Terrace	Source	Dating method
SP1	4.8 ± 0.6	2		HCO	This thesis	ESR
EKA.6	10.5 ± 5	10		HCO	Lecolle *et al*. 1990	U/Th
17-t	76 ± 5	27	+13	MIS 5a	Bloom *et al*. 1978	U/Th
ULW1	76.2 ± 9.8	35		MIS 5a	This thesis	ESR
MP1	69.8 ± 6.5	40		MIS 5a	This thesis	ESR
E AK 1	86 ± 4		+13	MIS 5a	Jouannic *et al*. 1982	U/Th
EY-t	92 ± 5	60	+13	MIS 5a	Bloom *et al*. 1978	U/Th
Efaté 235	120 ± 7	72		MIS 5e	Neef & Veeh 1977	U/Th
EKB.5	106.4 ± 6	80		MIS 5c?	Lecolle *et al*. 1990	U/Th
MP64	70.9 ± 6.6	80		MIS 5a ?	This thesis	ESR
EX-2	130 ± 7	81	+15	MIS 5e	Bloom *et al.* 1978	U/Th
EX-4	114 ± 6	81	+15	MIS 5e	Bloom *et al*. 1978	U/Th
UL2	140.3 ± 10.7	90		MIS 5e or MIS 7	This thesis	ESR
Efaté X	118 ± 7	100		MIS 5e	Neef & Veeh 1977	U/Th
EKA.4	121.6 ± 12.5	100		MIS 5e	Lecolle *et al*. 1990	U/Th
EKB.4	125 ± 16	100		MIS 5e	Lecolle *et al*. 1990	U/Th
ET-2	141 ± 8	105	-6	MIS 5e or MIS 7	Bloom *et al*. 1978	U/Th
MP2	79.2 ± 7.1	105		MIS 5a ?	This thesis	ESR
EL-3	141 ± 8	120	-6	MIS 5e or MIS 7	Bloom *et al*. 1978	U/Th
EKA.3	157.4 ± 11	120		MIS 5e or MIS 7	Lecolle *et al*. 1990	U/Th
EKB.3	175.2 ± 10.5	120		MIS 5e or MIS 7	Lecolle *et al*. 1990	U/Th

Site	Age (ka)	Altitude (m)	Paleo-sea level	Terrace	Source	Dating method
EL-1	131 ± 11	127	-6	MIS 5e or MIS 7	Bloom *et al*. 1978	U/Th
17-5	124 ± 7	130	-6	MIS 5e or MIS 7	Bloom *et al*. 1978	U/Th
MP3	34.8 ± 4.6	130			This thesis	ESR
EKA.1	300	250		MIS 9	Lecolle *et al*. 1990	estimation
MP4	237.5 ± 29.7	297		MIS 7 or 9	This thesis	ESR
MP5	350	393		MIS 9 or 11	This thesis	estimation

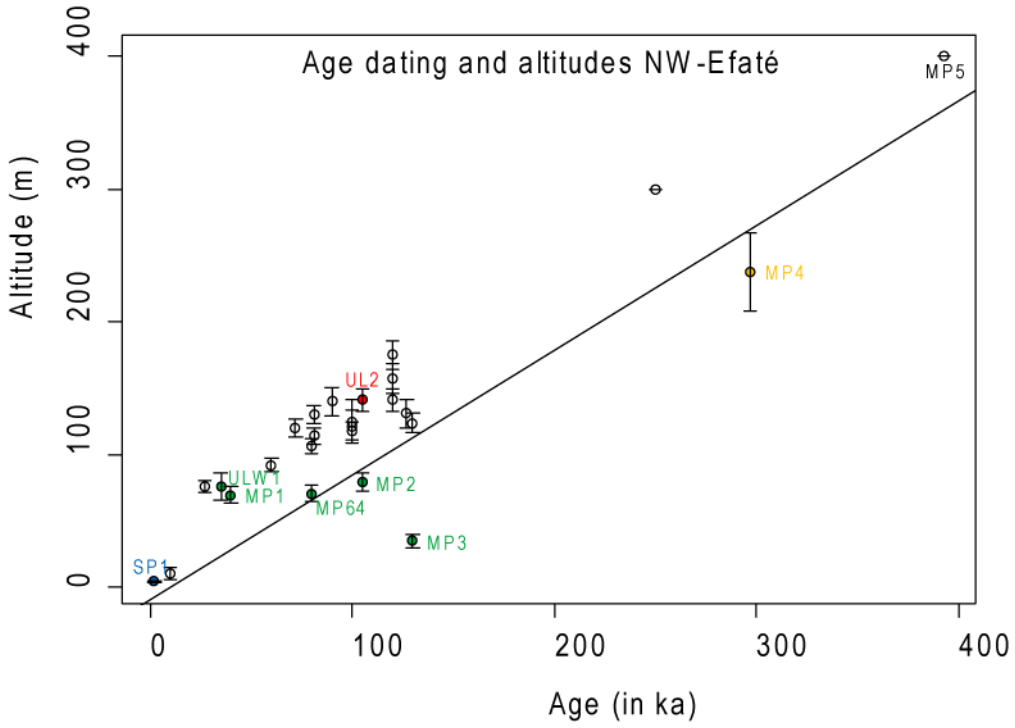

Figure 4.4.1: Scatterplot of age and altitude data from this thesis and studies listed in Table 4.4.1. A linear regression (p = 7.7E-11) can be plotted along the graph, indicating a constant uplift rate. Distribution of results from this study are marked with previously used color scheme and labeled respectively.

A scatterplot (Figure 4.4.1) of the literature and my dating results with altitudes reveals a significant (p = 7.7E-11) linear regression with R^2 = 0.83. This means that 83% of the pattern can be explained by this simple model. If my ESR-results are removed from the regression, R^2 is 95%, which is a significance of 1.2E-14.

The discrepancy between the ESR results and the literature data occur when interpreting the results of samples from above 60 m. There are two main sources of error that I can define: the complex structural geology and the precision of sites on the map and within the elevation-profiles. The topographic map in Figure 4.1.1d displays a fault system dividing Mt. Paopakoa. Our profiles are from each side of the fault, while Lecolle *et al*. (1990) and the other authors worked on the southern side of the fault, at our MP-profile. As such, the results of the UL-profile are only listed in the table for the interest of completeness. Nevertheless, my UL-dating results fit better into the existing dataset. The lower (Pleistocene 1) terrace is evenly wide on each side of the fault, while the middle terraces are compacted within a short distance in the MP-profile. This again reveals several new sources of error. Earthquakes and landslides may have led to these disturbances in terrace morphology.

The positions of sites in this study have been taken with the help of two GPS-devices in the field, and altitude values were corrected when drawing the profile and matching the positions on the map, which presumes correct values of the position given by the GPS-device. Studies from the 1970s, 80s and probably also from the early 90s could not use GPS devices and are based on correct orientation in the field. Consequently it cannot be excluded that the discrepancy in ages between my data and literature data is a result of incorrect correlation of sites, especially regarding the MP-profile where terraces of different ages are apparently densely packed.

The older terrace (our MP4) could not be dated previously; our study is the first that provides a measured age of this terrace, even though this cannot be tested and compared but only discussed with respect to its altitude. All results will be discussed in detail for every terrace below. Figure 4.4.2 gives a rough picture of the distribution of our ESR-results within/through time.

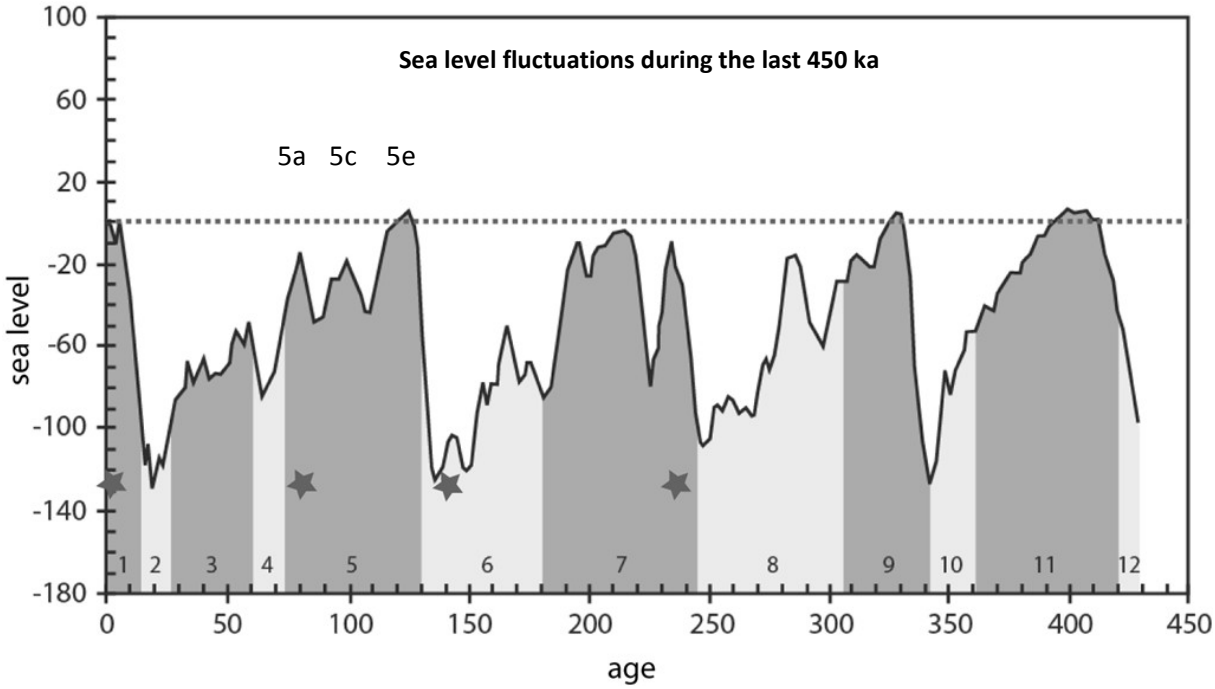

Figure 4.4.2: ESR-dating results (stars) within the context of Marine Isotopic stages, redrawn after Waelbroeck et al. (2002). Results from one reef building episode (MIS 5a in this case) have been summarized in one star. The dotted line presents today's sea level, the numbers in the grey fields give the marine isotopic stages, light grey are glacial episodes, and dark grey represents the interglacial episodes. 5a, 5c, and 5e mark the peaks within the last glacial episode.

4.4.3 Holocene

The youngest of the examined reef terraces comprises the sites at Samoa Point, Saama Village and Lakenasua. The dating results from Saama Village and Samoa Point suggest an age of c. 5,000 years, considering the systematic 5-10% underestimation of age in ESR dating results in comparison to U/Th dating (Schellmann *et al*. 2004, Schellmann & Radtke 2004). This was a time when sea level already reached the level of today, and the preservation of reefs of this age on land is only the result of the tectonic uplift in this region. As already mentioned above, the diversity is strongly underestimated. Two different reef environments can be distinguished in this study: Samoa Point with its 'lagoonal' (according to the environmental fitting) facies and Saama village with significantly distinct facies. The latter contains a high number of *Goniastrea*, but also contains *Porites* and *Lobophyllia*, and the robust branching *Acropora monticulosa*. Coralline algae are also abundant. According to Done and Navin (1990) Sa1 represents a reef crest environment at outer reef slopes. In contrast to the reefs at Samoa Point, the reefs at Saama Village are not protected by offshore islands. Samoa Point rather represents the fourth community type defined by Done and Navin (1990): the sheltered embayment. The islands of Moso and Lelepa protect the fringing reefs growing along the shore of NW-Efaté from outer sea conditions and lead to lagoonal or backreef (=sheltered)

conditions. The "allenocs" data shows that a large number of taxa from Samoa Point occur in slope, lagoonal and backreef habitats. Branching *Porites* and *Acropora* are very common, along with domal *Porites*. *Lobophyllia* as typical slope taxon is also common, next to *Goniopora* as typical backreef taxon.

4.4.4 Pleistocene 1 - MIS 5a

This terrace is the best sampled one, and also the one that comprises the most outcrops and different reef environments. Including all sites that might belong to the same interglacial period according to our dating results - namely all sites between 35 and 130 m, this is by far the best sampled terrace and contains at least two reef environments (exposed slope and sheltered areas). MP1 and MP64 represent sheltered fringing reef slope communities in probably deeper water than the slope community of MP 55, which contains several taxa that prefer shallower and more exposed habitats (e.g. *Goniastrea* and *Lobophyllia*). The rank abundance distribution (RAD) curve of this terrace bears a lognormal distribution, which is the most common distribution in Mesozoic-Cenozoic marine communities (Wagner *et al.* 2006) and is typical of mature communities with moderate complexity (McGill *et al.* 2007). As such, this terrace seems to represent a well established and undisturbed reef with different reef habitats. Nevertheless, this terrace is problematic concerning its age, especially when comparing our results to those of previous studies (Table 4.4.1.). The results from different authors in the lower part of the terrace until about 60 m are similar and clearly suggest an age of about 75 to 90 ka, which corresponds to MIS 5a - the last interglacial peak before the youngest glacial episode when sea level was distinctively below today's level. Our samples from higher altitudes (105 m and 130 m) at the Mt. Paopakoa profile still suggest the same episode, so that those sites are combined together as Pleistocene 1 in my analyses. Older studies gained ages from MIS 5c and 5 e at the latter altitudes. As the linear regression in Figure 4.4.1 suggests, the uplift rate in this region has been constant throughout the at least last 150,000 years (excluding the estimated ages of the older samples still leads to a significant linear regression). Consequently it can be excluded that samples collected in 105 or 130 m belong to MIS 5a, unless the uplift rate was higher in this profile, which is unlikely. MP2 and MP3 would thus rather be of Eemian age and would have to be moved to Pleistocene 2, which, as I tested, would not change the results. Pleistocene 2 would have a larger sample size and higher species richness and diversity, but the discrepancy between transect data and all levels of standardization and identification in the bulk sampling data remain the same. Even the lognormal RAD of Pleistocene 1 and the broken-stick RAD of Pleistocene 2 do not change. The small datasets of MP2 and MP3 apparently do not influence the results.

4.4.5 Pleistocene 2 - MIS uncertain

This terrace contains three sites (UL1, Ul2, UL3) in the Ulei profile, but only one dating result of about 140 ka from UL2. Preservation is poor and most samples were not suitable for dating. From the Mt. Paopakoa profile no sample approached that age, so that the sites from the Ulei profile were treated as one distinct unit. Ul1 and Ul3 were included based on the topology in the profile. It is likely that they were formed during the same reef building episode. The age of 140 ka would represent a glacial episode, so that I cannot give a reliable correlation with a certain interglacial episode. Pleistocene 2 could either represent the late MIS 5e, or - if underestimated - the early MIS7. However, regarding its present elevation of 90 m, none of the stages would fit to the uplift rate of 0.9-1 mm/a. The elevation of 90 m would be excepted for MIS 5c. In contrast to the phenomenon in Pleistocene 1 of the MP-profile, where younger samples occurred in higher altitudes, in the UL-profile apparently older samples occur in lower altitudes. As such, geomorphological events, such as landslides would deliver a robust explanation for the phenomenon in the UL-profile. This explanation, however, cannot solve the problem if UL2 grew during MIS5e or MIS 7. Inferring from the distinct underestimation in ESR-ages of MP2 and MP3, an underestimation of age in UL2, which also is partly recrystallized, appears to be more plausible. If so, this terrace would remain distinct from MP2 and MP3.

UL-sites are the poorest sampled ones in the bulk sampling data, but the best in terms of transect data (88 specimens versus 47 in the bulk sampling data). In both datasets the community of this terrace is the most even, and it is the least diverse along with Pleistocene 3 in comparison to Pleistocene 1 and Holocene in the bulk sampling terrace. When regarding the evenness of the transect data, there is no difference to most of the other terraces. The rank-abundance distribution shows a broken-stick community (Macarthur 1957). This community type indicates that a major factor is being roughly evenly apportioned among the taxa of this community (May 1975), especially in contrast to the lognormal distribution, which suggests an interplay of many independent factors. The broken-stick is typically found in narrowly defined communities of closely related species (MacArthur 1957). Caution must be exerted, because the small dataset might be the main reason for this result, but this result is robust even if MP2 and MP3 are moved to this terrace. Identification to species level was mostly not possible in the samples, but noticeable massive "faviids" dominate the community, along with *Porites.* No *Acropora* could be found, even though other branching taxa (*Stylophora*) were relatively common. This indicates that the underrepresentation of *Acropora* in Pleistocene terraces (discussed below) is not only due to taphonomical bias. The few identified taxa are relatively unspecific concerning their preferred environments. According to the NMDS plots UL2 is most likely an upper slope community.

4.4.6 Pleistocene 3 - MIS 9

Only one site, MP4, could be studied in that terrace. This was probably located within an exposed upper slope or crest environment, supported by the outcome of the analyses and the occurrence of environmentally distinct genera. *Goniastrea* is most common, but also several other massive taxa and massive branching *Acropora monticulosa*. The environmental conditions were probably similar to those in Sa1, to which MP4 shows the most affinities in the cluster dendrogram. The islands of Moso and Lelepa were probably only were low elevations in front of the shore 300 ka years ago when this reef developed. As such, the protected environment found nowadays was not given in that time. The community structure is relatively simple with a Zipf rank-abundance distribution, taking the raw bulk sampling data. Raw data and preservation-standardized data were identical in this dataset, because no branching, fragile and/or solitary taxa were identified. Zipf's law (Zipf, 1935) says that relatively few species occur very frequently, while a large number of taxa occurs rarely within a community. When considering the evenness of the transect data there is no difference to most of the other terraces, and with respect to the differences of the AIC of this model and the log-normal model for this community, the Zipf community pattern might just be a sampling artifact.

The result of the ESR-dating of one sample suggests an age of around 230 ka, which would fit into the late MIS 7. However, considering the altitude of this terrace (almost 300 m) the more likely explanation as observed in the ESR-results of the other terraces is again an underestimation in the dating. The ESR-dating results are lower, but also along a constant and linear level (Figure 4.4.1). When adding the error of 30 ka to the result and the 10% underestimation that ESR results usually reveal in comparison to U/Th-dating (Schellmann *et al.* 2004) we get an age of 293 ka, which is almost MIS 9. Inferred from the elevation of this terrace and assuming that the uplift rate remained constant, it can confidently be assigned to MIS 9.

4.4.7 Pleistocene 4 - MIS 11

This terrace at 393 m altitude could neither be dated nor studied in detail. The preservation is poor, the limestone is 100% recrystallized and only a few rocks with fossil corals are accessible. Only a few massive taxa, such as *Dipsastraea*, *Platygyra* and *Cyphastrea*, could be observed, so that any statement on the ecology would be speculative. Nevertheless, the age can be approximately calculated from the altitude, considering a constant uplift rate of between 0.9 - 1 mm a year and using the equation provided by Chappel *et al*. (1996) as in Section 4.3.1, i.e. t=(H -S)/U. The top of the mountain was at 393 m altitude, and reconstructions of ancient sea level vary between -10 and + 22

m (Siddall et. al. 2007). The resulting calculation gives an age of around 400 ka. Thus, the fourth Pleistocene terrace of Vanuatu can be correlated with MIS 11.

4.4.8 Diagenesis, taphonomy and the *Acropora* enigma

As shown in section 4.3.1 the recrystallization is independent of the age of the samples, leading to the fact that samples from MP4 (MIS 7 or 9) are not diagenetically altered, while younger samples might have experienced severe recrystallization processes. Here, exposure to tropical weathering played a major role. The samples from MP4 have been buried and sampled in a fresh road section, while stronger recrystallized samples were gathered from more exposed sites, where tropical weathering have influenced the limestone for a much longer time. The corals are mostly preserved in-situ and given that there is a 100% aragonitic preservation at about 300 m altitude, it seems that the fossil reefs have not undergone any major taphonomical changes. The only exception is MP5, where fossils and matrix became recrystallized probably within only 100 ka before MP4 was fossilized, as it otherwise should also have been affected. If there was some influence from the basalt layers that we found between MP4 and MP5 would be worth further investigations.

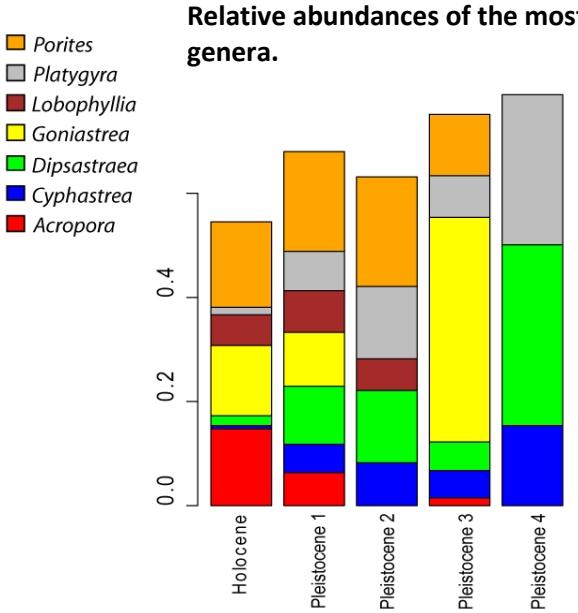

Figure 4.4.3: Relative abundances of taxa that have an overall abundance > 20% in the complete dataset and their distribution between and within the different terraces.

Figure 4.4.3 shows the relative abundance of the most common genera. This includes all taxa that have a relative abundance of more than 20% in the complete dataset. The figure shows how these abundances are distributed among the terraces. Pleistocene 4 is also shown, but only for completeness. As mentioned before, Pleistocene 3 is represented by one site and one environment only. Its intertidal origin explains the dominance of *Goniastrea*. It also has to be considered that some datasets are small, and the frequency of some genera is only based on their good preservation properties (*Dipsastraea* and *Cyphastrea*). This fact also explains why these few genera form up to 80% of the assemblage in the older terraces. *Porites* is a common (except in Pleistocene 4), but not dominating genus in all terraces, as is *Lobophyllia*, which is a typical slope taxon and therefore does not occur in Pleistocene 3 (MP4). What is very telling in this figure is the *Acropora* enigma. The fast-growing *Acropora* is the most diverse genus in recent Indo-Pacific coral reefs and usually very abundant, which is also reflected in the Holocene terrace. In the Pleistocene, however, *Acropora* is remarkably scarce. Especially Pleistocene 1 contains other branching corals like *Seriatropora* and *Stylophora*. Even the poorer preserved samples from Pleistocene 2 contain the branching taxa *Stylophora* and *Porites*. This fact renders taphonomy implausible as the sole cause for the under-representation of *Acropora*, at least for Pleistocene 1 and 2. In Pleistocene 3 only relatively massive

specimens of *Acropora* are preserved, but here the reef crest/flat situation might play the major role. However, Pleistocene 1 and 2 contain slope communities so that the absence of *Acropora* cannot be explained by the ecology of the locality in the reef. It seems that *Acropora* played only a minor role in the Pleistocene reef communities of Vanuatu, whereas any controlling or other responsible factors could not be identified within the frame of this study. However, ongoing research by Kiessling *et al.* (pers. comm.) indicate that this observation might be a general pattern in Pleistocene reefs throughout the Indo-Pacific.

4.5 Conclusions

This study provided for the first time insights into the taxonomy and ecology of the Pleistocene reefs of Vanuatu. Four Pleistocene (from MIS 5a to probably MIS 11) and one Holocene (around 5ka old) terrace have been identified and dated. The more recrystallized the samples are, the less reliable are the U/Th-dating results provided by other authors, whereas the ESR results do not seem to be significantly influenced by a larger calcite content (Schellmann & Radtke 2004; Schellmann *et al.* 2004). The ESR-dating method is the method of choice when comparing fossil reef terraces over several hundreds of thousands of years. However, as already indicated by above authors, ESR ages have the tendency to be underestimated and only deliver reliable results in statistically significant numbers and then using the oldest results (Schellmann & Radtke 2004; Schellmann *et al.* 2004). In this study, ESR ages follow the pattern of U/Th dating results of other authors, but are underestimations of those inferring from uplift rate and elevation of the terraces. The age discrepancy between my dating results can largely be explained by those underestimations, but problems in correlating correct altitudes and positions of sites gained with modern methods and those gained without GPS-devices on the map cannot be excluded. Some of the discrepancies, especially those between profiles might be the result of geomorphological disturbances.

My results show that the recrystallization is not generally dependent on the age of the samples, but more strongly influenced by other parameters, such as exposition to environmental forces (vegetation, climate, carst) after uplift. They also show that older terraces (up to MP4) are well enough preserved for age dating. A detailed mapping and dating of the terraces in NW-Efaté is possible and should precede further studies on the ecology of the Pleistocene assemblages. The UL-profile appears to be the more disturbed of the two profiles, and further studies should consequently concentrate on the profile south of the fault in Mt. Paopakoa.

Several reef environments could be identified on the basis of the species composition. Differences among terraces are mainly the result of the unbalanced sampling of different reef environments. ADONIS and ANOVA have shown that there are significant differences among environments rather than among terraces and a pairwise permutation of the multivariate analysis of variance reveals a significant difference between some of the environments. Slope communities, however, are not significantly different from all other communities, because they cover a large range of exposures, depths, disturbances, whereas crest and lagoonal communities are more specialized with distinctively different requirements to inhabiting species.

My study also shows that bulk sampling data should be handled with care when performing diversity analyses, because even a high level of standardization and identification cannot compensate the bias that becomes obvious when comparing bulk sampling data to transect data. However, bulk sampling allows to gain some insight into the ecology of fossil reefs by the identification of key genera, when the outcrop situation does not allow sufficient transect sampling. Transects should always be the first choice for quantitative ecological studies, because they give a more balanced picture on diversity distributions among different assemblages. The Pleistocene reefs of Vanuatu appear to be stable in the sense that there are no significant differences in species composition among terraces of different ages, apart from *Acropora* that becomes scarce in older terraces, and which cannot be explained by taphonomical biases alone.

5. PLEISTOCENE AND RECENT REEFS OF SINAI, EGYPT

Figure 4.5: Recent reefs and reef adjacent interglacial reefs at *Shark Observatory*, Ras Mohammed, show spectacularly well that it is possible to directly compare recent and fossil communities and environments in this region.

The fossil reef terraces along the northern Red Sea/Gulf of Aqaba coast provide an excellent opportunity for studying Pleistocene reef communities: There is (almost) no vegetation and a constant tectonic uplift, so that the terraces are well exposed within a narrow strip in parallel along the recent coastline (see Figure 5.1). Due to the low humidity and the absence of vegetation preservation is much better than in tropical areas like Vanuatu. It also explains why the lowermost preserved terrace shows only minor diagenetic alteration (Gvirtzman & Friedman 1977; Dullo 1990; El Moursi 1993). The reefs of the Gulf of Aqaba occur at relatively high latitudes (ca. 29°N), which makes them especially interesting when studying the effect of Pleistocene climatic fluctuations on reef communities. A poleward shift of coral reef development may be a reasonable scenario when SST further increases, and thus subtropical habitats like the northern Red Sea may become potential refuges (Kiessling *et al.* 2012; Fine *et al.* 2013; Descombes *et al.* 2015). Modern coral diversity in the Red Sea, and especially in the central Red Sea, is the highest for the western Indian Ocean (Spalding *et al.* 2001).

In this chapter, data are examined at different scales. First, I look at the large-scale distribution of coral communities in the Red Sea and adjacent regions. A presence-absence dataset is used to compare the Pleistocene coral distributions with those of modern reefs in the Red Sea. The next scale includes the analysis of PIT data from two different localities, Ras Mohammed National Park and *The Canyon* dive site north of Dahab, both Sinai peninsula, in relation to data from recent reefs at the dive site *The Islands* in Dahab. The third scale, and the smallest one here, focuses on a large reef complex at *The Canyon* dive site that reveals ecological succession.

5.1 Geographic situation and geological background

The Red Sea is a branch of the Great Rift Valley, a continuous rift system that ranges over approximately 6000 km from Syria to Mozambique. It represents a highly active rifting zone analogous to the mid-ocean ridges, with the major tectonic units being the Arabian and African plates. Figure 5.1.1 provides a detailed overview of the complex tectonical background of this region, along with an overview of the locations of this study. The Red Sea extends 2270 km from 30°N in the Gulf of Suez to 13 °N at Bab-el-Mandeb in the southeast. The Red Sea is a narrow, max. 350 km wide and up to 2920 m deep oceanic basin. The only 137 m deep and 30 km wide Bab-el-Mandeb Straight restricts water exchange between the Red Sea and the Gulf of Aden. The sill at Bab-el Mandeb is also a biological barrier for some species, largely because of the upwelling of 16° C cool deep water currents from the Gulf of Aden. The land surrounding the Red Sea is mostly hot and dry with minimal freshwater inflows and high evaporation. Therefore, surface waters enter the Red Sea from the Gulf of Aden to compensate for evaporation loss. The salinity varies along the length of the Red Sea from 36.5 ppt (normal seawater) at the southern entrance to more than 41 ppt in the northern Gulf of Aqaba in summer. Water temperatures and nutrient concentrations decrease in surface waters towards the northern end of the Red Sea, where the water is generally clearer.

The narrow basin and the rectilinear coast of the Red Sea do not favor tropical storms or tsunami waves and the coast was thus rarely exposed to extreme hydro-dynamic events. These special climatic, geographic and sedimentary conditions favored the development of low-energy coral reef terraces during Quaternary sea level highstand (Plaziat *et al.* 1995, 1998). Also, during the recent highstand coral reefs are well developed along the Red Sea, with fringing reefs lining most of both shores and into the Gulf of Aqaba.

The Egyptian localities investigated in this study are located on the Sinai Peninsula, which is a sub- or microplate, located between the African and Arabian plates, and bordered by the Suez and Red Sea rifts and the Dead Sea transform fault. Due to tectonic activity associated with the widening of the Red Sea, Pleistocene reef terraces are well preserved along the Red Sea coast. In contrast to most other uplifted reef terraces (e.g. Vanuatu), which are superimposed on convergent plates in a subduction system with much higher uplift rates, the coral reefs of Sinai are growing on a lateral-moving plate margin being part of a transform system (Gvirtzman 1994). The latter author calculated an average uplift rate of only 0.085 mm year^{-1}, resulting in relatively narrow terraces close to the recent coast. This relative low uplift rate makes the fossil reefs of Sinai ideal sea level recorders.

The Gulf of Aqaba is a northward extension of the Red Sea that separates Sinai from the Arabian plate. The Gulf of Aqaba is characterized by a maximum depth of 1830 m, a length of 180 km, and a width 5 to 26 km (Al-Rousan *et al.* 2002). The morphology of the fossil reefs is largely a result of the coastal morphology. Reefs in the Gulf of Aqaba now and then are usually fringing reefs along steep narrow cliffs (Dullo & Montaggioni 1998), because a true continental shelf is missing and the offshore profile is very steep (Gvirtzman & Buchbinder 1978).

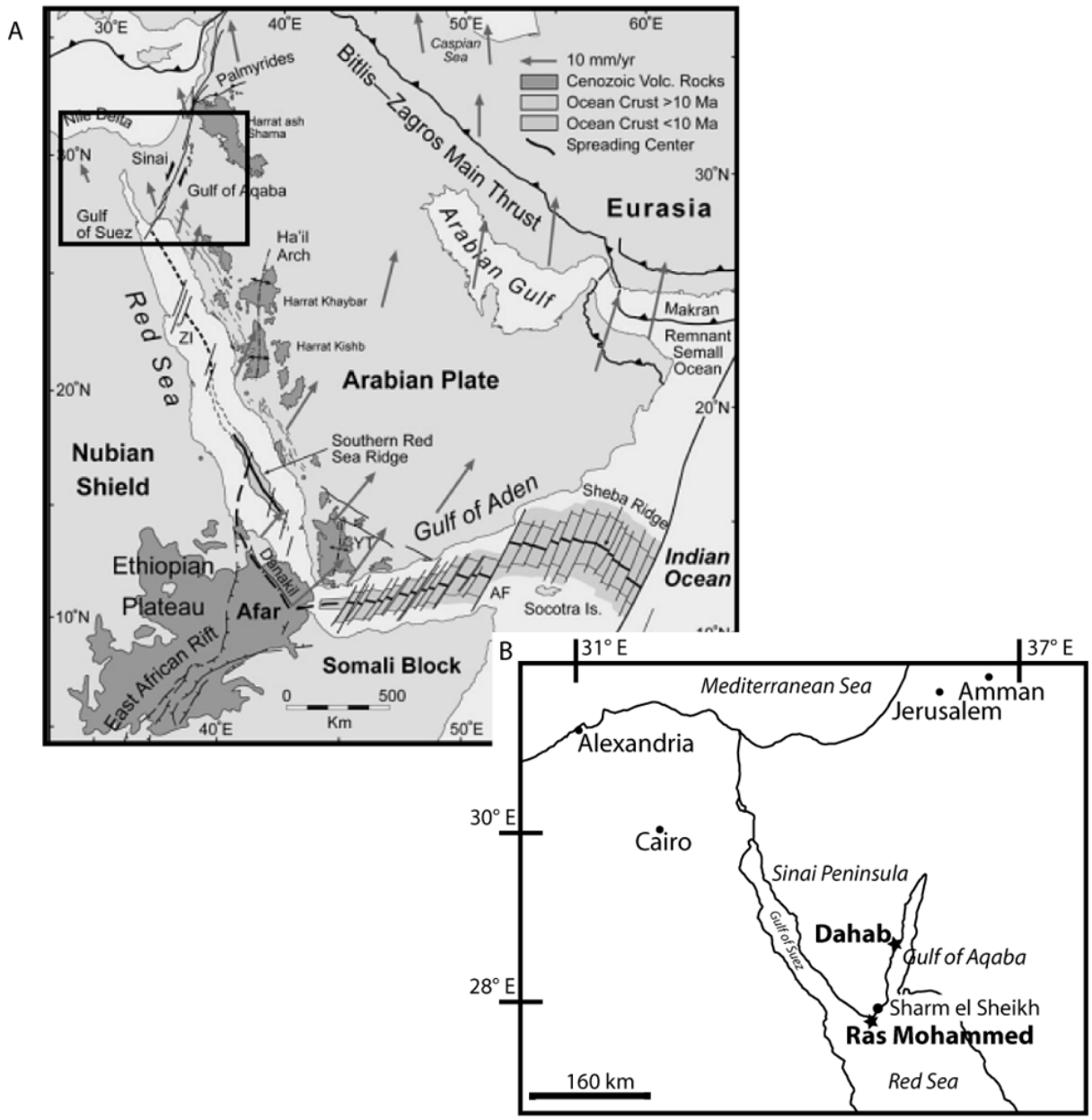

Figure 5.1.1: Overview of the study area. A (taken from Bosworth 2015) - Tectonic features of the greater Red Sea rift system, including the East African rift, Afar, and the Gulf of Aden, Aqaba and Suez. AF = Alula Fartak fracture zone, YT = Yemen traps, ZI = Zabargad Island, Red arrows are GPS velocities in an Eurasia-fixed reference frame from ArRajehi *et al.* (2010). B - Close-up of the Sinai Peninsula and adjacent regions. The two localities of this study are highlighted. Dahab is located in the central Gulf of Aqaba, while Ras Mohammed is the southernmost tip of the Sinai Peninsula where faunas from the Gulf of Aqaba, from the Gulf of Suez and the open Red Sea meet.

5.1.1 Age of the reef terraces and sea level implications

The coastal lowlands on both sides of the Red Sea are mostly formed by eroded escarpment uplifted since the early Miocene (e.g. Bosworth 2015) and for sea level studies it is important to know whether this uplift has continued into the present or whether it has ceased in recent time, as it was also suggested by Plaziat *et al.* (1998) for some sectors of the African Plate in Egypt. In Dahab only one Pleistocene terrace could be identified, while there where at least three of them forming the landscape in Ras Mohammed (Figure 5.1.2). A fourth one is probably formed as patchy structure further inland. Subject of this study is only the youngest terrace (I), because it is preserved in both localities and has not undergone much diagenetic alteration in contrast to the strongly eroded (Plaziat *et al.* 2008) and poorly preserved older terraces. While all previously published ages obtained from the lowermost fossil reef terraces along the Red Sea coast from Djibouti to Egypt can be

correlated to the last interglacial high-stand sea-level, marine isotopic stage (MIS) 5e (Veeh & Giegengack 1970; Buss & Jackson 1979; Faure *et al.* 1980; Andres *et al.* 1988; Hoang & Taviani 1991; El Moursi *et al.* 1994; Gvirtzman 1994; El-Asmar 1997; Strasser & Strohmenger 1997; Parker *et al.* 2012b), there is little consensus about the elevation of the lowermost terrace. Lambeck *et al.* (2011) correlated all previous studies on altitude and age of Pleistocene terraces along the Red Sea coast and came to the conclusion that all of them obtain an elevation between 5 - 9 m, with a mean of 7 ±1.5 m, above the recent sea level for the lowermost terrace, with the exception of the terraces studied by Gvirtzmann *et al.* (1992), Gvirtzmann (1994), and El-Asmar (1997) in southern Sinai (Um Seed and Ras Mohammed), which are substantially lower and about 3 - 6 m in elevation. This corresponds with the elevation of the lowermost terrace in Ras Mohammed studied here. Lambeck *et al.* (2011) argue that Pleistocene terraces may not always correspond to the maximum elevation of reef development during the particular interglacial and that regional differences in tectonics should be considered. For the main fossil terrace in Dahab the elevation fits well to Lambeck *et al.*'s reconstruction and correlations of the elevation of the lowermost terrace, while some of the patch reefs along the coast in Dahab correspond to the elevation of the lowermost terrace in Ras Mohammed. However, in terms of preservation all these terraces are similar and clearly distinct from the second terrace in Ras Mohammed, which is recrystallized and can be distinguished already by its preservation.

Figure 5.1.2: Fossil marine terraces in Ras Mohammed, view from the northern coast on the top of terrace I towards the entrance of the Marsa Bareika and the tongue that separates the Marsa Bareika from the bay of Ras Ghozlani in the east. This land tongue is called *Ras Ghozlani* within this study, and terrace I on this picture is exactly where the transects of *Ras Ghozlani* were taken. Here the terraces are distinct.

Thus, apart from two transects that have been taken in older terraces, all fossil sites of this study can be confidentially assigned to MIS 5e (Eemian stage) with an age of 115 - 130 ka before present. Several authors (Hoang & Taviani 1991; Bosworth & Taviani 1996; Hoang *et al.* 1996; El-Asmar 1997; Plaziat *et al.* 2008) argue that the height of this terrace indicate the absence of

tectonical uplift in the last 125,000 years, and the occurrence of older and higher terraces indicate that uplift existed before the last interglacial (Plaziat *et al.* 2008). However, Lambeck *et al.* (2011) presented new calculations and correlations of the sea level history in the Red Sea considering the effects of isostasy. The authors calculated that if there was no tectonic uplift, the Eemian terrace would be barely above sea level because of the influence of the Eurasian ice sheets during MIS 2 and MIS 6. As most Eemian terraces are between 5 - 9 m above sea level, a site-specific near uniform long-term uplift is the most plausible explanation (Lambeck *et al.* 2011). Terraces II and III are assigned to MIS7 and MIS 9 along the entire Red Sea coast (Lambeck *et al.* 2011). However, in a complex tectonic system like the Red Sea it has to be accepted that there are local exceptions, and especially Ras Mohammed shows variations in the elevation of the lowermost terrace. As Nir (1971) has shown, the height and especially the width of the lowermost terrace in Ras Mohammed depends on the topography, and, most importantly, that there is much tectonic disturbance exhibited in all terraces on the peninsula. The lowermost terrace is narrow along the coast of Marsa Bareika, a bay separating the Ras Mohammed peninsula from the rest of Sinai, similar to the narrow recent fringing reefs. Present reef flats in the Red Sea are typically between 0.5 and 1 m below present sea level (Dullo 1990; Dullo & Montaggioni 1998) and the identification of a reef flat in fossil reefs is useful to infer the paleo sea level.

During the last glacial maximum (LGM), when sea level was ~ 120 m below recent (Peltier 1994, 2004; Siddall *et al.* 2007) the water exchange at Bab-el-Mandeb was dramatically restricted (Rohling *et al.* 1998; Siddall *et al.* 2004), but not completely interrupted (Lambeck *et al.* 2011). Salinity in the Red Sea increased up to 55 ppt (Reiss *et al.* 1980; Brachert 1999; Siddall *et al.* 2003; Almogi-Labin *et al.* 2008), the water column was stratified and there was a stronger, shallower oxygen minimum zone (Almogi-Labin *et al.* 1998, 2008), which led to local decimation of corals (Braithwaite 1987) and plankton (Fenton *et al.* 2000), but allowed the growth of stromatolites on the deep shelf. The reestablishment of coral reefs started only after sea level returned to within 20 m of the present level, around 8 ka ago (Braithwaite 1987). The situation was probably similar in other Quaternary glacial cycles (Lambeck *et al.* 2011) . The sea level reconstructions for the glacial episode MIS6 was similarly low as the sea level during the LGM (e.g., Siddall *et al.* 2007).

5.2 Localities

Two localities on the Sinai Peninsula are analyzed herein. One of them is located about 5 km north of Dahab, a small town popular among divers, at the coast of the Gulf of Aqaba. Data on modern corals were collected by Alter (2004) from the diving sport *The Islands* directly in Dahab and made accessible to me. The other locality is the Ras Mohammed National Park at the very southern tip of the Sinai Peninsula (Figure 5.1.1A). Table 5.2.1 shows the recent species richness in the Red Sea region. Alter (2004) provided these numbers from an unpublished report by Abou Zaid (2000). They show that the Gulf of Aqaba hosts a high diversity of corals despite its high latitude.

Ras Mohammed is a National Park that marks the southern tip of the Gulf of Aqaba on the Egyptian side, and one of originally four marine protected areas in southern Sinai. The others are Nabq, Ras Abu Galum, and Taba. These protected areas have been combined with the St. Katherine protectorate, including Mt. Sinai, to the Southern Sinai Protectorates Network and are now covering 11,000 km^2 of marine and terrestrial habitats, including 52% of the Egyptian shoreline along the Gulf of Aqaba. The coast north of Dahab, including the fossil reefs, belongs to this protected area as well, as does Ras Mohammed National Park.

Table 5.2.1: Number of genera and species of reef-building corals in the Egyptian Red Sea (Alter 2004)

Region	Genera	Species
Gulf of Aqaba	47	120
Gulf of Suez	25	47
Northern Red Sea	45	128
Central Red Sea	49	143
Southern Red Sa	31	74

5.2.1 Locality 1: From Dahab to the Blue Hole along the Gulf of Aqaba

The Canyon, a popular dive site, is situated approximately 5 km north from the northern city limits of Dahab (Figure 5.2.1). The southernmost exposure of the fossil terrace directly faces the diving spot, and from there stretches 2700m northward up to the *Blue Hole*, which is another dive site (Figure 5.2.2). Only one reef terrace has been preserved along this narrow coast, where the Sinai mountains (aka Red Sea Hills), which represent the uplifted Neoproterozoic crystalline basement of the Red Sea (Bosworth *et al.* 2005), reach to the shore. Along the foothills of these mountains, interrupted by wadis, recent and Eemian reefs find and found the necessary hard substrate to develop, respectively. Older terraces have probably been eroded along the steep mountains. Holocene reefs with an age of about 6 ka have been dated within 0.2 - 0.5 m above the recent sea level along the Gulf of Aqaba (Gvirtzman *et al.* 1992; Gvirtzman 1994). The fossil reef flats merging into the recent reef flat, exposed at some places between The Canyon and the Blue Hole can thus be interpreted as top of the mid Holocene reef flat (Figure 5.2.3).

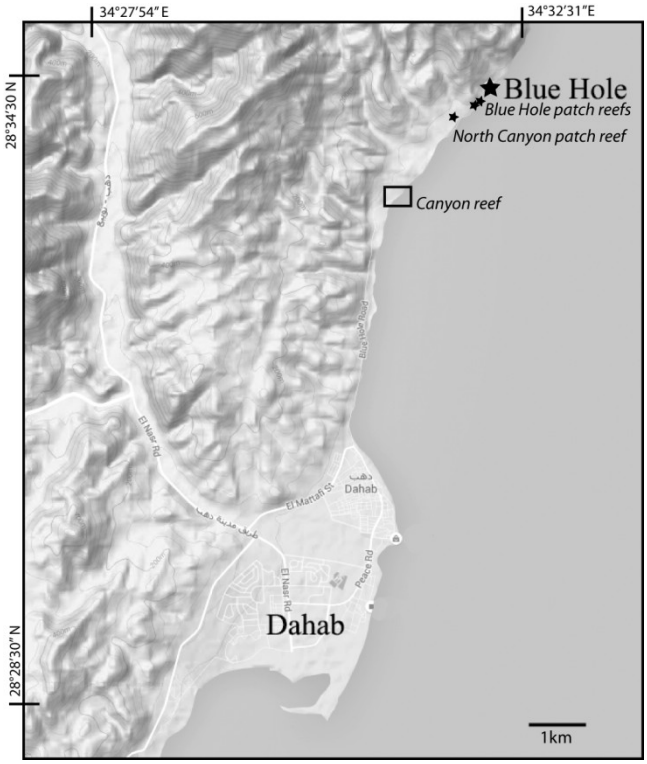

Figure 5.2.1 (left): Overview of the area north of Dahab with the sites marked. The rectangle marks the location of the Canyon reef and Figure 5.2.2. It contains GPS-Points 42, 43, 44, 48, 51, 52. North Canyon patch reef is GPS-Point 41, the Blue Hole patch reefs comprises GPS-Points 49 and 50 (Appendix II-IV).

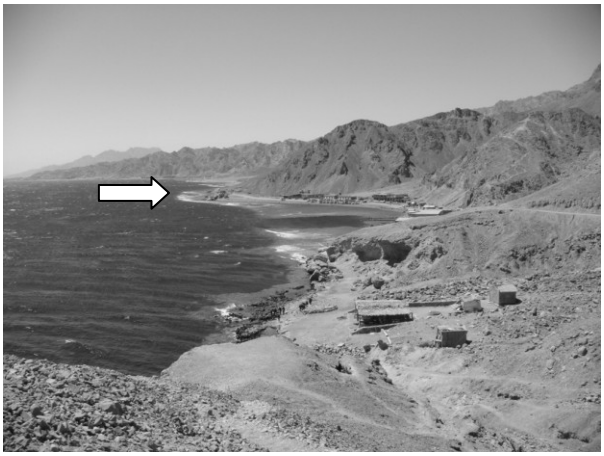

Figure 5.2.2: View over the *Blue Hole*, a submarine sinkhole in the recent reef. This picture illustrates how narrow the recent fringing reefs follow the coast, and how close the Sinai mountains aka Red Sea Hills (crystalline Precambrian basement) are to the shore. Only one fossil reef terrace is preserved in form of patchy structures along the beach. One of these outcrops can be seen in the middle of the picture (arrow), directly in front of the Blue Hole.

Figure 5.2.3: The recent reef flat during low tide, and the mid Holocene (~6 ka) reef flat in the front.

The *Canyon Reef* (28°33'19"N, 34°31'15"E)

This well preserved coral reef at Wadi Abu Ma' (Figure 5.2.2) has been studied in detail, and I will refer to it as *Canyon reef* in the following. The Canyon reef represents a morphologically well defined reef body (Figure 5.2.3) that includes three clearly distinguishable zones. The main reef body reaches a thickness of 7.7 m and can be traced laterally for about 150 m. It is a narrow fringing reef that stretches along a foothill of the close-by Sinai Mountains. Seaward the reef ends abruptly as a steep cliff, as it is typical for the fringing reefs in the Gulf of Aqaba. Landward it thins out rapidly. The base of the reef is 5 m above the recent sea level. The Canyon reef is underlain by 3.5 m of siliciclastic fanglomerates, which are conglomerates deposited by alluvial fans (or wadis) in arid areas. Fanglomerates are compositionally immature and matrix-supported. The angular to subangular

shape of clasts suggests that a minimum or non-intensive abrasion has occurred before sedimentation. Terrigenous fanglomerates also cover the reef top. Twenty transects with a total of 1153 datapoints have been collected at this site.

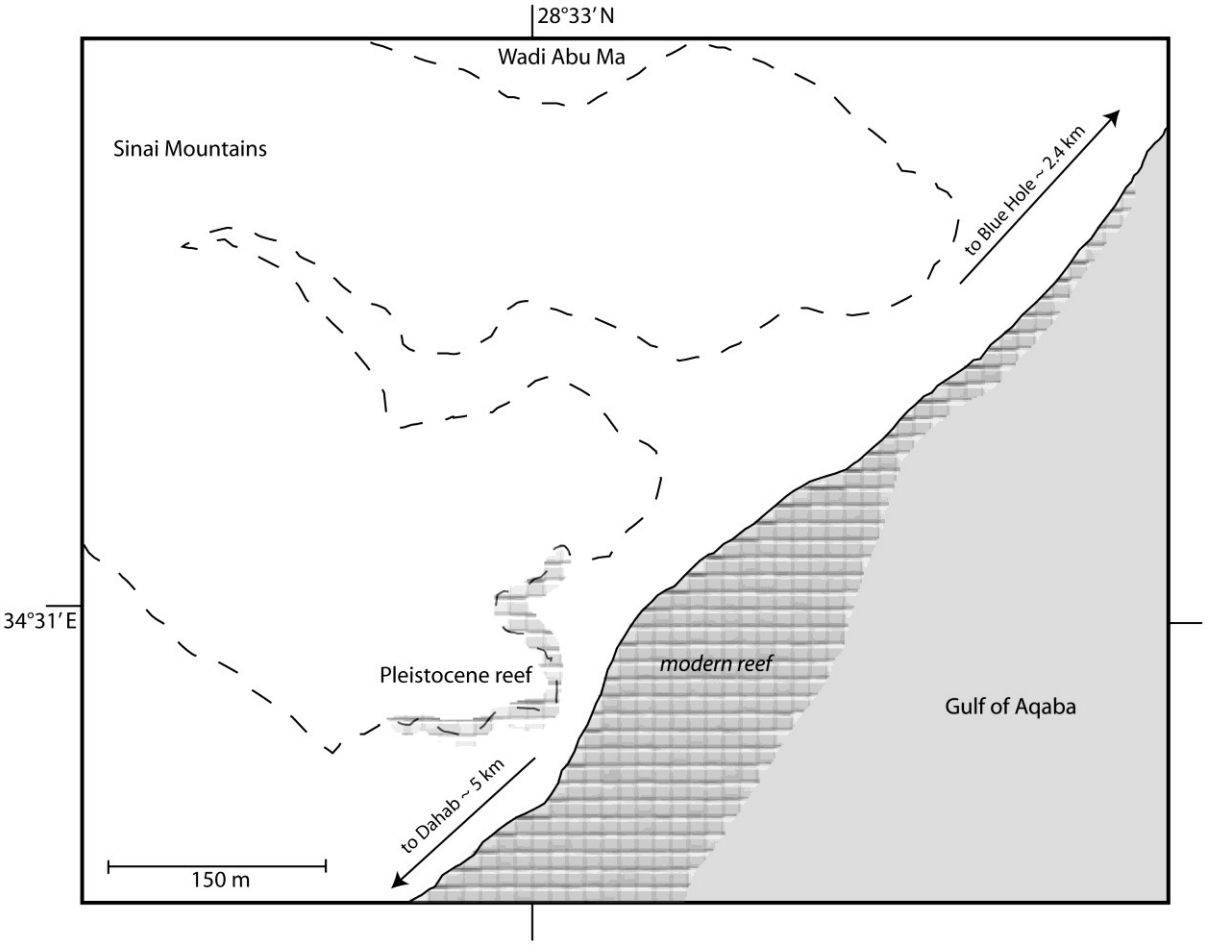

Figure 5.2.2: Locality map of the Canyon reef (Sinai, Egypt). Modified from Mewis & Kiessling (2013).

Figure 5.2.3: Reef front of the Canyon reef, directly above the diving spot *The Canyon*. The front is a steep cliff that comprises three clearly distinguishable zones.

North Canyon patch reefs and Blue Hole

All further transects from Dahab have been taken in patch reefs along the Gulf of Aqaba, between the Canyon reef and the Blue Hole (Figure 5.2.1). The site *North Canyon patch reef* contains five in parallel transects with a total of 126 datapoints from the same patch reef at 28°33'59.13" N and 34°31'49.65" E. This patch is mainly made up by lose gravel, covering a layer of beach rock above a reef framestone of about 3 m height and 4 m width (Figure 5.2.4). This small patch contains a rich coral fauna. The shortest distance from the patch reef to the shore is about 80 m, and the elevation is approximately 2 m above sea level.

Figure 5.2.4: North Canyon patch reef - a hill mainly built by gravel and containing a small patch of reef limestone. A layer of beach rock covers the patch.

Figure 5.2.5: Patch reef directly south of the Blue Hole at WP50. Reef limestones here are located directly on the shore and are less elevated than the Canyon reef or the North Canyon patch reef.

Six transects with a total of 330 datapoints have been taken close to the Blue Hole between 28°34'5.52" and 28°34'12.08" E, and between 34°32'2.18" and 34°32'2.18" N from three small patch reefs within a distance of 280 m. They have been summarized to one site *Blue Hole*, because otherwise the sample size of each patch would have been too small to be compared to the much larger samplings at other sites. Also the short distance between the patches along a recently relative uniform shore justified this procedure. All three patch reefs are located directly at the shore, in contrast to the North Canyon patch reef and the Canyon reef. They connect directly to the Holocene beach rocks and are elevated up to 5 m above recent sea level (Figure 5.2.5). Similar to the Canyon reef they are covered by beach rock und unconsolidated gravel from the wadi. However, differences in the communities have already been obvious in the field, but also other sites as, for example, the Canyon reef comprise communities from different water depths within one reef. One of the patch reefs at the Blue Hole is exclusively built by *Porites nodifera*, similar to one of the zones in the Canyon reef. The other two patches are more diverse.

5.2.2 Locality 2: Ras Mohammed National Park

Ras Mohammed National Park is the southernmost point of the Sinai Peninsula, about 10 km south of Sharm El-Sheikh. The park spans an area of 480 km², including 135 km² of surface land area and 345 km² area over water. Ras Mohammed is separated from the Sinai Peninsula by a shallow bay inlet called the *Marsa Bareika*. Only a narrow land bridge of 3.5 km length and a maximum width of 800 m connects the Ras Mohammed peninsula with the rest of Sinai. The peninsula represents a single block of uplifted fossil reef terraces. In the *Mangrove Channel* at the very southern tip of the peninsula the second most northern mangroves worldwide can be found. (The northernmost mangroves grow in Nabq, only a few kilometers north of Sharm El-Sheikh.) Water masses from the Gulf of Suez, the Gulf of Aqaba, and the open Red Sea meet around the Ras Mohammed peninsula, and so does the contained life, which is supposed to be the highest diverse around Sinai. Coral reefs are well developed around Ras Mohammed. The climate is very dry, with only minimal rainfall during winter. During summer, temperatures often exceed 40°C. Temperatures are mild during the winter, with daytime high temperatures averaging around 23°C and low temperatures of about 14°C. This results in desert dominated inland habitats. Vegetation is scarce. The sites of this study are all located along the northern shore of Marsa Bareika.

5.2.2.1 Sites in Ras Mohammed

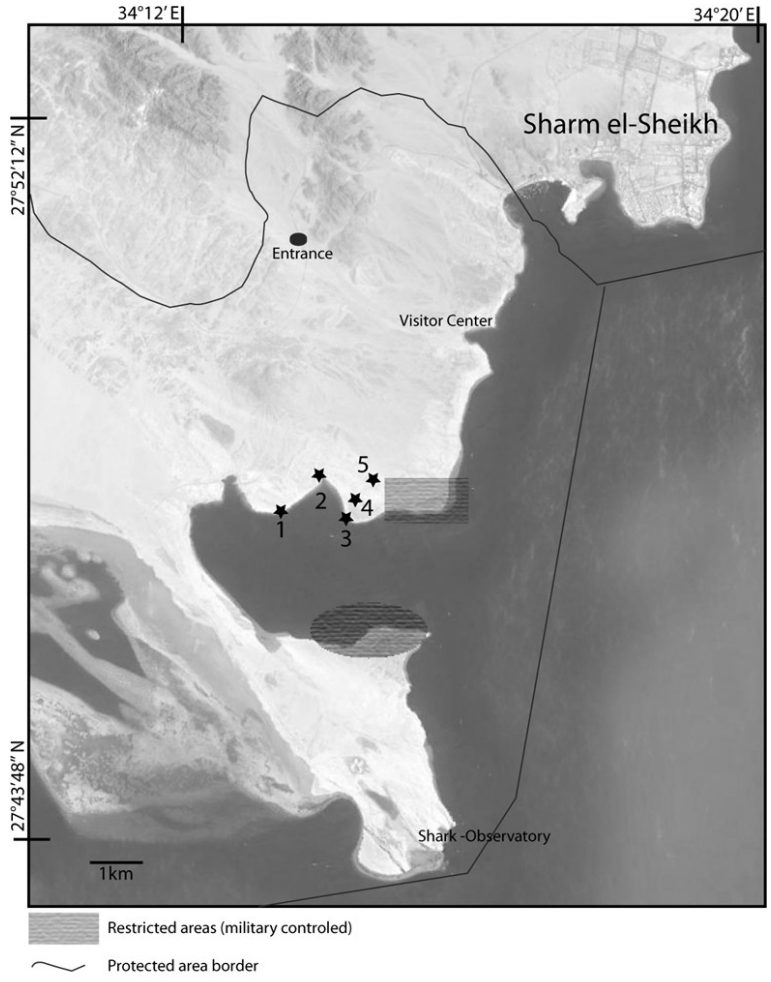

Figure 5.2.6: Map of the Ras Mohammed peninsula and a large part of the National Park (bordered). Sites are marked with numbers: 1 - Ras Mohammed Camp, 2 - Turtle Bay, 3 - Ras Ghozlani, 4 - Ras Ghozlani inland (terrace II), 5 - Ras Mohammed inland (terrace III).

Ras Mohammed Camp (27°47'19.71"N, 34°13'31.24"E)

The first site in the Ras Mohammed National Park is the terrace located directly next to the camp in the park, at the northern shore of Marsa Bareika (Figure 5.2.7). The terrace begins directly above recent sea level and reaches a height of max. 3 m above sea level. It can be followed eastwards to the next wadi, but the surface increases gradually in elevation until it meets the lowermost terrace within the wadi described in the next section (site *Turtle Bay*). This terrace has been dated by El-Asmar (1997) as 118 - 125 ka, which represents MIS 5e. Because of its low elevation, the author argues that this area does not have experienced any significant uplift in the last 125 ka, which also explains why terraces from MIS 5a and MIS 5c are not preserved in this region. Sea level during the latter stages was lower than in the present and the terraces must now be located beneath the recent reefs. All reef terraces along the shore are marked with a notch at their base. However, the elevation and the width of this lowermost terrace (terrace I) varies greatly among sites within the park, which is probably mainly the result of antecedent topography, but fault displacement cannot be excluded either at some places. At the camp the terrace reaches a width of about 60 m. It is a well preserved fringing reef that is covered by beach rock and loose gravel. It contains many coralline algae. Four transects with a total of 421 points were taken.

Figure 5.2.7: The camp at the northern shore of Marsa Bareika in the Ras Mohammed National Park. It is located at a beach directly next to the lowermost reef terrace and below the second terrace (Figure 5.2.13).

Turtle Bay, 27°47'44.27" N, 34°13'55.66" E

Turtle Bay is the best studied site in Ras Mohammed. This site is situated at the end of an alluvial fan in a small sandy embayment within Marsa Bareika. Two larger blocks of one terrace are preserved about 5 m above recent sea level (during low tide) between several wadi structures, a southern block (reef 1, Figure 5.2.8) and a northern block (reef 2, Figure 5.2.9). Several small patches, which are mainly built by fanglomerates and coral rubble flank the western side of the wadi shorewards (Plate 5.1), while the eastern flank of the wadi contains loose debris only (Plate 5.1b), with older limestone terraces on top of them. The preserved fossil reefs are covered by a thick layer of beach rock and wadi sediments. Also, there are several layers of siliciclastic sediments in between the corals, getting more landwards where the reef limestone thins out rapidly.

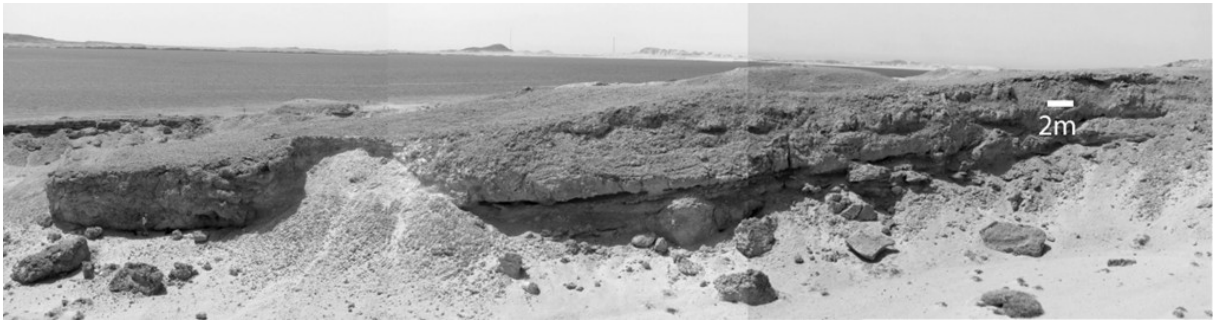

Figure 5.2.8: Southern block (reef 1) within the wadi discharging into a small embayment within the northern Marsa Bareika. A distinct bedding can be observed within the more inland part of the block, while the seaward end bears a diverse coral fauna and has been less heavily disturbed by alluvial deposits. The red circle marks a small patch where *Tubastraea micranthus*, a azooxanthellate coral, was observed in life position.

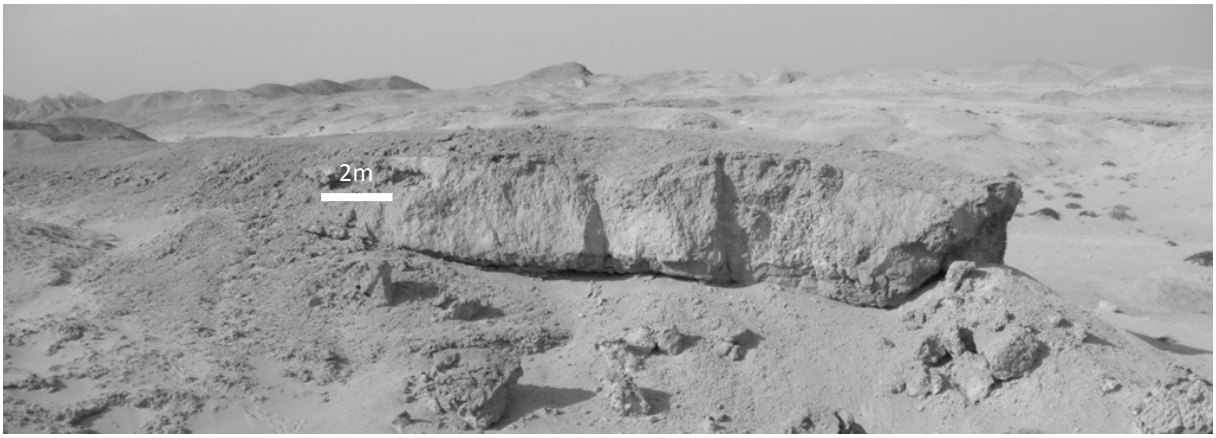

Figure 5.2.9: Northern reef block (reef 2) seen from reef 1 in the middle between the large main wadi, and a smaller wadi stream separating this block from the reef. This reef exhibits a distinct notch at its base, but less distinct bedding. The block has the same maximum height as reef 1 above.

The maximum thickness observed is about 4 m. The coral reefs grew on unconsolidated gravel of different height. The sorting is very poor and is here interpreted as debris flow deposit. Several debris flow deposits also interrupt the reef limestones, especially in the southern block, but the reef recovered after deposition of the debris flow and the upper facies of the next unit is comparable to the lower. These reef deposits are again capped by gravel deposits. The depositional environment of the gravel is interpreted as fluvial. The uppermost layer is preserved as a thin layer with well rounded gravel in cm-size, mixed with marine mollusks and coral fragments. This layer is interpreted as beach deposits. Lateral facies variations can be observed in the larger southern block. Towards the shore, coral growth enhances and bedding is less distinct, while landwards, coral and mollusk debris are the main components in the limestone, and the bedding between mudstone and sandstone/fanglomerates becomes more distinct . Reef 2 consist mainly of debris and contains fewer in-situ corals than the seaward front of reef 1. It also exhibits less bedding than reef 1. Farther into the wadi, on top of the gravel above reef 2, a large *Porites lobata/lutea* colony (Plate 5.1d) could be found. Derived from its size (3 m width and almost 2 m height), it probably grew undisturbed for about two hundred years, based on a mean growth rate of about 0.8-1.2 cm/year (Supriharyono 2013). Because it is situated in the middle of an unconsolidated gravel it is hard to say if it is the onset of the same terrace as the two reef blocks, or if it belongs to an older terrace. Farther in the hinterland of Turtle Bay, sandstone of aeolian origin outcrops on the top of terrace II (Figure 5.2.12). The sandstone consists of finely grained siliciclastic material, exhibits high-angle cross bedding, and contains no fossils.

The interpretation of this site is not trivial. The two single blocks resemble the lowermost fossil terrace closer to the shore. They possess a notch at their bases and are covered by beach rock. They are also similar in thickness and hardly diagenetically altered - in contrast to the older terraces

sitting on top of siliciclastic debris at the northern flank of the wadi, which are also found at a higher altitude. Wadis have been shown to be correlated with tectonic settings (Saqqa & Atallah 2013) and graben structures, so that a local tectonic event cannot be excluded causing the displacement. All terraces around this site embayment are highly fissured and it is sometimes difficult to distinguish between the terraces, especially between terrace 2 and 3, which are similarly strongly altered diagenetically.

Similar, but smaller and more patchy structures of similar elevation, occur at the southwestern side of the wadi between reef 1 and the shore, and merge with the lowermost terrace towards the camp. However, some uncertainties remain, and radiometric dating of these two reef blocks is needed for the final interpretation concerning the age of these terraces. Transect data (10 transects with a total of 546 datapoints) have been collected where corals could be identified in growth position.

When leaving Turtle Bay, small patch reefs occur close the beach, and grow into a larger reef outside the embayment (Plate 5.1c). Beach rock of probably early Holocene age occurs along the sandy beach (Plate 5.1a). As Nir (1971) has shown, the fossil terraces much resemble their recent counterparts in terms of width and steepness. Here, the fossil embayment seems as much siliciclastically dominated as the recent embayment.

Figure 5.2.10: Sandstone of aeolian origin in the hinterland of Turtle Bay. Picture taken by W. Kiessling.

Plate 5.1 (next page):

- **a) Holocene beach rocks that cover the Holocene reefs, and that provide the hard substrate for the corals in the fossil reefs.**
- **b) Turtle Bay with the beach where the wadi opens into the sea. Also the eastern flank of the wadi can be seen here, with a lowermost terrace built by unconsolidated gravel and topped by older limestone terraces.**
- **c) Beginning patch reefs in the small embayment of Marsa Bareika, Turtle Bay. The patchy structure is mirrored in the fossil reefs at the entrance of the embayment.**
- **d) A large *Porites lobata* colony growing landwards above the northern block.**

a)

b)

c)

d)

a)

b)

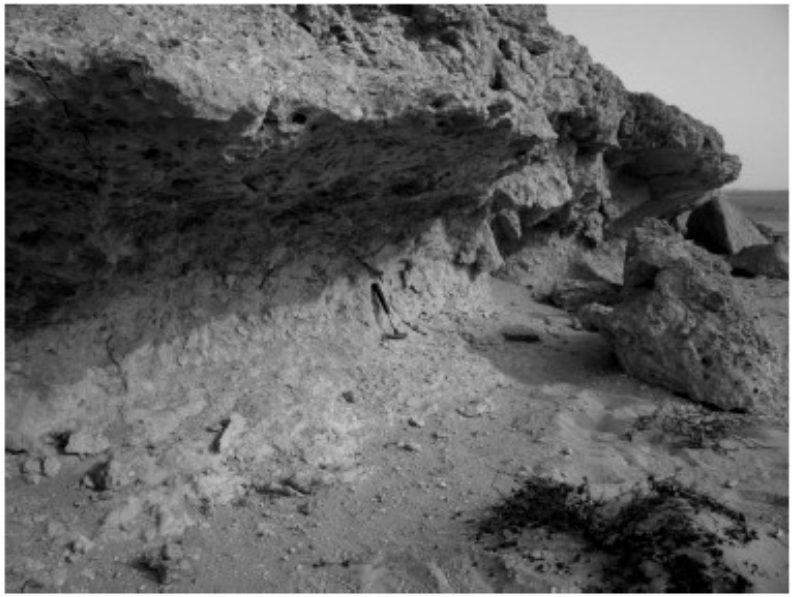

c)

d)

Plate 5.2 (previous page):

a) The lowermost terrace at Ras Ghozlani. The fossil reef flat is well preserved and not covered by beach rock and gravel.
b) A distinct notch marking the base of Terrace II. Picture taken by W. Kießling.
c) The second terrace is well exposed behind the camp, but contains only coral debris and mainly gravel.
d) Ras Ghozlani inland with beach rock layer and gravel surface.

Ras Ghozlani, 27°47'13.98"N, 34°14'19.01"E

This site is located on a well exposed patch of the lowermost terrace at the entrance of Marsa Bareika at about 2 m above the recent sea level. In contrast to most other sites, it is not covered by beach rock and gravel. The fossil reef flat is directly accessible and well preserved (Plate 5.2a). The site is part of the lowermost terrace that stretches along the northern shore of Marsa Bareika, interrupted only by the wadi described above. It has a maximum width of 10 m at this spot, which is similar to the recent fringing reef. Three transects with 192 datapoints were collected here.

Terrace II and III

Directly behind the camp the second terrace (terrace II) is well exposed with a nearly horizontal surface ranging in height from 8 - 12 m (Plate 5.2c). This terrace is covered by at least 1 m of coral debris, gravel and silt. In-situ corals can hardly be found. If they occur, they are strongly recrystallized. At some places the second terrace is preserved with a distinct notch at its base (Plate 5.2b). The site *Ras Ghozlani inland* (LT46 at 27°47'19.85"N and 34°14'24.35"E) is located within this terrace, but the one transect with 149 datapoints contains mostly gravel, and in-situ corals are scarce. A beach rock layer could be identified as well (Plate 5.2d). Previous dating of this terrace suggests an age of about 200 ka (e.g., El-Asmar 1997; Gvirtzman 1994), which represents MIS 7. Terrace III has a similarly poor preservation, the limestone is strongly recrystallized, but it contains more in-situ corals than terrace II. However, corals are 100% calcified. The site *Ras Mohammed inland* (LT33 at 27°47'40.92"N and 34°14'42.47"E) is located within this terrace at an altitude of about 40 m, and contains one transect with 20 points. The third terrace has been correlated with MIS 9 by several authors (e.g., El-Asmar 1997; Gvirtzman 1994).

5.3 Results

5.3.1 Presence/absence data

A binary (presence/absence) dataset was created out of my quantitative dataset in order to compare it to the list of present coral occurrences in the Red Sea and adjacent regions provided by Sheppard and Sheppard (1991). Figure 5.3.1 provides a map of the regions defined by these authors. Additional Pleistocene data from the northern Red Sea published by El-Sorogy (2002, 2008) and Kora *et al.* (2014) led to a comprehensive list of 78 Pleistocene species included in the analyses. The raw dataset with occurrences of 184 species (Appendix II-I) from the whole region, including the Arabian Sea (here mainly Dhofar region and Gulf of Aden), Gulf of Oman and Persian Gulf, was delimited to exclusively those species that occur in the Pleistocene of the northern Red Sea, in order to reduce sampling bias (Kiessling *et al.* 2012). For the purpose of comparison analyses have been repeated with taxa that were observed in this study. Table 5.3.1 shows the number of species and the percentages of recent taxa that could be found in the Pleistocene. The probability of being preserved and/or found in the Pleistocene corresponds with the size of the dataset. Nevertheless, including the literature data, around 50% of the recent data could be identified in the lowermost Pleistocene terrace in Egypt.

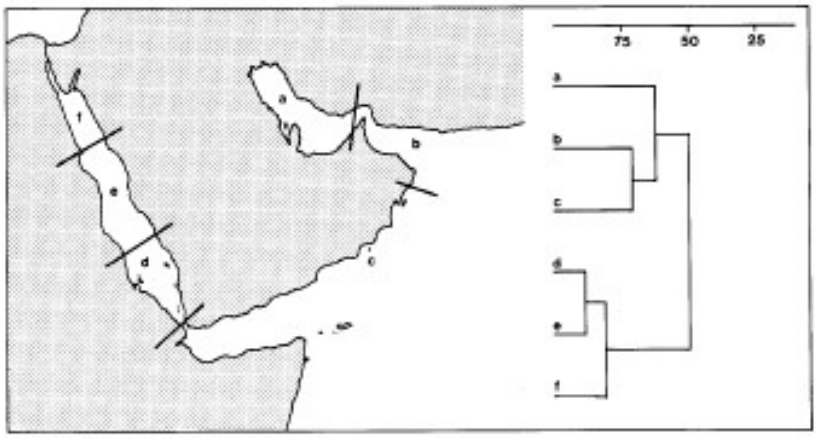

Figure 5.3.1 (from Sheppard & Sheppard 1991): This figure shows the boundaries of the regions as defined by Sheppard & Sheppard (1991). a - Persian Gulf, b - Gulf of Oman, c - Arabian Sea, d - southern Red Sea, e - central Red Sea, f - northern Red Sea. The cluster dendrogram shows their result of the analysis of the coral species present in the respective regions.

Table 5.3.1: Number of species in the binary (presence/absence) dataset. The second row (Pleistocene occurrences) shows the species number in the sampling-standardized dataset, which contains only taxa that occurred in the Pleistocene. The third row (Pleistocene occurrences) shows the percentage of recent taxa from the different areas that occurred also in the Pleistocene. Rows four and five are similar, but contain the number of species collected within this study, and the respective percentages of recent taxa occurring in the Pleistocene. NRS = northern Red Sea, CRS = central Red Sea, SRS = southern Red Sea, AS = Arabian Sea, GO = Gulf of Oman, Gulf = Persian Gulf.

	Pleistocene	NRS	CRS	SRS	AS	GO	Gulf
Raw data	78	139	148	112	82	69	45
Pleistocene occurrences	78	66	71	62	44	38	29
% in Pleistocene		47.5	48	55.4	53.7	55.1	64.4
Data exclusively from this study	34	32	33	31	24	20	15
% in Pleistocene		23	22.3	27.7	29.3	29	33.3

The Sørensen indices (Table 5.3.2 & 5.3.3) mirror largely the cluster dendrogram of Figure 5.3.1 from Sheppard & Sheppard (1991) with adjacent regions being more similar to each other than to more distant regions. However, in both matrices the Pleistocene assemblage from the northern Red Sea is most similar to the recent assemblage from the central Red Sea, and all Red Sea assemblages are very similar to each other.

Table 5.3.2: Sørensen similarity between assemblages from the different regions, including the Pleistocene data from El-Sorogy (2002, 2008) and Kora *et al.* (2014). NRS = northern Red Sea, CRS = central Red Sea, SRS = southern Red Sea, AS = Arabian Sea, GO = Gulf of Oman, Gulf = Persian Gulf.

	NRS	CRS	SRS	Gulf	GO	AS
CRS	0.92					
SRS	0.88	0.90				
Gulf	0.57	0.52	0.57			
GO	0.60	0.62	0.70	0.81		
AS	0.75	0.70	0.74	0.71	0.71	
Pleistocene	0.92	0.95	0.89	0.54	0.66	0.72

Table 5.3.3: Sørensen similarity between assemblages from the different regions, including only Pleistocene corals found in this study.

	NRS	CRS	SRS	Gulf	GO	AS
CRS	0.98					
SRS	0.92	0.94				
Gulf	0.64	0.63	0.65			
GO	0.69	0.72	0.78	0.80		
AS	0.86	0.84	0.84	0.77	0.78	
Pleistocene	0.97	0.99	0.95	0.61	0.74	0.83

The dissimilarities (=1-Sørensen similarity = binary Bray-Curtis dissimilarity) were used to cluster the results with hierarchical clustering using Ward's method (Figure 5.3.2). Both dendrograms reflect the high similarity of the Pleistocene with the recent central Red Sea assemblage. The recent coral assemblages in the dendrogram are sorted by their geographic distribution: The community from the northern Red Sea is most similar to the community of the central Red Sea. The community of the southern Red Sea is most similar to both. Here, with Ward's method, the Gulf of Oman and the Persian Gulf are most similar to each other, whereas the assemblage of the Arabian Sea is similar to both. In Sheppard & Sheppard (1991) the community of the Arabian Sea is most similar to the assemblage from the Gulf of Oman, and the Persian Gulf assemblages is the sister of both. These differences are probably the result of the standardization. Rare taxa that do not occur in the Pleistocene have been deleted from the dataset, and do not distort the geometry of the presence/absence dataset. According to the geographic distribution the result of the sampling-standardized dataset used in this study makes the most sense. The cluster dendrogram of the smaller dataset including my data only reveals the same pattern as the larger dataset including Pleistocene literature data, with the Pleistocene assemblage being most similar to the assemblage from the central Red Sea. Only the Arabian Sea changes its position and is more similar to the Red Sea data than to the assemblages from the two Gulfs.

The NMDS result (Figure 5.3.3) reveals the true distances better than the cluster dendrogram. Here, only the larger Pleistocene dataset was plotted. The Arabian Sea community plots

as much distant from the Red Sea assemblages as from the Persian Gulf, which means that in the cluster dendrograms its position is imprecise. All Red Sea communities are relatively close together, but the Pleistocene assemblage from the northern Red is identical to the assemblage from the central Red Sea. Almost all assemblages, except the ones from the Arabian Sea and the Pleistocene, plot largely along their geographical gradient. The Arabian Sea plots well in the middle between the other two Gulfs and the Red Sea, as its geographical position would suggest, and the NMDS does not reflect the latitudinal position. The position of the Pleistocene community is the most interesting, because geographical reasons cannot explain its similarity to the assemblage from the recent central Red Sea.

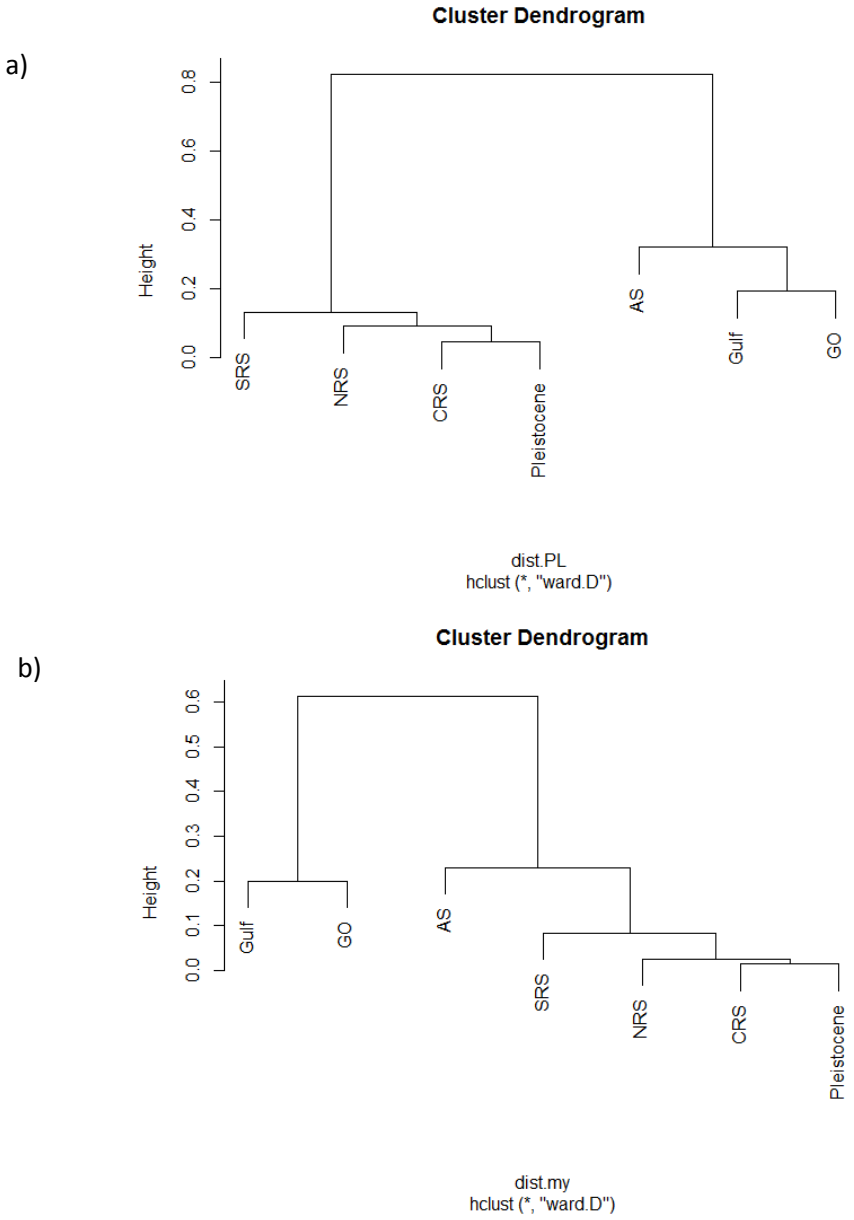

Figure 5.3.2: Cluster dendrograms based on Sørensen dissimilarity matrices and Ward's method. a) Dissimilarities between the different regions containing all available Pleistocene data, b) Dissimilarities between the different regions containing only Pleistocene data recorded within this study. NRS = northern Red Sea, CRS = central Red Sea, SRS = southern Red Sea, AS = Arabian Sea, GO = Gulf of Oman, Gulf = Persian Gulf.

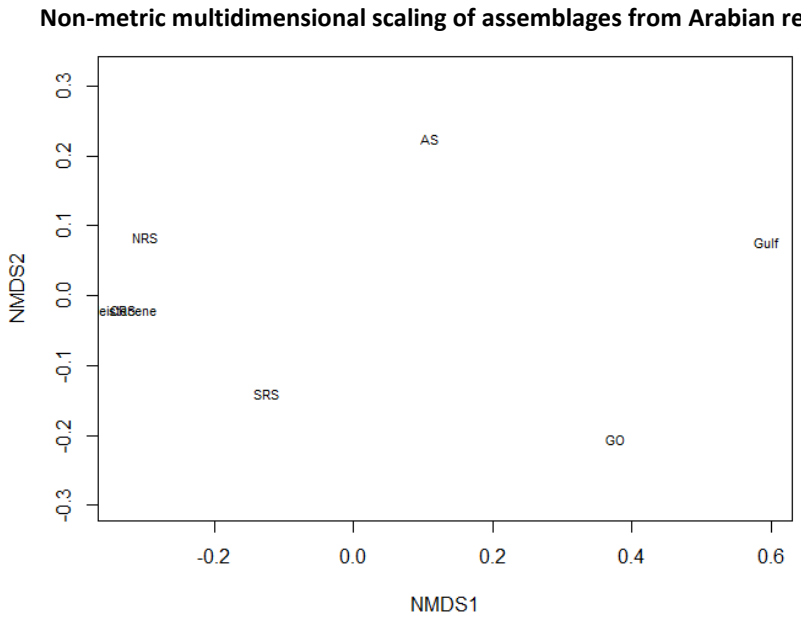

Figure 5.3.3: Non-metric multidimensional scaling (NMDS) of the different geographic regions. The NMDS was calculated in two dimensions. Distance is based on a binary Bray-Curtis matrix (Sørensen dissimilarity). The minimum stress = 3.15E-5. NRS = northern Red Sea, CRS = central Red Sea, SRS = southern Red Sea, AS = Arabian Sea, GO = Gulf of Oman, Gulf = Persian Gulf.

5.3.2 Quantitative data

The quantitative data from this study was used to examine the differences between the fossil localities and sites. These were also compared to quantitative data from recent reefs in Dahab at the dive site *The Islands* (Alter 2004), which is located only about 10 km south of our fossil reef. Table 5.3.4 provides an overview of the available cleaned data, including Scleractinia and *Millepora*, and the recent data has been constrained to taxa that occur also in the Pleistocene. The complete raw dataset is available in Appendix II-II. The two sites that are represented by only one transect each were excluded from further analyses: Ras Mohammed inland and Ras Ghozlani inland. Both sites are situated farther away from the coast and show a higher diagenetic alteration. The preservation is poor and there are hardly any scleractinians in the respective transects. They belong to older terraces, and can thus not be compared by the same means to the other fossil sites that all belong to the last interglacial. Consequently there are three sites from Dahab, three from Ras Mohammed and three recent sites that remain in the centre of the following analyses.

The first striking difference between the recent data and the fossil data is the sample size, but each station at *The Islands* contained several transects, so that N(LT) and S_{obs}(LT) are already the summed specimen and species numbers, respectively. When comparing the specimen number of the fossil reef at *The Canyon* to the single recent stations, differences become less striking. For this reason these three stations were not summarized for all analyses.

Table 5.3.4: Overview of line transects and site distribution in Dahab and Ras Mohammed and recent sites, respectively. The mean coral coverage per site is the mean of the coral coverage in each transect. SD (coverage) = standard deviation of the mean coverage, S*obs* = number of observed species in LT and site, *N* = number of observed specimens in LT and site, *H* = Shannon–Wiener Index of Diversity, *J* = evenness, S_{R80} = number of species after rarefaction (*N* = 80), S_{R200} = number of species after rarefaction (*N* = 200), ACE = coverage-based richness estimation that gives the estimate for the minimum total number of species we might observe at the respective sites, SE (ACE) = standard error of ACE, SQS = shareholder quorum subsampling for a coverage level of 70% after 1000 trials.

Locality	LT	Coral coverage	*N* (LT)	S_{obs} (LT)	Site	Mean Coverage ± SD (in %)	*N* (site)	S_{obs} (site)	*H*	*J*	$S_{R\,(80)}$	$S_{R\,(200)}$	ACE ± SE	SQS q = 0.7
Dahab	LT20	70.3	44	15	Blue Hole	64.8 ± 14.8	216	24	2.34	0.74	18.88	23.62	26.75 ± 2.2	8.59
	LT21	56.3	27	9										
	LT22	46	21	13										
	LT23	76.3	29	4										
	LT24	85.1	74	3										
	LT25	54.8	21	6										
	LT01	76.1	35	10	Canyon North Patch Reef	61.6 ± 22	80	17	2.55	0.90	17		18.28 ± 1.6	8.94
	LT02	81	17	6										
	LT03	25	6	2										
	LT04	61.9	13	5										
	LT05	64.3	9	4										
	LT06	37.6	37	2	Canyon Reef	48.2 ± 20.3	540	42	2.80	0.75	22.1	32	47.17 ± 3.2	9.82
	LT07	64	46	18										
	LT08	64	32	6										
	LT09	9.8	4	3										
	LT10	26.7	8	3										
	LT11	34.7	17	1										
	LT12	31	9	3										
	LT13	76.2	32	2										
	LT14	79.1	34	8										
	LT15	47.4	36	10										

Locality	LT	Coral coverage	*N* (LT)	S_{obs} (LT)	Site	Mean Coverage ± SD (in %)	*N* (site)	S_{obs} (site)	*H*	*J*	$S_{R\,(80)}$	$S_{R\,(200)}$	ACE ± SE	SQS q = 0.7
	LT16	40.9	56	8										
	LT17	42.4	14	5										
	LT18	55.9	19	8										
	LT19	52.6	10	6										
	LT26	52.9	9	3										
	LT27	49.4	38	15										
	LT28	52.6	48	15										
	LT29	88.9	56	3										
	LT30	45.0	26	10										
	LT31	13.6	9	4										
Ras Mohammed	LT32	41.1	22	2	Turtle Bay	52.7 ± 14.5	281	21	1.85	0.61	14.13	19.12	26.37 ± 2.7	4.39
	LT37	67.5	26	4										
	LT38	72.7	23	5										
	LT40	76.3	56	7										
	LT41	55.3	41	10										
	LT42	44.3	27	8										
	LT43	45.7	16	3										
	LT44	35.3	12	4										
	LT45	46.7	27	6										
	LT47	42.7	31	6										
	LT48	49.2	30	7	Ras Ghozlani	63.2 ± 15.8	120	14	1.70	0.65	12.58		15.35 ± 1.8	3.45
	LT49	60.0	37	7										
	LT50	80.3	53	9										

Locality	LT	Coral coverage	*N* (LT)	S_{obs} (LT)	Site	Mean Coverage ± SD (in %)	*N* (site)	S_{obs} (site)	*H*	*J*	$S_{R\,(80)}$	$S_{R\,(200)}$	ACE ± SE	SQS q = 0.7
	LT46	12.8	19	2	Ras Ghozlani-inland	12.84	19	2	0.21	0.30				
	LT34	39.7	48	9	Ras Mohammed Camp	46.4 ± 11.7	173	19	1.93	0.66	14.39		25.63 ± 2.57	4.36
	LT35	47.4	55	10										
	LT36	36.1	26	8										
	LT39	62.5	44	8										
	LT33	20	3	1	Ras Mohammed inland	20.0	3	1						
Recent (Dahab)	Station1		888	38	The Islands		2579	40	2.75 ± 0.08 (mean)	0.77 ± 0.04 (mean)	22.38	29.24	40.3 ± 2.9	12.14
	Station2		1227	38										
	Station3		464	30										

However, despite the differences in sampling size the diversity of the fossil site at *The Canyon* is comparable to the recent reef sites. The Shannon-Wiener-Index of the Canyon reef (H = 2.8) is even higher than the mean Shannon-Wiener-Index of the three recent stations (H = 2.75). The same pattern is observed in the sampling-standardized analysis. When comparing the subsampled species richness of 80 specimens, which is the number of specimens given by the smallest sampling at the patch reefs north of the Canyon reef, the recent reef and the Canyon reef have almost the same number of specimens, but when subsampled by the fairer number of 200 specimens, the Canyon reef has a species richness of 32, while there are only 29.4 in the recent reef, and the rarefaction curve (Figure 5.3.5) shows that not all common taxa have been found yet at this point. As mentioned before rarefaction curves flatten when sampling size is sufficient and only rare taxa remain to be found. Trusting the results of the estimated species richness (ACE) the Canyon reef would be even more distinctively diverse than the recent reef. The five other fossil sites are less well sampled, so that the results also mirror the sampling bias, but nevertheless, at first sight they appear to be remarkably less diverse than *The Canyon* and *The Islands* sites. The SQS curves (Figure 5.3.4) reflect this. Also *The Canyon* and *The Islands* sites are less distinct from each other, and run almost in parallel.

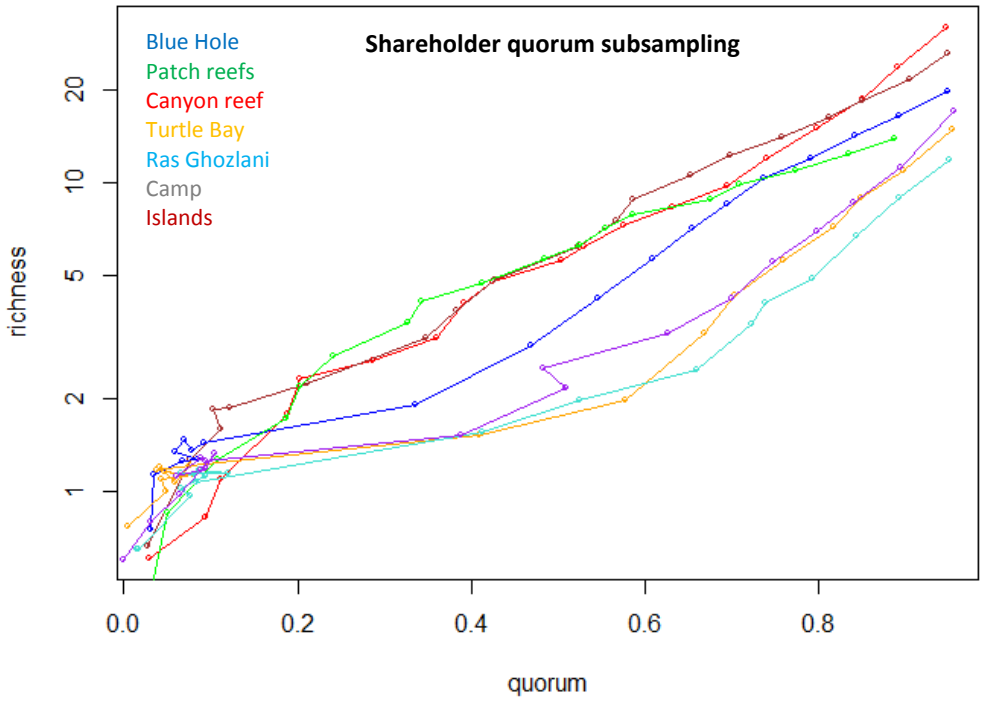

Figure 5.3.4: Shareholder quorum subsampling curves, showing the subsampled richness for different coverages after 1000 trials.

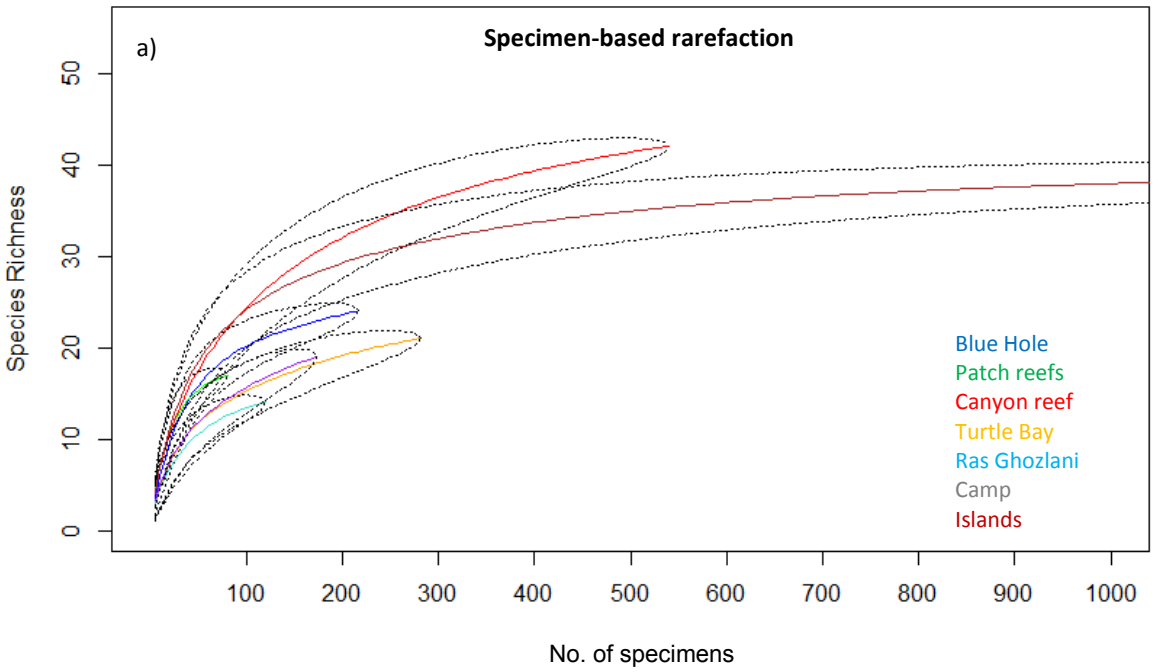

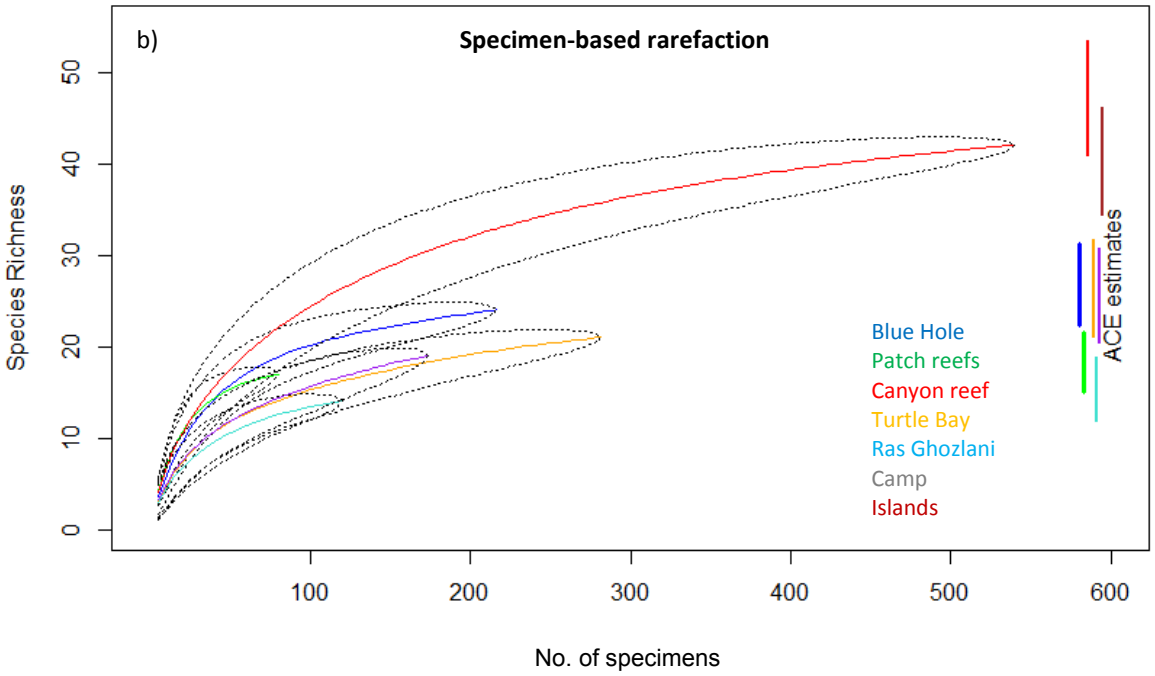

Figure 5.3.5: Rarefaction curves and abundance-based coverage estimator (ACE) of transect data by site using individual-based rarefaction. a) includes the summarized recent data, but stopped at 1000 specimens, b) enlarged rarefaction curves of fossil sites only, but including the recent ACE value (in brown as shown in the legend of a). The total richness estimator (ACE) was plotted in intervals (expected values +/- 2*SE).

Regarding the Sørensen similarity (Table 5.3.5) among sites, the diversity seems to play a major role: The Canyon reef is more similar to Station 1 than Station 1 is to Station 3. Ras Ghozlani and Ras Mohammed Camp show the smallest similarities to most of the other sites.

Table 5.3.5: Sørensen similarities among sites.

	Station 1	Station 2	Station 3	Blue Hole	Patch reefs	Canyon	Turtle Bay	Ras Ghozlani
Station 2	0.95							
Station 3	0.82	0.88						
Blue Hole	0.66	0.62	0.52					
Patch reefs	0.64	0.64	0.67	0.53				
Canyon	0.85	0.85	0.76	0.64	0.55			
Turtle Bay	0.62	0.66	0.60	0.60	0.63	0.60		
Ras Ghozlani	0.44	0.44	0.48	0.56	0.53	0.40	0.44	
Ras Mohammed Camp	0.54	0.50	0.50	0.63	0.44	0.51	0.53	0.47

To reconstruct the environmental conditions of the sites, I grouped them by their species compositions. For that purpose Table 3.1 (Chapter 3) was used again to group the sites by the preferred environments of their contained taxa. Table 5.3.6 provides the resulting data that was used to calculate the environmental fit of the sites in vegan (`envfit`). In comparison to Vanuatu the sites in Egypt contain a lot of taxa that prefer a certain environment. Also obviously some of the sites contain groups of taxa that prefer different environmental conditions. Table 5.3.7 contains the Bray-Curtis-dissimilarities between the fossil sites on which the non-metric-multidimensional scaling is based.

Table 5.3.6: Summary of the number of specimens at each site that have preferred environments.

	Backreef	Intertidal	Lagoon	Slope
Blue Hole	27	15	0	5
Patch reefs	5	0	0	0
Canyon reef	117	6	0	48
Turtle Bay	18	2	0	0
Ras Ghozlani	1	64	0	0
Ras Mohammed Camp	19	83	0	5

Table 5.3.7: Bray-Curtis-dissimilarity matrix used for the environmental fitting. Data has been square rooted before submitted to Wisconsin double standardization.

	Blue Hole	Patch reefs	Canyon reef	Turtle Bay	Ras Ghozlani
Patch reefs	0.79				
Canyon reef	0.51	0.73			
Turtle Bay	0.62	0.66	0.57		
Ras Ghozlani	0.59	0.67	0.76	0.69	
Ras Mohammed Camp	0.59	0.72	0.67	0.60	0.58

Only three environmental settings seem to be preserved in the fossil reefs, which is not surprising when regarding the recent reefs of this region, which are almost all fringing reefs and do not possess lagoons. The intertidal environment includes the reef crest/flat environments, which are identical in recent reefs of this regions (see introduction). Figure 5.3.6 shows the non-metric multidimensional scaling and the environmental fit of the respective sites, based on Bray-Curtis-dissimilarities. Ras Mohammed Camp comprises largely species that prefer intertidal/ flat habitats, while Turtle Bay has a strong fit with backreef environments. The species of the Canyon reef and the Blue Hole show a strong slope affinity. These results are significant for backreef and flat environments, and help to group the sites according to their environmental preferences. The recent data was not included, because their environment is well-known, but each station comprises several environments that are not itemized in the dataset, so that I cannot distinguish which species occurred in which environment during sampling. Otherwise it would have been interesting to test the exact accuracy of this method.

The same NMDS plot was used to show the salinity tolerance of taxa (Table 5.3.8) comprised at each site (Figure 5.3.7). The result fits to the outcome of reconstruction of the preferred environment. The sites that contain a lot of species that prefer intertidal habitat also contain more species that can tolerate high salinities. This fitting is significant (p = 0.03). Turtle Bay comprises several species that are sensitive and cannot tolerate variations of salinity well, which is also a significant result with p = 0.03. Most species, however, are unspecific or data is not available, but certainly a high number of taxa at each site have the ability to tolerate high salinities.

Table 5.3.8: Summary of the number of taxa at each site and their ability to tolerate variations in salinity.

	High tolerance	Low tolerance	Unspecific/ unknown
Blue Hole	106	0	63
Patch reefs	10	1	54
Canyon reef	111	2	204
Turtle Bay	20	1	45
Ras Ghozlani	64	0	26
Ras Mohammed Camp	90	0	57

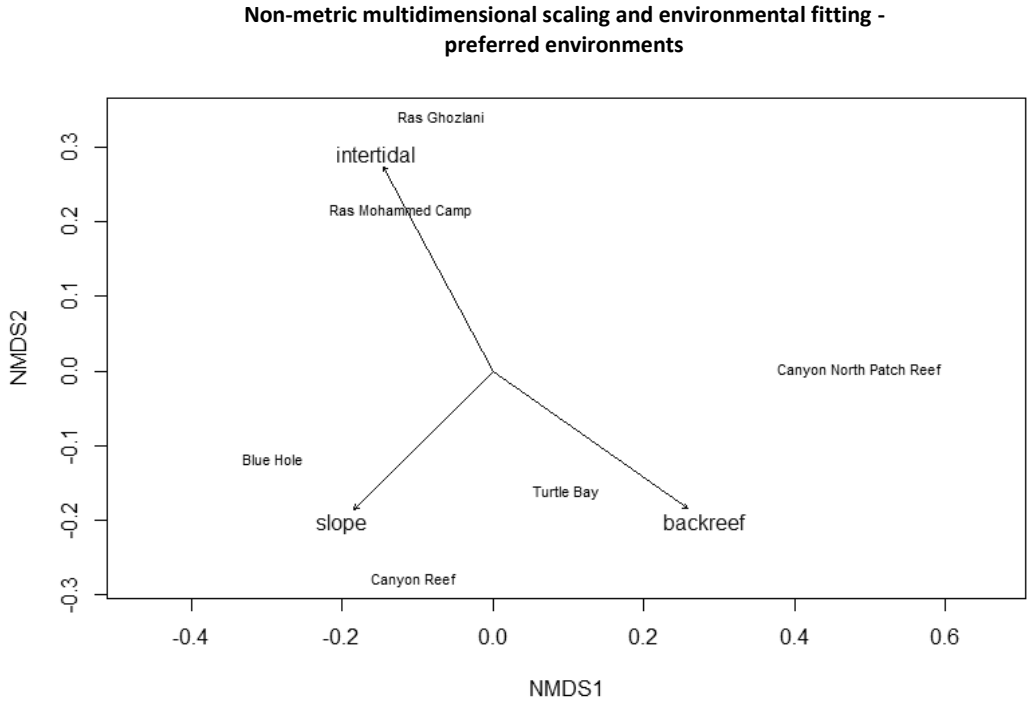

Figure 5.3.6: Non-metric multidimensional scaling (NMDS) ordination of sites, species and their preferred environments. Species are not displayed here, because of their high number and the purpose of intelligibility. The NMDS was calculated in two dimensions. Distance is based on a Bray-Curtis matrix. Both datasets are square rooted before submitted to Wisconsin double standardization. The minimum stress value was 0.07. *P*-values of the environmental fitting: backreef = 0.02, intertidal = 0.03, slope = 0.2.

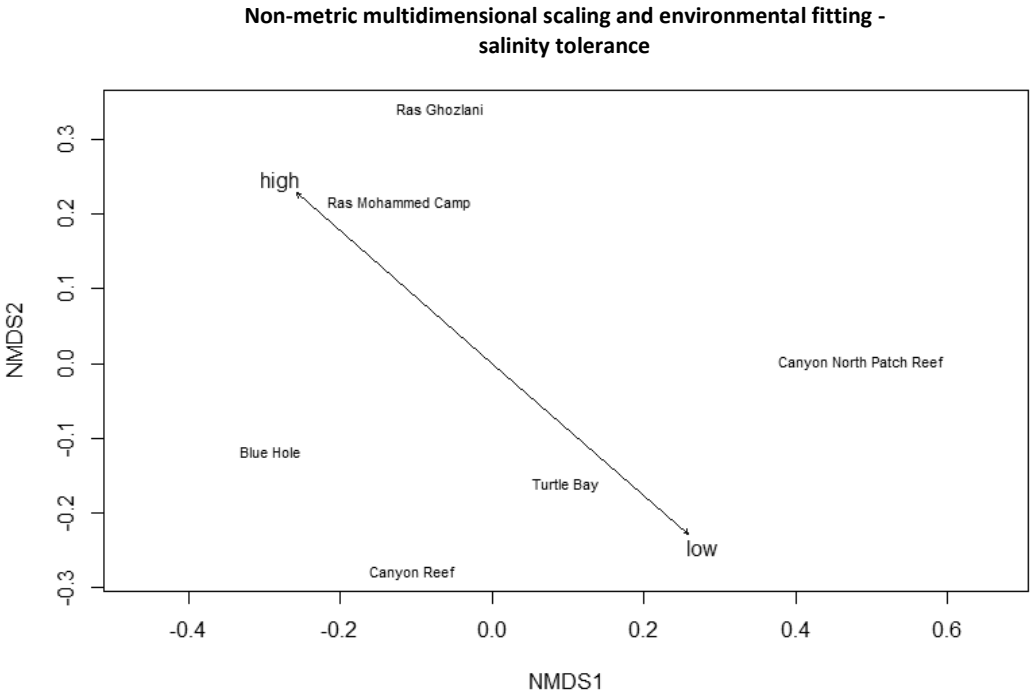

Figure 5.3.7: Non-metric multidimensional scaling (NMDS) ordination of sites, species and there salinity tolerance. Species are not displayed here, because of their high number and the purpose of intelligibility. The NMDS was calculated in two dimensions. Distance is based on a Bray-Curtis matrix. Both datasets were square rooted before submitted to Wisconsin double standardization. The minimum stress value was 0.06. *P*-values of the environmental fitting: high salinity tolerance = 0.03, low salinity tolerance = 0.03.

The plot of the preferred environments was used to create groups of sites: Ras Mohammed Camp and Ras Ghozlani are interpreted as reef flat communities, Blue Hole and the Canyon reef as slope communities, and Turtle Bay and the patch reefs north of the Canyon reef as backreef communities, keeping in mind that at least some of the communities might contain more than one reef zone. But these groups were needed to test the distinctiveness of the sites and localities. Also, the recent sites were included here as separate environments. Table 5.3.9 provides the beta diversities of standardized occurrences (Wisconsin standardization) between the sites with the assigned environments marked in colors. In accordance with the similarity before, the beta diversity (Arrhenius species-area model) between the Canyon reef and the recent reefs appears to be remarkably small in contrast to most of the other beta diversities between fossil and recent sites, as well as among fossil sites. Usually a value of $z \approx 0.3$ implies random sampling variability, and only higher values mean real systematic differences (Oksanen 2015), which means that most of sites are really different from each other, whereas the Canyon reef and the recent sites are not systematically different from each other.

Table 5.3.9: Beta diversity based on the Arrhenius species-area model between sites. The higher the beta diversity, the more the communities differ. The colors mark the different environments reconstructed above. R= Recent, S= Slope, B = Backreef, I = Intertidal/very shallow.

	Station 1 (R)	Station 2 (R)	Station 3 (R)	Blue Hole (S)	Patch reefs (B)	Canyon (S)	Turtle Bay (B)	Ras Ghozlani (I)
Station 2 (R)	0.07							
Station 3 (R)	0.23	0.16						
Blue Hole (S)	0.43	0.46	0.57					
Patch reefs (B)	0.44	0.44	0.42	0.56				
Canyon (S)	0.21	0.21	0.31	0.44	0.54			
Turtle Bay (B)	0.46	0.43	0.49	0.49	0.45	0.48		
Ras Ghozlani (I)	0.64	0.64	0.61	0.52	0.55	0.68	0.64	
Ras Mohammed Camp (I)	0.55	0.58	0.58	0.45	0.64	0.58	0.56	0.62

Table 5.3.10: Bray-Curtis dissimilarity matrix used in the analyses including the recent sites.

	Station 1	Station 2	Station 3	Blue Hole	Patch reefs	Canyon reef	Turtle Bay	Ras Ghozlani
Station 2	0.33							
Station 3	0.46	0.47						
Blue Hole	0.74	0.72	0.87					
Patch reefs	0.75	0.71	0.67	0.86				
Canyon reef	0.54	0.51	0.62	0.57	0.79			
Turtle Bay	0.74	0.70	0.73	0.80	0.85	0.75		
Ras Ghozlani	0.81	0.77	0.81	0.74	0.78	0.82	0.77	
Ras Mohammed Camp	0.82	0.83	0.85	0.67	0.86	0.75	0.66	0.64

A Bray-Curtis dissimilarity of the standardized dataset (Table 5.3.10) including the recent sites was used to cluster the sites (Figure 5.3.8). The sites plot largely along their spatial distribution. A further NMDS analysis (Figure 5.3.9) including the recent sites provides a similar picture. It seems that there is a geographical difference in addition to an ecological one.

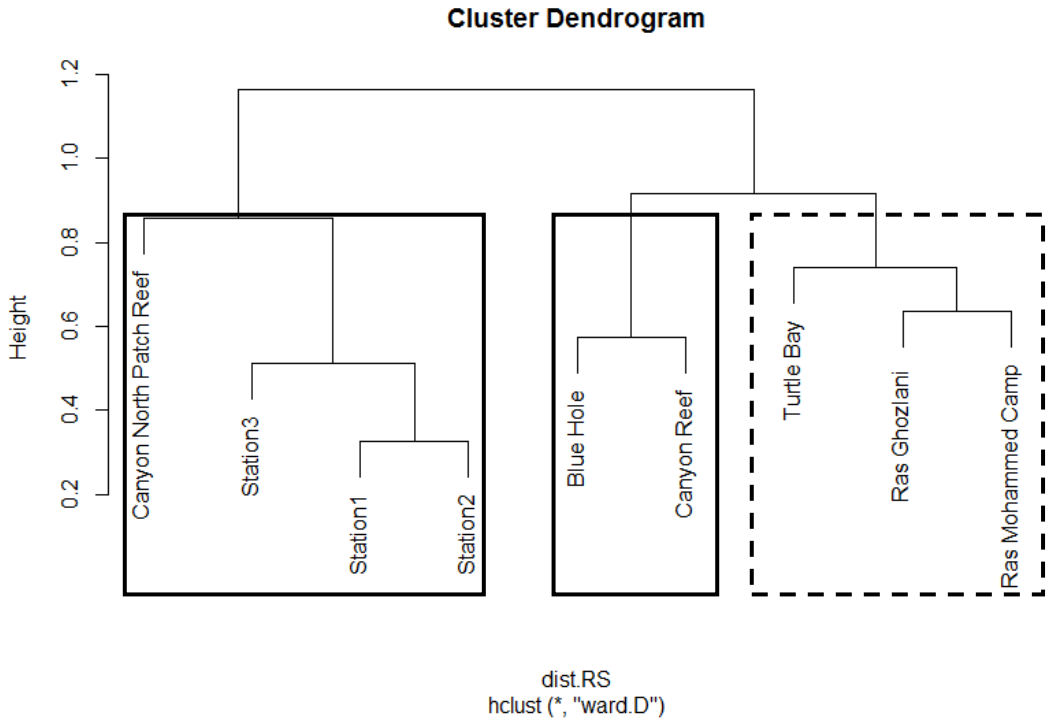

Figure 5.3.8: Cluster dendrogram based on Bray-Curtis dissimilarity matrices and Ward's method. Black rectangles = sites in Dahab, dashed line= sites in Ras Mohammed,

.

For comparison the plot of the detrended correspondence analysis is shown in Figure 5.3.10. The results are relatively similar, apart from the Canyon reef being eve closer to the recent data, and Ras Ghozlani and Ras Mohammed Camp being closer to each other.

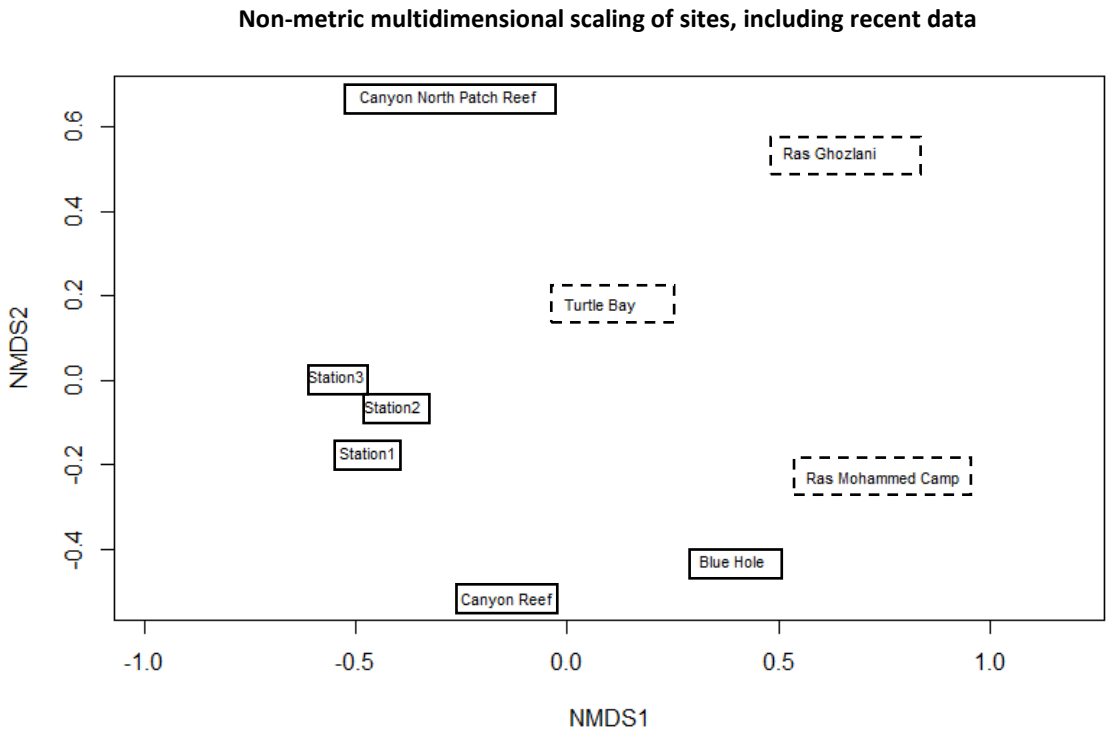

Figure 5.3.9: Non-metric multidimensional scaling (NMDS) ordination including the recent sites and species. Species are not displayed here, because of their high number and the purpose of intelligibility. The NMDS was calculated in two dimensions. Dataset was standardized by Wisconsin double standardization. Distance is based on a Bray-Curtis matrix. The minimum stress value was 0.1. Black rectangles = sites at Dahab, dashed = sites at Ras Mohammed.

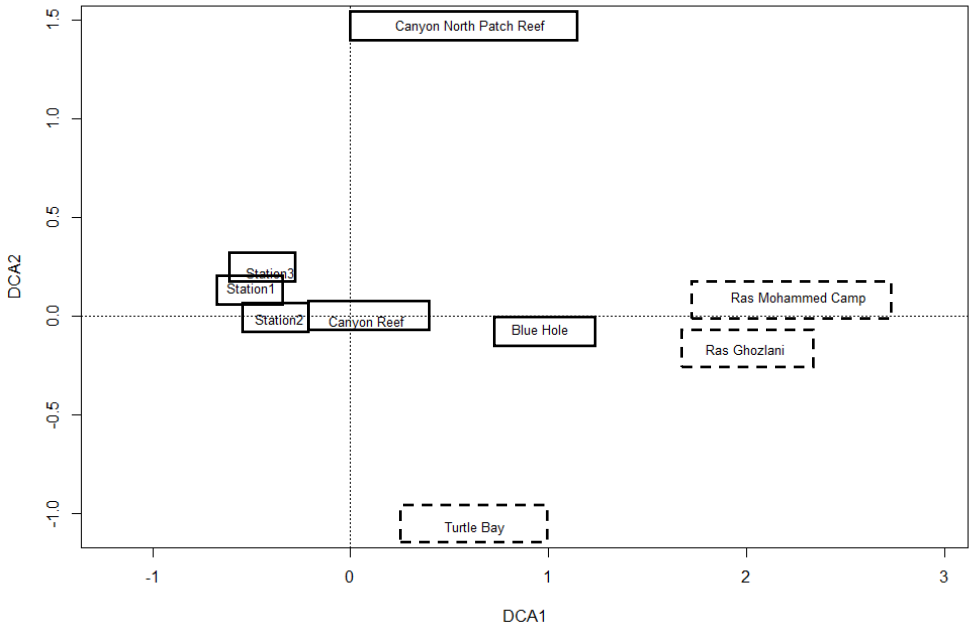

Figure 5.3.10: Detrended correspondence analysis of the same dataset as in Figure 5.3.9. Black rectangles = sites at Dahab, dashed = sites at Ras Mohammed.

The significance of the distinctiveness between the localities was tested, as was the distinctiveness of environmental groups. Table 5.3.11 provides an overview of all metrics and their results. ANOSIM uses the Bray-Curtis-dissimilarity matrix, while ADONIS analyses the beta diversity (*z*) provided in Table 5.3.9 grouped by localities and environments, respectively. The recent sites were also treated as distinct locality and environment, in order to test their environmental affinities. ANOVA and permutation tests analyze the significance of the analysis of multivariate homogeneity of group dispersions (`betadisper()`). The parametric Tukey's HSD test analyzes the pairwise differences between the respective groups.

Table 5.3.11: Summary of metrics used to assess the degree of similarity among reef communities from different ages/fossil sites and reef environments from Sinai/Egypt.

	Red Sea data, including recent	
	Grouped by locality	**Grouped by reef environment as defined above**
ADONIS	R^2 = 0.33; *P* = 0.17	R^2 = 0.58; *P* = 0.01
ANOSIM	R = 0.47; *P* = 0.02	R = 0.64; *P* = 0.006
ANOVA (Betadisper)	F = 2.08; *P* = 0.21	F = 4.6; *P* = 0.07
Permutation test for F		
Pairwise comparisons		
Dahab - Ras Mohammed	Observed/permuted *P* = 0.81/0.83	
Dahab - Recent	Observed/permuted *P* = 0.17/0.15	
Ras Mohammed - recent	Observed/permuted *P* = 0.09/0.10	
Backreef - flat		Observed/permuted *P* = 1.8.E-30 /0.002
Backreef - recent		Observed/permuted *P* = 0.07/0.04
Backreef - slope		Observed/permuted *P* = 1.57E-31/0.004
Slope - flat		Observed/permuted *P* = 2.24E-29/0.007
Slope - recent		Observed/permuted *P* = 0.52/0.55
Recent - flat		Observed/permuted *P* = 0.32/0.37
Tukey's HSD test		
95% family-wise confidence level		
Dahab - Ras Mohammed	*P* = 0.96	
Dahab - Recent	*P* = 0.22	
Recent - Ras Mohammed	*P* = 0.31	
Backreef - flat		*P* = 0.32
Backreef - recent		*P* = 0.05
Backreef - slope		*P* = 0.18
Slope - flat		*P* = 0.94
Slope - recent		*P* = 0.80
Recent - flat		*P* = 0.49

When grouped by locality all but the ANOSIM show no significant model fitting. The ANOSIM is the least robust of the provided measurements (Oksanen 2015) and as such shows that it is always good to evaluate different metrics in order to get a reliable result. When grouped by reef environments ADONIS, ANOSIM and ANOVA of group dispersion show a strong significance, but looking at the pairwise comparisons of the permutation test, it becomes obvious that two of six sites

are not significantly different: Slope - recent communities and recent - flat communities. The Tukey test gives even less significances for almost all sites, but confirms the significant differences of the recent assemblage from the fossil backreef community.

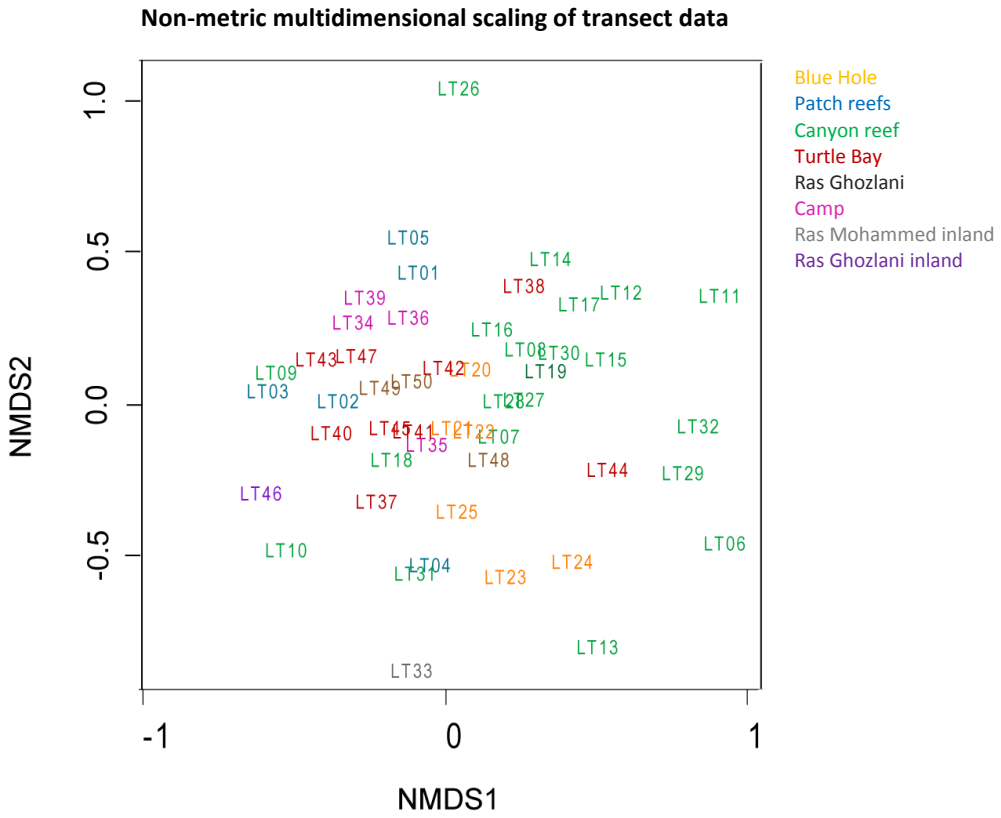

Figure 5.3.11: Non-metric multidimensional scaling of the line transect data, based on a Bray-Curtis-dissimilarity matrix. Raw data has been square rooted and Wisconsin double standardized. Stress = 0.2, dimensions =2.

Figure 5.3.11 shows the dissimilarities between transects of the fossil sites and gives an explanation why a grouping by environment based on sites does not always deliver significant results. Especially large sites contain more than one reef environment, and so do the recent sites. The latter comprise transects from reef flats to reef slope communities. The above figure also shows that especially the Canyon reef deserves a closer look in the following section, since it shows an environmental gradient and contains sufficient data.

5.3.3 Ecological succession in the Canyon reef (Mewis & Kiessling 2013)

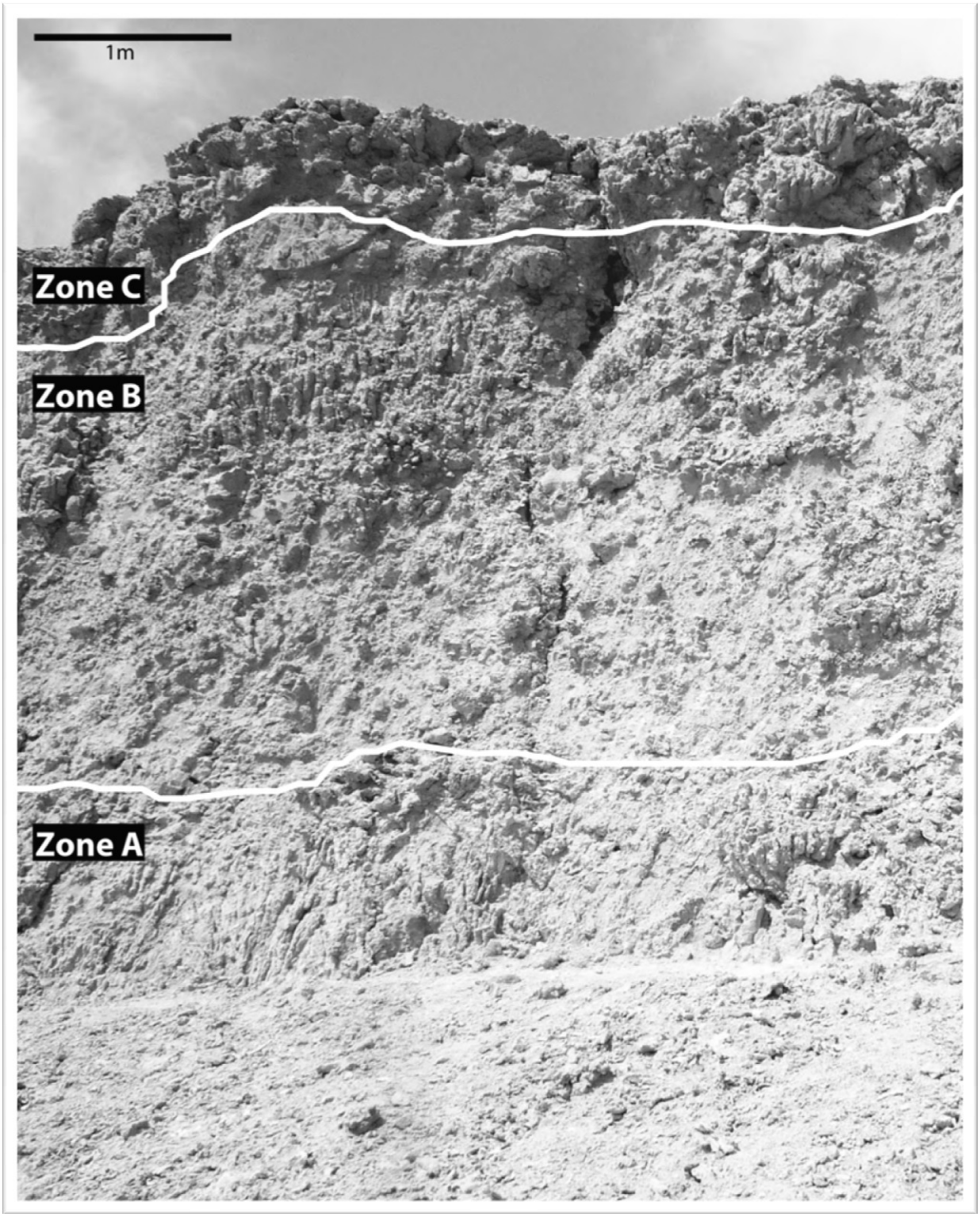

Figure 5.3.12: Photograph of the reef front of the Canyon reef, with the three zones (A, B, and C) marked respectively.

The fossil reef complex at *The Canyon* provides an ideal setting to be studied in more detail, because it represents a complete and distinct reef body where ecological succession can be observed. The Canyon reef shows a distinct vertical zonation. A "zone" is a local, lithologically distinct reef unit, where distinctiveness is created by the dominant growth forms of corals and the proportion and composition of matrix. Each zone is also characterized by a distinctive set of species

(Table 5.3.12), species diversities (Table 5.3.13), and paleoenvironmental conditions. Three zones can be identified (Figure 5.3.12): The lowermost Zone A is up to 3.3 m thick, but thins out rapidly northwards according to the underlying topography, and consists mainly of large colonies of *Porites nodifera*, which forms extensive single species stands (89 % of the specimens, Plate 5.3A). Other genera are *Millepora, Pavona*, and *Cyphastrea*. Some of the patch reefs forming the northward extension of the Canyon reef are almost exclusively built by *P. nodifera*. The abundance of corals measured as the proportion of corals in line transects is 63.3 % ± 36.3 % (mean ± SD). The matrix is siliciclastic and contains only few bioclasts, such as small molluscs. It also contains some pockets with loose sandy material.

Species	Zone A	Zone B	Zone C
Acanthastrea echinata	0	0	0
Acropora formosa	0	43	0
Acropora sp.	0	71	8
Astreopora myriophthalma	0	2	0
Astreopora sp.	0	0	2
Coscinaraea monile	0	0	1
Cyphastrea serailia	2	4	0
Cyphastrea sp.	0	3	2
Echinopora forskaliana	0	16	0
Echinopora sp.	0	1	0
Favia pallida	0	0	0
Favia rotundata	0	1	0
Favia sp.	0	11	6
Favites flexuosa	0	1	0
Favites pentagona	0	0	0
Favites sp.	0	3	6
Favites spinosa	0	0	0
Fungia sp.	0	5	0
Galaxea fascicularis	0	6	3
Goniastrea aspera	0	0	0
Goniastrea edwardsi	0	0	6
Goniastrea peresi	0	4	0
Goniastrea retiformis	0	0	0
Goniastrea sp.	0	2	0
Goniopora sp.	0	1	0
Gyrosmilia interrupta	0	0	0
Hydnophora microconos	0	0	0
Leptastrea bottae	0	2	0
Leptastrea sp.	0	5	0
Leptastrea transversa	0	2	0
Leptoseris sp.	0	2	0
Lobophyllia corymbosa	0	3	4
Lobophyllia hemprichii	0	1	1
Lobophyllia sp.	0	4	0
Millepora sp.	7	6	1
Montipora sp.	0	32	2
Mycedium sp.	0	3	0
Pavona cactus	0	2	0
Pavona sp.	1	3	0
Platygyra crosslandi	0	0	0
Platygyra daedalea	0	13	4
Platygyra lamellina	0	3	0
Platygyra sp.	0	13	4
Pocillopora damicornis	0	1	0
Pocillopora verrucosa	0	0	0
Porites lobata/lutea	0	31	61
Porites nodifera	83	16	0
Porites sp.	0	8	0
Psammocora sp.	0	7	0
Stylophora sp.	0	2	1
Turbinaria reniformis	0	1	0
Turbinaria sp.	0	1	0

Table 5.3.12: Species occurrences in the three zones of the Canyon reef.

Table 5.3.13: Overview of line transect distribution in the three zones of the Canyon reef. The mean coral coverage per zone is the mean of the coral coverage in each transect. SD (mean) is the standard deviation of the mean coverage. *Sobs* = number of observed species in each zone, *N* = number of observed specimens in each zone, S_{R90} = number of species after rarefaction (*N* = 90), *H* = Shannon–Wiener Index of Diversity, *J* = evenness, ACE = coverage-based richness estimation that gives the estimate for the minimum total number of species we might observe at the respective sites, SE (ACE) = standard error of ACE.

LT	Zone	Coral coverage (mean, in %)	*N*	S_{obs}	*H*	*J*	S_{R90}	ACE	SE (ACE)
LT06	**A**	63.3 ± 36.2	93	4	0.43	0.31	3.97	5.03	1.07
LT29									
LT07	**B**	57.1 ± 12.3	335	39	2.90	0.79	25.24	43.68	3.00
LT08									
LT13									
LT14									
LT15									
LT17									
LT18									
LT19									
LT27									
LT28									
LT30									
LT09	**C**	30.00 ± 15	112	16	1.83	0.66	15.10	18.31	1.60
LT10									
LT11									
LT12									
LT16									
LT26									
LT31									

The middle Zone B is about as thick (3.2 m) as Zone A and characterized by a high diversity of coral growth forms and species (Plate 5.B, C). It consists of smaller coral colonies, mainly branching, platy or encrusting, and coralline algae. The coral coverage of 57.25% ± 12.25% is similar to that of Zone A, but the matrix in Zone B is less siliciclastic. The uppermost Zone C (Plate 5.D–F), which is only 1.20 m thick at its thickest part, is characterized by massive coral colonies, coral microatolls, and abundant rhodoliths. Microatolls are massive corals that are truncated at their top by subaerial exposure and weathering (Woodroffe & McLean 1990). Massive *Porites lutea/lobata* (treated as a species complex because I could not confidentially distinguish the species from each other) and faviids are the most common taxa, but there are no clearly dominant species within that zone. Due to the abundance of red algae, the proportion of corals is only 30% ± 15%. The matrix is siliciclastic but contains many bioclasts such as sea urchin spines, barnacles, and molluscs. The molluscs are predominantly oysters and boring bivalves.

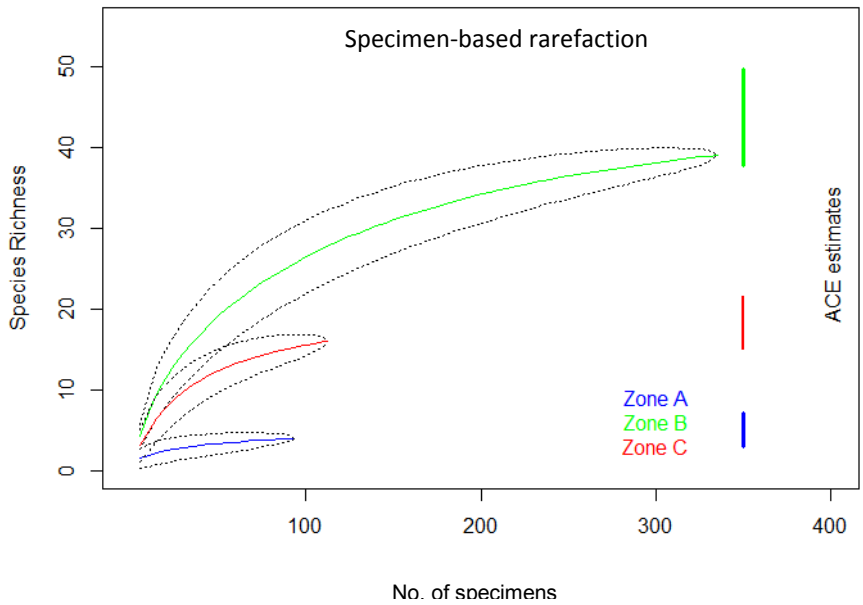

Figure 5.3.13: Specimen-based rarefaction and ACE estimates. The total richness estimator (ACE) was plotted in intervals (expected values +/- 2*SE). Rarefaction as well as ACE estimates confirm Zone B being most diverse, and Zone A being least diverse.

The minimum diversity and evenness is observed in Zone A and the maximum in Zone B (Figure 5.3.13). The ACE analysis supports this and suggests significant differences in diversity among all three zones. Multidimensional scaling indicates that each zone is characterized by a distinct species composition (Figure 5.3.14). Bray–Curtis dissimilarity indices based on square root transformed and Wisconsin standardized data indicate the highest dissimilarity between Zone A and Zone C (Table 5.3.14).

Plate 5.3: Close-up photographs of the three zones in the Canyon reef. A - Zone A with a typical P. nodifera colony; B - Zone B with its diverse fauna of smaller coral colonies; C - Zone B with Pavona sp.; D - Zone C with rhodoliths (white) and coarse siliciclastic material between massive coral colonies; E - Zone C with a small microatoll indicating the fossil sea level; F - Zone C with typical bioclasts, mainly barnacles, on strongly eroded massive coral colonies.

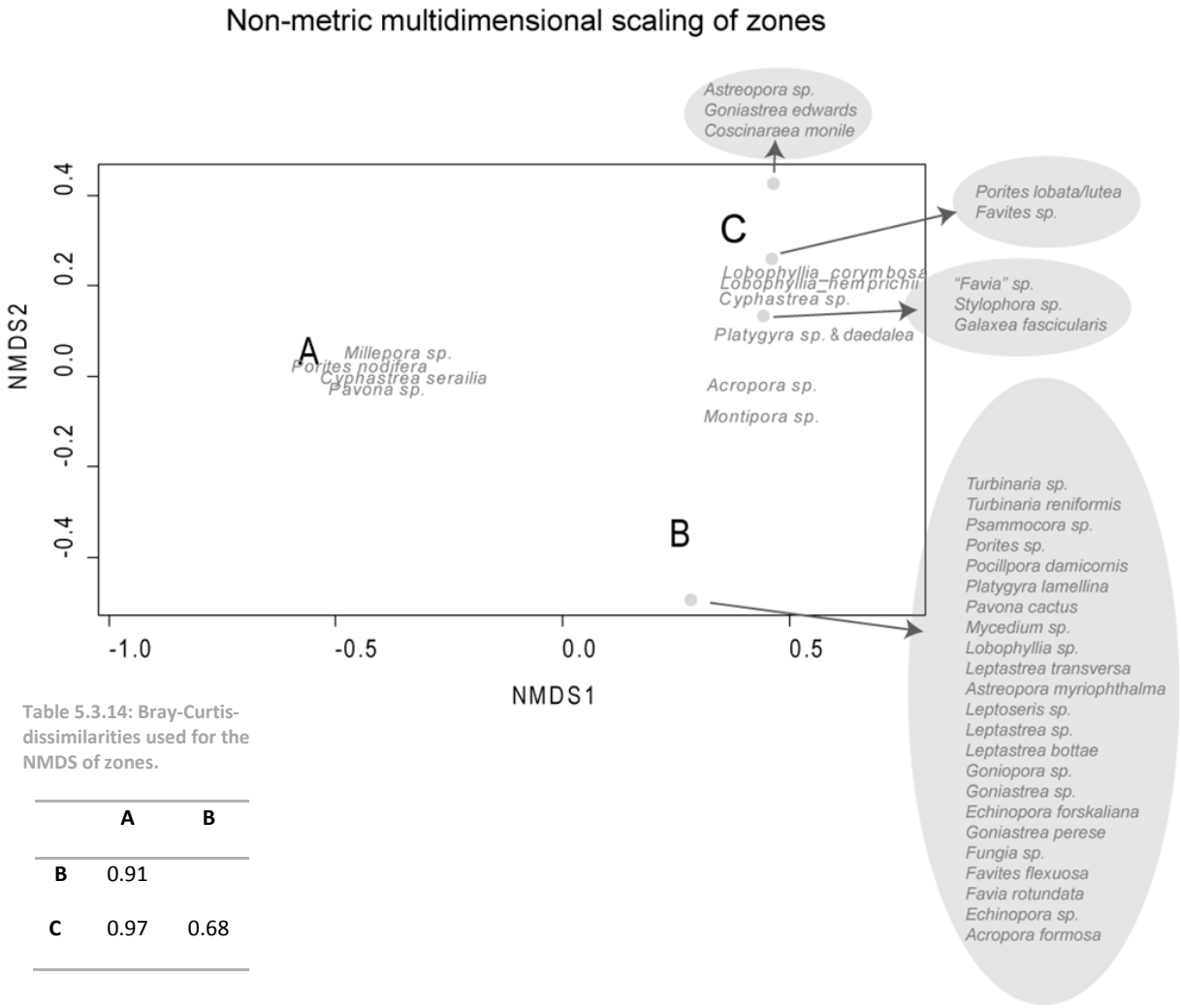

Table 5.3.14: Bray-Curtis-dissimilarities used for the NMDS of zones.

	A	B
B	0.91	
C	0.97	0.68

Figure 5.3.14: Non-metric multidimensional scaling (NMDS) ordination of the three zones, plotted onto two dimensions., with their typical species compositions. The NMDS was calculated in two dimensions. Distance is based on a Bray-Curtis matrix. Data has been square rooted before submitted to Wisconsin double standardization. Stress =0.

Table 5.3.15 provides a summary of the number of species at each site that have a preferred environment. Zone A inhabits too few species and cannot provide information, but Zone C shows a distinct affinity to a backreef environment. Zone B is not uniform, but consists of two groups of species of about equal size, i.e. one group preferring a slope environment and one a backreef environment.

Table 5.3.15: Summary of the number of specimens in each zone that have preferred environments. Zone A lacks species with preferences, while Zone B consists of two groups with different preferences. Only Zone C has distinct environmental preferences.

Zone	Backreef	Intertidal	Lagoon	Slope
A	0	0	0	0
B	48	0	0	47
C	69	6	0	1

The distinctiveness of the zones has been tested with the metrics used before in the thesis. ADNOS, ANOSIM and ANOVA (of the beta diversity) show a highly significant difference among the zones (Table 5.3.16). The permutation test and Tukey's HSD test confirm that there are significant differences in the compositions between Zone A and Zone B, and between Zone A and Zone C, respectively. There is no significant difference between Zones B and C.

Table 5.3.16: Summary of metrics used to assess the degree of similarity among reef communities from the three different zones of the Canyon reef.

Metric	Canyon reef zonation
ADONIS	R^2 = 0.19; *P* = 0.005
ANOSIM	R = 0.31; *P* = 0.03
ANOVA (Betadisper)	F = 7.6; *P* = 0.004
Permutation test for F	
Pairwise comparisons	
Zone A - Zone B	Observed/permuted *P* = 0.002/0.004
Zone A - Zone C	Observed/permuted *P* = 0.01/0.013
Zone B - Zone C	Observed/permuted *P* = 0.46/0.45
Tukey's HSD test	
95% family-wise confidence level	
Zone A - Zone B	*P* = 0.007
Zone A - Zone C	*P* = 0.003
Zone B - Zone C	*P* = 0.72

All three zones exhibit a similar rank abundance distribution (RAD). Among the various models, the Zipf-model and the Zipf-Mandelbrot-model have the best model fits (Table 5.3.17, Figure 5.3.15). In a classical autochthonous succession we would expect a directional change toward more complex RADs (McGill *et al.* 2007).

Table 5.3.17: Rank-abundance distribution (RAD) results for the three zones. The default family is poisson. The best modelfit (marked with bold numbers) has the lowest AIC.

	Zone A		**Zone B**		**Zone C**	
No. of species	4		39		16	
No. of specimens	93		335		112	
Model	**Deviance**	**AIC**	**Deviance**	**AIC**	**Deviance**	**AIC**
Null	60.3	74.98	73.84	202.52	62.42	111.92
Preemption	3.45	20.13	44.78	175.46	53.17	104.66
Lognormal	2.42	21.1	10.62	143.3	23.45	76.94
Zipf	**0.17**	**18.85**	18.28	150.97	**13.88**	**67.37**
Zipf-Mandelbrot	0.17	20.85	**4.14**	**138.82**	13.88	69.37

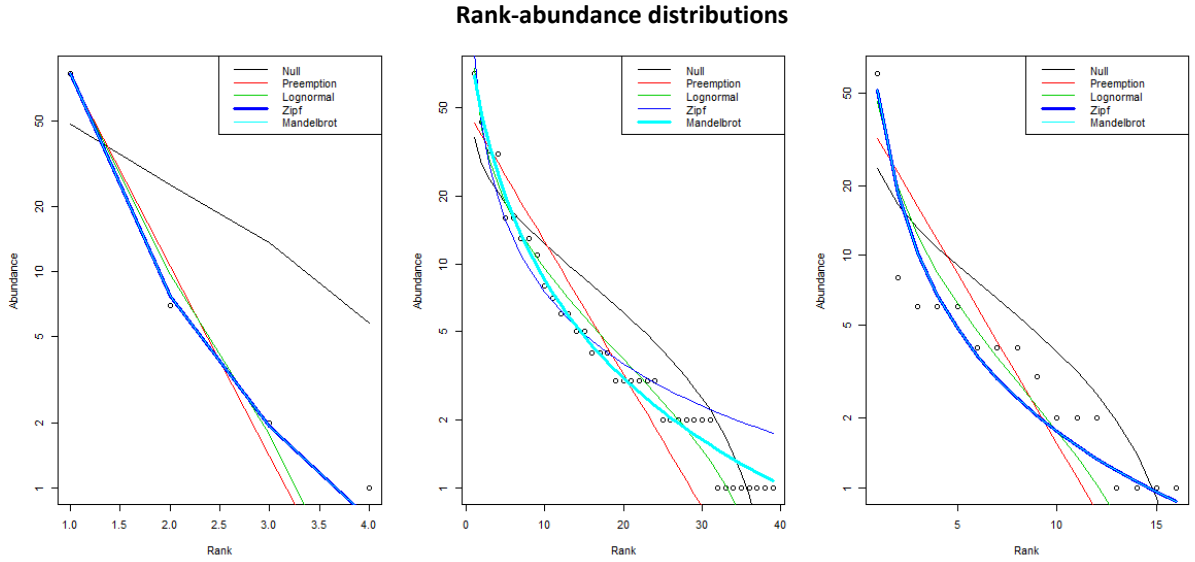

Figure 5.3.15: Rank–abundance curves for the three zones of the Pleistocene reef from Dahab. Various models have been added. The best fit based on the lowest Akaike information criterion (AIC) is marked with thicker lines. The respective AIC values are listed in Table 5.3.17.

5.4 Discussion

5.4.1 Community shifts in the Red Sea during the Eemian

The Pleistocene presence/absence data of the southern Sinai is more similar to the recent assemblage of the central Red Sea than to the Northern Red Sea. This suggests that range shifts have occurred between MIS5e and today. Kiessling *et al.* (2012) have shown that coral species range shifted towards higher latitudes during MIS5e, in combination with a contraction in diversity at low latitudes. During this time the ocean temperature was about 0.78 °C warmer than today (McKay *et al.* 2011; Kiessling *et al.* 2012). Descombes *et al.* (2015) forecast expansion of coral reef habitats under warmer climate, and also calculated a retraction of coral reefs from low latitudes, similar do other studies that generally estimate future distributions of marine biodiversity (Molinos *et al.* 2015). The central Red Sea is located in the outer tropics, but summer temperature often exceeds 32 °C (Figure 5.4.1), primarily in shallow water (Fine *et al.* 2013). Fine *et al.* (2013) also argue that due to the 'warm barrier' in the southern Red Sea where the summer SST reach up to 34 °C, corals and their zooxanthellae in the central and northern Red Sea must be well adapted to high temperatures. However, these warm areas are characterized by a lower density of zooxanthellae (Fine *et al.* 2013). And despite the adaption, corals in the central Red Sea live close to their bleaching threshold and, as records from 2007 and 2010 show, occasionally bleach (Fine *et al.* 2013; Furby *et al.* 2013). During the last interglacial, when SST was even higher, corals in the central Red Sea might have reached the bleaching threshold even more often, and a community shift towards the Gulf of Aqaba is a feasible explanation for the remarkable similarity of Pleistocene reef assemblages from the northern Red Sea to modern reef communities from the central Red Sea. Fine *et al.* (2013) even suggested that this shift might happen in the future. The latter authors also propose that the Gulf of Aqaba might serve as refuge for Red Sea corals. Because the Gulf's surface

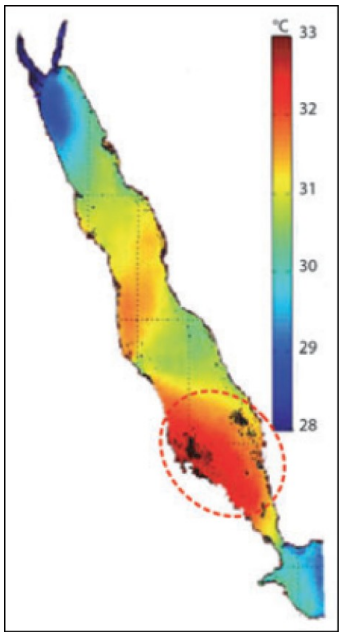

Figure 5.4.1 (Fine et al. 2013): Red Sea summer temperatures demonstrating the sharp latitudinal temperature gradient between the warm southern section of the Red Sea and cooler water in the Gulf of Aqaba. Dashed red circle indicates the 'warm barrier' in the southern Red Sea.

water temperature is much lower than in the central and southern Red Sea (27.5 °C = summer average), it will take much longer until corals will reach their bleaching threshold.

The quantitative data support the conclusion that a northward shift of coral diversity occurred during the Eemian, because the analyses show a higher diversity in the Pleistocene than in the recent reef of Dahab, despite the much larger sampling size in the recent reef. The estimated species richness (ACE) of my quantitative data from the Canyon reef is 47 species, while it is 40 in the nearby recent reefs (Table 5.3.4). Today, diversity is highest in the central Red Sea, even relative to the whole western Indian Ocean (Spalding *et al.* 2001), because there is no such temperature drop in winter as in the northern Red Sea, and the salinity is more stable. Since Pleistocene data explicitly from the central Red Sea was not available to me, it cannot be shown if the shift northwards is accompanied by a decrease in diversity in this region. A special role for the Gulf of Aqaba cannot be derived from this result, since El-Sorogy (2002, 2008) collected his data in Hurghada and Safaga, and Kora *et al*. (2014) in Marsa Alam, which all are located along the mainland Egyptian coast of the northern Red Sea. However, when excluding the occurrences provided by Kora *et al.* (2014) either because of their location farther south and/or because at least some of their taxonomic identifications are misleading (see below) the signals gained from the dataset become even stronger.

5.4.2 Community ecology of Pleistocene reefs in Dahab and Ras Mohammed

The reef communities in Dahab differ from those in Ras Mohammed. The results of testing for significant differences indicate a difference in environments rather than geography. The differences between these localities are to be traced back to their different environmental conditions. All sites in Dahab show a distinctly higher diversity than the sites in Ras Mohammed. About 6% of Red Sea coral species are believed to be endemic (Sheppard *et al.* 1992), but no endemic species was identified within this study. All species identified in this study still occur in the recent Red Sea. However, 14 Pleistocene taxa from the binary dataset are not found in the dataset provided by Sheppard & Sheppard (1991). These taxa thus appear to occur as singletons only during the Pleistocene of the northern Red Sea, but in none of the recent Arabian regions, raising the question if this absence is a true biological signal or a sampling artifact. Including them would lead to a different picture with a large regional extinction event, a species loss of about 15%, and provide a picture of instability and impersistence. Of the 14 singletons, four were identified by myself: *Echinopora forskaliana*, *Favites spinosa*, *Coelastrea aspera*, *Leptastrea bottae*. The first one was used as synonym of *Echinopora gemmacea* by Sheppard & Sheppard (1991), and was included as such in the analyses. All four species occur in the modern Red Sea (Veron 2000). Similarly, four further species identified by El Sorogy (2002, 2008) in the Pleistocene appear to be singletons not been observed by Sheppard & Sheppard (1991): *Acropora latistella*, *Dipsastraea veroni*, *Stylophora kuehlmanni*, *Porites undulata*. The remaining singletons come from Kora *et al.* (2014): *Acropora stoddarti*, *Acropora spicifera*, *Acanthastrea hemprichii*, *Plesiastrea devantieri*, *Leptastrea pruinosa*, *Echinopora hirsutissima*. Some of them can be deduced to incorrect taxonomy: I consider their identification of *Echinopora hirsutissima* to be synonymous to *Echinopora forskalina*, and their identification of *Plesiastrea devantieri* cannot be distinguished from *Astrea curta*. Other identifications remain at least questionable. Between all these datasets also correct synonymization appears to be a large problem that could not always be solved - especially when questionable taxonomic identifications meet incorrect synonymy. All the 14 singletons occur in the Red Sea region today (Veron 2000) and none of them is an endemic species. The occurrences provided by Veron (2000) and in the online database based on this book http://coral.aims.gov.au/ are coarse and do not allow a resolution of occurrences within the region defined by Sheppard & Sheppard (1991). Hence, all these singletons were confidentially excluded, because they could not be used for a comparison at the regional level. Also instability cannot be assumed from the occurrences of the alleged singletons.

All sites contain a large number of specimens that can tolerate high salinities, in reef flat communities it is even the majority of specimens. This observation indicates that the coral species that were able to successfully establish in the Red Sea are not only selected by their ability to

tolerate high temperatures in the 'warm barrier', but also by their ability to tolerate high salinities. Since these species also occur in other Indo-Pacific regions, this is not a signal of adaption but of filtering.

5.4.2.1 Dahab

The fossil reef at *The Canyon* is in many ways comparable to the recent reefs at *the Islands* studied by Alter (2004): Both represent classical fringing reefs as they are typical for the Gulf of Aqaba. They comprise communities from reef flat to reef slope, there is a high similarity in the overall community composition (up to 84%), and the sites have the highest diversities of all sites studied here. Surprisingly, the fossil site appears to be even more diverse than the recent site, despite the smaller sample size. Of course, the recent data has been delimited to species that occur in the Pleistocene data, but Alter (2004) has calculated a mean diversity (*H*) of 2.8 for station 1 and 2 respectively, and 2.67 for station 3. This corresponds to the fossil reef (*H* = 2.8), but the latter one is a strong underestimation, as the ACE-estimate suggests. The Canyon reef comprises three significantly distinct zones in terms of diversity and species composition, which will be discussed in Chapter 5.4.3 (below). That the recent site contains flat to slope environments might explain why this community is not significantly distinct from fossil flat and slope communities.

The sites *Patch reefs* and *Blue Hole* represent an artificial combination of transects according to their spatial distribution (see site descriptions). Both sites consist of different patch reefs, which obviously do not represent homogenous environmental backgrounds, as can be inferred from the preferred environments of the contained taxa. Especially the Blue Hole comprises three different patch reefs from different environments. The patch reefs grew on base rocks and fanglomerates providing different water depths, so that the community composition on each patch differs depending on the depth of the fundament. One of them is almost exclusively built by *Porites nodifera*, comparable to Zone A in the Canyon reef. The locality *Patch reef* between the Blue Hole and the Canyon reef comprises line transects from one patch only and is inhabited by only a few species that prefer backreef environments. Nevertheless, in the NMDS it plots closer to Turtle Bay than to any other site, and was thus grouped with the first one, which also contains a huge number of backreef preferring coral taxa. This patch reef likely grew in a backreef channel that consolidated in the small embayment behind the reef flat. The site is a little more offset from the recent beach than the other patch reefs at the Blue Hole. The diversity at the *Patch reef* is high (*H* = 2.55) in comparison to most of the other sites and it has the most even community of all sites (*J* = 90), despite the small sample size. The reason is probably that it contains data from one environmental background only, and represents a sheltered undisturbed reef environment.

5.4.2.2 Ras Mohammed

Especially the site Turtle Bay at Ras Mohammed offers a different habitat for coral species than the narrow fringing reefs in the Gulf of Aqaba. Three study sites are located at the shore of Marsa Bareika, the main study site kept this name in the small embayment Turtle Bay, Ras Mohammed Camp at the northern coast of Marsa Bareika, and *Ras Ghozlani* at the northern entrance of Marsa Bareika. The species at *Turtle Bay* that have a preferred environment mostly prefer the calmer backreef area. Also, there is a significant number of species occurrences at Turtle Bay that cannot tolerate high salinities. Marsa Bareika is a relatively shallow bay, but with a large opening towards the open Red Sea, so that salinity does not exceed the usual Red Sea salinity. Fishelson (1980) refers to the reef type that the site in the Turtle Bay represents as *Sharem reef*, which is a quite common type of reef in surrounding embayments where wadis terminate into. Shifting alluvial sediments on the bottom of the bay prevents coral development in the internal part of the bay, and corals grow along the sides of the bay usually starting as small patches and reef structures that gradually increase in size towards the opening of the embayment (see outcrop description).

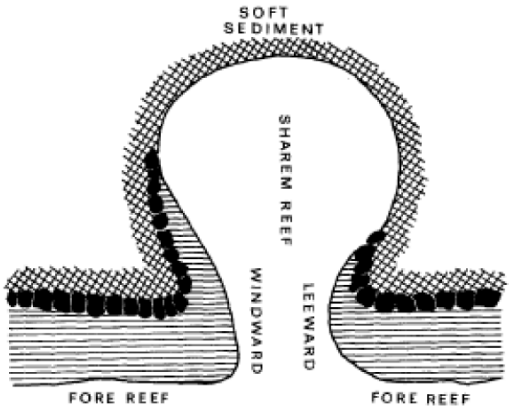

Figure 5.4.2: (Fishelson 1980): Aerial view of a Sharem reef. Black structure = beach rock, crossed = soft sediments, lines = reef.

Figure 5.4.3: Turtle Bay is a small embayment in Marsa Bareika with a large wadi entering the bay in the left part of the picture.

Diversity also increases only towards the opening. Additionally there are differences in the communities between leeward and windward sides (Fishelson 1980), which we could also observe in the Pleistocene reefs (see description of sites). Diversity is generally lower than in the large fossil reef at the Canyon or in the recent reefs of Dahab, but it is still higher than in the other sites at Ras Mohammed. Several species of *Porites* (branching and massive forms) are abundant, as is *Echinopora forskaliana.* The fossil reefs along the wadi in this embayment have been frequently disturbed, especially in the inner embayment. The disturbances can be observed in the fossil reefs in form of huge siliciclastic inputs within the reef body Figure 5.4.2. Only azooxanthellate corals were abundant in the most landward part of reef 1, indicating that the stronger sedimentation prevented zooxanthellate corals from settling.

Figure 5.4.2: Siliciclastic layers switch with reef carbonates in the inner embayment (reef 1, position marked by a dot in the sketch of Figure 5.4.3, close to the edge of reef growth. The siliciclastic layers become rarer towards the opening of the embayment.

This special situation explains the low diversity of this site in comparison to the Canyon reef and Dahab patch reef. The recent wadi seems to have been already existent during the last interglacial, and structures remained similar during at least the last ~125,000 years. The fossil reefs of the lowest terrace reach relatively deep into the recent wadi. Next to the uplift of the reefs, especially the higher sea level during MIS5e can explain this pattern. Also, derived from the distribution of the fossil reefs in comparison to the recent reefs (Figure 5.4.3), the predominating wind direction seems to have changed since the last glacation, according to the sketch of Fishelson (1980).

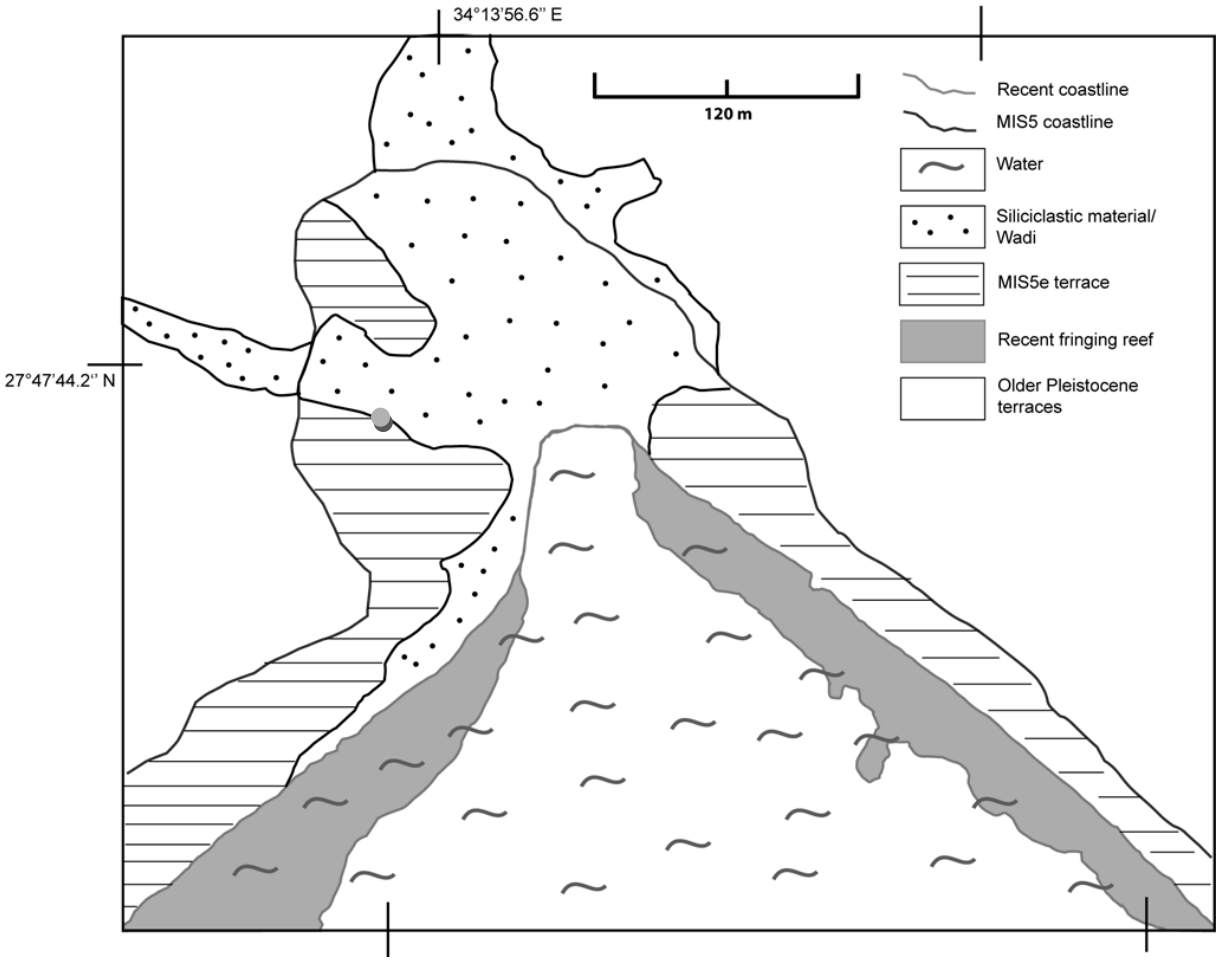

Figure 5.4.3: Sketch of the site *Marsa Bareika* or *Turtle Bay* in a small embayment of the Marsa Bareika. The MIS5e coastline is a rough estimate but is sufficient to show the distribution of MIS5e reefs in the embayment. The dot marks the position of Figure 5.4.4.

The communities at the sites at *Ras Mohammed Camp* and *Ras Ghozlani* show a strong affiliation towards intertidal/reef flat communities. The analyses confirmed the first impressions from the field. *Goniastrea retiformis* is a dominating species in both sites, but especially at *Ras Ghozlani*. At *Ras Mohammed Camp* the occurrence of *Favites*, *Platygyra*, and especially *Lobophyllia* suggest that the water was probably shallow, but calmer and the reef not as exposed as the reef at *Ras Ghozlani*. However, the communities of both sites contain a significant number of species that are able to cope well with high salinities. Diversity at *Ras Mohammed Camp* is slightly higher than at *Turtle Bay*. The distance between these sites is only about 1 km, but grouped by their environmental conditions, and the communities of these sites are significantly distinct in the analyses. The diversity at *Ras Ghozlani* is the lowest in this study (apart from the older terraces ignored in the further analyses), which can be ascribed to its exposed reef flat environment that has special requirements for its inhabitants. The strong dominance of *Goniastrea retiformis* is typical for a reef flat

environment and regular aerial exposure during low tides, as it can be observed in recent fringing reefs in the Gulf of Aqaba. Its position at the entrance of Marsa Bareika makes it a less sheltered environment than *Ras Mohammed Camp*, which is located further inland.

5.4.3 Ecological succession in the Canyon reef (Mewis & Kiessling 2013)

Different environmental conditions can be inferred for the three reef zones. The dominant species of Zone A (*Porites nodifera*) is tolerant of high salinities and prefers shallow water (Veron 2000), which suggests a salinity-controlled marginal marine setting. Zone B is a typical reef slope community, with *Acropora* being the most common but not dominating genus. Platy and encrusting taxa are only common in this zone. Zone C is typical of a reef flat or backreef facies as *Porites lutea* and *Porites lobata* are commonly found together today in backreef margins and intertidal areas (Veron 2000).

Porites nodifera is a shallow-water species, generally living in less than 5 m depth and tolerating salinities of up to 48 % (Sheppard & Sheppard 1991). Its presence is especially notable in highly saline, shallow areas where sea grass dominates (Sheppard & Sheppard 1991). *P. nodifera* is also supposed to be common on reef slopes with normal Red Sea salinities (about 40–42 %), but there it does not form extensive single species stands that we observed in the lowermost reef zone at the fossil reef of Dahab. The dominance of *P. nodifera* at the base of the Canyon reef is a first hint that these reefs do not show a classical ecological succession that usually shallows upward (Copper 1988). Reef growth did not start in deeper water, e.g. on a slope, but during a transgression in very shallow water. The siliciclastic fanglomerate below provided the hard substrate for colonization. Due to the particular geological setting of the Red Sea and the extreme aridity in this region (Reiss & Hottinger 1984), salinity was significantly higher during glacial episodes, when the Red Sea was disconnected from the Indian Ocean than during interglacial periods, and salinity decreased only gradually during deglaciation (Thunell *et al.* 1988). The high siliciclastic content of the framework between the *Porites* columns also indicate a near-shore environment. I thus conclude that species diversity was constrained by high salinities at the beginning of the reef development after the preceding glacation.

The coral community of Zone B is a typical reef slope community, based on the composition of the community and the relative abundance of *Acropora*. Although Zone B might also be regarded as a classical diversification stage in an autogenic ecological succession, it is more likely that sea-level rise during deglaciation caused normal salinities, which triggered diversification. This observation is in accordance with other studies of Pleistocene coral reefs in the Gulf of Aqaba (e.g. Dullo 1990). Therefore, although the transition from Zone A to Zone B is similar to what might be expected from an autogenic ecological succession, I interpret this as the result of environmental change. Also, the community of Zone B is grouped into a community that prefers backreef environments and a community that prefers slope environments. This can be explained by the size of the reef complex. At first, the sheltered areas of the reef, further away from the reef front, contain a larger amount of typical backreef species, such as *Porites lobata* and *lutea*. Second, there was presumably some change in water depth and turbidity during reef growth, which might have led to some change in preferences, but this change was neither distinct in the field nor in the resulting data. And third and most important, many of the species that prefer one specific environment do also occur in several other environments. There is mostly no exclusiveness in the information about preferences. As such, the observation in the field is much more important than the theoretical approach about reconstructing environments.

The coral community at the top of Zone C is a typical reef flat community, similar to the recent coast of the Gulf of Aqaba (personal observation; Dullo 1990; Dullo & Montaggioni 1998). Typical intertidal organisms such as oysters and barnacles grew on large, massive coral colonies. Microatolls mark the sea level, and a high amount of bioclasts prove substantial erosion. Here, an autogenic succession cannot be excluded but is again unlikely, because obviously a decrease in water depth as a consequence of its own upward growth led to the abrupt change of the community structure in zone C. This case represents allogenic succession (Walker & Alberstadt 1975). *Porites lobata/lutea* is dominating the community with about 54% abundance. Thus, the origin of Zone C is

likely related to the reef reaching the sea level rather than autogenic community replacement. Especially the patch of *Acropora muricata* in the uppermost edge of zone B already indicates a shallowing upward inside zone B. Alter (2004) has shown that this species occurs in depths of 1 -2 m in a comparable recent reef in Dahab. Within Zone C, the community changes from a typical backreef community with several *P. lutea*/*lobata* colonies to an intertidal facies with microatolls.

Altogether, the Canyon reef shows a distinct transgression–regression cycle from beach—very shallow habitat—reef slope—shallow backreef—intertidal, and to beach facies again. All three communities show a Zipf or Zipf-Mandelbrot rank abundance distribution (RAD). Especially at a pioneer stage in the true ecological sense we would expect a more linear model such as pre-emption, which is typical for simple, species-poor communities. Nevertheless, the AICs of the pre-emption and Zipf-Mandelbrot model of the lowermost zone are very similar, which may be due to an underestimation of diversity of Zone A and the low sample size. But despite the low sample size, the RAD does not suggest a simple community. Even though one species is overwhelmingly dominating the community, the other species do not follow the geometric series. Likewise, the RAD in Zone B suggests a Zipf-Mandelbrot, but the AIC values are similar to the log-normal distribution. As my data is likely to underestimate true diversity, the Zipf-Mandelbrot distribution might also be an underestimation of a lognormal distribution. This information, together with the information about diversity and evenness, indicates that Zone B was a highly diverse and complex reef community that could cope with disturbances. That such disturbances indeed occurred can be seen in the *Acropora muricata* patch at the uppermost slope of the reef body (Figure 5.4.4), indicating regular catastrophic siliciclastic input from adjacent wadis.

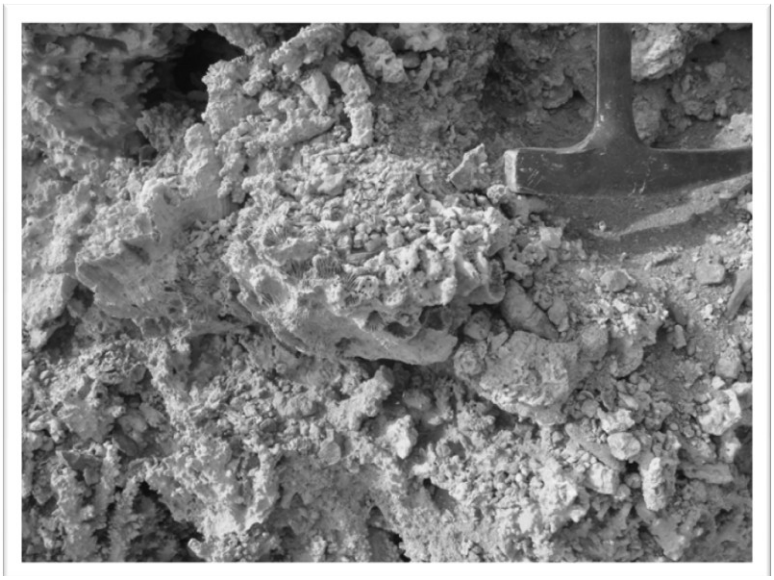

Figure 5.4.4: Patch at the outer edge of the Canyon reef that is almost exclusively built by *Acropora muricata* and a few other species, as e.g. *Lobophyllia corymbosa* in this picture. The hammer marks a disturbance in this *Acropora* community, where coarse siliciclastic material and several gastropods indicate a sediment input from the adjacent wadi. But *Acropora* recovered well and the community above the disturbance is the same as below.

5.5 Conclusions

This study directly and quantitatively compared coral species from the Eemian of the Gulf of Aqaba to recent reef data from the same region, and binary recent data from the whole Arabian region to Pleistocene data from the northern Red Sea. I could show a spatial community shift from the central Red Sea to the Northern Red Sea in the Eemian. Current hotspots of coral diversity occur in regions with the warmest SST, such as the coral triangular and the central Red Sea, because those regions served as refugia during cold periods of the Quaternary (Pellissier *et al.* 2014). Descombes *et al.* (2015) predict that those regions will also be the first to show a reduction in habitat suitability under a warmer climate. Whereas this could not be directly proved in this study because Pleistocene data from the central and southern Red Sea are missing, it could be shown that diversity in the northern Red Sea and the Gulf of Aqaba during the last interglacial have been more similar to the diversity in the recent central Red Sea than to the recent northern Red Sea, which is a strong hint for a community shift during elevated temperatures. However, the coral sensitivity to thermal stress is probably even increased by ocean acidification (Anthony *et al.* 2008), so that predictions about recent climate warming derived from Pleistocene data need to be carefully evaluated with respect to these additional problems.

The Eemian community shift also explains why the fossil data collected in Dahab reveals a higher diversity than the recent data collected by Alter (2004), even when compared to the latter author's raw data results. This is a surprising observation and calls for further work on this topic.

The Eemian communities from Dahab and Ras Mohammed differ distinctively from each other, which can largely be explained by different sedimentary environments. Especially the site *Turtle Bay* provides a complex sedimentary system that strongly influences and also restricts coral growth. The seasonal alluvial input from the wadis limits coral diversity. The other sides in Ras Mohammed represent reef flat and shallow slope environments, and are therefore not directly comparable to the completely preserved fossil fringing reef at *The Canyon*. However, the latter site has shown that the Red Sea comprises a special geological and climatic setting facilitating allogenic succession. The narrow shelf area as well as the high aridity and salinity lead to harder competition for space and stronger effects of sea level change than in most other coral reef habitats in tropical seas.

6. DISCUSSION SYNTHESIS AND FINAL CONCLUSIONS

In the previous chapters the results of the analyses of two different study areas have been discussed largely within their local context. In Vanuatu, four reef terraces could be studied in more detail despite the difficult access to suitable outcrops and the poor preservation. Age datings were used to group sites into at least 4, but rather 5 interglacial episodes ranging from mid-Holocene age to MIS 9. MIS 11 is also preserved, but 100% recrystallized. The communities of the terraces do not significantly differ from each other, whereas a grouping by reconstructed reef environments independent of age revealed significant differences. A similar pattern can be observed when comparing LIG and recent terraces in the northern Red Sea, where spatial and environmental reasons for differences between sites play a larger role than time.

The understanding of ecosystem dynamics is dependent on the scale at which ecological observations are made (Pandolfi 2002). Pandolfi (2002) showed that reef coral communities studied over small spatial and temporal scales do not display ecological equilibrium, whereas studies conducted over large temporal scales show persistence in coral community structure through tens of thousands of years. Before discussing my results on regional and global scales and taking a closer look at persistence and community shifts, I will shortly compare the study areas Vanuatu and Egypt to each other, and evaluate some of the methods that I used in this study.

6.1 Vanuatu and Egypt - a comparison

During two field work seasons in Vanuatu and Egypt a suitable number of data could be collected: 48 coral taxa (including the hydrozoan genus *Millepora*) could be identified out of 541 specimens from bulk sampling data in Vanuatu, of which 26 were identified at species level. In Egypt, 52 coral taxa (including the hydrozoan genus *Millepora*), of which 31 taxa were identified at species level, were determined out of 1432 specimens from transect data. Four additional species have been identified outside the transects. The total diversity (Shannon-Wiener-Index *H*) is 3.02 in Egypt, and 3.06 in Vanuatu. With 31 identified genera, genus diversity is higher in Vanuatu than in Egypt with only 26 different genera. In conjunction with the fact that more than 50% of the taxa identified in Vanuatu were only identified at genus level, and considering that preservation was much worse than in Egypt, it is only logical to assume that the total diversity of Vanuatu is a strong underestimation of the true diversity. This underestimation is also indicated by the rarefaction curves of the two study areas (Figure 6.1.1).

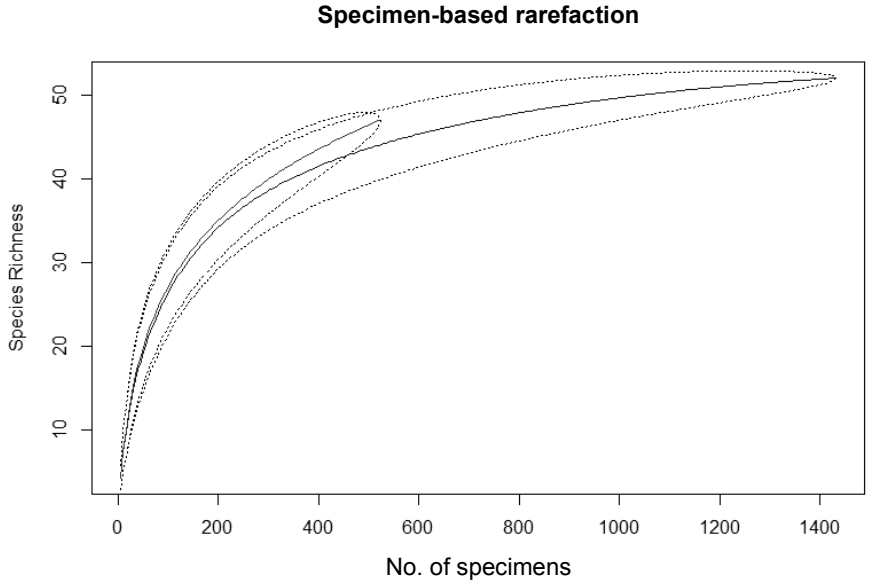

Figure 6.1.1: Specimen-based rarefaction curves of the total species and specimen number from Vanuatu (upper line) and Egypt (lower line).

6.2 Evaluation of methods used in this study

Pandolfi (2001b) has shown that there are differences between species and genus level patterns in Quaternary coral communities, but that they have little effect on paleoecological interpretations. Whereas in principle, I agree with this statement, I could also show in the Vanuatu study that if sampling is not sufficient, an identification down to species level of as many samples as possible helps to gain more distinctive results. By contrast, a sampling at genus level might give misleading, or at least imprecise signals, as standardized species data showed a less strong correlation between diversity (*H*) and age of the terraces than standardized genus data. Also, when based on genus level identification, diversity analyses show fewer differences among communities than if species identifications are considered, especially in the standardized dataset. Shareholder quorum subsampling of genera shows only minor differences among terraces, which das not reflect the SQS curves based on species level identification. Pandolfi's (2001) study is based on Caribbean data with a low genus/species ratio, while Indo-Pacific genera are often presented by a much larger number of species. The Vanuatu data has a relatively low level of species identification and the results already suggest that genus identification might be not enough for datasets with a high species richness as typical for indo-Pacific reefs. For paleoecological interpretations the identification of some key species in addition to genus determinations seems to be a good solution. With the help of relatively few taxa with certain ecological preferences reasonable environmental reconstructions could be obtained.

In this context, the present study could also show that the `envfit` function in vegan is useful to reconstruct environmental conditions when both outcrop situation and access to data from facies-diagnostic fossils were limited. The calculated environmental zones fit well to the field observations and subjective faunal interpretations. Bulk sampling appears to be useful to collect a larger number of specimens when the outcrop situation limits more rigorous collection approaches like the transect method. The collected data is useful for ecological interpretations, but the interpretation of diversity parameters derived from bulk sampling data should be handled with care and used only for a first assessment. In combination with transect data, however, bulk sampling can provide some valuable information. For example, Pleistocene 2, which was overrepresented in the transect data and underrepresented in the bulk sampling data, gives contradicting results regarding its species richness and diversity. In fact, it is the most diverse of all terraces in the transect data, but reveals a low diversity in bulk sampling data. In the bulk sampling size. However, only subsampling (rarefaction and SQS) of transect data could even out the differences in diversity between Pleistocene 2 and the other terraces. Subsampling of bulk sampling even strengthened patterns reflected by the raw data, which in this case were the distinct differences between Holocene and youngest Pleistocene on the one hand, and the two older Pleistocene terraces on the other. In this case, the small transect dataset prevented me from overinterpreting this pattern suggested by the bulk sampling data. Also, the reduction of presence/absence data reflected by the Sørensen similarity helped to minor differences among terraces. But again, genus level identification leads to stronger similarities among terraces and thus biases the signal revealed by similarities at species level. The standardized species presence/absence similarities are most similar to the presence/absence transect similarities, especially for the middle Pleistocene terraces where transect sampling was more sufficient than in the Holocene and the oldest Pleistocene terrace, respectively. This result suggests that presence/absence bulk sampling could be a strong alternative to abundance based bulk sampling, because it is less biased.

The results gained in the Vanuatu study are the reason why I did not perform any analyses at the genus level in Egypt, where transect data and species level identifications yielded much more robust results. The results of the Egypt study are, therefore, much more reliable and indicate to me that the selected approach was sufficiently comprehensive, which is why the methods used there require less technical discussion than for Vanuatu.

6.3 Stability, persistence, and disturbance

The results of the present study indicate that Pleistocene reef coral diversity in Vanuatu was higher than the diversity of the Red Sea (see above), just as it is today. In Vanuatu, four terraces from four interglacial episodes were compared in terms of their community composition, environmental background, and age. The signal gained from the bulk sampling data with Holocene and youngest Pleistocene being most similar to each other and being much more diverse than the older Pleistocene terraces is not biologically relevant, but can be ascribed to sampling artifacts. If combining the signals gained from the transect and bulk sampling data, Pleistocene and Holocene terraces reveal a much more similar diversity. Especially when testing for significant differences in species composition, it becomes obvious that differences between the community compositions of different reef environments play a larger role than differences between terraces of different interglacial episodes. Reef coral communities within the same environment are most similar to each other, even if they differ in age by almost 300 kyr. Differences in the community compositions between the terraces can be largely inferred from unbalanced sampling of different environments due to the dense vegetation growing on the surface of the fossil terraces. Also a greater spatial than temporal variability, as for example between the sheltered Holocene community from Samoa Point versus the exposed Holocene community from Saama village could be shown. However, Pandolfi (1996, 1999) did not only observe a persistence in diversity, but also a persistence in taxonomic composition during the at least last 95 kyr on Huon Peninsula, Papua New Guinea (PNG). In Vanuatu, the taxonomic composition is largely stable, with the most common genera *Porites*, *Platygyra*, *Lobophyllia*, *Goniastrea,* and *Dipsastraea* occurring relatively even throughout the terraces, and differences can be ascribed to different reef environments. For example, *Lobophyllia* as a typical slope taxon occurs evenly distributed among the three younger terraces, whereas it is lacking in Pleistocene 3, which is represented by one environment (exposed reef crest) only. At the same time, *Goniastrea* is very abundant in Pleistocene 3, and its absence in Pleistocene 2 can be explained by the low resolution at genus level among "faviid" corals. However, the rise of *Acropora* abundance in MIS 5a, and especially in the mid-Holocene of Vanuatu, is an observation that cannot only be explained by taphonomic biases. Other branching corals, such as *Stylophora* and branching *Porites* occur even in the poorly preserved outcrops of Pleistocene 2, but *Acropora* is completely missing. Also the especially delicate *Seriatropora hystrix* could be identified in Pleistocene 1, but *Acropora* is rare compared to today. *Acropora* is a fast growing genus that is common and often even dominating a wide range of reef habitats (Veron 2000). A recent study (Renema *et al.* in review) could show a correlation between increasing sea level fluctuations during the Quaternary and the increase in *Acropora* dominated reef communities during the Pleistocene. The switch to *Acropora* dominated communities increased the accretion rates of reefs and allowed them to keep up with Pleistocene sea level rise (Renema *et al.* in review). In the study site in Vanuatu, the tectonic uplift was probably largely fast enough to allow reefs to keep up with the rising lea level throughout the older Pleistocene terraces. I see mainly two possibilities for explaining the sudden rise of *Acropora* in Pleistocene 1, and especially in the Holocene: Either sea level fluctuations in the younger MIS 5 (a - c) were too fast, so that the uplift rate was not high enough to allow the reef corals to keep up, or some kind of disturbance allowed *Acropora* to occupy a niche, in which it could outcompete other coral taxa due to its reproductive abilities and high growth rates making *Acropora* one of the fastest taxa to recover from environmental disturbances (Sweatman *et al.* 2011). Both scenarios suggest that Pleistocene reefs in Vanuatu do not reveal the same strong persistence similar to the PNG reefs studied by Pandolfi (1996, 1999). To evaluate if this is a rather local phenomenon of Efaté, further quantitative studies of Pleistocene Indo-Pacific reefs would be necessary. However, in LIG reefs of the Gulf of Aqaba *Acropora* is a fairly abundant genus with a maximum of over 30% of specimens belonging to this genus in Zone B (slope community) of the Canyon reef.

In Egypt only one fossil terrace was examined in detail, but the analyses suggest a strong persistence in community composition and diversity within the last ~125 ka. The community preserved in a large fossil reef body from Dahab shows the highest similarity to a comparable recent reef. Within the LIG terrace significant differences occur between sites from different reef

environments. Disturbance of coral communities must have occurred during glacial episodes, because several studies have shown that the Red Sea has undergone dramatic changes during glacial episodes, caused by the limited water exchange at Bab-el Mandeb (Lambeck *et al.* 2011). Glacial and interglacial sea level changes play a much greater role for the health of Red Sea communities than for any other oceanic system (Siddall *et al.* 2004). Salinity in the Red Sea increased up to 55 ppt (Reiss *et al.* 1980; Siddall *et al.* 2003; Almogi-Labin *et al.* 2008), the water column was stratified and there was a stronger, shallower oxygen minimum zone (Almogi-Labin *et al.* 1998, 2008), which led to local decimation of corals (Braithwaite 1987) and plankton (Fenton *et al.* 2000), resulting in a starved greenhouse-type ocean allowing the growth of stromatolites (Brachert 1999). The reestablishment of coral reefs started only after sea level returned to within 20 m of the present level, around 8 ka ago (Braithwaite 1987). The situation was probably similar in other Quaternary glacial cycles (Lambeck *et al.* 2011). Sea level reconstructions for the glacial episode MIS6 suggest that seal level was as low as in the LGM (e.g., Siddall *et al.* 2007), so that similar conditions can be assumed. Nevertheless, the community composition appears to be stable in terms of diversity and species composition, and Red Sea coral communities must therefore have found some kind of refuge during glacial episodes. It is unlikely that reefs disappeared during glacial episodes in the Red Sea and invaded again afterwards with the same composition. All identified taxa still occur in the Red Sea today, whereas this and other studies on Pleistocene reefs from the Red Sea region did not identify any endemic species. However, these endemic species (largely also occurring in the Gulf of Aden) also are represented by rather rare species such as *Erythrastrea flabellata* and especially delicate taxa such as *Anacroprora spumosa*. Only four out of 47 species of *Acropora* are endemic in the Red Sea and Gulf of Aden today, but seven out of 29 *Montipora* species (Alter 2004). However, both genera largely lack identifications at species level in the fossil record. Drawing a signal out of the lack of endemic species in the fossil record would therefore run the risk of overinterpretation, because this observation is probably the result of a sampling artifact. There are two distinct, but not mutually exclusive hypotheses for what happened to the Red Sea biota during glacial episodes: 1) marine organisms survived glacial conditions within the Red Sea or 2) outside of the Red Sea, particularly in the Gulf of Aden. Recent studies (DiBattista *et al.* 2015a, b) reviewed paleontological, biological and genetic evidence in several marine groups, but found no consistent pattern across taxa with respect to the causes and processes underlying endemism in the Red Sea. Similar to other endemic coral hotspots like Hawaii, endemism seems to be largely related to restricted access to other diverse regions. Whereas for Hawaii the restriction is caused by geographic distance. In case of the Red Sea it is the very narrow and shallow Bab-el-Mandeb straight that restricts exchange even during the present sea level highstand (Siddall *et al.* 2004). Because many Red Sea endemics also occur in the Gulf of Aden (DiBattista *et al.* 2015a, b), some believe that the adjacent regions of cold-water upwelling off Somalia and Oman, as well as seasonal current patterns, are of greater importance as isolating mechanisms than the physical isolation at Bab al Mandeb (Kemp 1998, 2000). DiBattista *et al.* (2015a) find that apart from a few locations indicating a loss of most planktonic organisms, there is little direct evidence supporting the complete loss of species within the entire Red Sea during glacial episodes. These authors especially suggest that the strongest evidence for the persistence of some Red Sea fish taxa during glaciation events is the genetic evidence that many endemic taxa (or lineages) diverged from their Indian Ocean relatives long before the most recent glaciations, and that some endemics are restricted to narrow areas, especially in the northern Red Sea. The range of ages of Red Sea endemics suggests that peripatric speciation has been an ongoing process in this region, a pattern also seen in other hotspots of endemism in the Indo-Pacific (DiBattista *et al.* 2015a). To solve the question if corals persisted in the Red Sea during glacials, a calculation of molecular divergence estimates would be useful. Similar to Red Sea fish species, also coral endemics occur in several not closely related genera and appear to be randomly scattered across the phylogeny. There is evidence that endemic deep water bivalves from the Red Sea persisted and evolved during glacial periods (Turkay 1996), whereas shallow-water species contracted to refugia outside of the Red Sea (Grill & Zuschin 2001). Thus, there is indication that tolerance to elevated salinities allowed some species to survive through glacial cycles within the Red Sea and evolve into endemics (DiBattista *et al.* 2015a).

All study sites show a high number of specimens belonging to taxa that can tolerate high salinities. All species identified in this study are not endemics, and do occur also in other Indo-Pacific regions. However, in the Red Sea the salinity tolerant species seem to form larger proportion of the communities than in other oceanic regions, which also is to be expected given salinity in the Red Sea is higher than in any other ocean basin in the world. Apparently, salinity tolerance did not only lead to endemism, but species were also filtered according their physiological capabilities. If this filtering was enhanced due species persisting in the Red Sea during glacial episodes remains to be solved. But it is also a possibility that corals found a refuge in the western Gulf of Aden where they were similarly isolated from the western Indian Ocean through the above mentioned upwelling barrier. However, the question remains why also the western Gulf of Aden shows a much lower diversity than any of the Red Sea regions today, and why even in the Gulf of Aqaba the recent communities are almost identical in composition to LIG communities. Would a local and temporarily restricted extinction during the hostile glacial episodes in the Red Sea lead to almost identical communities across such a large distance, without different species getting the chance to occupy new niches? The distance between the Gulf of Aqaba and Bab-el-Mandeb is almost 2000 km. It appears unlikely that almost the same recent community as the LIG community established again in Dahab across this extensive temporal and spatial scale, especially when taking in account that diversity was also higher during the LIG. A refuge somewhere in the Gulf of Aqaba appears to be more plausible. But no matter where the corals found their refugium, the ability of regenerating in very similar manners reveals a strong persistence of these communities. Whereas the underlying reasons for such a persistence are still being discussed (see e.g. DiMichele *et al.* 2004 for a detailed discussion on this topic), Pandolfi (1996, 1999, 2000) suggested that niche differentiation and limited memberships are the primary causes of persistence. The concept of limited memberships within communities has been proposed by Elton (1933), meaning that only a fraction of the forms that could theoretically do so actually form a certain community at any one time (Pandolfi 1996). Alternatively, Hubbell (1997, 2001) claims that patterns of persistence in community structure might be produced by a 'law of large numbers'. The case studies and discussion presented by DiMichele *et al*. (2004) point to several different possible causes for these patterns and provide a range of possibilities; next to the above mentioned explanations they also discuss the issue of environmental control, because all in of their reviewed studies species distribution is neither random nor continuous across the landscape. I agree with this explanation, because the establishment of similar and almost identical communities after strong disturbances and environmental changes, especially in the Red Sea region, cannot be solely explained by the large number of species. Communities do not appear to assemble randomly after destruction and reorganization after interglacial sea level rise, but within certain bounds, which are probably determined by environmental conditions. Especially in the Red Sea, both salinity and thermal tolerances seem to be the primary factors.

6.4 Community shift

Even though Red Sea reefs show a strong persistence, they also display patterns of a community shift when compared at larger biogeographic scale. My results demonstrate that LIG coral reef communities from the Red Sea expanded their geographic ranges northwards relative to today. Eemian Red Sea reefs show a higher similarity to recent reefs from the central Red Sea than to recent reefs from the northern Red Sea. This is inferred from binary data, and fossil data from the central Red Sea are needed to verify this pattern and to explore if this expansion is accompanied by a contraction in diversity in the central Red Sea. Nevertheless, the observation in the northern Red Sea is in concordance with the higher diversity in the fossil reef at Dahab in comparison to the recent reef at the same locality shown by the quantitative data. The shift was probably a response to sea surface temperature changes that increased about 0.7° C in global average (McKay *et al.* 2011) during the last interglacial. These range expansions had an effect on regional beta diversity, and alpha diversity in the Pleistocene northern Red Sea was higher than in comparable recent reefs. The warmer Eemian may have caused a shift (or at least expansion) of central Red Sea communities towards the northern Red Sea. This is in accordance with several studies that observed shifts in diversity from lower

towards higher latitudes in the past (Greenstein & Pandolfi 2008; Kiessling *et al.* 2012; Descombes *et al.* 2015) and that predict a future shift under further climate warming (Hoegh-Guldberg 1999; Carpenter *et al.* 2008; Fine *et al.* 2013; Molinos *et al.* 2015). Because all reef communities within the Red Sea, recent and LIG, show a high similarity and low beta diversity, talking about persistence does not contradict the observation of a shift within this frame. When excluding the Kora *et al.* (2014) study, because several taxa in there have likely been taxonomically misidentified and their study sites are located close to the southern limits of the northern Red Sea, the signals gained from my analyses become even stronger. Apparently the Red Sea has the potential to serve as a model for range shifts correlated to thermal variations, due to its well defined geographical end environmental bounds. Future studies on Pleistocene reefs especially from the central Red Sea might help provide more precise predictions for possible future refugia.

6.5 Ecological succession in Egyptian Pleistocene reefs

Neogene and Quaternary reefs generally exhibit little evidence of succession, especially in comparison to their Paleozoic and Mesozoic counterparts. Budd *et al*. (1989) studied Miocene reefs of the Anguilla Formation of Anguilla (Lesser Antilles), where three coral species assemblages usually occur within the different units. The diversity within these assemblages is similar and a vertical zonation is lacking, so that these three assemblages were interpreted to represent parts of one major reef zone (Budd *et al.* 1989). The authors concluded that the occurrences of distinguishable assemblages in fossil reefs alone do not necessarily imply ecological succession or large-scale physical environmental change. Only a few studies of ecological succession have been performed on Pleistocene coral reefs. Jackson (1992) observed a remarkable similarity of zonation patterns in Pleistocene and recent coral communities in the Caribbean. Both typically culminate in a climax stage dominated by *Acropora palmata*, *Acropora cervicornis* and *Montastraea annularis*. This repeated pattern leads to a long-term stability and equilibrium in contrast to short-term fluctuations due to regular disturbances in historical times (Jackson 1992). A quantitative study from the Caribbean (Pandolfi & Jackson 2001) identified a strong consistence of communities within environments, indicating nonrandom species associations. Differences in community composition occur only along environmental gradients. The authors concluded that pre-1980s and ancient Caribbean reefs are very similar and the instability of recent reefs is caused either by anthropogenic influences or a problem of scaling. A study of ecological succession in Kenyan Pleistocene reefs found several types of successions at different sites (Crame 1980), but a pronounced zonation is lacking. This has been interpreted as evidence that the observed patterns are strongly controlled by local environmental conditions (Crame 1980). There are also paleoecological studies of Pleistocene reefs from the Caribbean (e.g., Geister 1984), which emphasize the role of physical environmental factors, such as water depth, for vertical successions. Changes in water depth, caused by sea-level fluctuations or reef growth, are responsible for the vertical arrangement of communities. Here, the concept of Neumann & Macintyre (1985) plays a large role: keep-up, catch-up, and give-up reefs are defined by their ability to react to changes in sea levels (Neumann & Macintyre 1985). The Canyon reef succession well represents the development of a catch-up reef. The initial reef growth at Dahab is not a classical pioneer stage, characterized by limited recruitment on bare substrates. Although pioneer stages have been suggested for some Pleistocene reefs (Crame 1980), the pioneer-like community at Dahab was caused by high salinity and thus external factors. Although salinity during interglacial highstand was probably more normally marine than today (Parker *et al.* 2012b), this does not conflict with my interpretation, because reef growth obviously started in very shallow waters where high evaporation might have led to increased salinities. After transgression the slope community (zone B) grew on the hard substrate provided by the *Porites nodifera* zone (zone A). The reef caught-up with sea level by upward growth and then was limited vertically when it reached the sea level by forming a typical reef flat community (zone C). The vertical accommodation space was limited as it is typical in fringing reefs, and hence succession is interpreted to be allogenic throughout the whole reef development of this site. A change of sea level can be inferred only between the zones A and B, while from zone B to C the reef grew upwards and reached sea level through upward

growth. A regression leading to the establishment of the reef flat zone, however, can neither be excluded nor derived from the collected data.

As only detailed analyses revealed the allogenic nature of the Dahab succession, it can be assumed that allogenic succession may often have been overlooked in ancient reefs and might indeed be much more widespread than commonly assumed. The results emphasize the importance of investigating individual species and their habitats for environmental reconstructions. Successional sequences, however, are less likely to occur in active tectonic settings. The relatively narrow Holocene terraces along northwestern Efaté, Vanuatu, separated by gentle slopes without notches, may indicate continuous and rapid uplift with keep-up reefs, preventing the formation of extensive reef flats. Cabioch *et al.* (2003) have studied drill cores and shown that only during sea level rise after deglaciations reefs probably had to catch-up with the higher sea level, because the rate of sea level rise exceeded the uplift rate. This could not be confirmed at our study site in Vanuatu, because no sequence was well enough preserved to be studied.

6.6 Future implications

The fossil record was able to provide observations from the geological past of coral reefs for all scenarios that are also discussed for the future of coral reefs, i.e. adaptation/acclimatization, migration and extinction (Pandolfi & Kiessling 2014). Migration towards higher latitudes is currently the most intensively discussed scenario for marine and terrestrial biota (Hoegh-Guldberg 1999; Carpenter *et al.* 2008; Greenstein & Pandolfi 2008; Sorte *et al.* 2010; Chen *et al.* 2011; Kiessling *et al.* 2012; Descombes *et al.* 2015; Graham *et al.* 2015). My results from the Red Sea would support this scenario, but it is not only temperature that influences the distribution of coral reefs. Even if migration towards higher latitudes was an option in the past, this happened before anthropogenic influences additionally disturbed coral reef growth: ocean acidification due to CO_2 increase, pollution, disease, and associated habitat loss or availability will affect the ability of reef corals to expand their latitudinal ranges over the next century or longer (Greenstein & Pandolfi 2008). Especially concentrations of CO_2 are predicted to increase the most at high latitudes (Kleypas *et al.* 1999b), which will probably limit the absolute expansion of the geographical ranges of corals (Greenstein & Pandolfi 2008; Descombes *et al.* 2015). Rodolfo-Metalpa *et al.* (2015), however, could not find a disruption in calcification rates in coldwater corals during laboratory and field tests during acidification processes, whereas Maier *et al.* (2012) have calculated that calcification of cold-water corals in the Mediterranean Sea has already declined by 50%. Muir *et al.* (2015) show that also the lower dose of photosynthetically available radiation during winter in higher latitudes would severely constrain reef development of zooxanthellate corals to very shallow waters.

When evaluating persistence, the respective scale is most important. Coral composition appears to be most variable at small temporal scales because communities are frequently disturbed (Pandolfi 2002), which could also be shown within the succession preserved in the Canyon reef. Viewed over intermediate time scales of several thousands of years, the same communities continually reoccur and reassemble after disturbance, both in Vanuatu as well as in Egypt. Not only the communities within this study, but global Pleistocene reefs, and especially those in the Indo-Pacific were able to cope with climate and sea level changes that occurred throughout the Pleistocene within fairly short timeframes of a few millennia, and even after sudden deglaciation events. However, when talking about the threats for recent reefs, then the scales are decades, and it is questionable if a shift towards higher latitudes or adaption to thermal stress can happen within such a short temporal frame. Along the Japanese coast, Yamano *et al.* (2011) observed poleward range expansions by 14 km/year within the last 80 years without contraction in diversity at lower latitudes, so some shifts might indeed be possible. However, this shift occurred along warm water current northwards along the shore. Cantin *et al.* (2010) could show that coral reef growth in a Red Sea species (*Diploastrea heliopora*) slowed by 30% since 1978, correlated with an increase of SST of 0.4° - 1° C since the mid-1970s, and it remains doubtful if the observation from Japan can be used for deriving global predictions. In fact, the deceleration of growth might counteract the necessary speed of expansion in the future. Also, the species examined by Cantin *et al.* (2010) did not acquire

enhanced resistance, despite a decade of exposure to persistent thermal stress (Cantin *et al.* 2010). Other recent studies (Loya 2004; Mohamed *et al.* 2012) have documented that Egyptian Red Sea reefs are currently impacted by a number of diseases, syndromes, and bleaching events, which might hamper a future migration. Additionally, the direct human impact (physical damage, overfishing, pollution, influx of fertilizers from agriculture) plays a further unpredictable role and is probably a larger threat to coral reefs than shifting climate regimes themselves.

Reef corals from remote Pacific regions are less threatened than the global average (Carpenter *et al.* 2008), which is presumably the result of the absence of comparable human disturbance such as in the densely inhabited Coral Triangle or Caribbean. Maybe these remote areas can serve as refuges for a longer period of time than other tropical regions, but I agree with Hoegh-Guldberg (2011) that it is highly unlikely that coral-dominated reef systems will be present in future oceans given the current rate of warming and acidification of the world's tropical oceans.

References

Abou Zaid, M. (2000). *Overview of the status of red Sea coral reefs in Egypt*.

Akaike, H. (1974). A new look at the statistical model identification. *IEEE Trans. Automat. Contr.*, 19, 716–723.

Alberstadt, L.P., Walker, K.R. & Zurawski R. P. (1974). Patch Reefs in the Carters Limestone (Middle Ordovician) in Tennessee, and Vertical Zonation in Ordovician Reefs. *Geol. Soc. Am. Bull.*, 85, 1171–1182.

Almogi-Labin, A., Hemleben, C. & Meischner, D. (1998). Carbonate preservation and climatic changes in the central Red Sea during the last 380 kyr as recorded by pteropods. *Mar. Micropaleontol.*, 33, 87–107.

Almogi-Labin, A.., Edelman-Furstenberg; & Y. Hemleben, C. (2008). Variations in biodiversity of thecostomatous pteropods during the Late Quaternary as a response to environmental changes in the Gulf of Aden–Red Sea–Gulf of Aqaba ecosystems. In: *Aqaba–Eilat, the Improbable Gulf. : Environment, Biodiversity and Preservation* (ed. Por, D.). The Hebrew University Magnes Press, Jerusalem, pp. 31–48.

Al-Rousan, S., Al-Moghrabi, S., Patzold, J. & Wefer, G. (2002). Environmental and biological effects on the stable oxygen isotope records of corals in the northern Gulf of Aqaba, Red Sea. *Mar. Ecol. Ser.*, 239, 301–310.

Alroy, J. (2010a). Fair sampling of taxonomic richness and unbiased estimation of origination and extinction rates. *Paleontol. Soc. Pap.*, 16, 55–80.

Alroy, J. (2010b). Geographical, environmental and intrinsic biotic controls on Phanerozoic marine diversification. *Palaeontology*, 53, 1211–1235.

Alroy, J. (2011). *SQS version 3.2*. Available at: http://bio.mq.edu.au/~jalroy/SQS-3-3.R. Last accessed .

Alter, C. (2004). Diversity, community structure and zonation of zooxanthellate, hermatypic corals of the reef complex at The Islands dive site, Dahab, in the Gulf of Aqaba. *Diploma Thesis.* Universität Heidelberg.

Andersen, K.K., Azuma, N., Barnola, J.-M., Bigler, M., Biscaye, P., Caillon, N., *et al.* (2004). High-resolution record of Northern Hemisphere climate extending into the last interglacial period. *Nature*, 431, 147–51.

Anderson, M.J. (2001). A new method for non-parametric multivariate analysis of variance. *Austral Ecol.*, 26, 32–46.

Anderson, M.J. (2006). Distance-Based Tests for Homogeneity of Multivariate Dispersions. *Biometrics*, 62, 245–253.

Anderson, M.J., Ellingsen, K.E. & McArdle, B.H. (2006). Multivariate dispersion as a measure of beta diversity. *Ecol. Lett.*, 9, 683–693.

Andres, W., Radtke, U. & Mangini, A. (1988). Quartäre Strandterrassen an der Küste des Gebel Zeit (Golf von Suez, Ägypten). *Erdkunde*, 42, 7–16.

Anthony, K.R.N., Kline, D.I., Diaz-Pulido, G., Dove, S. & Hoegh-Guldberg, O. (2008). Ocean acidification causes bleaching and productivity loss in coral reef builders. *Proc. Natl. Acad. Sci. U. S. A.*, 105, 17442–17446.

Aronson, R.B., Macintyre, I.G., Precht, W.F., Murdoch, T.J.T. & Wapnick, C.M. (2002). The expanding scale of species turnover events on coral reefs in Belize. *Ecol. Monogr.*, 72, 233–249.

Aronson, R.B. & Precht, W.F. (1997). Stasis, biological disturbance, and community structure of a Holocene coral reef. *Paleobiology*, 23, 326–346.

Aronson, R.B. & Precht, W.F. (2008). Stasis , Biological Disturbance , and Community Structure of a Holocene Coral Reef Published by : Paleontological Society Stable URL : http://www.jstor.org/stable/2401107, 23, 326–346.

ArRajehi, A., McClusky, S., Reilinger, R., Daoud, M., Alchalbi, A., Ergintav, S., *et al.* (2010). Geodetic constraints on present-day motion of the Arabian Plate: Implications for Red Sea and Gulf of Aden rifting. *Tectonics*, 29, n/a–n/a.

Arrhenius, O. (1921). Species and area. *J. Ecol.*, 9, 95–99.

Benzoni, F., Bianchi, C.N. & Morri, C. (2003). Coral communities of the northwestern Gulf of Aden (Yemen): variation in framework building related to environmental factors and biotic conditions. *Coral Reefs*, 22, 475–484.

Bianchi, C.N., Morri, C., Pichon, M., Benzoni, F., Colantoni, P., Baldelli, G., *et al.* (2006). Dynamics and pattern of coral recolonization following the 1998 bleaching event in the reefs of the Maldives. In: *Proceedings of the 10th International Coral Reef Symposium*. pp. 30–37.

Blanchon, P., Jones, B. & Kalbfleisch, W. (1997). Anatomy of a Fringing Reef Around Grand Cayman: Storm Rubble, Not Coral Framework. *J. Sediment. Res.*, 67.

loom, A.L., Jouannic, C. & Taylor, F.W. (1978). Preliminary radiometric ages from the uplifted Quaternary coral reefs of Efate, New Hebrides. *Reg. Rep. Geol. Surv. New Hebrides*, 47–49.

Borcard, D., Gillet, F. & Legendre, P. (2011). *Numerical Ecology with R*. Springer, New York.

Bosworth, W. (2015). Geological Evolution of the Red Sea: Historical Background, Review, and Synthesis. In: *The Red Sea: The Formation, Morphology, Oceanography and Environment of a Young Ocean Basin* (eds. Rasul, N.M.A. & Stewart, I.C.F.). Springer-Verlag Berlin Heidelberg, pp. 45–78.

Bosworth, W., Huchon, P. & McClay, K. (2005). The Red Sea and Gulf of Aden Basins. *J. African Earth Sci.*, 43, 334–378.

Bosworth, W. & Taviani, M. (1996). Late Quaternary reorientation of stress field and extension direction in the southern Gulf of Suez, Egypt: Evidence from uplifted coral terraces, mesoscopic fault arrays, and borehole breakouts. *Tectonics*, 15, 791–802.

Brachert, T.C. (1999). Non-skeletal carbonate production and stromatolite growth within a pleistocene deep ocean (Last glacial maximum, Red Sea). *Facies*, 40, 211–228.

Brachert, T.C. & Dullo, W.-C. (1991). Laminar Micrite Crusts and Associated Foreslope Processes, Red Sea. *SEPM J. Sediment. Res.*, Vol. 61, 354–363.

Braithwaite, C.J.R. (1987). Geology and paleogeography of the red sea region. In: *Red Sea* (eds. Edwards, A.J. & Head, S.M.). Pergamon Press, Oxford, pp. 22–44.

Bray, J.R. & Curtis, J.T. (1957). An Ordination of the Upland Forest Communities of Southern Wisconsin. *Ecol. Monogr.*, 27, 326–349.

Bromfield, K. (2013). Neogene corals from the Indo-Pacific: Indonesia, Papua New Guinea, and Fiji. *Bull. Am. Paleontol.*, 387, 1–60.

Budd, A.F., Fukami, H., Smith, N.D. & Knowlton, N. (2012). Taxonomic classification of the reef coral family Mussidae (Cnidaria: Anthozoa: Scleractinia). *Zool. J. Linn. Soc.*, 166, 465–529.

Budd, A.F., Johnson, K.G. & Edwards, J.C. (1989). Miocene Coral Assemblages in Anguilla, B.W.I., and Their Implications for the Interpretation of Vertical Succession on Fossil Reefs. *Palaios*, 4, 264–275.

Budd, A.F., Romano, S.L., Smith, N.D. & Barbeitos, M.S. (2010). Rethinking the phylogeny of scleractinian corals: a review of morphological and molecular data. *Integr. Comp. Biol.*, 50, 411–27.

Budd, A.F. & Stolarski, J. (2011). Corallite wall and septal microstructure in scleractinian reef corals: comparison of molecular clades within the family Faviidae. *J. Morphol.*, 272, 66–88.

Bunge, J. & Fitzpatrick, M. (1993). Estimating the number of species: a review. *J. Am. Stat. Assoc.*, 88, 364–373.

Burchard, J.E. (1979). *Coral fauna of the western Arabian Gulf*. Aramco, Environmental Affairs, Dhahran, Saudi Arabia.

Burchard, J.E. (1983). *Synopsis of the Arabian Gulf Corals*.

Buss, L.W. & Jackson, J.B. (1979). Competitive networks: nontransitive competitive relationships in cryptic coral reef environments. *Am. Nat.*, 113, 223–234.

Cabioch, G. (2003). Postglacial reef development in the South-West Pacific: case studies from New Caledonia and Vanuatu. *Sediment. Geol.*, 159, 43–59.

Cabioch, G. & Ayliffe, L.K. (2001). Raised Coral Terraces at Malakula, Vanuatu, Southwest Pacific, Indicate High Sea Level During Marine Isotope Stage 3. *Quat. Res.*, 56, 357–365.

Cabioch, G., Banks-Cutler, K.A., Beck, W.J., Burr, G.S., Corrège, T., Edwards, R.L., *et al.* (2003). Continuous reef growth during the last 23 cal kyr BP in a tectonically active zone (Vanuatu, SouthWest Pacific). *Quat. Sci. Rev.*, 22, 1771–1786.

Cabioch, G., Camoin, G., Webb, G.E., Cornec, F. Le, Molina, M.G., Pierre, C., *et al.* (2006). Contribution of microbialites to the development of coral reefs during the last deglacial period: Case study from Vanuatu (South-West Pacific). *Sediment. Geol.*, 185, 297–318.

Cairns, S.D. (2000). A revision of the shallow-water azooxanthellate scleractinia of the Western Atlantic. *Stud. fauna Curacao other Caribb. Islands*, 125, 1–235.

Cairns, S.D. (2001). A generic revision and phylogenetic analysis of the Dendrophylliidae (Cnidaria: Scleractinia). *Smithonian Contrib. to Zool.*, 615, 75 pp.

Cantin, N.E., Cohen, A.L., Karnauskas, K.B., Tarrant, A.M. & McCorkle, D.C. (2010). Ocean Warming Slows Coral Growth in the Central Red Sea. *Science (80-.).*, 329, 322–325.

Carpenter, K.E., Abrar, M., Aeby, G., Aronson, R.B., Banks, S., Bruckner, A., *et al.* (2008). One-third of reef-building corals face elevated extinction risk from climate change and local impacts. *Science*, 321, 560–563.

Chao, A. & Lee, S.-M. (1992). Estimating the Number of Classes via Sample Coverage. *J. Am. Stat. Assoc.*, 87, 210–217.

Chao, A. & Yang, M.C.K. (1993). Stopping rules and estimation for recapture debugging with unequal failure rates. *Biometrika*, 80, 193–201.

Chappell, J. (1974). Geology of coral terraces, Huon Peninsula, New Guinea: A study of quaternary Tectonic movements and sea-level changes. *Geol. Soc. Am. Bull.*, 85, 553.

Chappell, J. (1983). Evidence for smoothly falling sea level relative to north Queensland, Australia, during the past 6,000 yr. *Nature*, 302, 406–408.

Chappell, J. (1986). A revised sea-level record for the last 300,000 years from Papua New Guinea. *Search*, 14, 99–101.

Chappell, J., Omura, A., Esat, T., McCulloch, M., Pandolfi, J., Ota, Y., *et al.* (1996). Reconciliaion of late Quaternary sea levels derived from coral terraces at Huon Peninsula with deep sea oxygen isotope records. *Earth Planet. Sci. Lett.*, 141, 227–236.

Chappell, J., Ota, Y. & Campbell, C. (1998). Decoupling post-glacial tectonism and eustasy at Huon Peninsula, Papua New Guinea. *Geol. Soc. London, Spec. Publ.*, 146, 31–40.

Chappell, J. & Polach, H. (1991). Post-glacial sea-level rise from a coral record at Huon Peninsula, Papua New Guinea. *Nature*, 349, 147–149.

Chen, I.-C., Hill, J.K., Ohlemüller, R., Roy, D.B. & Thomas, C.D. (2011). Rapid range shifts of species associated with high levels of climate warming. *Science*, 333, 1024–6.

Clarke, K.. R. (1993). Non-parametric multivariate analyses of changes in community structure. *Austral Ecol.*, 18, 117–143.

Cohen, K.M. & Gibbard, P. (2011). *Global chronostratigraphical correlation table for the last 2.7 million years*. Cambridge, England.

Coles, S.L. & Riegl, B.M. (2013). Thermal tolerances of reef corals in the Gulf: a review of the potential for increasing coral survival and adaptation to climate change through assisted translocation. *Mar. Pollut. Bull.*, 72, 323–32.

Colwell, R.K. & Coddington, J.A. (1994). Estimating terrestrial biodiversity through extrapolation. *Philos. Trans. R. Soc. London B Biol. Sci.*, 345, 101–118.

Connell, J.H. & Slatyer, R.O. (1977). Mechanisms of Succession in Natural Communities and Their Role in Community Stability and Organization. *Am. Nat.*, 111, 1119–1144.

Copper, P. (1988). Ecological Succession in Phanerozoic Reef Ecosystems: Is It Real? *Palaios*, 3, 136–151.

Copper, P. & Grawbarger, D.J. (1978). Paleoecological succession leading to a late Ordovician biostrome on Manitoulin Island, Ontario. *Can. J. Earth Sci.*, 15, 1987–2005.

Crame, J.A. (1980). Succession and diversity in the Pleistocene coral reefs of the Kenya coast. *Palaeontology*, 23, 1–37.

Cullity, B.D. (1956). *Elements of X Ray diffraction*. Addison-Wesley.

Darwin, C. (1842). *The structure and distribution of coral reefs. Being the first part of the geology of the voyage of the Beagle, under the command of Capt. Fitzroy, R.N. during the years 1832 to 1836*. Smith Elder and Co., London.

Davis, W.M. (1928). *The coral reef problem*. American Geographical Society, New York.

Descombes, P., Wisz, M.S., Leprieur, F., Parravicini, V., Heine, C., Olsen, S.M., *et al.* (2015). Forecasted coral reef decline in marine biodiversity hotspots under climate change. *Glob. Chang. Biol.*

DiBattista, J.D., Howard Choat, J., Gaither, M.R., Hobbs, J.-P.A., Lozano-Cortés, D.F., Myers, R.F., *et al.* (2015a). On the origin of endemic species in the Red Sea. *J. Biogeogr.*, doi:10.1111/jbi.12631.

DiBattista, J.D., Roberts, M.B., Bouwmeester, J., Bowen, B.W., Coker, D.J., Lozano-Cortés, D.F., *et al.* (2015b). A review of contemporary patterns of endemism for shallow water reef fauna in the Red Sea. *J. Biogeogr.*, 10.1111/jbi.12649.

Dickinson, W.R. (2001). Paleoshoreline record of relative Holocene sea levels on Pacific islands. *Earth-Science Rev.*, 55, 191–234.

DiMichele, W. a., Behrensmeyer, A.K., Olszewski, T.D., Labandeira, C.C., Pandolfi, J.M., Wing, S.L., *et al.* (2004). Long-term stasis in ecological assemblages: Evidence from the fossil record. *Annu. Rev. Ecol. Evol. Syst.*, 35, 285–322.

Dodge, R.E., Logan, A. & Antonius, A. (1982). Quantitative reef assessment studies in Bermuda: a comparison of methods and preliminary results. *Bull. Mar. Sci.*, 32, 745–760.

Done, T. & Navin, K. (1990). Shallow water benthic communities on coral reefs. In: *Vanuatu Marine Resources: Report of a Biological Survey* (eds. Done, T. & Navin, K.). Australian Institute of Marine Science (AIMS), Townsville, pp. 10–37.

Dullo, W.-C. (1990). Facies, fossil record, and age of Pleistocene reefs from the Red Sea (Saudi Arabia). *Facies*, 22, 1–46.

Dullo, W.-C. (2005). Coral growth and reef growth: a brief review. *Facies*, 51, 33–48.

Dullo, W.C. & Montaggioni, L.F. (1998). Modern Red Sea coral reefs: a review of their morphologies and zonation. In: *Sedimentary and tectonic evolution of rift basins: Red Sea - Gulf of Aden* (eds. Purser, B.H. & Bosence, D.W.J.). Chapman Hall-Kluwers, London (UK), pp. 583–594.

Dutton, A. & Lambeck, K. (2012). Ice volume and sea level during the last interglacial. *Science*, 337, 216–9.

Eakin, C.M., Morgan, J.A., Heron, S.F., Smith, T.B., Liu, G., Alvarez-Filip, L., *et al.* (2010). Caribbean corals in crisis: record thermal stress, bleaching, and mortality in 2005. *PLoS One*, 5, e13969.

Edinger, E.N., Pandolfi, J.M. & Kelley, R.A. (2001). Community structure of Quaternary coral reefs compared with Recent life and death assemblages. *Paleobiology*, 27, 669–694.

Edmunds, P.J., Adjeroud, M., Baskett, M.L., Baums, I.B., Budd, A.F., Carpenter, R.C., *et al.* (2014). Persistence and change in community composition of reef corals through present, past, and future climates. *PLoS One*, 9, e107525.

El-Asmar, H.M. (1997). Quaternary isotope stratigraphy and paleoclimate of coral reef terraces, Gulf of Aqaba, South Sinai, Egypt. *Quat. Sci. Rev.*, 16, 911–924.

El-Sorogy, A.S. (2002). Paleontology and depositional environments of the Pleistocene coral reefs of the Gulf of Suez, Egypt. *Neues Jahrb. für Geol. und Paläontologie, Abhandlungen*, 225, 337–371.

El-Sorogy, A.S. (2008). Contributions to the Pleistocene coral reefs of the Red Sea coast, Egypt. *Arab Gulf J. Sci. Res.*, 26, 63–85.

Elton, C. (1933). *The ecology of animals*. Jarrold and Sons LTD, Norwich.

English, S., Wilkinson, C.R. & Baker, V.J. (1997). *Survey Manual for Tropical Marine Resources, 2nd edition*.

Facon, M., Pinault, M., Obura, D., Pioch, S., Pothin, K., Bigot, L., *et al.* (2016). A comparative study of the accuracy and effectiveness of Line and Point Intercept Transect methods for coral reef monitoring in the southwestern Indian Ocean islands. *Ecol. Indic.*, 60.

Faichney, I.D.E., Webster, J.M., Clague, D.A., Braga, J.C., Renema, W. & Potts, D.C. (2011). The impact of the Mid-Pleistocene Transition on the composition of submerged reefs of the Maui Nui Complex, Hawaii. *Palaeogeogr. Palaeoclimatol. Palaeoecol.*, 299, 493–506.

Faichney, I.D.E., Webster, J.M., Clague, D.A., Kelley, C., Appelgate, B. & Moore, J.G. (2009). The morphology and distribution of submerged reefs in the Maui-Nui Complex, Hawaii: New insights into their evolution since the Early Pleistocene. *Mar. Geol.*, 265, 130–145.

Fairbanks, R.G. (1989). A 17,000-year glacio-eustatic sea level record: influence of glacial melting rates on the Younger Dryas event and deep-ocean circulation. *Nature*, 342, 637–642.

Faith, D.P., Minchin, P.R. & Belbin, L. (1987). Compositional dissimilarity as a robust measure of ecological distance. *Vegetatio*, 69, 57–68.

Faure, H., Hoang, C.T. & Lalou, C. (1980). Datations 230Th/234U des calcaires coralliens et mouvements verticaux a Djibouti. *Bull. la Soc. Geol. Fr.*, 22, 659–692.

Fenton, M., Geiselhart, S., Rohling, E.J. & Hemleben, C. (2000). Aplanktonic zones in the Red Sea. *Mar. Micropaleontol.*, 40, 277–294.

Fine, M., Gildor, H. & Genin, A. (2013). A coral reef refuge in the Red Sea. *Glob. Chang. Biol.*, 19, 3640–7.

Fishelson, L. (1980). Marine reserves along the Sinai Peninsula (northern Red Sea). *Helgol. Mar. Res.*, 33, 624–640.

Fukami, H., Budd, A.F., Paulay, G., Sole-Cava, A., Allen Chen, C., Iwao, K., *et al.* (2004). Conventional taxonomy obscures deep divergence between Pacific and Atlantic corals. *Nature*, 427, 832–835.

Fukami, H., Chen, C.A., Budd, A.F., Collins, A., Wallace, C., Chuang, Y.-Y., *et al.* (2008). Mitochondrial and nuclear genes suggest that stony corals are monophyletic but most families of stony corals are not (Order Scleractinia, Class Anthozoa, Phylum Cnidaria). *PLoS One*, 3, e3222.

Furby, K.A., Bouwmeester, J. & Berumen, M.L. (2013). Susceptibility of central Red Sea corals during a major bleaching event. *Coral Reefs*, 32, 505–513.

Gagan, M.K., Ayliffe, L.K., Hopley, D., Cali, J.A., Mortimer, G.E., Chappell, J., *et al.* (1998). Temperature and Surface-Ocean Water Balance of the Mid-Holocene Tropical Western Pacific. *Science (80-.).*, 279, 1014–1018.

Gattuso, J.P. & Buddemeier, R.W. (2000). Ocean biogeochemistry. Calcification and CO2. *Nature*, 407, 311–313.

Geister, J. (1984). Récifs pleistocènes de la mer des Caraïbes: Aspects géologiques et paléoécologiques. In: *Géologie et Paléoécologie des Récifs* (eds. Geister, J. & Herb, R.). Éme Cycle Romand En Sciences De La Terre: Institut de Géologie de l'Université de Berne, Berne, pp. 3.1–3.34.

Gibbard, P.L., Head, M.J. & Walker, M.J.C. (2010). Formal ratification of the Quaternary System/Period and the Pleistocene Series/Epoch with a base at 2.58 Ma. *J. Quat. Sci.*, 25, 96–102.

Glynn, P.W. (1993). Coral reef bleaching: ecological perspectives. *Coral Reefs*, 12, 1–17.

Gotelli, N.J. & Colwell, R.K. (2001). Quantifying biodiversity: procedures and pitfalls in the measurement and comparison of species richness. *Ecol. Lett.*, 4, 379–391.

Graham, N.A.J., Jennings, S., MacNeil, M.A., Mouillot, D. & Wilson, S.K. (2015). Predicting climate-driven regime shifts versus rebound potential in coral reefs. *Nature*.

Gray, J.S. (1987). Species abundance patterns. In: *Organization of communities – past and present* (eds. Gee, J.H.R. & Giller, P.S.). Blackwell Publishing, Oxford, UK, pp. 53–67.

Greenstein, B.J., Curran, H. a. & Pandolfi, J.M. (1998). Shifting ecological baselines and the demise of Acropora cervicornis in the western North Atlantic and Caribbean Province: a Pleistocene perspective. *Coral Reefs*, 17, 249–261.

Greenstein, B.J. & Pandolfi, J.M. (2008). Escaping the heat: range shifts of reef coral taxa in coastal Western Australia. *Glob. Chang. Biol.*, 14, 513–528.

Grill, B. & Zuschin, M. (2001). Modern shallow- to deep-water bivalve death assemblages in the Red Sea — ecology and biogeography. *Palaeogeogr. Palaeoclimatol. Palaeoecol.*, 168, 75–96.

Grossman, E.E., Fletcher III, C.H. & Richmond, B.M. (1998). The Holocene sea-level highstand in the equatorial Pacific: analysis of the insular paleosea-level database. *Coral Reefs*, 17, 309–327.

Guilcher, A. (1974). Coral reefs of the New Hebrides, Melanesia, with particular reference to open-sea, not fringing, reefs. In: *Second International Coral Reef Sympoposium, Vol. 2.* (eds. Cameron, J.S. Jell, O.A. Jones, P. Mather & F.H. Talbot). The Great Barrier Reef Committee, Brisbane, pp. 523–536.

Guilcher, A. (1988). *Coral Reef Geomorphology*. Wiley, New York.

Gvirtzman, G. (1994). Fluctuations of sea level during the past 400 000 years: the record of Sinai, Egypt (northern Red Sea). *Coral Reefs*, 13, 203–214.

Gvirtzman, G. & Buchbinder, B. (1978). Recent and Pleistocene coral reefs and coastal sediments of the Gulf of Elat. In: *Guidebook lOth International Congress Sedimentology*. Jerusalem, pp. 162–191.

Gvirtzman, G. & Friedman, G.M. (1977). Sequence of progressive diagenesis in coral reefs. In: *Studies in Geology 4*. American Association of Petroleum Geologists, pp. 357–380.

Gvirtzman, G., Kronfeld, J. & Buchbinder, B. (1992). Dated coral reefs of southern Sinai (Red Sea) and their implication to late Quaternary sea levels. *Mar. Geol.*, 108, 29–37.

Harrell Jr, F.E. & with contributions from C. Dupont and many other. (2015). Hmisc: Harrell Miscellaneous. R package version 3.15-0.

Harris, P.T. & Davies, P.J. (1989). Submerged reefs and terraces on the shelf edge of the Great Barrier Reef, Australia. *Coral Reefs*, 8, 87–98.

Hill, J. & Wilkinson, C. (2004). *Methods for Ecological Monitoring of Coral Reefs*. Townsville.

Hill, M.O. & Gauch H.G. (1980). Detrended correspondence analysis: An improved ordination technique. *Vegetatio,* 42, 47-58.

Hoang, C.T. & Taviani, M. (1991). Stratigraphic and tectonic implications of uranium-series-dated coral reefs from uplifted Red Sea islands. *Quat. Res.*, 35, 264–273.

Hoegh-Guldberg, O. (1999). Climate change, coral bleaching and the future of the world's coral reefs. *Mar. Freshw. Res.*, 50, 839.

Hoegh-Guldberg, O. (2011). Coral reef ecosystems and anthropogenic climate change. *Reg. Environ. Chang.*, 11, S215–S227.

Hoegh-Guldberg, O. (2014). Coral reef sustainability through adaptation: glimmer of hope or persistent mirage? *Curr. Opin. Environ. Sustain.*, 7, 127–133.

Hoegh-Guldberg, O., Mumby, P.J., Hooten, a J., Steneck, R.S., Greenfield, P., Gomez, E., *et al.* (2007). Coral reefs under rapid climate change and ocean acidification. *Science*, 318, 1737–42.

Hoeksema, B.W. (1989). Taxonomy, phylogeny and biogeography of mushroom corals (Scleractinia: Fungiidae). *Zool. Verh. Leiden*, 254, 1–295.

Huang, D., Benzoni, F., Arrigoni, R., Baird, A.H., Berumen, M.L., Bouwmeester, J., *et al.* (2014a). Towards a phylogenetic classification of reef corals: the Indo-Pacific genera Merulina , Goniastrea and Scapophyllia (Scleractinia, Merulinidae). *Zool. Scr.*, 43, 531–548.

Huang, D., Benzoni, F., Fukami, H., Knowlton, N., Smith, N.D. & Budd, A.F. (2014b). Taxonomic classification of the reef coral families Merulinidae, Montastraeidae, and Diploastraeidae (Cnidaria: Anthozoa: Scleractinia). *Zool. J. Linn. Soc.*, 171, 277–355.

Huang, D., Licuanan, W.Y., Baird, A.H. & Fukami, H. (2011). Cleaning up the "Bigmessidae": molecular phylogeny of scleractinian corals from Faviidae, Merulinidae, Pectiniidae and Trachyphylliidae. *BMC Evol. Biol.*, 11, 37.

Hubbard, D.K. (1997). Reefs as dynamic systems. In: *Life and Death of Coral Reefs* (ed. Birkeland, C.). Chapman & Hall, New York, pp. 43–67.

Hubbell, S.P. (1997). Aunified theory of biogeog- raphy and relative species abundance and its application to tropical rain forests and coral reefs. In: *Proceedings of the 8th Int. Coral Reef Symposium*. pp. 33–42.

Hubbell, S.P. (2001). *The unified neutral theory of biodiversity and biogeography (MPB-32)*. Princeton University Press, Princeton, NJ.

Humblet, M., Hongo, C. & Sugihara, K. (2015). An identification guide to some major Quaternary fossil reef-building coral genera (Acropora , Isopora , Montipora , and Porites). *Isl. Arc*, 24, 16–30.

Ikeya, M. (1975). Dating a stalactite by electron paramagnetic resonance. *Nature*, 255, 48–50.

Jackson, J.B.C. (1992). Pleistocene perspectives on coral reef community structure. *Am. Zool.*, 32, 719–731.

Jouannic, C., Taylor, F.W. & Bloom, A.L. (1982). Sur la surrection et la déformation d'un arc jeune : l'arc des Nouvelles-Hébrides, 223–246.

Jouzel, J., Masson-Delmotte, V., Cattani, O., Dreyfus, G., Falourd, S., Hoffmann, G., *et al.* (2007). Orbital and millennial Antarctic climate variability over the past 800,000 years. *Science*, 317, 793–6.

Karlson, R.H. (1999). Dynamics of coral communities. *Popul. Community Biol. Ser.*, 23, i.

Kemp, J. (1998). Zoogeography of the coral reef fishes of the Socotra Archipelago. *J. Biogeogr.*, 25, 919–933.

Kemp, J.M. (2000). Zoogeography of the coral reef fishes of the north-eastern Gulf of Aden, with eight new records of coral reef fishes from Arabia. *Fauna Arab.*, 18, 293–321.

Kenkel, N.C. & Orloci, L. (1986). Applying Metric and Nonmetric Multidimensional Scaling to Ecological Studies: Some New Results. *Ecology*, 67, 919.

Kennedy, D.M. & Woodroffe, C.D. (2002). Fringing reef growth and morphology : a review, 57, 255–277.

Kenneth J. Mesolella, H.A.S.R.K.M. (1970). Facies Geometries Within Pleistocene Reefs of Barbados, West Indies. *Am. Assoc. Pet. Geol. Bull.*, 54, 1899–1917.

Kiessling, W. (2005). Long-term relationships between ecological stability and biodiversity in Phanerozoic reefs. *Nature*, 433, 410–413.

Kiessling, W. (2009). Geologic and Biologic Controls on the Evolution of Reefs. *Annu. Rev. Ecol. Evol. Syst.*, 40, 173–192.

Kiessling, W., Fluegel, E. & Golonka, J. (1999). Paleoreef maps; evaluation of a comprehensive database on Phanerozoic reefs. *Am. Assoc. Pet. Geol. Bull.*, 83, 1552–1587.

Kiessling, W., Kumar Pandey, D., Schemm-Gregory, M., Mewis, H. & Aberhan, M. (2011). Marine benthic invertebrates from the Upper Jurassic of northern Ethiopia and their biogeographic affinities. *J. African Earth Sci.*, 59, 195–214.

Kiessling, W., Simpson, C., Beck, B., Mewis, H. & Pandolfi, J.M. (2012). Equatorial decline of reef corals during the last Pleistocene interglacial. *Proc. Natl. Acad. Sci.*, 109, 21378–21383.

Kitahara, M. V, Cairns, S.D., Stolarski, J., Blair, D. & Miller, D.J. (2010). A comprehensive phylogenetic analysis of the Scleractinia (Cnidaria, Anthozoa) based on mitochondrial CO1 sequence data. *PLoS One*, 5, e11490.

Kitahara, M. V., Stolarski, J., Cairns, S.D., Benzoni, F., Stake, J.L. & Miller, D.J. (2012). The first modern solitary Agariciidae (Anthozoa, Scleractinia) revealed by molecular and microstructural analysis. *Invertebr. Syst.*

Kitano, Y.F., Benzoni, F., Arrigoni, R., Shirayama, Y., Wallace, C.C. & Fukami, H. (2014). A phylogeny of the family Poritidae (Cnidaria, Scleractinia) based on molecular and morphological analyses. *PLoS One*, 9, e98406.

Klaus, J.S. & Budd, A.F. (2003). Comparison of Caribbean coral reef communities before and after Plio-Pleistocene faunal turnover: analyses of two Dominican Republic reef sequences. *Palaios*, 18, 3–21.

Kleypas, J.A., Buddemeier, R.W., Archer, D., Gattuso, J.-P., Langdon, C. & Opdyke, B.N. (1999a). Geochemical Consequences of Increased Atmospheric Carbon Dioxide on Coral Reefs. *Science (80-.).*, 284, 118–120.

Kleypas, J.A., Mcmanus, J.W. & Menez, L.A. (1999b). Environmental limits to coral reef development: where do we draw the line? *Am. J. Bot.*, 39, 146–159.

Knowlton, N., Brainard, R.E., R., F., M., M., L., P. & Caley, M.J. (2010). Coral reef biodiversity. In: *Life in the World's Oceans: Diversity, Distribution, and Abundance* (ed. McIntyre, A.D.). Wiley-Blackwell, Oxford, UK, pp. 65–74.

Koleff, P., Gaston, K.J. & Lennon, J.J. (2003). Measuring beta diversity for presence-absence data. *J. Anim. Ecol.*, 72, 367–382.

Kora, M.A., Ayyad, S.N. & El-Desouky, H.M. (2014). Pleistocene scleractinian corals from Marsa Alam area, Red Sea Coast, Egypt: systematics and biogeography. *Swiss J. Palaeontol.*, 133, 77–97.

Kruskal, J.B. (1964). Multidimensional scaling by optimizing goodness of fit to a nonmetric hypothesis. *Psychometrika*, 29, 1–27.

Lambeck, K., Esat, T.M. & Potter, E.-K. (2002). Links between climate and sea levels for the past three million years. *Nature*, 419, 199–206.

Lambeck, K., Purcell, A., Flemming, N.C., Vita-Finzi, C., Alsharekh, A.M. & Bailey, G.N. (2011). Sea level and shoreline reconstructions for the Red Sea: isostatic and tectonic considerations and implications for hominin migration out of Africa. *Quat. Sci. Rev.*, 30, 3542–3574.

Langer, M.R., Silk, M.T. & Lipps, J.H. (1997). Global ocean carbonate and carbon dioxide production; the role of reef Foraminifera. *J. Foraminifer. Res.*, 27, 271–277.

Lecolle, J.., Bokilo, J.. & Bernat, M. (1990). Soulèvement et tectonique de l'île d'Efaté (Vanuatu) arc insulaire des Nouvelles-Hébrides, au cours du Quaternaire récent. Datations de terrasses soulevées par la méthode U/Th. *Mar. Geol.*, 94, 251–270.

Lecolle, J.F. & Bernat, M. (1985). Histoire de la surrection de l'île d'Efaté, au cours du Quaternaire recent datations de terrasses soulevées par la methode U/Th. In: *Proceedings of the Fifth International Coral Reef Congress*. Tahiti, pp. 179–184.

Lesson, R.P. (1829). *Histoire naturelle des oiseaux-mouches. Ouvrage orné de planches dessinées et gravées par les meilleurs artistes*. Arthus Bertrand, Paris.

Levene, H. (1960). Robust tests for equality of variances. In Contributions to Probability and Statistics: Essays in Honor of Harold Hotelling. In: *Contributions to Probability and Statistics: Essays in Honor of Harold Hotelling* (eds. Olkin, I., Ghurye, S.G., Hoeffding, W., Madow, W.G. & Mann, H.B.). Stanford University Press, pp. 278–292.

Lidz, B.H., Reich, C.D. & Shinn, E.A. (2003). Regional quaternary submarine geomorphology in the Florida Keys. *Bull. Geol. Soc. Am.*, 115, 845–866.

Linnaeus, C. (1758). *Systema Naturae*. 10. Auflag.

Lisiecki, L.E. (2005). A Pliocene-Pleistocene stack of 57 globally distributed benthic δ 18 O records. *Paleoceanography*, 20, PA1003.

Loya, Y. (1972). Community structure and species diversity of hermatypic corals at Eilat, Red Sea. *Mar. Biol.*, 13, 100–123.

Loya, Y. (2004). The Coral Reefs of Eilat – Past, Present and Future: Three Decades of Coral Community Structure Studies. In: *Coral Health and Disease* (eds. Rosenberg, E. & Loya, Y.). Springer-Verlag, Heidelberg, pp. 1–34.

MacArthur, R.H. (1957). On the relative abundance of bird species. *Proc. Natl. Acad. Sci. U. S. A.*, 43, 293–295.

Macarthur, R.H. (1957). ON THE RELATIVE ABUNDANCE OF BIRD SPECIES. *Proc. Natl. Acad. Sci. U. S. A.*, 43, 293–5.

Macintyre, I.G. (1972). Submerged Reefs of Eastern Caribbean. *Am. Assoc. Pet. Geol. Bull.*, 56, 720–738.

Macintyre, I.G. (1988). Modern coral reefs of western Atlantic; new geological perspective. *Am. Assoc. Pet. Geol. Bull.*, 72, 1360–1369.

Maier, C., Watremez, P., Taviani, M., Weinbauer, M.G. & Gattuso, J.P. (2012). Calcification rates and the effect of ocean acidification on Mediterranean cold-water corals. *Proc. Biol. Sci.*, 279, 1716–23.

Mandelbrot, B. (1977). *Fractals: Form, Chance and Dimension*. W. H. Freeman and Co, New York.

Mandelbrot, B. (1982). *The Fractal Geometry of Nature*. W. H. Freeman & Co, New York.

Martin, J.M., Braga, J.C. & Rivas, P. (1989). Coral successions in Upper Tortonian reefs in SE Spain. *Lethaia*, 22, 271–286.

May, R.M. (1975). Patterns of species abundance and diversity. In: *Ecology and evolution of communities* (eds. Cody, M.L. & Diamond, J.M.). Harvard University Press, Cambridge, pp. 81–120.

McArdle, B.H. & Anderson, M.J. (2001). Fitting multivariate models to community data: A comment on distance-based redundancy analysis. *Ecology*, 82, 290–297.

McGill, B.J., Etienne, R.S., Gray, J.S., Alonso, D., Anderson, M.J., Benecha, H.K., *et al.* (2007). Species abundance distributions: moving beyond single prediction theories to integration within an ecological framework. *Ecol. Lett.*, 10, 995–1015.

McKay, N.P., Overpeck, J.T. & Otto-Bliesner, B.L. (2011). The role of ocean thermal expansion in Last Interglacial sea level rise. *Geophys. Res. Lett.*, 38, L14605, doi:10.1029/2011GL048280.

Medina-Elizalde, M. (2013). A global compilation of coral sea-level benchmarks: Implications and new challenges. *Earth Planet. Sci. Lett.*, 362, 310–318.

Meffre, S. & Crawford, A.J. (2001). Collision tectonics in the New Hebrides arc (Vanuatu). *Isl. Arc*, 10, 33–50.

Méndez-Bedia, I. & Soto, F. (1984). Paleoecological succession in a devonian organic buildup (Moniello FM., Cantabrian mountains, NW Spain). *Geobios*, 17, Supple, 151–157.

Mewis, H. & Kiessling, W. (2013). Environmentally controlled succession in a late Pleistocene coral reef (Sinai, Egypt). *Coral Reefs*, 32, 49–58.

Meyer, D., Bries, J., Greenstein, B. & Debrot, A. (2003). Preservation of in situ reef framework in regions of low hurricane frequency: Pleistocene of Curaçao and Bonaire, southern Caribbean. *Lethaia*, 36, 273–285.

Millet, J. & Kiessling, W. (2009). First record of coralline demosponges in the Pleistocene: implications for reef ecology. *Coral Reefs*, 28, 867–870.

Milliman, J.D. (1993). Production and accumulation of calcium carbonate in the ocean: Budget of a nonsteady state. *Global Biogeochem. Cycles*, 7, 927–957.

Milliman, J.D. & Droxler, A.W. (1996). Neritic and pelagic carbonate sedimentation in the marine environment: ignorance is not bliss. *Geol. Rundschau*, 85, 496–504.

Minchin, P.R. (1987). An evaluation of the relative robustness of techniques for ecological ordination. *Vegetatio*, 69, 89–107.

Mitrovica, J.X. & Peltier, W.R. (1991). On postglacial geoid subsidence over the equatorial oceans. *J. Geophys. Res.*, 96, 20053.

Mittermeier, R.A., Myers, N., Thomsen, J.B., da Fonseca, G.A.B. & Olivieri, S. (1998). Biodiversity Hotspots and Major Tropical Wilderness Areas: Approaches to Setting Conservation Priorities. *Conserv. Biol.*, 12, 516–520.

Moberg, F. & Folke, C. (1999). Ecological goods and services of coral reef ecosystems. *Ecol. Econ.*, 29, 215–233.

Mohamed, A.R., Ali, A.-H.A.M. & Abdel-Salam, H.A. (2012). Status of coral reef health in the northern Red Sea, Egypt. In: *Proceedings of the 12th International Coral Reef Symposium*. Cairns.

Molinos, J.G., Halpern, B.S., Schoeman, D.S., Brown, C.J., Kiessling, W., Moore, P.J., *et al.* (2015). Climate velocity and the future global redistribution of marine biodiversity. *Nat. Clim. Chang.*, doi:10.1038/nclimate2769.

Montaggioni, L.F. (2005). History of Indo-Pacific coral reef systems since the last glaciation: Development patterns and controlling factors. *Earth-Science Rev.*, 71, 1–75.

Montaggioni, L.F. & Braithwaite, C.J.R. (2009). *Quaternary coral reef systems: History, development processes and controlling factors*. Developmen. Elsevier.

Motomura, I. (1932). “A statistical treatment of associations” (in Japanese). *Japanese J. Zool.*, 44, 379–383.

El Moursi, M.E.E. (1993). Pleistocene evolution of the reef terraces of the Red Sea coastal plain between Hurghada and Marsa Alam, Egypt. *J. African Earth Sci. (and Middle East)*, 17, 125–127.

El Moursi, M.M.E., Hoang, C.T., Fayoumy, I.F. El, Hegab, O. & Faure, H. (1994). Pleistocene evolution of the Red Sea coastal plain, Egypt: Evidence from uranium-series dating of emerged reef terraces. *Quat. Sci. Rev.*, 13, 345–359.

Muir, P.R., Wallace, C.C., Done, T. & Aguirre, J.D. (2015). Coral reefs. Limited scope for latitudinal extension of reef corals. *Science*, 348, 1135–8.

Murray-Wallace, C. V. (2002). Pleistocene coastal stratigraphy, sea-level highstands and neotectonism of the southern Australian passive continental margin?a review. *J. Quat. Sci.*, 17, 469–489.

Murray-Wallace, C. V. & Woodroffe, C.D. (2014). *Quaternary Sea-Level Changes: A Global Perspective*. Cambridge University Press.

Naeem, S. & Li, S. (1997). Biodiversity enhances ecosystem reliability. *Nature*, 390, 507.

Nakamori, T., Campbell, C.R. & Wallensky, E. (1995). Living Hermatypic Coral Assemblages at Huon Peninsula, Papua New Guinea. *J. Geogr. (Chigaku Zasshi)*, 104, 743–757.

Neef, G. & McCulloch, M.T. (2001). Pliocene-Quaternary history of Futuna Island, south Vanuatu, southwest Pacific. *Aust. J. Earth Sci.*, 48, 805–814.

Neef, G. & Veeh, H.H. (1977). Uranium series ages and late Quaternary uplift in the New Hebrides. *Nature*, 269, 682–683.

Nenadic, O. & Greenacre, M. (2007). Correspondence Analysis in R, with two- and three-dimensional graphics: The ca package. *J. Stat. Softw.*, 20, 1–13.

Neumann, A.. & Macintyre, I. (1985). Reef response to sea level rise: keep-up, catch-up or give-up. In: *Proceedings Of The Fifth International Coral Reef Congress, Vol. 3* (eds. Gabrie, C., Toffart, J.L. & Salvat, B.). Tahiti, pp. 105–110.

Nir, D. (1971). Marine terraces of southern Siani. *Geogr. Rev.*, 61, 32–50.

Nir, Y. (1969). *Survey of embayments in the western coast of the Gulf of Elat, between Nuweiba and Ras Muhamad (in Hebrew)*.

O'Hara, R.B. (2005). Species richness estimators: how many species can dance on the head of a pin? *J. Anim. Ecol.*, 74, 375–386.

Oksanen, J. (2015). *Multivariate Analysis of Ecological Communities in R: vegan tutorial*.

Oksanen, J., Blanchet, F.G., Kindt, R., Legendre, P., Minchin, P.R., O'Hara, R.B., *et al.* (2014). *vegan: Community Ecology Package. R package version 2.2-0.* Available at: http://cran.r-project.org/package=vegan. Last accessed .

Ota, Y. & Chappell, J. (1999). Holocene sea-level rise and coral reef growth on a tectonically rising coast, Huon Peninsula, Papua New Guinea. *Quat. Int.*, 55, 51–59.

Palmer, M.W. (1990). The Estimation of Species Richness by Extrapolation. *Ecology*, 71, 1195–1198.

Palumbi, S.R., Barshis, D.J., Traylor-Knowles, N. & Bay, R.A. (2014). Mechanisms of reef coral resistance to future climate change. *Science*, 344, 895–8.

Pandolfi, J.M. (1996). Limited membership in Pleistocene reef coral assemblages from the Huon Peninsula, PapuaNew Guinea: Constancy during global change. *Paleobiology*, 22, 152–176.

Pandolfi, J.M. (1999). Response of Pleistocene coral reefs to environmental change over long temporal scales. *Am. Zool.*, 39, 113–130.

Pandolfi, J.M. (2000). Persistence in Caribbean coral communities over broad spatial and temporal scales. In: *Presented at 9th Int. Coral Reef Congress*. Bali.

Pandolfi, J.M. (2001a). Community structure of Pleistocene coral reefs of Curacao, Netherlands Antilles. *Ecol. Monogr.*, 71, 49–67.

Pandolfi, J.M. (2001b). Numerical and taxonomic scale of analysis in paleoecological data sets: Examples from neo-tropical Pleistocene reef coral communities. *J. Paleontol.*, 75, 546–563.

Pandolfi, J.M. (2002). Coral community dynamics at multiple scales. *Coral Reefs*, 21, 13–23.

Pandolfi, J.M. (2010). The Paleoecology of coral reefs. In: *Coral Reefs: An Ecosystem in Transition* (eds. Dubinsky, Z. & Stambler, N.). Springer Netherlands, Dordrecht, pp. 13–24.

Pandolfi, J.M., Connolly, S.R., Marshall, D.J. & Cohen, A.L. (2011). Projecting Coral Reef Futures Under Global Warming and Ocean Acidification . *Sci.* , 333 , 418–422.

Pandolfi, J.M. & Jackson, J.B.C. (2001). Community Structure of Pleistocene Coral Reefs of Curaçao, Netherlands Antilles. *Ecol. Monogr.*, 71, 49–67.

Pandolfi, J.M. & Jackson, J.B.C. (2006). Ecological persistence interrupted in Caribbean coral reefs. *Ecol. Lett.*, 9, 818–26.

Pandolfi, J.M. & Kiessling, W. (2014). Gaining insights from past reefs to inform understanding of coral reef response to global climate change. *Curr. Opin. Environ. Sustain.*, 7, 52–58.

Pandolfi, J.M., Lovelock, C.E. & Budd, A.F. (2002). Character release following extinction in a Caribbean reef coral species complex . *Evolution (N. Y).*, 56.

Pandolfi, J.M., Tudhope, A.W., Burr, G., Chappell, J., Edinger, E.N., Frey, M., *et al.* (2006). Mass mortality following disturbance in Holocene coral reefs from Papua New Guinea. *Geology*, 34, 949–952.

Parker, J.H., Gischler, E. & Eisenhauer, A. (2012a). Biodiversity of foraminifera from Late Pleistocene to Holocene coral reefs, South Sinai, Egypt. *Mar. Micropaleontol.*, 86–87, 59–75.

Parker, J.H., Gischler, E. & Eisenhauer, A. (2012b). Biodiversity of foraminifera from Late Pleistocene to Holocene coral reefs, South Sinai, Egypt. *Mar. Micropaleontol.*, 86-87, 59–75.

Pellissier, L., Leprieur, F., Parravicini, V., Cowman, P.F., Kulbicki, M., Litsios, G., *et al.* (2014). Quaternary coral reef refugia preserved fish diversity. *Science (80-.).*, 344, 1016–1019.

Peltier, W.R. (1994). Ice Age Paleotopography. *Science (80-.).*, 265, 195–201.

Peltier, W.R. (2004). Global glacial isostasy and the surface of the ice-age earth: The ICE-5G (VM2) Model and GRACE. *Annu. Rev. Earth Planet. Sci.*, 32, 111–149.

Pirazzoli, P. a., Montaggioni, L.F., Salvat, B. & Faure, G. (1988). Late Holocene sea level indicators from twelve atolls in the central and eastern Tuamotus (Pacific Ocean). *Coral Reefs*, 7, 57–68.

Pirazzoli, P.A., Radtke, U., Hantoro, W.S., Jouannic, C., Hoang, C.T., Causse, C., *et al.* (1991). Quaternary raised coral-reef terraces on sumba island, indonesia. *Science*, 252, 1834–6.

Pirazzoli, P.A., Reyss, J.-L., Fontugne, M., Haghipour, A., Hilgers, A., H.U. Kasper, *et al.* (2004). Quaternary coral-reef terraces from Kish and Qeshm Islands, Persian Gulf: new radiometric ages and tectonic implications. *Quat. Int.*, 120, 15–27.

Plaziat, J.-C., Baltzer, F., Choukri, A., Conchon, O., Freytet, P., Orszag-Sperber, F., *et al.* (1995). Quaternary changes in the Egyptian shoreline of the Northwestern Red Sea and Gulf of Suez. *Quat. Int.*, 29-30, 11–22.

Plaziat, J.-C., Baltzer, F., Choukri, A., Conchon, O., Freytet, P., Orszag-Sperber, F., *et al.* (1998). Quaternary marine and continental sedimentation in the northern Red Sea and Gulf of Suez (Egyptian coast): influences of rift tectonics, climatic changes and sea-level fluctuations. In: *Sedimentation and Tectonics in Rift Basins Red Sea:- Gulf of Aden* (eds. Purser, B.H. & Bosence, D.W.J.). Springer Netherlands, Dordrecht, pp. 537–573.

Plaziat, J.-C., Reyss, J.-L., Choukri, A. & Cazala, C. (2008). Diagenetic rejuvenation of raised coral reefs and precision of dating. The contribution of the Red Sea reefs to the question of reliability of the Uranium-series datings of middle to late Pleistocene key reef-terraces of the world.

Preston, F.W. (1948). The commonness, and rarity, of species. *Ecology*, 29, 254–283.

R Core Team. (2014). R: A language and environment for statistical computing.

Radtke, U., Schellmann, G., Scheffers, A., Kelletat, D., Kromer, B. & Kasper, H. (2003). Electron spin resonance and radiocarbon dating of coral deposited by Holocene tsunami events on Curaçao, Bonaire and Aruba (Netherlands Antilles). *Quat. Sci. Rev.*

Raup, D.M. (1975). Taxonomic diversity estimation using rarefaction. *Paleobiology*, 1, 333–342.

Reiss, Z. & Hottinger, L. (1984). The Gulf of Aqaba. Ecological micropaleontology. *Ecol. Stud.*, 50, i–viii, 1–354.

Reiss, Z., Luz, B., Almogi-Labin, A., Halicz, E., Winter, A., Wolf, M., *et al.* (1980). Late Quaternary Paleoceanography of the Gulf of Aqaba (Elat), Red SEa. *Quat. Res.*, 14, 294–308.

Renema, W., Wallace, C., Kiessling, W., Pandolfi, J., Webster, J., Bosellini, F., *et al.* (in review.). Are coral reefs victims of their own past success? *Sci. Adv.*

Ricklefs, R.E. (1990). *Ecology*. New York.

Riegl, B. & Piller, W.E. (2003). Possible refugia for reefs in times of environmental stress. *Int. J. Earth Sci.*, 92, 520–531.

Rodolfo-Metalpa, R., Montagna, P., Aliani, S., Borghini, M., Canese, S., Hall-Spencer, J.M., *et al.* (2015). Calcification is not the Achilles' heel of cold-water corals in an acidifying ocean. *Glob. Chang. Biol.*, 21, 2238–48.

Rohling, E.J., Fenton, M., Jorissen, F.J., Bertrand, P., Ganssen, G. & Caulet, J.P. (1998). Magnitudes of sea-level lowstands of the past 500,000 years. *Nature*, 394, 162–165.

Rohling, E.J., Grant, K., Bolshaw, M., Roberts, A.P., Siddall, M., Hemleben, C., *et al.* (2009). Antarctic temperature and global sea level closely coupled over the past five glacial cycles. *Nat. Geosci.*, 2, 500–504.

Rohling, E.J., Medina-Elizalde, M., Shepherd, J.G., Siddall, M. & Stanford, J.D. (2012). Sea Surface and High-Latitude Temperature Sensitivity to Radiative Forcing of Climate over Several Glacial Cycles. *J. Clim.*, 25, 1635–1656.

Saqqa, W.A. & Atallah, M.Y. (2013). Tectonic geomorphology of alluvial fans east of the Wadi Araba Fault (Dead Sea Transform), Jordan. *Jordan J. Earth Environ. Sci.*, 5, 79–86.

Scheer, G. & Pillai, C.S.G. (1983). Report on the stony Corals from the Red Sea. *Zoologica*, 133, 198.

Schellmann, G., Beerten, K. & Radtke, U. (2008). Electron spin resonance (ESR) dating of Quaternary materials. *" Eiszeitalter und Gegenwart", Quat. Sci. J.*, 57, 150–178.

Schellmann, G. & Radtke, U. (2001). Progress in ESR dating of Pleistocene corals — a new approach for DE determination. *Quat. Sci. Rev.*, 20, 1015–1020.

Schellmann, G. & Radtke, U. (2004). *The marine quaternary of Barbados*. 81st edn. Kölner Geographische Schriften, Köln.

Schellmann, G., Radtke, U., Potter, E.-K., Esat, T.M. & McCulloch, M.T. (2004). Comparison of ESR and TIMS U/Th dating of marine isotope stage (MIS) 5e, 5c, and 5a coral from Barbados—implications for palaeo sea-level changes in the Caribbean. *Quat. Int.*, 120, 41–50.

Segal, B. & Castro, C.B.A. (2001). A proposed method for coral cover assessment: a case study in Abrolhos, Brazil. *Bull. Mar. Sci.*, 69, 487–496.

Shackleton, N.J. & Opdyke, N.D. (1973). Oxygen isotope and palaeomagnetic stratigraphy of equatorial Pacific core V28-238: oxygen isotope temperatures and ice volumes on a 105 year scale and 106 year scale. *Quat. Res.*, 3, 39–55.

Sheppard, C., Roberts, C. & Price, A. (1992). *Marine Ecology of the Arabian Region: Patterns and Processes in Extreme Tropical Environments*. Academic Press, London.

Sheppard, C.R.C. & Sheppard, A.L.S. (1991). Corals and coral communities of Arabia. *Fauna Saudi Arab.*, 12, 3–170.

Siddall, M., Chappell, J. & Potter, E.-K. (2007). *The Climate of Past Interglacials*. *Dev. Quat. Sci.*, Developments in Quaternary Sciences. Elsevier.

Siddall, M., Rohling, E.J., Almogi-Labin, A., Hemleben, C., Meischner, D., Schmelzer, I., *et al.* (2003). Sea-level fluctuations during the last glacial cycle. *Nature*, 423, 853–8.

Siddall, M., Smeed, D.A., Hemleben, C., Rohling, E.J., Schmelzer, I. & Peltier, W.R. (2004). Understanding the Red Sea response to sea level. *Earth Planet. Sci. Lett.*, 225, 421–434.

Sørensen, T. (1948). *A method of establishing groups of equal amplitude in plant sociology based on similarity of species content and its application to analyses of the vegetation on Danish commons.* I kommission hos E. Munksgaard, København.

Sorte, C.J.B., Williams, S.L. & Carlton, J.T. (2010). Marine range shifts and species introductions: comparative spread rates and community impacts. *Glob. Ecol. Biogeogr.*, 19, 303–316.

Spalding, M.D., Ravilious, C. & Green, E.P. (2001). *World Atlas of Coral Reefs*. University of California Press, Berkeley, California, USA.

Steers, J.A. & Stoddart, D.R. (1977). The origin of fringing reefs, barrier reefs, and atolls. In: *Biology and Geology of Coral Reefs* (eds. Jones, O.A. & Endean, R.). Academic Press, New York, pp. 21–57.

Stirling, C.H., Esat, T.M., Lambeck, K. & McCulloch, M.T. (1998). Timing and duration of the Last Interglacial: Evidence for a restricted interval of widespread coral reef growth. *Earth Planet. Sci. Lett.*, 160, 745–762.

Stolarski, J., Kitahara, M. V, Miller, D.J., Cairns, S.D., Mazur, M. & Meibom, A. (2011). The ancient evolutionary origins of Scleractinia revealed by azooxanthellate corals. *BMC Evol. Biol.*, 11, 316.

Strasser, A. & Strohmenger, C. (1997). Early diagenesis in Pleistocene coral reefs, southern Sinai, Egypt: response to tectonics, sea-level and climate. *Sedimentology*, 44, 537-558.

Strasser, A., Strohmenger, C., Davaud, E. & Bach, A. (1992). Sequential evolution and diagenesis of Pleistocene coral reefs (South Sinai, Egypt). *Sediment. Geol.*, 78, 59–79.

Supriharyono. (2013). Growth rates of the massive coral Porites lutea Edward and Haime, on the coast of Botang, East Kalimantan, Indonesia. *J. Coast. Dev.*

Suzuki, A. & Kawahata, H. (2003). Carbon budget of coral reef systems: an overview of observations in fringing reefs, barrier reefs and atolls in the Indo-Pacific regions. *Tellus B*, 55.

Sweatman, H., Delean, S. & Syms, C. (2011). Assessing loss of coral cover on Australia's Great Barrier Reef over two decades, with implications for longer-term trends. *Coral Reefs*, 30, 521–531.

Tager, D., Webster, J.M., Potts, D.C., Renema, W., Braga, J.C. & Pandolfi, J.M. (2010). Community dynamics of Pleistocene coral reefs during alternative climatic regimes. *Ecology*, 91, 191–200.

Thompson, W.G. & Goldstein, S.L. (2005). Open-system coral ages reveal persistent suborbital sea-level cycles. *Science*, 308, 401–4.

Thunell, R.C., Locke, S.M. & Williams, D.F. (1988). Glacio-eustatic sea-level control on Red Sea salinity. *Nature*, 334, 601–604.

Tokeshi, M. (1993). *Advances in Ecological Research Volume 24*. *Adv. Ecol. Res.*, Advances in Ecological Research. Elsevier.

Tuomisto, H. (2010a). A diversity of beta diversities: straightening up a concept gone awry. Part 1. Defining beta diversity as a function of alpha and gamma diversity. *Ecography (Cop.).*, 33, 2–22.

Tuomisto, H. (2010b). A diversity of beta diversities: straightening up a concept gone awry. Part 2. Quantifying beta diversity and related phenomena. *Ecography (Cop.).*, 33, 23–45.

Turkay, M. (1996). Composition of the deep Red Sea macro- and megabenthic invertebrate fauna. Zoogeographic and ecological implications. In: *Deep-sea and extreme shallow-water habitats: affinities and adaptations.* (eds. Uiblein, F., Ott, F. & Stachowitsch, M.). Verlag der Osterreichischen Akademie der Wissenschaften, Vienna, Austria, pp. 43–59.

Turney, C.S.M. & Jones, R.T. (2010). Does the Agulhas Current amplify global temperatures during super-interglacials? *J. Quat. Sci.*, 25, 839–843.

Vaughan, T.W. & Wells, J.W. (1943). Revision of the suborders, families and genera of the Scleractinia. *Spec. Pap. Geol. Soc. Am.*, 44, 1–363.

Vaughan, T.W.. (1907). Some Madreporarian corals from French Somaliland, East Africa, collected by Dr. Charles Gravier. *Proc. U.S. Nat. Hist. Museum*, 32, 249–265.

Vecsei, A. (2004). A new estimate of global reefal carbonate production including the fore-reefs. *Glob. Planet. Change*, 43, 1–18.

Veeh, H.H. & Giegengack, R. (1970). Uranium-series ages of corals from the Red Sea. *Nature, Lond.*, 226, 155–156.

Vernon, R.H. & Clarke, G.L. (2008). *Principles of metamorphic petrology*. Cambridge University Press.

Veron, E.N. (1990). Checklist of the hermatypic corals of Vanuatu. *Pacific Sci.*, 44, 51–70.

Veron, J.E.N. (1995). *Corals in space and time: the biogeography and evolution of the scleractinia*. Cornell University Press, Ithaca.

Veron, J.E.N. (2000). *Corals of the world*. Australian Institute of Marine Science, Townsville, 3 Volumes.

Veron, J.E.N., DeVantier, L.M., Turak, E., Green, A.L., Kininmonth, S., Stafford-Smith, M., *et al.* (2011). The Coral Triangle. In: *Coral Reefs: An Ecosystem in Transition* (eds. Dubinsky, Z. & Stambler, N.). Springer Netherlands, Dordrecht, pp. 47–55.

Veron, J.E.N., Hoegh-Guldberg, O., Lenton, T.M., Lough, J.M., Obura, D.O., Pearce-Kelly, P., *et al.* (2009). The coral reef crisis: The critical importance of < 350 ppm CO2. *Mar. Pollut. Bull.*, 58, 1428–1436.

Veron, J.E.N., Pichon, M. & Wijsman-Best, M. (1977). *Schleractinia of Eastern Australia Part 2, Families Faviidae, Trachyphylliidae*. Australian Institute of Marine Science (AIMS). Australian Government Publishing Service, Canberra.

Waelbroeck, C., Labeyrie, L., Michel, E., Duplessy, J.C., McManus, J.F., Lambeck, K., *et al.* (2002). Sea-level and deep water temperature changes derived from benthic foraminifera isotopic records. *Quat. Sci. Rev.*, 21, 295–305.

Wagner, P.J., Kosnik, M.A. & Lidgard, S. (2006). Abundance distributions imply elevated complexity of post-Paleozoic marine ecosystems. *Science*, 314, 1289–92.

Walker, K.R. & Alberstadt, L.P. (1975). Ecological succession as an aspect of structure in fossil communities. *Paleobiology*, 1, 238–257.

Ward Jr., J.H. (1963). Hierarchical Grouping to Optimize an Objective Function. *J. Am. Stat. Assoc.*, 58, 236–244.

Webster, J.M. & Davies, P.J. (2003). Coral variation in two deep drill cores: significance for the Pleistocene development of the Great Barrier Reef. *Sediment. Geol.*, 159, 61–80.

Wefer, G. & Berger, W.H. (2000). Klima und Ozean. In: *Klimazeugnisse der Erdgeschichte: Perspektiven für die Zukunft* (eds. Huch, M., Warnecke, G. & Germann, K.). Springer Berlin / Heidelberg, pp. 51–108.

Wells, J.W. (1956). Scleractinia. In: *Treatise on invertebrate paleontology. Part F: Coelenterata.* (ed. Moore, R.C.). Geological Society of America and University of Kansas Press, Lawrence, Kansas, pp. F328–F444.

Whittaker, R.H. (1960). Vegetation of the Siskiyou Mountains, Oregon and California. *Ecol. Monogr.*, 30, 407.

Whittaker, R.H. (1965). Dominance and Diversity in Land Plant Communities: Numerical relations of species express the importance of competition in community function and evolution. *Science*, 147, 250–60.

Wirrmann, D., Eagar, S.H., Harper, M.A., Leroy, E. & Semah, A.-M. (2011). First insights into mid-Holocene environmental change in central Vanuatu inferred from a terrestrial record from Emaotfer Swamp, Efate Island. *Quat. Sci. Rev.*, 30, 3908–3924.

Witze, A. (2015). Corals worldwide hit by bleaching. *Nature*.

van Woesik, R., Franklin, E.C., O'Leary, J., McClanahan, T.R., Klaus, J.S. & Budd, A.F. (2012). Hosts of the Plio-Pleistocene past reflect modern-day coral vulnerability. *Proc. Biol. Sci.*, 279, 2448–56.

Woodley, J.D., Chornesky, E.A., Clifford, P.A., Jackson, J.B., Kaufman, L.S., Knowlton, N., *et al.* (1981). Hurricane Allen's Impact on Jamaican Coral Reefs. *Science*, 214, 749–55.

Woodroffe, C. & McLean, R. (1990). Microatolls and recent sea level change on coral atolls. *Nature*, 344, 531–534.

Woodroffe, C.D. & Webster, J.M. (2014). Coral reefs and sea-level change. *Mar. Geol.*, 352, 248–267.

Wooldridge, S.A. (2013). Breakdown of the coral-algae symbiosis: towards formalising a linkage between warm-water bleaching thresholds and the growth rate of the intracellular zooxanthellae. *Biogeosciences*, 10, 1647–1658.

WoRMS Editorial Board. (2015). *World Register of Marine Species*. *http//www.marinespecies.org VLIZ*.

Yamano, H., Sugihara, K. & Nomura, K. (2011). Rapid poleward range expansion of tropical reef corals in response to rising sea surface temperatures. *Geophys. Res. Lett.*, 38, L04601.

Yokoyama, Y., Esat, T.M. & Lambeck, K. (2001). Coupled climate and sea-level changes deduced from Huon Peninsula coral terraces of the last ice age. *Earth Planet. Sci. Lett.*, 193, 579–587.

Zipf, G.K. (1949). *Human behavior and the principle of least effort*. Addison-Wesley Press, Oxford, UK.

Selbstständigkeitserklärung

Hiermit erkläre ich, die Dissertation selbstständig und nur unter Verwendung der angegebenen Hilfen und Hilfsmittel angefertigt zu haben.

Ich habe mich anderwärts nicht um einen Doktorgrad beworben und besitze einen entsprechenden Doktorgrad nicht.

Ich erkläre die Kenntnisnahme der dem Verfahren zugrunde liegenden Promotionsordnung der Mathematisch-Naturwissenschaftlichen Fakultät I der Humboldt-Universität zu Berlin vom 01. September 2005.

Datum Unterschrift

Appendix I - Data from Vanuatu

The following Table I-I contains the complete dataset from all transects performed in Vanuatu. Table I-II contains the bulk sampling data. The GPS points are listed in TableI-III.

Table 6-I: Complete transect dataset from Vanuatu.

LT	Locality	Altitude (in m)	Terrace	Taxon	sample
LT1	UL2	90	Pleistocene 2	red algae	UL2a
LT1	UL2	90	Pleistocene 2	*Alveopora sp.*	
LT1	UL2	90	Pleistocene 2	*Alveopora sp.*	
LT1	UL2	90	Pleistocene 2	gap	
LT1	UL2	90	Pleistocene 2	red algae	
LT1	UL2	90	Pleistocene 2	gap	
LT1	UL2	90	Pleistocene 2	red algae	
LT1	UL2	90	Pleistocene 2	gap	
LT1	UL2	90	Pleistocene 2	gap	
LT1	UL2	90	Pleistocene 2	gap	
LT1	UL2	90	Pleistocene 2	gap	
LT1	UL2	90	Pleistocene 2	gap	
LT1	UL2	90	Pleistocene 2	gap	
LT1	UL2	90	Pleistocene 2	gap	
LT1	UL2	90	Pleistocene 2	*Favites sp.*	
LT1	UL2	90	Pleistocene 2	gap	
LT1	UL2	90	Pleistocene 2	gap	
LT1	UL2	90	Pleistocene 2	gap	
LT1	UL2	90	Pleistocene 2	gap	
LT1	UL2	90	Pleistocene 2	gap	
LT1	UL2	90	Pleistocene 2	gap	
LT1	UL2	90	Pleistocene 2	red algae	
LT1	UL2	90	Pleistocene 2	red algae	
LT1	UL2	90	Pleistocene 2	gap	
LT1	UL2	90	Pleistocene 2	gap	
LT1	UL2	90	Pleistocene 2	red algae	
LT1	UL2	90	Pleistocene 2	red algae	
LT1	UL2	90	Pleistocene 2	gap	
LT1	UL2	90	Pleistocene 2	gap	
LT1	UL2	90	Pleistocene 2	gap	
LT1	UL2	90	Pleistocene 2	gap	
LT1	UL2	90	Pleistocene 2	gap	
LT1	UL2	90	Pleistocene 2	gap	
LT1	UL2	90	Pleistocene 2	gap	
LT1	UL2	90	Pleistocene 2	gap	
LT1	UL2	90	Pleistocene 2	gap	
LT1	UL2	90	Pleistocene 2	gap	
LT1	UL2	90	Pleistocene 2	gap	
LT1	UL2	90	Pleistocene 2	gap	
LT1	UL2	90	Pleistocene 2	gap	

LT	Locality	Altitude (in m)	Terrace	Taxon	sample
LT1	UL2	90	Pleistocene 2	gap	
LT1	UL2	90	Pleistocene 2	gap	
LT1	UL2	90	Pleistocene 2	gap	
LT1	UL2	90	Pleistocene 2	red algae	
LT1	UL2	90	Pleistocene 2	red algae	
LT1	UL2	90	Pleistocene 2	red algae	
LT1	UL2	90	Pleistocene 2	*Favites sp.*	
LT1	UL2	90	Pleistocene 2	*Favites sp.*	
LT1	UL2	90	Pleistocene 2	*Favites sp.*	
LT1	UL2	90	Pleistocene 2	*Favites sp.*	
LT1	UL2	90	Pleistocene 2	*Favites sp.*	
LT1	UL2	90	Pleistocene 2	*Favites sp.*	
LT1	UL2	90	Pleistocene 2	red algae	
LT1	UL2	90	Pleistocene 2	red algae	
LT1	UL2	90	Pleistocene 2	red algae	
LT1	UL2	90	Pleistocene 2	*Porites sp.*	UL2b
LT1	UL2	90	Pleistocene 2	*Porites sp.*	UL2b
LT1	UL2	90	Pleistocene 2	gap

LT	Locality	Altitude (in m)	Terrace	Taxon	sample
LT1	UL2	90	Pleistocene 2	gap	

LT	Locality	Altitude (in m)	Terrace	Taxon	sample
LT1	UL2	90	Pleistocene 2	gap	
LT1	UL2	90	Pleistocene 2	red algae	
LT1	UL2	90	Pleistocene 2	red algae	
LT1	UL2	90	Pleistocene 2	red algae	
LT1	UL2	90	Pleistocene 2	red algae	
LT1	UL2	90	Pleistocene 2	red algae	
LT1	UL2	90	Pleistocene 2	*Favites sp.*	
LT1	UL2	90	Pleistocene 2	*Leptoria phrygia*	UL2e
LT1	UL2	90	Pleistocene 2	*Porites sp.*	
LT1	UL2	90	Pleistocene 2	matrix	
LT1	UL2	90	Pleistocene 2	matrix	
LT1	UL2	90	Pleistocene 2	matrix	
LT1	UL2	90	Pleistocene 2	matrix	
LT1	UL2	90	Pleistocene 2	matrix	
LT1	UL2	90	Pleistocene 2	matrix	
LT1	UL2	90	Pleistocene 2	matrix	
LT1	UL2	90	Pleistocene 2	matrix	
LT1	UL2	90	Pleistocene 2	matrix	
LT1	UL2	90	Pleistocene 2	matrix	
LT1	UL2	90	Pleistocene 2	matrix	
LT1	UL2	90	Pleistocene 2	matrix	
LT2	UL2	90	Pleistocene 2	gap	
LT2	UL2	90	Pleistocene 2	gap	
LT2	UL2	90	Pleistocene 2	gap	
LT2	UL2	90	Pleistocene 2	gap	
LT2	UL2	90	Pleistocene 2	gap	
LT2	UL2	90	Pleistocene 2	matrix	
LT2	UL2	90	Pleistocene 2	*Goniastrea sp.*	
LT2	UL2	90	Pleistocene 2	*Goniastrea sp.*	
LT2	UL2	90	Pleistocene 2	*Goniastrea sp.*	
LT2	UL2	90	Pleistocene 2	matrix	
LT2	UL2	90	Pleistocene 2	matrix	
LT2	UL2	90	Pleistocene 2	matrix	
LT2	UL2	90	Pleistocene 2	matrix	
LT2	UL2	90	Pleistocene 2	matrix	
LT2	UL2	90	Pleistocene 2	gap	
LT2	UL2	90	Pleistocene 2	gap	
LT2	UL2	90	Pleistocene 2	gap	
LT2	UL2	90	Pleistocene 2	gap	
LT2	UL2	90	Pleistocene 2	gap	
LT2	UL2	90	Pleistocene 2	gap	
LT2	UL2	90	Pleistocene 2	gap	
LT2	UL2	90	Pleistocene 2	gap	
LT2	UL2	90	Pleistocene 2	gap	
LT2	UL2	90	Pleistocene 2	gap	
LT2	UL2	90	Pleistocene 2	gap	
LT2	UL2	90	Pleistocene 2	gap	

LT	Locality	Altitude (in m)	Terrace	Taxon	sample
LT2	UL2	90	Pleistocene 2	gap	
LT2	UL2	90	Pleistocene 2	gap	
LT2	UL2	90	Pleistocene 2	gap	
LT2	UL2	90	Pleistocene 2	gap	
LT2	UL2	90	Pleistocene 2	gap	
LT2	UL2	90	Pleistocene 2	gap	
LT2	UL2	90	Pleistocene 2	gap	
LT2	UL2	90	Pleistocene 2	gap	
LT2	UL2	90	Pleistocene 2	gap	
LT2	UL2	90	Pleistocene 2	*Favites sp.*	UL2h
LT2	UL2	90	Pleistocene 2	*Favites sp.*	UL2h
LT2	UL2	90	Pleistocene 2	*Favites sp.*	UL2h
LT2	UL2	90	Pleistocene 2	*Stylocoeniella guentheri*	UL2i
LT2	UL2	90	Pleistocene 2	red algae	
LT2	UL2	90	Pleistocene 2	red algae	
LT2	UL2	90	Pleistocene 2	red algae	
LT2	UL2	90	Pleistocene 2	red algae	
LT2	UL2	90	Pleistocene 2	"Faviidae" indet.	
LT2	UL2	90	Pleistocene 2	gap	
LT2	UL2	90	Pleistocene 2	gap	
LT2	UL2	90	Pleistocene 2	gap	
LT2	UL2	90	Pleistocene 2	gap	
LT2	UL2	90	Pleistocene 2	gap	
LT2	UL2	90	Pleistocene 2	gap	
LT2	UL2	90	Pleistocene 2	gap	
LT2	UL2	90	Pleistocene 2	gap	
LT2	UL2	90	Pleistocene 2	gap	
LT2	UL2	90	Pleistocene 2	red algae	
LT2	UL2	90	Pleistocene 2	gap	
LT2	UL2	90	Pleistocene 2	gap	
LT2	UL2	90	Pleistocene 2	red algae	
LT2	UL2	90	Pleistocene 2	gap	
LT2	UL2	90	Pleistocene 2	matrix	
LT2	UL2	90	Pleistocene 2	gap	
LT2	UL2	90	Pleistocene 2	gap	
LT2	UL2	90	Pleistocene 2	gap	
LT2	UL2	90	Pleistocene 2	gap	
LT2	UL2	90	Pleistocene 2	gap	
LT2	UL2	90	Pleistocene 2	gap	
LT2	UL2	90	Pleistocene 2	gap	
LT2	UL2	90	Pleistocene 2	gap	
LT2	UL2	90	Pleistocene 2	gap	
LT2	UL2	90	Pleistocene 2	gap	
LT2	UL2	90	Pleistocene 2	gap	
LT2	UL2	90	Pleistocene 2	gap	
LT2	UL2	90	Pleistocene 2	gap	
LT2	UL2	90	Pleistocene 2	gap	

LT	Locality	Altitude (in m)	Terrace	Taxon	sample
LT2	UL2	90	Pleistocene 2	gap	
LT2	UL2	90	Pleistocene 2	gap	
LT2	UL2	90	Pleistocene 2	gap	
LT2	UL2	90	Pleistocene 2	gap	
LT2	UL2	90	Pleistocene 2	red algae	
LT2	UL2	90	Pleistocene 2	red algae	
LT2	UL2	90	Pleistocene 2	red algae	
LT2	UL2	90	Pleistocene 2	gap	
LT2	UL2	90	Pleistocene 2	gap	
LT2	UL2	90	Pleistocene 2	gap	
LT2	UL2	90	Pleistocene 2	gap	
LT2	UL2	90	Pleistocene 2	gap	
LT2	UL2	90	Pleistocene 2	red algae	
LT2	UL2	90	Pleistocene 2	red algae	
LT2	UL2	90	Pleistocene 2	*Stylocoeniella sp.*	
LT2	UL2	90	Pleistocene 2	*Stylocoeniella sp.*	
LT2	UL2	90	Pleistocene 2	gap	
LT2	UL2	90	Pleistocene 2	gap	
LT2	UL2	90	Pleistocene 2	gap	
LT2	UL2	90	Pleistocene 2	gap	
LT2	UL2	90	Pleistocene 2	gap	
LT2	UL2	90	Pleistocene 2	gap	
LT2	UL2	90	Pleistocene 2	red algae	
LT2	UL2	90	Pleistocene 2	"Faviidae" indet.	
LT2	UL2	90	Pleistocene 2	red algae	
LT2	UL2	90	Pleistocene 2	gap	
LT2	UL2	90	Pleistocene 2	gap	
LT2	UL2	90	Pleistocene 2	gap	
LT2	UL2	90	Pleistocene 2	gap	
LT2	UL2	90	Pleistocene 2	gap	
LT2	UL2	90	Pleistocene 2	gap	
LT2	UL2	90	Pleistocene 2	gap	
LT2	UL2	90	Pleistocene 2	gap	
LT2	UL2	90	Pleistocene 2	matrix	
LT2	UL2	90	Pleistocene 2	matrix	
LT2	UL2	90	Pleistocene 2	matrix	
LT2	UL2	90	Pleistocene 2	Scleractinia indet.	
LT2	UL2	90	Pleistocene 2	red algae	
LT2	UL2	90	Pleistocene 2	red algae	
LT2	UL2	90	Pleistocene 2	red algae	
LT2	UL2	90	Pleistocene 2	"Faviidae" indet.	
LT2	UL2	90	Pleistocene 2	"Faviidae" indet.	
LT2	UL2	90	Pleistocene 2	red algae	
LT2	UL2	90	Pleistocene 2	red algae	
LT2	UL2	90	Pleistocene 2	gap	
LT2	UL2	90	Pleistocene 2	gap	
LT2	UL2	90	Pleistocene 2	gap	

LT	Locality	Altitude (in m)	Terrace	Taxon	sample
LT2	UL2	90	Pleistocene 2	gap	
LT2	UL2	90	Pleistocene 2	gap	
LT2	UL2	90	Pleistocene 2	gap	
LT2	UL2	90	Pleistocene 2	gap	
LT2	UL2	90	Pleistocene 2	gap	
LT2	UL2	90	Pleistocene 2	*Dipsastraea sp.*	UL2k
LT2	UL2	90	Pleistocene 2	*Dipsastraea sp.*	UL2k
LT2	UL2	90	Pleistocene 2	*Dipsastraea sp.*	UL2k
LT2	UL2	90	Pleistocene 2	*Dipsastraea sp.*	UL2k
LT2	UL2	90	Pleistocene 2	gap	
LT2	UL2	90	Pleistocene 2	gap	
LT2	UL2	90	Pleistocene 2	gap	
LT2	UL2	90	Pleistocene 2	gap	
LT2	UL2	90	Pleistocene 2	red algae	
LT2	UL2	90	Pleistocene 2	red algae	
LT2	UL2	90	Pleistocene 2	red algae	
LT2	UL2	90	Pleistocene 2	gap	
LT2	UL2	90	Pleistocene 2	gap	
LT2	UL2	90	Pleistocene 2	gap	
LT2	UL2	90	Pleistocene 2	gap	
LT2	UL2	90	Pleistocene 2	gap	
LT2	UL2	90	Pleistocene 2	gap	
LT2	UL2	90	Pleistocene 2	gap	
LT2	UL2	90	Pleistocene 2	gap	
LT2	UL2	90	Pleistocene 2	gap	
LT2	UL2	90	Pleistocene 2	gap	
LT2	UL2	90	Pleistocene 2	gap	
LT2	UL2	90	Pleistocene 2	gap	
LT2	UL2	90	Pleistocene 2	gap	
LT2	UL2	90	Pleistocene 2	gap	
LT2	UL2	90	Pleistocene 2	gap	
LT2	UL2	90	Pleistocene 2	gap	
LT2	UL2	90	Pleistocene 2	gap	
LT2	UL2	90	Pleistocene 2	gap	
LT2	UL2	90	Pleistocene 2	gap	
LT2	UL2	90	Pleistocene 2	gap	
LT2	UL2	90	Pleistocene 2	gap	
LT2	UL2	90	Pleistocene 2	gap	
LT2	UL2	90	Pleistocene 2	gap	
LT2	UL2	90	Pleistocene 2	gap	
LT2	UL2	90	Pleistocene 2	gap	
LT2	UL2	90	Pleistocene 2	gap	
LT2	UL2	90	Pleistocene 2	gap	
LT2	UL2	90	Pleistocene 2	gap	
LT2	UL2	90	Pleistocene 2	gap	
LT2	UL2	90	Pleistocene 2	gap	
LT3	UL2	90	Pleistocene 2	gap	
LT3	UL2	90	Pleistocene 2	gap	
LT3	UL2	90	Pleistocene 2	gap	
LT3	UL2	90	Pleistocene 2	gap	
LT3	UL2	90	Pleistocene 2	gap	
LT3	UL2	90	Pleistocene 2	gap	
LT3	UL2	90	Pleistocene 2	gap	
LT3	UL2	90	Pleistocene 2	gap	
LT3	UL2	90	Pleistocene 2	gap	
LT3	UL2	90	Pleistocene 2	gap	
LT3	UL2	90	Pleistocene 2	gap	
LT3	UL2	90	Pleistocene 2	gap	
LT3	UL2	90	Pleistocene 2	gap	
LT3	UL2	90	Pleistocene 2	gap	
LT3	UL2	90	Pleistocene 2	gap	

LT	Locality	Altitude (in m)	Terrace	Taxon	sample
LT3	UL2	90	Pleistocene 2	gap	
LT3	UL2	90	Pleistocene 2	gap	
LT3	UL2	90	Pleistocene 2	gap	
LT3	UL2	90	Pleistocene 2	gap	
LT3	UL2	90	Pleistocene 2	gap	
LT3	UL2	90	Pleistocene 2	gap	
LT3	UL2	90	Pleistocene 2	gap	
LT3	UL2	90	Pleistocene 2	gap	
LT3	UL2	90	Pleistocene 2	gap	
LT3	UL2	90	Pleistocene 2	gap	
LT3	UL2	90	Pleistocene 2	gap	
LT3	UL2	90	Pleistocene 2	gap	
LT3	UL2	90	Pleistocene 2	gap	
LT3	UL2	90	Pleistocene 2	gap	
LT3	UL2	90	Pleistocene 2	gap	
LT3	UL2	90	Pleistocene 2	gap	
LT3	UL2	90	Pleistocene 2	gap	
LT3	UL2	90	Pleistocene 2	gap	
LT3	UL2	90	Pleistocene 2	gap	
LT3	UL2	90	Pleistocene 2	gap	
LT3	UL2	90	Pleistocene 2	gap	
LT3	UL2	90	Pleistocene 2	gap	
LT3	UL2	90	Pleistocene 2	gap	
LT3	UL2	90	Pleistocene 2	gap	
LT3	UL2	90	Pleistocene 2	gap	
LT3	UL2	90	Pleistocene 2	Scleractinia indet.	
LT3	UL2	90	Pleistocene 2	Scleractinia indet.	
LT3	UL2	90	Pleistocene 2	Scleractinia indet.	
LT3	UL2	90	Pleistocene 2	Scleractinia indet.	
LT3	UL2	90	Pleistocene 2	red algae	
LT3	UL2	90	Pleistocene 2	gap	
LT3	UL2	90	Pleistocene 2	gap	
LT3	UL2	90	Pleistocene 2	red algae	
LT3	UL2	90	Pleistocene 2	red algae	
LT3	UL2	90	Pleistocene 2	red algae	
LT3	UL2	90	Pleistocene 2	red algae	
LT3	UL2	90	Pleistocene 2	gap	
LT3	UL2	90	Pleistocene 2	gap	
LT3	UL2	90	Pleistocene 2	gap	
LT3	UL2	90	Pleistocene 2	gap	
LT3	UL2	90	Pleistocene 2	gap	
LT3	UL2	90	Pleistocene 2	gap	
LT3	UL2	90	Pleistocene 2	gap	
LT3	UL2	90	Pleistocene 2	gap	
LT3	UL2	90	Pleistocene 2	gap	
LT3	UL2	90	Pleistocene 2	gap	
LT3	UL2	90	Pleistocene 2	gap	
LT3	UL2	90	Pleistocene 2	gap	
LT3	UL2	90	Pleistocene 2	gap	
LT3	UL2	90	Pleistocene 2	gap	

LT	Locality	Altitude (in m)	Terrace	Taxon	sample
LT3	UL2	90	Pleistocene 2	gap	
LT3	UL2	90	Pleistocene 2	gap	
LT3	UL2	90	Pleistocene 2	gap	
LT3	UL2	90	Pleistocene 2	gap	
LT3	UL2	90	Pleistocene 2	gap	
LT3	UL2	90	Pleistocene 2	gap	
LT3	UL2	90	Pleistocene 2	gap	
LT3	UL2	90	Pleistocene 2	gap	
LT3	UL2	90	Pleistocene 2	gap	
LT3	UL2	90	Pleistocene 2	gap	
LT3	UL2	90	Pleistocene 2	gap	
LT3	UL2	90	Pleistocene 2	gap	
LT3	UL2	90	Pleistocene 2	gap	
LT3	UL2	90	Pleistocene 2	gap	
LT3	UL2	90	Pleistocene 2	gap	
LT3	UL2	90	Pleistocene 2	gap	
LT3	UL2	90	Pleistocene 2	gap	
LT3	UL2	90	Pleistocene 2	gap	
LT3	UL2	90	Pleistocene 2	gap	
LT3	UL2	90	Pleistocene 2	Scleractinia indet.	
LT3	UL2	90	Pleistocene 2	red algae	
LT3	UL2	90	Pleistocene 2	red algae	
LT3	UL2	90	Pleistocene 2	"Faviidae" indet.	
LT3	UL2	90	Pleistocene 2	red algae	
LT3	UL2	90	Pleistocene 2	red algae	
LT3	UL2	90	Pleistocene 2	gap	
LT3	UL2	90	Pleistocene 2	gap	
LT3	UL2	90	Pleistocene 2	gap	
LT3	UL2	90	Pleistocene 2	gap	
LT3	UL2	90	Pleistocene 2	*Goniastrea sp.*	UL2l
LT3	UL2	90	Pleistocene 2	*Goniastrea sp.*	UL2l
LT3	UL2	90	Pleistocene 2	*Goniastrea sp.*	UL2l
LT3	UL2	90	Pleistocene 2	gap	
LT3	UL2	90	Pleistocene 2	gap	
LT3	UL2	90	Pleistocene 2	gap	
LT3	UL2	90	Pleistocene 2	gap	
LT3	UL2	90	Pleistocene 2	gap	
LT3	UL2	90	Pleistocene 2	gap	
LT3	UL2	90	Pleistocene 2	gap	
LT3	UL2	90	Pleistocene 2	gap	
LT3	UL2	90	Pleistocene 2	gap	
LT3	UL2	90	Pleistocene 2	gap	
LT3	UL2	90	Pleistocene 2	gap	
LT3	UL2	90	Pleistocene 2	gap	
LT3	UL2	90	Pleistocene 2	gap	
LT3	UL2	90	Pleistocene 2	gap	
LT3	UL2	90	Pleistocene 2	gap	
LT3	UL2	90	Pleistocene 2	gap	
LT3	UL2	90	Pleistocene 2	gap	
LT3	UL2	90	Pleistocene 2	gap	
LT3	UL2	90	Pleistocene 2	gap	
LT3	UL2	90	Pleistocene 2	gap	
LT3	UL2	90	Pleistocene 2	gap	
LT3	UL2	90	Pleistocene 2	gap	
LT3	UL2	90	Pleistocene 2	gap	

LT	Locality	Altitude (in m)	Terrace	Taxon	sample
LT3	UL2	90	Pleistocene 2	gap	
LT3	UL2	90	Pleistocene 2	gap	
LT3	UL2	90	Pleistocene 2	gap	
LT3	UL2	90	Pleistocene 2	gap	
LT3	UL2	90	Pleistocene 2	gap	
LT3	UL2	90	Pleistocene 2	gap	
LT3	UL2	90	Pleistocene 2	"Faviidae" indet.	
LT3	UL2	90	Pleistocene 2	gap	
LT3	UL2	90	Pleistocene 2	gap	
LT3	UL2	90	Pleistocene 2	Scleractinia indet.	
LT3	UL2	90	Pleistocene 2	Scleractinia indet.	
LT3	UL2	90	Pleistocene 2	red algae	
LT3	UL2	90	Pleistocene 2	red algae	
LT3	UL2	90	Pleistocene 2	red algae	
LT3	UL2	90	Pleistocene 2	red algae	
LT3	UL2	90	Pleistocene 2	gap	
LT3	UL2	90	Pleistocene 2	*Montipora sp.*	UL2m
LT3	UL2	90	Pleistocene 2	*Montipora sp.*	UL2m
LT3	UL2	90	Pleistocene 2	*Montipora sp.*	UL2m
LT3	UL2	90	Pleistocene 2	*Montipora sp.*	UL2m
LT3	UL2	90	Pleistocene 2	*Montipora sp.*	UL2m
LT3	UL2	90	Pleistocene 2	*Montipora sp.*	UL2m
LT3	UL2	90	Pleistocene 2	*Montipora sp.*	UL2m
LT3	UL2	90	Pleistocene 2	*Montipora sp.*	UL2m
LT4	UL3	125	Pleistocene 2	matrix	
LT4	UL3	125	Pleistocene 2	matrix	
LT4	UL3	125	Pleistocene 2	matrix	
LT4	UL3	125	Pleistocene 2	red algae	
LT4	UL3	125	Pleistocene 2	red algae	
LT4	UL3	125	Pleistocene 2	red algae	
LT4	UL3	125	Pleistocene 2	red algae	
LT4	UL3	125	Pleistocene 2	red algae	
LT4	UL3	125	Pleistocene 2	red algae	
LT4	UL3	125	Pleistocene 2	red algae	
LT4	UL3	125	Pleistocene 2	red algae	
LT4	UL3	125	Pleistocene 2	matrix	
LT4	UL3	125	Pleistocene 2	matrix	
LT4	UL3	125	Pleistocene 2	matrix	
LT4	UL3	125	Pleistocene 2	gap	
LT4	UL3	125	Pleistocene 2	gap	
LT4	UL3	125	Pleistocene 2	gap	
LT4	UL3	125	Pleistocene 2	gap	
LT4	UL3	125	Pleistocene 2	gap	
LT4	UL3	125	Pleistocene 2	gap	
LT4	UL3	125	Pleistocene 2	gap	
LT4	UL3	125	Pleistocene 2	matrix	

LT	Locality	Altitude (in m)	Terrace	Taxon	sample
LT4	UL3	125	Pleistocene 2	matrix	
LT4	UL3	125	Pleistocene 2	matrix	
LT4	UL3	125	Pleistocene 2	matrix	
LT4	UL3	125	Pleistocene 2	gap	
LT4	UL3	125	Pleistocene 2	gap	
LT4	UL3	125	Pleistocene 2	gap	
LT4	UL3	125	Pleistocene 2	gap	
LT4	UL3	125	Pleistocene 2	matrix	UL3a
LT4	UL3	125	Pleistocene 2	matrix	UL3a
LT4	UL3	125	Pleistocene 2	matrix	UL3a
LT4	UL3	125	Pleistocene 2	matrix	UL3a
LT4	UL3	125	Pleistocene 2	matrix	UL3a
LT4	UL3	125	Pleistocene 2	"Faviidae" indet.	
LT4	UL3	125	Pleistocene 2	"Faviidae" indet.	
LT4	UL3	125	Pleistocene 2	"Faviidae" indet.	
LT4	UL3	125	Pleistocene 2	matrix	UL3b
LT4	UL3	125	Pleistocene 2	matrix	UL3b
LT4	UL3	125	Pleistocene 2	matrix	UL3b
LT4	UL3	125	Pleistocene 2	"Faviidae" indet.	UL3c
LT4	UL3	125	Pleistocene 2	"Faviidae" indet.	UL3c
LT4	UL3	125	Pleistocene 2	matrix	
LT4	UL3	125	Pleistocene 2	gap	
LT4	UL3	125	Pleistocene 2	Fungia sp.	UL3d
LT4	UL3	125	Pleistocene 2	matrix	
LT4	UL3	125	Pleistocene 2	matrix	
LT4	UL3	125	Pleistocene 2	matrix	
LT4	UL3	125	Pleistocene 2	matrix	
LT4	UL3	125	Pleistocene 2	gap	
LT4	UL3	125	Pleistocene 2	matrix	UL3e
LT4	UL3	125	Pleistocene 2	matrix	UL3e
LT4	UL3	125	Pleistocene 2	"Faviidae" indet.	
LT4	UL3	125	Pleistocene 2	matrix	
LT4	UL3	125	Pleistocene 2	matrix	
LT4	UL3	125	Pleistocene 2	matrix	
LT4	UL3	125	Pleistocene 2	matrix	
LT4	UL3	125	Pleistocene 2	matrix	
LT4	UL3	125	Pleistocene 2	gap	
LT4	UL3	125	Pleistocene 2	gap	
LT4	UL3	125	Pleistocene 2	gap	
LT4	UL3	125	Pleistocene 2	gap	
LT4	UL3	125	Pleistocene 2	gap	
LT4	UL3	125	Pleistocene 2	gap	
LT4	UL3	125	Pleistocene 2	gap	
LT4	UL3	125	Pleistocene 2	gap	
LT4	UL3	125	Pleistocene 2	gap	
LT4	UL3	125	Pleistocene 2	gap	

LT	Locality	Altitude (in m)	Terrace	Taxon	sample
LT4	UL3	125	Pleistocene 2	gap	
LT4	UL3	125	Pleistocene 2	gap	
LT4	UL3	125	Pleistocene 2	gap	
LT4	UL3	125	Pleistocene 2	gap	
LT4	UL3	125	Pleistocene 2	gap	
LT4	UL3	125	Pleistocene 2	gap	
LT4	UL3	125	Pleistocene 2	gap	
LT4	UL3	125	Pleistocene 2	gap	
LT4	UL3	125	Pleistocene 2	gap	
LT4	UL3	125	Pleistocene 2	gap	
LT4	UL3	125	Pleistocene 2	gap	
LT4	UL3	125	Pleistocene 2	gap	
LT4	UL3	125	Pleistocene 2	gap	
LT4	UL3	125	Pleistocene 2	matrix	
LT4	UL3	125	Pleistocene 2	matrix	
LT4	UL3	125	Pleistocene 2	matrix	
LT4	UL3	125	Pleistocene 2	matrix	
LT4	UL3	125	Pleistocene 2	gap	
LT4	UL3	125	Pleistocene 2	gap	
LT4	UL3	125	Pleistocene 2	gap	
LT4	UL3	125	Pleistocene 2	matrix	
LT4	UL3	125	Pleistocene 2	matrix	
LT4	UL3	125	Pleistocene 2	gap	
LT4	UL3	125	Pleistocene 2	gap	
LT4	UL3	125	Pleistocene 2	gap	
LT4	UL3	125	Pleistocene 2	gap	
LT4	UL3	125	Pleistocene 2	matrix	
LT4	UL3	125	Pleistocene 2	matrix	
LT4	UL3	125	Pleistocene 2	matrix	
LT4	UL3	125	Pleistocene 2	matrix	
LT4	UL3	125	Pleistocene 2	matrix	
LT4	UL3	125	Pleistocene 2	*Dipsastraea sp.*	UL3f
LT4	UL3	125	Pleistocene 2	matrix	
LT4	UL3	125	Pleistocene 2	Fungiidae indet.	
LT4	UL3	125	Pleistocene 2	gap	
LT4	UL3	125	Pleistocene 2	gap	
LT4	UL3	125	Pleistocene 2	gap	
LT4	UL3	125	Pleistocene 2	gap	
LT4	UL3	125	Pleistocene 2	gap	
LT4	UL3	125	Pleistocene 2	gap	
LT4	UL3	125	Pleistocene 2	gap	
LT4	UL3	125	Pleistocene 2	matrix	
LT4	UL3	125	Pleistocene 2	gap	
LT4	UL3	125	Pleistocene 2	gap	
LT4	UL3	125	Pleistocene 2	gap	
LT4	UL3	125	Pleistocene 2	gap	
LT4	UL3	125	Pleistocene 2	gap	

LT	Locality	Altitude (in m)	Terrace	Taxon	sample
LT4	UL3	125	Pleistocene 2	gap	
LT4	UL3	125	Pleistocene 2	gap	
LT4	UL3	125	Pleistocene 2	gap	
LT4	UL3	125	Pleistocene 2	gap	
LT4	UL3	125	Pleistocene 2	gap	
LT4	UL3	125	Pleistocene 2	gap	
LT4	UL3	125	Pleistocene 2	matrix	
LT4	UL3	125	Pleistocene 2	matrix	
LT4	UL3	125	Pleistocene 2	matrix	
LT4	UL3	125	Pleistocene 2	Scleractinia indet.	
LT5	UL1	80	Pleistocene 2	matrix	
LT5	UL1	80	Pleistocene 2	matrix	
LT5	UL1	80	Pleistocene 2	matrix	
LT5	UL1	80	Pleistocene 2	matrix	
LT5	UL1	80	Pleistocene 2	matrix	
LT5	UL1	80	Pleistocene 2	matrix	
LT5	UL1	80	Pleistocene 2	matrix	
LT5	UL1	80	Pleistocene 2	Scleractinia indet.	
LT5	UL1	80	Pleistocene 2	Favites sp.	
LT5	UL1	80	Pleistocene 2	matrix	
LT5	UL1	80	Pleistocene 2	matrix	
LT5	UL1	80	Pleistocene 2	matrix	
LT5	UL1	80	Pleistocene 2	matrix	
LT5	UL1	80	Pleistocene 2	matrix	
LT5	UL1	80	Pleistocene 2	matrix	
LT5	UL1	80	Pleistocene 2	*Cyphastrea sp.*	
LT5	UL1	80	Pleistocene 2	*Tridacna sp.*	
LT5	UL1	80	Pleistocene 2	*Tridacna sp.*	
LT5	UL1	80	Pleistocene 2	matrix	
LT5	UL1	80	Pleistocene 2	matrix	
LT5	UL1	80	Pleistocene 2	gap	
LT5	UL1	80	Pleistocene 2	gap	
LT5	UL1	80	Pleistocene 2	*Favites sp.*	
LT5	UL1	80	Pleistocene 2	*Favites sp.*	
LT5	UL1	80	Pleistocene 2	*Favites sp.*	
LT5	UL1	80	Pleistocene 2	"Faviidae" indet.	
LT5	UL1	80	Pleistocene 2	"Faviidae" indet.	
LT5	UL1	80	Pleistocene 2	gap	
LT5	UL1	80	Pleistocene 2	gap	
LT5	UL1	80	Pleistocene 2	gap	
LT5	UL1	80	Pleistocene 2	gap	
LT5	UL1	80	Pleistocene 2	gap	
LT5	UL1	80	Pleistocene 2	gap	
LT5	UL1	80	Pleistocene 2	gap	
LT5	UL1	80	Pleistocene 2	gap	
LT5	UL1	80	Pleistocene 2	gap	

LT	Locality	Altitude (in m)	Terrace	Taxon	sample
LT5	UL1	80	Pleistocene 2	gap	
LT5	UL1	80	Pleistocene 2	gap	
LT5	UL1	80	Pleistocene 2	gap	
LT5	UL1	80	Pleistocene 2	gap	
LT5	UL1	80	Pleistocene 2	gap	
LT5	UL1	80	Pleistocene 2	gap	
LT5	UL1	80	Pleistocene 2	gap	
LT5	UL1	80	Pleistocene 2	gap	
LT5	UL1	80	Pleistocene 2	gap	
LT5	UL1	80	Pleistocene 2	gap	
LT5	UL1	80	Pleistocene 2	gap	
LT5	UL1	80	Pleistocene 2	gap	
LT5	UL1	80	Pleistocene 2	red algae	
LT5	UL1	80	Pleistocene 2	*Goniastrea retiformis*	UL1b
LT5	UL1	80	Pleistocene 2	*Goniastrea retiformis*	UL1b
LT5	UL1	80	Pleistocene 2	*Goniastrea retiformis*	UL1b
LT5	UL1	80	Pleistocene 2	*Goniastrea retiformis*	UL1b
LT5	UL1	80	Pleistocene 2	*Goniastrea retiformis*	UL1b
LT5	UL1	80	Pleistocene 2	matrix	
LT5	UL1	80	Pleistocene 2	gap	
LT5	UL1	80	Pleistocene 2	gap	
LT5	UL1	80	Pleistocene 2	*Goniastrea retiformis*	
LT5	UL1	80	Pleistocene 2	*Goniastrea retiformis*	
LT5	UL1	80	Pleistocene 2	gap	
LT5	UL1	80	Pleistocene 2	gap	
LT5	UL1	80	Pleistocene 2	gap	
LT5	UL1	80	Pleistocene 2	gap	
LT5	UL1	80	Pleistocene 2	gap	
LT5	UL1	80	Pleistocene 2	gap	
LT5	UL1	80	Pleistocene 2	gap	
LT5	UL1	80	Pleistocene 2	gap	
LT5	UL1	80	Pleistocene 2	gap	
LT5	UL1	80	Pleistocene 2	gap	
LT5	UL1	80	Pleistocene 2	gap	
LT5	UL1	80	Pleistocene 2	gap	
LT5	UL1	80	Pleistocene 2	gap	
LT5	UL1	80	Pleistocene 2	gap	
LT5	UL1	80	Pleistocene 2	gap	
LT5	UL1	80	Pleistocene 2	gap	
LT5	UL1	80	Pleistocene 2	gap	
LT5	UL1	80	Pleistocene 2	gap	
LT5	UL1	80	Pleistocene 2	gap	
LT5	UL1	80	Pleistocene 2	gap	
LT5	UL1	80	Pleistocene 2	gap	
LT5	UL1	80	Pleistocene 2	*Goniastrea sp.*	
LT5	UL1	80	Pleistocene 2	*Goniastrea sp.*	
LT5	UL1	80	Pleistocene 2	*Goniastrea sp.*	
LT5	UL1	80	Pleistocene 2	*Goniastrea sp.*	
LT5	UL1	80	Pleistocene 2	*Goniastrea sp.*	
LT5	UL1	80	Pleistocene 2	*Goniastrea sp.*	
LT5	UL1	80	Pleistocene 2	*Goniastrea sp.*	

LT	Locality	Altitude (in m)	Terrace	Taxon	sample
LT5	UL1	80	Pleistocene 2	*Goniastrea sp.*	
LT5	UL1	80	Pleistocene 2	*Dipsastraea sp.*	UL1c
LT5	UL1	80	Pleistocene 2	*Dipsastraea sp.*	UL1c
LT5	UL1	80	Pleistocene 2	*Dipsastraea sp.*	UL1c
LT5	UL1	80	Pleistocene 2	*Dipsastraea sp.*	UL1c
LT5	UL1	80	Pleistocene 2	*Dipsastraea sp.*	UL1c
LT5	UL1	80	Pleistocene 2	*Dipsastraea sp.*	UL1c
LT5	UL1	80	Pleistocene 2	*Dipsastraea sp.*	UL1c
LT5	UL1	80	Pleistocene 2	*Dipsastraea sp.*	UL1c
LT5	UL1	80	Pleistocene 2	*Dipsastraea sp.*	UL1c
LT5	UL1	80	Pleistocene 2	*Dipsastraea sp.*	UL1c
LT5	UL1	80	Pleistocene 2	*Dipsastraea sp.*	UL1c
LT5	UL1	80	Pleistocene 2	*Dipsastraea sp.*	UL1c
LT5	UL1	80	Pleistocene 2	gap	
LT5	UL1	80	Pleistocene 2	gap	
LT5	UL1	80	Pleistocene 2	gap	
LT5	UL1	80	Pleistocene 2	gap	
LT5	UL1	80	Pleistocene 2	gap	
LT5	UL1	80	Pleistocene 2	*Porites sp.*	UL1d
LT5	UL1	80	Pleistocene 2	*Porites sp.*	UL1d
LT5	UL1	80	Pleistocene 2	*Porites sp.*	UL1d
LT5	UL1	80	Pleistocene 2	*Stylophora sp.*	UL1e
LT5	UL1	80	Pleistocene 2	*Stylophora sp.*	UL1e
LT5	UL1	80	Pleistocene 2	*Stylophora sp.*	UL1e
LT5	UL1	80	Pleistocene 2	*Platygyra sp.*	UL1f
LT5	UL1	80	Pleistocene 2	*Platygyra sp.*	UL1f
LT5	UL1	80	Pleistocene 2	*Stylophora sp.*	UL1g
LT5	UL1	80	Pleistocene 2	*Stylophora sp.*	UL1g
LT5	UL1	80	Pleistocene 2	*Cyphastrea sp.*	
LT5	UL1	80	Pleistocene 2	*Cyphastrea sp.*	
LT5	UL1	80	Pleistocene 2	*Cyphastrea sp.*	
LT5	UL1	80	Pleistocene 2	matrix	
LT5	UL1	80	Pleistocene 2	matrix	
LT5	UL1	80	Pleistocene 2	matrix	
LT5	UL1	80	Pleistocene 2	matrix	
LT5	UL1	80	Pleistocene 2	matrix	
LT5	UL1	80	Pleistocene 2	matrix	
LT6	MP4	297	Pleistocene 3	gap	
LT6	MP4	297	Pleistocene 3	gap	
LT6	MP4	297	Pleistocene 3	*Dipsastraea sp.*	MP4a
LT6	MP4	297	Pleistocene 3	*Dipsastraea sp.*	MP4a
LT6	MP4	297	Pleistocene 3	matrix	
LT6	MP4	297	Pleistocene 3	matrix	
LT6	MP4	297	Pleistocene 3	matrix	
LT6	MP4	297	Pleistocene 3	*Porites sp.*	MP4b

LT	Locality	Altitude (in m)	Terrace	Taxon	sample
LT6	MP4	297	Pleistocene 3	*Porites sp.*	MP4b
LT6	MP4	297	Pleistocene 3	gap	
LT6	MP4	297	Pleistocene 3	gap	
LT6	MP4	297	Pleistocene 3	*Porites sp.*	MP4c
LT6	MP4	297	Pleistocene 3	*Porites sp.*	MP4c
LT6	MP4	297	Pleistocene 3	*Porites sp.*	MP4c
LT6	MP4	297	Pleistocene 3	matrix	MP4d
LT6	MP4	297	Pleistocene 3	matrix	MP4d
LT6	MP4	297	Pleistocene 3	matrix	MP4d
LT6	MP4	297	Pleistocene 3	matrix	MP4d
LT6	MP4	297	Pleistocene 3	gap	
LT6	MP4	297	Pleistocene 3	gap	
LT6	MP4	297	Pleistocene 3	gap	
LT6	MP4	297	Pleistocene 3	gap	
LT6	MP4	297	Pleistocene 3	gap	
LT6	MP4	297	Pleistocene 3	gap	
LT6	MP4	297	Pleistocene 3	gap	
LT6	MP4	297	Pleistocene 3	gap	
LT6	MP4	297	Pleistocene 3	*Platygyra sp.*	MP4e
LT6	MP4	297	Pleistocene 3	Scleractinia indet.	
LT6	MP4	297	Pleistocene 3	Scleractinia indet.	
LT6	MP4	297	Pleistocene 3	red algae	
LT6	MP4	297	Pleistocene 3	red algae	
LT6	MP4	297	Pleistocene 3	red algae	
LT6	MP4	297	Pleistocene 3	red algae	
LT6	MP4	297	Pleistocene 3	*Goniastrea sp.*	MP4f
LT6	MP4	297	Pleistocene 3	gap	
LT6	MP4	297	Pleistocene 3	gap	
LT6	MP4	297	Pleistocene 3	gap	
LT6	MP4	297	Pleistocene 3	gap	
LT6	MP4	297	Pleistocene 3	gap	
LT6	MP4	297	Pleistocene 3	gap	
LT6	MP4	297	Pleistocene 3	gap	
LT6	MP4	297	Pleistocene 3	*Porites sp.*	MP4g
LT6	MP4	297	Pleistocene 3	matrix	
LT6	MP4	297	Pleistocene 3	gap	
LT6	MP4	297	Pleistocene 3	gap	
LT6	MP4	297	Pleistocene 3	gap	
LT6	MP4	297	Pleistocene 3	gap	
LT6	MP4	297	Pleistocene 3	gap	
LT6	MP4	297	Pleistocene 3	gap	
LT6	MP4	297	Pleistocene 3	gap	
LT6	MP4	297	Pleistocene 3	gap	
LT6	MP4	297	Pleistocene 3	gap	
LT6	MP4	297	Pleistocene 3	gap	
LT6	MP4	297	Pleistocene 3	gap	

LT	Locality	Altitude (in m)	Terrace	Taxon	sample
LT6	MP4	297	Pleistocene 3	gap	
LT6	MP4	297	Pleistocene 3	gap	
LT6	MP4	297	Pleistocene 3	gap	
LT6	MP4	297	Pleistocene 3	gap	
LT6	MP4	297	Pleistocene 3	gap	
LT6	MP4	297	Pleistocene 3	gap	
LT6	MP4	297	Pleistocene 3	gap	
LT6	MP4	297	Pleistocene 3	gap	
LT6	MP4	297	Pleistocene 3	gap	
LT6	MP4	297	Pleistocene 3	red algae	
LT6	MP4	297	Pleistocene 3	red algae	
LT6	MP4	297	Pleistocene 3	red algae	
LT6	MP4	297	Pleistocene 3	gap	
LT6	MP4	297	Pleistocene 3	gap	
LT6	MP4	297	Pleistocene 3	*Dipsastraea sp.*	MP4i
LT6	MP4	297	Pleistocene 3	*Goniastrea retiformis*	MP4i
LT6	MP4	297	Pleistocene 3	red algae	
LT6	MP4	297	Pleistocene 3	gap	
LT6	MP4	297	Pleistocene 3	gap	
LT6	MP4	297	Pleistocene 3	*Pocillopora sp.*	MP4j
LT6	MP4	297	Pleistocene 3	gap	
LT6	MP4	297	Pleistocene 3	gap	
LT6	MP4	297	Pleistocene 3	gap	
LT6	MP4	297	Pleistocene 3	gap	
LT6	MP4	297	Pleistocene 3	matrix	
LT6	MP4	297	Pleistocene 3	matrix	
LT6	MP4	297	Pleistocene 3	matrix	
LT6	MP4	297	Pleistocene 3	gap

LT	Locality	Altitude (in m)	Terrace	Taxon	sample
LT6	MP4	297	Pleistocene 3	gap	
LT6	MP4	297	Pleistocene 3	gap	
LT6	MP4	297	Pleistocene 3	gap	
LT6	MP4	297	Pleistocene 3	gap	
LT6	MP4	297	Pleistocene 3	gap	
LT6	MP4	297	Pleistocene 3	red algae	
LT6	MP4	297	Pleistocene 3	gap	
LT6	MP4	297	Pleistocene 3	matrix	
LT6	MP4	297	Pleistocene 3	matrix	
LT6	MP4	297	Pleistocene 3	matrix	
LT6	MP4	297	Pleistocene 3	matrix	
LT6	MP4	297	Pleistocene 3	*Montipora sp.*	MP4k
LT6	MP4	297	Pleistocene 3	gap	
LT6	MP4	297	Pleistocene 3	gap	
LT6	MP4	297	Pleistocene 3	gap	
LT6	MP4	297	Pleistocene 3	red algae	
LT6	MP4	297	Pleistocene 3	gap	
LT6	MP4	297	Pleistocene 3	gap	
LT6	MP4	297	Pleistocene 3	*Porites sp.*	
LT6	MP4	297	Pleistocene 3	*Porites sp.*	
LT6	MP4	297	Pleistocene 3	gap	
LT6	MP4	297	Pleistocene 3	gap	
LT6	MP4	297	Pleistocene 3	gap	
LT6	MP4	297	Pleistocene 3	gap	
LT6	MP4	297	Pleistocene 3	gap	
LT6	MP4	297	Pleistocene 3	gap	
LT6	MP4	297	Pleistocene 3	gap	
LT6	MP4	297	Pleistocene 3	gap	
LT6	MP4	297	Pleistocene 3	gap	
LT6	MP4	297	Pleistocene 3	gap	
LT6	MP4	297	Pleistocene 3	gap	
LT6	MP4	297	Pleistocene 3	gap	
LT6	MP4	297	Pleistocene 3	gap	
LT6	MP4	297	Pleistocene 3	*Favites pentagona*	MP4l
LT6	MP4	297	Pleistocene 3	*Favites pentagona*	MP4l
LT6	MP4	297	Pleistocene 3	gap	
LT6	MP4	297	Pleistocene 3	gap	
LT6	MP4	297	Pleistocene 3	gap	
LT6	MP4	297	Pleistocene 3	gap	
LT6	MP4	297	Pleistocene 3	gap	
LT6	MP4	297	Pleistocene 3	gap	
LT6	MP4	297	Pleistocene 3	gap	
LT6	MP4	297	Pleistocene 3	gap	
LT6	MP4	297	Pleistocene 3	gap	
LT6	MP4	297	Pleistocene 3	gap	
LT6	MP4	297	Pleistocene 3	gap	
LT6	MP4	297	Pleistocene 3	red algae	
LT6	MP4	297	Pleistocene 3	red algae	

LT	Locality	Altitude (in m)	Terrace	Taxon	sample
LT6	MP4	297	Pleistocene 3	red algae	
LT6	MP4	297	Pleistocene 3	red algae	
LT6	MP4	297	Pleistocene 3	red algae	
LT6	MP4	297	Pleistocene 3	red algae	
LT6	MP4	297	Pleistocene 3	*Goniastrea sp.*	MP4m
LT6	MP4	297	Pleistocene 3	*Goniastrea sp.*	MP4m
LT6	MP4	297	Pleistocene 3	*Goniastrea sp.*	MP4m
LT6	MP4	297	Pleistocene 3	*Goniastrea sp.*	MP4m
LT7	MP2	105	Pleistocene 1	Porites sp.	MP2a
LT7	MP2	105	Pleistocene 1	Porites sp.	MP2a
LT7	MP2	105	Pleistocene 1	Porites sp.	MP2b
LT7	MP2	105	Pleistocene 1	Porites sp.	
LT7	MP2	105	Pleistocene 1	*Dipsastraea sp.*	MP2c
LT7	MP2	105	Pleistocene 1	red algae	
LT7	MP2	105	Pleistocene 1	red algae	
LT7	MP2	105	Pleistocene 1	red algae	
LT7	MP2	105	Pleistocene 1	*Platygyra sp.*	
LT7	MP2	105	Pleistocene 1	*Platygyra sp.*	
LT7	MP2	105	Pleistocene 1	matrix	
LT7	MP2	105	Pleistocene 1	matrix	
LT7	MP2	105	Pleistocene 1	matrix	
LT7	MP2	105	Pleistocene 1	Scleractinia indet.	
LT7	MP2	105	Pleistocene 1	Scleractinia indet.	
LT7	MP2	105	Pleistocene 1	*Dipsastraea sp.*	MP2d
LT7	MP2	105	Pleistocene 1	*Dipsastraea sp.*	MP2d
LT7	MP2	105	Pleistocene 1	gap	
LT7	MP2	105	Pleistocene 1	Scleractinia indet.	
LT7	MP2	105	Pleistocene 1	red algae	
LT7	MP2	105	Pleistocene 1	red algae	
LT7	MP2	105	Pleistocene 1	gap	
LT7	MP2	105	Pleistocene 1	gap	
LT7	MP2	105	Pleistocene 1	gap	
LT7	MP2	105	Pleistocene 1	*Platygyra sp.*	MP2e
LT7	MP2	105	Pleistocene 1	*Platygyra sp.*	MP2e
LT7	MP2	105	Pleistocene 1	*Platygyra sp.*	MP2e
LT7	MP2	105	Pleistocene 1	gap	
LT7	MP2	105	Pleistocene 1	gap	
LT7	MP2	105	Pleistocene 1	gap	
LT7	MP2	105	Pleistocene 1	gap	
LT7	MP2	105	Pleistocene 1	gap	
LT7	MP2	105	Pleistocene 1	*Porites sp.*	MP2f
LT7	MP2	105	Pleistocene 1	*Porites sp.*	MP2f
LT7	MP2	105	Pleistocene 1	matrix	
LT7	MP2	105	Pleistocene 1	matrix	
LT7	MP2	105	Pleistocene 1	gap	
LT7	MP2	105	Pleistocene 1	gap	

LT	Locality	Altitude (in m)	Terrace	Taxon	sample
LT7	MP2	105	Pleistocene 1	gap	
LT7	MP2	105	Pleistocene 1	gap	
LT7	MP2	105	Pleistocene 1	gap	
LT7	MP2	105	Pleistocene 1	gap	
LT7	MP2	105	Pleistocene 1	gap	
LT7	MP2	105	Pleistocene 1	gap	
LT7	MP2	105	Pleistocene 1	gap	
LT7	MP2	105	Pleistocene 1	gap	
LT7	MP2	105	Pleistocene 1	gap	
LT7	MP2	105	Pleistocene 1	gap	
LT7	MP2	105	Pleistocene 1	gap	
LT7	MP2	105	Pleistocene 1	gap	
LT7	MP2	105	Pleistocene 1	matrix	
LT7	MP2	105	Pleistocene 1	*Platygyra sp.*	MP2g
LT7	MP2	105	Pleistocene 1	gap	
LT7	MP2	105	Pleistocene 1	matrix	
LT7	MP2	105	Pleistocene 1	matrix	
LT7	MP2	105	Pleistocene 1	gap	
LT7	MP2	105	Pleistocene 1	gap	
LT7	MP2	105	Pleistocene 1	gap	
LT7	MP2	105	Pleistocene 1	*Dipsastraea sp.*	MP2h
LT7	MP2	105	Pleistocene 1	matrix	
LT7	MP2	105	Pleistocene 1	matrix	
LT7	MP2	105	Pleistocene 1	matrix	
LT7	MP2	105	Pleistocene 1	*Porites sp.*	MP2i
LT7	MP2	105	Pleistocene 1	*Porites sp.*	MP2i
LT7	MP2	105	Pleistocene 1	*Porites sp.*	MP2i
LT7	MP2	105	Pleistocene 1	matrix	
LT7	MP2	105	Pleistocene 1	gap	
LT7	MP2	105	Pleistocene 1	gap	
LT7	MP2	105	Pleistocene 1	gap	
LT7	MP2	105	Pleistocene 1	gap	
LT7	MP2	105	Pleistocene 1	gap	
LT7	MP2	105	Pleistocene 1	gap	
LT7	MP2	105	Pleistocene 1	gap	
LT7	MP2	105	Pleistocene 1	gap	
LT7	MP2	105	Pleistocene 1	gap	
LT7	MP2	105	Pleistocene 1	gap	
LT7	MP2	105	Pleistocene 1	gap	
LT7	MP2	105	Pleistocene 1	gap	
LT7	MP2	105	Pleistocene 1	gap	
LT7	MP2	105	Pleistocene 1	gap	
LT7	MP2	105	Pleistocene 1	gap	
LT7	MP2	105	Pleistocene 1	gap	
LT7	MP2	105	Pleistocene 1	gap	
LT7	MP2	105	Pleistocene 1	matrix	MP2j
LT7	MP2	105	Pleistocene 1	gap	
LT7	MP2	105	Pleistocene 1	gap	
LT7	MP2	105	Pleistocene 1	gap	

LT	Locality	Altitude (in m)	Terrace	Taxon	sample
LT7	MP2	105	Pleistocene 1	gap	
LT7	MP2	105	Pleistocene 1	gap	
LT7	MP2	105	Pleistocene 1	gap	
LT7	MP2	105	Pleistocene 1	gap	
LT7	MP2	105	Pleistocene 1	gap	
LT7	MP2	105	Pleistocene 1	matrix	
LT7	MP2	105	Pleistocene 1	matrix	
LT7	MP2	105	Pleistocene 1	gap	
LT7	MP2	105	Pleistocene 1	gap	
LT7	MP2	105	Pleistocene 1	gap	
LT7	MP2	105	Pleistocene 1	gap	
LT7	MP2	105	Pleistocene 1	matrix	
LT7	MP2	105	Pleistocene 1	matrix	
LT7	MP2	105	Pleistocene 1	matrix	
LT7	MP2	105	Pleistocene 1	matrix	
LT7	MP2	105	Pleistocene 1	matrix	
LT7	MP2	105	Pleistocene 1	matrix	
LT7	MP2	105	Pleistocene 1	gap	
LT7	MP2	105	Pleistocene 1	*Galaxea astreata*	MP2l
LT7	MP2	105	Pleistocene 1	gap	
LT7	MP2	105	Pleistocene 1	gap	
LT7	MP2	105	Pleistocene 1	gap	
LT7	MP2	105	Pleistocene 1	gap	
LT7	MP2	105	Pleistocene 1	gap	
LT7	MP2	105	Pleistocene 1	matrix	
LT7	MP2	105	Pleistocene 1	Scleractinia indet.	
LT7	MP2	105	Pleistocene 1	*Porites sp.*	MP2m
LT7	MP2	105	Pleistocene 1	*Porites sp.*	MP2m
LT7	MP2	105	Pleistocene 1	*Porites sp.*	MP2m
LT7	MP2	105	Pleistocene 1	*Porites sp.*	MP2m
LT7	MP2	105	Pleistocene 1	*Porites sp.*	MP2m
LT7	MP2	105	Pleistocene 1	*Porites sp.*	MP2m
LT7	MP2	105	Pleistocene 1	*Porites sp.*	MP2m
LT7	MP2	105	Pleistocene 1	*Porites sp.*	MP2m
LT7	MP2	105	Pleistocene 1	*Porites sp.*	MP2m
LT7	MP2	105	Pleistocene 1	*Porites sp.*	MP2m
LT7	MP2	105	Pleistocene 1	*Porites sp.*	MP2m
LT7	MP2	105	Pleistocene 1	*Porites sp.*	
LT7	MP2	105	Pleistocene 1	*Porites sp.*	
LT7	MP2	105	Pleistocene 1	*Porites sp.*	
LT7	MP2	105	Pleistocene 1	matrix	
LT7	MP2	105	Pleistocene 1	matrix	
LT7	MP2	105	Pleistocene 1	matrix	
LT7	MP2	105	Pleistocene 1	"Faviidae" indet.	MP2n
LT7	MP2	105	Pleistocene 1	matrix	
LT7	MP2	105	Pleistocene 1	matrix	

LT	Locality	Altitude (in m)	Terrace	Taxon	sample
LT7	MP2	105	Pleistocene 1	matrix	
LT7	MP2	105	Pleistocene 1	matrix	
LT7	MP2	105	Pleistocene 1	matrix	
LT7	MP2	105	Pleistocene 1	matrix	
LT7	MP2	105	Pleistocene 1	matrix	
LT7	MP2	105	Pleistocene 1	matrix	
LT7	MP2	105	Pleistocene 1	Porites sp.	
LT7	MP2	105	Pleistocene 1	Porites sp.	
LT7	MP2	105	Pleistocene 1	matrix	
LT7	MP2	105	Pleistocene 1	matrix	
LT7	MP2	105	Pleistocene 1	matrix	
LT7	MP2	105	Pleistocene 1	Porites sp.	MP2o
LT7	MP2	105	Pleistocene 1	Porites sp.	MP2o
LT7	MP2	105	Pleistocene 1	"Faviidae" indet.	MP2p
LT7	MP2	105	Pleistocene 1	matrix	
LT7	MP2	105	Pleistocene 1	matrix	
LT7	MP2	105	Pleistocene 1	gap	
LT7	MP2	105	Pleistocene 1	gap	
LT7	MP2	105	Pleistocene 1	gap	
LT7	MP2	105	Pleistocene 1	gap	
LT7	MP2	105	Pleistocene 1	gap	
LT8	MP2	105	Pleistocene 1	matrix	
LT8	MP2	105	Pleistocene 1	matrix	
LT8	MP2	105	Pleistocene 1	matrix	
LT8	MP2	105	Pleistocene 1	matrix	
LT8	MP2	105	Pleistocene 1	matrix	
LT8	MP2	105	Pleistocene 1	red algae	
LT8	MP2	105	Pleistocene 1	red algae	
LT8	MP2	105	Pleistocene 1	gap	
LT8	MP2	105	Pleistocene 1	red algae	
LT8	MP2	105	Pleistocene 1	matrix	
LT8	MP2	105	Pleistocene 1	matrix	
LT8	MP2	105	Pleistocene 1	matrix	
LT8	MP2	105	Pleistocene 1	matrix	
LT8	MP2	105	Pleistocene 1	"Faviidae" indet.	MP2q
LT8	MP2	105	Pleistocene 1	matrix	
LT8	MP2	105	Pleistocene 1	matrix	
LT8	MP2	105	Pleistocene 1	matrix	
LT8	MP2	105	Pleistocene 1	gap	
LT8	MP2	105	Pleistocene 1	matrix	
LT8	MP2	105	Pleistocene 1	matrix	
LT8	MP2	105	Pleistocene 1	*Dipsastraea sp.*	MP2r
LT8	MP2	105	Pleistocene 1	*Dipsastraea sp.*	MP2r
LT8	MP2	105	Pleistocene 1	matrix	
LT8	MP2	105	Pleistocene 1	matrix	
LT8	MP2	105	Pleistocene 1	matrix	

LT	Locality	Altitude (in m)	Terrace	Taxon	sample
LT8	MP2	105	Pleistocene 1	matrix	
LT8	MP2	105	Pleistocene 1	matrix	
LT8	MP2	105	Pleistocene 1	matrix	
LT8	MP2	105	Pleistocene 1	matrix	
LT8	MP2	105	Pleistocene 1	matrix	
LT8	MP2	105	Pleistocene 1	matrix	
LT8	MP2	105	Pleistocene 1	matrix	
LT8	MP2	105	Pleistocene 1	matrix	
LT8	MP2	105	Pleistocene 1	matrix	
LT8	MP2	105	Pleistocene 1	*Porites sp.*	MP2s
LT8	MP2	105	Pleistocene 1	matrix	
LT8	MP2	105	Pleistocene 1	matrix	
LT8	MP2	105	Pleistocene 1	*Leptoria phrygia*	MP2t
LT8	MP2	105	Pleistocene 1	*Leptoria phrygia*	MP2t
LT8	MP2	105	Pleistocene 1	matrix	
LT8	MP2	105	Pleistocene 1	matrix	
LT8	MP2	105	Pleistocene 1	matrix	
LT8	MP2	105	Pleistocene 1	matrix	
LT8	MP2	105	Pleistocene 1	Dipsastraea sp.	MP2u
LT8	MP2	105	Pleistocene 1	matrix	
LT8	MP2	105	Pleistocene 1	matrix	
LT8	MP2	105	Pleistocene 1	*Porites sp.*	
LT8	MP2	105	Pleistocene 1	matrix	
LT8	MP2	105	Pleistocene 1	matrix	
LT8	MP2	105	Pleistocene 1	matrix	
LT8	MP2	105	Pleistocene 1	matrix	
LT8	MP2	105	Pleistocene 1	matrix	
LT8	MP2	105	Pleistocene 1	gap	
LT8	MP2	105	Pleistocene 1	gap	
LT8	MP2	105	Pleistocene 1	gap	
LT8	MP2	105	Pleistocene 1	*Porites sp.*	MP2v
LT8	MP2	105	Pleistocene 1	*Porites sp.*	MP2v
LT8	MP2	105	Pleistocene 1	*Porites sp.*	MP2v
LT8	MP2	105	Pleistocene 1	*Porites sp.*	MP2v
LT8	MP2	105	Pleistocene 1	gap	
LT8	MP2	105	Pleistocene 1	matrix	
LT8	MP2	105	Pleistocene 1	*Montipora sp.*	MP2w
LT8	MP2	105	Pleistocene 1	matrix	
LT8	MP2	105	Pleistocene 1	matrix	
LT8	MP2	105	Pleistocene 1	*Porites sp.*	MP2x
LT8	MP2	105	Pleistocene 1	*Porites sp.*	MP2x
LT8	MP2	105	Pleistocene 1	*Porites sp.*	MP2x
LT8	MP2	105	Pleistocene 1	*Porites sp.*	MP2x
LT8	MP2	105	Pleistocene 1	*Leptoria phrygia*	MP2y
LT8	MP2	105	Pleistocene 1	matrix	
LT8	MP2	105	Pleistocene 1	*Porites sp.*	MP2z

LT	Locality	Altitude (in m)	Terrace	Taxon	sample
LT8	MP2	105	Pleistocene 1	matrix	
LT8	MP2	105	Pleistocene 1	*Leptoria phrygia*	MP2a1
LT8	MP2	105	Pleistocene 1	*Leptoria phrygia*	MP2a1
LT8	MP2	105	Pleistocene 1	matrix	
LT8	MP2	105	Pleistocene 1	matrix	
LT8	MP2	105	Pleistocene 1	*Dipsastraea sp.*	MP2a3
LT8	MP2	105	Pleistocene 1	*Dipsastraea sp.*	MP2a3
LT8	MP2	105	Pleistocene 1	matrix	
LT8	MP2	105	Pleistocene 1	"Faviidae" indet.	MP2a4
LT8	MP2	105	Pleistocene 1	matrix	
LT8	MP2	105	Pleistocene 1	matrix	
LT8	MP2	105	Pleistocene 1	matrix	
LT8	MP2	105	Pleistocene 1	matrix	
LT8	MP2	105	Pleistocene 1	*Porites sp.*	
LT8	MP2	105	Pleistocene 1	*Porites sp.*	
LT8	MP2	105	Pleistocene 1	*Porites sp.*	
LT8	MP2	105	Pleistocene 1	matrix	
LT8	MP2	105	Pleistocene 1	matrix	
LT8	MP2	105	Pleistocene 1	matrix	
LT8	MP2	105	Pleistocene 1	matrix	
LT8	MP2	105	Pleistocene 1	matrix	
LT8	MP2	105	Pleistocene 1	matrix	
LT8	MP2	105	Pleistocene 1	matrix	
LT8	MP2	105	Pleistocene 1	*Porites sp.*	MP2a5
LT8	MP2	105	Pleistocene 1	matrix	
LT8	MP2	105	Pleistocene 1	*Galaxea sp.*	MP2a6
LT8	MP2	105	Pleistocene 1	*Porites sp.*	MP2a7
LT8	MP2	105	Pleistocene 1	*Porites sp.*	MP2a7
LT8	MP2	105	Pleistocene 1	matrix	
LT8	MP2	105	Pleistocene 1	*Lobophyllia sp.*	MP2a8
LT8	MP2	105	Pleistocene 1	matrix	
LT8	MP2	105	Pleistocene 1	matrix	
LT8	MP2	105	Pleistocene 1	matrix	
LT8	MP2	105	Pleistocene 1	matrix	
LT8	MP2	105	Pleistocene 1	matrix	
LT8	MP2	105	Pleistocene 1	matrix	
LT8	MP2	105	Pleistocene 1	matrix	
LT8	MP2	105	Pleistocene 1	matrix	
LT8	MP2	105	Pleistocene 1	matrix	
LT8	MP2	105	Pleistocene 1	matrix	
LT8	MP2	105	Pleistocene 1	matrix	
LT8	MP2	105	Pleistocene 1	matrix	
LT8	MP2	105	Pleistocene 1	*Porites sp.*	
LT8	MP2	105	Pleistocene 1	*Porites sp.*	MP2a9
LT8	MP2	105	Pleistocene 1	matrix	
LT8	MP2	105	Pleistocene 1	*Porites sp.*	
LT8	MP2	105	Pleistocene 1	matrix	

LT	Locality	Altitude (in m)	Terrace	Taxon	sample
LT8	MP2	105	Pleistocene 1	*Porites sp.*	MP2a10
LT9	Sa1	0	Holocene	matrix	
LT9	Sa1	0	Holocene	matrix	
LT9	Sa1	0	Holocene	matrix	
LT9	Sa1	0	Holocene	matrix	
LT9	Sa1	0	Holocene	matrix	
LT9	Sa1	0	Holocene	matrix	
LT9	Sa1	0	Holocene	matrix	
LT9	Sa1	0	Holocene	matrix	
LT9	Sa1	0	Holocene	matrix	
LT9	Sa1	0	Holocene	*Favites sp.*	
LT9	Sa1	0	Holocene	*Montipora sp.*	Sa1a
LT9	Sa1	0	Holocene	matrix	
LT9	Sa1	0	Holocene	*Montipora sp.*	Sa1b
LT9	Sa1	0	Holocene	matrix	
LT9	Sa1	0	Holocene	matrix	
LT9	Sa1	0	Holocene	matrix	
LT9	Sa1	0	Holocene	*Dipsastraea sp.*	
LT9	Sa1	0	Holocene	*Dipsastraea sp.*	
LT9	Sa1	0	Holocene	*Platygyra sp.*	
LT9	Sa1	0	Holocene	*Platygyra sp.*	
LT9	Sa1	0	Holocene	matrix	
LT9	Sa1	0	Holocene	matrix	
LT9	Sa1	0	Holocene	matrix	
LT9	Sa1	0	Holocene	matrix	
LT9	Sa1	0	Holocene	matrix	
LT9	Sa1	0	Holocene	matrix	
LT9	Sa1	0	Holocene	red algae	
LT9	Sa1	0	Holocene	matrix	
LT9	Sa1	0	Holocene	matrix	
LT9	Sa1	0	Holocene	matrix	
LT9	Sa1	0	Holocene	matrix	
LT9	Sa1	0	Holocene	matrix	
LT9	Sa1	0	Holocene	matrix	
LT9	Sa1	0	Holocene	*Goniastrea sp.*	
LT9	Sa1	0	Holocene	*Goniastrea sp.*	
LT9	Sa1	0	Holocene	matrix	
LT9	Sa1	0	Holocene	*Acropora monticulosa*	
LT9	Sa1	0	Holocene	*Acropora monticulosa*	
LT9	Sa1	0	Holocene	matrix	
LT9	Sa1	0	Holocene	matrix	
LT9	Sa1	0	Holocene	matrix	
LT9	Sa1	0	Holocene	matrix	
LT9	Sa1	0	Holocene	*Acropora monticulosa*	Sa1c
LT9	Sa1	0	Holocene	*Acropora monticulosa*	Sa1c
LT9	Sa1	0	Holocene	*Acropora monticulosa*	Sa1c

LT	Locality	Altitude (in m)	Terrace	Taxon	sample
LT9	Sa1	0	Holocene	*Acropora monticulosa*	Sa1c
LT9	Sa1	0	Holocene	matrix	
LT9	Sa1	0	Holocene	*Porites sp.*	
LT9	Sa1	0	Holocene	gap	
LT9	Sa1	0	Holocene	*Pocillopora sp.*	Sa1d
LT9	Sa1	0	Holocene	red algae	
LT9	Sa1	0	Holocene	*Porites sp.*	
LT9	Sa1	0	Holocene	red algae	
LT9	Sa1	0	Holocene	matrix	
LT9	Sa1	0	Holocene	*Porites sp.*	Sa1e
LT9	Sa1	0	Holocene	*Porites sp.*	Sa1e
LT9	Sa1	0	Holocene	*Porites sp.*	Sa1e
LT9	Sa1	0	Holocene	*Porites sp.*	Sa1e
LT9	Sa1	0	Holocene	*Goniastrea sp.*	
LT9	Sa1	0	Holocene	*Goniastrea sp.*	
LT9	Sa1	0	Holocene	*Porites sp.*	
LT9	Sa1	0	Holocene	*Goniastrea sp.*	Sa1f
LT9	Sa1	0	Holocene	matrix	SA1g
LT9	Sa1	0	Holocene	*Porites sp.*	
LT9	Sa1	0	Holocene	*Goniastrea sp.*	
LT9	Sa1	0	Holocene	*Goniastrea sp.*	
LT9	Sa1	0	Holocene	*Goniastrea sp.*	Sa1h
LT9	Sa1	0	Holocene	*Goniastrea sp.*	Sa1h
LT9	Sa1	0	Holocene	*Goniastrea sp.*	Sa1h
LT9	Sa1	0	Holocene	*Dipsastraea sp.*	
LT9	Sa1	0	Holocene	*Porites sp.*	Sa1i
LT9	Sa1	0	Holocene	*Cyphastrea sp.*	Sa1k
LT9	Sa1	0	Holocene	*Cyphastrea sp.*	Sa1k
LT9	Sa1	0	Holocene	*Cyphastrea sp.*	Sa1k
LT9	Sa1	0	Holocene	matrix	
LT9	Sa1	0	Holocene	matrix	
LT9	Sa1	0	Holocene	gap	
LT9	Sa1	0	Holocene	gap	
LT9	Sa1	0	Holocene	gap	
LT9	Sa1	0	Holocene	gap	
LT9	Sa1	0	Holocene	gap	
LT9	Sa1	0	Holocene	gap	
LT9	Sa1	0	Holocene	gap	
LT9	Sa1	0	Holocene	gap	
LT9	Sa1	0	Holocene	gap	
LT9	Sa1	0	Holocene	gap	
LT9	Sa1	0	Holocene	gap	
LT9	Sa1	0	Holocene	gap	
LT9	Sa1	0	Holocene	gap	
LT9	Sa1	0	Holocene	gap	
LT9	Sa1	0	Holocene	gap	

LT	Locality	Altitude (in m)	Terrace	Taxon	sample
LT9	Sa1	0	Holocene	gap	
LT9	Sa1	0	Holocene	gap	
LT9	Sa1	0	Holocene	gap	
LT9	Sa1	0	Holocene	gap	
LT9	Sa1	0	Holocene	gap	
LT9	Sa1	0	Holocene	red algae	
LT9	Sa1	0	Holocene	*Porites sp.*	
LT9	Sa1	0	Holocene	gap	
LT9	Sa1	0	Holocene	gap	
LT9	Sa1	0	Holocene	matrix	
LT9	Sa1	0	Holocene	matrix	
LT9	Sa1	0	Holocene	matrix	
LT9	Sa1	0	Holocene	matrix	
LT9	Sa1	0	Holocene	*Acropora monticulosa*	Sa1m
LT9	Sa1	0	Holocene	red algae	
LT9	Sa1	0	Holocene	red algae	
LT9	Sa1	0	Holocene	*Porites sp.*	Sa1n
LT9	Sa1	0	Holocene	*Porites sp.*	Sa1n
LT9	Sa1	0	Holocene	*Porites sp.*	Sa1o
LT9	Sa1	0	Holocene	*Porites sp.*	Sa1o
LT9	Sa1	0	Holocene	red algae	
LT9	Sa1	0	Holocene	*Goniastrea sp.*	Sa1q
LT9	Sa1	0	Holocene	*Cyphastrea sp.*	Sa1r
LT9	Sa1	0	Holocene	*Cyphastrea sp.*	Sa1r
LT9	Sa1	0	Holocene	red algae	
LT9	Sa1	0	Holocene	red algae	
LT9	Sa1	0	Holocene	red algae	
LT9	Sa1	0	Holocene	*Favites sp.*	
LT9	Sa1	0	Holocene	red algae	
LT9	Sa1	0	Holocene	red algae	
LT9	Sa1	0	Holocene	matrix	
LT9	Sa1	0	Holocene	Porites sp.	
LT9	Sa1	0	Holocene	Porites sp.	
LT9	Sa1	0	Holocene	Porites sp.	
LT9	Sa1	0	Holocene	matrix	

Table 6-II: Complete bulk-sampling dataset from Vanuatu:

Locality	Altitude	Terrace	Taxon	Sample
SP1	0	Holocene	*Goniopora minor*	SP1f
SP1	0	Holocene	*Lobophyllia hemprichii*	
SP1	0	Holocene	*Porites cylindrica*	
SP1	0	Holocene	*Goniopora sp.*	
SP1	0	Holocene	*Acropora sp.*	
SP1	0	Holocene	*Goniopora sp.*	
SP1	0	Holocene	*Lobophyllia sp.*	SP1a
SP1	0	Holocene	*Dipsastraea sp.*	
SP1	0	Holocene	*Stylophora pistillata*	SP1b
SP1	0	Holocene	*Tubipora musica*	
SP1	0	Holocene	*Fungia sp.*	
SP1	0	Holocene	*Porites sp.*	SP1d
SP1	0	Holocene	*Lobophyllia corymbosa*	SP1c
SP1	0	Holocene	*Cyphastrea sp.*	SP1e
SP1	0	Holocene	*Pavona varians*	SP1g
SP1	0	Holocene	*Dipsastraea sp.*	SP1h
SP1	0	Holocene	*Astreopora myriophthalma*	SP1i
SP1	0	Holocene	*Acropora sp.*	SP1j
SP1	0	Holocene	*Goniopora minor*	SP1k
SP1	0	Holocene	*Tridacna sp.*	
SP1	0	Holocene	*Montipora sp.*	
SP1	0	Holocene	*Porites sp.*	SP1l
SP1	0	Holocene	*Dipsastraea sp.*	SP1m
SP1	0	Holocene	*Goniastrea edwardsi*	
SP1	0	Holocene	*Acropora sp.*	SP1n
SP1	0	Holocene	*Porites sp.*	SP1o
SP1	0	Holocene	*Fungia sp.*	SP1p
SP1	0	Holocene	*Galaxea sp.*	SP1q
Sa1	0	Holocene	*Goniastrea sp.*	
Sa1	0	Holocene	*Goniastrea sp.*	
Sa1	0	Holocene	*Goniastrea sp.*	
Sa1	0	Holocene	*Goniastrea sp.*	
Sa1	0	Holocene	*Goniastrea sp.*	
Sa1	0	Holocene	*Porites sp.*	
Sa1	0	Holocene	*Porites sp.*	
Sa1	0	Holocene	*Goniastrea sp.*	
Sa1	0	Holocene	*Goniastrea sp.*	
Sa1	0	Holocene	*Porites sp.*	
Sa1	0	Holocene	*Astrea sp.*	
Sa1	0	Holocene	*Lobophyllia hemprichii*	
Sa1	0	Holocene	*Pocillopora sp.*	SA1Ba
Sa1	0	Holocene	*Goniastrea sp.*	
Sa1	0	Holocene	*Goniastrea sp.*	
Sa1	0	Holocene	*Goniastrea sp.*	
Sa1	0	Holocene	*Goniastrea sp.*	
Sa1	0	Holocene	*Favites sp.*	
Sa1	0	Holocene	*Goniastrea sp.*	
Sa1	0	Holocene	*Goniastrea sp.*	
Sa1	0	Holocene	*Goniastrea sp.*	
Sa1	0	Holocene	*Platygyra sp.*	
Sa1	0	Holocene	*Goniastrea sp.*	
Sa1	0	Holocene	*Platygyra sp.*	

Locality	Altitude	Terrace	Taxon	Sample
Sa1	0	Holocene	*Symphyllia sp.*	
Sa1	0	Holocene	*Porites sp.*	
Sa1	0	Holocene	*Porites sp.*	
Sa1	0	Holocene	*Goniastrea sp.*	
Sa1	0	Holocene	*Goniastrea sp.*	
Sa1	0	Holocene	*Porites sp.*	
Sa1	0	Holocene	*Porites sp.*	
Sa1	0	Holocene	*Goniopora sp.*	
Sa1	0	Holocene	*Goniastrea sp.*	
Sa1	0	Holocene	*Porites sp.*	
Sa1	0	Holocene	*Montipora sp.*	
SP	0	Holocene	*Sandalolitha robusta*	SPJa
SP	0	Holocene	*Fungia sp.*	SPJb
SP	0	Holocene	*Goniopora tenuidens*	SPJc
SP	0	Holocene	*Turbinaria sp.*	SPJd
SP	0	Holocene	*Porites sp.*	SPJe
SP	0	Holocene	*Porites lobata/lutea*	SPJf
SP	0	Holocene	*Montipora sp.*	SPJg
SP	0	Holocene	*Acanthastrea echinata*	SPJh
SP	0	Holocene	*Acropora sp.*	SPJi
SP	0	Holocene	*Pavona varians*	SPJj
SP	0	Holocene	*Pavona cactus*	SPJk
SP	0	Holocene	*Montipora sp.*	SPJl
SP	0	Holocene	*Pocillopora damicornis*	SPJm
SP	0	Holocene	*Porites lobata/lutea*	SPJn
SP	0	Holocene	*Porites sp.*	SPJo
SP	0	Holocene	*Acropora sp.*	SPJp
SP	0	Holocene	*Fungia sp.*	SPJq
SP	0	Holocene	*Fungia sp.*	SPJr
SP	0	Holocene	*Stylophora sp.*	SPJs
SP	0	Holocene	*Porites sp.*	SPJt
SP	0	Holocene	*Porites sp.*	SPJu
SP	0	Holocene	*Porites sp.*	SPJv
SP	0	Holocene	*Sandalolitha robusta*	SPJx
SP	0	Holocene	*Montipora sp.*	SPJy
SP	0	Holocene	*Acropora sp.*	SPJz
SP	0	Holocene	*Stylophora pistillata*	SPJaa
SP	0	Holocene	*Galaxea sp.*	SPJab
SP	0	Holocene	*Acropora sp.*	SPJad
SP	0	Holocene	*Porites sp.*	SPJae
SP	0	Holocene	*Lobophyllia sp.*	SPJaf
SP	0	Holocene	*Acropora sp.*	SPJaf
SP	0	Holocene	*Acropora sp.*	SPJag
SP	0	Holocene	*Acropora sp.*	SPJah
SP	0	Holocene	*Goniopora sp.*	SPJah
SP	0	Holocene	*Fungia sp.*	SPJai
SP	0	Holocene	*Goniastrea sp.*	SPJaj
SP	0	Holocene	*Acropora sp.*	SPJak
SP	0	Holocene	*Acropora sp.*	SPJak
SP	0	Holocene	*Acropora sp.*	SPJak
SP	0	Holocene	*Acropora sp.*	SPJak
SP	0	Holocene	*Acropora sp.*	SPJak
SP	0	Holocene	*Acropora sp.*	SPJak
SP	0	Holocene	*Acropora sp.*	SPJak

Locality	Altitude	Terrace	Taxon	Sample
SP	0	Holocene	*Acropora sp.*	SPJak
SP	0	Holocene	*Acropora sp.*	SPJak
SP	0	Holocene	*Acropora sp.*	SPJak
SP	0	Holocene	*Porites sp.*	SPJak
SP	0	Holocene	*Pocillopora damicornis*	SPJal
SP	0	Holocene	*Porites sp.*	SPJam
SP	0	Holocene	*Montipora sp.*	SPJan
SP	0	Holocene	*Goniopora sp.*	SPJao
SP	0	Holocene	*Porites sp.*	SPJap
SP	0	Holocene	*Stylophora sp.*	SPJaq
SP	0	Holocene	*Alveopora sp.*	SPJar
SP	0	Holocene	*Lobophyllia sp*	SPJas
SP	0	Holocene	*Porites sp.*	SPJat
SP	0	Holocene	*Goniastrea sp.*	SPJau
SP	0	Holocene	*Montipora sp.*	SPJax
SP	0	Holocene	*Montipora sp.*	SPJay
SP	0	Holocene	*Montipora sp.*	SPJaz
SP	0	Holocene	*Pocillopora verrucosa*	Pocillopora_sp_SA.tif
SP	0	Holocene	*Pavona varians*	Pavona_SA.tif
SP	0	Holocene	*Acanthastrea echinata*	Acanthastrea_sp_SA.tif
SP	0	Holocene	*Galaxea sp.*	Galaxea_sp_SA.tif
SP	0	Holocene	*Lobophyllia corymbosa*	Lobophyllia_corymbosa_SA.tif
SP	0	Holocene	*Lobophyllia hemprichii*	Lobophyllia_hemprichii_SA.tif
SP	0	Holocene	*Lobophyllia hemprichii*	Lobophyllia_hemprichii2_SA.tif
SP	0	Holocene	*Tubipora musica*	Tubipora_musica_SA.tif
SP	0	Holocene	*Astreopora myriophthalma*	Astreopora_ myriophthalmy_SA.tif
SP	0	Holocene	*Mycedium sp.*	SPJba
SP	0	Holocene	*Echinopora sp.*	SPJbb
SP	0	Holocene	*Echinopora sp.*	SPJbc
SP	0	Holocene	*Acropora sp.*	SPJbd
SP	0	Holocene	*Turbinaria sp.*	SPJbe
SP	0	Holocene	*Porites sp.*	SPJbf
SP	0	Holocene	*Goniopora sp.*	SPJbg
SP	0	Holocene	*Fungia sp.*	SPJbh
SP	0	Holocene	*Porites sp.*	SPJbi
SP	0	Holocene	*Alveopora sp.*	SPJbj
SP	0	Holocene	Scleractinia indet.	SPJbk
SP	0	Holocene	*Acropora sp.*	SPJbl
SP	0	Holocene	Scleractinia indet.	SPJbm
SP	0	Holocene	*Acropora sp.*	SPJbn
SP	0	Holocene	Argariciidae indet.	SPJbo
SP	0	Holocene	*Goniopora sp.*	SPJbp
SP	0	Holocene	*Montipora sp.*	SPJbq
SP	0	Holocene	*Montipora sp.*	SPJbr
La	10	Pleistocene 1	*Porites sp.*	La1S1
LA	10	Pleistocene 1	*Porites sp.*	La1S2
ULW	20	Pleistocene 1	*Porites sp.*	ULW1
MP1	40	Pleistocene 1	*Porites sp.*	
MP1	40	Pleistocene 1	*Porites sp.*	MP1Ba
MP1	40	Pleistocene 1	*Porites sp.*	
MP1	40	Pleistocene 1	"Faviidae" indet.	MP1Bb
MP1	40	Pleistocene 1	*Porites sp.*	
MP1	40	Pleistocene 1	*Dipsastraea sp.*	
MP1	40	Pleistocene 1	*Porites sp.*	

Locality	Altitude	Terrace	Taxon	Sample
MP1	40	Pleistocene 1	*Porites sp.*	
MP1	40	Pleistocene 1	*Porites sp.*	
MP1	40	Pleistocene 1	*Porites sp.*	
MP1	40	Pleistocene 1	*Porites sp.*	
MP1	40	Pleistocene 1	*Porites sp.*	
MP1	40	Pleistocene 1	*Dipsastraea sp.*	
MP1	40	Pleistocene 1	Scleractinia indet.	
MP1	40	Pleistocene 1	*Porites sp.*	
MP1	40	Pleistocene 1	*Goniastrea sp.*	
MP1	40	Pleistocene 1	*Porites sp.*	
MP1	40	Pleistocene 1	*Millepora sp.*	MP1Bc
MP1	40	Pleistocene 1	"Faviidae" indet.	
MP1	40	Pleistocene 1	"Faviidae" indet.	
MP1	40	Pleistocene 1	"Faviidae" indet.	
MP1	40	Pleistocene 1	*Porites sp.*	MP1Be
MP1	40	Pleistocene 1	*Goniastrea sp.*	MP1Bd
MP1	40	Pleistocene 1	*Favits sp.*	
MP1	40	Pleistocene 1	*Goniastrea sp.*	
MP1	40	Pleistocene 1	*Porites sp.*	MP1Bf
MP1	40	Pleistocene 1	*Goniastrea sp.*	
MP1	40	Pleistocene 1	*Lobophyllia sp.*	MP1Bg
MP1	40	Pleistocene 1	*Montipora sp.*	
MP1	40	Pleistocene 1	*Cyphastrea sp.*	
MP1	40	Pleistocene 1	*Goniastrea sp.*	
MP1	40	Pleistocene 1	*Porites lobata/lutea*	
MP1	40	Pleistocene 1	*Astrea sp.*	
MP1	40	Pleistocene 1	*Porites sp.*	
MP1	40	Pleistocene 1	*Platygyra sp.*	
MP1	40	Pleistocene 1	*Galaxea astreata*	
MP1	40	Pleistocene 1	*Porites lobata/lutea*	
MP1	40	Pleistocene 1	*Porites lobata/lutea*	
MP1	40	Pleistocene 1	*Lobophyllia sp.*	
MP1	40	Pleistocene 1	*Leptoseris sp.*	MP1Bh
MP1	40	Pleistocene 1	*Porites lobata/lutea*	same sample
MP1	40	Pleistocene 1	*Fungia sp.*	
MP1	40	Pleistocene 1	*Acropora sp.*	MP1Bi
MP1	40	Pleistocene 1	*Leptoria phrygia*	
MP1	40	Pleistocene 1	*Porites sp.*	
MP1	40	Pleistocene 1	*Acropora sp.*	MP1Bi
MP1	40	Pleistocene 1	*Acropora sp.*	MP1Bi
MP1	40	Pleistocene 1	"Faviidae" indet.	
MP1	40	Pleistocene 1	*Montipora sp.*	
MP1	40	Pleistocene 1	*Lobophyllia sp.*	
MP1	40	Pleistocene 1	*Fungia sp.*	
MP1	40	Pleistocene 1	*Lobophyllia sp.*	
MP1	40	Pleistocene 1	*Montipora sp.*	
MP1	40	Pleistocene 1	*Stylocoeniella guentheri*	
MP1	40	Pleistocene 1	*Dipsastraea sp.*	
MP1	40	Pleistocene 1	*Dipsastraea sp.*	
MP1	40	Pleistocene 1	*Goniopora sp.*	
MP1	40	Pleistocene 1	*Goniastrea sp.*	
MP1	40	Pleistocene 1	*Goniastrea sp.*	
MP1	40	Pleistocene 1	*Porites sp.*	
MP1	40	Pleistocene 1	*Acropora sp.*	MP1Bi

Locality	Altitude	Terrace	Taxon	Sample
MP1	40	Pleistocene 1	*Acropora sp.*	MP1Bi
MP1	40	Pleistocene 1	*Cyphastrea sp.*	
MP1	40	Pleistocene 1	*Porites sp.*	
MP1	40	Pleistocene 1	*Turbinaria sp.*	MP1Bk
MP1	40	Pleistocene 1	*Seriatopora hystrix*	MP1Bi
MP1	40	Pleistocene 1	*Fungia sp.*	MP1Bl
MP1	40	Pleistocene 1	*Echinopora sp.*	
MP1	40	Pleistocene 1	*Echinopora sp.*	
MP1	40	Pleistocene 1	*Platygyra sp.*	MP1t
MP1	40	Pleistocene 1	Scleractinia indet.	MP1u
MP1	40	Pleistocene 1	*Porites sp.*	MP1v
MP1	40	Pleistocene1	*Porites sp.*	MP1Ja
MP1	40	Pleistocene1	*Platygyra sp.*	MP1Jb
MP55	55	Pleistocene 1	*Fungia sp.*	
MP55	55	Pleistocene 1	*Fungia sp.*	
MP55	55	Pleistocene 1	*Lobophyllia hemprichii*	MP55c
MP55	55	Pleistocene 1	*Lobophyllia hemprichii*	
MP55	55	Pleistocene 1	*Lobophyllia hemprichii*	
MP55	55	Pleistocene 1	*Lobophyllia hemprichii*	
MP55	55	Pleistocene 1	*Galaxea sp.*	MP55a
MP55	55	Pleistocene 1	*Galaxea sp.*	
MP55	55	Pleistocene 1	*Galaxea sp.*	
MP55	55	Pleistocene 1	*Galaxea sp.*	
MP55	55	Pleistocene 1	*Galaxea sp.*	
MP55	55	Pleistocene 1	"Faviidae" indet.	MP55b
MP55	55	Pleistocene 1	"Faviidae" indet.	
MP55	55	Pleistocene 1	*Goniastrea sp.*	MP55d
MP55	55	Pleistocene 1	*Goniastrea sp.*	
MP55	55	Pleistocene 1	*Goniastrea sp.*	
MP55	55	Pleistocene 1	*Dipsastraea sp.*	MP55e
MP55	55	Pleistocene 1	*Dipsastraea sp.*	MP55f
MP55	55	Pleistocene 1	*Pocillopora damicornis*	MP55g
MP55	55	Pleistocene 1	*Pocillopora damicornis*	
MP55	55	Pleistocene 1	*Porites sp.*	MP55h
MP55	55	Pleistocene 1	*Seriatopora hystrix*	
MP55	55	Pleistocene 1	*Porites sp.*	MP55i
MP55	55	Pleistocene 1	*Porites sp.*	
MP55	55	Pleistocene 1	*Porites sp.*	MP55j
MP55	55	Pleistocene 1	*Acropora monticulosa*	MP55k
MP55	55	Pleistocene 1	*Platygyra pini*	MP55l
MP55	55	Pleistocene 1	*Platygyra pini*	
MP64	80	Pleistocene 1	*Platygyra sp.*	MP64a
MP64	80	Pleistocene 1	*Platygyra sp.*	MP64b
MP64	80	Pleistocene 1	*Dipsastraea sp.*	
MP64	80	Pleistocene 1	*Stylophora pistillata*	MP64c
MP64	80	Pleistocene 1	*Porites sp.*	MP64d
MP64	80	Pleistocene 1	*Dipsastraea sp.*	
MP64	80	Pleistocene 1	*Playtygyra sp.*	MP64e
MP64	80	Pleistocene 1	*Acropora sp.*	MP64e
MP64	80	Pleistocene 1	*Dipsastraea sp.*	MP64f
MP64	80	Pleistocene 1	*Leptoria phrygia*	MP64g
MP64	80	Pleistocene 1	*Dipsastraea sp.*	
MP64	80	Pleistocene 1	*Fungia sp.*	
MP64	80	Pleistocene 1	*Acropora monticulosa*	

Locality	Altitude	Terrace	Taxon	Sample
MP64	80	Pleistocene 1	Scleractinia indet.	
MP64	80	Pleistocene 1	*Dipsastraea sp.*	
MP64	80	Pleistocene 1	Scleractinia indet.	
MP64	80	Pleistocene 1	*Stylophora pistillata*	
MP64	80	Pleistocene 1	*Lobophyllia hemprichii*	
MP64	80	Pleistocene 1	*Platygyra sp.*	
MP64	80	Pleistocene 1	*Lobophyllia hemprichii*	
MP64	80	Pleistocene 1	*Stylophora pistillata*	
MP64	80	Pleistocene 1	*Acropora sp.*	
MP64	80	Pleistocene 1	*Porites sp.*	
MP64	80	Pleistocene 1	*Platygyra sp.*	
MP64	80	Pleistocene 1	*Galaxea sp.*	MP64h
MP64	80	Pleistocene 1	*Acropora monticulosa*	
MP64	80	Pleistocene 1	*Stylocoeniella guentheri*	MP64i
MP64	80	Pleistocene 1	*Porites sp.*	MP64j
MP64	80	Pleistocene 1	*Acropora monticulosa*	
MP64	80	Pleistocene 1	"Faviidae" indet.	
MP64	80	Pleistocene 1	*Stylophora pistillata*	MP64k
MP64	80	Pleistocene 1	*Goniastrea sp.*	
MP64	80	Pleistocene 1	*Goniastrea sp.*	
MP64	80	Pleistocene 1	*Fungia sp.*	
MP64	80	Pleistocene 1	"Faviidae" indet.	
MP64	80	Pleistocene 1	*Goniastrea sp.*	
MP64	80	Pleistocene 1	*Cyphastrea sp.*	
MP64	80	Pleistocene 1	*Porites sp.*	
MP64	80	Pleistocene 1	*Acropora monticulosa*	
MP64	80	Pleistocene 1	*Acropora monticulosa*	MP64l
MP64	80	Pleistocene 1	"Faviidae" indet.	
MP64	80	Pleistocene 1	*Goniastrea sp.*	
MP64	80	Pleistocene 1	"Faviidae" indet.	
MP64	80	Pleistocene 1	*Coelastrea aspera*	
MP64	80	Pleistocene 1	*Stylophora pistillata*	
MP64	80	Pleistocene 1	Poritidae indet.	
MP64	80	Pleistocene 1	Scleractinia indet.	MP64m
MP64	80	Pleistocene 1	*Cyphastrea sp.*	
MP64	80	Pleistocene 1	Scleractinia indet.	
MP64	80	Pleistocene 1	*Porites sp.*	
MP64	80	Pleistocene 1	*Galaxea astreata*	
MP64	80	Pleistocene 1	*Acropora sp.*	
MP64	80	Pleistocene 1	*Porites sp.*	
MP64	80	Pleistocene 1	*Dipsastraea sp.*	
MP64	80	Pleistocene 1	*Lobophyllia sp.*	
MP64	80	Pleistocene 1	*Fungia sp.*	
MP64	80	Pleistocene 1	*Porites sp.*	
MP64	80	Pleistocene 1	*Acropora sp.*	
MP64	80	Pleistocene 1	Scleractinia indet.	
MP64	80	Pleistocene 1	*Goniopora sp.*	
MP64	80	Pleistocene 1	*Seriatopora hystrix*	
MP64	80	Pleistocene 1	*Acropora sp.*	
MP64	80	Pleistocene 1	*Cyphastrea sp.*	
MP64	80	Pleistocene 1	*Goniopora sp.*	
MP64	80	Pleistocene 1	*Goniopora sp.*	
MP64	80	Pleistocene 1	*Lobophyllia sp.*	
MP64	80	Pleistocene 1	*Cyphastrea sp.*	

Locality	Altitude	Terrace	Taxon	Sample
MP64	80	Pleistocene 1	*Cyphastrea sp.*	
MP64	80	Pleistocene 1	"Faviidae" indet.	MP64n
MP64	80	Pleistocene 1	*Cyphastrea sp.*	
MP64	80	Pleistocene 1	*Dipsastraea sp.*	MP64o
MP64	80	Pleistocene 1	*Porites sp.*	
MP64	80	Pleistocene 1	*Platygyra sp.*	MP64p
MP64	80	Pleistocene 1	*Dipsastraea sp.*	MP64q
MP64	80	Pleistocene 1	*Goniastrea sp.*	MP64r
MP64	80	Pleistocene 1	Scleractinia indet.	
MP64	80	Pleistocene 1	*Lobophyllia sp.*	
MP64	80	Pleistocene 1	*Galaxea sp.*	MP64aa
MP64	80	Pleistocene 1	*Galaxea sp.*	
MP64	80	Pleistocene 1	*Galaxea sp.*	
MP64	80	Pleistocene 1	*Galaxea sp.*	
MP64	80	Pleistocene 1	*Lobophyllia corymbosa*	MP64t
MP64	80	Pleistocene 1	*Lobophyllia corymbosa*	
MP64	80	Pleistocene 1	*Lobophyllia corymbosa*	
MP64	80	Pleistocene 1	*Porites sp.*	MP64u
MP64	80	Pleistocene 1	*Porites sp.*	
MP64	80	Pleistocene 1	*Cyphastrea sp.*	MP64v
MP64	80	Pleistocene 1	*Stylophora pistillata*	MP64w
MP64	80	Pleistocene 1	*Stylophora pistillata*	
MP64	80	Pleistocene 1	*Leptoria phrygia*	MP64w
MP64	80	Pleistocene 1	*Stylophora sp.*	Julien Probe
MP64	80	Pleistocene 1	*Porites sp.*	MP64y
MP64	80	Pleistocene 1	*Acropora sp.*	MP64x
MP64	80	Pleistocene 1	*Dipsastraea sp.*	MP64z
MP64	80	Pleistocene 1	*Dipsastraea sp.*	
MP64	80	Pleistocene 1	Scleractinia indet.	MP64z
MP64	80	Pleistocene 1	*Alveopora sp.*	MP64ab
MP64	80	Pleistocene 1	*Alveopora sp.*	MP64ac
MP64	80	Pleistocene 1	*Porites sp.*	
MP64	80	Pleistocene 1	*Porites sp.*	
MP64	80	Pleistocene 1	*Porites sp.*	
MP64	80	Pleistocene 1	*Platygyra sp.*	
MP64	80	Pleistocene 1	Scleractinia indet.	MP64TH
UL2	90	Pleistocene 2	*Stylophora pistillata*	UL2B1
UL2	90	Pleistocene 2	*Dipsastraea sp.*	UL2B3
UL2	90	Pleistocene 2	*Porites sp.*	
UL2	90	Pleistocene 2	*Porites sp.*	
UL2	90	Pleistocene 2	*Porites sp.*	
UL2	90	Pleistocene 2	*Porites sp.*	
UL2	90	Pleistocene 2	*Porites sp.*	
UL2	90	Pleistocene 2	*Porites sp.*	
UL2	90	Pleistocene 2	*Lobophyllia corymbosa*	
UL2	90	Pleistocene 2	"Faviidae" indet.	
UL2	90	Pleistocene 2	"Faviidae" indet.	
UL2	90	Pleistocene 2	"Faviidae" indet.	
UL2	90	Pleistocene 2	"Faviidae" indet.	
UL2	90	Pleistocene 2	"Faviidae" indet.	
UL2	90	Pleistocene 2	"Faviidae" indet.	
UL2	90	Pleistocene 2	"Faviidae" indet.	
UL2	90	Pleistocene 2	"Faviidae" indet.	
UL2	90	Pleistocene 2	"Faviidae" indet.	

Locality	Altitude	Terrace	Taxon	Sample
UL2	90	Pleistocene 2	"Faviidae" indet.	
UL2	90	Pleistocene 2	"Faviidae" indet.	
UL2	90	Pleistocene 2	"Faviidae" indet.	
UL2	90	Pleistocene 2	"Faviidae" indet.	
UL2	90	Pleistocene 2	"Faviidae" indet.	
UL2	90	Pleistocene 2	"Faviidae" indet.	
UL2	90	Pleistocene 2	"Faviidae" indet.	
UL2	90	Pleistocene 2	"Faviidae" indet.	
UL2	90	Pleistocene 2	"Faviidae" indet.	
UL2	90	Pleistocene 2	"Faviidae" indet.	
UL2	90	Pleistocene 2	"Faviidae" indet.	
UL2	90	Pleistocene 2	"Faviidae" indet.	
UL2	90	Pleistocene 2	"Faviidae" indet.	
UL2	90	Pleistocene 2	"Faviidae" indet.	
UL2	90	Pleistocene 2	"Faviidae" indet.	
UL2	90	Pleistocene 2	"Faviidae" indet.	
UL2	90	Pleistocene 2	"Faviidae" indet.	
UL2	90	Pleistocene 2	"Faviidae" indet.	
UL2	90	Pleistocene 2	"Faviidae" indet.	
UL2	90	Pleistocene 2	"Faviidae" indet.	
UL2	90	Pleistocene 2	"Faviidae" indet.	
UL2	90	Pleistocene 2	*Porites sp.*	
UL2	90	Pleistocene 2	*Platygyra sp.*	
UL2	90	Pleistocene 2	*Platygyra sp.*	
UL2	90	Pleistocene 2	*Platygyra sp.*	
UL2	90	Pleistocene 2	*Porites sp.*	
UL2	90	Pleistocene 2	*Lobophyllia sp.*	
UL2	90	Pleistocene 2	*Platygyra sp.*	
UL2	90	Pleistocene 2	*Platygyra sp.*	
UL2	90	Pleistocene 2	*Cyphastrea sp.*	
UL2	90	Pleistocene 2	*Dipsastraea sp.*	
UL2	90	Pleistocene 2	*Dipsastraea sp.*	
UL2	90	Pleistocene 2	*Dipsastraea sp.*	
UL2	90	Pleistocene 2	*Dipsastraea sp.*	
UL2	90	Pleistocene 2	*Dipsastraea sp.*	
UL2	90	Pleistocene 2	*Dipsastraea sp.*	
UL2	90	Pleistocene 2	"Faviidae" indet.	
UL2	90	Pleistocene 2	*Porites sp.*	
UL2	90	Pleistocene 2	*Galaxea sp.*	UL2B2
UL2	90	Pleistocene 2	*Galaxea sp.*	
UL2	90	Pleistocene 2	*Galaxea sp.*	
MP2	105	Pleistocene 1	*Dipsastraea sp.*	
MP2	105	Pleistocene 1	*Dipsastraea sp.*	
MP2	105	Pleistocene 1	*Favites sp.*	
MP2	105	Pleistocene 1	*Favites sp.*	
MP2	105	Pleistocene 1	*Favites sp.*	
MP2	105	Pleistocene 1	*Platygyra sp.*	
MP2	105	Pleistocene 1	*Porites sp.*	
MP2	105	Pleistocene 1	*Porites sp.*	
MP2	105	Pleistocene 1	*Porites sp.*	
MP2	105	Pleistocene 1	*Porites sp.*	
MP2	105	Pleistocene 1	*Lobophyllia corymbosa*	
MP2	105	Pleistocene 1	*Cyphastrea sp.*	
MP2	105	Pleistocene 1	*Cyphastrea sp.*	

Locality	Altitude	Terrace	Taxon	Sample
MP2	105	Pleistocene 1	*Cyphastrea sp.*	
MP2	105	Pleistocene 1	*Porites sp*	
MP2	105	Pleistocene 1	*Dipsastraea sp.*	
MP2	105	Pleistocene 1	*Dipsastraea sp.*	
MP2	105	Pleistocene 1	*Dipsastraea sp.*	
MP2	105	Pleistocene 1	*Dipsastraea sp.*	
MP2	105	Pleistocene 1	*Dipsastraea sp.*	
MP2	105	Pleistocene 1	*Platygyra sp.*	MP2Ba
MP2	105	Pleistocene 1	*Goniastrea retiformis*	MP2Bf
MP2	105	Pleistocene 1	*Goniastrea retiformis*	
MP2	105	Pleistocene 1	*Goniastrea retiformis*	
MP2	105	Pleistocene 1	*Goniastrea retiformis*	
MP2	105	Pleistocene 1	*Goniastrea retiformis*	
MP2	105	Pleistocene 1	*Goniastrea retiformis*	
MP2	105	Pleistocene 1	*Goniastrea retiformis*	
MP2	105	Pleistocene 1	*Goniastrea retiformis*	
MP2	105	Pleistocene 1	*Goniastrea retiformis*	
MP2	105	Pleistocene 1	*Goniastrea retiformis*	MP2Bb
MP2	105	Pleistocene 1	*Platygyra pini*	MP2Bc & MP2Bd
MP2	105	Pleistocene 1	*Platygyra pini*	
MP2	105	Pleistocene 1	*Platygyra pini*	
MP2	105	Pleistocene 1	*Platygyra pini*	MP2Be
MP2	105	Pleistocene 1	*Platygyra sp.*	
MP2	105	Pleistocene 1	*Lobophyllia sp.*	MP2Bg
MP2	105	Pleistocene 1	*Lobophyllia sp.*	
MP2	105	Pleistocene 1	*Platygyra pini*	MP2Bh
MP2	105	Pleistocene1	*Lobophyllia sp.*	MP2sa
MP2	105	Pleistocene1	*Dipsastraea sp.*	MP2Sc
UL3	125	Pleistocene 2	*Favites sp.*	
UL3	125	Pleistocene 2	*Favites sp.*	
UL3	125	Pleistocene 2	*Favites sp.*	
UL3	125	Pleistocene 2	*Favites sp.*	
UL3	125	Pleistocene 2	*Favites sp.*	
UL3	125	Pleistocene 2	*Cyphastrea sp.*	
UL3	125	Pleistocene 2	*Cyphastrea sp.*	
UL3	125	Pleistocene 2	*Cyphastrea sp.*	
UL3	125	Pleistocene 2	*Fungia sp.*	
UL3	125	Pleistocene 2	*Fungia sp.*	
UL3	125	Pleistocene 2	*Fungia sp.*	
UL3	125	Pleistocene 2	*Fungia sp.*	
UL3	125	Pleistocene 2	*Fungia sp.*	
UL3	125	Pleistocene 2	*Astrea sp.*	
UL3	125	Pleistocene 2	Scleractinia indet.	
UL3	125	Pleistocene 2	"Faviidae" indet.	
UL3	125	Pleistocene 2	"Faviidae" indet.	
UL3	125	Pleistocene 2	"Faviidae" indet.	
UL3	125	Pleistocene 2	*Lobophyllia sp.*	UL3B1
UL3	125	Pleistocene 2	*Platygyra sp.*	
UL3	125	Pleistocene 2	*Platygyra sp.*	
UL3	125	Pleistocene 2	*Porites sp.*	
UL3	125	Pleistocene 2	*Porites sp.*	
MP3	130	Pleistocene 1	*Galaxea sp.*	MP3Sa
MP3	130	Pleistocene 1	*Goniastrea sp.*	
MP3	130	Pleistocene 1	*Dipsastraea sp.*	
MP3	130	Pleistocene 1	*Dipsastraea sp.*	

Locality	Altitude	Terrace	Taxon	Sample
MP3	130	Pleistocene 1	*Dipsastraea sp.*	
MP3	130	Pleistocene 1	*Echinopora sp.*	MP3Sb
MP3	130	Pleistocene 1	*Porites sp.*	Mp3Sc
MP3	130	Pleistocene 1	*Porites sp.*	
MP3	130	Pleistocene 1	*Porites sp.*	MP3Sd
MP3	130	Pleistocene 1	*Porites sp.*	
MP3	130	Pleistocene 1	*Porites sp.*	
MP3	130	Pleistocene 1	*Dipsastraea sp.*	MP3Se
MP3	130	Pleistocene 1	*Symphyllia recta*	
MP3	130	Pleistocene 1	*Echinopora sp.*	MP3Sf
MP3	130	Pleistocene 1	*Echinopora sp.*	
MP3	130	Pleistocene 1	*Echinopora sp.*	
MP3	130	Pleistocene 1	*Echinopora sp.*	
MP3	130	Pleistocene 1	*Goniastrea sp.*	MP3Sg
MP3	130	Pleistocene 1	*Cyphastrea sp.*	
MP3	130	Pleistocene 1	*Lobophyllia sp.*	
MP3	130	Pleistocene 1	*Lobophyllia sp.*	
MP3	130	Pleistocene 1	*Dipsastraea sp.*	MP3Sh
MP3	130	Pleistocene 1	*Dipsastraea sp.*	
MP3	130	Pleistocene 1	*Fungia sp.*	
MP3	130	Pleistocene 1	*Echinopora sp.*	MP3Si
MP3	130	Pleistocene 1	*Goniastrea sp.*	
MP3	130	Pleistocene 1	*Leptoria phrygia*	
MP3	130	Pleistocene 1	*Leptoria phrygia*	
MP3	130	Pleistocene 1	*Leptoria phrygia*	
MP3	130	Pleistocene 1	*Porites sp.*	MP3Sj
MP3	130	Pleistocene 1	*Turbinaria sp.*	
MP3	130	Pleistocene 1	*Cyphastrea sp.*	
MP3	130	Pleistocene 1	*Cyphastrea sp.*	
MP3	130	Pleistocene 1	*Platygyra pini*	
MP3	130	Pleistocene 1	*Leptoria phrygia*	
MP3	130	Pleistocene 1	*Goniastrea sp.*	
MP3	130	Pleistocene 1	*Goniastrea sp.*	
MP3	130	Pleistocene 1	*Goniopora sp.*	MP3Sk
MP3	130	Pleistocene 1	*Dipsastraea sp.*	
MP4	297	Pleistocene 3	*Goniastrea sp.*	
MP4	297	Pleistocene 3	*Porites sp.*	MP4Sa
MP4	297	Pleistocene 3	*Goniastrea sp.*	
MP4	297	Pleistocene 3	*Platygyra sp.*	
MP4	297	Pleistocene 3	*Platygyra sp.*	
MP4	297	Pleistocene 3	*Goniastrea sp.*	
MP4	297	Pleistocene 3	*Astrea sp.*	
MP4	297	Pleistocene 3	*Goniastrea edwardsi*	
MP4	297	Pleistocene 3	*Goniastrea edwardsi*	
MP4	297	Pleistocene 3	*Platygyra sp.*	
MP4	297	Pleistocene 3	*Platygyra sp.*	
MP4	297	Pleistocene 3	*Dipsastraea sp.*	
MP4	297	Pleistocene 3	*Dipsastraea sp.*	
MP4	297	Pleistocene 3	"Faviidae" indet.	sample?
MP4	297	Pleistocene 3	*Goniastrea sp.*	
MP4	297	Pleistocene 3	*Goniastrea sp.*	
MP4	297	Pleistocene 3	*Goniastrea sp.*	MP4Sb
MP4	297	Pleistocene 3	*Porites sp.*	MP4Sc
MP4	297	Pleistocene 3	*Goniastrea sp.*	

Locality	Altitude	Terrace	Taxon	Sample
MP4	297	Pleistocene 3	*Goniastrea sp.*	
MP4	297	Pleistocene 3	*Goniastrea retiformis*	
MP4	297	Pleistocene 3	*Cyphastrea sp.*	MP4Sd
MP4	297	Pleistocene 3	*Goniastrea sp.*	
MP4	297	Pleistocene 3	*Goniastrea sp.*	
MP4	297	Pleistocene 3	*Goniastrea retiformis*	
MP4	297	Pleistocene 3	*Porites sp.*	MP4Se
MP4	297	Pleistocene 3	*Leptoria phrygia*	
MP4	297	Pleistocene 3	*Goniastrea retiformis*	
MP4	297	Pleistocene 3	*Goniastrea retiformis*	
MP4	297	Pleistocene 3	*Goniastrea sp.*	MP4Sf
MP4	297	Pleistocene 3	*Cyphastrea sp.*	
MP4	297	Pleistocene 3	*Cyphastrea sp.*	
MP4	297	Pleistocene 3	*Porites sp.*	
MP4	297	Pleistocene 3	*Leptoria phrygia*	
MP4	297	Pleistocene 3	*Porites sp.*	
MP4	297	Pleistocene 3	*Porites sp.*	
MP4	297	Pleistocene 3	"Faviidae" indet.	
MP4	297	Pleistocene 3	*Goniastrea sp.*	
MP4	297	Pleistocene 3	"Faviidae" indet.	MP4Sg
MP4	297	Pleistocene 3	*Goniastrea retiformis*	
MP4	297	Pleistocene 3	*Goniastrea retiformis*	MP4Sh
MP4	297	Pleistocene 3	*Goniastrea sp.*	
MP4	297	Pleistocene 3	"Faviidae" indet.	
MP4	297	Pleistocene 3	*Platygyra sp.*	
MP4	297	Pleistocene 3	*Platygyra sp.*	
MP4	297	Pleistocene 3	"Faviidae" indet.	
MP4	297	Pleistocene 3	*Goniastrea sp*	
MP4	297	Pleistocene 3	*Acropora monticulosa*	MP4Si
MP4	297	Pleistocene 3	*Goniastrea sp.*	
MP4	297	Pleistocene 3	*Goniastrea sp.*	
MP4	297	Pleistocene 3	*Goniastrea sp.*	
MP4	297	Pleistocene 3	*Goniastrea sp.*	
MP4	297	Pleistocene 3	*Goniastrea sp.*	
MP4	297	Pleistocene 3	*Favites sp.*	
MP4	297	Pleistocene 3	*Goniastrea sp.*	
MP4	297	Pleistocene 3	*Goniastrea sp.*	
MP4	297	Pleistocene 3	*Dipsastraea sp.*	
MP4	297	Pleistocene 3	*Goniastrea sp.*	
MP4	297	Pleistocene 3	*Dipsastraea sp.*	
MP4	297	Pleistocene 3	*Goniastrea sp.*	
MP4	297	Pleistocene 3	*Goniastrea sp.*	
MP4	297	Pleistocene 3	*Goniastrea edwardsi*	
MP4	297	Pleistocene 3	*Goniastrea edwardsi*	
MP4	297	Pleistocene 3	*Goniastrea edwardso*	
MP4	297	Pleistocene 3	*Porites sp.*	
MP4	297	Pleistocene 3	*Leptoria phrygia*	
MP4	297	Pleistocene 3	*Goniastrea sp.*	
MP4	297	Pleistocene 3	*Cyphastrea sp.*	
MP4	297	Pleistocene 3	*Montipora sp.*	
MP4	297	Pleistocene 3	*Leptoria phrygia*	
MP4	297	Pleistocene 3	*Goniastrea sp.*	
MP4	297	Pleistocene 3	*Goniastrea sp.*	
MP4	297	Pleistocene 3	*Goniastrea sp.*	

Locality	Altitude	Terrace	Taxon	Sample
MP4	297	Pleistocene 3	Scleractinia indet.	MP4Sj
MP4	297	Pleistocene3	*Favites sp.*	MP4_faviid
MP4	297	Pleistocene3	*Favites pentagona*	MP4B1
MP4	297	Pleistocene3	*Porites sp.*	MP4Ja
MP4	297	Pleistocene3	*Porites sp.*	MP4Jb
MP5	393	Pleistocene 4	*Platygyra sp.*	MP5a
MP5	393	Pleistocene 4	*Platygyra sp.*	
MP5	393	Pleistocene 4	*Platygyra sp.*	
MP5	393	Pleistocene 4	*Dipsastraea sp.*	
MP5	393	Pleistocene 4	*Dipsastraea sp.*	
MP5	393	Pleistocene 4	*Dipsastraea sp.*	
MP5	393	Pleistocene 4	*Dipsastraea sp.*	
MP5	393	Pleistocene 4	*Dipsastraea sp.*	MP5b
MP5	393	Pleistocene 4	*Cyphastrea sp.*	
MP5	393	Pleistocene 4	*Cyphastrea sp.*	
MP5	393	Pleistocene 4	*Platygyra sp.*	
MP5	393	Pleistocene 4	*Leptoria phrygia*	
MP5	393	Pleistocene 4	"Faviidae" indet.	MP5c

Table 6-III: GPS data from respective localities.

Locality	Latitude (S)	Longitude (E)
UL1	17°34'18.61"	168°16'8.81"
UL2	17°34'21.86"	168°16'12.63"
UL3	17°34'31.83"	168°16'18.27"
MP1	17°34'33.81"	168°15'18.45"
MP64	17°34'39.30"	168°15'19.78"
MP2	17°34'44.85"	168°15'17.01"
MP3	17°34'54.71"	168°15'15.76"
MP4	17°35'25.83"	168°16'5.99"
MP5	17°35'40.94"	168°16'57.91"
Sa1	17°32'28.70"	168°21'49.07"
La	17°32'37.62"	168°21'28.89"
SP	17°34'38.42"	168°14'45.14"
SP1	17°34'30.95"	168°14'51.06"

Appendix II - Data from Egypt

The following table II-I contains the binary dataset used for the comparison of assemblages on regional level. The complete data from all transects performed in Egypt (March - April 2009) can be found in table II-II. The GPS points are marked in Figure 5.2.1 (chapter 5) and listed in detail in table II-IV. Table II-III contains the summarized and standardized data including the recent data provided by Alter (2004) used for the analyses.

Table 6-IV: Binary data set used in den analyses of Chapter 5. NRS = northern Red Sea, CRS = central Red Sea , SRS = southern Red Sea, Gulf = Persian Gulf, GO = Gulf of Oman, AS = Arabian Sea. The recent data is taken from Sheppard & Sheppard (1991). The authors of the Pleistocene data are designated in the table, including the collection number of the Paleobiology Database (PBDB) where they are deposited.

Species	NRS	CRS	SRS	Gulf	GO	AS	Pleistocene	Author (Pleistocene data)	PBDB collection
Acanthastrea echinata	1	1	1	1	1	1	1	This thesis	
Acanthastrea hillae	0	0	0	1	1	1	0		
Acanthastrea maxima	0	0	0	0	1	1	0		
Acropora clathrata	1	1	1	1	1	1	1	El-Sorogy 2002	87873
Acropora cythera	1	1	1	0	0	0	0		
Acropora danai	1	1	1	0	0	0	0		
Acropora digitifera	1	1	1	0	0	0	0		
Acropora eurystoma	1	1	1	0	0	0	0		
Acropora muricata	1	0	1	0	0	1	1	This thesis	
Acropora granulosa	1	1	1	0	0	1	0		
Acropora hemprichii	1	1	1	0	0	0	1	El-Sorogy 2008	120205
Acropora horrida	1	0	1	1	1	1	1	El-Sorogy 2002	87873
Acropora humilis	1	1	1	0	0	0	0		
Acropora hyacinthus	1	1	1	0	0	1	0		
Acropora latistella	0	0	0	0	0	0	1	El-Sorogy 2008	120203
Acropora nasuta	1	1	1	1	0	0	0		
Acropora nobilis	0	1	1	0	0	0	0		
Acropora pharaonis	1	1	1	1	1	1	1	Kora et al. 2014	
Acropora poylstoma	0	0	1	0	0	0	0		
Acropora robusta	0	1	1	0	0	0	1	El-Sorogy 2008	120205
Acropora squarrosa	1	1	0	0	0	0	0		
Acropora valenciennesi	1	1	0	1	1	0	1	El-Sorogy 2008	120203
Acropora valida	1	1	1	0	1	1	1	El-Sorogy 2008	120203
Alveopora allingi	1	1	0	0	0	0	0		
Alveopora ocellata	1	1	0	0	0	0	0		
Alveopora spongiosa	1	1	0	0	0	0	0		
Alveopora tizardi	0	1	0	0	0	0	0		
Alveopora viridis	1	0	0	0	0	0	0		
Astreopora explanata	0	0	0	0	1	0	0		
Astreopora myriophthalma	1	1	1	0	1	0	1	This thesis	
Blastomussa merleti	1	1	1	1	1	1	1	El-Sorogy 2002	87876
Caulastrea tumida	1	0	0	0	0	0	0		
Coscinaraea columna	0	1	1	0	1	1	1	El-Sorogy 2002	87876
Coscinaraea monile	1	1	1	1	1	1	1	This thesis	
Ctenactis echinata	1	1	1	0	0	0	1	Kora et al. 2014	

Species	NRS	CRS	SRS	Gulf	GO	AS	Pleistocene	Author (Pleistocene data)	PBDB collection
Cycloseris costulata	1	1	0	0	0	0	0		
Cycloseris cyclolites	1	0	0	1	0	1	1	El-Sorogy 2008	120203
Cycloseris doederleini	1	1	0	0	0	0	0		
Cycloseris marginata	1	1	0	0	0	0	0		
Cycloseris patelliformis	1	1	1	0	0	0	1	El-Sorogy 2008	120204
Cycloseris tenuis	0	0	0	0	0	1	0		
Cynarina lacrymalis	1	0	0	0	0	0	0		
Cyphastrea microphthalma	1	1	1	1	1	1	1	Kora et al. 2014	
Cyphastrea serailia	1	1	1	1	1	1	1	This thesis	
Diaseris distorta	1	1	0	0	0	1	0		
Diploastrea heliopora	1	1	1	0	0	0	0		
Echinophyllia aspera	1	1	1	1	1	1	0		
Echinopora cf. fruticulosa	1	1	1	0	0	0	1	El-Sorogy 2008	120206
Echinopora gemmacea	1	1	1	0	1	1	1	This thesis	
Echinopora lamellosa	1	1	1	0	1	0	1	El-Sorogy 2002	87876
Echinopora forskaliana	0	0	0	0	0	0	1	This thesis	
Erythrastrea flabellata	1	0	0	0	0	1	0		
Euphyllia glabrescens	1	0	0	0	0	1	0		
Dipsastraea speciosa	1	1	1	0	1	1	0		
Dipsastraea favus	1	1	1	1	0	0	0		
Dipsastraea laxa	1	1	1	0	0	0	1	El-Sorogy 2008	120128
Dipsastraea lizardensis	0	1	0	0	0	0	1	El-Sorogy 2008	120211
Dipsastraea matthai	1	1	0	0	0	0	0		
Dipsastraea pallida	1	1	1	1	1	1	1	This thesis	
Dipsastraea rotumana	0	0	0	0	1	0	1	El-Sorogy 2008	120209
Favites rotundata	1	1	0	0	0	0	1	This thesis	
Dipsastraea stelligera	1	1	1	0	0	0	1	El-Sorogy 2002	87876
Dipsastraea veroni	0	0	0	0	0	0	1	El-Sorogy 2008	120203
Dipsastraea wisseli	0	1	0	0	0	0	0		
Favites abdita	1	1	1	0	0	1	1	Kora et al. 2014	
Favites chinensis	1	1	1	1	1	1	1	Kora et al. 2014	
Favites complanata	1	1	0	1	0	1	0		
Favites flexuosa	1	1	1	0	0	1	1	This thesis	
Favites halicora	1	1	1	0	0	0	0		
Favites pentagona	1	1	1	1	1	1	1	This thesis	
Favites spinosa	0	0	0	0	0	0	1	This thesis	
Fungia concinna	1	1	1	0	0	0	1	El-Sorogy 2008	120203
Fungia corona	0	1	0	0	0	0	1	El-Sorogy 2002	87873
Fungia fungites	1	1	1	0	0	1	1	El-Sorogy 2002	87873
Fungia granulosa	1	1	0	0	0	0	1	El-Sorogy 2008	120207
Fungia horrida	1	1	0	0	0	0	0		
Fungia klunzingeri	1	1	0	0	0	0	1	El-Sorogy 2008	120204
Fungia moluccensis	1	0	0	0	0	0	1	El-Sorogy 2008	120205
Fungia paumotensis	1	1	0	0	0	1	1	El-Sorogy 2008	120205
Fungia repanda	0	1	0	0	0	0	0		

Species	NRS	CRS	SRS	Gulf	GO	AS	Pleistocene	Author (Pleistocene data)	PBDB collection
Fungia scruposa	1	1	0	0	0	0	0		
Fungia scutaria	1	1	1	0	0	0	1	Kora et al. 2014	
Fungia valida	0	1	0	0	0	0	1	El-Sorogy 2002	87873
Galaxea astreata	0	0	0	0	0	1	1	Kora et al. 2014	
Galaxea fascicularis	1	1	1	0	1	1	1	This thesis	
Gardineroseris planulata	1	1	1	0	0	1	1	This thesis	
Coelastrea aspera	0	0	0	0	0	0	1	This thesis	
Paragoniastrea australensis	1	1	1	0	0	0	0		
Goniastrea edwardsi	1	1	1	0	0	0	1	This thesis	
Goniastrea pectinata	1	1	1	0	0	1	1	El-Sorogy 2008	120128
Paramontastraea peresi	1	1	1	0	0	1	1	This thesis	
Goniastrea retiformis	1	1	0	0	0	1	1	This thesis	
Goniopora columna	1	1	1	0	1	1	0		
Goniopora djiboutinensis	0	0	0	0	1	1	0		
Goniopora minor	1	1	0	0	0	0	1	El-Sorogy 2008	120128
Goniopora somaliensis	1	1	1	0	0	1	0		
Goniopora stokesi	1	1	0	0	0	0	0		
Goniopora tenella	0	1	0	0	0	0	0		
Goniopora tenuidens	0	0	0	0	1	1	0		
Gyrosmilia interrupta	1	1	1	0	0	0	1	This thesis	
Herpolitha limax	1	1	1	0	0	0	0		
Hydnophora exesa	1	1	1	1	1	1	1	El-Sorogy 2008	120203
Hydnophora microconos	1	1	1	0	1	1	1	This thesis	
Leptastrea bottae	0	0	0	0	0	0	1	This thesis	
Leptastrea inaequalis	1	1	1	0	1	1	0		
Leptastrea purpurea	1	1	1	1	1	1	1	Kora et al. 2014	
Leptastrea transversa	1	1	1	1	1	1	1	This thesis	
Leptoria phrygia	1	1	1	0	0	1	1	El-Sorogy 2008	120129
Leptoseris explanata	1	1	0	0	0	0	0		
Leptoseris foliosa	1	1	1	0	1	0	0		
Leptoseris hawaiiensis	1	1	1	0	0	0	0		
Leptoseris mycetoseroides	1	1	1	0	1	0	0		
Leptoseris scabra	1	1	1	0	0	0	0		
Leptoseris yabei	1	1	1	0	0	0	0		
Lobophyllia corymbosa	1	1	1	0	0	0	1	This thesis	
Lobophyllia hattai	0	1	0	0	0	1	0		
Lobophyllia hemprichii	1	1	1	0	0	1	1	This thesis	
Merulina scheeri	1	1	1	0	0	0	0		
Astrea curta	1	1	1	0	0	0	1	This thesis	
Favites magnistellata	0	1	0	0	0	0	0		
Montipora aequituberculata	1	1	1	1	1	1	0		
Montipora circumvallata	1	1	1	1	1	1	0		
Montipora danae	1	1	1	0	0	0	0		
Montipora digitata	0	0	0	0	0	1	0		
Montipora informis	1	1	1	0	0	0	0		

Species	NRS	CRS	SRS	Gulf	GO	AS	Pleistocene	Author (Pleistocene data)	PBDB collection
Montipora monasteriata	1	1	1	0	1	1	0		
Montipora spongiosa	0	1	1	0	1	0	1	El-Sorogy 2002	87876
Montipora stilosa	1	1	0	0	1	1	0		
Montipora tuberculosa	1	1	0	0	0	0	0		
Montipora venosa	1	1	0	1	1	1	0		
Montipora verrucosa	0	1	1	0	0	1	0		
Montipora sp.	1	1	1	1	1	1	1	This thesis	
Mycedium elephantotus	1	1	1	0	0	0	1	This thesis	
Oulophyllia crispa	1	1	1	0	0	0	0		
Oxypora lacera	1	1	1	0	1	0	0		
Pachyseris speciosa	1	1	1	0	0	0	0		
Pararimplastrea simplicitexta	0	0	0	0	1	1	0		
Pavona cactus	1	1	1	1	1	1	1	This thesis	
Pavona decussata	1	1	1	0	1	1	0		
Pavona diffluens	0	1	0	1	1	1	0		
Pavona duerdeni	1	1	0	0	0	0	0		
Pavona explanulata	1	1	1	1	1	1	0		
Pavona maldivensis	1	1	1	0	0	0	0		
Pavona minuta	0	0	0	0	1	0	0		
Pavona varians	1	1	1	1	0	1	0		
Pavona venosa	0	0	0	0	0	1	0		
Platygyra crosslandi	1	1	0	0	0	0	1	This thesis	
Platygyra daedalea	1	1	1	1	1	1	1	This thesis	
Platygyra lamellina	1	1	1	1	1	1	1	This thesis	
Plerogyra sinensis	0	1	1	1	1	0	1	El-Sorogy 2008	120208
Plesiastrea versipora	1	1	1	1	1	1	0		
Pocillopora damicornis	1	1	1	1	1	1	1	This thesis	
Pocillopora verrucosa	1	1	1	1	0	1	1	This thesis	
Podabacia crustacea	1	1	1	0	0	0	0		
Porites compressa	1	1	1	1	1	0	1	El-Sorogy 2008	120210
Porites echinulata	1	1	1	0	0	1	0		
Porites lobata/lutea	1	1	1	1	1	1	1	This thesis	
Porites nodifera	1	1	1	1	1	1	1	This thesis	
Porites rus	1	1	0	0	0	0	0		
Porites solida	1	1	1	0	1	1	0		
Porites undulata	0	0	0	0	0	0	1	El-Sorogy 2008	120203
Psammocora contigua	0	0	0	1	1	1	0		
Psammocora explanulata	1	1	1	0	0	0	0		
Psammocora haimeana	1	1	1	1	1	1	1	Kora et al. 2014	
Pseudosiderastrea tayamai	0	0	0	1	1	1	1	Kora et al. 2014	
Seriatopora caliendrum	1	1	1	0	0	1	1	El-Sorogy 2008	120203
Seriatopora hystrix	1	1	1	0	0	0	1	Kora et al. 2014	
Siderastrea savignyana	1	1	1	1	1	1	0		
Stylocoeniella armata	0	1	0	0	0	0	0		
Stylocoeniella guentheri	1	1	1	0	1	0	0		

Species	NRS	CRS	SRS	Gulf	GO	AS	Pleistocene	Author (Pleistocene data)	PBDB collection
Stylophora kuehlmanni	0	0	0	0	0	0	1	El-Sorogy 2008	120209
Stylophora mamillata	1	1	0	0	0	0	0		
Stylophora pistillata	1	1	1	1	1	1	1	This thesis	
Stylophora wellsi	1	1	1	0	0	0	1	Kora et al. 2014	
Symphyllia eythraea	1	1	1	0	0	0	0		
Symphyllia radians	0	0	0	0	1	1	0		
Trachyphyllia geoffroyi	1	0	0	0	0	0	0		
Tubastraea aurea	0	1	1	1	0	0	0		
Tubastraea diphana	1	0	0	0	0	0	0		
Tubastraea coccinea	1	1	1	0	1	1	0		
Tubastraea micranthus	0	1	1	0	1	0	1	This thesis	
Turbinaria mesenterina	1	1	1	1	1	0	0		
Turbinaria peltata	0	0	0	0	1	1	0		
Turbinaria reniformis	0	0	1	0	1	0	1	This thesis	
Acropora stoddarti	0	0	0	0	0	0	1	Kora et al. 2014	
Acropora spicifera	0	0	0	0	0	0	1	Kora et al. 2014	
Acanthastrea hemprichii	0	0	0	0	0	0	1	Kora et al. 2014	
Plesiastrea devantieri	0	0	0	0	0	0	1	Kora et al. 2014	
Leptastrea pruinosa	0	0	0	0	0	0	1	Kora et al. 2014	
Echinopora hirsutissima	0	0	0	0	0	0	1	Kora et al. 2014	

Table 6-V: Complete transect data collected in Egypt during field work in 2009. If no GPS point is mentioned for some transects, then these were taken close to the preceding transect.

LT	Locality	Site	GPS	Layer	*Name*	Sample
LT01	Dahab	Canyon North Patch Reef	WP41		*Dipsastraea pallida*	
LT01	Dahab	Canyon North Patch Reef	WP41		*Dipsastraea pallida*	
LT01	Dahab	Canyon North Patch Reef	WP41		red algae	
LT01	Dahab	Canyon North Patch Reef	WP41		matrix	
LT01	Dahab	Canyon North Patch Reef	WP41		matrix	
LT01	Dahab	Canyon North Patch Reef	WP41		matrix	
LT01	Dahab	Canyon North Patch Reef	WP41		*Dipsastraea sp.*	LT1a
LT01	Dahab	Canyon North Patch Reef	WP41		matrix	
LT01	Dahab	Canyon North Patch Reef	WP41		*Galaxea fascicularis*	
LT01	Dahab	Canyon North Patch Reef	WP41		*Dipsastraea pallida*	
LT01	Dahab	Canyon North Patch Reef	WP41		*Dipsastraea pallida*	
LT01	Dahab	Canyon North Patch Reef	WP41		*Dipsastraea pallida*	
LT01	Dahab	Canyon North Patch Reef	WP41		*Dipsastraea pallida*	
LT01	Dahab	Canyon North Patch Reef	WP41		*Dipsastraea pallida*	
LT01	Dahab	Canyon North Patch Reef	WP41		*Galaxea fascicularis*	
LT01	Dahab	Canyon North Patch Reef	WP41		matrix	
LT01	Dahab	Canyon North Patch Reef	WP41		*Galaxea fascicularis*	
LT01	Dahab	Canyon North Patch Reef	WP41		*Hydnophora microconos*	LT1b
LT01	Dahab	Canyon North Patch Reef	WP41		*Pocillopora verrucosa*	
LT01	Dahab	Canyon North Patch Reef	WP41		*Porites lobata/lutea*	
LT01	Dahab	Canyon North Patch Reef	WP41		*Porites lobata/lutea*	

LT	Locality	Site	GPS	Layer	*Name*	Sample
LT01	Dahab	Canyon North Patch Reef	WP41		matrix	
LT01	Dahab	Canyon North Patch Reef	WP41		*Pocillopora verrucosa*	
LT01	Dahab	Canyon North Patch Reef	WP41		*Pocillopora verrucosa*	
LT01	Dahab	Canyon North Patch Reef	WP41		*Pocillopora verrucosa*	
LT01	Dahab	Canyon North Patch Reef	WP41		*Pocillopora verrucosa*	
LT01	Dahab	Canyon North Patch Reef	WP41		*Pocillopora verrucosa*	
LT01	Dahab	Canyon North Patch Reef	WP41		*Porites lobata/lutea*	
LT01	Dahab	Canyon North Patch Reef	WP41		*Porites lobata/lutea*	
LT01	Dahab	Canyon North Patch Reef	WP41		*Galaxea fascicularis*	
LT01	Dahab	Canyon North Patch Reef	WP41		*Platygyra lamellina*	
LT01	Dahab	Canyon North Patch Reef	WP41		*Platygyra lamellina*	
LT01	Dahab	Canyon North Patch Reef	WP41		*Platygyra lamellina*	
LT01	Dahab	Canyon North Patch Reef	WP41		*Platygyra lamellina*	
LT01	Dahab	Canyon North Patch Reef	WP41		*Platygyra lamellina*	
LT01	Dahab	Canyon North Patch Reef	WP41		*Platygyra lamellina*	
LT01	Dahab	Canyon North Patch Reef	WP41		red algae	
LT01	Dahab	Canyon North Patch Reef	WP41		red algae	
LT01	Dahab	Canyon North Patch Reef	WP41		*Acropora sp.*	LT1c
LT01	Dahab	Canyon North Patch Reef	WP41		matrix	
LT01	Dahab	Canyon North Patch Reef	WP41		matrix	
LT01	Dahab	Canyon North Patch Reef	WP41		*Pocillopora damicornis*	
LT01	Dahab	Canyon North Patch Reef	WP41		*Pocillopora damicornis*	
LT01	Dahab	Canyon North Patch Reef	WP41		*Astreopora myriophthalma*	
LT01	Dahab	Canyon North Patch Reef	WP41		*Astreopora myriophthalma*	
LT01	Dahab	Canyon North Patch Reef	WP41		*Astreopora myriophthalma*	
LT02	Dahab	Canyon North Patch Reef	WP41		*Porites sp.*	
LT02	Dahab	Canyon North Patch Reef	WP41		*Porites sp.*	
LT02	Dahab	Canyon North Patch Reef	WP41		*Porites sp.*	
LT02	Dahab	Canyon North Patch Reef	WP41		*Echinopora forskaliana*	LT2a
LT02	Dahab	Canyon North Patch Reef	WP41		*Pocillopora damicornis*	
LT02	Dahab	Canyon North Patch Reef	WP41		red algae	
LT02	Dahab	Canyon North Patch Reef	WP41		red algae	
LT02	Dahab	Canyon North Patch Reef	WP41		*Pocillopora damicornis*	
LT02	Dahab	Canyon North Patch Reef	WP41		*Galaxea fascicularis*	
LT02	Dahab	Canyon North Patch Reef	WP41		*Dipsastraea sp.*	
LT02	Dahab	Canyon North Patch Reef	WP41		*Dipsastraea sp.*	
LT02	Dahab	Canyon North Patch Reef	WP41		*Dipsastraea sp.*	
LT02	Dahab	Canyon North Patch Reef	WP41		*Galaxea fascicularis*	
LT02	Dahab	Canyon North Patch Reef	WP41		*Galaxea fascicularis*	
LT02	Dahab	Canyon North Patch Reef	WP41		*Hydnophora microconos*	LT2b
LT02	Dahab	Canyon North Patch Reef	WP41		*Hydnophora microconos*	
LT02	Dahab	Canyon North Patch Reef	WP41		matrix	
LT02	Dahab	Canyon North Patch Reef	WP41		*Galaxea fascicularis*	
LT02	Dahab	Canyon North Patch Reef	WP41		*Galaxea fascicularis*	
LT02	Dahab	Canyon North Patch Reef	WP41		matrix	
LT02	Dahab	Canyon North Patch Reef	WP41		*Pocillopora damicornis*	

LT	Locality	Site	GPS	Layer	*Name*	Sample
LT03	Dahab	Canyon North Patch Reef	WP41		*Galaxea fascicularis*	
LT03	Dahab	Canyon North Patch Reef	WP41		matrix	
LT03	Dahab	Canyon North Patch Reef	WP41		matrix	
LT03	Dahab	Canyon North Patch Reef	WP41		matrix	
LT03	Dahab	Canyon North Patch Reef	WP41		matrix	
LT03	Dahab	Canyon North Patch Reef	WP41		matrix	
LT03	Dahab	Canyon North Patch Reef	WP41		matrix	
LT03	Dahab	Canyon North Patch Reef	WP41		matrix	
LT03	Dahab	Canyon North Patch Reef	WP41		matrix	
LT03	Dahab	Canyon North Patch Reef	WP41		red algae	
LT03	Dahab	Canyon North Patch Reef	WP41		matrix	
LT03	Dahab	Canyon North Patch Reef	WP41		*Galaxea fascicularis*	
LT03	Dahab	Canyon North Patch Reef	WP41		matrix	
LT03	Dahab	Canyon North Patch Reef	WP41		red algae	
LT03	Dahab	Canyon North Patch Reef	WP41		*Dipsastraea sp.*	
LT03	Dahab	Canyon North Patch Reef	WP41		red algae	
LT03	Dahab	Canyon North Patch Reef	WP41		matrix	
LT03	Dahab	Canyon North Patch Reef	WP41		matrix	
LT03	Dahab	Canyon North Patch Reef	WP41		red algae	
LT03	Dahab	Canyon North Patch Reef	WP41		matrix	
LT03	Dahab	Canyon North Patch Reef	WP41		matrix	
LT03	Dahab	Canyon North Patch Reef	WP41		*Galaxea fascicularis*	
LT03	Dahab	Canyon North Patch Reef	WP41		*Galaxea fascicularis*	
LT03	Dahab	Canyon North Patch Reef	WP41		*Galaxea fascicularis*	
LT04	Dahab	Canyon North Patch Reef	WP41		red algae	
LT04	Dahab	Canyon North Patch Reef	WP41		*Cyphastrea sp.*	LT4a
LT04	Dahab	Canyon North Patch Reef	WP41		*Cyphastrea sp.*	
LT04	Dahab	Canyon North Patch Reef	WP41		matrix	
LT04	Dahab	Canyon North Patch Reef	WP41		matrix	
LT04	Dahab	Canyon North Patch Reef	WP41		matrix	
LT04	Dahab	Canyon North Patch Reef	WP41		matrix	
LT04	Dahab	Canyon North Patch Reef	WP41		*Stylophora sp.*	
LT04	Dahab	Canyon North Patch Reef	WP41		matrix	
LT04	Dahab	Canyon North Patch Reef	WP41		*Galaxea fascicularis*	
LT04	Dahab	Canyon North Patch Reef	WP41		*Paramontastraea peresi*	
LT04	Dahab	Canyon North Patch Reef	WP41		*Goniastrea Paramontastraea peresi*	
LT04	Dahab	Canyon North Patch Reef	WP41		*Paramontastraea peresi*	
LT04	Dahab	Canyon North Patch Reef	WP41		*Paramontastraea peresi*	
LT04	Dahab	Canyon North Patch Reef	WP41		Serpulid	
LT04	Dahab	Canyon North Patch Reef	WP41		*Porites nodifera*	
LT04	Dahab	Canyon North Patch Reef	WP41		*Porites nodifera*	
LT04	Dahab	Canyon North Patch Reef	WP41		*Porites nodifera*	
LT04	Dahab	Canyon North Patch Reef	WP41		matrix	
LT04	Dahab	Canyon North Patch Reef	WP41		*Galaxea fascicularis*	
LT04	Dahab	Canyon North Patch Reef	WP41		*Stylophora sp.*	
LT05	Dahab	Canyon North Patch Reef	WP41		*Favites pentagona*	

LT	Locality	Site	GPS	Layer	*Name*	Sample
LT05	Dahab	Canyon North Patch Reef	WP41		*Porites lobata/lutea*	
LT05	Dahab	Canyon North Patch Reef	WP41		red algae	
LT05	Dahab	Canyon North Patch Reef	WP41		matrix	
LT05	Dahab	Canyon North Patch Reef	WP41		*Dipsastraea sp.*	
LT05	Dahab	Canyon North Patch Reef	WP41		*Dipsastraea sp.*	
LT05	Dahab	Canyon North Patch Reef	WP41		*Platygyra lamellina*	
LT05	Dahab	Canyon North Patch Reef	WP41		matrix	
LT05	Dahab	Canyon North Patch Reef	WP41		red algae	
LT05	Dahab	Canyon North Patch Reef	WP41		*Platygyra lamellina*	
LT05	Dahab	Canyon North Patch Reef	WP41		*Platygyra lamellina*	
LT05	Dahab	Canyon North Patch Reef	WP41		*Platygyra lamellina*	
LT05	Dahab	Canyon North Patch Reef	WP41		*Platygyra lamellina*	
LT05	Dahab	Canyon North Patch Reef	WP41		Bivalve	
LT06	Dahab	Canyon Reef	WP42	A	*Porites nodifera*	
LT06	Dahab	Canyon Reef	WP42	A	matrix	
LT06	Dahab	Canyon Reef	WP42	A	matrix	
LT06	Dahab	Canyon Reef	WP42	A	*Porites nodifera*	
LT06	Dahab	Canyon Reef	WP42	A	*Porites nodifera*	
LT06	Dahab	Canyon Reef	WP42	A	matrix	
LT06	Dahab	Canyon Reef	WP42	A	matrix	
LT06	Dahab	Canyon Reef	WP42	A	matrix	
LT06	Dahab	Canyon Reef	WP42	A	matrix	
LT06	Dahab	Canyon Reef	WP42	A	matrix	
LT06	Dahab	Canyon Reef	WP42	A	matrix	
LT06	Dahab	Canyon Reef	WP42	A	*Pavona sp.*	LT6a
LT06	Dahab	Canyon Reef	WP42	A	matrix	
LT06	Dahab	Canyon Reef	WP42	A	matrix	
LT06	Dahab	Canyon Reef	WP42	A	matrix	LT6b
LT06	Dahab	Canyon Reef	WP42	A	matrix	
LT06	Dahab	Canyon Reef	WP42	A	matrix	
LT06	Dahab	Canyon Reef	WP42	A	matrix	
LT06	Dahab	Canyon Reef	WP42	A	matrix	
LT06	Dahab	Canyon Reef	WP42	A	matrix	
LT06	Dahab	Canyon Reef	WP42	A	matrix	
LT06	Dahab	Canyon Reef	WP42	A	matrix	
LT06	Dahab	Canyon Reef	WP42	A	matrix	
LT06	Dahab	Canyon Reef	WP42	A	matrix	
LT06	Dahab	Canyon Reef	WP42	A	matrix	
LT06	Dahab	Canyon Reef	WP42	A	matrix	
LT06	Dahab	Canyon Reef	WP42	A	matrix	
LT06	Dahab	Canyon Reef	WP42	A	*Porites nodifera*	
LT06	Dahab	Canyon Reef	WP42	A	matrix	
LT06	Dahab	Canyon Reef	WP42	A	matrix	
LT06	Dahab	Canyon Reef	WP42	A	*Porites nodifera*	
LT06	Dahab	Canyon Reef	WP42	A	matrix	
LT06	Dahab	Canyon Reef	WP42	A	*Porites nodifera*	

LT	Locality	Site	GPS	Layer	*Name*	Sample
LT06	Dahab	Canyon Reef	WP42	A	*Porites nodifera*	
LT06	Dahab	Canyon Reef	WP42	A	*Porites nodifera*	
LT06	Dahab	Canyon Reef	WP42	A	*Porites nodifera*	
LT06	Dahab	Canyon Reef	WP42	A	*Porites nodifera*	
LT06	Dahab	Canyon Reef	WP42	A	*Porites nodifera*	
LT06	Dahab	Canyon Reef	WP42	A	matrix	
LT06	Dahab	Canyon Reef	WP42	A	matrix	
LT06	Dahab	Canyon Reef	WP42	A	matrix	
LT06	Dahab	Canyon Reef	WP42	A	matrix	
LT06	Dahab	Canyon Reef	WP42	A	red algae	LT6c
LT06	Dahab	Canyon Reef	WP42	A	red algae	
LT06	Dahab	Canyon Reef	WP42	A	red algae	
LT06	Dahab	Canyon Reef	WP42	A	matrix	
LT06	Dahab	Canyon Reef	WP42	A	matrix	
LT06	Dahab	Canyon Reef	WP42	A	matrix	
LT06	Dahab	Canyon Reef	WP42	A	red algae	
LT06	Dahab	Canyon Reef	WP42	A	red algae	
LT06	Dahab	Canyon Reef	WP42	A	red algae	
LT06	Dahab	Canyon Reef	WP42	A	red algae	
LT06	Dahab	Canyon Reef	WP42	A	red algae	
LT06	Dahab	Canyon Reef	WP42	A	red algae	
LT06	Dahab	Canyon Reef	WP42	A	red algae	
LT06	Dahab	Canyon Reef	WP42	A	red algae	
LT06	Dahab	Canyon Reef	WP42	A	matrix	
LT06	Dahab	Canyon Reef	WP42	A	red algae	
LT06	Dahab	Canyon Reef	WP42	A	matrix	
LT06	Dahab	Canyon Reef	WP42	A	red algae	
LT06	Dahab	Canyon Reef	WP42	A	red algae	
LT06	Dahab	Canyon Reef	WP42	A	*Porites nodifera*	
LT06	Dahab	Canyon Reef	WP42	A	*Porites nodifera*	
LT06	Dahab	Canyon Reef	WP42	A	*Porites nodifera*	
LT06	Dahab	Canyon Reef	WP42	A	*Porites nodifera*	
LT06	Dahab	Canyon Reef	WP42	A	*Porites nodifera*	
LT06	Dahab	Canyon Reef	WP42	A	*Porites nodifera*	
LT06	Dahab	Canyon Reef	WP42	A	*Porites nodifera*	
LT06	Dahab	Canyon Reef	WP42	A	*Porites nodifera*	
LT06	Dahab	Canyon Reef	WP42	A	*Porites nodifera*	
LT06	Dahab	Canyon Reef	WP42	A	matrix	
LT06	Dahab	Canyon Reef	WP42	A	matrix	
LT06	Dahab	Canyon Reef	WP42	A	Scleractinia indet.	
LT06	Dahab	Canyon Reef	WP42	A	*Porites nodifera*	
LT06	Dahab	Canyon Reef	WP42	A	*Porites nodifera*	
LT06	Dahab	Canyon Reef	WP42	A	matrix	
LT06	Dahab	Canyon Reef	WP42	A	*Porites nodifera*	
LT06	Dahab	Canyon Reef	WP42	A	*Porites nodifera*	
LT06	Dahab	Canyon Reef	WP42	A	*Porites nodifera*	

LT	Locality	Site	GPS	Layer	*Name*	Sample
LT06	Dahab	Canyon Reef	WP42	A	matrix	
LT06	Dahab	Canyon Reef	WP42	A	matrix	
LT06	Dahab	Canyon Reef	WP42	A	matrix	
LT06	Dahab	Canyon Reef	WP42	A	matrix	
LT06	Dahab	Canyon Reef	WP42	A	matrix	
LT06	Dahab	Canyon Reef	WP42	A	*Porites nodifera*	
LT06	Dahab	Canyon Reef	WP42	A	*Porites nodifera*	
LT06	Dahab	Canyon Reef	WP42	A	*Porites nodifera*	
LT06	Dahab	Canyon Reef	WP42	A	matrix	
LT06	Dahab	Canyon Reef	WP42	A	*Porites nodifera*	
LT06	Dahab	Canyon Reef	WP42	A	*Porites nodifera*	
LT06	Dahab	Canyon Reef	WP42	A	*Porites nodifera*	
LT06	Dahab	Canyon Reef	WP42	A	*Porites nodifera*	
LT06	Dahab	Canyon Reef	WP42	A	*Porites nodifera*	
LT06	Dahab	Canyon Reef	WP42	A	*Porites nodifera*	
LT06	Dahab	Canyon Reef	WP42	A	matrix	
LT06	Dahab	Canyon Reef	WP42	A	*Porites nodifera*	
LT06	Dahab	Canyon Reef	WP42	A	*Porites nodifera*	
LT06	Dahab	Canyon Reef	WP42	A	matrix	
LT06	Dahab	Canyon Reef	WP42	A	matrix	
LT06	Dahab	Canyon Reef	WP42	A	matrix	
LT06	Dahab	Canyon Reef	WP42	A	matrix	
LT07	Dahab	Canyon Reef		B	*Astreopora myriophthalma*	
LT07	Dahab	Canyon Reef		B	*Echinopora forskaliana*	LT7a
LT07	Dahab	Canyon Reef		B	*Astreopora myriophthalma*	LT7b
LT07	Dahab	Canyon Reef		B	*Platygyra sp.*	LT7c
LT07	Dahab	Canyon Reef		B	*Platygyra sp.*	LT7d
LT07	Dahab	Canyon Reef		B	*Dipsastraea sp.*	
LT07	Dahab	Canyon Reef		B	matrix	
LT07	Dahab	Canyon Reef		B	*Stylophora sp.*	
LT07	Dahab	Canyon Reef		B	matrix	
LT07	Dahab	Canyon Reef		B	*Fungia sp.*	
LT07	Dahab	Canyon Reef		B	*Acropora sp.*	
LT07	Dahab	Canyon Reef		B	*Favites sp.*	
LT07	Dahab	Canyon Reef		B	*Favites sp.*	
LT07	Dahab	Canyon Reef		B	matrix	
LT07	Dahab	Canyon Reef		B	red algae	
LT07	Dahab	Canyon Reef		B	matrix	
LT07	Dahab	Canyon Reef		B	matrix	
LT07	Dahab	Canyon Reef		B	*Goniastrea sp.*	LT7e
LT07	Dahab	Canyon Reef		B	*Lobophyllia sp.*	
LT07	Dahab	Canyon Reef		B	matrix	
LT07	Dahab	Canyon Reef		B	matrix	
LT07	Dahab	Canyon Reef		B	*Galaxea fascicularis*	
LT07	Dahab	Canyon Reef		B	*Galaxea fascicularis*	
LT07	Dahab	Canyon Reef		B	*Galaxea fascicularis*	

LT	Locality	Site	GPS	Layer	*Name*	Sample
LT07	Dahab	Canyon Reef		B	*Pavona cactus*	LT7f
LT07	Dahab	Canyon Reef		B	matrix	
LT07	Dahab	Canyon Reef		B	*Acropora sp.*	
LT07	Dahab	Canyon Reef		B	matrix	
LT07	Dahab	Canyon Reef		B	matrix	
LT07	Dahab	Canyon Reef		B	red algae	
LT07	Dahab	Canyon Reef		B	*Turbinaria reniformis*	LT7g
LT07	Dahab	Canyon Reef		B	matrix	
LT07	Dahab	Canyon Reef		B	*Platygyra sp.*	
LT07	Dahab	Canyon Reef		B	*Platygyra sp.*	
LT07	Dahab	Canyon Reef		B	*Platygyra sp.*	
LT07	Dahab	Canyon Reef		B	matrix	
LT07	Dahab	Canyon Reef		B	*Acropora sp.*	
LT07	Dahab	Canyon Reef		B	matrix	
LT07	Dahab	Canyon Reef		B	Scleractinia indet.	LT7??
LT07	Dahab	Canyon Reef		B	*Leptastrea sp.*	LT7h
LT07	Dahab	Canyon Reef		B	*Acropora sp.*	
LT07	Dahab	Canyon Reef		B	*Porites lobata/lutea*	
LT07	Dahab	Canyon Reef		B	*Lobophyllia hemprichii*	
LT07	Dahab	Canyon Reef		B	red algae	
LT07	Dahab	Canyon Reef		B	red algae	
LT07	Dahab	Canyon Reef		B	red algae	
LT07	Dahab	Canyon Reef		B	matrix	
LT07	Dahab	Canyon Reef		B	Argariciidae indet.	LT7i
LT07	Dahab	Canyon Reef		B	*Acropora sp.*	
LT07	Dahab	Canyon Reef		B	*Porites lobata/lutea*	
LT07	Dahab	Canyon Reef		B	matrix	
LT07	Dahab	Canyon Reef		B	red algae	
LT07	Dahab	Canyon Reef		B	*Porites sp.*	LT7j
LT07	Dahab	Canyon Reef		B	*Porites sp.*	
LT07	Dahab	Canyon Reef		B	*Porites sp.*	
LT07	Dahab	Canyon Reef		B	*Porites sp.*	
LT07	Dahab	Canyon Reef		B	*Porites sp.*	
LT07	Dahab	Canyon Reef		B	matrix	
LT07	Dahab	Canyon Reef		B	*Lobophyllia sp.*	
LT07	Dahab	Canyon Reef		B	*Lobophyllia sp.*	
LT07	Dahab	Canyon Reef		B	*Acropora sp.*	
LT07	Dahab	Canyon Reef		B	*Fungia sp.*	
LT07	Dahab	Canyon Reef		B	matrix	
LT07	Dahab	Canyon Reef		B	matrix	
LT07	Dahab	Canyon Reef		B	matrix	
LT07	Dahab	Canyon Reef		B	*Acropora sp.*	
LT07	Dahab	Canyon Reef		B	*Acropora sp.*	
LT07	Dahab	Canyon Reef		B	matrix	
LT07	Dahab	Canyon Reef		B	*Acropora sp.*	
LT07	Dahab	Canyon Reef		B	*Cyphastrea sp.*	

LT	Locality	Site	GPS	Layer	*Name*	Sample
LT07	Dahab	Canyon Reef		B	*Acropora sp.*	
LT07	Dahab	Canyon Reef		B	matrix	
LT07	Dahab	Canyon Reef		B	*Acropora sp.*	LT7k
LT07	Dahab	Canyon Reef		B	*Acropora sp.*	LT7l
LT07	Dahab	Canyon Reef		B	*Acropora sp.*	
LT08	Dahab	Canyon Reef		B	*Acropora sp.*	LT8a
LT08	Dahab	Canyon Reef		B	*Acropora sp.*	
LT08	Dahab	Canyon Reef		B	*Acropora sp.*	
LT08	Dahab	Canyon Reef		B	*Acropora sp.*	
LT08	Dahab	Canyon Reef		B	*Acropora sp.*	
LT08	Dahab	Canyon Reef		B	*Acropora sp.*	
LT08	Dahab	Canyon Reef		B	*Acropora sp.*	
LT08	Dahab	Canyon Reef		B	matrix	
LT08	Dahab	Canyon Reef		B	matrix	
LT08	Dahab	Canyon Reef		B	*Montipora sp.*	LT8b
LT08	Dahab	Canyon Reef		B	*Montipora sp.*	
LT08	Dahab	Canyon Reef		B	*Montipora sp.*	
LT08	Dahab	Canyon Reef		B	matrix	
LT08	Dahab	Canyon Reef		B	matrix	
LT08	Dahab	Canyon Reef		B	*Montipora sp.*	
LT08	Dahab	Canyon Reef		B	Echinoid spine	
LT08	Dahab	Canyon Reef		B	*Acropora sp.*	
LT08	Dahab	Canyon Reef		B	*Acropora sp.*	
LT08	Dahab	Canyon Reef		B	red algae	
LT08	Dahab	Canyon Reef		B	*Acropora sp.*	
LT08	Dahab	Canyon Reef		B	matrix	
LT08	Dahab	Canyon Reef		B	*Porites lobata/lutea*	
LT08	Dahab	Canyon Reef		B	matrix	
LT08	Dahab	Canyon Reef		B	*Porites lobata/lutea*	
LT08	Dahab	Canyon Reef		B	red algae	
LT08	Dahab	Canyon Reef		B	red algae	
LT08	Dahab	Canyon Reef		B	*Porites lobata/lutea*	
LT08	Dahab	Canyon Reef		B	matrix	
LT08	Dahab	Canyon Reef		B	red algae	
LT08	Dahab	Canyon Reef		B	red algae	
LT08	Dahab	Canyon Reef		B	*Porites lobata/lutea*	
LT08	Dahab	Canyon Reef		B	*Porites lobata/lutea*	
LT08	Dahab	Canyon Reef		B	*Porites lobata/lutea*	
LT08	Dahab	Canyon Reef		B	*Porites lobata/lutea*	
LT08	Dahab	Canyon Reef		B	red algae	
LT08	Dahab	Canyon Reef		B	*Porites lobata/lutea*	
LT08	Dahab	Canyon Reef		B	*Porites lobata/lutea*	
LT08	Dahab	Canyon Reef		B	*Porites lobata/lutea*	
LT08	Dahab	Canyon Reef		B	red algae	
LT08	Dahab	Canyon Reef		B	red algae	
LT08	Dahab	Canyon Reef		B	*Leptastrea sp.*	LT8c

LT	Locality	Site	GPS	Layer	*Name*	Sample
LT08	Dahab	Canyon Reef		B	*Leptastrea sp.*	
LT08	Dahab	Canyon Reef		B	*Cyphastrea sp.*	
LT08	Dahab	Canyon Reef		B	*Cyphastrea sp.*	
LT08	Dahab	Canyon Reef		B	red algae	
LT08	Dahab	Canyon Reef		B	red algae	
LT08	Dahab	Canyon Reef		B	*Porites lobata/lutea*	
LT08	Dahab	Canyon Reef		B	*Dipsastraea sp.*	LT8d
LT08	Dahab	Canyon Reef		B	*Porites lobata/lutea*	
LT08	Dahab	Canyon Reef		B	*Porites lobata/lutea*	
LT09	Dahab	Canyon Reef	WP43	C	red algae	
LT09	Dahab	Canyon Reef	WP43	C	red algae	
LT09	Dahab	Canyon Reef	WP43	C	red algae	
LT09	Dahab	Canyon Reef	WP43	C	red algae	
LT09	Dahab	Canyon Reef	WP43	C	red algae	
LT09	Dahab	Canyon Reef	WP43	C	*Galaxea fascicularis*	
LT09	Dahab	Canyon Reef	WP43	C	red algae	
LT09	Dahab	Canyon Reef	WP43	C	red algae	
LT09	Dahab	Canyon Reef	WP43	C	red algae	
LT09	Dahab	Canyon Reef	WP43	C	red algae	
LT09	Dahab	Canyon Reef	WP43	C	red algae	
LT09	Dahab	Canyon Reef	WP43	C	red algae	
LT09	Dahab	Canyon Reef	WP43	C	red algae	
LT09	Dahab	Canyon Reef	WP43	C	red algae	
LT09	Dahab	Canyon Reef	WP43	C	red algae	
LT09	Dahab	Canyon Reef	WP43	C	red algae	
LT09	Dahab	Canyon Reef	WP43	C	red algae	
LT09	Dahab	Canyon Reef	WP43	C	red algae	
LT09	Dahab	Canyon Reef	WP43	C	red algae	
LT09	Dahab	Canyon Reef	WP43	C	red algae	
LT09	Dahab	Canyon Reef	WP43	C	*Dipsastraea sp.*	LT9a
LT09	Dahab	Canyon Reef	WP43	C	red algae	
LT09	Dahab	Canyon Reef	WP43	C	red algae	
LT09	Dahab	Canyon Reef	WP43	C	red algae	
LT09	Dahab	Canyon Reef	WP43	C	matrix	
LT09	Dahab	Canyon Reef	WP43	C	matrix	
LT09	Dahab	Canyon Reef	WP43	C	*Lobophyllia hemprichii*	
LT09	Dahab	Canyon Reef	WP43	C	red algae	
LT09	Dahab	Canyon Reef	WP43	C	*Dipsastraea sp.*	
LT09	Dahab	Canyon Reef	WP43	C	matrix	
LT09	Dahab	Canyon Reef	WP43	C	matrix	
LT09	Dahab	Canyon Reef	WP43	C	red algae	
LT09	Dahab	Canyon Reef	WP43	C	red algae	
LT09	Dahab	Canyon Reef	WP43	C	red algae	
LT09	Dahab	Canyon Reef	WP43	C	Scleractinia indet.	LT9b
LT09	Dahab	Canyon Reef	WP43	C	red algae	
LT09	Dahab	Canyon Reef	WP43	C	red algae	

LT	Locality	Site	GPS	Layer	*Name*	Sample
LT09	Dahab	Canyon Reef	WP43	C	red algae	
LT09	Dahab	Canyon Reef	WP43	C	red algae	
LT09	Dahab	Canyon Reef	WP43	C	red algae	
LT09	Dahab	Canyon Reef	WP43	C	matrix	
LT09	Dahab	Canyon Reef	WP43	C	red algae	
LT09	Dahab	Canyon Reef	WP43	C	matrix	
LT09	Dahab	Canyon Reef	WP43	C	red algae	
LT09	Dahab	Canyon Reef	WP43	C	red algae	
LT09	Dahab	Canyon Reef	WP43	C	red algae	
LT09	Dahab	Canyon Reef	WP43	C	red algae	
LT09	Dahab	Canyon Reef	WP43	C	red algae	
LT09	Dahab	Canyon Reef	WP43	C	matrix	
LT09	Dahab	Canyon Reef	WP43	C	matrix	
LT09	Dahab	Canyon Reef	WP43	C	matrix	
LT10	Dahab	Canyon Reef	WP43	C	red algae	
LT10	Dahab	Canyon Reef	WP43	C	red algae	
LT10	Dahab	Canyon Reef	WP43	C	red algae	
LT10	Dahab	Canyon Reef	WP43	C	red algae	
LT10	Dahab	Canyon Reef	WP43	C	red algae	
LT10	Dahab	Canyon Reef	WP43	C	*Favites sp.*	
LT10	Dahab	Canyon Reef	WP43	C	*Favites sp.*	
LT10	Dahab	Canyon Reef	WP43	C	*Favites sp.*	
LT10	Dahab	Canyon Reef	WP43	C	*Favites sp.*	
LT10	Dahab	Canyon Reef	WP43	C	red algae	
LT10	Dahab	Canyon Reef	WP43	C	matrix	
LT10	Dahab	Canyon Reef	WP43	C	matrix	
LT10	Dahab	Canyon Reef	WP43	C	red algae	
LT10	Dahab	Canyon Reef	WP43	C	red algae	
LT10	Dahab	Canyon Reef	WP43	C	red algae	
LT10	Dahab	Canyon Reef	WP43	C	red algae	
LT10	Dahab	Canyon Reef	WP43	C	red algae	
LT10	Dahab	Canyon Reef	WP43	C	red algae	
LT10	Dahab	Canyon Reef	WP43	C	red algae	
LT10	Dahab	Canyon Reef	WP43	C	red algae	
LT10	Dahab	Canyon Reef	WP43	C	*Stylophora sp.*	
LT10	Dahab	Canyon Reef	WP43	C	*Lobophyllia corymbosa*	
LT10	Dahab	Canyon Reef	WP43	C	red algae	
LT10	Dahab	Canyon Reef	WP43	C	*Lobophyllia corymbosa*	
LT10	Dahab	Canyon Reef	WP43	C	red algae	
LT10	Dahab	Canyon Reef	WP43	C	*Lobophyllia corymbosa*	
LT10	Dahab	Canyon Reef	WP43	C	red algae	
LT10	Dahab	Canyon Reef	WP43	C	red algae	
LT10	Dahab	Canyon Reef	WP43	C	red algae	
LT11	Dahab	Canyon Reef	WP44	C	matrix	
LT11	Dahab	Canyon Reef	WP44	C	Bivalve	

LT	Locality	Site	GPS	Layer	*Name*	Sample
LT11	Dahab	Canyon Reef	WP44	C	matrix	
LT11	Dahab	Canyon Reef	WP44	C	red algae	
LT11	Dahab	Canyon Reef	WP44	C	red algae	
LT11	Dahab	Canyon Reef	WP44	C	red algae	
LT11	Dahab	Canyon Reef	WP44	C	red algae	
LT11	Dahab	Canyon Reef	WP44	C	red algae	
LT11	Dahab	Canyon Reef	WP44	C	red algae	
LT11	Dahab	Canyon Reef	WP44	C	red algae	
LT11	Dahab	Canyon Reef	WP44	C	red algae	
LT11	Dahab	Canyon Reef	WP44	C	Bivalve	
LT11	Dahab	Canyon Reef	WP44	C	red algae	
LT11	Dahab	Canyon Reef	WP44	C	red algae	
LT11	Dahab	Canyon Reef	WP44	C	red algae	
LT11	Dahab	Canyon Reef	WP44	C	red algae	
LT11	Dahab	Canyon Reef	WP44	C	red algae	
LT11	Dahab	Canyon Reef	WP44	C	red algae	
LT11	Dahab	Canyon Reef	WP44	C	red algae	
LT11	Dahab	Canyon Reef	WP44	C	red algae	
LT11	Dahab	Canyon Reef	WP44	C	red algae	
LT11	Dahab	Canyon Reef	WP44	C	red algae	
LT11	Dahab	Canyon Reef	WP44	C	*Porites lobata/lutea*	
LT11	Dahab	Canyon Reef	WP44	C	red algae	
LT11	Dahab	Canyon Reef	WP44	C	*Porites lobata/lutea*	
LT11	Dahab	Canyon Reef	WP44	C	red algae	
LT11	Dahab	Canyon Reef	WP44	C	*Porites lobata/lutea*	
LT11	Dahab	Canyon Reef	WP44	C	*Porites lobata/lutea*	
LT11	Dahab	Canyon Reef	WP44	C	red algae	
LT11	Dahab	Canyon Reef	WP44	C	red algae	
LT11	Dahab	Canyon Reef	WP44	C	red algae	
LT11	Dahab	Canyon Reef	WP44	C	red algae	
LT11	Dahab	Canyon Reef	WP44	C	matrix	
LT11	Dahab	Canyon Reef	WP44	C	*Porites lobata/lutea*	
LT11	Dahab	Canyon Reef	WP44	C	*Porites lobata/lutea*	
LT11	Dahab	Canyon Reef	WP44	C	*Porites lobata/lutea*	
LT11	Dahab	Canyon Reef	WP44	C	*Porites lobata/lutea*	
LT11	Dahab	Canyon Reef	WP44	C	*Porites lobata/lutea*	
LT11	Dahab	Canyon Reef	WP44	C	red algae	
LT11	Dahab	Canyon Reef	WP44	C	red algae	
LT11	Dahab	Canyon Reef	WP44	C	*Porites lobata/lutea*	
LT11	Dahab	Canyon Reef	WP44	C	*Porites lobata/lutea*	
LT11	Dahab	Canyon Reef	WP44	C	*Porites lobata/lutea*	
LT11	Dahab	Canyon Reef	WP44	C	*Porites lobata/lutea*	
LT11	Dahab	Canyon Reef	WP44	C	*Porites lobata/lutea*	
LT11	Dahab	Canyon Reef	WP44	C	*Porites lobata/lutea*	
LT11	Dahab	Canyon Reef	WP44	C	*Porites lobata/lutea*	

LT	Locality	Site	GPS	Layer	*Name*	Sample
LT11	Dahab	Canyon Reef	WP44	C	*Porites lobata/lutea*	
LT12	Dahab	Canyon Reef	WP44	C	*Porites lobata/lutea*	
LT12	Dahab	Canyon Reef	WP44	C	*Porites lobata/lutea*	
LT12	Dahab	Canyon Reef	WP44	C	*Porites lobata/lutea*	
LT12	Dahab	Canyon Reef	WP44	C	*Porites lobata/lutea*	
LT12	Dahab	Canyon Reef	WP44	C	*Porites lobata/lutea*	
LT12	Dahab	Canyon Reef	WP44	C	red algae	
LT12	Dahab	Canyon Reef	WP44	C	*Platygyra sp.*	
LT12	Dahab	Canyon Reef	WP44	C	red algae	
LT12	Dahab	Canyon Reef	WP44	C	red algae	
LT12	Dahab	Canyon Reef	WP44	C	matrix	
LT12	Dahab	Canyon Reef	WP44	C	*Platygyra sp.*	
LT12	Dahab	Canyon Reef	WP44	C	red algae	
LT12	Dahab	Canyon Reef	WP44	C	red algae	
LT12	Dahab	Canyon Reef	WP44	C	red algae	
LT12	Dahab	Canyon Reef	WP44	C	red algae	
LT12	Dahab	Canyon Reef	WP44	C	red algae	
LT12	Dahab	Canyon Reef	WP44	C	red algae	
LT12	Dahab	Canyon Reef	WP44	C	red algae	
LT12	Dahab	Canyon Reef	WP44	C	red algae	
LT12	Dahab	Canyon Reef	WP44	C	*Acropora sp.*	
LT12	Dahab	Canyon Reef	WP44	C	*Acropora sp.*	
LT12	Dahab	Canyon Reef	WP44	C	red algae	
LT12	Dahab	Canyon Reef	WP44	C	red algae	
LT12	Dahab	Canyon Reef	WP44	C	red algae	
LT12	Dahab	Canyon Reef	WP44	C	red algae	
LT12	Dahab	Canyon Reef	WP44	C	red algae	
LT12	Dahab	Canyon Reef	WP44	C	red algae	
LT12	Dahab	Canyon Reef	WP44	C	red algae	
LT13	Dahab	Canyon Reef	WP48	B	Basalt	
LT13	Dahab	Canyon Reef	WP48	B	*Acropora muricata*	
LT13	Dahab	Canyon Reef	WP48	B	*Acropora muricata*	
LT13	Dahab	Canyon Reef	WP48	B	red algae	
LT13	Dahab	Canyon Reef	WP48	B	fanglomerate	
LT13	Dahab	Canyon Reef	WP48	B	red algae	
LT13	Dahab	Canyon Reef	WP48	B	red algae	
LT13	Dahab	Canyon Reef	WP48	B	red algae	
LT13	Dahab	Canyon Reef	WP48	B	*Acropora muricata*	
LT13	Dahab	Canyon Reef	WP48	B	*Acropora muricata*	
LT13	Dahab	Canyon Reef	WP48	B	*Acropora muricata*	
LT13	Dahab	Canyon Reef	WP48	B	red algae	
LT13	Dahab	Canyon Reef	WP48	B	*Acropora muricata*	
LT13	Dahab	Canyon Reef	WP48	B	*Acropora muricata*	
LT13	Dahab	Canyon Reef	WP48	B	*Acropora muricata*	
LT13	Dahab	Canyon Reef	WP48	B	*Acropora muricata*	

LT	Locality	Site	GPS	Layer	*Name*	Sample
LT13	Dahab	Canyon Reef	WP48	B	*Acropora muricata*	
LT13	Dahab	Canyon Reef	WP48	B	*Acropora muricata*	
LT13	Dahab	Canyon Reef	WP48	B	*Acropora muricata*	
LT13	Dahab	Canyon Reef	WP48	B	*Acropora muricata*	
LT13	Dahab	Canyon Reef	WP48	B	*Acropora muricata*	
LT13	Dahab	Canyon Reef	WP48	B	*Acropora muricata*	
LT13	Dahab	Canyon Reef	WP48	B	*Acropora muricata*	
LT13	Dahab	Canyon Reef	WP48	B	*Acropora muricata*	
LT13	Dahab	Canyon Reef	WP48	B	*Acropora muricata*	
LT13	Dahab	Canyon Reef	WP48	B	*Acropora muricata*	
LT13	Dahab	Canyon Reef	WP48	B	*Acropora muricata*	
LT13	Dahab	Canyon Reef	WP48	B	*Acropora muricata*	
LT13	Dahab	Canyon Reef	WP48	B	*Acropora muricata*	
LT13	Dahab	Canyon Reef	WP48	B	fanglomerate	
LT13	Dahab	Canyon Reef	WP48	B	fanglomerate	
LT13	Dahab	Canyon Reef	WP48	B	*Acropora muricata*	
LT13	Dahab	Canyon Reef	WP48	B	*Acropora muricata*	
LT13	Dahab	Canyon Reef	WP48	B	*Acropora muricata*	
LT13	Dahab	Canyon Reef	WP48	B	*Acropora muricata*	
LT13	Dahab	Canyon Reef	WP48	B	*Acropora muricata*	
LT13	Dahab	Canyon Reef	WP48	B	*Acropora muricata*	
LT13	Dahab	Canyon Reef	WP48	B	*Acropora muricata*	
LT13	Dahab	Canyon Reef	WP48	B	*Goniastrea sp.*	
LT13	Dahab	Canyon Reef	WP48	B	*Acropora muricata*	
LT13	Dahab	Canyon Reef	WP48	B	red algae	
LT14	Dahab	Canyon Reef	WP48	B	red algae	
LT14	Dahab	Canyon Reef	WP48	B	fanglomerate	
LT14	Dahab	Canyon Reef	WP48	B	*Cyphastrea serailia*	LT14a
LT14	Dahab	Canyon Reef	WP48	B	*Montipora sp.*	
LT14	Dahab	Canyon Reef	WP48	B	*Montipora sp.*	
LT14	Dahab	Canyon Reef	WP48	B	*Montipora sp.*	
LT14	Dahab	Canyon Reef	WP48	B	*Montipora sp.*	
LT14	Dahab	Canyon Reef	WP48	B	*Montipora sp.*	
LT14	Dahab	Canyon Reef	WP48	B	*Montipora sp.*	
LT14	Dahab	Canyon Reef	WP48	B	*Montipora sp.*	
LT14	Dahab	Canyon Reef	WP48	B	*Montipora sp.*	
LT14	Dahab	Canyon Reef	WP48	B	*Montipora sp.*	
LT14	Dahab	Canyon Reef	WP48	B	*Acropora muricata*	
LT14	Dahab	Canyon Reef	WP48	B	*Montipora sp.*	
LT14	Dahab	Canyon Reef	WP48	B	*Montipora sp.*	
LT14	Dahab	Canyon Reef	WP48	B	*Montipora sp.*	
LT14	Dahab	Canyon Reef	WP48	B	*Montipora sp.*	
LT14	Dahab	Canyon Reef	WP48	B	*Montipora sp.*	
LT14	Dahab	Canyon Reef	WP48	B	red algae	
LT14	Dahab	Canyon Reef	WP48	B	red algae	

LT	Locality	Site	GPS	Layer	*Name*	Sample
LT14	Dahab	Canyon Reef	WP48	B	*Lobophyllia corymbosa*	
LT14	Dahab	Canyon Reef	WP48	B	*Lobophyllia corymbosa*	
LT14	Dahab	Canyon Reef	WP48	B	*Lobophyllia corymbosa*	
LT14	Dahab	Canyon Reef	WP48	B	*Acropora sp.*	
LT14	Dahab	Canyon Reef	WP48	B	*Montipora sp.*	
LT14	Dahab	Canyon Reef	WP48	B	*Montipora sp.*	
LT14	Dahab	Canyon Reef	WP48	B	*Montipora sp.*	
LT14	Dahab	Canyon Reef	WP48	B	red algae	
LT14	Dahab	Canyon Reef	WP48	B	*Platygyra sp.*	
LT14	Dahab	Canyon Reef	WP48	B	*Platygyra sp.*	
LT14	Dahab	Canyon Reef	WP48	B	*Montipora sp.*	
LT14	Dahab	Canyon Reef	WP48	B	*Montipora sp.*	
LT14	Dahab	Canyon Reef	WP48	B	*Montipora sp.*	
LT14	Dahab	Canyon Reef	WP48	B	*Platygyra sp.*	
LT14	Dahab	Canyon Reef	WP48	B	*Goniopora sp.*	
LT14	Dahab	Canyon Reef	WP48	B	red algae	
LT14	Dahab	Canyon Reef	WP48	B	red algae	
LT14	Dahab	Canyon Reef	WP48	B	red algae	
LT14	Dahab	Canyon Reef	WP48	B	*Montipora sp.*	
LT14	Dahab	Canyon Reef	WP48	B	*Montipora sp.*	
LT14	Dahab	Canyon Reef	WP48	B	*Montipora sp.*	
LT14	Dahab	Canyon Reef	WP48	B	fanglomerate	
LT14	Dahab	Canyon Reef	WP48	B	*Leptastrea sp.*	
LT15	Dahab	Canyon Reef	WP48	B	red algae	
LT15	Dahab	Canyon Reef	WP48	B	red algae	
LT15	Dahab	Canyon Reef	WP48	B	red algae	
LT15	Dahab	Canyon Reef	WP48	B	red algae	
LT15	Dahab	Canyon Reef	WP48	B	*Acropora muricata*	
LT15	Dahab	Canyon Reef	WP48	B	*Acropora muricata*	
LT15	Dahab	Canyon Reef	WP48	B	red algae	
LT15	Dahab	Canyon Reef	WP48	B	red algae	
LT15	Dahab	Canyon Reef	WP48	B	*Acropora muricata*	
LT15	Dahab	Canyon Reef	WP48	B	*Acropora muricata*	
LT15	Dahab	Canyon Reef	WP48	B	*Acropora muricata*	
LT15	Dahab	Canyon Reef	WP48	B	*Acropora muricata*	
LT15	Dahab	Canyon Reef	WP48	B	*Acropora muricata*	
LT15	Dahab	Canyon Reef	WP48	B	*Acropora muricata*	
LT15	Dahab	Canyon Reef	WP48	B	*Acropora muricata*	
LT15	Dahab	Canyon Reef	WP48	B	*Acropora muricata*	
LT15	Dahab	Canyon Reef	WP48	B	red algae	
LT15	Dahab	Canyon Reef	WP48	B	red algae	
LT15	Dahab	Canyon Reef	WP48	B	red algae	
LT15	Dahab	Canyon Reef	WP48	B	matrix	
LT15	Dahab	Canyon Reef	WP48	B	*Millepora sp.*	LT15a
LT15	Dahab	Canyon Reef	WP48	B	*Millepora sp.*	

LT	Locality	Site	GPS	Layer	*Name*	Sample
LT15	Dahab	Canyon Reef	WP48	B	red algae	
LT15	Dahab	Canyon Reef	WP48	B	red algae	
LT15	Dahab	Canyon Reef	WP48	B	red algae	
LT15	Dahab	Canyon Reef	WP48	B	red algae	
LT15	Dahab	Canyon Reef	WP48	B	red algae	
LT15	Dahab	Canyon Reef	WP48	B	red algae	
LT15	Dahab	Canyon Reef	WP48	B	red algae	
LT15	Dahab	Canyon Reef	WP48	B	red algae	
LT15	Dahab	Canyon Reef	WP48	B	*Psammocora sp.*	LT15b
LT15	Dahab	Canyon Reef	WP48	B	*Psammocora sp.*	
LT15	Dahab	Canyon Reef	WP48	B	*Millepora sp.*	LT15c
LT15	Dahab	Canyon Reef	WP48	B	*Porites lobata/lutea*	
LT15	Dahab	Canyon Reef	WP48	B	*Leptastrea transversa*	
LT15	Dahab	Canyon Reef	WP48	B	*Acropora sp.*	
LT15	Dahab	Canyon Reef	WP48	B	*Acropora sp.*	
LT15	Dahab	Canyon Reef	WP48	B	red algae	
LT15	Dahab	Canyon Reef	WP48	B	*Porites nodifera*	
LT15	Dahab	Canyon Reef	WP48	B	Bivalve	
LT15	Dahab	Canyon Reef	WP48	B	*Montipora sp.*	LT15d
LT15	Dahab	Canyon Reef	WP48	B	*Montipora sp.*	
LT15	Dahab	Canyon Reef	WP48	B	*Montipora sp.*	
LT15	Dahab	Canyon Reef	WP48	B	*Montipora sp.*	
LT15	Dahab	Canyon Reef	WP48	B	*Acropora sp.*	
LT15	Dahab	Canyon Reef	WP48	B	red algae	
LT15	Dahab	Canyon Reef	WP48	B	*Porites nodifera*	
LT15	Dahab	Canyon Reef	WP48	B	red algae	
LT15	Dahab	Canyon Reef	WP48	B	red algae	
LT15	Dahab	Canyon Reef	WP48	B	red algae	
LT15	Dahab	Canyon Reef	WP48	B	red algae	
LT15	Dahab	Canyon Reef	WP48	B	red algae	
LT15	Dahab	Canyon Reef	WP48	B	*Acropora sp.*	
LT15	Dahab	Canyon Reef	WP48	B	red algae	
LT15	Dahab	Canyon Reef	WP48	B	red algae	
LT15	Dahab	Canyon Reef	WP48	B	*Acropora sp.*	
LT15	Dahab	Canyon Reef	WP48	B	*Porites nodifera*	
LT15	Dahab	Canyon Reef	WP48	B	red algae	
LT15	Dahab	Canyon Reef	WP48	B	red algae	
LT15	Dahab	Canyon Reef	WP48	B	red algae	
LT15	Dahab	Canyon Reef	WP48	B	red algae	
LT15	Dahab	Canyon Reef	WP48	B	matrix	
LT15	Dahab	Canyon Reef	WP48	B	matrix	
LT15	Dahab	Canyon Reef	WP48	B	red algae	
LT15	Dahab	Canyon Reef	WP48	B	red algae	
LT15	Dahab	Canyon Reef	WP48	B	*Leptastrea transversa*	
LT15	Dahab	Canyon Reef	WP48	B	red algae	
LT15	Dahab	Canyon Reef	WP48	B	*Acropora sp.*	

LT	Locality	Site	GPS	Layer	*Name*	Sample
LT15	Dahab	Canyon Reef	WP48	B	*Pocillopora damicornis*	LT15e
LT15	Dahab	Canyon Reef	WP48	B	red algae	
LT15	Dahab	Canyon Reef	WP48	B	red algae	
LT15	Dahab	Canyon Reef	WP48	B	*Acropora sp.*	LT15f
LT15	Dahab	Canyon Reef	WP48	B	*Acropora sp.*	
LT15	Dahab	Canyon Reef	WP48	B	red algae	
LT15	Dahab	Canyon Reef	WP48	B	*Cyphastrea serailia*	LT15g
LT16	Dahab	Canyon Reef	WP48	C	*Acropora sp.*	
LT16	Dahab	Canyon Reef	WP48	C	*Acropora sp.*	
LT16	Dahab	Canyon Reef	WP48	C	*Porites lobata/lutea*	
LT16	Dahab	Canyon Reef	WP48	C	*Porites lobata/lutea*	
LT16	Dahab	Canyon Reef	WP48	C	*Porites lobata/lutea*	
LT16	Dahab	Canyon Reef	WP48	C	*Porites lobata/lutea*	
LT16	Dahab	Canyon Reef	WP48	C	*Lobophyllia corymbosa*	
LT16	Dahab	Canyon Reef	WP48	C	*Platygyra sp.*	
LT16	Dahab	Canyon Reef	WP48	C	red algae	
LT16	Dahab	Canyon Reef	WP48	C	red algae	
LT16	Dahab	Canyon Reef	WP48	C	*Porites lobata/lutea*	
LT16	Dahab	Canyon Reef	WP48	C	red algae	
LT16	Dahab	Canyon Reef	WP48	C	*Porites lobata/lutea*	
LT16	Dahab	Canyon Reef	WP48	C	*Porites lobata/lutea*	
LT16	Dahab	Canyon Reef	WP48	C	*Porites lobata/lutea*	
LT16	Dahab	Canyon Reef	WP48	C	red algae	
LT16	Dahab	Canyon Reef	WP48	C	matrix	
LT16	Dahab	Canyon Reef	WP48	C	red algae	
LT16	Dahab	Canyon Reef	WP48	C	red algae	
LT16	Dahab	Canyon Reef	WP48	C	red algae	
LT16	Dahab	Canyon Reef	WP48	C	red algae	
LT16	Dahab	Canyon Reef	WP48	C	red algae	
LT16	Dahab	Canyon Reef	WP48	C	red algae	
LT16	Dahab	Canyon Reef	WP48	C	red algae	
LT16	Dahab	Canyon Reef	WP48	C	matrix	
LT16	Dahab	Canyon Reef	WP48	C	matrix	
LT16	Dahab	Canyon Reef	WP48	C	red algae	
LT16	Dahab	Canyon Reef	WP48	C	red algae	
LT16	Dahab	Canyon Reef	WP48	C	red algae	
LT16	Dahab	Canyon Reef	WP48	C	*Porites lobata/lutea*	
LT16	Dahab	Canyon Reef	WP48	C	red algae	
LT16	Dahab	Canyon Reef	WP48	C	red algae	
LT16	Dahab	Canyon Reef	WP48	C	red algae	
LT16	Dahab	Canyon Reef	WP48	C	Gastropod	
LT16	Dahab	Canyon Reef	WP48	C	red algae	
LT16	Dahab	Canyon Reef	WP48	C	matrix	
LT16	Dahab	Canyon Reef	WP48	C	*Millepora sp.*	LT16a
LT16	Dahab	Canyon Reef	WP48	C	red algae	
LT16	Dahab	Canyon Reef	WP48	C	red algae	

LT	Locality	Site	GPS	Layer	*Name*	Sample
LT16	Dahab	Canyon Reef	WP48	C	*Platygyra sp.*	
LT16	Dahab	Canyon Reef	WP48	C	red algae	
LT16	Dahab	Canyon Reef	WP48	C	red algae	
LT16	Dahab	Canyon Reef	WP48	C	red algae	
LT16	Dahab	Canyon Reef	WP48	C	*Porites lobata/lutea*	
LT16	Dahab	Canyon Reef	WP48	C	*Porites lobata/lutea*	
LT16	Dahab	Canyon Reef	WP48	C	*Porites lobata/lutea*	
LT16	Dahab	Canyon Reef	WP48	C	*Porites lobata/lutea*	
LT16	Dahab	Canyon Reef	WP48	C	red algae	
LT16	Dahab	Canyon Reef	WP48	C	*Porites lobata/lutea*	
LT16	Dahab	Canyon Reef	WP48	C	*Porites lobata/lutea*	
LT16	Dahab	Canyon Reef	WP48	C	*Dipsastraea sp.*	
LT16	Dahab	Canyon Reef	WP48	C	*Porites lobata/lutea*	
LT16	Dahab	Canyon Reef	WP48	C	*Porites lobata/lutea*	
LT16	Dahab	Canyon Reef	WP48	C	*Porites lobata/lutea*	
LT16	Dahab	Canyon Reef	WP48	C	*Porites lobata/lutea*	
LT16	Dahab	Canyon Reef	WP48	C	*Porites lobata/lutea*	
LT16	Dahab	Canyon Reef	WP48	C	*Porites lobata/lutea*	
LT16	Dahab	Canyon Reef	WP48	C	*Porites lobata/lutea*	
LT16	Dahab	Canyon Reef	WP48	C	*Porites lobata/lutea*	
LT16	Dahab	Canyon Reef	WP48	C	red algae	
LT16	Dahab	Canyon Reef	WP48	C	red algae	
LT16	Dahab	Canyon Reef	WP48	C	*Porites lobata/lutea*	
LT16	Dahab	Canyon Reef	WP48	C	*Dipsastraea sp.*	
LT16	Dahab	Canyon Reef	WP48	C	*Favites sp.*	
LT16	Dahab	Canyon Reef	WP48	C	*Favites sp.*	
LT16	Dahab	Canyon Reef	WP48	C	red algae	
LT16	Dahab	Canyon Reef	WP48	C	red algae	
LT16	Dahab	Canyon Reef	WP48	C	red algae	
LT16	Dahab	Canyon Reef	WP48	C	red algae	
LT16	Dahab	Canyon Reef	WP48	C	red algae	
LT16	Dahab	Canyon Reef	WP48	C	*Porites lobata/lutea*	
LT16	Dahab	Canyon Reef	WP48	C	red algae	
LT16	Dahab	Canyon Reef	WP48	C	red algae	
LT16	Dahab	Canyon Reef	WP48	C	*Acropora sp.*	
LT16	Dahab	Canyon Reef	WP48	C	*Acropora sp.*	
LT16	Dahab	Canyon Reef	WP48	C	red algae	
LT16	Dahab	Canyon Reef	WP48	C	*Acropora sp.*	
LT16	Dahab	Canyon Reef	WP48	C	red algae	
LT16	Dahab	Canyon Reef	WP48	C	red algae	
LT16	Dahab	Canyon Reef	WP48	C	*Porites lobata/lutea*	
LT16	Dahab	Canyon Reef	WP48	C	fanglomerate	
LT16	Dahab	Canyon Reef	WP48	C	*Porites lobata/lutea*	
LT16	Dahab	Canyon Reef	WP48	C	*Porites lobata/lutea*	
LT16	Dahab	Canyon Reef	WP48	C	Barnacles	
LT16	Dahab	Canyon Reef	WP48	C	*Montipora sp.*	

LT	Locality	Site	GPS	Layer	*Name*	Sample
LT16	Dahab	Canyon Reef	WP48	C	red algae	
LT16	Dahab	Canyon Reef	WP48	C	red algae	
LT16	Dahab	Canyon Reef	WP48	C	*Acropora sp.*	
LT16	Dahab	Canyon Reef	WP48	C	red algae	
LT16	Dahab	Canyon Reef	WP48	C	red algae	
LT16	Dahab	Canyon Reef	WP48	C	red algae	
LT16	Dahab	Canyon Reef	WP48	C	*Porites lobata/lutea*	
LT16	Dahab	Canyon Reef	WP48	C	*Porites lobata/lutea*	
LT16	Dahab	Canyon Reef	WP48	C	*Porites lobata/lutea*	
LT16	Dahab	Canyon Reef	WP48	C	*Porites lobata/lutea*	
LT16	Dahab	Canyon Reef	WP48	C	red algae	
LT16	Dahab	Canyon Reef	WP48	C	red algae	
LT16	Dahab	Canyon Reef	WP48	C	red algae	
LT16	Dahab	Canyon Reef	WP48	C	red algae	
LT16	Dahab	Canyon Reef	WP48	C	red algae	
LT16	Dahab	Canyon Reef	WP48	C	red algae	
LT16	Dahab	Canyon Reef	WP48	C	red algae	
LT16	Dahab	Canyon Reef	WP48	C	red algae	
LT16	Dahab	Canyon Reef	WP48	C	red algae	
LT16	Dahab	Canyon Reef	WP48	C	red algae	
LT16	Dahab	Canyon Reef	WP48	C	red algae	
LT16	Dahab	Canyon Reef	WP48	C	red algae	
LT16	Dahab	Canyon Reef	WP48	C	red algae	
LT16	Dahab	Canyon Reef	WP48	C	red algae	
LT16	Dahab	Canyon Reef	WP48	C	red algae	
LT16	Dahab	Canyon Reef	WP48	C	red algae	
LT16	Dahab	Canyon Reef	WP48	C	red algae	
LT16	Dahab	Canyon Reef	WP48	C	*Porites lobata/lutea*	
LT16	Dahab	Canyon Reef	WP48	C	*Porites lobata/lutea*	
LT16	Dahab	Canyon Reef	WP48	C	red algae	
LT16	Dahab	Canyon Reef	WP48	C	fanglomerate	
LT16	Dahab	Canyon Reef	WP48	C	red algae	
LT16	Dahab	Canyon Reef	WP48	C	red algae	
LT16	Dahab	Canyon Reef	WP48	C	red algae	
LT16	Dahab	Canyon Reef	WP48	C	*Porites lobata/lutea*	
LT16	Dahab	Canyon Reef	WP48	C	red algae	
LT16	Dahab	Canyon Reef	WP48	C	red algae	
LT16	Dahab	Canyon Reef	WP48	C	red algae	
LT16	Dahab	Canyon Reef	WP48	C	red algae	
LT16	Dahab	Canyon Reef	WP48	C	red algae	
LT16	Dahab	Canyon Reef	WP48	C	red algae	
LT16	Dahab	Canyon Reef	WP48	C	red algae	
LT16	Dahab	Canyon Reef	WP48	C	*Porites lobata/lutea*	
LT16	Dahab	Canyon Reef	WP48	C	*Porites lobata/lutea*	
LT16	Dahab	Canyon Reef	WP48	C	*Porites lobata/lutea*	
LT16	Dahab	Canyon Reef	WP48	C	red algae	

LT	Locality	Site	GPS	Layer	*Name*	Sample
LT16	Dahab	Canyon Reef	WP48	C	red algae	
LT16	Dahab	Canyon Reef	WP48	C	red algae	
LT16	Dahab	Canyon Reef	WP48	C	*Porites lobata/lutea*	
LT16	Dahab	Canyon Reef	WP48	C	red algae	
LT16	Dahab	Canyon Reef	WP48	C	*Dipsastraea sp.*	
LT16	Dahab	Canyon Reef	WP48	C	*Dipsastraea sp.*	
LT17	Dahab	Canyon Reef		B	*Porites lobata/lutea*	
LT17	Dahab	Canyon Reef		B	*Porites lobata/lutea*	
LT17	Dahab	Canyon Reef		B	*Porites lobata/lutea*	
LT17	Dahab	Canyon Reef		B	red algae	
LT17	Dahab	Canyon Reef		B	red algae	
LT17	Dahab	Canyon Reef		B	matrix	
LT17	Dahab	Canyon Reef		B	*Acropora sp.*	
LT17	Dahab	Canyon Reef		B	red algae	
LT17	Dahab	Canyon Reef		B	red algae	
LT17	Dahab	Canyon Reef		B	*Acropora sp.*	
LT17	Dahab	Canyon Reef		B	red algae	
LT17	Dahab	Canyon Reef		B	red algae	
LT17	Dahab	Canyon Reef		B	red algae	
LT17	Dahab	Canyon Reef		B	*Platygyra daedalea*	
LT17	Dahab	Canyon Reef		B	*Platygyra daedalea*	
LT17	Dahab	Canyon Reef		B	red algae	
LT17	Dahab	Canyon Reef		B	red algae	
LT17	Dahab	Canyon Reef		B	red algae	
LT17	Dahab	Canyon Reef		B	red algae	
LT17	Dahab	Canyon Reef		B	red algae	
LT17	Dahab	Canyon Reef		B	red algae	
LT17	Dahab	Canyon Reef		B	red algae	
LT17	Dahab	Canyon Reef		B	red algae	
LT17	Dahab	Canyon Reef		B	red algae	
LT17	Dahab	Canyon Reef		B	red algae	
LT17	Dahab	Canyon Reef		B	red algae	
LT17	Dahab	Canyon Reef		B	*Leptastrea sp.*	LT17a
LT17	Dahab	Canyon Reef		B	*Acropora sp.*	
LT17	Dahab	Canyon Reef		B	*Acropora sp.*	
LT17	Dahab	Canyon Reef		B	*Acropora sp.*	
LT17	Dahab	Canyon Reef		B	*Acropora sp.*	
LT17	Dahab	Canyon Reef		B	*Platygyra sp.*	
LT17	Dahab	Canyon Reef		B	*Platygyra sp.*	
LT18	Dahab	Canyon Reef		B	*Platygyra daedalea*	
LT18	Dahab	Canyon Reef		B	*Platygyra daedalea*	
LT18	Dahab	Canyon Reef		B	*Platygyra daedalea*	
LT18	Dahab	Canyon Reef		B	*Platygyra daedalea*	
LT18	Dahab	Canyon Reef		B	*Pavona cactus*	
LT18	Dahab	Canyon Reef		B	*Dipsastraea sp.*	
LT18	Dahab	Canyon Reef		B	*Dipsastraea sp.*	

LT	Locality	Site	GPS	Layer	*Name*	Sample
LT18	Dahab	Canyon Reef		B	*Dipsastraea sp.*	
LT18	Dahab	Canyon Reef		B	matrix	
LT18	Dahab	Canyon Reef		B	red algae	
LT18	Dahab	Canyon Reef		B	red algae	
LT18	Dahab	Canyon Reef		B	red algae	
LT18	Dahab	Canyon Reef		B	red algae	
LT18	Dahab	Canyon Reef		B	red algae	
LT18	Dahab	Canyon Reef		B	matrix	
LT18	Dahab	Canyon Reef		B	red algae	
LT18	Dahab	Canyon Reef		B	*Echinopora forskaliana*	
LT18	Dahab	Canyon Reef		B	*Platygyra daedalea*	
LT18	Dahab	Canyon Reef		B	*Platygyra daedalea*	
LT18	Dahab	Canyon Reef		B	*Platygyra daedalea*	
LT18	Dahab	Canyon Reef		B	*Platygyra daedalea*	
LT18	Dahab	Canyon Reef		B	red algae	
LT18	Dahab	Canyon Reef		B	*Turbinaria sp.*	
LT18	Dahab	Canyon Reef		B	red algae	
LT18	Dahab	Canyon Reef		B	matrix	
LT18	Dahab	Canyon Reef		B	red algae	
LT18	Dahab	Canyon Reef		B	*Stylophora sp.*	
LT18	Dahab	Canyon Reef		B	red algae	
LT18	Dahab	Canyon Reef		B	red algae	
LT18	Dahab	Canyon Reef		B	red algae	
LT18	Dahab	Canyon Reef		B	*Platygyra daedalea*	
LT18	Dahab	Canyon Reef		B	*Platygyra daedalea*	
LT18	Dahab	Canyon Reef		B	*Acropora sp.*	
LT18	Dahab	Canyon Reef		B	*Porites sp.*	
LT19	Dahab	Canyon Reef		B	*Acropora sp.*	
LT19	Dahab	Canyon Reef		B	matrix	
LT19	Dahab	Canyon Reef		B	red algae	
LT19	Dahab	Canyon Reef		B	matrix	
LT19	Dahab	Canyon Reef		B	red algae	
LT19	Dahab	Canyon Reef		B	*Lobophyllia sp.*	
LT19	Dahab	Canyon Reef		B	red algae	
LT19	Dahab	Canyon Reef		B	*Acropora sp.*	
LT19	Dahab	Canyon Reef		B	*Acropora sp.*	
LT19	Dahab	Canyon Reef		B	red algae	
LT19	Dahab	Canyon Reef		B	red algae	
LT19	Dahab	Canyon Reef		B	*Pavona sp.*	
LT19	Dahab	Canyon Reef		B	red algae	
LT19	Dahab	Canyon Reef		B	*Dipsastraea sp.*	
LT19	Dahab	Canyon Reef		B	*Dipsastraea sp.*	
LT19	Dahab	Canyon Reef		B	matrix	
LT19	Dahab	Canyon Reef		B	*Platygyra sp.*	
LT19	Dahab	Canyon Reef		B	*Psammocora sp.*	LT19a
LT19	Dahab	Canyon Reef		B	*Acropora sp.*	LT19b

LT	Locality	Site	GPS	Layer	*Name*	Sample
LT20	Dahab	Blue Hole	WP49		red algae	
LT20	Dahab	Blue Hole	WP49		red algae	
LT20	Dahab	Blue Hole	WP49		red algae	
LT20	Dahab	Blue Hole	WP49		*Lobophyllia corymbosa*	
LT20	Dahab	Blue Hole	WP49		*Lobophyllia corymbosa*	
LT20	Dahab	Blue Hole	WP49		*Porites lobata/lutea*	
LT20	Dahab	Blue Hole	WP49		*Dipsastraea sp.*	
LT20	Dahab	Blue Hole	WP49		*Acropora sp.*	
LT20	Dahab	Blue Hole	WP49		*Acropora sp.*	
LT20	Dahab	Blue Hole	WP49		*Acropora sp.*	
LT20	Dahab	Blue Hole	WP49		red algae	
LT20	Dahab	Blue Hole	WP49		red algae	
LT20	Dahab	Blue Hole	WP49		matrix	
LT20	Dahab	Blue Hole	WP49		matrix	
LT20	Dahab	Blue Hole	WP49		matrix	
LT20	Dahab	Blue Hole	WP49		*Acropora sp.*	
LT20	Dahab	Blue Hole	WP49		matrix	
LT20	Dahab	Blue Hole	WP49		*Porites sp.*	
LT20	Dahab	Blue Hole	WP49		matrix	
LT20	Dahab	Blue Hole	WP49		*Acropora sp.*	LT20a
LT20	Dahab	Blue Hole	WP49		*Fungia sp.*	LT20b
LT20	Dahab	Blue Hole	WP49		*Acropora sp.*	
LT20	Dahab	Blue Hole	WP49		matrix	
LT20	Dahab	Blue Hole	WP49		*Platygyra daedalea*	
LT20	Dahab	Blue Hole	WP49		*Porites lobata/lutea*	
LT20	Dahab	Blue Hole	WP49		matrix	
LT20	Dahab	Blue Hole	WP49		red algae	
LT20	Dahab	Blue Hole	WP49		gap	
LT20	Dahab	Blue Hole	WP49		*Platygyra lamellina*	
LT20	Dahab	Blue Hole	WP49		*Platygyra lamellina*	
LT20	Dahab	Blue Hole	WP49		*Platygyra lamellina*	
LT20	Dahab	Blue Hole	WP49		*Cyphastrea sp.*	LT20c
LT20	Dahab	Blue Hole	WP49		*Goniastrea edwardsi*	
LT20	Dahab	Blue Hole	WP49		*Goniastrea edwardsi*	
LT20	Dahab	Blue Hole	WP49		*Goniastrea edwardsi*	
LT20	Dahab	Blue Hole	WP49		*Montipora sp.*	
LT20	Dahab	Blue Hole	WP49		*Montipora sp.*	
LT20	Dahab	Blue Hole	WP49		*Echinopora forskaliana*	
LT20	Dahab	Blue Hole	WP49		*Echinopora forskaliana*	
LT20	Dahab	Blue Hole	WP49		*Echinopora forskaliana*	
LT20	Dahab	Blue Hole	WP49		*Echinopora forskaliana*	
LT20	Dahab	Blue Hole	WP49		*Platygyra crosslandi*	
LT20	Dahab	Blue Hole	WP49		*Platygyra crosslandi*	
LT20	Dahab	Blue Hole	WP49		*Platygyra crosslandi*	
LT20	Dahab	Blue Hole	WP49		*Platygyra crosslandi*	
LT20	Dahab	Blue Hole	WP49		*Platygyra crosslandi*	

LT	Locality	Site	GPS	Layer	*Name*	Sample
LT20	Dahab	Blue Hole	WP49		*Platygyra crosslandi*	
LT20	Dahab	Blue Hole	WP49		*Platygyra crosslandi*	
LT20	Dahab	Blue Hole	WP49		*Platygyra crosslandi*	
LT20	Dahab	Blue Hole	WP49		matrix	
LT20	Dahab	Blue Hole	WP49		matrix	
LT20	Dahab	Blue Hole	WP49		red algae	
LT20	Dahab	Blue Hole	WP49		*Acropora sp.*	
LT20	Dahab	Blue Hole	WP49		red algae	
LT20	Dahab	Blue Hole	WP49		*Platygyra sp.*	
LT20	Dahab	Blue Hole	WP49		*Galaxea fascicularis*	
LT20	Dahab	Blue Hole	WP49		matrix	
LT20	Dahab	Blue Hole	WP49		matrix	
LT20	Dahab	Blue Hole	WP49		Faviidae indet.	
LT20	Dahab	Blue Hole	WP49		*Platygyra sp.*	
LT20	Dahab	Blue Hole	WP49		*Goniastrea edwardsi*	
LT20	Dahab	Blue Hole	WP49		*Goniastrea edwardsi*	
LT20	Dahab	Blue Hole	WP49		*Goniastrea edwardsi*	
LT20	Dahab	Blue Hole	WP49		*Echinopora forskaliana*	
LT20	Dahab	Blue Hole	WP49		*Platygyra sp.*	
LT21	Dahab	Blue Hole			red algae	
LT21	Dahab	Blue Hole			*Porites lobata/lutea*	
LT21	Dahab	Blue Hole			*Porites lobata/lutea*	
LT21	Dahab	Blue Hole			matrix	
LT21	Dahab	Blue Hole			matrix	
LT21	Dahab	Blue Hole			*Echinopora forskaliana*	
LT21	Dahab	Blue Hole			*Echinopora forskaliana*	
LT21	Dahab	Blue Hole			*Platygyra daedalea*	
LT21	Dahab	Blue Hole			*Platygyra daedalea*	
LT21	Dahab	Blue Hole			*Dipsastraea sp.*	
LT21	Dahab	Blue Hole			*Platygyra daedalea*	
LT21	Dahab	Blue Hole			*Galaxea fascicularis*	
LT21	Dahab	Blue Hole			*Porites lobata/lutea*	
LT21	Dahab	Blue Hole			*Porites lobata/lutea*	
LT21	Dahab	Blue Hole			red algae	
LT21	Dahab	Blue Hole			*Platygyra sp.*	
LT21	Dahab	Blue Hole			red algae	
LT21	Dahab	Blue Hole			red algae	
LT21	Dahab	Blue Hole			*Porites lobata/lutea*	
LT21	Dahab	Blue Hole			*Porites lobata/lutea*	
LT21	Dahab	Blue Hole			*Porites lobata/lutea*	
LT21	Dahab	Blue Hole			red algae	
LT21	Dahab	Blue Hole			red algae	
LT21	Dahab	Blue Hole			*Fungia sp.*	
LT21	Dahab	Blue Hole			matrix	
LT21	Dahab	Blue Hole			Gastropod	
LT21	Dahab	Blue Hole			red algae	

LT	Locality	Site	GPS	Layer	*Name*	Sample
LT21	Dahab	Blue Hole			red algae	
LT21	Dahab	Blue Hole			red algae	
LT21	Dahab	Blue Hole			Bivalve	
LT21	Dahab	Blue Hole			red algae	
LT21	Dahab	Blue Hole			*Echinopora forskaliana*	
LT21	Dahab	Blue Hole			*Echinopora forskaliana*	
LT21	Dahab	Blue Hole			*Echinopora forskaliana*	
LT21	Dahab	Blue Hole			*Cyphastrea sp.*	
LT21	Dahab	Blue Hole			red algae	
LT21	Dahab	Blue Hole			matrix	
LT21	Dahab	Blue Hole			red algae	
LT21	Dahab	Blue Hole			matrix	
LT21	Dahab	Blue Hole			*Fungia sp.*	
LT21	Dahab	Blue Hole			*Fungia sp.*	
LT21	Dahab	Blue Hole			*Lobophyllia hemprichii*	
LT21	Dahab	Blue Hole			matrix	
LT21	Dahab	Blue Hole			matrix	
LT21	Dahab	Blue Hole			*Lobophyllia hemprichii*	
LT21	Dahab	Blue Hole			*Lobophyllia hemprichii*	
LT21	Dahab	Blue Hole			*Lobophyllia hemprichii*	
LT21	Dahab	Blue Hole			*Lobophyllia hemprichii*	
LT22	Dahab	Blue Hole			Scleractinia indet.	
LT22	Dahab	Blue Hole			Scleractinia indet.	
LT22	Dahab	Blue Hole			*Dipsastraea sp.*	
LT22	Dahab	Blue Hole			*Echinopora sp.*	
LT22	Dahab	Blue Hole			*Leptoseris sp.*	
LT22	Dahab	Blue Hole			red algae	
LT22	Dahab	Blue Hole			*Lobophyllia sp.*	
LT22	Dahab	Blue Hole			red algae	
LT22	Dahab	Blue Hole			matrix	
LT22	Dahab	Blue Hole			*Platygyra sp.*	
LT22	Dahab	Blue Hole			Barnacles	
LT22	Dahab	Blue Hole			*Echinopora forskaliana*	
LT22	Dahab	Blue Hole			*Echinopora forskaliana*	
LT22	Dahab	Blue Hole			matrix	
LT22	Dahab	Blue Hole			*Fungia sp.*	
LT22	Dahab	Blue Hole			*Gastropod*	
LT22	Dahab	Blue Hole			*Echinopora forskaliana*	
LT22	Dahab	Blue Hole			*Coelastrea aspera*	
LT22	Dahab	Blue Hole			matrix	
LT22	Dahab	Blue Hole			*Platygyra crosslandi*	
LT22	Dahab	Blue Hole			red algae	
LT22	Dahab	Blue Hole			*Galaxea fascicularis*	
LT22	Dahab	Blue Hole			*Galaxea fascicularis*	
LT22	Dahab	Blue Hole			*Platygyra crosslandi*	
LT22	Dahab	Blue Hole			matrix	

LT	Locality	Site	GPS	Layer	*Name*	Sample
LT22	Dahab	Blue Hole			*Acropora sp.*	
LT22	Dahab	Blue Hole			matrix	
LT22	Dahab	Blue Hole			*Acropora sp.*	
LT22	Dahab	Blue Hole			*Acropora sp.*	
LT22	Dahab	Blue Hole			matrix	
LT22	Dahab	Blue Hole			matrix	
LT22	Dahab	Blue Hole			red algae	
LT22	Dahab	Blue Hole			red algae	
LT22	Dahab	Blue Hole			matrix	
LT22	Dahab	Blue Hole			red algae	
LT22	Dahab	Blue Hole			red algae	
LT22	Dahab	Blue Hole			matrix	
LT22	Dahab	Blue Hole			Bivalve	
LT22	Dahab	Blue Hole			*Porites sp.*	
LT22	Dahab	Blue Hole			matrix	
LT22	Dahab	Blue Hole			matrix	
LT22	Dahab	Blue Hole			matrix	
LT22	Dahab	Blue Hole			*Porites sp.*	
LT22	Dahab	Blue Hole			red algae	
LT22	Dahab	Blue Hole			red algae	
LT22	Dahab	Blue Hole			red algae	
LT22	Dahab	Blue Hole			red algae	
LT22	Dahab	Blue Hole			matrix	
LT22	Dahab	Blue Hole			*Platygyra daedalea*	
LT22	Dahab	Blue Hole			*Platygyra daedalea*	
LT23	Dahab	Blue Hole	WP50		*Porites nodifera*	
LT23	Dahab	Blue Hole	WP50		*Porites nodifera*	
LT23	Dahab	Blue Hole	WP50		*Porites nodifera*	
LT23	Dahab	Blue Hole	WP50		red algae	
LT23	Dahab	Blue Hole	WP50		*Porites nodifera*	
LT23	Dahab	Blue Hole	WP50		*Porites nodifera*	
LT23	Dahab	Blue Hole	WP50		*Porites nodifera*	
LT23	Dahab	Blue Hole	WP50		*Porites nodifera*	
LT23	Dahab	Blue Hole	WP50		*Porites nodifera*	
LT23	Dahab	Blue Hole	WP50		*Cyphastrea sp.*	LT23a
LT23	Dahab	Blue Hole	WP50		fanglomerate	
LT23	Dahab	Blue Hole	WP50		matrix	
LT23	Dahab	Blue Hole	WP50		red algae	
LT23	Dahab	Blue Hole	WP50		*Porites nodifera*	
LT23	Dahab	Blue Hole	WP50		*Porites nodifera*	
LT23	Dahab	Blue Hole	WP50		*Porites nodifera*	
LT23	Dahab	Blue Hole	WP50		*Porites nodifera*	
LT23	Dahab	Blue Hole	WP50		matrix	
LT23	Dahab	Blue Hole	WP50		*Goniastrea sp.*	
LT23	Dahab	Blue Hole	WP50		*Goniastrea sp.*	
LT23	Dahab	Blue Hole	WP50		*Goniastrea sp.*	

LT	Locality	Site	GPS	Layer	*Name*	Sample
LT23	Dahab	Blue Hole	WP50		matrix	
LT23	Dahab	Blue Hole	WP50		*Porites sp.*	
LT23	Dahab	Blue Hole	WP50		*Goniastrea sp.*	LT23b
LT23	Dahab	Blue Hole	WP50		*Goniastrea sp.*	
LT23	Dahab	Blue Hole	WP50		*Porites sp.*	
LT23	Dahab	Blue Hole	WP50		*Porites sp.*	
LT23	Dahab	Blue Hole	WP50		matrix	
LT23	Dahab	Blue Hole	WP50		*Porites nodifera*	
LT23	Dahab	Blue Hole	WP50		*Porites nodifera*	
LT23	Dahab	Blue Hole	WP50		*Porites nodifera*	
LT23	Dahab	Blue Hole	WP50		*Porites nodifera*	
LT23	Dahab	Blue Hole	WP50		*Porites nodifera*	
LT23	Dahab	Blue Hole	WP50		*Porites nodifera*	
LT23	Dahab	Blue Hole	WP50		*Porites nodifera*	
LT23	Dahab	Blue Hole	WP50		matrix	
LT23	Dahab	Blue Hole	WP50		granite boulder	
LT23	Dahab	Blue Hole	WP50		*Cyphastrea sp.*	LT23c
LT24	Dahab	Blue Hole	WP50		*Porites nodifera*	
LT24	Dahab	Blue Hole	WP50		*Porites nodifera*	
LT24	Dahab	Blue Hole	WP50		*Porites nodifera*	
LT24	Dahab	Blue Hole	WP50		*Porites nodifera*	
LT24	Dahab	Blue Hole	WP50		*Porites nodifera*	
LT24	Dahab	Blue Hole	WP50		red algae	
LT24	Dahab	Blue Hole	WP50		red algae	
LT24	Dahab	Blue Hole	WP50		red algae	
LT24	Dahab	Blue Hole	WP50		red algae	
LT24	Dahab	Blue Hole	WP50		*Porites nodifera*	
LT24	Dahab	Blue Hole	WP50		*Goniastrea sp.*	
LT24	Dahab	Blue Hole	WP50		red algae	
LT24	Dahab	Blue Hole	WP50		red algae	
LT24	Dahab	Blue Hole	WP50		red algae	
LT24	Dahab	Blue Hole	WP50		*Porites nodifera*	
LT24	Dahab	Blue Hole	WP50		*Porites nodifera*	
LT24	Dahab	Blue Hole	WP50		*Porites nodifera*	
LT24	Dahab	Blue Hole	WP50		*Porites nodifera*	
LT24	Dahab	Blue Hole	WP50		*Porites nodifera*	
LT24	Dahab	Blue Hole	WP50		*Porites nodifera*	
LT24	Dahab	Blue Hole	WP50		*Porites nodifera*	
LT24	Dahab	Blue Hole	WP50		*Porites nodifera*	
LT24	Dahab	Blue Hole	WP50		*Porites nodifera*	
LT24	Dahab	Blue Hole	WP50		*Porites nodifera*	
LT24	Dahab	Blue Hole	WP50		*Porites nodifera*	
LT24	Dahab	Blue Hole	WP50		*Porites nodifera*	
LT24	Dahab	Blue Hole	WP50		*Porites nodifera*	
LT24	Dahab	Blue Hole	WP50		*Porites nodifera*	
LT24	Dahab	Blue Hole	WP50		*Porites nodifera*	
LT24	Dahab	Blue Hole	WP50		*Porites nodifera*	

LT	Locality	Site	GPS	Layer	*Name*	Sample
LT24	Dahab	Blue Hole	WP50		*Porites nodifera*	
LT24	Dahab	Blue Hole	WP50		*Porites nodifera*	
LT24	Dahab	Blue Hole	WP50		*Porites nodifera*	
LT24	Dahab	Blue Hole	WP50		*Porites nodifera*	
LT24	Dahab	Blue Hole	WP50		*Porites nodifera*	
LT24	Dahab	Blue Hole	WP50		*Porites nodifera*	
LT24	Dahab	Blue Hole	WP50		*Porites nodifera*	
LT24	Dahab	Blue Hole	WP50		*Porites nodifera*	
LT24	Dahab	Blue Hole	WP50		*Porites nodifera*	
LT24	Dahab	Blue Hole	WP50		*Porites nodifera*	
LT24	Dahab	Blue Hole	WP50		*Porites nodifera*	
LT24	Dahab	Blue Hole	WP50		red algae	
LT24	Dahab	Blue Hole	WP50		*Porites sp.*	
LT24	Dahab	Blue Hole	WP50		matrix	
LT24	Dahab	Blue Hole	WP50		*Porites nodifera*	
LT24	Dahab	Blue Hole	WP50		*Porites nodifera*	
LT24	Dahab	Blue Hole	WP50		*Porites nodifera*	
LT24	Dahab	Blue Hole	WP50		*Porites nodifera*	
LT24	Dahab	Blue Hole	WP50		*Porites nodifera*	
LT24	Dahab	Blue Hole	WP50		*Porites nodifera*	
LT24	Dahab	Blue Hole	WP50		*Porites nodifera*	
LT24	Dahab	Blue Hole	WP50		*Porites nodifera*	
LT24	Dahab	Blue Hole	WP50		*Porites nodifera*	
LT24	Dahab	Blue Hole	WP50		*Porites nodifera*	
LT24	Dahab	Blue Hole	WP50		*Porites nodifera*	
LT24	Dahab	Blue Hole	WP50		*Porites nodifera*	
LT24	Dahab	Blue Hole	WP50		*Porites nodifera*	
LT24	Dahab	Blue Hole	WP50		*Porites nodifera*	
LT24	Dahab	Blue Hole	WP50		matrix	
LT24	Dahab	Blue Hole	WP50		*Porites nodifera*	
LT24	Dahab	Blue Hole	WP50		*Porites nodifera*	
LT24	Dahab	Blue Hole	WP50		*Porites nodifera*	
LT24	Dahab	Blue Hole	WP50		*Porites nodifera*	
LT24	Dahab	Blue Hole	WP50		*Porites nodifera*	
LT24	Dahab	Blue Hole	WP50		*Porites nodifera*	
LT24	Dahab	Blue Hole	WP50		*Porites nodifera*	
LT24	Dahab	Blue Hole	WP50		*Porites nodifera*	
LT24	Dahab	Blue Hole	WP50		*Porites nodifera*	
LT24	Dahab	Blue Hole	WP50		matrix	
LT24	Dahab	Blue Hole	WP50		*Porites nodifera*	
LT24	Dahab	Blue Hole	WP50		*Porites nodifera*	
LT24	Dahab	Blue Hole	WP50		*Porites nodifera*	
LT24	Dahab	Blue Hole	WP50		*Porites nodifera*	
LT24	Dahab	Blue Hole	WP50		*Porites nodifera*	
LT24	Dahab	Blue Hole	WP50		matrix	

LT	Locality	Site	GPS	Layer	*Name*	Sample
LT24	Dahab	Blue Hole	WP50		*Porites nodifera*	
LT24	Dahab	Blue Hole	WP50		*Porites nodifera*	
LT24	Dahab	Blue Hole	WP50		*Porites nodifera*	
LT24	Dahab	Blue Hole	WP50		*Porites nodifera*	
LT24	Dahab	Blue Hole	WP50		*Porites nodifera*	
LT24	Dahab	Blue Hole	WP50		*Porites nodifera*	
LT24	Dahab	Blue Hole	WP50		matrix	
LT24	Dahab	Blue Hole	WP50		*Porites nodifera*	
LT24	Dahab	Blue Hole	WP50		*Porites nodifera*	
LT24	Dahab	Blue Hole	WP50		*Porites nodifera*	
LT24	Dahab	Blue Hole	WP50		*Porites nodifera*	
LT24	Dahab	Blue Hole	WP50		*Porites nodifera*	
LT25	Dahab	Blue Hole	WP50		*Porites lobata/lutea*	
LT25	Dahab	Blue Hole	WP50		*Porites lobata/lutea*	
LT25	Dahab	Blue Hole	WP50		red algae	
LT25	Dahab	Blue Hole	WP50		red algae	
LT25	Dahab	Blue Hole	WP50		*Galaxea fascicularis*	
LT25	Dahab	Blue Hole	WP50		matrix	
LT25	Dahab	Blue Hole	WP50		red algae	
LT25	Dahab	Blue Hole	WP50		*Goniastrea retiformis*	
LT25	Dahab	Blue Hole	WP50		*Goniastrea retiformis*	
LT25	Dahab	Blue Hole	WP50		*Goniastrea retiformis*	
LT25	Dahab	Blue Hole	WP50		*Goniastrea retiformis*	
LT25	Dahab	Blue Hole	WP50		*Goniastrea retiformis*	
LT25	Dahab	Blue Hole	WP50		*Goniastrea retiformis*	
LT25	Dahab	Blue Hole	WP50		*Goniastrea retiformis*	
LT25	Dahab	Blue Hole	WP50		*Goniastrea retiformis*	
LT25	Dahab	Blue Hole	WP50		red algae	
LT25	Dahab	Blue Hole	WP50		red algae	
LT25	Dahab	Blue Hole	WP50		matrix	
LT25	Dahab	Blue Hole	WP50		matrix	
LT25	Dahab	Blue Hole	WP50		*Platygyra daedalea*	
LT25	Dahab	Blue Hole	WP50		*Platygyra daedalea*	
LT25	Dahab	Blue Hole	WP50		*Platygyra daedalea*	
LT25	Dahab	Blue Hole	WP50		*Platygyra daedalea*	
LT25	Dahab	Blue Hole	WP50		*Platygyra daedalea*	
LT25	Dahab	Blue Hole	WP50		*Platygyra daedalea*	
LT25	Dahab	Blue Hole	WP50		*Platygyra daedalea*	
LT25	Dahab	Blue Hole	WP50		*Platygyra daedalea*	
LT25	Dahab	Blue Hole	WP50		fanglomerate	
LT25	Dahab	Blue Hole	WP50		fanglomerate	
LT25	Dahab	Blue Hole	WP50		fanglomerate	
LT25	Dahab	Blue Hole	WP50		fanglomerate	
LT25	Dahab	Blue Hole	WP50		fanglomerate	
LT25	Dahab	Blue Hole	WP50		fanglomerate	
LT25	Dahab	Blue Hole	WP50		fanglomerate	

LT	Locality	Site	GPS	Layer	*Name*	Sample
LT25	Dahab	Blue Hole	WP50		fanglomerate	
LT25	Dahab	Blue Hole	WP50		*Cyphastrea sp.*	
LT25	Dahab	Blue Hole	WP50		matrix	
LT25	Dahab	Blue Hole	WP50		Faviidae indet.	
LT25	Dahab	Blue Hole	WP50		matrix	
LT25	Dahab	Blue Hole	WP50		*Favites sp.*	
LT25	Dahab	Blue Hole	WP50		matrix	
LT25	Dahab	Blue Hole	WP50		Faviidae indet.	
LT26	Dahab	Canyon Reef		C	*Montipora sp.*	
LT26	Dahab	Canyon Reef		C	*Astreopora sp.*	
LT26	Dahab	Canyon Reef		C	*Astreopora sp.*	
LT26	Dahab	Canyon Reef		C	*Goniastrea edwardsi*	
LT26	Dahab	Canyon Reef		C	matrix	
LT26	Dahab	Canyon Reef		C	matrix	
LT26	Dahab	Canyon Reef		C	Gastropod	
LT26	Dahab	Canyon Reef		C	*Goniastrea edwardsi*	
LT26	Dahab	Canyon Reef		C	*Goniastrea edwardsi*	
LT26	Dahab	Canyon Reef		C	matrix	
LT26	Dahab	Canyon Reef		C	red algae	
LT26	Dahab	Canyon Reef		C	*Goniastrea edwardsi*	
LT26	Dahab	Canyon Reef		C	*Goniastrea edwardsi*	
LT26	Dahab	Canyon Reef		C	matrix	
LT26	Dahab	Canyon Reef		C	*Goniastrea edwardsi*	
LT26	Dahab	Canyon Reef		C	red algae	
LT26	Dahab	Canyon Reef		C	red algae	
LT27	Dahab	Canyon Reef	WP51	B	*Porites nodifera*	
LT27	Dahab	Canyon Reef	WP51	B	*Porites nodifera*	
LT27	Dahab	Canyon Reef	WP51	B	*Porites nodifera*	
LT27	Dahab	Canyon Reef	WP51	B	*Porites nodifera*	
LT27	Dahab	Canyon Reef	WP51	B	*Porites nodifera*	
LT27	Dahab	Canyon Reef	WP51	B	*Porites nodifera*	
LT27	Dahab	Canyon Reef	WP51	B	*Porites nodifera*	
LT27	Dahab	Canyon Reef	WP51	B	*Porites nodifera*	
LT27	Dahab	Canyon Reef	WP51	B	matrix	
LT27	Dahab	Canyon Reef	WP51	B	matrix	
LT27	Dahab	Canyon Reef	WP51	B	*Echinopora forskaliana*	
LT27	Dahab	Canyon Reef	WP51	B	*Echinopora forskaliana*	
LT27	Dahab	Canyon Reef	WP51	B	red algae	
LT27	Dahab	Canyon Reef	WP51	B	*Psammocora sp.*	LT27a
LT27	Dahab	Canyon Reef	WP51	B	red algae	
LT27	Dahab	Canyon Reef	WP51	B	matrix	
LT27	Dahab	Canyon Reef	WP51	B	matrix	
LT27	Dahab	Canyon Reef	WP51	B	matrix	
LT27	Dahab	Canyon Reef	WP51	B	*Galaxea fascicularis*	
LT27	Dahab	Canyon Reef	WP51	B	red algae	
LT27	Dahab	Canyon Reef	WP51	B	*Porites lobata/lutea*	

LT	Locality	Site	GPS	Layer	*Name*	Sample
LT27	Dahab	Canyon Reef	WP51	B	*Cyphastrea serailia*	
LT27	Dahab	Canyon Reef	WP51	B	*Millepora sp.*	
LT27	Dahab	Canyon Reef	WP51	B	red algae	
LT27	Dahab	Canyon Reef	WP51	B	*Psammocora sp.*	
LT27	Dahab	Canyon Reef	WP51	B	matrix	
LT27	Dahab	Canyon Reef	WP51	B	matrix	
LT27	Dahab	Canyon Reef	WP51	B	*Galaxea fascicularis*	
LT27	Dahab	Canyon Reef	WP51	B	matrix	
LT27	Dahab	Canyon Reef	WP51	B	*Mycedium sp.*	LT27b
LT27	Dahab	Canyon Reef	WP51	B	*Acropora sp.*	
LT27	Dahab	Canyon Reef	WP51	B	red algae	
LT27	Dahab	Canyon Reef	WP51	B	matrix	
LT27	Dahab	Canyon Reef	WP51	B	matrix	
LT27	Dahab	Canyon Reef	WP51	B	*Acropora sp.*	
LT27	Dahab	Canyon Reef	WP51	B	*Acropora sp.*	
LT27	Dahab	Canyon Reef	WP51	B	red algae	
LT27	Dahab	Canyon Reef	WP51	B	red algae	
LT27	Dahab	Canyon Reef	WP51	B	*Galaxea fascicularis*	
LT27	Dahab	Canyon Reef	WP51	B	matrix	
LT27	Dahab	Canyon Reef	WP51	B	*Favites rotundata*	
LT27	Dahab	Canyon Reef	WP51	B	red algae	
LT27	Dahab	Canyon Reef	WP51	B	Scleractinia indet.	LT27c
LT27	Dahab	Canyon Reef	WP51	B	*Psammocora sp.*	LT27d
LT27	Dahab	Canyon Reef	WP51	B	matrix	
LT27	Dahab	Canyon Reef	WP51	B	*Acropora sp.*	
LT27	Dahab	Canyon Reef	WP51	B	matrix	
LT27	Dahab	Canyon Reef	WP51	B	*Leptastrea bottae*	LT27e
LT27	Dahab	Canyon Reef	WP51	B	*Echinopora forskaliana*	
LT27	Dahab	Canyon Reef	WP51	B	*Montipora sp.*	LT27f
LT27	Dahab	Canyon Reef	WP51	B	Faviidae indet.	LT7g
LT27	Dahab	Canyon Reef	WP51	B	red algae	
LT27	Dahab	Canyon Reef	WP51	B	matrix	
LT27	Dahab	Canyon Reef	WP51	B	matrix	
LT27	Dahab	Canyon Reef	WP51	B	*Porites lobata/lutea*	
LT27	Dahab	Canyon Reef	WP51	B	*Acropora sp.*	
LT27	Dahab	Canyon Reef	WP51	B	*Acropora sp.*	
LT27	Dahab	Canyon Reef	WP51	B	red algae	
LT27	Dahab	Canyon Reef	WP51	B	matrix	
LT27	Dahab	Canyon Reef	WP51	B	*Fungia sp.*	
LT27	Dahab	Canyon Reef	WP51	B	red algae	
LT27	Dahab	Canyon Reef	WP51	B	matrix	
LT27	Dahab	Canyon Reef	WP51	B	red algae	
LT27	Dahab	Canyon Reef	WP51	B	*Acropora sp.*	
LT27	Dahab	Canyon Reef	WP51	B	matrix	
LT27	Dahab	Canyon Reef	WP51	B	matrix	
LT27	Dahab	Canyon Reef	WP51	B	matrix	

LT	Locality	Site	GPS	Layer	*Name*	Sample
LT27	Dahab	Canyon Reef	WP51	B	matrix	
LT27	Dahab	Canyon Reef	WP51	B	matrix	
LT27	Dahab	Canyon Reef	WP51	B	*Favites sp.*	LT27h
LT27	Dahab	Canyon Reef	WP51	B	matrix	
LT27	Dahab	Canyon Reef	WP51	B	matrix	
LT27	Dahab	Canyon Reef	WP51	B	Scleractinia indet.	
LT27	Dahab	Canyon Reef	WP51	B	matrix	
LT27	Dahab	Canyon Reef	WP51	B	*Millepora sp.*	
LT27	Dahab	Canyon Reef	WP51	B	matrix	
LT27	Dahab	Canyon Reef	WP51	B	red algae	
LT27	Dahab	Canyon Reef	WP51	B	*Dipsastraea sp.*	
LT27	Dahab	Canyon Reef	WP51	B	*Mycedium sp.*	
LT27	Dahab	Canyon Reef	WP51	B	matrix	
LT27	Dahab	Canyon Reef	WP51	B	red algae	
LT27	Dahab	Canyon Reef	WP51	B	red algae	
LT27	Dahab	Canyon Reef	WP51	B	*Porites lobata/lutea*	
LT28	Dahab	Canyon Reef	WP51	B	matrix	
LT28	Dahab	Canyon Reef	WP51	B	matrix	
LT28	Dahab	Canyon Reef	WP51	B	*Acropora sp.*	
LT28	Dahab	Canyon Reef	WP51	B	matrix	
LT28	Dahab	Canyon Reef	WP51	B	*Pavona sp.*	LT28a
LT28	Dahab	Canyon Reef	WP51	B	matrix	
LT28	Dahab	Canyon Reef	WP51	B	red algae	
LT28	Dahab	Canyon Reef	WP51	B	red algae	
LT28	Dahab	Canyon Reef	WP51	B	red algae	
LT28	Dahab	Canyon Reef	WP51	B	red algae	
LT28	Dahab	Canyon Reef	WP51	B	matrix	
LT28	Dahab	Canyon Reef	WP51	B	matrix	
LT28	Dahab	Canyon Reef	WP51	B	*Leptoseris sp.*	LT28b
LT28	Dahab	Canyon Reef	WP51	B	matrix	
LT28	Dahab	Canyon Reef	WP51	B	matrix	
LT28	Dahab	Canyon Reef	WP51	B	matrix	
LT28	Dahab	Canyon Reef	WP51	B	*Porites lobata/lutea*	
LT28	Dahab	Canyon Reef	WP51	B	red algae	
LT28	Dahab	Canyon Reef	WP51	B	red algae	
LT28	Dahab	Canyon Reef	WP51	B	*Leptastrea bottae*	
LT28	Dahab	Canyon Reef	WP51	B	*matrix*	
LT28	Dahab	Canyon Reef	WP51	B	*matrix*	
LT28	Dahab	Canyon Reef	WP51	B	*Porites lobata/lutea*	
LT28	Dahab	Canyon Reef	WP51	B	matrix	
LT28	Dahab	Canyon Reef	WP51	B	*Psammocora sp.*	LT28c
LT28	Dahab	Canyon Reef	WP51	B	*Acropora sp.*	
LT28	Dahab	Canyon Reef	WP51	B	matrix	
LT28	Dahab	Canyon Reef	WP51	B	red algae	
LT28	Dahab	Canyon Reef	WP51	B	matrix	
LT28	Dahab	Canyon Reef	WP51	B	red algae	

LT	Locality	Site	GPS	Layer	*Name*	Sample
LT28	Dahab	Canyon Reef	WP51	B	matrix	
LT28	Dahab	Canyon Reef	WP51	B	matrix	
LT28	Dahab	Canyon Reef	WP51	B	matrix	
LT28	Dahab	Canyon Reef	WP51	B	*Fungia sp.*	
LT28	Dahab	Canyon Reef	WP51	B	matrix	
LT28	Dahab	Canyon Reef	WP51	B	*Acropora sp.*	
LT28	Dahab	Canyon Reef	WP51	B	*Acropora sp.*	
LT28	Dahab	Canyon Reef	WP51	B	*Acropora sp.*	
LT28	Dahab	Canyon Reef	WP51	B	red algae	
LT28	Dahab	Canyon Reef	WP51	B	*Echinopora sp.*	
LT28	Dahab	Canyon Reef	WP51	B	red algae	
LT28	Dahab	Canyon Reef	WP51	B	Scleractinia indet.	
LT28	Dahab	Canyon Reef	WP51	B	matrix	
LT28	Dahab	Canyon Reef	WP51	B	matrix	
LT28	Dahab	Canyon Reef	WP51	B	*Echinopora forskaliana*	
LT28	Dahab	Canyon Reef	WP51	B	*Echinopora forskaliana*	
LT28	Dahab	Canyon Reef	WP51	B	red algae	
LT28	Dahab	Canyon Reef	WP51	B	*Mycedium sp.*	LT28d
LT28	Dahab	Canyon Reef	WP51	B	matrix	
LT28	Dahab	Canyon Reef	WP51	B	*Porites nodifera*	
LT28	Dahab	Canyon Reef	WP51	B	*Porites nodifera*	
LT28	Dahab	Canyon Reef	WP51	B	*Acropora sp.*	
LT28	Dahab	Canyon Reef	WP51	B	*Echinopora forskaliana*	
LT28	Dahab	Canyon Reef	WP51	B	*Echinopora forskaliana*	
LT28	Dahab	Canyon Reef	WP51	B	matrix	
LT28	Dahab	Canyon Reef	WP51	B	red algae	
LT28	Dahab	Canyon Reef	WP51	B	matrix	
LT28	Dahab	Canyon Reef	WP51	B	*Porites sp.*	
LT28	Dahab	Canyon Reef	WP51	B	matrix	
LT28	Dahab	Canyon Reef	WP51	B	matrix	
LT28	Dahab	Canyon Reef	WP51	B	matrix	
LT28	Dahab	Canyon Reef	WP51	B	*Porites lobata/lutea*	
LT28	Dahab	Canyon Reef	WP51	B	Faviidae indet.	
LT28	Dahab	Canyon Reef	WP51	B	*Porites lobata/lutea*	
LT28	Dahab	Canyon Reef	WP51	B	*Porites lobata/lutea*	
LT28	Dahab	Canyon Reef	WP51	B	*Echinopora forskaliana*	
LT28	Dahab	Canyon Reef	WP51	B	*Echinopora forskaliana*	LT28e
LT28	Dahab	Canyon Reef	WP51	B	*Echinopora forskaliana*	
LT28	Dahab	Canyon Reef	WP51	B	*Echinopora forskaliana*	
LT28	Dahab	Canyon Reef	WP51	B	*Porites lobata/lutea*	
LT28	Dahab	Canyon Reef	WP51	B	*Porites lobata/lutea*	
LT28	Dahab	Canyon Reef	WP51	B	*Platygyra daedalea*	
LT28	Dahab	Canyon Reef	WP51	B	matrix	
LT28	Dahab	Canyon Reef	WP51	B	*Leptoseris sp.*	LT28f
LT28	Dahab	Canyon Reef	WP51	B	*Dipsastraea sp.*	
LT28	Dahab	Canyon Reef	WP51	B	*Acropora sp.*	

LT	Locality	Site	GPS	Layer	*Name*	Sample
LT28	Dahab	Canyon Reef	WP51	B	red algae	
LT28	Dahab	Canyon Reef	WP51	B	*Platygyra lamellina*	
LT28	Dahab	Canyon Reef	WP51	B	matrix	
LT28	Dahab	Canyon Reef	WP51	B	*Acropora sp.*	
LT28	Dahab	Canyon Reef	WP51	B	*Platygyra lamellina*	
LT28	Dahab	Canyon Reef	WP51	B	*Platygyra lamellina*	
LT28	Dahab	Canyon Reef	WP51	B	matrix	
LT28	Dahab	Canyon Reef	WP51	B	*Fungia sp.*	
LT28	Dahab	Canyon Reef	WP51	B	*Acropora sp.*	
LT28	Dahab	Canyon Reef	WP51	B	*Acropora sp.*	
LT28	Dahab	Canyon Reef	WP51	B	*Acropora sp.*	
LT28	Dahab	Canyon Reef	WP51	B	*Echinopora forskaliana*	
LT28	Dahab	Canyon Reef	WP51	B	*Echinopora forskaliana*	
LT28	Dahab	Canyon Reef	WP51	B	*Echinopora forskaliana*	
LT28	Dahab	Canyon Reef	WP51	B	matrix	
LT28	Dahab	Canyon Reef	WP51	B	red algae	
LT28	Dahab	Canyon Reef	WP51	B	*Dipsastraea sp.*	LT28g
LT28	Dahab	Canyon Reef	WP51	B	*Porites sp.*	
LT28	Dahab	Canyon Reef	WP51	B	matrix	
LT29	Dahab	Canyon Reef	WP52	A	*Porites nodifera*	
LT29	Dahab	Canyon Reef	WP52	A	*Porites nodifera*	
LT29	Dahab	Canyon Reef	WP52	A	*Porites nodifera*	
LT29	Dahab	Canyon Reef	WP52	A	*Porites nodifera*	
LT29	Dahab	Canyon Reef	WP52	A	*Porites nodifera*	
LT29	Dahab	Canyon Reef	WP52	A	*Porites nodifera*	
LT29	Dahab	Canyon Reef	WP52	A	*Porites nodifera*	
LT29	Dahab	Canyon Reef	WP52	A	*Porites nodifera*	
LT29	Dahab	Canyon Reef	WP52	A	*Porites nodifera*	
LT29	Dahab	Canyon Reef	WP52	A	*Porites nodifera*	
LT29	Dahab	Canyon Reef	WP52	A	*Porites nodifera*	
LT29	Dahab	Canyon Reef	WP52	A	*Porites nodifera*	
LT29	Dahab	Canyon Reef	WP52	A	*Porites nodifera*	
LT29	Dahab	Canyon Reef	WP52	A	*Porites nodifera*	
LT29	Dahab	Canyon Reef	WP52	A	*Millepora sp.*	LT29a
LT29	Dahab	Canyon Reef	WP52	A	*Millepora sp.*	
LT29	Dahab	Canyon Reef	WP52	A	*Millepora sp.*	
LT29	Dahab	Canyon Reef	WP52	A	*Millepora sp.*	
LT29	Dahab	Canyon Reef	WP52	A	*Millepora sp.*	
LT29	Dahab	Canyon Reef	WP52	A	*Millepora sp.*	
LT29	Dahab	Canyon Reef	WP52	A	*Millepora sp.*	
LT29	Dahab	Canyon Reef	WP52	A	*Porites nodifera*	
LT29	Dahab	Canyon Reef	WP52	A	*Porites nodifera*	
LT29	Dahab	Canyon Reef	WP52	A	*Porites nodifera*	
LT29	Dahab	Canyon Reef	WP52	A	*Porites nodifera*	
LT29	Dahab	Canyon Reef	WP52	A	*Porites nodifera*	

LT	Locality	Site	GPS	Layer	*Name*	Sample
LT29	Dahab	Canyon Reef	WP52	A	*Porites nodifera*	
LT29	Dahab	Canyon Reef	WP52	A	*Porites nodifera*	
LT29	Dahab	Canyon Reef	WP52	A	sandy pocket	
LT29	Dahab	Canyon Reef	WP52	A	sandy pocket	
LT29	Dahab	Canyon Reef	WP52	A	sandy pocket	
LT29	Dahab	Canyon Reef	WP52	A	sandy pocket	
LT29	Dahab	Canyon Reef	WP52	A	sandy pocket	
LT29	Dahab	Canyon Reef	WP52	A	sandy pocket	
LT29	Dahab	Canyon Reef	WP52	A	*Porites nodifera*	
LT29	Dahab	Canyon Reef	WP52	A	*Cyphastrea serailia*	
LT29	Dahab	Canyon Reef	WP52	A	*Cyphastrea serailia*	
LT29	Dahab	Canyon Reef	WP52	A	*Porites nodifera*	
LT29	Dahab	Canyon Reef	WP52	A	*Porites nodifera*	
LT29	Dahab	Canyon Reef	WP52	A	*Porites nodifera*	
LT29	Dahab	Canyon Reef	WP52	A	*Porites nodifera*	
LT29	Dahab	Canyon Reef	WP52	A	*Porites nodifera*	
LT29	Dahab	Canyon Reef	WP52	A	*Porites nodifera*	
LT29	Dahab	Canyon Reef	WP52	A	*Porites nodifera*	
LT29	Dahab	Canyon Reef	WP52	A	*Porites nodifera*	
LT29	Dahab	Canyon Reef	WP52	A	*Porites nodifera*	
LT29	Dahab	Canyon Reef	WP52	A	*Porites nodifera*	
LT29	Dahab	Canyon Reef	WP52	A	*Porites nodifera*	
LT29	Dahab	Canyon Reef	WP52	A	*Porites nodifera*	
LT29	Dahab	Canyon Reef	WP52	A	*Porites nodifera*	
LT29	Dahab	Canyon Reef	WP52	A	*Porites nodifera*	
LT29	Dahab	Canyon Reef	WP52	A	*Porites nodifera*	
LT29	Dahab	Canyon Reef	WP52	A	sandy pocket	
LT29	Dahab	Canyon Reef	WP52	A	*Porites nodifera*	
LT29	Dahab	Canyon Reef	WP52	A	*Porites nodifera*	
LT29	Dahab	Canyon Reef	WP52	A	*Porites nodifera*	
LT29	Dahab	Canyon Reef	WP52	A	*Porites nodifera*	
LT29	Dahab	Canyon Reef	WP52	A	*Porites nodifera*	
LT29	Dahab	Canyon Reef	WP52	A	*Porites nodifera*	
LT29	Dahab	Canyon Reef	WP52	A	*Porites nodifera*	
LT29	Dahab	Canyon Reef	WP52	A	*Porites nodifera*	
LT29	Dahab	Canyon Reef	WP52	A	*Porites nodifera*	
LT30	Dahab	Canyon Reef		B	matrix	
LT30	Dahab	Canyon Reef		B	matrix	
LT30	Dahab	Canyon Reef		B	matrix	
LT30	Dahab	Canyon Reef		B	matrix	
LT30	Dahab	Canyon Reef		B	matrix	
LT30	Dahab	Canyon Reef		B	matrix	
LT30	Dahab	Canyon Reef		B	matrix	
LT30	Dahab	Canyon Reef		B	*Porites nodifera*	
LT30	Dahab	Canyon Reef		B	*Porites nodifera*	
LT30	Dahab	Canyon Reef		B	matrix	

LT	Locality	Site	GPS	Layer	*Name*	Sample
LT30	Dahab	Canyon Reef		B	matrix	
LT30	Dahab	Canyon Reef		B	matrix	
LT30	Dahab	Canyon Reef		B	matrix	
LT30	Dahab	Canyon Reef		B	matrix	
LT30	Dahab	Canyon Reef		B	matrix	
LT30	Dahab	Canyon Reef		B	Scleractinia indet.	LT30a
LT30	Dahab	Canyon Reef		B	*Millepora sp.*	LT30b
LT30	Dahab	Canyon Reef		B	red algae	
LT30	Dahab	Canyon Reef		B	red algae	
LT30	Dahab	Canyon Reef		B	*Paramontastraea peresi*	
LT30	Dahab	Canyon Reef		B	*Paramontastraea peresi*	
LT30	Dahab	Canyon Reef		B	*Paramontastraea peresi*	
LT30	Dahab	Canyon Reef		B	*Paramontastraea peresi*	
LT30	Dahab	Canyon Reef		B	matrix	
LT30	Dahab	Canyon Reef		B	*Acropora sp.*	
LT30	Dahab	Canyon Reef		B	matrix	LT30c
LT30	Dahab	Canyon Reef		B	*Porites lobata/lutea*	
LT30	Dahab	Canyon Reef		B	matrix	
LT30	Dahab	Canyon Reef		B	matrix	
LT30	Dahab	Canyon Reef		B	red algae	
LT30	Dahab	Canyon Reef		B	matrix	
LT30	Dahab	Canyon Reef		B	matrix	
LT30	Dahab	Canyon Reef		B	matrix	
LT30	Dahab	Canyon Reef		B	*Platygyra sp.*	
LT30	Dahab	Canyon Reef		B	*Platygyra sp.*	
LT30	Dahab	Canyon Reef		B	*Porites lobata/lutea*	
LT30	Dahab	Canyon Reef		B	*Acropora sp.*	
LT30	Dahab	Canyon Reef		B	*Acropora sp.*	
LT30	Dahab	Canyon Reef		B	*Acropora sp.*	
LT30	Dahab	Canyon Reef		B	matrix	
LT30	Dahab	Canyon Reef		B	matrix	
LT30	Dahab	Canyon Reef		B	*Acropora sp.*	
LT30	Dahab	Canyon Reef		B	*Acropora sp.*	
LT30	Dahab	Canyon Reef		B	*Porites nodifera*	
LT30	Dahab	Canyon Reef		B	*Acropora sp.*	
LT30	Dahab	Canyon Reef		B	*Cyphastrea serailia*	LT30d
LT30	Dahab	Canyon Reef		B	*Acropora sp.*	
LT30	Dahab	Canyon Reef		B	*Acropora sp.*	
LT30	Dahab	Canyon Reef		B	*Acropora sp.*	
LT30	Dahab	Canyon Reef		B	*Pavona sp.*	LT30e
LT30	Dahab	Canyon Reef		B	matrix	
LT30	Dahab	Canyon Reef		B	*Dipsastraea sp.*	
LT30	Dahab	Canyon Reef		B	matrix	
LT30	Dahab	Canyon Reef		B	matrix	
LT30	Dahab	Canyon Reef		B	*Favites flexuosa*	
LT30	Dahab	Canyon Reef		B	matrix	

LT	Locality	Site	GPS	Layer	*Name*	Sample
LT30	Dahab	Canyon Reef		B	debris	
LT30	Dahab	Canyon Reef		B	debris	
LT30	Dahab	Canyon Reef		B	debris	
LT30	Dahab	Canyon Reef		B	debris	
LT31	Dahab	Canyon Reef		C	red algae	
LT31	Dahab	Canyon Reef		C	red algae	
LT31	Dahab	Canyon Reef		C	red algae	
LT31	Dahab	Canyon Reef		C	red algae	
LT31	Dahab	Canyon Reef		C	matrix	
LT31	Dahab	Canyon Reef		C	matrix	
LT31	Dahab	Canyon Reef		C	red algae	
LT31	Dahab	Canyon Reef		C	red algae	
LT31	Dahab	Canyon Reef		C	red algae	
LT31	Dahab	Canyon Reef		C	fanglomerate	
LT31	Dahab	Canyon Reef		C	fanglomerate	
LT31	Dahab	Canyon Reef		C	fanglomerate	
LT31	Dahab	Canyon Reef		C	fanglomerate	
LT31	Dahab	Canyon Reef		C	fanglomerate	
LT31	Dahab	Canyon Reef		C	fanglomerate	
LT31	Dahab	Canyon Reef		C	red algae	
LT31	Dahab	Canyon Reef		C	red algae	
LT31	Dahab	Canyon Reef		C	red algae	
LT31	Dahab	Canyon Reef		C	red algae	
LT31	Dahab	Canyon Reef		C	red algae	
LT31	Dahab	Canyon Reef		C	red algae	
LT31	Dahab	Canyon Reef		C	red algae	
LT31	Dahab	Canyon Reef		C	red algae	
LT31	Dahab	Canyon Reef		C	red algae	
LT31	Dahab	Canyon Reef		C	*Cyphastrea sp.*	
LT31	Dahab	Canyon Reef		C	red algae	
LT31	Dahab	Canyon Reef		C	red algae	
LT31	Dahab	Canyon Reef		C	red algae	
LT31	Dahab	Canyon Reef		C	red algae	
LT31	Dahab	Canyon Reef		C	red algae	
LT31	Dahab	Canyon Reef		C	red algae	
LT31	Dahab	Canyon Reef		C	red algae	
LT31	Dahab	Canyon Reef		C	red algae	
LT31	Dahab	Canyon Reef		C	red algae	
LT31	Dahab	Canyon Reef		C	red algae	
LT31	Dahab	Canyon Reef		C	red algae	
LT31	Dahab	Canyon Reef		C	red algae	
LT31	Dahab	Canyon Reef		C	red algae	
LT31	Dahab	Canyon Reef		C	*Platygyra daedalea*	
LT31	Dahab	Canyon Reef		C	*Platygyra daedalea*	
LT31	Dahab	Canyon Reef		C	*Platygyra daedalea*	
LT31	Dahab	Canyon Reef		C	*Platygyra daedalea*	

LT	Locality	Site	GPS	Layer	*Name*	Sample
LT31	Dahab	Canyon Reef		C	red algae	
LT31	Dahab	Canyon Reef		C	red algae	
LT31	Dahab	Canyon Reef		C	red algae	
LT31	Dahab	Canyon Reef		C	red algae	
LT31	Dahab	Canyon Reef		C	red algae	
LT31	Dahab	Canyon Reef		C	red algae	
LT31	Dahab	Canyon Reef		C	red algae	
LT31	Dahab	Canyon Reef		C	red algae	
LT31	Dahab	Canyon Reef		C	red algae	
LT31	Dahab	Canyon Reef		C	red algae	
LT31	Dahab	Canyon Reef		C	red algae	
LT31	Dahab	Canyon Reef		C	*Galaxea fascicularis*	
LT31	Dahab	Canyon Reef		C	red algae	
LT31	Dahab	Canyon Reef		C	red algae	
LT31	Dahab	Canyon Reef		C	red algae	
LT31	Dahab	Canyon Reef		C	red algae	
LT31	Dahab	Canyon Reef		C	*Cyphastrea sp.*	
LT31	Dahab	Canyon Reef		C	red algae	
LT31	Dahab	Canyon Reef		C	*Galaxea fascicularis*	
LT31	Dahab	Canyon Reef		C	*Coscinaraea monile*	LT31a
LT31	Dahab	Canyon Reef		C	red algae	
LT31	Dahab	Canyon Reef		C	red algae	
LT31	Dahab	Canyon Reef		C	red algae	
LT31	Dahab	Canyon Reef		C	red algae	
LT32	Ras Mohammed	Turtle Bay	WP54		*Porites lobata/lutea*	
LT32	Ras Mohammed	Turtle Bay	WP54		*Porites lobata/lutea*	
LT32	Ras Mohammed	Turtle Bay	WP54		*Porites lobata/lutea*	
LT32	Ras Mohammed	Turtle Bay	WP54		*Porites lobata/lutea*	
LT32	Ras Mohammed	Turtle Bay	WP54		*Porites lobata/lutea*	
LT32	Ras Mohammed	Turtle Bay	WP54		*Porites lobata/lutea*	
LT32	Ras Mohammed	Turtle Bay	WP54		*Porites lobata/lutea*	
LT32	Ras Mohammed	Turtle Bay	WP54		*Porites lobata/lutea*	
LT32	Ras Mohammed	Turtle Bay	WP54		*Porites lobata/lutea*	
LT32	Ras Mohammed	Turtle Bay	WP54		*Porites lobata/lutea*	
LT32	Ras Mohammed	Turtle Bay	WP54		*Porites lobata/lutea*	
LT32	Ras Mohammed	Turtle Bay	WP54		matrix	
LT32	Ras Mohammed	Turtle Bay	WP54		matrix	
LT32	Ras Mohammed	Turtle Bay	WP54		matrix	
LT32	Ras Mohammed	Turtle Bay	WP54		red algae	
LT32	Ras Mohammed	Turtle Bay	WP54		red algae	
LT32	Ras Mohammed	Turtle Bay	WP54		*Porites nodifera*	
LT32	Ras Mohammed	Turtle Bay	WP54		*Porites nodifera*	
LT32	Ras Mohammed	Turtle Bay	WP54		*Porites nodifera*	
LT32	Ras Mohammed	Turtle Bay	WP54		*Porites nodifera*	
LT32	Ras Mohammed	Turtle Bay	WP54		*Porites nodifera*	

LT	Locality	Site	GPS	Layer	*Name*	Sample
LT32	Ras Mohammed	Turtle Bay	WP54		*Porites nodifera*	
LT32	Ras Mohammed	Turtle Bay	WP54		*Porites nodifera*	
LT32	Ras Mohammed	Turtle Bay	WP54		*Porites nodifera*	
LT32	Ras Mohammed	Turtle Bay	WP54		red algae	
LT32	Ras Mohammed	Turtle Bay	WP54		red algae	
LT32	Ras Mohammed	Turtle Bay	WP54		red algae	
LT32	Ras Mohammed	Turtle Bay	WP54		red algae	
LT32	Ras Mohammed	Turtle Bay	WP54		matrix	
LT32	Ras Mohammed	Turtle Bay	WP54		matrix	
LT32	Ras Mohammed	Turtle Bay	WP54		matrix	
LT32	Ras Mohammed	Turtle Bay	WP54		matrix	
LT32	Ras Mohammed	Turtle Bay	WP54		matrix	
LT32	Ras Mohammed	Turtle Bay	WP54		Scleractinia indet.	
LT32	Ras Mohammed	Turtle Bay	WP54		red algae	
LT32	Ras Mohammed	Turtle Bay	WP54		red algae	
LT32	Ras Mohammed	Turtle Bay	WP54		red algae	
LT32	Ras Mohammed	Turtle Bay	WP54		*Porites nodifera*	
LT32	Ras Mohammed	Turtle Bay	WP54		*Porites nodifera*	
LT32	Ras Mohammed	Turtle Bay	WP54		red algae	
LT32	Ras Mohammed	Turtle Bay	WP54		red algae	
LT32	Ras Mohammed	Turtle Bay	WP54		red algae	
LT32	Ras Mohammed	Turtle Bay	WP54		red algae	
LT32	Ras Mohammed	Turtle Bay	WP54		red algae	
LT32	Ras Mohammed	Turtle Bay	WP54		red algae	
LT32	Ras Mohammed	Turtle Bay	WP54		red algae	
LT32	Ras Mohammed	Turtle Bay	WP54		red algae	
LT32	Ras Mohammed	Turtle Bay	WP54		red algae	
LT32	Ras Mohammed	Turtle Bay	WP54		red algae	
LT32	Ras Mohammed	Turtle Bay	WP54		red algae	
LT32	Ras Mohammed	Turtle Bay	WP54		red algae	
LT32	Ras Mohammed	Turtle Bay	WP54		red algae	
LT32	Ras Mohammed	Turtle Bay	WP54		red algae	
LT32	Ras Mohammed	Turtle Bay	WP54		red algae	
LT33	Ras Mohammed	Ras Mohammed inland	WP57		matrix	
LT33	Ras Mohammed	Ras Mohammed inland	WP57		matrix	
LT33	Ras Mohammed	Ras Mohammed inland	WP57		matrix	
LT33	Ras Mohammed	Ras Mohammed inland	WP57		matrix	
LT33	Ras Mohammed	Ras Mohammed inland	WP57		matrix	
LT33	Ras Mohammed	Ras Mohammed inland	WP57		*Cyphastrea sp.*	
LT33	Ras Mohammed	Ras Mohammed inland	WP57		matrix	
LT33	Ras Mohammed	Ras Mohammed inland	WP57		matrix	
LT33	Ras Mohammed	Ras Mohammed inland	WP57		matrix	
LT33	Ras Mohammed	Ras Mohammed inland	WP57		matrix	
LT33	Ras Mohammed	Ras Mohammed inland	WP57		matrix	
LT33	Ras Mohammed	Ras Mohammed inland	WP57		matrix	

LT	Locality	Site	GPS	Layer	*Name*	Sample
LT33	Ras Mohammed	Ras Mohammed inland	WP57		matrix	
LT33	Ras Mohammed	Ras Mohammed inland	WP57		matrix	
LT33	Ras Mohammed	Ras Mohammed inland	WP57		matrix	
LT33	Ras Mohammed	Ras Mohammed inland	WP57		matrix	
LT33	Ras Mohammed	Ras Mohammed inland	WP57		matrix	
LT33	Ras Mohammed	Ras Mohammed inland	WP57		Argariciidae indet.	
LT33	Ras Mohammed	Ras Mohammed inland	WP57		*Cyphastrea sp.*	
LT33	Ras Mohammed	Ras Mohammed inland	WP57		*Cyphastrea sp.*	
LT34	Ras Mohammed	Ras Mohammed Camp	WP62		red algae	
LT34	Ras Mohammed	Ras Mohammed Camp	WP62		red algae	
LT34	Ras Mohammed	Ras Mohammed Camp	WP62		matrix	
LT34	Ras Mohammed	Ras Mohammed Camp	WP62		matrix	
LT34	Ras Mohammed	Ras Mohammed Camp	WP62		*Goniastrea retiformis*	LT34 1690a-c
LT34	Ras Mohammed	Ras Mohammed Camp	WP62		*Goniastrea retiformis*	
LT34	Ras Mohammed	Ras Mohammed Camp	WP62		*Goniastrea retiformis*	
LT34	Ras Mohammed	Ras Mohammed Camp	WP62		*Dipsastraea sp.*	LT34 1693a-c
LT34	Ras Mohammed	Ras Mohammed Camp	WP62		*Dipsastraea sp.*	
LT34	Ras Mohammed	Ras Mohammed Camp	WP62		*Dipsastraea sp.*	
LT34	Ras Mohammed	Ras Mohammed Camp	WP62		gap	
LT34	Ras Mohammed	Ras Mohammed Camp	WP62		gap	
LT34	Ras Mohammed	Ras Mohammed Camp	WP62		matrix	
LT34	Ras Mohammed	Ras Mohammed Camp	WP62		matrix	
LT34	Ras Mohammed	Ras Mohammed Camp	WP62		matrix	
LT34	Ras Mohammed	Ras Mohammed Camp	WP62		*Goniastrea retiformis*	LT34 1701
LT34	Ras Mohammed	Ras Mohammed Camp	WP62		*Goniastrea retiformis*	
LT34	Ras Mohammed	Ras Mohammed Camp	WP62		*Goniastrea retiformis*	
LT34	Ras Mohammed	Ras Mohammed Camp	WP62		*Goniastrea retiformis*	
LT34	Ras Mohammed	Ras Mohammed Camp	WP62		*Goniastrea retiformis*	
LT34	Ras Mohammed	Ras Mohammed Camp	WP62		*Goniastrea retiformis*	
LT34	Ras Mohammed	Ras Mohammed Camp	WP62		matrix	
LT34	Ras Mohammed	Ras Mohammed Camp	WP62		matrix	
LT34	Ras Mohammed	Ras Mohammed Camp	WP62		red algae	
LT34	Ras Mohammed	Ras Mohammed Camp	WP62		red algae	
LT34	Ras Mohammed	Ras Mohammed Camp	WP62		matrix	
LT34	Ras Mohammed	Ras Mohammed Camp	WP62		matrix	
LT34	Ras Mohammed	Ras Mohammed Camp	WP62		matrix	
LT34	Ras Mohammed	Ras Mohammed Camp	WP62		red algae	
LT34	Ras Mohammed	Ras Mohammed Camp	WP62		red algae	
LT34	Ras Mohammed	Ras Mohammed Camp	WP62		matrix	
LT34	Ras Mohammed	Ras Mohammed Camp	WP62		*Galaxea fascicularis*	
LT34	Ras Mohammed	Ras Mohammed Camp	WP62		matrix	
LT34	Ras Mohammed	Ras Mohammed Camp	WP62		matrix	
LT34	Ras Mohammed	Ras Mohammed Camp	WP62		matrix	
LT34	Ras Mohammed	Ras Mohammed Camp	WP62		matrix	
LT34	Ras Mohammed	Ras Mohammed Camp	WP62		matrix	
LT34	Ras Mohammed	Ras Mohammed Camp	WP62		matrix	

LT	Locality	Site	GPS	Layer	*Name*	Sample
LT34	Ras Mohammed	Ras Mohammed Camp	WP62		Scleractinia indet.	
LT34	Ras Mohammed	Ras Mohammed Camp	WP62		gap	
LT34	Ras Mohammed	Ras Mohammed Camp	WP62		gap	
LT34	Ras Mohammed	Ras Mohammed Camp	WP62		gap	
LT34	Ras Mohammed	Ras Mohammed Camp	WP62		red algae	
LT34	Ras Mohammed	Ras Mohammed Camp	WP62		matrix	
LT34	Ras Mohammed	Ras Mohammed Camp	WP62		matrix	
LT34	Ras Mohammed	Ras Mohammed Camp	WP62		matrix	
LT34	Ras Mohammed	Ras Mohammed Camp	WP62		matrix	
LT34	Ras Mohammed	Ras Mohammed Camp	WP62		*Goniastrea retiformis*	
LT34	Ras Mohammed	Ras Mohammed Camp	WP62		matrix	
LT34	Ras Mohammed	Ras Mohammed Camp	WP62		*Galaxea fascicularis*	
LT34	Ras Mohammed	Ras Mohammed Camp	WP62		matrix	
LT34	Ras Mohammed	Ras Mohammed Camp	WP62		matrix	
LT34	Ras Mohammed	Ras Mohammed Camp	WP62		matrix	
LT34	Ras Mohammed	Ras Mohammed Camp	WP62		red algae	
LT34	Ras Mohammed	Ras Mohammed Camp	WP62		red algae	
LT34	Ras Mohammed	Ras Mohammed Camp	WP62		*Goniastrea retiformis*	
LT34	Ras Mohammed	Ras Mohammed Camp	WP62		matrix	
LT34	Ras Mohammed	Ras Mohammed Camp	WP62		matrix	
LT34	Ras Mohammed	Ras Mohammed Camp	WP62		red algae	
LT34	Ras Mohammed	Ras Mohammed Camp	WP62		red algae	
LT34	Ras Mohammed	Ras Mohammed Camp	WP62		red algae	
LT34	Ras Mohammed	Ras Mohammed Camp	WP62		*Goniastrea retiformis*	
LT34	Ras Mohammed	Ras Mohammed Camp	WP62		red algae	
LT34	Ras Mohammed	Ras Mohammed Camp	WP62		red algae	
LT34	Ras Mohammed	Ras Mohammed Camp	WP62		*Goniastrea retiformis*	
LT34	Ras Mohammed	Ras Mohammed Camp	WP62		*Favites flexuosa*	
LT34	Ras Mohammed	Ras Mohammed Camp	WP62		*Favites flexuosa*	
LT34	Ras Mohammed	Ras Mohammed Camp	WP62		*Favites flexuosa*	
LT34	Ras Mohammed	Ras Mohammed Camp	WP62		red algae	
LT34	Ras Mohammed	Ras Mohammed Camp	WP62		red algae	
LT34	Ras Mohammed	Ras Mohammed Camp	WP62		*Echinopora forskaliana*	
LT34	Ras Mohammed	Ras Mohammed Camp	WP62		*Echinopora forskaliana*	
LT34	Ras Mohammed	Ras Mohammed Camp	WP62		*Echinopora forskaliana*	
LT34	Ras Mohammed	Ras Mohammed Camp	WP62		red algae	
LT34	Ras Mohammed	Ras Mohammed Camp	WP62		matrix	
LT34	Ras Mohammed	Ras Mohammed Camp	WP62		*Lobophyllia corymbosa*	
LT34	Ras Mohammed	Ras Mohammed Camp	WP62		*Lobophyllia corymbosa*	
LT34	Ras Mohammed	Ras Mohammed Camp	WP62		*Lobophyllia corymbosa*	
LT34	Ras Mohammed	Ras Mohammed Camp	WP62		*Montipora sp.*	
LT34	Ras Mohammed	Ras Mohammed Camp	WP62		red algae	
LT34	Ras Mohammed	Ras Mohammed Camp	WP62		Bivalve	
LT34	Ras Mohammed	Ras Mohammed Camp	WP62		Scleractinia indet.	
LT34	Ras Mohammed	Ras Mohammed Camp	WP62		matrix	
LT34	Ras Mohammed	Ras Mohammed Camp	WP62		*Favites spinosa*	

LT	Locality	Site	GPS	Layer	*Name*	Sample
LT34	Ras Mohammed	Ras Mohammed Camp	WP62		matrix	
LT34	Ras Mohammed	Ras Mohammed Camp	WP62		gap	
LT34	Ras Mohammed	Ras Mohammed Camp	WP62		red algae	
LT34	Ras Mohammed	Ras Mohammed Camp	WP62		*Goniastrea retiformis*	
LT34	Ras Mohammed	Ras Mohammed Camp	WP62		red algae	
LT34	Ras Mohammed	Ras Mohammed Camp	WP62		*Goniastrea retiformis*	
LT34	Ras Mohammed	Ras Mohammed Camp	WP62		matrix	
LT34	Ras Mohammed	Ras Mohammed Camp	WP62		matrix	
LT34	Ras Mohammed	Ras Mohammed Camp	WP62		matrix	
LT34	Ras Mohammed	Ras Mohammed Camp	WP62		red algae	
LT34	Ras Mohammed	Ras Mohammed Camp	WP62		*Goniastrea retiformis*	
LT34	Ras Mohammed	Ras Mohammed Camp	WP62		*Goniastrea retiformis*	
LT34	Ras Mohammed	Ras Mohammed Camp	WP62		*Goniastrea retiformis*	
LT34	Ras Mohammed	Ras Mohammed Camp	WP62		matrix	
LT34	Ras Mohammed	Ras Mohammed Camp	WP62		matrix	
LT34	Ras Mohammed	Ras Mohammed Camp	WP62		matrix	
LT34	Ras Mohammed	Ras Mohammed Camp	WP62		red algae	
LT34	Ras Mohammed	Ras Mohammed Camp	WP62		red algae	
LT34	Ras Mohammed	Ras Mohammed Camp	WP62		red algae	
LT34	Ras Mohammed	Ras Mohammed Camp	WP62		*Echinopora forskaliana*	
LT34	Ras Mohammed	Ras Mohammed Camp	WP62		*Echinopora forskaliana*	
LT34	Ras Mohammed	Ras Mohammed Camp	WP62		*Echinopora forskaliana*	
LT34	Ras Mohammed	Ras Mohammed Camp	WP62		matrix	
LT34	Ras Mohammed	Ras Mohammed Camp	WP62		matrix	
LT34	Ras Mohammed	Ras Mohammed Camp	WP62		*Lobophyllia hemprichii*	
LT34	Ras Mohammed	Ras Mohammed Camp	WP62		*Lobophyllia hemprichii*	
LT34	Ras Mohammed	Ras Mohammed Camp	WP62		*Lobophyllia hemprichii*	
LT34	Ras Mohammed	Ras Mohammed Camp	WP62		red algae	
LT34	Ras Mohammed	Ras Mohammed Camp	WP62		red algae	
LT34	Ras Mohammed	Ras Mohammed Camp	WP62		matrix	
LT34	Ras Mohammed	Ras Mohammed Camp	WP62		*Lobophyllia hemprichii*	
LT34	Ras Mohammed	Ras Mohammed Camp	WP62		*Lobophyllia hemprichii*	
LT34	Ras Mohammed	Ras Mohammed Camp	WP62		red algae	
LT34	Ras Mohammed	Ras Mohammed Camp	WP62		matrix	
LT34	Ras Mohammed	Ras Mohammed Camp	WP62		*Favites flexuosa*	
LT34	Ras Mohammed	Ras Mohammed Camp	WP62		*Favites flexuosa*	
LT34	Ras Mohammed	Ras Mohammed Camp	WP62		red algae	
LT34	Ras Mohammed	Ras Mohammed Camp	WP62		red algae	
LT34	Ras Mohammed	Ras Mohammed Camp	WP62		*Goniastrea retiformis*	
LT34	Ras Mohammed	Ras Mohammed Camp	WP62		matrix	
LT34	Ras Mohammed	Ras Mohammed Camp	WP62		matrix	
LT34	Ras Mohammed	Ras Mohammed Camp	WP62		matrix	
LT34	Ras Mohammed	Ras Mohammed Camp	WP62		matrix	
LT34	Ras Mohammed	Ras Mohammed Camp	WP62		*Echinopora forskaliana*	
LT34	Ras Mohammed	Ras Mohammed Camp	WP62		*Echinopora forskaliana*	
LT34	Ras Mohammed	Ras Mohammed Camp	WP62		matrix	

LT	Locality	Site	GPS	Layer	*Name*	Sample
LT34	Ras Mohammed	Ras Mohammed Camp	WP62		matrix	
LT34	Ras Mohammed	Ras Mohammed Camp	WP62		*Echinopora forskaliana*	
LT35	Ras Mohammed	Ras Mohammed Camp	WP62		*Platygyra sp.*	
LT35	Ras Mohammed	Ras Mohammed Camp	WP62		red algae	
LT35	Ras Mohammed	Ras Mohammed Camp	WP62		red algae	
LT35	Ras Mohammed	Ras Mohammed Camp	WP62		matrix	
LT35	Ras Mohammed	Ras Mohammed Camp	WP62		matrix	
LT35	Ras Mohammed	Ras Mohammed Camp	WP62		*Stylophora sp.*	
LT35	Ras Mohammed	Ras Mohammed Camp	WP62		matrix	
LT35	Ras Mohammed	Ras Mohammed Camp	WP62		matrix	
LT35	Ras Mohammed	Ras Mohammed Camp	WP62		*Goniastrea retiformis*	
LT35	Ras Mohammed	Ras Mohammed Camp	WP62		*Goniastrea retiformis*	
LT35	Ras Mohammed	Ras Mohammed Camp	WP62		*Goniastrea retiformis*	
LT35	Ras Mohammed	Ras Mohammed Camp	WP62		*Goniastrea retiformis*	
LT35	Ras Mohammed	Ras Mohammed Camp	WP62		matrix	
LT35	Ras Mohammed	Ras Mohammed Camp	WP62		matrix	
LT35	Ras Mohammed	Ras Mohammed Camp	WP62		*Echinopora forskaliana*	
LT35	Ras Mohammed	Ras Mohammed Camp	WP62		matrix	
LT35	Ras Mohammed	Ras Mohammed Camp	WP62		matrix	
LT35	Ras Mohammed	Ras Mohammed Camp	WP62		*Dipsastraea sp.*	
LT35	Ras Mohammed	Ras Mohammed Camp	WP62		*Dipsastraea sp.*	
LT35	Ras Mohammed	Ras Mohammed Camp	WP62		*Favites sp.*	
LT35	Ras Mohammed	Ras Mohammed Camp	WP62		*Favites sp.*	
LT35	Ras Mohammed	Ras Mohammed Camp	WP62		red algae	
LT35	Ras Mohammed	Ras Mohammed Camp	WP62		*Echinopora forskaliana*	
LT35	Ras Mohammed	Ras Mohammed Camp	WP62		*Acanthastrea echinata*	
LT35	Ras Mohammed	Ras Mohammed Camp	WP62		red algae	
LT35	Ras Mohammed	Ras Mohammed Camp	WP62		matrix	
LT35	Ras Mohammed	Ras Mohammed Camp	WP62		gap	
LT35	Ras Mohammed	Ras Mohammed Camp	WP62		gap	
LT35	Ras Mohammed	Ras Mohammed Camp	WP62		gap	
LT35	Ras Mohammed	Ras Mohammed Camp	WP62		gap	
LT35	Ras Mohammed	Ras Mohammed Camp	WP62		*Goniastrea retiformis*	
LT35	Ras Mohammed	Ras Mohammed Camp	WP62		matrix	
LT35	Ras Mohammed	Ras Mohammed Camp	WP62		gap	
LT35	Ras Mohammed	Ras Mohammed Camp	WP62		matrix	
LT35	Ras Mohammed	Ras Mohammed Camp	WP62		matrix	
LT35	Ras Mohammed	Ras Mohammed Camp	WP62		*Goniastrea retiformis*	
LT35	Ras Mohammed	Ras Mohammed Camp	WP62		*Goniastrea retiformis*	
LT35	Ras Mohammed	Ras Mohammed Camp	WP62		gap	
LT35	Ras Mohammed	Ras Mohammed Camp	WP62		red algae	
LT35	Ras Mohammed	Ras Mohammed Camp	WP62		red algae	
LT35	Ras Mohammed	Ras Mohammed Camp	WP62		gap	
LT35	Ras Mohammed	Ras Mohammed Camp	WP62		gap	
LT35	Ras Mohammed	Ras Mohammed Camp	WP62		gap	
LT35	Ras Mohammed	Ras Mohammed Camp	WP62		gap	

LT	Locality	Site	GPS	Layer	*Name*	Sample
LT35	Ras Mohammed	Ras Mohammed Camp	WP62		gap	
LT35	Ras Mohammed	Ras Mohammed Camp	WP62		gap	
LT35	Ras Mohammed	Ras Mohammed Camp	WP62		gap	
LT35	Ras Mohammed	Ras Mohammed Camp	WP62		gap	
LT35	Ras Mohammed	Ras Mohammed Camp	WP62		gap	
LT35	Ras Mohammed	Ras Mohammed Camp	WP62		red algae	
LT35	Ras Mohammed	Ras Mohammed Camp	WP62		*Goniastrea retiformis*	
LT35	Ras Mohammed	Ras Mohammed Camp	WP62		*Goniastrea retiformis*	
LT35	Ras Mohammed	Ras Mohammed Camp	WP62		*Goniastrea retiformis*	
LT35	Ras Mohammed	Ras Mohammed Camp	WP62		*Goniastrea retiformis*	
LT35	Ras Mohammed	Ras Mohammed Camp	WP62		*Goniastrea retiformis*	
LT35	Ras Mohammed	Ras Mohammed Camp	WP62		*Goniastrea retiformis*	
LT35	Ras Mohammed	Ras Mohammed Camp	WP62		*Goniastrea retiformis*	
LT35	Ras Mohammed	Ras Mohammed Camp	WP62		red algae	
LT35	Ras Mohammed	Ras Mohammed Camp	WP62		*Goniastrea retiformis*	
LT35	Ras Mohammed	Ras Mohammed Camp	WP62		matrix	
LT35	Ras Mohammed	Ras Mohammed Camp	WP62		*Goniastrea retiformis*	
LT35	Ras Mohammed	Ras Mohammed Camp	WP62		*Goniastrea retiformis*	
LT35	Ras Mohammed	Ras Mohammed Camp	WP62		*Goniastrea retiformis*	
LT35	Ras Mohammed	Ras Mohammed Camp	WP62		*Goniastrea retiformis*	
LT35	Ras Mohammed	Ras Mohammed Camp	WP62		*Goniastrea retiformis*	
LT35	Ras Mohammed	Ras Mohammed Camp	WP62		*Goniastrea retiformis*	
LT35	Ras Mohammed	Ras Mohammed Camp	WP62		matrix	
LT35	Ras Mohammed	Ras Mohammed Camp	WP62		matrix	
LT35	Ras Mohammed	Ras Mohammed Camp	WP62		matrix	
LT35	Ras Mohammed	Ras Mohammed Camp	WP62		matrix	
LT35	Ras Mohammed	Ras Mohammed Camp	WP62		matrix	
LT35	Ras Mohammed	Ras Mohammed Camp	WP62		red algae	
LT35	Ras Mohammed	Ras Mohammed Camp	WP62		matrix	
LT35	Ras Mohammed	Ras Mohammed Camp	WP62		matrix	
LT35	Ras Mohammed	Ras Mohammed Camp	WP62		matrix	
LT35	Ras Mohammed	Ras Mohammed Camp	WP62		*Cyphastrea sp.*	
LT35	Ras Mohammed	Ras Mohammed Camp	WP62		matrix	
LT35	Ras Mohammed	Ras Mohammed Camp	WP62		*Favites sp.*	
LT35	Ras Mohammed	Ras Mohammed Camp	WP62		matrix	
LT35	Ras Mohammed	Ras Mohammed Camp	WP62		*Favites sp.*	
LT35	Ras Mohammed	Ras Mohammed Camp	WP62		matrix	
LT35	Ras Mohammed	Ras Mohammed Camp	WP62		*Echinopora forskaliana*	
LT35	Ras Mohammed	Ras Mohammed Camp	WP62		matrix	
LT35	Ras Mohammed	Ras Mohammed Camp	WP62		matrix	
LT35	Ras Mohammed	Ras Mohammed Camp	WP62		matrix	
LT35	Ras Mohammed	Ras Mohammed Camp	WP62		*Goniastrea retiformis*	
LT35	Ras Mohammed	Ras Mohammed Camp	WP62		matrix	
LT35	Ras Mohammed	Ras Mohammed Camp	WP62		matrix	
LT35	Ras Mohammed	Ras Mohammed Camp	WP62		gap	
LT35	Ras Mohammed	Ras Mohammed Camp	WP62		gap	

LT	Locality	Site	GPS	Layer	*Name*	Sample
LT35	Ras Mohammed	Ras Mohammed Camp	WP62		gap	
LT35	Ras Mohammed	Ras Mohammed Camp	WP62		gap	
LT35	Ras Mohammed	Ras Mohammed Camp	WP62		gap	
LT35	Ras Mohammed	Ras Mohammed Camp	WP62		gap	
LT35	Ras Mohammed	Ras Mohammed Camp	WP62		gap	
LT35	Ras Mohammed	Ras Mohammed Camp	WP62		matrix	
LT35	Ras Mohammed	Ras Mohammed Camp	WP62		red algae	
LT35	Ras Mohammed	Ras Mohammed Camp	WP62		red algae	
LT35	Ras Mohammed	Ras Mohammed Camp	WP62		matrix	
LT35	Ras Mohammed	Ras Mohammed Camp	WP62		matrix	
LT35	Ras Mohammed	Ras Mohammed Camp	WP62		matrix	
LT35	Ras Mohammed	Ras Mohammed Camp	WP62		matrix	
LT35	Ras Mohammed	Ras Mohammed Camp	WP62		*Goniastrea retiformis*	
LT35	Ras Mohammed	Ras Mohammed Camp	WP62		gap	
LT35	Ras Mohammed	Ras Mohammed Camp	WP62		matrix	
LT35	Ras Mohammed	Ras Mohammed Camp	WP62		*Goniastrea retiformis*	
LT35	Ras Mohammed	Ras Mohammed Camp	WP62		matrix	
LT35	Ras Mohammed	Ras Mohammed Camp	WP62		*Goniastrea retiformis*	
LT35	Ras Mohammed	Ras Mohammed Camp	WP62		*Goniastrea retiformis*	
LT35	Ras Mohammed	Ras Mohammed Camp	WP62		matrix	
LT35	Ras Mohammed	Ras Mohammed Camp	WP62		red algae	
LT35	Ras Mohammed	Ras Mohammed Camp	WP62		gap	
LT35	Ras Mohammed	Ras Mohammed Camp	WP62		gap	
LT35	Ras Mohammed	Ras Mohammed Camp	WP62		*Platygyra crosslandi*	
LT35	Ras Mohammed	Ras Mohammed Camp	WP62		*Platygyra crosslandi*	
LT35	Ras Mohammed	Ras Mohammed Camp	WP62		matrix	
LT35	Ras Mohammed	Ras Mohammed Camp	WP62		*Fungia sp.*	
LT35	Ras Mohammed	Ras Mohammed Camp	WP62		matrix	
LT35	Ras Mohammed	Ras Mohammed Camp	WP62		gap	
LT35	Ras Mohammed	Ras Mohammed Camp	WP62		gap	
LT35	Ras Mohammed	Ras Mohammed Camp	WP62		gap	
LT35	Ras Mohammed	Ras Mohammed Camp	WP62		matrix	
LT35	Ras Mohammed	Ras Mohammed Camp	WP62		*Goniastrea retiformis*	
LT35	Ras Mohammed	Ras Mohammed Camp	WP62		*Goniastrea retiformis*	
LT35	Ras Mohammed	Ras Mohammed Camp	WP62		*Goniastrea retiformis*	
LT35	Ras Mohammed	Ras Mohammed Camp	WP62		*Goniastrea retiformis*	
LT35	Ras Mohammed	Ras Mohammed Camp	WP62		*Goniastrea retiformis*	
LT35	Ras Mohammed	Ras Mohammed Camp	WP62		gap	
LT35	Ras Mohammed	Ras Mohammed Camp	WP62		matrix	
LT35	Ras Mohammed	Ras Mohammed Camp	WP62		*Goniastrea retiformis*	
LT35	Ras Mohammed	Ras Mohammed Camp	WP62		*Goniastrea retiformis*	
LT35	Ras Mohammed	Ras Mohammed Camp	WP62		*Goniastrea retiformis*	
LT35	Ras Mohammed	Ras Mohammed Camp	WP62		*Goniastrea retiformis*	
LT35	Ras Mohammed	Ras Mohammed Camp	WP62		*Goniastrea retiformis*	
LT35	Ras Mohammed	Ras Mohammed Camp	WP62		matrix	
LT35	Ras Mohammed	Ras Mohammed Camp	WP62		matrix	

LT	Locality	Site	GPS	Layer	*Name*	Sample
LT35	Ras Mohammed	Ras Mohammed Camp	WP62		matrix	
LT35	Ras Mohammed	Ras Mohammed Camp	WP62		matrix	
LT35	Ras Mohammed	Ras Mohammed Camp	WP62		matrix	
LT35	Ras Mohammed	Ras Mohammed Camp	WP62		matrix	
LT35	Ras Mohammed	Ras Mohammed Camp	WP62		*Echinopora forskaliana*	
LT35	Ras Mohammed	Ras Mohammed Camp	WP62		*Echinopora forskaliana*	
LT35	Ras Mohammed	Ras Mohammed Camp	WP62		*Echinopora forskaliana*	
LT35	Ras Mohammed	Ras Mohammed Camp	WP62		matrix	
LT35	Ras Mohammed	Ras Mohammed Camp	WP62		matrix	
LT36	Ras Mohammed	Ras Mohammed Camp			*Echinopora forskaliana*	
LT36	Ras Mohammed	Ras Mohammed Camp			*Echinopora forskaliana*	
LT36	Ras Mohammed	Ras Mohammed Camp			red algae	
LT36	Ras Mohammed	Ras Mohammed Camp			red algae	
LT36	Ras Mohammed	Ras Mohammed Camp			matrix	
LT36	Ras Mohammed	Ras Mohammed Camp			matrix	
LT36	Ras Mohammed	Ras Mohammed Camp			matrix	
LT36	Ras Mohammed	Ras Mohammed Camp			matrix	
LT36	Ras Mohammed	Ras Mohammed Camp			red algae	
LT36	Ras Mohammed	Ras Mohammed Camp			red algae	
LT36	Ras Mohammed	Ras Mohammed Camp			matrix	
LT36	Ras Mohammed	Ras Mohammed Camp			*Goniastrea retiformis*	
LT36	Ras Mohammed	Ras Mohammed Camp			*Goniastrea retiformis*	
LT36	Ras Mohammed	Ras Mohammed Camp			*Goniastrea retiformis*	
LT36	Ras Mohammed	Ras Mohammed Camp			matrix	
LT36	Ras Mohammed	Ras Mohammed Camp			matrix	
LT36	Ras Mohammed	Ras Mohammed Camp			matrix	
LT36	Ras Mohammed	Ras Mohammed Camp			matrix	
LT36	Ras Mohammed	Ras Mohammed Camp			matrix	
LT36	Ras Mohammed	Ras Mohammed Camp			red algae	
LT36	Ras Mohammed	Ras Mohammed Camp			*Goniastrea retiformis*	
LT36	Ras Mohammed	Ras Mohammed Camp			*Goniastrea retiformis*	
LT36	Ras Mohammed	Ras Mohammed Camp			matrix	
LT36	Ras Mohammed	Ras Mohammed Camp			red algae	
LT36	Ras Mohammed	Ras Mohammed Camp			red algae	
LT36	Ras Mohammed	Ras Mohammed Camp			matrix	
LT36	Ras Mohammed	Ras Mohammed Camp			matrix	
LT36	Ras Mohammed	Ras Mohammed Camp			matrix	
LT36	Ras Mohammed	Ras Mohammed Camp			matrix	
LT36	Ras Mohammed	Ras Mohammed Camp			*Dipsastraea pallida*	
LT36	Ras Mohammed	Ras Mohammed Camp			*Dipsastraea pallida*	
LT36	Ras Mohammed	Ras Mohammed Camp			matrix	
LT36	Ras Mohammed	Ras Mohammed Camp			red algae	
LT36	Ras Mohammed	Ras Mohammed Camp			*Goniastrea retiformis*	
LT36	Ras Mohammed	Ras Mohammed Camp			*Platygyra sp.*	
LT36	Ras Mohammed	Ras Mohammed Camp			red algae	
LT36	Ras Mohammed	Ras Mohammed Camp			red algae	

LT	Locality	Site	GPS	Layer	*Name*	Sample
LT36	Ras Mohammed	Ras Mohammed Camp			matrix	
LT36	Ras Mohammed	Ras Mohammed Camp			matrix	
LT36	Ras Mohammed	Ras Mohammed Camp			matrix	
LT36	Ras Mohammed	Ras Mohammed Camp			matrix	
LT36	Ras Mohammed	Ras Mohammed Camp			*Dipsastraea sp.*	
LT36	Ras Mohammed	Ras Mohammed Camp			*Dipsastraea sp.*	
LT36	Ras Mohammed	Ras Mohammed Camp			*Dipsastraea sp.*	
LT36	Ras Mohammed	Ras Mohammed Camp			*Dipsastraea sp.*	
LT36	Ras Mohammed	Ras Mohammed Camp			red algae	
LT36	Ras Mohammed	Ras Mohammed Camp			red algae	
LT36	Ras Mohammed	Ras Mohammed Camp			red algae	
LT36	Ras Mohammed	Ras Mohammed Camp			matrix	
LT36	Ras Mohammed	Ras Mohammed Camp			red algae	
LT36	Ras Mohammed	Ras Mohammed Camp			red algae	
LT36	Ras Mohammed	Ras Mohammed Camp			matrix	
LT36	Ras Mohammed	Ras Mohammed Camp			matrix	
LT36	Ras Mohammed	Ras Mohammed Camp			matrix	
LT36	Ras Mohammed	Ras Mohammed Camp			red algae	
LT36	Ras Mohammed	Ras Mohammed Camp			red algae	
LT36	Ras Mohammed	Ras Mohammed Camp			*Cyphastrea serailia*	
LT36	Ras Mohammed	Ras Mohammed Camp			matrix	
LT36	Ras Mohammed	Ras Mohammed Camp			matrix	
LT36	Ras Mohammed	Ras Mohammed Camp			matrix	
LT36	Ras Mohammed	Ras Mohammed Camp			*Goniastrea retiformis*	
LT36	Ras Mohammed	Ras Mohammed Camp			*Goniastrea retiformis*	
LT36	Ras Mohammed	Ras Mohammed Camp			*Goniastrea retiformis*	
LT36	Ras Mohammed	Ras Mohammed Camp			*Favites flexuosa*	
LT36	Ras Mohammed	Ras Mohammed Camp			red algae	
LT36	Ras Mohammed	Ras Mohammed Camp			*Goniastrea retiformis*	
LT36	Ras Mohammed	Ras Mohammed Camp			*Goniastrea retiformis*	
LT36	Ras Mohammed	Ras Mohammed Camp			*Platygyra sp.*	
LT36	Ras Mohammed	Ras Mohammed Camp			*Acanthastrea echinata*	
LT36	Ras Mohammed	Ras Mohammed Camp			red algae	
LT36	Ras Mohammed	Ras Mohammed Camp			*Goniastrea retiformis*	
LT36	Ras Mohammed	Ras Mohammed Camp			*Goniastrea retiformis*	
LT37	Ras Mohammed	Turtle Bay	WP69		matrix	
LT37	Ras Mohammed	Turtle Bay	WP69		*Dipsastraea sp.*	
LT37	Ras Mohammed	Turtle Bay	WP69		matrix	
LT37	Ras Mohammed	Turtle Bay	WP69		matrix	
LT37	Ras Mohammed	Turtle Bay	WP69		*Porites sp.*	
LT37	Ras Mohammed	Turtle Bay	WP69		*Porites sp.*	
LT37	Ras Mohammed	Turtle Bay	WP69		matrix	
LT37	Ras Mohammed	Turtle Bay	WP69		*Porites sp.*	
LT37	Ras Mohammed	Turtle Bay	WP69		Pectinidae indet.	
LT37	Ras Mohammed	Turtle Bay	WP69		*Porites sp.*	
LT37	Ras Mohammed	Turtle Bay	WP69		matrix	

LT	Locality	Site	GPS	Layer	*Name*	Sample
LT37	Ras Mohammed	Turtle Bay	WP69		*Porites sp.*	
LT37	Ras Mohammed	Turtle Bay	WP69		*Porites sp.*	
LT37	Ras Mohammed	Turtle Bay	WP69		*Porites sp.*	
LT37	Ras Mohammed	Turtle Bay	WP69		matrix	
LT37	Ras Mohammed	Turtle Bay	WP69		matrix	
LT37	Ras Mohammed	Turtle Bay	WP69		*Porites sp.*	
LT37	Ras Mohammed	Turtle Bay	WP69		*Porites sp.*	
LT37	Ras Mohammed	Turtle Bay	WP69		*Porites sp.*	
LT37	Ras Mohammed	Turtle Bay	WP69		*Porites sp.*	
LT37	Ras Mohammed	Turtle Bay	WP69		*Porites sp.*	
LT37	Ras Mohammed	Turtle Bay	WP69		*Porites sp.*	
LT37	Ras Mohammed	Turtle Bay	WP69		matrix	
LT37	Ras Mohammed	Turtle Bay	WP69		matrix	
LT37	Ras Mohammed	Turtle Bay	WP69		matrix	
LT37	Ras Mohammed	Turtle Bay	WP69		*Porites sp.*	
LT37	Ras Mohammed	Turtle Bay	WP69		*red algae*	
LT37	Ras Mohammed	Turtle Bay	WP69		*Porites sp.*	
LT37	Ras Mohammed	Turtle Bay	WP69		*Porites sp.*	
LT37	Ras Mohammed	Turtle Bay	WP69		matrix	
LT37	Ras Mohammed	Turtle Bay	WP69		*Porites sp.*	
LT37	Ras Mohammed	Turtle Bay	WP69		*Porites sp.*	
LT37	Ras Mohammed	Turtle Bay	WP69		*Porites sp.*	
LT37	Ras Mohammed	Turtle Bay	WP69		*Cyphastrea sp.*	
LT37	Ras Mohammed	Turtle Bay	WP69		*Goniastrea sp.*	
LT37	Ras Mohammed	Turtle Bay	WP69		*Porites sp.*	
LT37	Ras Mohammed	Turtle Bay	WP69		matrix	
LT37	Ras Mohammed	Turtle Bay	WP69		*Porites sp.*	
LT37	Ras Mohammed	Turtle Bay	WP69		*Porites sp.*	
LT37	Ras Mohammed	Turtle Bay	WP69		*Porites sp.*	
LT38	Ras Mohammed	Turtle Bay			*Pocillopora verrucosa*	LT38a
LT38	Ras Mohammed	Turtle Bay			*Pocillopora verrucosa*	
LT38	Ras Mohammed	Turtle Bay			matrix	
LT38	Ras Mohammed	Turtle Bay			matrix	
LT38	Ras Mohammed	Turtle Bay			matrix	
LT38	Ras Mohammed	Turtle Bay			*Porites sp.*	
LT38	Ras Mohammed	Turtle Bay			matrix	
LT38	Ras Mohammed	Turtle Bay			matrix	
LT38	Ras Mohammed	Turtle Bay			matrix	
LT38	Ras Mohammed	Turtle Bay			matrix	
LT38	Ras Mohammed	Turtle Bay			*Millepora sp.*	
LT38	Ras Mohammed	Turtle Bay			*Porites sp.*	
LT38	Ras Mohammed	Turtle Bay			*Millepora sp.*	
LT38	Ras Mohammed	Turtle Bay			*Millepora sp.*	
LT38	Ras Mohammed	Turtle Bay			*Porites sp.*	LT38b
LT38	Ras Mohammed	Turtle Bay			*Millepora sp.*	
LT38	Ras Mohammed	Turtle Bay			*Acropora sp.*	

LT	Locality	Site	GPS	Layer	*Name*	Sample
LT38	Ras Mohammed	Turtle Bay			*Acropora sp.*	
LT38	Ras Mohammed	Turtle Bay			*Porites sp.*	
LT38	Ras Mohammed	Turtle Bay			*Acropora sp.*	
LT38	Ras Mohammed	Turtle Bay			Scleractinia indet.	
LT38	Ras Mohammed	Turtle Bay			*Acropora sp.*	
LT38	Ras Mohammed	Turtle Bay			*Porites sp.*	
LT38	Ras Mohammed	Turtle Bay			*Porites sp.*	
LT38	Ras Mohammed	Turtle Bay			*Gastropod*	
LT38	Ras Mohammed	Turtle Bay			*Porites sp.*	
LT38	Ras Mohammed	Turtle Bay			*Montipora sp.*	LT38c
LT38	Ras Mohammed	Turtle Bay			*Montipora sp.*	
LT38	Ras Mohammed	Turtle Bay			*Montipora sp.*	
LT38	Ras Mohammed	Turtle Bay			*Montipora sp.*	
LT38	Ras Mohammed	Turtle Bay			matrix	
LT38	Ras Mohammed	Turtle Bay			*Acropora sp.*	
LT38	Ras Mohammed	Turtle Bay			*Acropora sp.*	
LT39	Ras Mohammed	Ras Mohammed Camp	WP70		*Echinopora forskaliana*	
LT39	Ras Mohammed	Ras Mohammed Camp	WP70		*Echinopora forskaliana*	
LT39	Ras Mohammed	Ras Mohammed Camp	WP70		*Echinopora forskaliana*	
LT39	Ras Mohammed	Ras Mohammed Camp	WP70		red algae	
LT39	Ras Mohammed	Ras Mohammed Camp	WP70		*Echinopora forskaliana*	
LT39	Ras Mohammed	Ras Mohammed Camp	WP70		*Echinopora forskaliana*	
LT39	Ras Mohammed	Ras Mohammed Camp	WP70		*Echinopora forskaliana*	
LT39	Ras Mohammed	Ras Mohammed Camp	WP70		*Favites sp.*	
LT39	Ras Mohammed	Ras Mohammed Camp	WP70		*Favites sp.*	
LT39	Ras Mohammed	Ras Mohammed Camp	WP70		*Favites sp.*	
LT39	Ras Mohammed	Ras Mohammed Camp	WP70		*Dipsastraea pallida*	
LT39	Ras Mohammed	Ras Mohammed Camp	WP70		*Dipsastraea pallida*	
LT39	Ras Mohammed	Ras Mohammed Camp	WP70		*Dipsastraea pallida*	
LT39	Ras Mohammed	Ras Mohammed Camp	WP70		*Dipsastraea pallida*	
LT39	Ras Mohammed	Ras Mohammed Camp	WP70		*Favites flexuosa*	
LT39	Ras Mohammed	Ras Mohammed Camp	WP70		*Favites flexuosa*	
LT39	Ras Mohammed	Ras Mohammed Camp	WP70		*Favites flexuosa*	
LT39	Ras Mohammed	Ras Mohammed Camp	WP70		*Favites flexuosa*	
LT39	Ras Mohammed	Ras Mohammed Camp	WP70		matrix	
LT39	Ras Mohammed	Ras Mohammed Camp	WP70		matrix	
LT39	Ras Mohammed	Ras Mohammed Camp	WP70		matrix	
LT39	Ras Mohammed	Ras Mohammed Camp	WP70		*Goniastrea retiformis*	
LT39	Ras Mohammed	Ras Mohammed Camp	WP70		*Goniastrea retiformis*	
LT39	Ras Mohammed	Ras Mohammed Camp	WP70		*Goniastrea retiformis*	
LT39	Ras Mohammed	Ras Mohammed Camp	WP70		*Goniastrea retiformis*	
LT39	Ras Mohammed	Ras Mohammed Camp	WP70		*Goniastrea retiformis*	
LT39	Ras Mohammed	Ras Mohammed Camp	WP70		*Goniastrea retiformis*	
LT39	Ras Mohammed	Ras Mohammed Camp	WP70		matrix	
LT39	Ras Mohammed	Ras Mohammed Camp	WP70		red algae	
LT39	Ras Mohammed	Ras Mohammed Camp	WP70		*Goniastrea retiformis*	

LT	Locality	Site	GPS	Layer	*Name*	Sample
LT39	Ras Mohammed	Ras Mohammed Camp	WP70		*Goniastrea retiformis*	
LT39	Ras Mohammed	Ras Mohammed Camp	WP70		*Goniastrea retiformis*	
LT39	Ras Mohammed	Ras Mohammed Camp	WP70		*Goniastrea retiformis*	
LT39	Ras Mohammed	Ras Mohammed Camp	WP70		red algae	
LT39	Ras Mohammed	Ras Mohammed Camp	WP70		red algae	
LT39	Ras Mohammed	Ras Mohammed Camp	WP70		red algae	
LT39	Ras Mohammed	Ras Mohammed Camp	WP70		red algae	
LT39	Ras Mohammed	Ras Mohammed Camp	WP70		*Goniastrea retiformis*	
LT39	Ras Mohammed	Ras Mohammed Camp	WP70		red algae	
LT39	Ras Mohammed	Ras Mohammed Camp	WP70		red algae	
LT39	Ras Mohammed	Ras Mohammed Camp	WP70		*Dipsastraea sp.*	
LT39	Ras Mohammed	Ras Mohammed Camp	WP70		red algae	
LT39	Ras Mohammed	Ras Mohammed Camp	WP70		red algae	
LT39	Ras Mohammed	Ras Mohammed Camp	WP70		red algae	
LT39	Ras Mohammed	Ras Mohammed Camp	WP70		red algae	
LT39	Ras Mohammed	Ras Mohammed Camp	WP70		red algae	
LT39	Ras Mohammed	Ras Mohammed Camp	WP70		*Platygyra lamellina*	
LT39	Ras Mohammed	Ras Mohammed Camp	WP70		*Echinopora forskaliana*	
LT39	Ras Mohammed	Ras Mohammed Camp	WP70		*Platygyra lamellina*	
LT39	Ras Mohammed	Ras Mohammed Camp	WP70		*Echinopora forskaliana*	
LT39	Ras Mohammed	Ras Mohammed Camp	WP70		*Goniastrea retiformis*	
LT39	Ras Mohammed	Ras Mohammed Camp	WP70		*Goniastrea retiformis*	
LT39	Ras Mohammed	Ras Mohammed Camp	WP70		red algae	
LT39	Ras Mohammed	Ras Mohammed Camp	WP70		red algae	
LT39	Ras Mohammed	Ras Mohammed Camp	WP70		*Goniastrea retiformis*	
LT39	Ras Mohammed	Ras Mohammed Camp	WP70		Faviidae indet.	
LT39	Ras Mohammed	Ras Mohammed Camp	WP70		matrix	
LT39	Ras Mohammed	Ras Mohammed Camp	WP70		red algae	
LT39	Ras Mohammed	Ras Mohammed Camp	WP70		red algae	
LT39	Ras Mohammed	Ras Mohammed Camp	WP70		matrix	
LT39	Ras Mohammed	Ras Mohammed Camp	WP70		matrix	
LT39	Ras Mohammed	Ras Mohammed Camp	WP70		*Goniastrea retiformis*	
LT39	Ras Mohammed	Ras Mohammed Camp	WP70		red algae	
LT39	Ras Mohammed	Ras Mohammed Camp	WP70		matrix	
LT39	Ras Mohammed	Ras Mohammed Camp	WP70		*Dipsastraea sp.*	
LT39	Ras Mohammed	Ras Mohammed Camp	WP70		matrix	
LT39	Ras Mohammed	Ras Mohammed Camp	WP70		*Lobophyllia corymbosa*	
LT39	Ras Mohammed	Ras Mohammed Camp	WP70		*Lobophyllia corymbosa*	
LT39	Ras Mohammed	Ras Mohammed Camp	WP70		*Lobophyllia corymbosa*	
LT39	Ras Mohammed	Ras Mohammed Camp	WP70		*Lobophyllia corymbosa*	
LT39	Ras Mohammed	Ras Mohammed Camp	WP70		*Lobophyllia corymbosa*	
LT39	Ras Mohammed	Ras Mohammed Camp	WP70		*Lobophyllia corymbosa*	
LT40	Ras Mohammed	Turtle Bay			*Dipsastraea sp.*	
LT40	Ras Mohammed	Turtle Bay			red algae	
LT40	Ras Mohammed	Turtle Bay			*Porites sp.*	
LT40	Ras Mohammed	Turtle Bay			red algae	

LT	Locality	Site	GPS	Layer	*Name*	Sample
LT40	Ras Mohammed	Turtle Bay			*Porites sp.*	
LT40	Ras Mohammed	Turtle Bay			*Porites sp.*	
LT40	Ras Mohammed	Turtle Bay			*Porites sp.*	
LT40	Ras Mohammed	Turtle Bay			*Porites sp.*	
LT40	Ras Mohammed	Turtle Bay			*Porites sp.*	
LT40	Ras Mohammed	Turtle Bay			Faviidae indet.	
LT40	Ras Mohammed	Turtle Bay			red algae	
LT40	Ras Mohammed	Turtle Bay			*Porites sp.*	
LT40	Ras Mohammed	Turtle Bay			matrix	
LT40	Ras Mohammed	Turtle Bay			matrix	
LT40	Ras Mohammed	Turtle Bay			matrix	
LT40	Ras Mohammed	Turtle Bay			red algae	
LT40	Ras Mohammed	Turtle Bay			*Porites sp.*	LT40a
LT40	Ras Mohammed	Turtle Bay			*Porites sp.*	
LT40	Ras Mohammed	Turtle Bay			*Porites sp.*	
LT40	Ras Mohammed	Turtle Bay			*Porites sp.*	
LT40	Ras Mohammed	Turtle Bay			*Porites sp.*	
LT40	Ras Mohammed	Turtle Bay			red algae	
LT40	Ras Mohammed	Turtle Bay			*Porites sp.*	
LT40	Ras Mohammed	Turtle Bay			Faviidae indet.	
LT40	Ras Mohammed	Turtle Bay			matrix	
LT40	Ras Mohammed	Turtle Bay			*Porites sp.*	
LT40	Ras Mohammed	Turtle Bay			*Porites sp.*	
LT40	Ras Mohammed	Turtle Bay			*Gyrosmilia interrupta*	LT40d
LT40	Ras Mohammed	Turtle Bay			*Gyrosmilia interrupta*	
LT40	Ras Mohammed	Turtle Bay			*Gyrosmilia interrupta*	
LT40	Ras Mohammed	Turtle Bay			*Gyrosmilia interrupta*	
LT40	Ras Mohammed	Turtle Bay			*Gyrosmilia interrupta*	
LT40	Ras Mohammed	Turtle Bay			matrix	
LT40	Ras Mohammed	Turtle Bay			red algae	
LT40	Ras Mohammed	Turtle Bay			*Porites sp.*	LT40b
LT40	Ras Mohammed	Turtle Bay			*Porites sp.*	
LT40	Ras Mohammed	Turtle Bay			*Porites sp.*	
LT40	Ras Mohammed	Turtle Bay			*Porites sp.*	
LT40	Ras Mohammed	Turtle Bay			*Porites sp.*	
LT40	Ras Mohammed	Turtle Bay			*Porites sp.*	
LT40	Ras Mohammed	Turtle Bay			*Porites sp.*	
LT40	Ras Mohammed	Turtle Bay			matrix	
LT40	Ras Mohammed	Turtle Bay			*Porites sp.*	
LT40	Ras Mohammed	Turtle Bay			*Porites sp.*	
LT40	Ras Mohammed	Turtle Bay			*Porites sp.*	
LT40	Ras Mohammed	Turtle Bay			*Porites sp.*	
LT40	Ras Mohammed	Turtle Bay			*Porites sp.*	
LT40	Ras Mohammed	Turtle Bay			*Porites sp.*	
LT40	Ras Mohammed	Turtle Bay			*Porites sp.*	

LT	Locality	Site	GPS	Layer	*Name*	Sample
LT40	Ras Mohammed	Turtle Bay			matrix	
LT40	Ras Mohammed	Turtle Bay			*Favites spinosa*	
LT40	Ras Mohammed	Turtle Bay			matrix	
LT40	Ras Mohammed	Turtle Bay			*Galaxea fascicularis*	
LT40	Ras Mohammed	Turtle Bay			*Porites sp.*	LT40c
LT40	Ras Mohammed	Turtle Bay			*Porites sp.*	
LT40	Ras Mohammed	Turtle Bay			*Porites sp.*	
LT40	Ras Mohammed	Turtle Bay			*Porites sp.*	
LT40	Ras Mohammed	Turtle Bay			*Porites sp.*	
LT40	Ras Mohammed	Turtle Bay			*Porites sp.*	
LT40	Ras Mohammed	Turtle Bay			*Porites sp.*	
LT40	Ras Mohammed	Turtle Bay			*Porites sp.*	
LT40	Ras Mohammed	Turtle Bay			*Porites sp.*	
LT40	Ras Mohammed	Turtle Bay			*Porites sp.*	
LT40	Ras Mohammed	Turtle Bay			*Porites sp.*	
LT40	Ras Mohammed	Turtle Bay			*Porites sp.*	
LT40	Ras Mohammed	Turtle Bay			matrix	
LT40	Ras Mohammed	Turtle Bay			*Favites sp.*	
LT40	Ras Mohammed	Turtle Bay			*Stylophora sp.*	
LT40	Ras Mohammed	Turtle Bay			matrix	
LT40	Ras Mohammed	Turtle Bay			matrix	
LT40	Ras Mohammed	Turtle Bay			*Dipsastraea sp.*	
LT40	Ras Mohammed	Turtle Bay			*Dipsastraea sp.*	
LT40	Ras Mohammed	Turtle Bay			*Dipsastraea sp.*	
LT40	Ras Mohammed	Turtle Bay			matrix	
LT40	Ras Mohammed	Turtle Bay			*Dipsastraea sp.*	
LT40	Ras Mohammed	Turtle Bay			*Dipsastraea sp.*	
LT41	Ras Mohammed	Turtle Bay			matrix	
LT41	Ras Mohammed	Turtle Bay			*Porites sp.*	
LT41	Ras Mohammed	Turtle Bay			matrix	
LT41	Ras Mohammed	Turtle Bay			matrix	
LT41	Ras Mohammed	Turtle Bay			*Porites sp.*	
LT41	Ras Mohammed	Turtle Bay			*Porites sp.*	
LT41	Ras Mohammed	Turtle Bay			*Porites sp.*	
LT41	Ras Mohammed	Turtle Bay			*matrix*	
LT41	Ras Mohammed	Turtle Bay			*matrix*	
LT41	Ras Mohammed	Turtle Bay			*Porites sp.*	
LT41	Ras Mohammed	Turtle Bay			matrix	
LT41	Ras Mohammed	Turtle Bay			red algae	
LT41	Ras Mohammed	Turtle Bay			matrix	
LT41	Ras Mohammed	Turtle Bay			*Porites sp.*	
LT41	Ras Mohammed	Turtle Bay			*Porites sp.*	
LT41	Ras Mohammed	Turtle Bay			*Goniopora sp.*	LT41a
LT41	Ras Mohammed	Turtle Bay			*Porites sp.*	
LT41	Ras Mohammed	Turtle Bay			*Porites sp.*	
LT41	Ras Mohammed	Turtle Bay			*Porites sp.*	
LT41	Ras Mohammed	Turtle Bay			*Porites sp.*	

LT	Locality	Site	GPS	Layer	*Name*	Sample
LT41	Ras Mohammed	Turtle Bay			red algae	
LT41	Ras Mohammed	Turtle Bay			red algae	
LT41	Ras Mohammed	Turtle Bay			red algae	
LT41	Ras Mohammed	Turtle Bay			red algae	
LT41	Ras Mohammed	Turtle Bay			*Porites nodifera*	
LT41	Ras Mohammed	Turtle Bay			*Porites nodifera*	
LT41	Ras Mohammed	Turtle Bay			*Porites nodifera*	
LT41	Ras Mohammed	Turtle Bay			red algae	
LT41	Ras Mohammed	Turtle Bay			red algae	
LT41	Ras Mohammed	Turtle Bay			red algae	
LT41	Ras Mohammed	Turtle Bay			*Gyrosmilia interrupta*	
LT41	Ras Mohammed	Turtle Bay			*Gyrosmilia interrupta*	
LT41	Ras Mohammed	Turtle Bay			*Dipsastraea sp.*	
LT41	Ras Mohammed	Turtle Bay			*Dipsastraea sp.*	
LT41	Ras Mohammed	Turtle Bay			red algae	
LT41	Ras Mohammed	Turtle Bay			*Dipsastraea pallida*	
LT41	Ras Mohammed	Turtle Bay			*Dipsastraea pallida*	
LT41	Ras Mohammed	Turtle Bay			red algae	
LT41	Ras Mohammed	Turtle Bay			red algae	
LT41	Ras Mohammed	Turtle Bay			red algae	
LT41	Ras Mohammed	Turtle Bay			Pectinidae indet.	LT41b
LT41	Ras Mohammed	Turtle Bay			red algae	
LT41	Ras Mohammed	Turtle Bay			*Porites sp.*	
LT41	Ras Mohammed	Turtle Bay			*Porites sp.*	
LT41	Ras Mohammed	Turtle Bay			matrix	
LT41	Ras Mohammed	Turtle Bay			matrix	
LT41	Ras Mohammed	Turtle Bay			matrix	
LT41	Ras Mohammed	Turtle Bay			*Porites sp.*	
LT41	Ras Mohammed	Turtle Bay			*Porites sp.*	
LT41	Ras Mohammed	Turtle Bay			*Porites sp.*	
LT41	Ras Mohammed	Turtle Bay			matrix	
LT41	Ras Mohammed	Turtle Bay			*Porites sp.*	
LT41	Ras Mohammed	Turtle Bay			red algae	
LT41	Ras Mohammed	Turtle Bay			red algae	
LT41	Ras Mohammed	Turtle Bay			matrix	
LT41	Ras Mohammed	Turtle Bay			red algae	
LT41	Ras Mohammed	Turtle Bay			red algae	
LT41	Ras Mohammed	Turtle Bay			*Fungia sp.*	
LT41	Ras Mohammed	Turtle Bay			*Goniastrea sp.*	
LT41	Ras Mohammed	Turtle Bay			*Porites sp.*	
LT41	Ras Mohammed	Turtle Bay			*Porites sp.*	
LT41	Ras Mohammed	Turtle Bay			*Porites sp.*	
LT41	Ras Mohammed	Turtle Bay			*Porites sp.*	
LT41	Ras Mohammed	Turtle Bay			*Porites sp.*	
LT41	Ras Mohammed	Turtle Bay			matrix	
LT41	Ras Mohammed	Turtle Bay			matrix	

LT	Locality	Site	GPS	Layer	*Name*	Sample
LT41	Ras Mohammed	Turtle Bay			matrix	
LT41	Ras Mohammed	Turtle Bay			*Cyphastrea sp.*	
LT41	Ras Mohammed	Turtle Bay			red algae	
LT41	Ras Mohammed	Turtle Bay			*Echinopora forskaliana*	
LT41	Ras Mohammed	Turtle Bay			*Echinopora forskaliana*	
LT41	Ras Mohammed	Turtle Bay			*Echinopora forskaliana*	
LT41	Ras Mohammed	Turtle Bay			*Echinopora forskaliana*	
LT41	Ras Mohammed	Turtle Bay			*Dipsastraea sp.*	
LT41	Ras Mohammed	Turtle Bay			*Dipsastraea sp.*	
LT41	Ras Mohammed	Turtle Bay			red algae	
LT42	Ras Mohammed	Turtle Bay			*Dipsastraea sp.*	
LT42	Ras Mohammed	Turtle Bay			matrix	
LT42	Ras Mohammed	Turtle Bay			*Porites sp.*	
LT42	Ras Mohammed	Turtle Bay			matrix	
LT42	Ras Mohammed	Turtle Bay			matrix	
LT42	Ras Mohammed	Turtle Bay			matrix	
LT42	Ras Mohammed	Turtle Bay			*Porites sp.*	
LT42	Ras Mohammed	Turtle Bay			*Porites sp.*	
LT42	Ras Mohammed	Turtle Bay			*Echinopora forskaliana*	
LT42	Ras Mohammed	Turtle Bay			*Echinopora forskaliana*	LT42a
LT42	Ras Mohammed	Turtle Bay			*Porites lobata/lutea*	
LT42	Ras Mohammed	Turtle Bay			matrix	
LT42	Ras Mohammed	Turtle Bay			*Acropora sp.*	
LT42	Ras Mohammed	Turtle Bay			*Acropora sp.*	
LT42	Ras Mohammed	Turtle Bay			red algae	
LT42	Ras Mohammed	Turtle Bay			*Porites sp.*	
LT42	Ras Mohammed	Turtle Bay			*Porites sp.*	
LT42	Ras Mohammed	Turtle Bay			*Porites sp.*	
LT42	Ras Mohammed	Turtle Bay			*Porites sp.*	
LT42	Ras Mohammed	Turtle Bay			*Porites sp.*	
LT42	Ras Mohammed	Turtle Bay			*Porites sp.*	
LT42	Ras Mohammed	Turtle Bay			*Gyrosmilia interrupta*	
LT42	Ras Mohammed	Turtle Bay			red algae	
LT42	Ras Mohammed	Turtle Bay			red algae	
LT42	Ras Mohammed	Turtle Bay			*Porites sp.*	
LT42	Ras Mohammed	Turtle Bay			*Porites sp.*	
LT42	Ras Mohammed	Turtle Bay			matrix	
LT42	Ras Mohammed	Turtle Bay			*Porites sp.*	
LT42	Ras Mohammed	Turtle Bay			*Porites sp.*	
LT42	Ras Mohammed	Turtle Bay			*Porites sp.*	
LT42	Ras Mohammed	Turtle Bay			matrix	
LT42	Ras Mohammed	Turtle Bay			matrix	
LT42	Ras Mohammed	Turtle Bay			matrix	
LT42	Ras Mohammed	Turtle Bay			matrix	
LT42	Ras Mohammed	Turtle Bay			matrix	
LT42	Ras Mohammed	Turtle Bay			matrix	

LT	Locality	Site	GPS	Layer	*Name*	Sample
LT42	Ras Mohammed	Turtle Bay			matrix	
LT42	Ras Mohammed	Turtle Bay			matrix	
LT42	Ras Mohammed	Turtle Bay			matrix	
LT42	Ras Mohammed	Turtle Bay			matrix	
LT42	Ras Mohammed	Turtle Bay			*Fungia sp.*	
LT42	Ras Mohammed	Turtle Bay			matrix	
LT42	Ras Mohammed	Turtle Bay			matrix	
LT42	Ras Mohammed	Turtle Bay			*Porites sp.*	
LT42	Ras Mohammed	Turtle Bay			*Goniastrea edwardsi*	
LT42	Ras Mohammed	Turtle Bay			*Goniastrea edwardsi*	
LT42	Ras Mohammed	Turtle Bay			matrix	
LT42	Ras Mohammed	Turtle Bay			matrix	
LT42	Ras Mohammed	Turtle Bay			matrix	
LT42	Ras Mohammed	Turtle Bay			matrix	
LT42	Ras Mohammed	Turtle Bay			*Acropora sp.*	
LT42	Ras Mohammed	Turtle Bay			matrix	
LT42	Ras Mohammed	Turtle Bay			matrix	
LT42	Ras Mohammed	Turtle Bay			matrix	
LT42	Ras Mohammed	Turtle Bay			matrix	
LT42	Ras Mohammed	Turtle Bay			matrix	
LT42	Ras Mohammed	Turtle Bay			matrix	
LT42	Ras Mohammed	Turtle Bay			matrix	
LT42	Ras Mohammed	Turtle Bay			*Porites sp.*	
LT42	Ras Mohammed	Turtle Bay			matrix	
LT42	Ras Mohammed	Turtle Bay			red algae	
LT43	Ras Mohammed	Turtle Bay			*Porites sp.*	
LT43	Ras Mohammed	Turtle Bay			matrix	
LT43	Ras Mohammed	Turtle Bay			red algae	
LT43	Ras Mohammed	Turtle Bay			*Porites sp.*	
LT43	Ras Mohammed	Turtle Bay			matrix	
LT43	Ras Mohammed	Turtle Bay			matrix	
LT43	Ras Mohammed	Turtle Bay			matrix	
LT43	Ras Mohammed	Turtle Bay			*Dipsastraea sp.*	
LT43	Ras Mohammed	Turtle Bay			*Dipsastraea sp.*	
LT43	Ras Mohammed	Turtle Bay			*Dipsastraea sp.*	
LT43	Ras Mohammed	Turtle Bay			*Porites sp.*	
LT43	Ras Mohammed	Turtle Bay			*Montipora sp.*	
LT43	Ras Mohammed	Turtle Bay			*Montipora sp.*	
LT43	Ras Mohammed	Turtle Bay			*Montipora sp.*	
LT43	Ras Mohammed	Turtle Bay			*Montipora sp.*	
LT43	Ras Mohammed	Turtle Bay			matrix	
LT43	Ras Mohammed	Turtle Bay			matrix	
LT43	Ras Mohammed	Turtle Bay			matrix	
LT43	Ras Mohammed	Turtle Bay			matrix	
LT43	Ras Mohammed	Turtle Bay			red algae	
LT43	Ras Mohammed	Turtle Bay			red algae	

LT	Locality	Site	GPS	Layer	*Name*	Sample
LT43	Ras Mohammed	Turtle Bay			red algae	
LT43	Ras Mohammed	Turtle Bay			*Porites sp.*	
LT43	Ras Mohammed	Turtle Bay			*Porites sp.*	
LT43	Ras Mohammed	Turtle Bay			*Porites sp.*	
LT43	Ras Mohammed	Turtle Bay			red algae	
LT43	Ras Mohammed	Turtle Bay			red algae	
LT43	Ras Mohammed	Turtle Bay			red algae	
LT43	Ras Mohammed	Turtle Bay			*Dipsastraea sp.*	
LT43	Ras Mohammed	Turtle Bay			*Dipsastraea sp.*	
LT43	Ras Mohammed	Turtle Bay			matrix	
LT43	Ras Mohammed	Turtle Bay			matrix	
LT43	Ras Mohammed	Turtle Bay			matrix	
LT43	Ras Mohammed	Turtle Bay			matrix	
LT43	Ras Mohammed	Turtle Bay			*Porites sp.*	
LT44	Ras Mohammed	Turtle Bay			*Porites sp.*	LT44a
LT44	Ras Mohammed	Turtle Bay			matrix	
LT44	Ras Mohammed	Turtle Bay			matrix	
LT44	Ras Mohammed	Turtle Bay			matrix	
LT44	Ras Mohammed	Turtle Bay			matrix	
LT44	Ras Mohammed	Turtle Bay			matrix	
LT44	Ras Mohammed	Turtle Bay			matrix	
LT44	Ras Mohammed	Turtle Bay			*Millepora sp.*	LT44b
LT44	Ras Mohammed	Turtle Bay			*Millepora sp.*	
LT44	Ras Mohammed	Turtle Bay			matrix	
LT44	Ras Mohammed	Turtle Bay			*Millepora sp.*	
LT44	Ras Mohammed	Turtle Bay			matrix	
LT44	Ras Mohammed	Turtle Bay			matrix	
LT44	Ras Mohammed	Turtle Bay			matrix	
LT44	Ras Mohammed	Turtle Bay			matrix	
LT44	Ras Mohammed	Turtle Bay			matrix	
LT44	Ras Mohammed	Turtle Bay			matrix	
LT44	Ras Mohammed	Turtle Bay			Tridacna sp.	
LT44	Ras Mohammed	Turtle Bay			matrix	
LT44	Ras Mohammed	Turtle Bay			matrix	
LT44	Ras Mohammed	Turtle Bay			*Porites lobata/lutea*	
LT44	Ras Mohammed	Turtle Bay			*Porites lobata/lutea*	
LT44	Ras Mohammed	Turtle Bay			*Porites lobata/lutea*	
LT44	Ras Mohammed	Turtle Bay			*Porites lobata/lutea*	
LT44	Ras Mohammed	Turtle Bay			*Porites lobata/lutea*	
LT44	Ras Mohammed	Turtle Bay			matrix	
LT44	Ras Mohammed	Turtle Bay			*Coscinaraea monile*	
LT44	Ras Mohammed	Turtle Bay			matrix	
LT44	Ras Mohammed	Turtle Bay			*Porites sp.*	
LT44	Ras Mohammed	Turtle Bay			matrix	
LT44	Ras Mohammed	Turtle Bay			*Millepora sp.*	
LT44	Ras Mohammed	Turtle Bay			matrix	

LT	Locality	Site	GPS	Layer	*Name*	Sample
LT44	Ras Mohammed	Turtle Bay			matrix	
LT44	Ras Mohammed	Turtle Bay			red algae	
LT45	Ras Mohammed	Turtle Bay			*Porites sp.*	
LT45	Ras Mohammed	Turtle Bay			*Porites sp.*	
LT45	Ras Mohammed	Turtle Bay			*Echinopora forskaliana*	
LT45	Ras Mohammed	Turtle Bay			matrix	
LT45	Ras Mohammed	Turtle Bay			*Porites sp.*	
LT45	Ras Mohammed	Turtle Bay			matrix	
LT45	Ras Mohammed	Turtle Bay			*Porites sp.*	
LT45	Ras Mohammed	Turtle Bay			matrix	
LT45	Ras Mohammed	Turtle Bay			*Porites sp.*	
LT45	Ras Mohammed	Turtle Bay			*Porites sp.*	
LT45	Ras Mohammed	Turtle Bay			*Porites sp.*	
LT45	Ras Mohammed	Turtle Bay			*Porites sp.*	
LT45	Ras Mohammed	Turtle Bay			Faviidae indet.	
LT45	Ras Mohammed	Turtle Bay			*Porites sp.*	
LT45	Ras Mohammed	Turtle Bay			*Porites sp.*	
LT45	Ras Mohammed	Turtle Bay			matrix	
LT45	Ras Mohammed	Turtle Bay			red algae	
LT45	Ras Mohammed	Turtle Bay			matrix	
LT45	Ras Mohammed	Turtle Bay			red algae	
LT45	Ras Mohammed	Turtle Bay			*Porites sp.*	
LT45	Ras Mohammed	Turtle Bay			*Porites sp.*	
LT45	Ras Mohammed	Turtle Bay			matrix	
LT45	Ras Mohammed	Turtle Bay			matrix	
LT45	Ras Mohammed	Turtle Bay			*Echinopora forskaliana*	
LT45	Ras Mohammed	Turtle Bay			*Porites sp.*	
LT45	Ras Mohammed	Turtle Bay			matrix	
LT45	Ras Mohammed	Turtle Bay			matrix	
LT45	Ras Mohammed	Turtle Bay			matrix	
LT45	Ras Mohammed	Turtle Bay			matrix	
LT45	Ras Mohammed	Turtle Bay			matrix	
LT45	Ras Mohammed	Turtle Bay			*Porites sp.*	
LT45	Ras Mohammed	Turtle Bay			*Porites sp.*	
LT45	Ras Mohammed	Turtle Bay			*Dipsastraea sp.*	
LT45	Ras Mohammed	Turtle Bay			red algae	
LT45	Ras Mohammed	Turtle Bay			matrix	
LT45	Ras Mohammed	Turtle Bay			red algae	
LT45	Ras Mohammed	Turtle Bay			*Porites sp.*	
LT45	Ras Mohammed	Turtle Bay			red algae	
LT45	Ras Mohammed	Turtle Bay			matrix	
LT45	Ras Mohammed	Turtle Bay			*Dipsastraea sp.*	
LT45	Ras Mohammed	Turtle Bay			*Dipsastraea sp.*	
LT45	Ras Mohammed	Turtle Bay			matrix	
LT45	Ras Mohammed	Turtle Bay			matrix	
LT45	Ras Mohammed	Turtle Bay			*Porites sp.*	

LT	Locality	Site	GPS	Layer	*Name*	Sample
LT45	Ras Mohammed	Turtle Bay			matrix	
LT45	Ras Mohammed	Turtle Bay			*Cyphastrea sp.*	LT45a
LT45	Ras Mohammed	Turtle Bay			matrix	
LT45	Ras Mohammed	Turtle Bay			*Stylophora sp.*	
LT45	Ras Mohammed	Turtle Bay			red algae	
LT45	Ras Mohammed	Turtle Bay			*Porites sp.*	
LT45	Ras Mohammed	Turtle Bay			red algae	
LT45	Ras Mohammed	Turtle Bay			red algae	
LT45	Ras Mohammed	Turtle Bay			*Dipsastraea sp.*	
LT45	Ras Mohammed	Turtle Bay			*Acropora sp.*	
LT45	Ras Mohammed	Turtle Bay			matrix	
LT45	Ras Mohammed	Turtle Bay			red algae	
LT45	Ras Mohammed	Turtle Bay			matrix	
LT45	Ras Mohammed	Turtle Bay			matrix	
LT45	Ras Mohammed	Turtle Bay			matrix	
LT45	Ras Mohammed	Turtle Bay			red algae	
LT46	Ras Mohammed	Ras Ghozlani-inland	WP78		*Porites sp.*	
LT46	Ras Mohammed	Ras Ghozlani-inland	WP78		*Porites sp.*	
LT46	Ras Mohammed	Ras Ghozlani-inland	WP78		*Porites sp.*	
LT46	Ras Mohammed	Ras Ghozlani-inland	WP78		red algae	
LT46	Ras Mohammed	Ras Ghozlani-inland	WP78		red algae	
LT46	Ras Mohammed	Ras Ghozlani-inland	WP78		red algae	
LT46	Ras Mohammed	Ras Ghozlani-inland	WP78		gap	
LT46	Ras Mohammed	Ras Ghozlani-inland	WP78		*Porites sp.*	
LT46	Ras Mohammed	Ras Ghozlani-inland	WP78		*Porites sp.*	LT46a
LT46	Ras Mohammed	Ras Ghozlani-inland	WP78		matrix	LT46b
LT46	Ras Mohammed	Ras Ghozlani-inland	WP78		matrix	
LT46	Ras Mohammed	Ras Ghozlani-inland	WP78		matrix	
LT46	Ras Mohammed	Ras Ghozlani-inland	WP78		matrix	
LT46	Ras Mohammed	Ras Ghozlani-inland	WP78		matrix	
LT46	Ras Mohammed	Ras Ghozlani-inland	WP78		matrix	
LT46	Ras Mohammed	Ras Ghozlani-inland	WP78		matrix	
LT46	Ras Mohammed	Ras Ghozlani-inland	WP78		matrix	
LT46	Ras Mohammed	Ras Ghozlani-inland	WP78		matrix	
LT46	Ras Mohammed	Ras Ghozlani-inland	WP78		matrix	
LT46	Ras Mohammed	Ras Ghozlani-inland	WP78		matrix	
LT46	Ras Mohammed	Ras Ghozlani-inland	WP78		matrix	
LT46	Ras Mohammed	Ras Ghozlani-inland	WP78		matrix	
LT46	Ras Mohammed	Ras Ghozlani-inland	WP78		matrix	
LT46	Ras Mohammed	Ras Ghozlani-inland	WP78		red algae	
LT46	Ras Mohammed	Ras Ghozlani-inland	WP78		red algae	
LT46	Ras Mohammed	Ras Ghozlani-inland	WP78		matrix	
LT46	Ras Mohammed	Ras Ghozlani-inland	WP78		matrix	
LT46	Ras Mohammed	Ras Ghozlani-inland	WP78		matrix	
LT46	Ras Mohammed	Ras Ghozlani-inland	WP78		matrix	

LT	Locality	Site	GPS	Layer	*Name*	Sample
LT46	Ras Mohammed	Ras Ghozlani-inland	WP78		matrix	
LT46	Ras Mohammed	Ras Ghozlani-inland	WP78		matrix	
LT46	Ras Mohammed	Ras Ghozlani-inland	WP78		matrix	
LT46	Ras Mohammed	Ras Ghozlani-inland	WP78		matrix	
LT46	Ras Mohammed	Ras Ghozlani-inland	WP78		matrix	
LT46	Ras Mohammed	Ras Ghozlani-inland	WP78		matrix	
LT46	Ras Mohammed	Ras Ghozlani-inland	WP78		matrix	
LT46	Ras Mohammed	Ras Ghozlani-inland	WP78		debris	
LT46	Ras Mohammed	Ras Ghozlani-inland	WP78		red algae	
LT46	Ras Mohammed	Ras Ghozlani-inland	WP78		red algae	
LT46	Ras Mohammed	Ras Ghozlani-inland	WP78		red algae	
LT46	Ras Mohammed	Ras Ghozlani-inland	WP78		red algae	
LT46	Ras Mohammed	Ras Ghozlani-inland	WP78		red algae	
LT46	Ras Mohammed	Ras Ghozlani-inland	WP78		red algae	
LT46	Ras Mohammed	Ras Ghozlani-inland	WP78		red algae	
LT46	Ras Mohammed	Ras Ghozlani-inland	WP78		red algae	
LT46	Ras Mohammed	Ras Ghozlani-inland	WP78		red algae	
LT46	Ras Mohammed	Ras Ghozlani-inland	WP78		red algae	
LT46	Ras Mohammed	Ras Ghozlani-inland	WP78		*Porites sp.*	
LT46	Ras Mohammed	Ras Ghozlani-inland	WP78		*Porites sp.*	
LT46	Ras Mohammed	Ras Ghozlani-inland	WP78		red algae	
LT46	Ras Mohammed	Ras Ghozlani-inland	WP78		red algae	
LT46	Ras Mohammed	Ras Ghozlani-inland	WP78		red algae	
LT46	Ras Mohammed	Ras Ghozlani-inland	WP78		red algae	
LT46	Ras Mohammed	Ras Ghozlani-inland	WP78		debris	
LT46	Ras Mohammed	Ras Ghozlani-inland	WP78		red algae	
LT46	Ras Mohammed	Ras Ghozlani-inland	WP78		red algae	
LT46	Ras Mohammed	Ras Ghozlani-inland	WP78		red algae	
LT46	Ras Mohammed	Ras Ghozlani-inland	WP78		red algae	
LT46	Ras Mohammed	Ras Ghozlani-inland	WP78		red algae	
LT46	Ras Mohammed	Ras Ghozlani-inland	WP78		matrix	
LT46	Ras Mohammed	Ras Ghozlani-inland	WP78		matrix	
LT46	Ras Mohammed	Ras Ghozlani-inland	WP78		matrix	
LT46	Ras Mohammed	Ras Ghozlani-inland	WP78		matrix	
LT46	Ras Mohammed	Ras Ghozlani-inland	WP78		matrix	
LT46	Ras Mohammed	Ras Ghozlani-inland	WP78		matrix	
LT46	Ras Mohammed	Ras Ghozlani-inland	WP78		debris	
LT46	Ras Mohammed	Ras Ghozlani-inland	WP78		red algae	
LT46	Ras Mohammed	Ras Ghozlani-inland	WP78		debris	
LT46	Ras Mohammed	Ras Ghozlani-inland	WP78		red algae	
LT46	Ras Mohammed	Ras Ghozlani-inland	WP78		debris	
LT46	Ras Mohammed	Ras Ghozlani-inland	WP78		debris	
LT46	Ras Mohammed	Ras Ghozlani-inland	WP78		debris	
LT46	Ras Mohammed	Ras Ghozlani-inland	WP78		debris	
LT46	Ras Mohammed	Ras Ghozlani-inland	WP78		red algae	
LT46	Ras Mohammed	Ras Ghozlani-inland	WP78		red algae	

LT	Locality	Site	GPS	Layer	*Name*	Sample
LT46	Ras Mohammed	Ras Ghozlani-inland	WP78		*Dipsastraea pallida*	
LT46	Ras Mohammed	Ras Ghozlani-inland	WP78		matrix	
LT46	Ras Mohammed	Ras Ghozlani-inland	WP78		matrix	
LT46	Ras Mohammed	Ras Ghozlani-inland	WP78		red algae	
LT46	Ras Mohammed	Ras Ghozlani-inland	WP78		debris

LT	Locality	Site	GPS	Layer	*Name*	Sample
LT46	Ras Mohammed	Ras Ghozlani-inland	WP78		debris	
LT46	Ras Mohammed	Ras Ghozlani-inland	WP78		debris	
LT46	Ras Mohammed	Ras Ghozlani-inland	WP78		debris	
LT46	Ras Mohammed	Ras Ghozlani-inland	WP78		debris	
LT46	Ras Mohammed	Ras Ghozlani-inland	WP78		debris	
LT46	Ras Mohammed	Ras Ghozlani-inland	WP78		debris	
LT46	Ras Mohammed	Ras Ghozlani-inland	WP78		red algae	
LT46	Ras Mohammed	Ras Ghozlani-inland	WP78		*Porites sp.*	
LT46	Ras Mohammed	Ras Ghozlani-inland	WP78		*Porites sp.*	
LT46	Ras Mohammed	Ras Ghozlani-inland	WP78		debris	
LT46	Ras Mohammed	Ras Ghozlani-inland	WP78		debris	
LT46	Ras Mohammed	Ras Ghozlani-inland	WP78		debris	
LT46	Ras Mohammed	Ras Ghozlani-inland	WP78		*Porites sp.*	
LT46	Ras Mohammed	Ras Ghozlani-inland	WP78		*Porites sp.*	
LT46	Ras Mohammed	Ras Ghozlani-inland	WP78		*Porites sp.*	
LT46	Ras Mohammed	Ras Ghozlani-inland	WP78		*Porites sp.*	
LT46	Ras Mohammed	Ras Ghozlani-inland	WP78		*Porites sp.*	
LT46	Ras Mohammed	Ras Ghozlani-inland	WP78		*Porites sp.*	
LT46	Ras Mohammed	Ras Ghozlani-inland	WP78		*Porites sp.*	
LT46	Ras Mohammed	Ras Ghozlani-inland	WP78		*Porites sp.*	
LT46	Ras Mohammed	Ras Ghozlani-inland	WP78		debris	
LT46	Ras Mohammed	Ras Ghozlani-inland	WP78		matrix	
LT46	Ras Mohammed	Ras Ghozlani-inland	WP78		matrix	
LT46	Ras Mohammed	Ras Ghozlani-inland	WP78		debris	
LT46	Ras Mohammed	Ras Ghozlani-inland	WP78		debris	
LT46	Ras Mohammed	Ras Ghozlani-inland	WP78		matrix	
LT46	Ras Mohammed	Ras Ghozlani-inland	WP78		debris	
LT47	Ras Mohammed	Turtle Bay			*Porites sp.*	LT47a
LT47	Ras Mohammed	Turtle Bay			*Porites sp.*	
LT47	Ras Mohammed	Turtle Bay			*Porites sp.*	
LT47	Ras Mohammed	Turtle Bay			matrix	
LT47	Ras Mohammed	Turtle Bay			matrix	
LT47	Ras Mohammed	Turtle Bay			*Porites sp.*	
LT47	Ras Mohammed	Turtle Bay			*Gyrosmilia interrupta*	
LT47	Ras Mohammed	Turtle Bay			*Gyrosmilia interrupta*	
LT47	Ras Mohammed	Turtle Bay			*Dipsastraea pallida*	LT47b
LT47	Ras Mohammed	Turtle Bay			*Dipsastraea pallida*	
LT47	Ras Mohammed	Turtle Bay			red algae	
LT47	Ras Mohammed	Turtle Bay			red algae	
LT47	Ras Mohammed	Turtle Bay			*Dipsastraea pallida*	
LT47	Ras Mohammed	Turtle Bay			red algae	
LT47	Ras Mohammed	Turtle Bay			red algae	
LT47	Ras Mohammed	Turtle Bay			red algae	
LT47	Ras Mohammed	Turtle Bay			matrix	
LT47	Ras Mohammed	Turtle Bay			*Porites sp.*	
LT47	Ras Mohammed	Turtle Bay			*Porites sp.*	LT47c

LT	Locality	Site	GPS	Layer	*Name*	Sample
LT47	Ras Mohammed	Turtle Bay			*Porites sp.*	
LT47	Ras Mohammed	Turtle Bay			matrix	
LT47	Ras Mohammed	Turtle Bay			red algae	
LT47	Ras Mohammed	Turtle Bay			*Porites sp.*	
LT47	Ras Mohammed	Turtle Bay			matrix	
LT47	Ras Mohammed	Turtle Bay			red algae	
LT47	Ras Mohammed	Turtle Bay			*Echinopora forskaliana*	
LT47	Ras Mohammed	Turtle Bay			matrix	
LT47	Ras Mohammed	Turtle Bay			matrix	
LT47	Ras Mohammed	Turtle Bay			matrix	
LT47	Ras Mohammed	Turtle Bay			matrix	
LT47	Ras Mohammed	Turtle Bay			matrix	
LT47	Ras Mohammed	Turtle Bay			*Porites sp.*	
LT47	Ras Mohammed	Turtle Bay			*Porites sp.*	
LT47	Ras Mohammed	Turtle Bay			*Porites sp.*	
LT47	Ras Mohammed	Turtle Bay			*Porites sp.*	
LT47	Ras Mohammed	Turtle Bay			matrix	
LT47	Ras Mohammed	Turtle Bay			*Montipora sp.*	LT47d
LT47	Ras Mohammed	Turtle Bay			*Montipora sp.*	
LT47	Ras Mohammed	Turtle Bay			matrix	
LT47	Ras Mohammed	Turtle Bay			matrix	
LT47	Ras Mohammed	Turtle Bay			matrix	
LT47	Ras Mohammed	Turtle Bay			matrix	
LT47	Ras Mohammed	Turtle Bay			*Echinopora forskaliana*	LT47e
LT47	Ras Mohammed	Turtle Bay			*Echinopora forskaliana*	
LT47	Ras Mohammed	Turtle Bay			*Dipsastraea sp.*	
LT47	Ras Mohammed	Turtle Bay			red algae	
LT47	Ras Mohammed	Turtle Bay			red algae	
LT47	Ras Mohammed	Turtle Bay			*Echinopora forskaliana*	
LT47	Ras Mohammed	Turtle Bay			*Echinopora forskaliana*	
LT47	Ras Mohammed	Turtle Bay			*Echinopora forskaliana*	
LT47	Ras Mohammed	Turtle Bay			matrix	
LT47	Ras Mohammed	Turtle Bay			matrix	
LT47	Ras Mohammed	Turtle Bay			matrix	
LT47	Ras Mohammed	Turtle Bay			*Porites sp.*	
LT47	Ras Mohammed	Turtle Bay			matrix	
LT47	Ras Mohammed	Turtle Bay			matrix	
LT47	Ras Mohammed	Turtle Bay			matrix	
LT47	Ras Mohammed	Turtle Bay			*Porites sp.*	
LT47	Ras Mohammed	Turtle Bay			matrix	
LT47	Ras Mohammed	Turtle Bay			matrix	
LT47	Ras Mohammed	Turtle Bay			matrix	
LT47	Ras Mohammed	Turtle Bay			*Porites sp.*	
LT47	Ras Mohammed	Turtle Bay			matrix	
LT47	Ras Mohammed	Turtle Bay			matrix	
LT47	Ras Mohammed	Turtle Bay			matrix	

LT	Locality	Site	GPS	Layer	*Name*	Sample
LT47	Ras Mohammed	Turtle Bay			*Porites sp.*	
LT47	Ras Mohammed	Turtle Bay			red algae	
LT47	Ras Mohammed	Turtle Bay			*Porites sp.*	
LT47	Ras Mohammed	Turtle Bay			matrix	
LT47	Ras Mohammed	Turtle Bay			matrix	
LT47	Ras Mohammed	Turtle Bay			matrix	
LT47	Ras Mohammed	Turtle Bay			matrix	
LT47	Ras Mohammed	Turtle Bay			matrix	
LT47	Ras Mohammed	Turtle Bay			matrix	
LT47	Ras Mohammed	Turtle Bay			Faviidae indet.	LT47f
LT48	Ras Mohammed	Ras Ghozlani	WP82		matrix	
LT48	Ras Mohammed	Ras Ghozlani	WP82		matrix	
LT48	Ras Mohammed	Ras Ghozlani	WP82		red algae	
LT48	Ras Mohammed	Ras Ghozlani	WP82		red algae	
LT48	Ras Mohammed	Ras Ghozlani	WP82		red algae	
LT48	Ras Mohammed	Ras Ghozlani	WP82		*Platygyra sp.*	
LT48	Ras Mohammed	Ras Ghozlani	WP82		red algae	
LT48	Ras Mohammed	Ras Ghozlani	WP82		red algae	
LT48	Ras Mohammed	Ras Ghozlani	WP82		matrix	
LT48	Ras Mohammed	Ras Ghozlani	WP82		Bivalve	
LT48	Ras Mohammed	Ras Ghozlani	WP82		red algae	
LT48	Ras Mohammed	Ras Ghozlani	WP82		red algae	
LT48	Ras Mohammed	Ras Ghozlani	WP82		red algae	
LT48	Ras Mohammed	Ras Ghozlani	WP82		red algae	
LT48	Ras Mohammed	Ras Ghozlani	WP82		*Echinopora forskaliana*	
LT48	Ras Mohammed	Ras Ghozlani	WP82		*Echinopora forskaliana*	
LT48	Ras Mohammed	Ras Ghozlani	WP82		*Echinopora forskaliana*	
LT48	Ras Mohammed	Ras Ghozlani	WP82		*Echinopora forskaliana*	
LT48	Ras Mohammed	Ras Ghozlani	WP82		matrix	
LT48	Ras Mohammed	Ras Ghozlani	WP82		matrix	
LT48	Ras Mohammed	Ras Ghozlani	WP82		*Goniastrea sp.*	LT48b
LT48	Ras Mohammed	Ras Ghozlani	WP82		red algae	
LT48	Ras Mohammed	Ras Ghozlani	WP82		*Platygyra daedalea*	
LT48	Ras Mohammed	Ras Ghozlani	WP82		*Acropora sp.*	
LT48	Ras Mohammed	Ras Ghozlani	WP82		*Acropora sp.*	
LT48	Ras Mohammed	Ras Ghozlani	WP82		red algae	
LT48	Ras Mohammed	Ras Ghozlani	WP82		*Goniastrea sp.*	LT48c
LT48	Ras Mohammed	Ras Ghozlani	WP82		red algae	
LT48	Ras Mohammed	Ras Ghozlani	WP82		red algae	
LT48	Ras Mohammed	Ras Ghozlani	WP82		*Goniastrea sp.*	
LT48	Ras Mohammed	Ras Ghozlani	WP82		red algae	
LT48	Ras Mohammed	Ras Ghozlani	WP82		*Goniastrea retiformis*	
LT48	Ras Mohammed	Ras Ghozlani	WP82		*Goniastrea retiformis*	
LT48	Ras Mohammed	Ras Ghozlani	WP82		red algae	
LT48	Ras Mohammed	Ras Ghozlani	WP82		red algae	
LT48	Ras Mohammed	Ras Ghozlani	WP82		red algae	

LT	Locality	Site	GPS	Layer	*Name*	Sample
LT48	Ras Mohammed	Ras Ghozlani	WP82		*Echinopora forskaliana*	
LT48	Ras Mohammed	Ras Ghozlani	WP82		*Echinopora forskaliana*	
LT48	Ras Mohammed	Ras Ghozlani	WP82		red algae	
LT48	Ras Mohammed	Ras Ghozlani	WP82		red algae	
LT48	Ras Mohammed	Ras Ghozlani	WP82		red algae	
LT48	Ras Mohammed	Ras Ghozlani	WP82		*Goniastrea retiformis*	
LT48	Ras Mohammed	Ras Ghozlani	WP82		red algae	
LT48	Ras Mohammed	Ras Ghozlani	WP82		red algae	
LT48	Ras Mohammed	Ras Ghozlani	WP82		*Echinopora forskaliana*	
LT48	Ras Mohammed	Ras Ghozlani	WP82		*Echinopora forskaliana*	
LT48	Ras Mohammed	Ras Ghozlani	WP82		*Echinopora forskaliana*	
LT48	Ras Mohammed	Ras Ghozlani	WP82		*Echinopora forskaliana*	
LT48	Ras Mohammed	Ras Ghozlani	WP82		red algae	
LT48	Ras Mohammed	Ras Ghozlani	WP82		red algae	
LT48	Ras Mohammed	Ras Ghozlani	WP82		*Galaxea fascicularis*	
LT48	Ras Mohammed	Ras Ghozlani	WP82		*Goniastrea retiformis*	
LT48	Ras Mohammed	Ras Ghozlani	WP82		*Goniastrea retiformis*	
LT48	Ras Mohammed	Ras Ghozlani	WP82		*Goniastrea retiformis*	
LT48	Ras Mohammed	Ras Ghozlani	WP82		red algae	
LT48	Ras Mohammed	Ras Ghozlani	WP82		*Goniastrea retiformis*	LT48d
LT48	Ras Mohammed	Ras Ghozlani	WP82		*Goniastrea retiformis*	
LT48	Ras Mohammed	Ras Ghozlani	WP82		*Goniastrea retiformis*	
LT48	Ras Mohammed	Ras Ghozlani	WP82		*Goniastrea retiformis*	
LT48	Ras Mohammed	Ras Ghozlani	WP82		*Goniastrea retiformis*	
LT48	Ras Mohammed	Ras Ghozlani	WP82		*Goniastrea retiformis*	
LT49	Ras Mohammed	Ras Ghozlani	WP82		*Porites sp.*	
LT49	Ras Mohammed	Ras Ghozlani	WP82		*Porites sp.*	
LT49	Ras Mohammed	Ras Ghozlani	WP82		*Porites sp.*	
LT49	Ras Mohammed	Ras Ghozlani	WP82		*Porites sp.*	
LT49	Ras Mohammed	Ras Ghozlani	WP82		red algae	
LT49	Ras Mohammed	Ras Ghozlani	WP82		red algae	
LT49	Ras Mohammed	Ras Ghozlani	WP82		*Porites sp.*	
LT49	Ras Mohammed	Ras Ghozlani	WP82		*Porites sp.*	
LT49	Ras Mohammed	Ras Ghozlani	WP82		*Porites sp.*	
LT49	Ras Mohammed	Ras Ghozlani	WP82		red algae	
LT49	Ras Mohammed	Ras Ghozlani	WP82		red algae	
LT49	Ras Mohammed	Ras Ghozlani	WP82		red algae	
LT49	Ras Mohammed	Ras Ghozlani	WP82		*Goniastrea retiformis*	
LT49	Ras Mohammed	Ras Ghozlani	WP82		*Goniastrea retiformis*	
LT49	Ras Mohammed	Ras Ghozlani	WP82		*Goniastrea retiformis*	
LT49	Ras Mohammed	Ras Ghozlani	WP82		*Platygyra lamellina*	
LT49	Ras Mohammed	Ras Ghozlani	WP82		*Platygyra lamellina*	
LT49	Ras Mohammed	Ras Ghozlani	WP82		*Goniastrea retiformis*	
LT49	Ras Mohammed	Ras Ghozlani	WP82		*Goniastrea retiformis*	
LT49	Ras Mohammed	Ras Ghozlani	WP82		*Goniastrea retiformis*	
LT49	Ras Mohammed	Ras Ghozlani	WP82		red algae	

LT	Locality	Site	GPS	Layer	*Name*	Sample
LT49	Ras Mohammed	Ras Ghozlani	WP82		red algae	
LT49	Ras Mohammed	Ras Ghozlani	WP82		red algae	
LT49	Ras Mohammed	Ras Ghozlani	WP82		red algae	
LT49	Ras Mohammed	Ras Ghozlani	WP82		red algae	
LT49	Ras Mohammed	Ras Ghozlani	WP82		Fungia sp.	
LT49	Ras Mohammed	Ras Ghozlani	WP82		*Goniastrea retiformis*	
LT49	Ras Mohammed	Ras Ghozlani	WP82		*Goniastrea retiformis*	
LT49	Ras Mohammed	Ras Ghozlani	WP82		*Goniastrea retiformis*	
LT49	Ras Mohammed	Ras Ghozlani	WP82		*Goniastrea retiformis*	
LT49	Ras Mohammed	Ras Ghozlani	WP82		*Goniastrea retiformis*	
LT49	Ras Mohammed	Ras Ghozlani	WP82		*Goniastrea retiformis*	
LT49	Ras Mohammed	Ras Ghozlani	WP82		*red algae*	
LT49	Ras Mohammed	Ras Ghozlani	WP82		*red algae*	
LT49	Ras Mohammed	Ras Ghozlani	WP82		*Echinopora forskaliana*	
LT49	Ras Mohammed	Ras Ghozlani	WP82		*Goniastrea retiformis*	
LT49	Ras Mohammed	Ras Ghozlani	WP82		*Goniastrea retiformis*	
LT49	Ras Mohammed	Ras Ghozlani	WP82		*Goniastrea retiformis*	
LT49	Ras Mohammed	Ras Ghozlani	WP82		*Goniastrea retiformis*	
LT49	Ras Mohammed	Ras Ghozlani	WP82		*Goniastrea retiformis*	
LT49	Ras Mohammed	Ras Ghozlani	WP82		*Goniastrea retiformis*	
LT49	Ras Mohammed	Ras Ghozlani	WP82		red algae	
LT49	Ras Mohammed	Ras Ghozlani	WP82		red algae	
LT49	Ras Mohammed	Ras Ghozlani	WP82		red algae	
LT49	Ras Mohammed	Ras Ghozlani	WP82		red algae	
LT49	Ras Mohammed	Ras Ghozlani	WP82		red algae	
LT49	Ras Mohammed	Ras Ghozlani	WP82		red algae	
LT49	Ras Mohammed	Ras Ghozlani	WP82		red algae	
LT49	Ras Mohammed	Ras Ghozlani	WP82		*Dipsastraea sp.*	LT49b
LT49	Ras Mohammed	Ras Ghozlani	WP82		red algae	
LT49	Ras Mohammed	Ras Ghozlani	WP82		red algae	
LT49	Ras Mohammed	Ras Ghozlani	WP82		*Fungia sp.*	
LT49	Ras Mohammed	Ras Ghozlani	WP82		*Goniastrea retiformis*	
LT49	Ras Mohammed	Ras Ghozlani	WP82		*Goniastrea retiformis*	
LT49	Ras Mohammed	Ras Ghozlani	WP82		Faviidae indet.	
LT49	Ras Mohammed	Ras Ghozlani	WP82		red algae	
LT49	Ras Mohammed	Ras Ghozlani	WP82		matrix	
LT49	Ras Mohammed	Ras Ghozlani	WP82		matrix	
LT49	Ras Mohammed	Ras Ghozlani	WP82		red algae	
LT49	Ras Mohammed	Ras Ghozlani	WP82		*Dipsastraea sp.*	
LT49	Ras Mohammed	Ras Ghozlani	WP82		*Dipsastraea sp.*	
LT49	Ras Mohammed	Ras Ghozlani	WP82		red algae	
LT49	Ras Mohammed	Ras Ghozlani	WP82		*Dipsastraea sp.*	
LT49	Ras Mohammed	Ras Ghozlani	WP82		Faviidae indet.	
LT49	Ras Mohammed	Ras Ghozlani	WP82		*Galaxea fascicularis*	
LT50	Ras Mohammed	Ras Ghozlani	WP82		*Porites sp.*	
LT50	Ras Mohammed	Ras Ghozlani	WP82		*Porites sp.*	

LT	Locality	Site	GPS	Layer	*Name*	Sample
LT50	Ras Mohammed	Ras Ghozlani	WP82		*Porites sp.*	
LT50	Ras Mohammed	Ras Ghozlani	WP82		*Porites sp.*	
LT50	Ras Mohammed	Ras Ghozlani	WP82		*Porites sp.*	
LT50	Ras Mohammed	Ras Ghozlani	WP82		*Porites sp.*	
LT50	Ras Mohammed	Ras Ghozlani	WP82		*Porites sp.*	
LT50	Ras Mohammed	Ras Ghozlani	WP82		red algae	
LT50	Ras Mohammed	Ras Ghozlani	WP82		red algae	
LT50	Ras Mohammed	Ras Ghozlani	WP82		*Acanthastrea echinata*	
LT50	Ras Mohammed	Ras Ghozlani	WP82		*Acanthastrea echinata*	
LT50	Ras Mohammed	Ras Ghozlani	WP82		*Acanthastrea echinata*	
LT50	Ras Mohammed	Ras Ghozlani	WP82		red algae	
LT50	Ras Mohammed	Ras Ghozlani	WP82		red algae	
LT50	Ras Mohammed	Ras Ghozlani	WP82		*Goniastrea retiformis*	LT50a
LT50	Ras Mohammed	Ras Ghozlani	WP82		*Goniastrea retiformis*	
LT50	Ras Mohammed	Ras Ghozlani	WP82		*Goniastrea retiformis*	
LT50	Ras Mohammed	Ras Ghozlani	WP82		*Goniastrea retiformis*	
LT50	Ras Mohammed	Ras Ghozlani	WP82		*Goniastrea retiformis*	
LT50	Ras Mohammed	Ras Ghozlani	WP82		*Goniastrea retiformis*	
LT50	Ras Mohammed	Ras Ghozlani	WP82		*Goniastrea retiformis*	
LT50	Ras Mohammed	Ras Ghozlani	WP82		*Goniastrea retiformis*	
LT50	Ras Mohammed	Ras Ghozlani	WP82		*Goniastrea retiformis*	
LT50	Ras Mohammed	Ras Ghozlani	WP82		red algae	
LT50	Ras Mohammed	Ras Ghozlani	WP82		*Goniastrea sp.*	LT50b
LT50	Ras Mohammed	Ras Ghozlani	WP82		*Pocillopora damicornis*	LT50c
LT50	Ras Mohammed	Ras Ghozlani	WP82		*Pocillopora damicornis*	
LT50	Ras Mohammed	Ras Ghozlani	WP82		*Pocillopora damicornis*	
LT50	Ras Mohammed	Ras Ghozlani	WP82		red algae	
LT50	Ras Mohammed	Ras Ghozlani	WP82		*Acropora sp.*	LT50d
LT50	Ras Mohammed	Ras Ghozlani	WP82		*Acropora sp.*	
LT50	Ras Mohammed	Ras Ghozlani	WP82		matrix	
LT50	Ras Mohammed	Ras Ghozlani	WP82		*Pocillopora verrucosa*	
LT50	Ras Mohammed	Ras Ghozlani	WP82		red algae	
LT50	Ras Mohammed	Ras Ghozlani	WP82		*Goniastrea retiformis*	LT50e
LT50	Ras Mohammed	Ras Ghozlani	WP82		*Goniastrea retiformis*	
LT50	Ras Mohammed	Ras Ghozlani	WP82		*Goniastrea retiformis*	
LT50	Ras Mohammed	Ras Ghozlani	WP82		*Goniastrea retiformis*	
LT50	Ras Mohammed	Ras Ghozlani	WP82		*Goniastrea retiformis*	
LT50	Ras Mohammed	Ras Ghozlani	WP82		*Goniastrea retiformis*	
LT50	Ras Mohammed	Ras Ghozlani	WP82		*Goniastrea retiformis*	
LT50	Ras Mohammed	Ras Ghozlani	WP82		*Goniastrea retiformis*	
LT50	Ras Mohammed	Ras Ghozlani	WP82		*Goniastrea retiformis*	
LT50	Ras Mohammed	Ras Ghozlani	WP82		*Goniastrea retiformis*	
LT50	Ras Mohammed	Ras Ghozlani	WP82		*Goniastrea retiformis*	
LT50	Ras Mohammed	Ras Ghozlani	WP82		*Goniastrea retiformis*	
LT50	Ras Mohammed	Ras Ghozlani	WP82		*Goniastrea retiformis*	
LT50	Ras Mohammed	Ras Ghozlani	WP82		*Goniastrea retiformis*	

LT	Locality	Site	GPS	Layer	*Name*	Sample
LT50	Ras Mohammed	Ras Ghozlani	WP82		red algae	
LT50	Ras Mohammed	Ras Ghozlani	WP82		*Echinopora forskaliana*	
LT50	Ras Mohammed	Ras Ghozlani	WP82		*Echinopora forskaliana*	
LT50	Ras Mohammed	Ras Ghozlani	WP82		*Echinopora forskaliana*	
LT50	Ras Mohammed	Ras Ghozlani	WP82		red algae	
LT50	Ras Mohammed	Ras Ghozlani	WP82		*Goniastrea retiformis*	
LT50	Ras Mohammed	Ras Ghozlani	WP82		*Goniastrea retiformis*	
LT50	Ras Mohammed	Ras Ghozlani	WP82		*Goniastrea retiformis*	
LT50	Ras Mohammed	Ras Ghozlani	WP82		*Goniastrea retiformis*	
LT50	Ras Mohammed	Ras Ghozlani	WP82		*Goniastrea retiformis*	
LT50	Ras Mohammed	Ras Ghozlani	WP82		*Goniastrea retiformis*	
LT50	Ras Mohammed	Ras Ghozlani	WP82		red algae	LT50f
LT50	Ras Mohammed	Ras Ghozlani	WP82		*Goniastrea retiformis*	
LT50	Ras Mohammed	Ras Ghozlani	WP82		*Goniastrea retiformis*	
LT50	Ras Mohammed	Ras Ghozlani	WP82		red algae	
LT50	Ras Mohammed	Ras Ghozlani	WP82		*Goniastrea retiformis*	
LT50	Ras Mohammed	Ras Ghozlani	WP82		*Dipsastraea sp.*	LT50g
LT50	Ras Mohammed	Ras Ghozlani	WP82		red algae	

Table 6-VI: Combined dataset with recent and fossil data. Station 1 -3 are the data from divesite *The Islands* provided by Alter (2004), standardized to Pleistocene occurences.

	Station 1	Station 2	Station 3	Blue Hole	Canyon north patch Reef	Canyon Reef	Turtle Bay	Ras Ghozlani-inland	Ras Ghozlani	Ras Mohammed Camp	Ras Mohammed inland
Acanthastrea echinata	15	28	14	0	0	0	0	0	3	2	0
Acropora muricata	18	35	4	0	0	43	0	0	0	0	0
Acropora sp.	212	422	87	10	1	79	10	0	4	0	0
Astreopora myriophthalma	1	2	4	0	3	2	0	0	0	0	0
Coscinerea monile	3	3	0	0	0	1	1	0	0	0	0
Cyphastrea serailia	13	3	4	0	0	6	0	0	0	1	0
Cyphastrea sp.	44	39	17	5	2	5	3	0	0	1	3
Echinopora forskaliana	10	6	1	13	1	16	14	0	14	25	0
Dipsastraea pallida	8	14	19	0	7	0	5	1	0	6	0
Favites rotundata	0	1	1	0	0	1	0	0	0	0	0
Dipsastraea sp.	11	22	38	3	7	17	22	0	5	11	0
Favites flexuosa	0	0	0	0	0	1	0	0	0	10	0
Favites pentagona	5	25	12	0	1	0	0	0	0	0	0
Favites spinosa	0	0	0	0	0	0	1	0	0	1	0
Favites sp.	27	20	5	1	1	1	1	0	0	7	0
Fungia sp.	10	22	2	5	0	5	2	0	2	1	0
Galaxea fascicularis	1	12	0	5	16	9	1	0	2	2	0
Coelastrea aspera	1	2	0	1	0	0	0	0	0	0	0
Goniastrea edwardsi	31	34	8	6	0	6	2	0	0	0	0
Paramontastraea peresi	4	5	1	0	4	4	0	0	0	0	0

	Station 1	Station 2	Station 3	Blue Hole	Canyon north patch Reef	Canyon Reef	Turtle Bay	Ras Ghozlani-inland	Ras Ghozlani	Ras Mohammed Camp	Ras Mohammed inland
Goniastrea retiformis	0	0	0	8	0	0	0	0	64	83	0
Goniopora sp.	0	8	1	0	0	1	1	0	0	0	0
Gyrosmilia interrupta	3	3	0	0	0	0	10	0	0	0	0
Hydnophora microconos	4	7	2	0	3	0	0	0	0	0	0
Leptastrea sp.	10	15	19	0	0	9	0	0	0	0	0
Leptoseris sp.	2	5	0	1	0	2	0	0	0	0	0
Lobophyllia sp.	1	2	0	6	0	6	0	0	0	5	0
Lobophyllia corymbosa	1	0	0	2	0	7	0	0	0	9	0
Millepora sp.	41	17	29	0	0	14	8	0	0	0	0
Montipora sp.	79	48	51	2	0	34	10	0	0	1	0
Mycedium sp.	7	0	0	0	0	3	0	0	0	0	0
Pavona sp.	72	20	23	0	0	6	0	0	0	0	0
Platygyra crosslandi	4	3	1	10	0	0	0	0	0	2	0
Platygyra daedalea	6	1	6	14	0	17	0	0	1	0	0
Platygyra lamellina	8	5	1	3	11	3	0	0	2	2	0
Pocillopora damicornis	31	41	10	0	5	1	0	0	3	0	0
Pocillopora verrucosa	17	42	11	0	6	0	2	0	1	0	0
Porites lobata/lutea	47	100	9	11	5	92	18	0	0	0	0
Porites nodifera	9	28	0	91	3	99	13	0	0	0	0
Porites sp.	20	110	16	7	3	8	153	18	14	0	0
Psammocora sp.	7	19	2	0	0	7	0	0	0	0	0
Stylophora sp.	104	57	66	0	2	3	2	0	0	1	0
Turbinaria sp.	1	1	0	0	0	2	0	0	0	0	0

Table 6-VII: GPS-coordinates of transects and sites, omplemented by coordinates of the data collected by Alter (2004) and the Miocene outcrop described in Chapter 5. WP = waypoint of GPS device.

WP	LT	Site	Latitude (N)	Longitude (E)
41	LT01	Canyon north patch reef	28°33'59.13"	34°31'49.65"
	LT02	Canyon north patch reef		
	LT03	Canyon north patch reef		
	LT04	Canyon north patch reef		
	LT05	Canyon north patch reef		
42	LT06	Canyon reef	28°33'19.38"	34°31'16.88''
	LT07	Canyon reef		
	LT08	Canyon reef		
43	LT09	Canyon reef	28°33'19.39"	34°31'12.95"
	LT10	Canyon reef		
44	LT11	Canyon reef	28°33'19.33"	34°31'15.05"
	LT12	Canyon reef		
48	LT13	Canyon reef		
	LT14	Canyon reef		
	LT15	Canyon reef		

WP	LT	Site	Latitude (N)	Longitude (E)
	LT16	Canyon reef		
	LT17	Canyon reef		
	LT18	Canyon reef		
	LT19	Canyon reef		
49	LT20	Blue Hole	28°34'5.52"	34°32'2.18"
	LT21	Blue Hole		
	LT22	Blue Hole		
50	LT23	Blue Hole	28°34'12.08"	34°32'8.43"
	LT24	Blue Hole		
	LT25	Blue Hole		
	LT26	Canyon reef		
51	LT27	Canyon reef	28°33'19.84"	34°31'15.47"
	LT28	Canyon reef		
52	LT29	Canyon reef	28°33'21.82"	34°31'15.41"
	LT30	Canyon reef		
	LT31	Canyon reef		
54	LT32	Turtle Bay	27°47'39.06"	34°13'55.28"
57	LT33	Ras Mohammed inland	27°47'40.92"	34°14'42.47"
62	LT34	Ras Mohammed camp	27°47'19.71"	34°13'31.24"
	LT35	Ras Mohammed camp		
	LT36	Ras Mohammed camp		
69	LT37	Turtle Bay	27°47'44.27"	34°13'55.66"
	LT38	Turtle Bay		
70	LT39	Ras Mohammed camp	27°47'20.08"	34°13'31.90"
	LT40	Turtle Bay		
	LT41	Turtle Bay		
	LT42	Turtle Bay		
	LT43	Turtle Bay		
	LT44	Turtle Bay		
	LT45	Turtle Bay		
78	LT46	Ras Ghozlani inland	27°47'19.85"	34°14'24.35"
	LT47	Turtle Bay		
82	LT48	Ras Ghozlani	27°47'13.98"	34°14'19.01"
82	LT49	Ras Ghozlani		
82	LT50	Ras Ghozlani		
63	Miocene terrace	Ras Mohammed peininsula	27°45'46.67"	34°14'40.50"
	Islands diving spot	Dahab	28°28'38.25"	34°30'45.61"